University of Belgrade, Technical faculty in Bor
Chamber of Commerce and Industry of Serbia

PROCEEDINGS

2021 IMPRO
INTERNATIONAL MINERAL PROCESSING & RECYCLING CONFERENCE

XIV INTERNATIONAL MINERAL PROCESSING AND RECYCLING CONFERENCE

Editors:
Jovica Sokolović
Milan Trumić

May 12-14, 2021, Belgrade, Serbia

University of Belgrade, Technical faculty in Bor
Chamber of Commerce and Industry of Serbia

PROCEEDINGS

2021 IMPRO
INTERNATIONAL MINERAL PROCESSING & RECYCLING CONFERENCE

XIV International
MINERAL PROCESSING and RECYCLING CONFERENCE

Editors:
Jovica Sokolović
Milan Trumić

May 12 – 14, 2021, Belgrade, Serbia

XIV INTERNATIONAL
MINERAL PROCESSING and RECYCLING CONFERENCE

PUBLISHER:
University of Belgrade, Technical Faculty in Bor

FOR THE PUBLISHER:
DEAN: Prof. Dr Nada Štrbac

EDITORS:
Prof. Dr Jovica Sokolović
Prof. Dr Milan Trumić

PROCEEDINGS COVER DESIGN:
Branislav Gapić

PRINTED BY:
Tercija d.o.o., Bor, Serbia
Printed: 100 copies

PUBLICATION YEAR:
2021

===========================
CIP - Каталогизација у публикацији
Народна библиотека Србије, Београд

622.7(082)
502.131.1:628.477.6(082)
628.477.6(082)

INTERNATIONAL Mineral Processing and Recycling Conference (14 ; 2021 ; Beograd)
Proceedings / XIV International Mineral Processing and Recycling Conference, IMPRC, May 12-14, 2021, Belgrade, Serbia ; editors Jovica Sokolović, Milan Trumić. - Bor : University of Belgrade, Technical Faculty, 2021 (Bor : Tercija). - XI, 514 str. : ilustr. ; 25 cm

Na vrhu nasl. str.: Chamber of Commerce and Industry of Serbia. - Tiraž 100. - Bibliografija uz svaki rad. - Registar.

ISBN 978-86-6305-113-3

а) Руде -- Припрема -- Зборници б) Отпадне материје -- Одрживи развој -- Зборници в) Отпадне материје -- Рециклажа -- Зборници

COBISS.SR-ID 37464585
===========================

Conference is financially supported by
Republic of Serbia,
Ministry of Education, Science and
Technological Development

SCIENTIFIC COMMITTEE

Prof. Dr Milan Trumić, Serbia, President
Prof. Dr Grozdanka Bogdanović, Serbia, Vice President
Prof. Dr Jovica Sokolović, Serbia, Vice President
Prof. Dr Mauricio Torem, Brazil
Prof. Dr Sanja Miskovic, Canada
Prof. Dr Qingqing Huang, USA
Prof. Dr Zhiyong Gao, China
Prof. Dr Wencheng Xia, China
Prof. Dr Takashi Nakamura, Japan
Prof. Dr Boris Albijanic, Australia
Prof. Dr Rraghupatruni Bhima Rao, India
Prof. Dr Przemyslaw Kowalczuk, Norway
Prof. Dr Junbeum Kim, France
Prof. Dr Srećko Stopić, Germany
Prof. Dr Alejandro Rodriguez Pascual, Spain
Prof. Dr Adele Muscolo, Italy
Prof. Dr Georgios Anastassakis, Greece
Prof. Dr Mehmet Polat, Turkey
Prof. Dr Leonid Vaisberg, Russia
Prof. Dr Vladimir Čablik, Czech Republic
Dr Slavomir Hredzak, Slovakia
Prof. Dr Gabor Musci, Hungary
Prof. Dr Francisc Popescu, Romania
Prof. Dr Ivan Nishkov, Bulgaria
Prof. Dr Jakob Lamut, Slovenia
Prof. Dr Aleksandra Anić Vučinić, Croatia
Prof. Dr Ilhan Bušatlić, Bosnia & Herzegovina
Prof. Dr Svjetlana Sredić, Republic of Srpska, Bosnia & Herzegovina
Prof. Dr Mirjana Golomeova, North Macedonia
Prof. Dr Nada Štrbac, Serbia
Prof. Dr Milan Antonijević, Serbia
Prof. Dr Miodrag Žikić, Serbia
Prof. Dr Zoran Stević, Serbia
Prof. Dr Dejan Tanikić, Serbia
Prof. Dr Snežana Šerbula, Serbia
Prof. Dr Mira Cocić, Serbia
Prof. Dr Ljubiša Andrić, Serbia

Prof. Dr Milena Kostović, Serbia
Prof. Dr Aleksandar Jovović, Serbia
Prof. Dr Željko Kamberović, Serbia
Prof. Dr Vlada Veljković, Serbia
Prof. Dr Goran Vujić, Serbia
Prof. Dr Jelena Radonić, Serbia
Prof. Dr Srđan Rončević, Serbia
Prof. Dr Irma Dervišević, Serbia
Prof. Dr Marina Stamenović, Serbia
Prof. Dr Vladimir Pavićević, Serbia
Prof. Dr Zoran Štirbanović, Serbia
Prof. Dr Maja Trumić, Serbia
Dr Miroslav Ignjatović, Serbia
Dr Ivana Smičiklas, Serbia
Dr Miroslav Sokić, Serbia
Dr Dragan Radulović, Serbia
Dr Vladan Milošević, Serbia
Dr Sonja Milićević, Serbia
Dr Milinko Radosavljević, Serbia
Dr Mile Bugarin, Serbia
Dr Zoran Stevanović, Serbia
Dr Radmila Marković, Serbia

ORGANIZING COMMITTEE

Prof. Dr Jovica Sokolović, Serbia, President
Prof. Dr Milan Trumić, Serbia
Prof. Dr Grozdanka Bogdanović, Serbia
Dr Miroslav Ignjatović, Serbia
Prof. Dr Zoran Štirbanović, Serbia
Prof. Dr Maja Trumić, Serbia
MSc Vladimir Nikolić, Serbia
MSc Dragana Marilović, Serbia
MSc Predrag Stolić, Serbia
MSc Katarina Balanović, Serbia
BSc Ivana Ilić, Serbia
BSc Sandra Vasković, Serbia
BSc Slavica Stevanović, Serbia
Dobrinka Trujić, Serbia

TABLE OF CONTENTS

PLENARY LECTURES

XIV International Mineral Processing
and Recycling Conference
Belgrade, Serbia, 12-14 May 2021

ATOMIC FORCE MICROSCOPY (AFM) FORCE MEASUREMENT IN SURFACE CHEMISTRY OF MINERAL FLOTATION

Zhiyong Gao#, Mengjie Tian, Jianyong He, Wanjia Zhang, Wei Sun, Jian Cao
[1] Central South University, School of Minerals Processing and Bioengineering,
Changsha, China
[2] Central South University, Key Laboratory of Hunan Province for Clean and
Efficient Utilization of Strategic Calcium-containing Mineral Resources,
Changsha, China

ABSTRACT – Flotation is a mineral separation technology by use of the surface hydrophobic difference between valuable minerals and their associated gangue minerals. Flotation collector adsorbs on the valuable mineral surface to improve its hydrophobicity, and metal ion is usually used as activator to enhance the collector adsorption. All those adsorptions and/or flotation behaviours are governed by mineral surface chemistry such as surface charging and reactivity. In our studies, atomic force microscopy (AFM) force measurement was employed, to study the surface chemistry of mineral flotation. The application of AFM force measurement lay the foundation for the specific regulation of mineral surface characteristics.

Keywords: Mineral, Flotation, Surface Chemistry, AFM.

INTRODUCTION

Scheelite ($CaWO_4$) is the most important mineral source of tungsten, an element used in lamp filaments, cutting steel, super hard moulds, and catalysts, to name a few [1]. Flotation is a mineral separation technology by use of the surface hydrophobic difference between valuable minerals and their associated gangue minerals, and is the important beneficiation method of scheelite from ore deposits. Recently, benzohydroxamic acid (BHA) has been extensively used in scheelite flotation, and shows excellent selectivity but limited collecting ability in [2]. Pb^{2+} ion is therefore commonly used as the activator to enhance BHA collecting ability [3]. According to the classical activation theory, Pb^{2+} ion is normally added prior to the addition of BHA to increase the number of active sites on oxide mineral surface, thus enhancing the subsequent adsorption of BHA collector [4]. Recent flotation studies demonstrated that a Pb-BHA complex prepared by mixing Pb^{2+} ion and BHA at a given molar ratio exhibited a more promising collectability than the sequential addition of Pb^{2+} and BHA (SAPB) on scheelite [5]. It is of both fundamental and practical importance to explore the adsorption mechanism of both Pb-BHA complex and BHA on the scheelite surface, which accurate measurement of scheelite surface charging (potential) is helpful to explore. Because Pb-BHA complex and BHA adsorption on the scheelite surface are governed by surface chemistry such as surface charging (potential).

---

corresponding author: zhiyong.gao@csu.edu.com

In this work, AFM was used to study the charging of scheelite surfaces with specific orientation including (112), (101) and (001) surfaces. The BHA-functionalized AFM tip was prepared and employed to measure the interaction forces between BHA and the Pb^{2+}-activated scheelite surface to mimic the SAPB. In contrast, the BHA-functionalized AFM tip was conditioned in Pb^{2+} solution to form a Pb-BHA complex, which was used to measure the interaction of Pb-BHA complex with the scheelite surface.

The study on the surface chemistry of mineral flotation are of both fundamental and practical importance on the development of flotation reagents and lay the foundation for the specific regulation of mineral surface characteristics. This method we reported is of great significance to design tailor-made reaction system in such fields as flotation reagent development, oriental growth of crystal, and powder modification.

EXPERIMENTAL

MATERIALS AND REAGENTS

Analytical grade lead nitrate ($Pb(NO_3)_2$, Tianjin Kermil Chemical Reagents Development Centre, China) as activator was used in the AFM force experiments. Potassium hydroxide (KOH) and hydrochloric acid (HCl) were used for pH modification. Milli-Q water (Millipore deionized, US) with resistivity of 18.2 MΩ × cm was used throughout the experiments.

N-hydroxy-4-mercaptobenzamide (MBHA) was synthesized by modifying carboxyl group (-COOH) of 4-mercaptobenzoic acid into hydroxamate group (-CONHOH), and the synthesis method is presented in one of our previous studies [6].

SCHEELITE CRYSTALS AND THEIR CHARACTERIZATION

Single crystals of scheelite with dimensions of 5 to 10 mm were obtained from an ore in the Huili Mine located in Sichuan, China. The crystallographic orientations of scheelite crystal specimens were determined by single-crystal X-ray diffraction. The X-ray diffraction (XRD) analysis was conducted on 20 scheelite crystal samples and 3 crystals were selected for the atomic functional microscopy (AFM) study. In total, 23 pieces of scheelite crystals were randomly picked up from the crushed ore samples and characterized with X-ray diffraction (XRD). The XRD results revealed 13 specimens with (112) surface, 7 specimens with (101) and only 3 specimens with (001), indicating that (112) plane is the most commonly exposed cleavage surface for scheelite crystal, followed by a moderate (101) and a weak (001), in agreement with the previous reports [7].

AFM FORCE MEASUREMENTS

In the AFM force measurements to study the scheelite surface charging (potential), contact-mode silicon nitride (Si_3N_4) AFM cantilevers of a V-frame shape (Bruker AFM Probes, Camarillo, CA) were used in this study. The colloidal force measurements were carried out in 1mM KCl solutions of varying pH (adjusted with KOH or HCl stock solutions) using a NanoscopeII AFM (Digital Instruments Inc. – currently Bruker Corp.) equipped with a fluid cell. Surface charge density and potential values reported are values calculated from experimental force curves after fitting the theoretical equations presented in previous study [8]. Prior to the AFM force measurements between BHA and scheelite surfaces, Au-coated AFM tips (B Triangular NPG-10, Bruker) were functionalized with a self-assembled monolayer of MBHA. Fig. 1 show the schematics of force measurements between functionalized AFM Au tips and scheelite surfaces in 1 mM KCl solution.

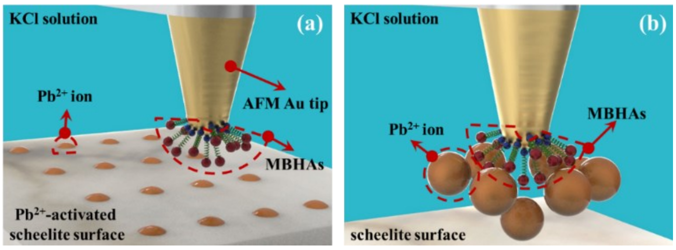

Figure 1 Schematics of force measurements between the MBHA-functionalized AFM Au tip and the Pb^{2+}-activated scheelite surface (a), and the Pb-MBHA complex-functionalized AFM Au tip and the scheelite surface in 10^{-3} mol/L KCl solution

RESULTS

AFM FORCE MEASUREMENTS TO STUDY THE SCHEELITE SURFACE CHARGING

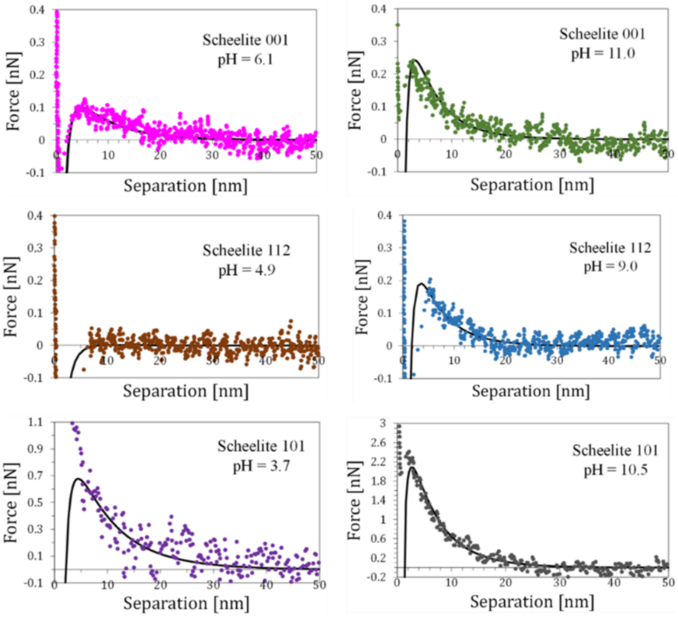

Figure 2 Examples of force-separation curves for the Si_3N_4 tips interacting with scheelite (001), (101) and (112) surfaces in 1 mM KCl solution of varying pH. Force measurements were done with two cantilevers of different spring constant and tip radius: scheelite (001) and (112), and scheelite (101). The solid lines represent theoretical fits

Previous work indicates that silicon nitride (AFM cantilever tip) is negatively charged over a pH range of 4–11 [9]. Therefore, the attractive or repulsive interaction force between cantilever tip and mineral surface is mainly controlled by the sign of the mineral surface charge. If the surface charge of mineral surface is negative, a repulsive force was observed, and positive for attractive force. For each of the scheelite specimens, examples of two force curves, together with theoretical fittings, are shown in Fig. 2.

Only repulsive forces were recorded for all three specimens, over a pH value from pH = 3.7–5.0 to pH = 10.5–11.2 (Fig. 2). Given the negative surface potential of silicon nitride tip for this range of pH values, it is obvious that all three specimens were negatively charged in this pH range.

THEORETICAL FITTING AND RESULTING SURFACE POTENTIALS

In plotting theoretical curves, the surface charge density values extrapolated from the values determined for Si_3N_4 AFM tips in the previous study were used [9]. The surface charge density values were calculated from fitting the experimental data with the theoretical force curve [10].

As shown in Fig. 3a, the most noticeable effect of pH on surface charge density variation is associated with the surface (112). The average surface charge density increased from about −1 $mC{\cdot}m^{-2}$ to −8 $mC{\cdot}m^{-2}$ for (112) when pH increased from pH=5.0 to pH=11.0. The surface charge density of (101) increased from about −4 $mC{\cdot}m^{-2}$ at pH=3.7 to over −8 $mC{\cdot}m^{-2}$ at pH=10.5. On the contrary, the surface (001) showed very small sensitivity to pH, and the surface charge density for this surface remained nearly constant at about −3 $mC{\cdot}m^{-2}$ over pH=5.0 to pH=9.0, with a small tendency to increase in more alkaline solutions.

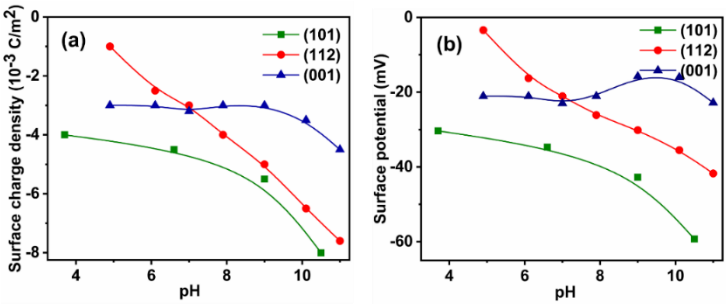

Figure 3 Surface charge densities (a) and potentials (b) for scheelite (001), (101) and (112) surfaces in 1mM KCl solution at varying pH

The surface potential values (Ψ) were calculated from the experimentally – determined surface charge density (σ) values as described in the previous contribution [9]. Average surface potential values are shown in Fig. 3b. The calculated negative surface potential increased from approximately −4 mV at pH=5.0 to over −40 mV for (112). For (101), the calculated negative surface potential increased from about −30 mV at pH=3.7 to about −60 mV at pH=10.5. A nearly constant surface potential of −20 mV (±5 mV) over the pH range of pH=5.0 to pH=11.0 was calculated for (001).

The surface potential values for three scheelite surfaces closely matched the zeta potential values reported for powdered scheelite in the literature [11, 12]. Powdered scheelite samples have been reported to carry negative charges in the pH range of 3–11. Since measurements on powdered scheelite reflect averaging contributions from all cleaved and exposed surfaces of this anisotropic mineral, with very predominant cleavage on (112), (101) and (001) surfaces, the agreement between results in Fig. 3b and previous literature is remarkably good.

AFM FORCE MEASUREMENTS BETWEEN BHA AND SCHEELITE SURFACES

The negative charging (potentials) of scheelite (112), (101) and (001) surfaces, the commonly exposed cleavage surfaces for scheelite crystal, was determined by AFM force measurement (Fig. 3). The limited collecting ability of benzohydroxamic acid (BHA) in scheelite flotation is because it is difficult for it to adsorb on scheelite surface, which is due to the electrostatic repulsion between negatively charged scheelite surface and BHA anion. Pb^{2+} ion can increase the scheelite surface potential to enhance BHA adsorption. Pb^{2+} ion pre-adsorbed on the scheelite surface acts as the active site for subsequent attachment of BHA. However, the hydrated layer of Pb^{2+} ion can inhibit its interaction with BHA. To mitigate the negative effect of Pb^{2+} ion hydration, Pb-BHA complex was prepared as the collector, which shows the stronger collecting ability than the SAPB (Fig. 4). To unravel the interaction mechanism between BHA molecule and scheelite surface in the presence of Pb^{2+} ion, MBHA with a structure similar to BHA was self-assembled on AFM tips. The scheelite crystal characterization results show that (112) surface is the most commonly exposed cleavage surface and was therefore selected as the studied surface in the following AFM force measurements.

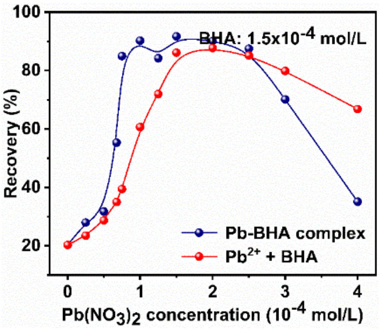

Figure 4 Scheelite flotation recovery as a function of $Pb(NO_3)_2$ concentration using different collector schedules [3]

The surface potentials of the MBHA-functionalized AFM tip and the Pb^{2+}-activated scheelite (112) surface were fitted to be approximately −230 mV and −200 mV, respectively. The adhesion and the effective adhesion energy (W_{adh}) of BHA on the Pb^{2+}-activated scheelite (112) surface in 1 mM KCl solution was 33 $mN\cdot m^{-1}$ and 5.25 $mJ\cdot m^{-2}$, respectively (Table 1). The MBHA-functionalized AFM tip was immersed in Pb^{2+} solution for 10 min to prepare the Pb-MBHA complex-functionalized AFM tip with the higher surface potential of −130 mV. The surface potential of the scheelite (112) surface of –

130 mV was also higher than the Pb^{2+}-activated scheelite (112) surface, which is due to the hydroxylation of Pb^{2+} ion adsorbed on the scheelite surface. The adhesion of Pb-BHA complex on the scheelite (112) surface in KCl solution was 65 mN·m^{-1} (Table 1). The W_{adh} of Pb-BHA complex was 10.35 mJ·m^{-2} (Table 1).

Table 1 Adhesion forces (energies) of BHA and Pb-BHA complex with scheelite surfaces.

Scheelite surface Adsorbent	Pb^{2+}-activated and hydroxylated BHA	Hydroxylated Pb-BHA complex
Normalized adhesion (mN·m^{-1})	33	65
Adhesion energy (mJ·m^{-2})	5.25	10.35

DISCUSSIONS

The negative charge of scheelite surfaces could be attributed to the semi-soluble nature of the scheelite mineral and the preferential dissolution of ions from the crystal [13, 14]. Ca^{2+} ion with a more negative free energy of hydration is favorably removed from the scheelite surface, leaving behind a slight stoichiometric excess of WO_4^{2-} in the near-surface region. As a result, the scheelite surface is negatively charged in the aqueous phase. Further, at acidic pH values, surface WO_4^{2-} could adsorb H+ from the solution to form HWO_4^-, which weakens the binding of surface WO_4^{2-} ion to Ca^{2+} ion and facilitates the dissolution of surface Ca^{2+} ion. Therefore, either WO_4^{2-} or HWO_4^{2-} could be the potential determining ion for scheelite, depending on the solution pH.

Figure 3 show the surface charge densities (σ) and surface potentials (Ψ), respectively. All three scheelite surfaces had different σ-pH and Ψ-pH correlations, most likely dictated by differences in distribution of Ca^{2+} and WO_4^{2-} ions, combined with a number of broken bonds for O^{2-}. Specifically, three surfaces have a different surface density of Ca^{2+} ions to be hydrated and hence a different surface density of WO_4^{2-} (or O^{2-}) ions is left in the near-surface region. The saturated coordination number of O^{2-} in the scheelite crystal cell is three, i.e., one with W and two with Ca. There are different types of O^{2-} in the structure of the surface WO_4^{2-} ion. They differ in the number of broken bonds: 1) O with no broken bond (O_0^{2-}, non-active below the surface top layer); 2) O with one broken bond (O_1^{2-}), and 3) O with two broken bonds (O_2^{2-}). Both 1) and 2) are active and positioned near the surface top layer. It is hypothesized that the active O^{2-} ions exert influence on surface charging while non-active ones do not. The surface density of WO_4^{2-} and active O^{2-} at each scheelite surface is summarized in Table 2.

The largest density of active O^{2-} equal to 9.1 sites·nm^{-2} was calculated for (101) (Table 2). The surface active O^{2-} attracts hydroxide ions (OH^-) from the solution via a hydrogen bonding interaction. As the solution pH increases, the concentration of OH^- in solution increases accordingly, and the magnitude of negative surface potential increases. A large number of OH^- are expected to adsorb on a surface with a larger density of active O^{2-} ions, leading to a more negatively charged surface. Consequently, the surface (101) bears the largest magnitude of negative surface potential, followed by (112) and then (001) surface, in agreement with results in Fig. 3. The surface (001) has the lowest density of surface active O^{2-} ions, and consequently OH^- adsorption on this surface can almost reach a saturation level at a low OH– concentration (at low pH). Therefore, with the increase of pH, the surface charging of (001) changes only slightly.

Table 2 Population of WO_4^{2-} or active O^{2-} on scheelite (112), (101) and (001) surfaces

Crystal surface	(112)	(101)	(001)
Surface unit cell area (nm^2)	0.504	0.328	0.275
Tungstate ion sites per unit cell (sites)	2	2	1
Active oxygen per unit cell (sites)	3	3	2
Active oxygen per unit cell area (sites/nm^2)	6.0	9.1	3.6

*Note: 1. On (112) surface, there are one O_2^{2-} in one WO_4^{2-} ion, while two O_1^{2-} in another. 2. On (101), there are one O_1^{2-} in one WO_4^{2-} ion and two in another. 3. On (001), there are two O_1^{2-} in one WO_4^{2-} ion.

The AFM force measurement results indicate the stronger adhesion strength of Pb-BHA complex on the scheelite surface that that of BHA on the Pb^{2+}-activated scheelite surface (Table 1), which is due to that Pb-BHA complex can actively interact with the scheelite surface without replacing the hydrated H_2O molecules (of Pb^{2+} ion) [15].

CONCLUSIONS

AFM colloidal force measurements for three different scheelite surfaces show strong anisotropy of scheelite. It was found that the surface (101) is the most negatively charged surface of scheelite, followed by (112) and (001). Surface potential for (001) was only slightly affected by pH whereas surface potentials of both (112) and (101) increased significantly with increasing pH.

Pb^{2+} ion can be used as the activator to enhance the benzohydroxamic acid (BHA) collectability in mineral flotation in two different ways: (i). adding Pb-BHA complex formed by mixing Pb^{2+} ion and BHA at a given molar ratio; (ii). sequential addition of Pb^{2+} and BHA. In this study, AFM was, for the first time, employed to investigate the activation role of Pb^{2+} ion in the BHA flotation of scheelite at the nanoscale. A BHA model molecule, i.e., N-hydroxy-4-mercaptobenzamide (MBHA), was synthesized to prepare a BHA-functionalized AFM probe. AFM force measurements demonstrate a much stronger adhesion energy (10.35 $mJ \cdot m^{-2}$) of Pb-BHA complex on scheelite surface than that (5.25 $mJ \cdot m^{-2}$) of BHA on the Pb^{2+}-activated scheelite surface, which is due to that Pb-BHA complex can actively interact with the scheelite surface without replacing the hydrated H_2O molecules (of Pb^{2+} ion).

ACKNOWLEDGEMENT

The authors acknowledge financial supports from the National Natural Science Foundation of China (51774328 and U2067201), the Key Program for International S & T Cooperation Projects of China (2019YFE012999), the Science Fund for Distinguished Young Scholars of Hunan Province, China (2020JJ2044), the Young Elite Scientists Sponsorship Program of Hunan province, China (2018RS3011) and the National 111 Project (B14034).

REFERENCES

1. Zhang, Z., Peng, H., Yan, J. (2013) Micro-cutting characteristics of EDM fabricated high-precision polycrystalline diamond tools. International Journal of Machine Tools and Manufacture, 65, 99-106.

2. Han, H., Hu, Y., Sun, W., Li, X., Cao, C., Liu, R., Yue, T., Meng, X., Guo, Y., Wang, J., Gao, Z., Chen, P., Huang, W., Liu, J., Xie, J., Chen, Y. (2017) Fatty acid flotation versus BHA flotation of tungsten minerals and their performance in flotation practice. International Journal of Mineral Processing, 159, 22-29.
3. Han, H., Hu, Y., Sun, W., Li, X., Chen, K., Zhu, Y., Nguyen, A.V., Tian, M., Wang, L., Yue, T., Liu, R., Gao, Z., Chen, P., Zhang, C., Wang, J., Wei, Z., Wang, R. (2018) Novel catalysis mechanisms of benzohydroxamic acid adsorption by lead ions and changes in the surface of scheelite particles. Minerals Engineering, 119, 11-22.
4. Tian, M., Zhang, C., Han, H., Liu, R., Gao, Z., Chen, P., He, J., Hu, Y., Sun, W., Yuan, D. (2018) Novel insights into adsorption mechanism of benzohydroxamic acid on lead (II)-activated cassiterite surface: An integrated experimental and computational study. Minerals Engineering, 122, 327-338.
5. He, J., Han, H., Zhang, C., Hu, Y., Yuan, D., Tian, M., Chen, D., Sun, W. (2018) New insights into the configurations of lead(II)-benzohydroxamic acid coordination compounds in aqueous solution: a combined experimental and computational study. Minerals, 8 (9), 16.
6. Hu, W., Tian, M., Cao, J., Xie, L., Gong, L., Sun, W., Gao, Z., Zeng, H. (2020) Probing the interaction mechanism between benzohydroxamic acid and mineral surface in the presence of Pb^{2+} Ions by AFM force measurements and first-principles calculations. Langmuir, 36, 8199-8208.
7. Mogilevsky, P., Parthasarathy, T., Petry, M. (2004) Anisotropy in room temperature microhardness and fracture of CaWO4 scheelite. Acta materialia, 52, 5529-5537.
8. Gao, Z., Xie, L., Cui, X., Hu, Y., Sun, W., Zeng, H. (2018) Probing anisotropic surface properties and surface forces of fluorite crystals. Langmuir, 34, 511-2521.
9. Yin, X., Drelich, J. (2008) Surface charge microscopy: novel technique for mapping charge-mosaic surfaces in electrolyte solutions. Langmuir, 24, 8013-8020.
10. Gao, Z., Hu, Y., Sun, W., Drelich, J.W. (2016) Surface-charge anisotropy of scheelite crystals. Langmuir, 32, 6282-6288.
11. Gao, Z., Sun, W., Hu, Y. (2015) New insights into the dodecylamine adsorption on scheelite and calcite: an adsorption model. Minerals Engineering, 79, 54-61.
12. Afanasiev, P. (2015) Non-aqueous metathesis as a general approach to prepare nanodispersed materials: case study of scheelites. Journal of Solid State Chemistry, 229, 112-123.
13. Atademir, M.R., Kitchener, J., Shergold, H. (1979) The surface chemistry and flotation of scheelite. I. Solubility and surface characteristics of precipitated calcium tungstate. Journal of Colloid and Interface Science, 71, 466-476.
14. Marinakis, K., Kelsall, G. (1987) The surface chemical properties of scheelite ($CaWO_4$) I. The scheelite/water interface and $CaWO_4$ solubility. Colloids and surfaces, 25, 369-385.
15. Tian, M., Gao, Z., Sun, W., Han, H., Sun, L., Hu, Y. (2018) Activation role of lead ions in benzohydroxamic acid flotation of oxide minerals: new perspective and new practice. Journal of Colloid and Interface Science, 529, 150-160.

XIV International Mineral Processing
and Recycling Conference
Belgrade, Serbia, 12-14 May 2021

WASTE AND WASTEWATER MANAGEMENT AS A POTENTIAL FOR REDUCTION OF GHG EMISSIONS

Aleksandar Jovović[1#], Danijela Božanić[2], Goran Vujić[3]
[1] University of Belgrade, Faculty of Mechanical Engineering, Belgrade, Serbia
[2] Climate Action Consulting, Belgrade, Serbia
[3] University of Novi Sad, Faculty of Technical Science, Novi Sad, Serbia

ABSTRACT – The main goal of this paper is to describe potential for GHG emission reduction in waste sector in the Republic of Serbia until 2050. Waste and wastewater sector covers emissions from the treatment and disposal of municipal solid waste (MSW) and wastewater treatment. During 2016 - 2021, the Republic of Serbia was developing a several national documents, which are currently in the draft form, to identify potentials for low-carbon economic development and to raise its reduction ambitions. Assessed GHG mitigation potential, based on comprehensive modeling through 4 mitigation scenarios, is result of analysis of technical, technological, and financial, as well as social and environmental conditions.

Keywords: Municipal Solid Waste, Wastewater, GHG, Emission, Scenarios.

INTRODUCTION

In previous years, Serbian climate change mitigation activities were shown in the national reporting documents (National Communications – NCs, Biennial update reports – BURs, National *Determined Contribution* - NDC) as sectoral actions presented through the GHG emission reduction [1-7]. The first climate change mitigation planning of the Republic of Serbia was conducted throughout development of a Low-Carbon Development Strategy (LCDS) and Action plan (AP), during the period 2016 – 2019, which is currently in the draft form [8]. The main goal of this document is to explore possibilities and identify potentials for low-carbon economic development, starting from possibilities for the GHG emission reduction until 2050. These possibilities were presented in the [3,5,8].

WASTE MANAGEMENT IN SERBIA

Approximately, 2.2-2.3 million tons of municipal waste are generated in Serbia every year, and a total of app. 2 million tons are collected and disposed. Of that amount, about 460,488 tons of waste, or 20% of the collected municipal waste, were disposed of at regional sanitary landfills in 2017 [9]. The average coverage of municipal waste collection is 82%. The municipal waste recycling rate is about 3%. There is no systematically organized separate collection, sorting, and recycling of municipal waste in the Republic of Serbia. Although the primary waste selection in Serbia has been set forth under the law which envisages which separation of paper, glass and metal in specially labelled

---

[#] corresponding author: ajovovic@mas.bg.ac.rs containers, recycling is not functioning in practice even low amounts of recyclables are collected. Serbia does not have the necessary infrastructure to reduce the disposal of biodegradable waste. Currently, composting sites exist only in Subotica and partially in Sremska Mitrovica regions.

Wastewater mainly comes from households (67%), and much less from industry (19%) and 14% from other users. The total amount of wastewater in 2018 was lower by 1.3% compared to 2017, while the amount of wastewater discharged into public sewerage systems was lower by 0.5%. In 2018, 1.1% less wastewater was treated than in 2017. The percentage of residents connected to the public sewerage system in 2018 was 63.0% and of the population included into wastewater treatment 14.1%.

GHG EMISSION FROM WASTE SECTOR IN SERBIA

In 2018, emissions from the waste sector amounted to 2,928 Gg CO2 eq, or 4.6% of total GHG emissions. In the period 2010-2018, emissions have decreased by 3.5%. Figure 1 presents trends of GHG emissions from source categories within the waste sector.

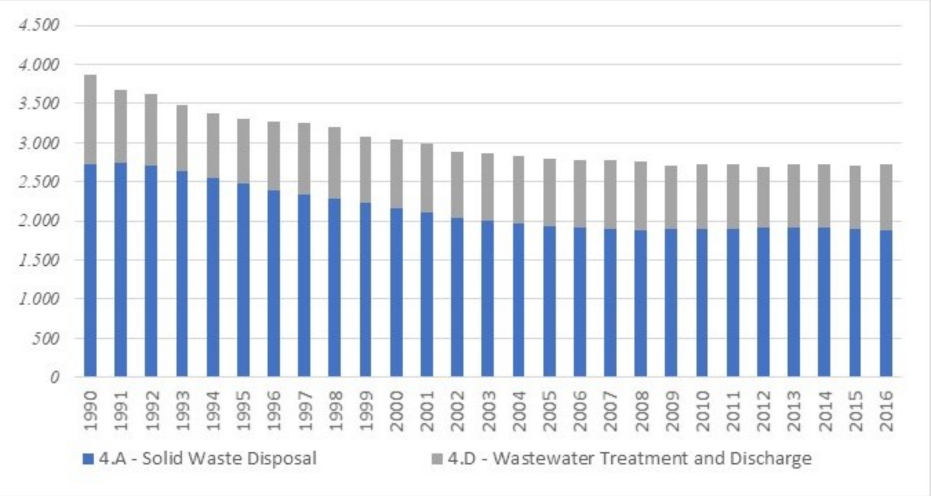

Figure 1 GHG emissions by categories in the waste sector, 1990-2018 (Gg CO2 eq)

Within the waste sector, 71.7% of total emissions in the year 2018 originated from solid waste disposal, and 28.3% from wastewater treatment. Despite improvements in waste and wastewater management practices in the recent period, the total number of waste management facilities and amounts of treated solid waste and wastewaters is still negligible and the share of GHG emissions from these categories have remained almost constant over the observed period.

MITIGATION SCENARIOS, DRIVERS, AND ASSUMPTIONS

Mitigation scenarios (up to 2050) developed for all sectors in LCDS [8] are:

- **Without Measures** (WOM), so-called Baseline (Business as usual, BaU) - Excludes all PAMs implemented, adopted and planned after the year 2015;

- **With Measures** (WEM) – Considers currently implemented, adopted, and planned PAMs (the whole EU 2030 acquis), assuming accession to the EU in 2025; and
- **With Additional Measures 1** (WAM1) - Considers a way of achieving the 2030 targets defined for the EU (-40% GHG emissions compared to 1990; 32% RES by 2030 and 32.5% enhanced energy efficiency) assuming accession to the EU in 2025.
- **With Additional Measures 2** (WAM 2) scenario - Serbia aiming to achieve 80% GHG cuts in 2050 compared to 1990 levels (the first EU target under the Paris Agreement).

Modelling has been conducted from 2015, while [2 and 4] the year 2010 is base year (for comparing GHG levels). For projecting the GHG emissions for the Waste sector, the IPCC 2006 Waste model was used [10].

As a most relevant scenario for all sectors (energy, IPPU, Agriculture, Forestry and Other Land Use, waste and wastewater) Scenario With Measures is chosen. In the waste and wastewater sector, this mitigation scenario is the same as the WOM/BaU scenario. In this scenario, the implementation of the relevant measures to achieve the goals is rescheduled.

MSW production is mainly driven by GDP and population. The emissions profile of the waste sector is, however, mostly determined by waste composition (organic vs non-organic) and waste treatment technology. Drivers for wastewater treatment are same as for MSW production. The emissions profile of the wastewater sector is, however, mostly determined by treatment technology. Wastewater treatment technology which considered tertiary treatment or treatment of sludge cause decreasing of emission.

Two key assumptions for the modelling of GHG emissions in the waste sector are the waste composition and the full implementation of the extensive agenda of EU approximation activities as a part of preparing of Serbia for the EU membership.

In order to develop a scenario, projected amount and composition of municipal waste in Serbia for period 2015 - 2050 was considered, assuming that the future characteristics of the waste by the end of 2050 will be changed in line with change of two key drivers, i.e. GDP and population growth/decrease. In other words, models for projection of the physical characteristics of the waste for the Republic of Serbia until 2050, were based on correlation between waste amount & composition with GDP and population. The amount of waste generated in Serbia in the period from 2015 to 2050, is projected to increase by 38.7%, which corresponds to approximately 1.1% per year. This means that the amount of municipal waste generated in the period from 2015 to 2050 will increase from 340.7 kg to 456.3 kg/capita/year.

The results related to the projected composition of municipal waste, shows that share of biodegradable categories consisting of garden and food waste, will be reduced by 21.9% in 2050.

The Republic of Serbia is preparing for the EU membership, which encompasses the transposition and implementation of EU environmental acquis, including requirements for waste management. Crucial legislative obligations include:

- Landfill Directive - 1999/31/EC,
- Directive on packaging and packaging waste - 1994/62/EC and
- Waste Framework Directive - 2008/98/EC.

Based on the estimation of the necessary time for each individual region to have a complete waste management system in compliance with EU requirements, it was projected how much the waste, by type, will be properly treated in relation to the time (table 1).

Table 1 Biodegradable waste treatment options and targets assumed in Scenario with measures

Relevant waste fractions for GHG emissions	Treatment option		Targets to be achieved			
			2025	2030	2040	2050
Food and garden waste	Landfilling		85%	75%	55%	35%
	Diversion	Composting	15%	25%	45%	65%
Paper and cardboard	Landfilling		85%	75%	55%	35%
	Diversion	Recycling	10%	15%	25%	45%
		Composting	5%	10%	10%	10%
		Incineration	5%	10%	10%	10%

GHG emission reduction is result of following measures:

- Construction of sanitary landfills – for 22 regions until 2025, and for four regions until 2030
- Introduction of source separation & Construction of Material Recovery Facilities - for 18 regions until 2025, and for eight regions until 2030.
- Construction of Biological Treatment Facilities (Composting Plants) – for one region until 2025, for 5 regions until 2030 and for rest 20 out of 26 after 2030.
- Construction of Thermal treatment (Incineration) Plant – only for Belgrade region until 2025.

In the field of wastewater collection and discharge systems, it is assumed that, by 2050, 95% of the major cities will have anaerobic digestion facilities installed. Facilities in the rest 5% of the cities would start with operation by 2062. The data are extrapolated without considering the industrial wastewater generation and discharge.

GHG EMISSIONS

Based on the results of modeling, it was concluded that for this scenario, GHG emissions in waste sector will increase 2% by 2020 compared to 2010 and decrease 7%, 17% and 39% by 2025, 2030 and 2050, respectively (table 2).

Table 2 CO_2eq emissions and emissions reductions for WEM scenario

Year	2010	2020	2025	2030	2050
CO2 eq, kt	1.920	1.960	1.791	1.585	1.167

The table below shows the dynamic of GHG emission in the wastewater sub-sector.

In last year (2050), CO_{2eq} emissions have been projected to be about 769 kt CO_{2eq} which represents 8,6% reduction compared to 2010 GHG emission levels.

Table 3 CO_2eq emissions from wastewater collection system for the chosen period 2010-2050 according to scenario WEM (kt CO_{2eq})

Year	2010	2015	2020	2025	2030	2040	2050
Emissions from wastewater	842	809	795	791	787	778	769
-of which from municipal wastewater	717	697	690	687	683	675	668

CONCLUSIONS

Described scenario represent the potential emissions pathway as a result of the transposition and implementation of the EU Acquis in Serbia, in a scenario of accession of Serbia to the EU in 2025.

Also, this scenario represents a minimum starting point for Serbia’s low carbon transition process since implementation of all relevant EU legal framework is considered.

In order to achieve the stated objectives of the EU, it is not enough to build functional sanitary landfills, but there must be other elements of waste treatment, i.e. most important is to establish recycling of certain suitable fraction and treatment of biodegradable waste. Therefore, in addition to sanitary landfills, other modern treatment of municipal waste (recycling and biological/thermal treatment plants) need to be implemented.

In accordance with the current level of infrastructure and status of waste management regions development, for the implementation of this scenario, estimations are that Serbia need to invest almost 45 million € for project preparation and additional 986 million € for the investment, in next 10-15 years.

REFERENCES

1. Initial National Communication of the Republic of Serbia under the United Nations Framework Convention on Climate Change, 2010.
2. Second National Communication of the Republic of Serbia under the United Nations Framework Convention on Climate Change, 2017.
3. Third National Communication of the Republic of Serbia under the United Nations Framework Convention on Climate Change, draft, 2021.
4. First Biennial Update Report of Serbia, 2016.
5. Second Biennial Update Report of Serbia, draft, 2020.
6. Intended Nationally Determined Contribution of the Republic of Serbia, 2015.
7. Revised Nationally Determined Contribution of the Republic of Serbia, draft, 2020
8. Low carbon development strategy of Republic of Serbia with action plan, draft, EuropeAid/1365966/DH/SER/RS, Service Contract No: 2016/375-531, January 2020.
9. National Waste Management Strategy including National Waste Management Plan for the period 2020-2025, draft, 2020.
10. https://www.ipcc-nggip.iges.or.jp/public/2006gl/vol5.html (accessed date 04.04.2021.).

SECTION LECTURES

XIV International Mineral Processing
and Recycling Conference
Belgrade, Serbia, 12-14 May 2021

APPROACH FOR SOLVING ENVIRONMENTAL ISSUES AT ABANDONED MINING WASTES IN REPUBLIC OF SERBIA

Zoran Stevanovic[1#], Peter Bayer[2], Stefan Kamsties[2], Radmila Markovic[1], Vojka Gardic[1], Aleksandar Doderovic[1], Nikola Stanic[1]
[1] Mining and Metallurgy Institute (MMI) Bor, Bor, Serbia
[2] PLEJADES, Griesheim, Germany

ABSTRACT – In Serbia exist numerous locations with larger and smaller quantities of mining wastes. Some of those wastes could be potentially characterized as “A” category wastes. One of the obligations of Republic of Serbia is harmonizing of national legislation with the EU Acquis Communautaire in the field of environment as a part of the negotiation process (Chapter 27). Regarding this fact, it was performed making of Cadastre of Mining Waste in Republic of Serbia with Consortium of German Companies PLEJADES GmbH and DMT GmbH & Co. KG with engagement of Mining and Metallurgy Institute Bor for implementation of all sites activities.

Keywords: Mining, Waste, Cadastre, Abandoned, Environmental.

INTRODUCTION

Mining industry in Serbia had a strong development during more than 100 years. Moreover, in Serbia exist archeological clues of mining activities from early V millennia BC (5400 BC) [1] on locality Rudna Glava which represent the oldest copper mine in Europe and probably world. Due to strong mining development in last few centuries, in Serbia exist numerous abandoned locations with larger or smaller quantities of mining wastes. According to EU Mining Waste Directive, mining wastes with potential for chemical and stability hazard is characterized as “A” category wastes [2].

One of the obligations of Republic of Serbia is harmonizing of national legislation with the EU Acquis Communautaire in the field of environment which is a part of the negotiation process for Chapter 27. Regarding this fact, Ministry for Mining and Energy of Republic of Serbia contracted and performed making of Cadastre of Mining Waste (CMW) in Republic of Serbia. The CMW project aims to support the sector of mining and environmental protection by developing and further improving the mining waste management system. The contracting authority for this project is the Ministry of Finance, the Department for Contracting and Financing of EU Funded Programmes (CFCU). The beneficiary of the project is the Ministry of Mining and Energy, and the project is implemented by a consortium of German companies PLEJADES GmbH and DMT GmbH & Co. KG which contracted MMI Bor for implementation of all sites activities including exploratory drilling, sampling, geotechnical testing and analyzing, chemical analyzing and interpretation of results. The CMW project began in 2017 and ends in early 2020. Total

---

[#] corresponding author: zoran.stevanovic@irmbor.co.rs

Project budget was 2.1 million EUR from which 90% was funded by the European Union and 10% by the Government of the Republic of Serbia.

METHODS

At the beginning of the CMW Project was performed initial consideration of potential abandoned mines sites based on available reports, historical data and Serbian map data. Based on this consideration was selected 250 abandoned Mining Waste Sites (MWS) for site visit. Site visits preparation included identification of accesses to abandoned mining sites and possible mining objects, preparation of rules for identifying of deterioration evidences, identifying of possible sampling locations, land usage, residential and industrial areas vicinity and similar data of importance.

Based on defined data which has to be collected during initial site visit, MMI Bor staff visited all 250 MWS and collected required data. One of the priorities during initial site visit was to confirm existing of Mine Waste Facilities (MWF) and indicate size and hazard potentiality. Collected data was a basis for the creation of Plan of Sampling and Exploration Works (PSEW). However, collected data was still not sufficient for selecting MWS for Detailed Sampling and Visiting Plan (DSVP) which has to be focused on Category "A" MWF.

Therefore, it was implemented Multi-criteria evaluation with Analytic Hierarchy Process (AHP) [3] which combines importance of collected parameters aiming on definition of MFW for DSVP. Based on this evaluation was selected 41 MWS for DSVP. The amount of waste in the selected sites accounts for 90% of the entire mining waste on all the visited abandoned mining waste sites (250 locations in total) [4].

DSVP included sampling of MWF by exploration drilling and test pits, sampling of surface waters and underground from installed monitoring wells. Collected solid and water samples were treated in MMI Bor laboratories with certified methods. Solid samples analyses included dry maters and solid leachate analyzes while water samples were analyzed on law defined limited parameters. Besides chemical analyzing, it was performed geotechnical sampling and testing objected on definition of stability hazards. All sampling points were recorded by licensed surveying company.

All of collected results from site activities and testing including three preliminary case studies will be part of CMW web application under administration of Ministry for Mining and Energy of Republic of Serbia.

RESULTS AND DISCUSSION

Preparation of MWS visits

Preparation included: Identification of access to the MWS; Preliminary identification of shafts, adits, open pits, processing plants, transport infrastructure and other facilities related to the exploitation in the vicinity of the MWS; Identification of evidence for deterioration of structural integrity, erosion, environmental pollution and other potentially adverse effects; Identification of potential sampling location; Identification of land-use in the vicinity of the MWS including location of residential areas, commercial and industrial areas and preparation of concept for field inspection of the individual

MWS. Map of selected 250 MWS (red triangles) for initial site visit in Republic of Serbia was presented on Figure 1a while on Figure 1b is shown example of prepared plan for visit of one MWS based on satellite imagery.

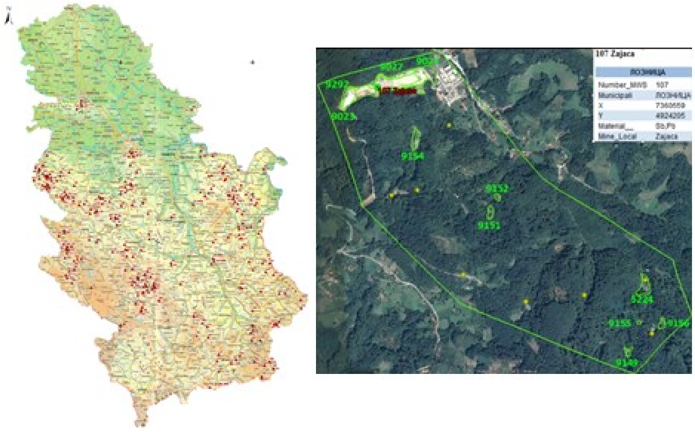

1(a) **1(b)**

Figure 1 (a) Map of selected 250 MWS for initial site visit in Republic of Serbia; **(b)** Plan for MWS visit based on satellite imagery

MWS visit and reporting

Reports from initial MWS visits included collected: General information (traffic, coordinates, mine elements, subsoil type); MWS geometry (lay-out, slope angles, inclination of base, volume estimation); Source potential (identification of type of deposited material, covering, etc.); Potential adverse effect and pollution (surface water management, seepage structures and rates, water treatment, erosion structures, slope failures); Potential receptors in the vicinity (waters, settlements, agriculture, nature areas); Verification of sampling locations and Photos. Figure 2 (a) and (b) shows example of map of MWS before and after the initial visit with included collected information's.

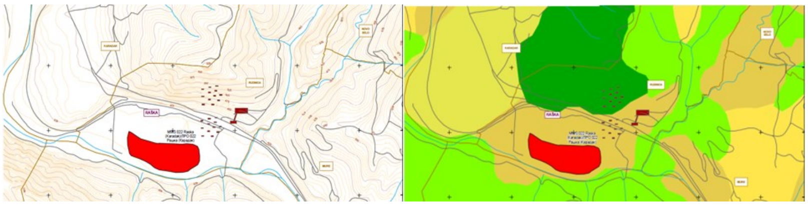

2(a) **2(b)**

Figure 2 (a) MWS map without collected data from initial site visit; **(b)** MWS map including collected data from initial site visit

Based on initial 250 MWS visit was also concluded:

- 63 MWS – without mining operations, No MWF
- 79 MWS – with mining operations but without mining waste or small

volumes of mining waste (≤ 50 m³). 39 sites did not show any mining waste

- ➢ 105 MWS – with large volumes of mining waste, totaling 215 MWF with individual vol. up to 3.5 mil.m³
  - 35 of 215 MWF – present at 24 active MWS
  - 179 of 215 MWF – found at abandoned sites
- ➢ 3 MWS (127, 142 and 146) – without available data due to force majeure (access impossible)

Multi-criteria evaluation

Having on mind that DSVP should be objected on category "A" MWF collected data were analyzed with Analytic Hierarchy Process (AHP) which combines importance of collected parameters as follows:

➢ MWF area (m²)	(1 – Not at all important)
➢ MWF volume (m³)	(2 – Low importance)
➢ Vicinity of agricultural soil (km)	(3 – Slightly important)
➢ Vicinity of nature protected areas (km)	(3 – Slightly important)
➢ Vicinity of surface/und. waters (km)	(5 – Moderately important)
➢ Vicinity of towns and settlements (km)	(5 – Moderately important)
➢ Chemical hazard	(6 – Very important)
➢ Stability hazard	(6 – Very important)
➢ MWF toxicity	(7 – Extremely important)

Results of Multi-criteria evaluation are presented on Figure 3(a) while map with locations of totally selected 41 MWS based on evaluation is presented on Figure 3(b).

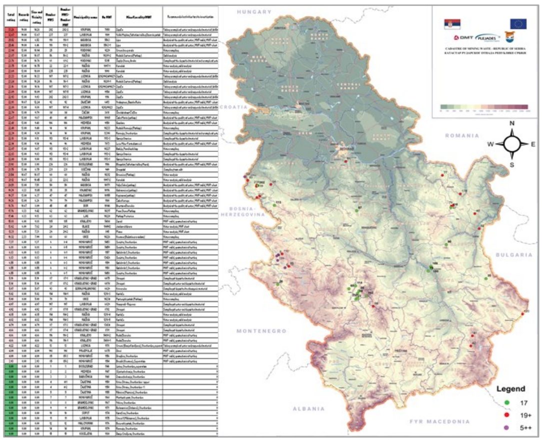

3(a) 3(b)

Figure 3 (a) Multi-criteria evaluation results (red hazardous – green non-hazardous); **(b)** Map of totally 41 selected MWS for DSVP

DSVP

Scope of site activities and laboratory testing are presented in following Tables:

Table 1 Sampling of solid and water samples

Activity	Specification	Unit	Total realized units
Test pit samples	0.2 x 0.2 x 0.2m	pcs	1465
Test pit samples	0.5 x 0.5 x 0.2m	pcs	67
Excavator samples	Depth 2m	pcs	245
Liner drilling	50-100mm	m	654
Install GWM-Well	Drilling and installation	m	96
Exist. GWM-Well	/	pcs	9
Surface water samples	/	pcs	107

Table 2 Water samples analyzing

Specification	Unit	Total realized units
pH, T, conductivity, redox (during sampling)	pcs	112
As, Pb, Cd, Cr(tot), Cu, Ni, Hg, Ti, Zn, V, Mo, Co	pcs	105
Total Fe, As	pcs	7
U	pcs	7
Sb	pcs	11
Sulfate	pcs	112
Flotation chemicals	pcs	17
Alkalinity	pcs	112

Table 3 Soil samples - dry matters

Specification	Unit	Total realized units
As, Pb, Cd, Cr(tot), Cu, Ni, Hg, Ti, Zn, V, Mo, Co	pcs	632
Total Fe, As	pcs	166
U	pcs	34
Sb	pcs	46
Asbestos	pcs	123
Mineral Phases (RDX)	pcs	108
TPH	pcs	10
PAH	pcs	10

Table 4 Soil samples - leachate

Specification	Unit	Total realized units
Leachate preparation	pcs	495
pH, conductivity, redox	pcs	495
As, Pb, Cd, Cr(tot), Cu, Ni, Hg, Ti, Zn, V, Mo, Co	pcs	380
Total Fe, As	pcs	163
U	pcs	16
Sb	pcs	15
TPH	pcs	10
PAH	pcs	10
Flotation chemicals	pcs	106
Alkalinity	pcs	482

Table 5 Geotechnical testing

Specification	Unit	Total realized units
Grain size distribution, fine grained materials	pcs	68
Moisture content	pcs	68
Atterberg Limits	pcs	13
Specific gravity	pcs	68
Undrained shear strength	pcs	68
Consolidation (Oedometer)	pcs	10

Total sampling points recorded by licensed surveying company – 1836 [5].

CONCLUSION

CMW Project was realized in very short time frame. 250 initial MWS for visits and later 41 MWS for detailed sampling and analyses indicate a strong and comprehensive organization and performing of all Project activities.

Defined approach for collecting data from site visits and laboratory testing and analyses ensured basis for implementation of Multi-criteria evaluation for determination of MWS priority for detailed consideration. Selected parameters and given importance indicators for Multi-criteria evaluation resulted with reliable results in determination of MWS priorities. Among selected 41 MWS for detailed sampling top three MWS with highest total and hazards ratings are Mine Zajaca near Krupanj, Veliki Majdan near Ljubovija and Lipa near Zagubica. During the CMW Project was collected huge amount of data, achieved results and information's and therefore it will be available on CMW web application.

Importance of performing CMW Project have to be considered as beginning of continual activities objected on solving of environmental and stability hazards on locations of abandoned mine locations all over Republic of Serbia. After the CMW Project, logical step forward is to start with planning of treatment of these locations. One possible way for continuation of those activities could be analyzing of methods for long term predicting of environmental performances on MWS. This approach should ensure basis for designing of measures for reduction of chemical and stability hazards on abandoned MWS.

ACKNOWLEDGEMENT

This work was financially supported by EU IPA – Cadastre of mining waste 2014/S 051-084387 through Department for Contracting and Financing EU Funded Programmes (CFCU).

REFERENCES

1. Jovanovic, B. (2009) Beginning of the Metal Age in the Central Balkans according to the results of the Archeometallurgy. Journal of Mining and Metallurgy, 45 (2) B, 143-148.
2. European Parliament and of the Council on the management of waste from extractive industries (2006) Directive 2006/21/EC.

3. Goepel, K. (2018) Implementation of an Online Software Tool for the Analytic Hierarchy Process (AHP-OS). International Journal of the Analytic Hierarchy Process, 10 (3).
4. Bayer, P. (2020) Serbia Gets Cadastre of Mining Waste with EU Support, https://cordmagazine.com/news/serbia-gets-cadastre-of-mining-waste-with-european-union-support/
5. Stevanovic, Z. (2020) Cadastre of Mining Waste in the Republic of Serbia – Fieldwork, chemical analyses, geotechnical assessment. In: Closing Conference of the Project. Belgrade, Serbia.

AVAILABILITY OF ESSENTIAL AND TRACE METALS IN AN ACIDIC SOIL AMENDED WITH BAUXITE RESIDUE (RED MUD)

Ivana Smičiklas[1#], Mihajlo Jović[1], Marija Egerić[1], Marija Šljivić-Ivanović[1], Slavko Smiljanić[2]
[1] "VINČA" Institute of Nuclear Sciences - National Institute of the Republic of Serbia, University of Belgrade, Belgrade, Serbia
[2] University of East Sarajevo, Faculty of Technology Zvornik, Zvornik, Republic of Srpska, Bosnia and Herzegovina

ABSTRACT –The availability of Cu, Zn, Fe, Mn, Ni, Pb, Co, and Cd in acidic soil amended with alkaline red mud (RM) (0.3%, 2%, and 5%) was addressed using the SRPS ISO 14870 method. The available fraction of elements decreased with increasing RM doses even though their total concentrations except for Cu were increased following RM addition. This indicates both the low availability of metals in RM and the stabilization of metals present in the soil. Regarding plants' needs, the micronutrients' status can be interpreted as sufficient for Zn and Mn, high for Fe, and very high for Cu, at the highest RM dose of 5%.

Keywords: Acidic Soil, Red Mud, Metal Availability, DTPA Extraction.

INTRODUCTION

The bioavailability of metals in soils depends on their distribution between the solid and solution phases, which is governed by soil properties (pH, cation exchange capacity, the content of organic matter, clay fraction, and Fe–Mn oxides), and the processes (the cation exchange, sorption, complexation, precipitation). Soil pH is the critical factor that affects chemical and biological processes. Most plants' nutrients exhibit optimal availability to plants at close to neutral soil pH (i.e., 6.5-7.5). In acidic soils, a significant increase in solubility and bioavailability of toxic elements occur with a concurrent decrease in available P, Mo, Ca, and Mg forms [1]. European Union Soil Thematic Strategy has recognized soil acidification and soil pollution as global degradation processes that threaten soil health [2]; therefore, sustainable measures for improving soil chemical properties are largely needed.

The periodical addition of alkaline agents such as limestone and lime is a widespread practice to restore optimal soil pH and enhance attenuation of toxic metals availability and leaching. As present-day society strives to protect natural resources and reduce the amount of landfill waste through its valorization and reuse, diverse alkaline waste materials and by-products (coal fly ash, blast furnace slag, bauxite residues, biochars, seashells, eggshells, etc.) are studied for their potential is soil pH regulation and stabilization of soil contaminants [3-5].

In our previous study, the bauxite residue from the aluminum industry (red mud,

---

[#] corresponding author: ivanat@vin.bg.ac.rs

RM) was investigated for its potential to increase the pH of the acidic soil sampled in the vicinity of the mining and metallurgical complex in Bor (Serbia) [6]. The addition of RM has caused a significant change in several essential soil properties, including the increase in pH and the increase in trace metals' total concentrations.

This study aimed to expand the RM impact assessment by analyzing the bioavailability of essential and trace elements to plants. The diethylenetriaminepentaacetic acid (DTPA) extractable concentrations of micronutrients and toxic metals correlate with their amounts in plants, particularly for near-neutral soils; thus, they represent important information for soil use, management, and protection.

EXPERIMENTAL

The agricultural soil (S) was sampled near the village Slatina (Serbia, 44° 01′ 31.2″ N, 22° 11′ 00.2″ E), from the surface to a depth of 20 cm, dried at room temperature, homogenized and sieved to <2 mm fraction. The red mud sample (Zvornik Alumina Refinery, Republic of Srpska, BiH) was washed with tap water to remove excess NaOH, dried at room temperature, and used as a fine powder (RM). The RM was rich in hematite and gibbsite (44% Fe_2O_3 and 18% Al_2O_3), with 12% SiO_2, 8% Na_2O, 4.7% TiO_2, and 3% CaO [7].

The RM was mixed with soil at the 0.3%, 2%, and 5% w/w bases (RM0.3, RM2, and RM5). The treated soil samples were transferred to the pots. The experiments have been carried out in triplicates. Only the deionized water was added to the pots periodically over the incubation time of two months [6].

The bioavailability of selected elements in the soil samples was assessed using the SRPS ISO 14870 method [8]. The standard applies to estimating the availability of micronutrients Cu, Fe, Mn, and Zn to plants, but the availability of potentially toxic elements such as Cd, Ni, Co, and Pb can also be evaluated. Each soil sample (10 g) was extracted with 20 mL of the solution prepared from 0.005 mol/L DTPA, 0.1 mol/L triethanolamine (TEA) and 0.01 mol/L $CaCl_2$. The solution pH was adjusted to 7.3 with 6 M HCl. The extraction was performed on a rotary shaker at 15 rpm for two hours, at room temperature.

The liquid phase was separated by membrane filtration (0.45 µm), while the metal concentrations in the extracts were measured by Inductively Coupled Plasma Atomic Emission Spectroscopy, ICP-OES (Thermo Scientific iCAP 6500 Duo ICP, Thermo Fisher Scientific, Cambridge, United Kingdom). The concentrations of elements are presented on a dry matter basis.

The Fisher's least significant difference (LSD) test was selected to identify the difference in metal availability between the samples at the confidence level of 95%. The DTPA-extracted metal concentrations were associated with selected soil properties using correlation analysis, and the Pearson's coefficients (r) are presented at the 0.05 alpha level of significance.

RESULTS AND DISCUSSION

The investigated soil and the additive exhibited contrasting properties. While the control soil was non-carbonate and acidic (pH_{H2O}=4.93), with a very low level of available P (3.61 mgP_2O_5/100 g), and a high total Cu concentration (219.2 mg/kg), the RM was alkaline (pH_{H2O}=10.0, 3.78% of $CaCO_3$), with a high level of available P (74.1 mgP_2O_5/100 g), and higher concentrations of trace metals compared to the control soil, except for Cu [6]. Consequently, after application of 0.3%, 2%, and 5% of RM, the soil pH respectively increased to 5.16, 6.48, and 7.50, available P increased to 5.91 mgP_2O_5/100g, 7.15 mgP_2O_5/100g, and 15.6 mgP_2O_5/100g, and the increase in total metal concentrations was evidenced (Table 1, [6]).

The DTPA test results revealed that the available content of essential micronutrients in the control soil followed the order Fe (82.6 mg/kg) > Mn (56.3 mg/kg) > Cu (47.2 mg/kg) > Zn (2.9 mg/kg) (Figure 1, a-d). The additive RM induced a decrease in the availability of essential elements, and the effect was more pronounced with the increase in the RM dose (Figure 1, a-d). The trend was most pronounced for Mn and Fe, which DTPA-concentrations were respectively reduced by 79.4% and 70.6% at the highest RM dose of 5%. The available fraction of Zn decreased maximally by 46.1%, while the effect on Cu was the lowest (34% decrease in RM5).

Given the range of factors affecting the availability of micronutrients and the levels needed by plants, the DTPA concentrations <0.3 mg/kg Cu, <0.5 mg/kg Zn, <4 mg/kg Mn, and <5 mg/kg Fe are generally rated as critical [9]. RM addition in all treatment variants did not reduce the availability of essential elements below levels suitable for plant growth and development. Even at the highest RM dose of 5%, the micronutrients' status can be interpreted as sufficient for Zn and Mn, high for Fe, and very high for Cu [9].

High available Cu concentrations may provoke toxic effects in the form of poor root development and leaf chlorosis. However, the phytotoxic levels of available Cu are mostly unknown as different plant cultures show different degrees of tolerance to elevated Cu concentrations. For instance, 20 mg/kg was found to be a critical upper limit of DTPA-bioavailable Cu for the yield of snap beans [10], while the concentrations of 50.6 mg/kg and 92.1 mg/kg reduced dry matter yield the Chinese cabbage and celery leaves by 10% [11].

The results from Figure 1, a indicate that bioavailable Cu concentration may have side effects on the growth and yield of more susceptible crops, but the risk decreases after RM application.

Simultaneously, soil samples exhibited decreased availability of Pb, Ni, Co, and Cd with the increase in RM dose, reaching a maximum reduction of 68.3% for Cd, 90.6% for Co, 84.3% for Ni, and 64.3% for Pb in the sample RM5 (Figure 1, e-h).

Since the total concentration of all investigated elements in the soil except for Cu increased following the RM addition [6], the bioavailable fraction of investigated elements relative to their total concentrations determined following the US EPA 3051A method [6] was determined and presented in Table 1. The DTPA test revealed that investigated metals' availability was not in positive correlation with their total concentrations. Quite contrary, a decrease in the available fraction of metals with increasing doses of RM in the soil was detected (Table 1), indicating the high stability of elements introduced in soil with RM.

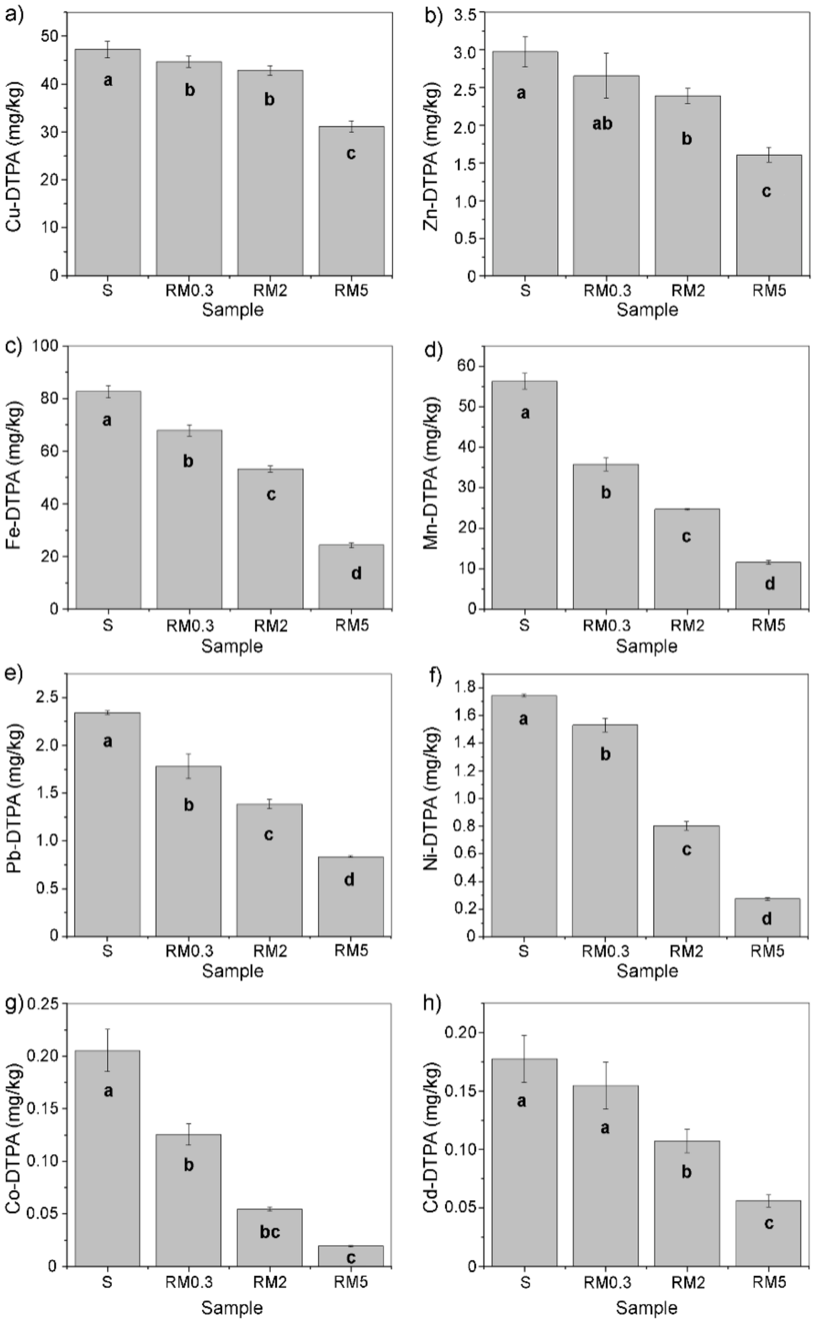

Figure 1 The DTPA-extractable concentrations of micronutrients and trace metals in the control soil (S) and samples amended with different RM doses (RM0.3, RM2, and RM5): a) Cu, b) Zn, c) Fe, d) Mn, e) Pb, f) Ni, g) Co, and h) Cd. The data presented are mean of three replicates ± standard deviation (SD); means that do not share a letter are significantly different

Table 1 The total concentrations of investigated elements in soil samples (US EPA 3051A, [6]), and the proportion of their bioavailable (DTPA) fraction

Sample		Cu	Zn	Mn	Fe	Ni	Cd	Co	Pb
S	Total (mg/kg)	219.2	106.5	1070	427500	19.80	0.524	19.49	27.56
	DTPA fraction (%)	21.5	2.79	5.26	0.193	8.81	33.8	1.05	8.50
RM0.3	Total (mg/kg)	213.4	102.7	1287	46560	21.30	0.542	23.10	26.83
	DTPA fraction (%)	20.2	2.58	2.78	0.146	7.19	28.5	0.543	6.64
RM2	Total (mg/kg)	223.0	102.4	1133	51860	42.70	0.575	24.59	31.32
	DTPA fraction (%)	19.2	2.33	2.18	0.103	1.88	18.6	0.221	4.42
RM5	Total (mg/kg)	223.0	116.1	1138	67290	61.31	0.687	31.77	37.73
	DTPA fraction (%)	13.9	1.38	1.02	0.036	0.448	8.20	0.061	2.21

The significant negative correlation was found between the total and available concentrations of Fe (-0.988, p=0.012), Ni (-0.993, p=0.007), and Cd (-0.961, p=0.039). Total Fe concentration in the soil samples was also in negative correlation with the available concentrations of Zn (-0.996, p=0.004), Cu (-0.993, P=0.007), Ni (-0.955, p=0.045) and Cd (-0.975, p=0.025), and the total Al concentration was in negative correlation with the available Zn (-0.981, p=0.019), Cu (-0.979, p=0.021), Ni (-0.963, p=0.037), and Cd (-0.974, p=0.026). These correlations confirm the metals' association with the Fe and Al oxides in RM, which contribute to their stability.

Furthermore, the pH of soil samples [6] was in negative correlation with the available Zn (-0.962, p=0.038), Fe (-0.975, p=0.025), Ni (-0.998, p=0.002), Pb (-0.958, p=0.042), and Cd (-0.994, p=0.006), whereas the amount of available P in the soil [6] was negatively correlated with the available concentrations of Cu (-0.999, p=0.001), Zn (-0.989, p=0.011) and Fe (-0.974, p=0.026).

Overall results demonstrate both the low availability of investigated metals in RM and the stabilization of metals present in the soil triggered by the increase in soil pH, the increased content of Fe and Al oxides and the increased content of available P.

CONCLUSION

Given that the total trace element concentration's determination does not provide information regarding their bioavailability, the effects of RM addition to the acidic soil were studied using the single extraction (DTPA) method for the evaluation of trace elements availability to plants. The decrease in metal availability was determined with increasing RM doses in the soil; however, micronutrients' availability was not reduced below the levels critical for plants. Although the addition of RM has led to a decrease in Cu availability, its levels may still be high for more sensitive plant cultures. The DTPA extracted amounts of Fe, Ni, Co, and Cd were negatively correlated with their total concentrations in the investigated soil samples, demonstrating that the metals in RM are highly stabile and inaccessible to plants. The increase in soil pH and content of available P after RM application contribute to the increased stability of metals present in the soil. The results point to the RM's usability as an alternative alkaline agent for soil pH adjustment, controlling its dose and monitoring its long-term effects.

ACKNOWLEDGEMENT

Financial support for this study is granted by the Ministry of Education, Science and Technological Development of the Republic of Serbia.

REFERENCES

1. Bolan, N.S., Adriano, D.C., Curtin, D. (2003) Soil acidification and liming interactions with nutrient and heavy metal transformation and bioavailability. Advances in Agronomy, 78, 215-272.
2. COM (2006) Communication from the Commission to the Council, the European Parliament, the European Economic and Social Committee and the Committee of the Regions — Thematic Strategy for Soil Protection (COM(2006) 231 Final), https://eur-lex.europa.eu/legal-content/EN/TXT/?uri=CELEX%3A52006DC0231, (Accessed 01.03.2021.).
3. Prasad, M., Chrysargyris, A., McDaniel, N., Kavanagh, A., Gruda, N.S., Tzortzakis, N. (2020) Plant nutrient availability and pH of biochars and their fractions, with the possible use as a component in a growing media. Agronomy, 10 (1), 1-17.
4. O'Day, P.A., Vlassopoulos, D. (2010) Mineral-based amendments for remediation. Elements, 6 (6), 375–381.
5. Hua, Y., Heal, K.V., Friesl-Hanl, W. (2017) The use of red mud as an immobiliser for metal/metalloid-contaminated soil: A review. Journal of Hazardous Materials, 325, 17–30.
6. Egerić, M., Smičiklas, I., Dojčinović, B., Sikirić, B., Jović, M., Šljivić-Ivanović, M., Čakmak, D. (2019) Interactions of acidic soil near copper mining and smelting complex and waste-derived alkaline additives. Geoderma, 352, 241–250.
7. Smiljanić, S., Smičiklas, I., Perić-Grujić, A., Lončar, B., Mitrić, M. (2010) Rinsed and thermally treated red mud sorbents for aqueous Ni^{2+} ions. Chemical Engineering Journal, 162 (1), 75–83.
8. SRPS ISO 14870:2005 (2005) Soil quality—Extraction of trace elements by buffered DTPA solution; SRPS, Institute for standardisation of Republic of Serbia: Belgrade, Serbia.
9. Barrett, L. et al. (2017) Agronomy Handbook, Soil and Plant Analysis Resource Handbook. Midwest laboratories, INC. NE, USA, Omaha.
10. Walsh, L.M., Erdardt, W.H., Seibel, H.D. (1972) Copper toxicity in snapbeans (*Phaseolus vulgaris L.*). Journal of Environmental Quality, 1 (3), 332–332.
11. Yang, X.-E., Long, X.-X., Ni, W.-Z., Ye, Z.-Q., He, Z.-L., Stoffella, P.J., Calvert, D.V. (2002) Assessing copper thresholds for phytotoxicity and potential dietary toxicity in selected vegetable crops. Journal of Environmental Science and Health, Part B, 37 (6), 625–635.

XIV International Mineral Processing
and Recycling Conference
Belgrade, Serbia, 12-14 May 2021

FUTURE QUESTIONS FOR RECYCLING SOCIETIES

Nemanja Stanisavljević[#], Nikolina Tošić, Bojan Batinić, Isidora Berežni
University of Novi Sad, Faculty of Technical Sciences, Novi Sad, Serbia

ABSTRACT – In order to achieve the goals of waste management (public health, environmental protection and resource conservation), a balanced quality and quantity approach is specifically important. It is particularly important for Republic of Serbia to examine how meeting the quantitative goals of the European Union by applying the various available technologies for waste treatment affects the quality of waste management through the achievement of waste management goals. It is incredibly challenging to remove hazardous substances from recyclables which contain them in small amounts (less than 1%), and this indicate that preferably small amounts of hazardous substances can lead to a huge impact on the circular use of large amounts of recyclables. The roles and obligations within a waste management system for consumers, producers and waste companies need to be specifically and plainly defined. Residence times of recyclables in the environment can be 100 years and more.

The goals of waste management can be successfully reached if a waste management system is formed in an adequate manner. It is necessary to merge individual processes that include generation, collection and transport, treatment and disposal of waste into complex waste management systems. More importantly is a treatment that meets the qualitative goals of public health and the environmental protection than the complete treatment of all recyclables. Advanced analytical models are necessary to integrate the analysis of material flows and the analysis of substance flows through waste management systems, the application of this tools will enable a complementary analysis of different recyclable flows within the system. The obtained results will be able to have their practical application precisely as a support in the development of future waste management systems that strive to meet the qualitative objectives of waste management while meeting the quantitative goals defined by EU.

Keywords: Waste Management, Qualitative Goals, Quantitative Goals, Recyclables.

[#] corresponding author: nemanjastanisavljevic@uns.ac.rs

PAPERS BY SECTIONS

COMMINUTION CHARACTERISTICS OF IRON ORES

Arun Kumar Jena[1#], Satya Sai Srikant[2], Shiv Kumar Angadi[3], Raghupatruni Bhima Rao[1]
[1] Aryan Institute of Engineering and Technology (BPUT), Bhubaneswar, India
[2] SRM Deemed University, New Delhi, India
[3] CSIR-IMMT, Bhubaneswar, India

ABSTRACT – Comminution is the process of crushing and grinding. In the present investigation, iron ore of two different associated gangue minerals in the form of banded hematite and quartzite and banded hematite and jasper are chosen. An attempt is made to estimate the energy and compressive strength required to crush. Experiments were carried out on single-particle breakage using an impact crusher by impacting from different heights and different feed sizes of the samples were used in the investigations. The results of these studies reveals that with an increase in the height of the impact head, the particle size decreases.

Keywords: Hematite, Crushing, Impact Crushing, Comminution, Iron Ore.

INTRODUCTION

Crushing is a complex process. Drop Weight Tests are measured by the method, reduction ratio of the sample and energy consumption. Sample requirement is at least 70 kg of representative broken rock in the size range -76+6 mm or 70 kg of whole uncut drill core at a diameter greater than 63 mm. This procedure repeated for 5, 10, 15 drops and stage crushed to generate narrow size ranges of rock fragments. The drop weight test is used to calculate the energy that is expanded in breaking the particle as given: [1-6]

$$E1 = Mg(h - XM) \tag{1}$$

where: *E1* - energy used for breakage,
M - drop weight mass,
g - gravitational constant,
h - initial height of drop weight above the anvil,
XM - final weight of the drop weight above the anvil.

EXPERIMENTAL

Raw Materials

Iron ore samples, hematite, banded hematite and quartzite and banded hematite jasper were collected from different parts of iron ore formations in Odisha.

[#] corresponding author: arunjena3@gmail.com

Typical iron ore samples are shown in Figure 1 and Figure 2.

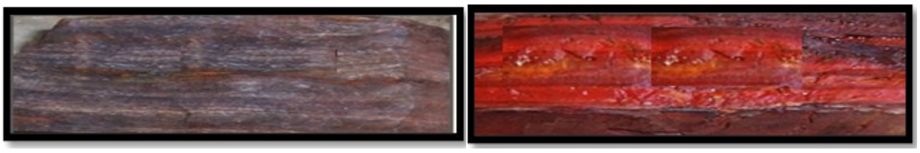

(a) (b)

Figure 1 (a) Banded hematite and quartzite, (b)Banded hematite and jasper

(a) (b) (c)

Figure 2 Iron ore formations in Odisha, India (a) hematite particle -20+10 mm size, (b) hematite-quartzite particle -20+10 mm size, (c) hematite-jasper particle -20+10 mm size

Compressive Strength Unit Operation

Fig.3 shows the experimental set up designed for the compressive strength test. The test apparatus consists of a drop surface on which the samples are kept in a material base, the drop weight is fixed to the head weight and it is released based on the lever system.

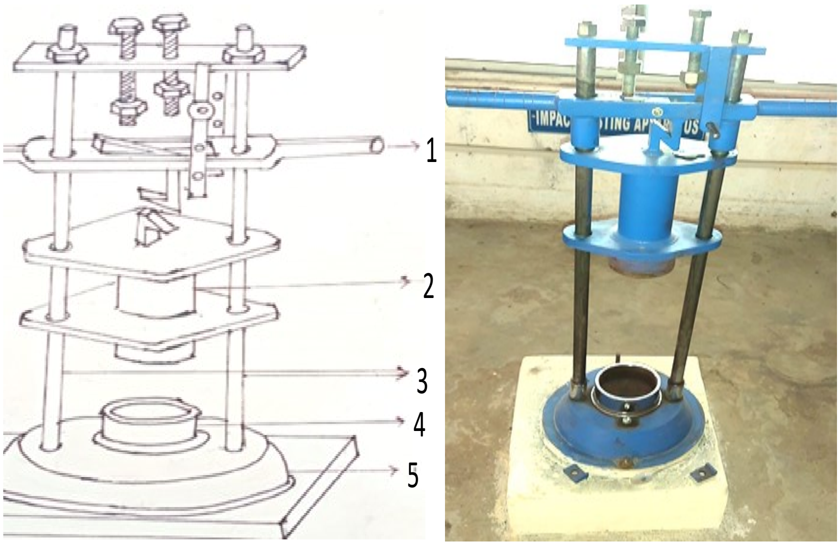

Figure 3 Impact crushing apparatus
(1 - lifting handle, 2 - hammer, 3 - vertical guide bar, 4 - cup, 5 - circular base)

Compressive Strength Tests

This particular test was carried out for determining the friability values (S1) for the selected samples from the different formations of iron ores 1) Hematite ore, 2) Banded Hematite and quartzite and 3) Banded Hematite and Jasper. All the three varieties of ore samples were screened between -20+10 mm sizes.

RESULTS AND DISCUSSION

Hematite Ore

The Response Surface Methodology study is attempted to find out the friability and energy required for crushing of the hematite ore. Where: A - Feed size, B - Drop Weight, C - Drop Height and the input variables are feed particle size, micron, $20*10^3$ and Drop weight, 13.5 kg are constants.

Friability Value(S) % = (amount of particles passing 200 mesh/Total Feed) x 100

Table 1 The results of particle size analysis of different ore samples

Input variables Feed Particle size, micron, $20*10^3$ and Drop weight, 13.5 kg are constants			Output variables	
Drop height, m	d80 passing size microns	S value, %	Joule	kWh
Hematite ore				
0.465	$2.8*10^3$	86.32	62.26	$1.6*10^{-5}$
0.537	$3.0*10^3$	88.35	71.9	$1.9*10^{-5}$
0.668	$3.1*10^3$	91.1	89.44	$2.4*10^{-5}$
Banded hematite and quartzite				
0.465	$2.8*10^3$	96.74	62.26	$1.6*10^{-5}$
0.537	$3.2*10^3$	98.63	71.9	$1.9*10^{-5}$
0.668	$3.4*10^3$	99.12	89.44	$2.4*10^{-5}$
Banded hematite and jasper				
0.465	$3.1*10^3$	88.42	62.26	$1.6*10^{-5}$
0.537	$4.2*10^3$	88.69	71.9	$1.9*10^{-5}$
0.668	$5*10^3$	90.15	89.44	$2.4*10^{-5}$

d80 passing size = - 969.55088 - 2.27649 X 10^{-11} A - 1.02757 X 10^{-9} B +12720.87057 C + 4.76381 X 10^{-15} A^2 + 1.68092 X 10^{-11} B^2 - 9923.24630 C^2 + 2.88043 X 10^{-13} AB + 2.03262 X 10^{-13} AC + 1.03809 X 10^{-11} BC, R-Squared = 100%.

S Value = + 64.35050 - (8.51124 X 10^{-13}) A + (2.33551 X 10^{-11}) B + 63.74362 C + 2.89261 X 10^{-16} A^2 + 6.00167 X 10^{-13} B^2 - 35.47822 C^2 - 2.03493 X 10^{-14} AB - 2.83259 X 10^{-14} AC + 1.82342 X 10^{-14} BC, R-Squared = 99.68%, Power = + 4.72650 X 10^{-3} - 9.77918 X 10^{-7} A - 1.84671 X 10^{-4} B + 133.89169 C, R, Squared = 100%, Energy = + 1.952 X 10^{-5} + 5.997 X 10^{-6} C - 3.878 X 10^{-7} C^2, R-Squared = 100%.

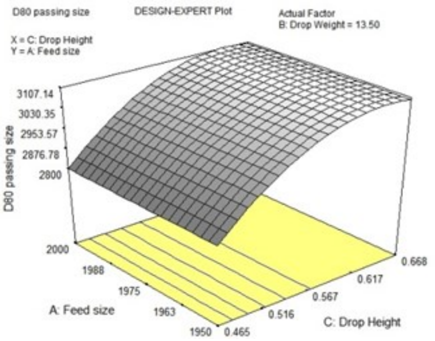

Figure 4 Hematite Ore d80 passing size

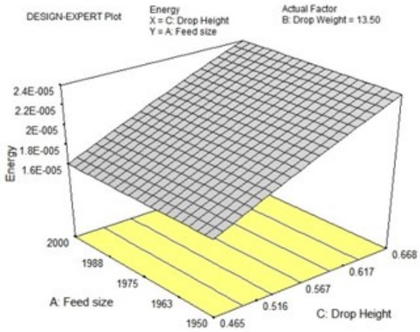

Figure 5 Hematite Ore – Energy Kwh

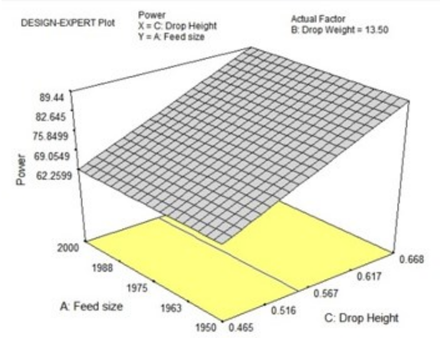

Figure 6 Hematite Ore – Power Joule

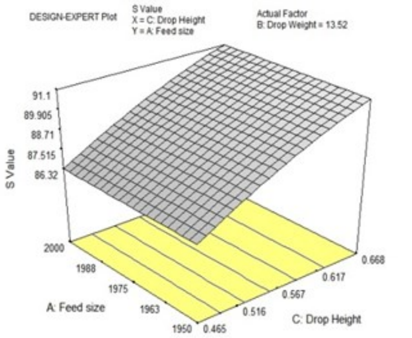

Figure 7 Hematite Ore – S value

Banded hematite and quartzite

d80 passing size = + 3272.22 + 0.0 A + 865.21 B + 833.33 C + 0.000 A^2 + 0.0 AB + 0.00 AC, R-Squared = 100%, S Value = + 98.97 + 0.000 A + 4.83 B + 3.94 C + 0.000 A^2 + 0.000 AB + 0.000 AC, R-Squared = 99.72%, Power = + 0.050847 - 1.85855 X 10^{-16} A - 3.64299 X 10^{-3} B + 133.88889 C, R-Squared = 100%, Energy = + 1.954 X 10^{-5} + 7.514 X 10^{-7} B + 6.25 X 10^{-6} C , R-Squared = 100%.

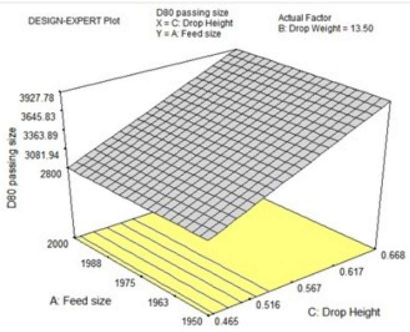

Figure 8 Banded Hematite and quartzite d80 particle passing size

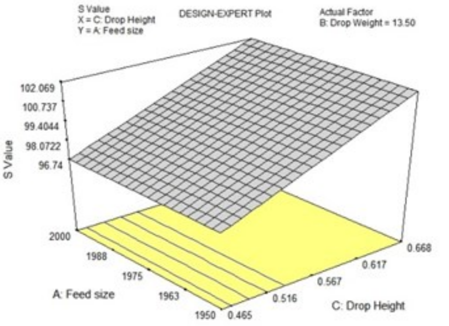

Figure 9 Banded Hematite and quartzite – S value

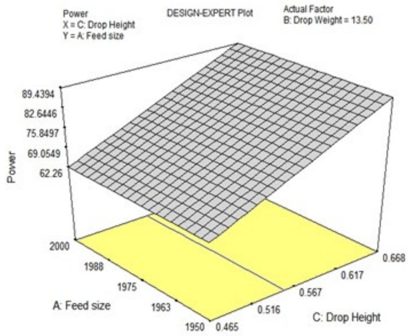

Figure 10 Banded Hematite and quartzite – Power

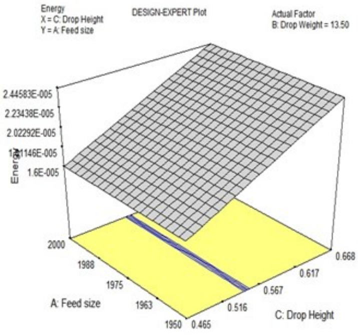

Figure 11 Banded Hematite and quartzite – Energy

Banded hematite and jasper

d80 passing size = + 4398.61 + 1969.49 B + 2291.67 C, R square = 100%, S Value = + 88.74 - 1.59 B + 0.56 C, R square = 99.34%, Power = + 73.64 - 9.107 X 10 – 4 B + 20.08 C, R square = 100%, Energy = + 1.954 X 10 – 5 + 7.514 X 10 – 7 B + 6.250 X 10 – C, R square = 100%. 3 D Curve almost same as Banded hematite and quartzite.

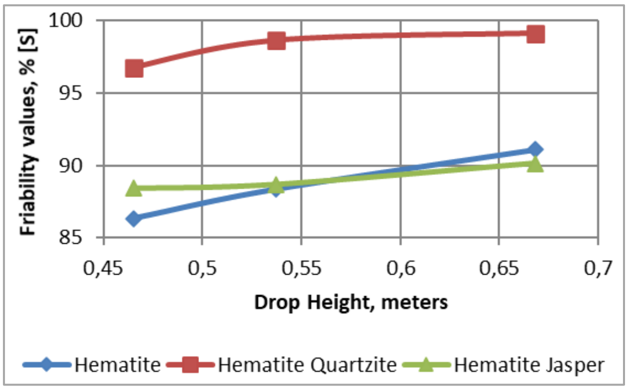

Figure 12 Drop height Vs Friability values for different types of iron ores

It is seen from Fig. 12 that as expected the friability values of any type of iron ore sample increases with increase the head height of compressive unit. 1) Hematite sample shows steep in increase friability value with increase of height weight. 2) Banded Hematite Quartzite sample also shows steep in increase friability value with increase of height weight and 3] the trend is similar with Banded Hematite Jasper sample.

CONCLUSION

Different heights of impact crushing were used in the investigations. The results of these studies reveal that as expected with an increase in the height of the impact head, the particle size decreases and accordingly the energy required for crushing of ore decreases the energy requirement and these observations are similar with all three types of ore samples. However, it is observed interestingly that the effect of impact crushing is more significant with reference higher production with Banded Hematite Quartzite sample and where as for Banded Hematite Jasper sample the effect of impact crushing is not significant with reference higher production with increase of height weight. Thus it is concluded that all three different iron ore formations have its own breakage properties.

ACKNOWLEDGEMENT

Two authors are thankful to the Chairman of Aryan Institute of Engineering and Technology for their encouragement to publish this paper.

REFERENCES

1. Bond, F.C. (1954) Crushing and Grinding Calculations. CIM Bulletin, 47 (507)466-472.
2. Bond, F.C. (1961) Crushing and Grinding Calculations, Part I. Br. Chem. Eng., 6 (6) 378-385.
3. Prasher, C.L. (1987) Crushing and grinding process handbook. John Wiley & Sons Ltd., New York, p 474.
4. Ozkahraman, T., Sirin, M. (1998) The use of brittleness test in determination of grindiability and crushing resistance of rocks and marbles. Innovations in mineral and coal processing, 33-36.
5. Altindag, R. (2003) Correlation of specific energy with rock brittleness concepts on rock cutting. The J. of the south African Institute of Mining and Metallurgy, 163-172.
6. Csoke, B., Hatvani, Z., Papanastassiou, D., Solymar, K. (2004) Investigation of grindiability of diosporic bauxites in dry, aqueous and alkaline media as well as after high pressure crushing. Int. J. Miner. Process 74S, 123-128.

XIV International Mineral Processing
and Recycling Conference
Belgrade, Serbia, 12-14 May 2021

DETERMINATION OF BOND WORK INDEX IN NON-STANDARD MILLS

Vladimir Nikolić[1#], Milan Trumić[1], Juan Maria Menéndez-Aguado[2]
[1] University of Belgrade, Technical Faculty in Bor, Bor, Serbia
[2] University of Oviedo, Escuela Politécnica de Mieres, Asturias, Spain

ABSTRACT – In mineral raw material processes, the Bond grinding procedure is widely used to obtain the grindability value of raw material, called the Bond working index. Determining the Bond work index is part of the design phase of a mining plant and can significantly affect the design costs associated with comminution. The Bond work index is very important, but the procedure itself takes a very long time and is prone to procedural errors, so for that reason a lot of work has been done that deals with this problem. One of the problems addressed by some researchers is whether the Bond work index can only be determined in a standard Bond ball mill. This paper gives an overview of previous research dealing with non-standard mills for determining the Bond work index.

Keywords: Bond Work Index, Comminution, Grindability, Non-Standard Mill, Bond ball mill test.

INTRODUCTION

The comminution of mineral raw materials is of great importance in many technological processes. Comminution is the process of reducing the size of raw materials for its direct use, preparation of raw materials for the concentration process or other type of technological processing. Apart from the technological one, comminution also has an important economic significance. It is estimated that over 5 % of the electricity produced in the world is spent on comminution various materials. The large share of energy in the total costs of mineral raw materials comminution is the reason why this process has been largely researched from the point of view of predicting the energy consumption from the changes in the size of the raw material.

One of the most important parameters for estimating the energy required when designing new plants or optimizing existing ones is the resistance of the raw material to comminution, which is called grindability. Although, today, new ways for designing the grinding process and determining the dimensions and power of mills, and thus the required amount of energy for the comminution process, are being intensively researched, the most widely used and most widespread one is the Fred Bond method. The basis of this method consists in the experimental determination of the Bond work index, which expresses the resistance of the raw material to comminution and is denoted (W_i). Bond developed the so-called standard test for determining the grindability of raw materials. In the test, the conditions for performing the test are precisely defined, the initial size of the sample is defined, as well as the standard mill with balls for performing the test. According to the standard Bond procedure, the work index is determined by the simulation of dry grinding in a closed cycle in a Bond ball mill until 250 % of the

---

[#] corresponding author: vnikolic@tfbor.bg.ac.rs circulating charge is reached [1-3]. The Bond test requires 7-10 grinding cycles, which shows that the procedure is long and complex, and therefore subject to errors. Due to the difficulty in determining the Bond work index by the standard method, many researchers have developed alternative methods, and some authors have suggested other mills to determine the Bond work index.

MATERIALS AND METHODS

Methods for testing the grindability of raw materials are used to determine the energy consumption for grinding products to the desired size. These procedures vary depending on the type of mill and the manufacturer. Mill manufacturers typically use the Bond test to dimension the size of grinding balls, although the standard Bond test does not lack ofsome difficulties. The test requires specific sample preparation for work and a precisely defined size of the initial sample. One Bond test requires around 10 kg of a sample, and usually the help of a professional technician to perform one test, which can take over 8 hours. The Bond work index is calculated using formula (1):

$$W_i = 1.1 \cdot \frac{44.5}{{P_c}^{0.23} \cdot G^{0.82} \cdot \left(\frac{10}{\sqrt{P_{80}}} - \frac{10}{\sqrt{F_{80}}}\right)}, [kWh/t] \tag{1}$$

where in:

W_i - Bond work index [kWh/t],
P_c - closing screen size [µm],
G - net mass of undersize product per unit revolution of the mill [g/rev],
F_{80} - the 80 % passing feed particle size [µm],
P_{80} - the 80 % passing product particle size [µm].

Determining the Bond index by the standard method gives very accurate and reliable results, but the method is very tedious and takes a long time. This section will present non-standard mills where it is possible to determine the Bond work index.

RESULTS AND DISCUSSION

Berry and Bruce (1966) [4] used an ordinary laboratory mill to compare the wet grinding of two ore samples, with one sample being the reference sample with known value of Bond work index. For identical sample weights of 2 kg, grinding time, and operating conditions, Bond's third comminution law was applied to calculate the estimated ore index of an unknown ore in a Bond ball mill.

Horst and Bassarear (1977) [5] gave a procedure similar to Berry and Bruce (1966) [4], except that this procedure is a little longer. The data of the reference ore and the unknown ore on which the Bond work index is determined are also compared. The only difference between these two processes is that the Horst and Bassarear (1977) procedure does not take into account the particle size distribution (PSD) of inputs and grinding products of an unknown sample but starts from the PSD of reference ore inputs, and the PSD of grinding products of unknown ore is calculated by the equation of the law of first-order kinetics. The test is performed in any laboratory ball mill on a sample of an initial weight of 1 kg.

Using copper ore as a reference ore, comparative results by the Berry-Bruce [4] method and the standard Bond method show that the largest error was 14.21 % and the smallest 1.36 %, while comparative results by the Horst-Bassarear [5] method and the standard method showed that the largest error was 2.16 % and the smallest 1 %.

A simple test for wet and dry grinding was developed by Outokumpu [6]. For this purpose, a laboratory mill was built, which is called Mergan's mill, smaller in size than the Bond's standard mill. The mill is equipped with variable speed and mechanical torque measurement which is integrated into the drive of the mill. This test differs from the Bond test in terms of sample weight (5 kg), initial PSD and the mill filling degree. Sample variability is calculated from the measured energy consumption.

Yap et al. (1982) [7] used a laboratory ball mill to determine the Bond work index. The sample is ground wet. The mill has a diameter of 251 mm and 2 kg of sample is needed for grinding. It is assumed that the adopted work index is proportional to the Bond work index for a constant desired sample size of 100 µm.

Nematollahi (1994) [8] designed a smaller mill to determine the Bond index and called it a calibrated Bond ball mill. The diameter of the mill was 200x200 mm and 85 steel balls were used for grinding. The weight of the balls was 5.9 kg, and the balls ranged in diameter from 16-38 mm.

The initial sample had a volume of 207 cm^3 instead of 700 cm^3, which is standard in the Bond test, and 3 kg of the initial sample is needed instead of 10 kg. The test is performed by dry grinding in a closed cycle until a 250 % circulating charge is reached. The Bond work index is calculated according to equation (2):

$$W_i = \frac{11.76}{{p_c}^{0.23}} \cdot \frac{1}{G^{0.75}} \cdot \frac{1}{\frac{10}{\sqrt{P_{80}}} - \frac{10}{\sqrt{F_{80}}}} \tag{2}$$

Table 1 shows the comparative values obtained with the standard Bond ball mill and with the new mill designed by Nematollahi (1994) [8].

Table 1 Comparative values of the Bond work index obtained in the standard Bond mill and the values of the Bond work index obtained in the Nematollahi mill [8]

Sample	Bond work index W_i (kWh/t)		Difference Δ (%)
	Bond mill	Nematollahi mill	
Barite	6.12	6.21	1.47
Feldspar	11.75	11.12	- 5.36
Hematite	13.89	14.31	3.02
Calcite	8.36	8.50	1.67
Chrome	14.98	15.70	4.81
Dolomite	21.77	19.18	- 11.90
Coke	30.43	28.75	- 5.52
Coal	12.99	12.33	- 5.08
Silicon	11.93	11.49	- 3.69
Fluorite	7.40	7.28	- 1.62
Magnetite	9.33	9.54	2.25

Menéndez-Aguado et al., (2005) [9] examined the possibility of determining the work index in a Denver laboratory mill (Figure 1). The research was performed on the size class of 100 % -3.35 mm on samples of gypsum, celestite, feldspar, clinker, limestone, fluorspar and copper slag. The initial sample volume was 326 cm^3, which results of applying the mill volume ratio (2.15) to 700 cm^3. The grinding test at the Denver mill followed Bond's methodology, with the only correction of the volume ratio when necessary. The Bond work index is calculated according to equation (3):

$$W_i = \frac{44.5}{{p_c}^{0.23} \cdot (2.15 \cdot G)^{0.82} \cdot \left(\frac{10}{\sqrt{P_{80}}} - \frac{10}{\sqrt{F_{80}}} \right)} \qquad (3)$$

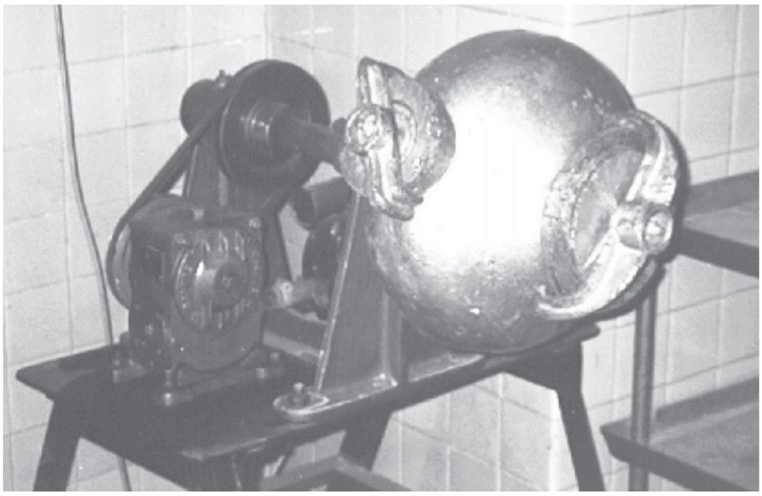

Figure 1 Denver laboratory mill [9]

Table 2 shows comparative value obtained with the Bond work mill and Denver laboratory mill.

Table 2 Comparative values of the Bond work index obtained in a standard Bond mill and the values of the Bond work index obtained in the Denver mill [9]

Sample	P_c (µm)	Bond work mill W_i (kWh/t)		Difference Δ (%)
		Bond mill	Denver mill	
Limestone	200	8.99	9.05	- 0.67
Feldspar	200	11.06	10.92	1.27
Celestite	200	5.41	5.57	- 2.96
Clinker	200	12.36	12.25	0.89
Gypsum	200	6.08	5.78	4.93
Fluorspar	200	6.94	7.41	- 6.77
Copper slag	200	18.40	19.10	- 3.80

Saeidi et al., (2013) [10] used a special mill to determine the Bond work index, designed by Nematollahi, (1994) [8]. The Bond work index is calculated by equation (3). On a representative sample (iron ore) of 2 kg, the PSD was determined, and then the representative sample was ground at time intervals of 20, 60, 120 and 180 seconds. After each grinding, the sample was sieved, the parameter P_{80} [µm] and the Bond work index were determined. The obtained results are shown in Table 3.

Table 3 Comparative results obtained of the standard Bond method and Saedi et al., (2013) method [10]

Mill time, s	Bond work index W_i (kWh/t)		Difference Δ (%)
	Bond	Saeidi et al.	
20	13.10	8.21	37.33
60	12.36	8.04	34.95
120	11.68	7.84	32.88
180	11.11	7.81	29.70

Due to large deviations in the values of the Bond work index, the authors defined a new equation (6) for determining the Bond work index based on the obtained results. They came up with a new formula by examining the relationship between the parameters G [g/rev] and P_{80} [µm] with the grinding time. It was necessary to create a relationship between these parameters, which could replace G [g/rev] and P_{80} [µm]. The relationship between G [g/rev] and P_{80} [µm] indicates that they are time-dependent, and can be represented by equations (4) and (5).

$$P_{80} = -0.1085 \cdot \mathrm{t} + 122.56 \tag{4}$$

$$G = -1E - 0.6 \cdot t^2 + 0.0004 \cdot t + 0.3397 \tag{5}$$

When equations (4) and (5) are inserted into equation (2), a new equation is obtained to determine the Bond work index (6):

$$W_i = \frac{5.6}{(-1E - 0.6 \cdot t^2 + 0.0004 \cdot t + 0.3397)^{0.75}} \cdot \frac{1}{\frac{10}{\sqrt{-0.1085 \cdot t + 122.56}} - \frac{10}{\sqrt{F_{80}}}} \tag{6}$$

To determine the accuracy of the equation (6), another experiment was performed, at a grinding time of 100 seconds, and the Bond working index was determined. The obtained values are given in Table 4.

Table 4 Comparative results obtained of the standard Bond method and Saedi et al., (2013) method [10]

Mill time, s	Bond work index w_i (kWh/t)		Difference Δ (%)
	Bond	Saeidi et al.	
100	12.18	12.13	0.41

Mwanga et al., (2017) [11] developed the Geometallurgical comminution test that requires a small amount of initial sample and a portable small mill (Capco) (Figure 2). The grinding test is performed on a sample of size class -3.35 mm with a starting weight of 220 g and can be performed within 2-3 hours. The sample is ground dry for 2, 5, 10, 17 and 25 minutes of grinding. After each grinding time, the PSD is determined through sieving, and the sample is returned to the mill for further grinding. The PSD is numerically estimated for parameter P_{80}. The recording of the total electricity consumption during the test is done using a conventional energy meter. When the test is performed at a constant sample mass and mill parameters (mill revolutions number, grinding batch), it is assumed that the energy supplied to the mill per unit time is constant. The Bond work index is calculated according to formula (7):

$$W_i = W_{i,GTC} \cdot \left(\frac{1}{\sqrt{\lambda}} \cdot \eta \cdot 1/4 \right) \tag{7}$$

where in:

λ - geometric factor of division and is $\lambda = 2.65$

η - mill drive and engine efficiency, up to $\eta = 0.64$

$W_{i,GTC}$ - performance index of the Geometallurgical comminution test, calculated as an old Bond equation.

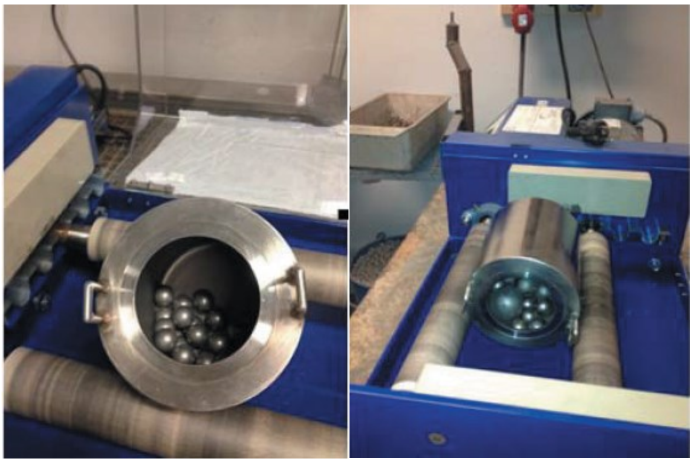

Figure 2 Small portable mill (Capco) (Mwanga et al., (2017) [11]

The authors stated that the test and performance of the presented method were confirmed on several types of ore and that the relative error ranged from 0.70 % to a maximum of 8.8 %.

CONCLUSION

The paper deals with existing methods for determining the grindability of raw materials in mills that differ from the standard Bond test. All methods used in different mills aim to give as close results as possible to the Bond work index compared to the results obtained in the Bond ball mill and to enable the determination of the Bond work index in conditions when the standard Bond ball mill is not available. Some of the presented methods are fast and practical because they eliminate certain steps in the work itself and reduce the number of grinding steps. Some methods also require a smaller initial mass, a smaller mass of grinding balls is required, and the grinding time itself is shorter than the Bond method. Notwithstanding the shortcomings of the Bond procedure for determining the Bond work index, and the shortcomings related to the size and precisely defined number of mill balls in the ball mill, the original procedure of the Bond procedure remains the industry standard.

REFERENCES

1. Bond F.C., Standard grindability test tabulated, Transactions of the American Institute of Mining and Metallurgical Engineers, 183, 1949, 313-329.
2. Bond F.C., The third theory of communition, Transactions of the American Institute of Mining and Metallurgical Engineers, 193, 1952, 484-494.
3. Bond F.C., Crushing and grinding calculation part I and II. British Chemical Engineering 6 (6 and 8), 1961,378-385 & 543-548.
4. Berry T. F., Bruce R.W., A simple method of determining the grindability of ores, Canadian Mining Journal, 87, 1966, 63-65,
5. Horst W. E., Bassarear J. H., Use of simplified ore grindability technique to evaluate plant performance, Transactions of the Metallurgical Society of AIME, 260, 1977, 348-351,
6. Niitti T., Rapid evaluation of grindability by a simple batch test, Proceedings of the International Mineral Processing Congress, Prague, Czechoslovakia, 1-6 June 1970, 1970, 41-46.
7. Yap R. F., Sepulveda J. L., Jauregui R., Determination of the Bond work index using an ordinary batch ball mill, In: Mular A. L., Jergensen, G. V. (Eds.), Design and Installation of Comminution Circuits, AIME, New York, 1982, 176-203,
8. Nematollahi H., New size laboratory ball mill for Bond work index determination, Mining Engineering, 46 (4), 1994, 352-353,
9. Menéndez-Aguado J.M., Dzioba B.R., Coello-Valazquez A.L., Determination of work index in a common laboratory mill, Minerals & Metallurgical Processing, 22 (3), 2005, 173-176,
10. Saeidi N., Noaparast M., Azizi D., Aslani S., Ramadi A., A developed approach based on grinding time to determine ore comminution properties, Journal of Mining & Environment, 4 (2), 2013, 105-112,
11. Mwanga A., Rosenkranz J., Lamberg P., Development and experimental validation of the Geometallurgical Comminution Test (GCT), Minerals Engineering, 108, 2017, 109-114.

XIV International Mineral Processing
and Recycling Conference
Belgrade, Serbia, 12-14 May 2021

EXPERIMENTAL STUDY ON THE GRINDING RATE CONSTANT OF QUARTZ IN A BALL MILL

Katarina Balanović#, Milan Trumić, Maja Trumić
University of Belgrade, Technical Faculty in Bor, Bor, Serbia

ABSTRACT – In this paper, the quartz grinding kinetics in a ball mill with charge of different ball size was analyzed. Three different ball charge were used (24, 15 and 10 mm), where each individual charge was composed of balls of the same diameter. By analyzing the obtained results, it was observed that the highest value of the quartz grinding efficiency (narrow range of quartz particle size) was achieved by using the charge with the 15 mm ball diameter.

Keywords: Quartz, Dry Grinding, Ball mill, Charge.

INTRODUCTION

In the comminution of materials, an understanding of how different components behave by themselves and how they interact with each other may be useful not only for understanding grinding mill action but also for optimizing the operation. Examination of the grinding process is performed in order to optimize the utilization of comminution energy and the recovery of minerals by minimizing overgrinding. Testing in industrial-scale grinding systems with variations in operating variables can be an expensive operation. On the other hand, laboratory-scale experimentation can provide detailed information about the grinding process which can be applied in full-scale comminution systems [1].

Ball mills such as tumbling, vibrating, and planetary mills are widely and frequently used as grinding devices in the field of chemical, materials, and recycling industries. The operational conditions in tumbling milling are generally determined experimentally. In order to determine the optimal operational conditions such as ball size, ball filling ratio, mill diameter, rotational speed of the mill, considerable effort and time are needed [2,3]. Size distribution of balls in ball mill has a significant impact on decrease of normative consumption as well as on quality of size distributions of grinding product, mill capacity and specific energy consumption. For each narrow size distribution of material there is a ball diameter which gives the highest grinding rate, and that is the optimal diameter of ball for the given grain size [4].

The quartz grinding kinetics in a ball mill with charge of different ball size was analyzed. The equation of the grinding kinetics law for the first order grinding was used. The differential form of the first order grinding kinetics equation is [5]:

$$\frac{dR}{dt} = -kR \tag{1}$$

[#] corresponding author: kbalanovic@tfbor.bg.ac.rs where is: $\frac{dR}{dt}$ – grinding speed of a large class; R – the content of the wide class in the mill at the moment (t); t – grinding time; k – grinding rate constant.

The integral form of equation (1) is:

$$R = R_0 \cdot e^{-kt} \tag{2}$$

Equation (2) can be written in the form:

$$ln\, R_0 - ln\, R = kt \tag{3}$$

Or otherwise:

$$ln \frac{R_0}{R} = kt \tag{4}$$

Equation (4) represents the equation of the linear line in the coordinate system $[t;\, ln(R_0/R)]$, with the coefficient of direction (k):

$$k = tg\alpha = \frac{Y}{X} = \frac{ln\frac{R_0}{R_2} - ln\frac{R_0}{R_1}}{t_2 - t_1} \tag{5}$$

MATERIALS AND METHODS

The test was carried out on samples of quartz which density is 2630 kg/m^3, and the Bond working index is Wi = 14.20 kWh/t. Three samples of 200 g (narrow range of particle size -0.850+0.600 mm) were formed. Grinding kinetics were monitored at the following time intervals: 0.5 min, 1 min, 2 min, 4 min, 8 min, 15 min. After grinding samples were sieved, the mass of unground feed particles was measured and put back into the mill, and the grinding was continued again for the prescribed time.

Grinding experiments have been performed in a laboratory ball mill with the following characteristics: mill diameter: D = 158 mm; mill length: L = 198 mm; relative rotational rate of the mill: ψ = 0.85 n_k; coefficient of ball mill filling: φ = 0.40; inside surface of cylinder mill: ribbed type; grinding method: dry. The ball mill (Fig. 1) is rolling using a roller device (Fig. 2). Inside surface of mill is ribbed to prevent sliding of balls during operation of mill (Fig. 3).

Figure 1 Outside view of the mill

Figure 2 Device with rollers

Figure 3 Ribbed inside surface of the mill

Three different ball charge were used (Fig. 4), where each individual charge was composed of balls of the same diameter. Characteristics of ball charge are given in Table 1.

Table 1 Characteristics of ball charge

Ball diameter in charge (mm)	Charge mass (g)	Number of balls in charge	Ball mass (g)
10	6775.8	1562	4.34
15	6945.1	482	14.41
24	6921.8	127	54.50

Figure 4 Three different charge made of balls of diameter 24, 15 and 10 mm

RESULTS AND DISCUSSION

The results of the quartz sample grinding kinetics with a 24 mm, 15 mm and 10 mm ball diameter charge, are shown in Figures 5, 6 and 7 respectively.

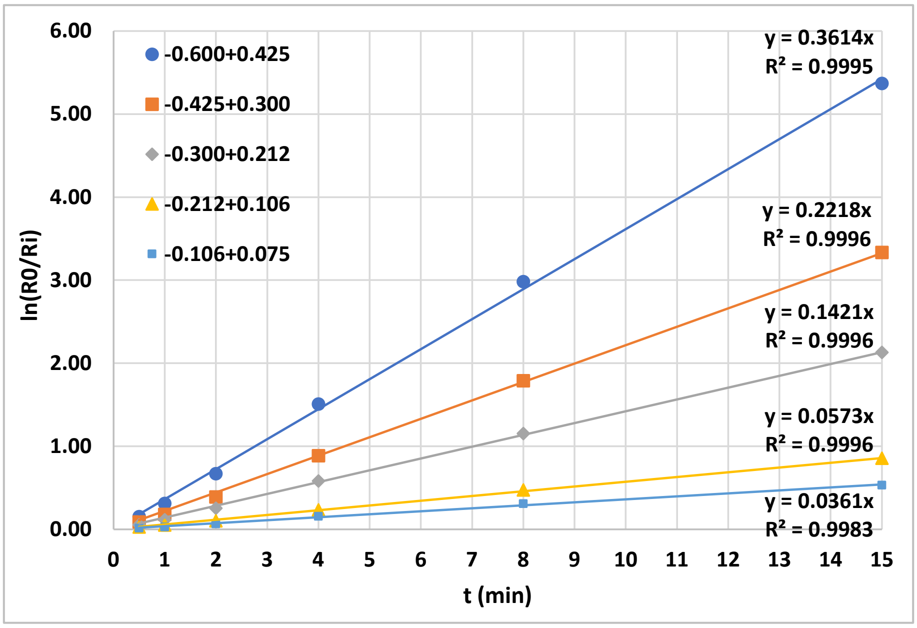

Figure 5 Quartz grinding kinetics with 24 mm ball diameter in charge

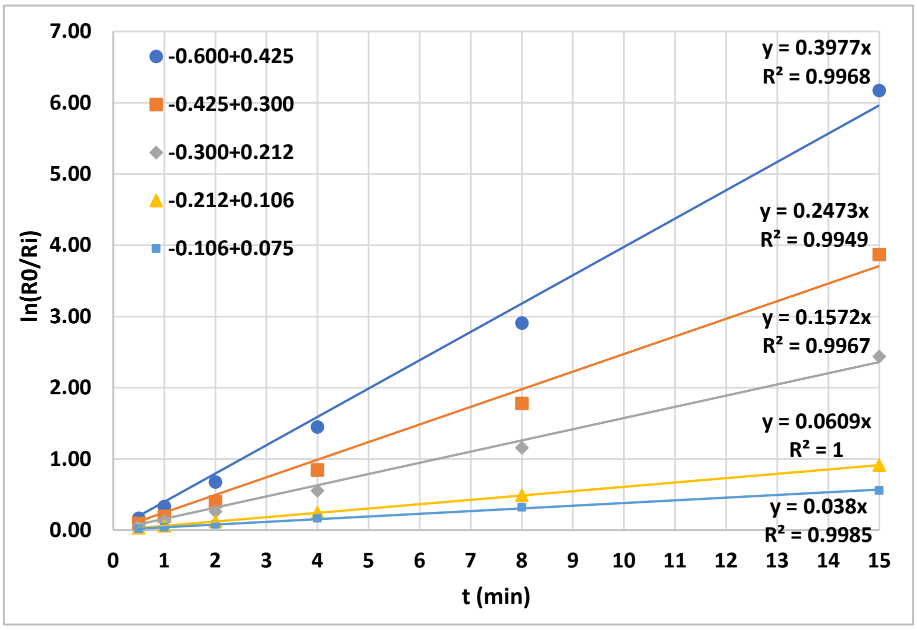

Figure 6 Quartz grinding kinetics with 15 mm ball diameter in charge

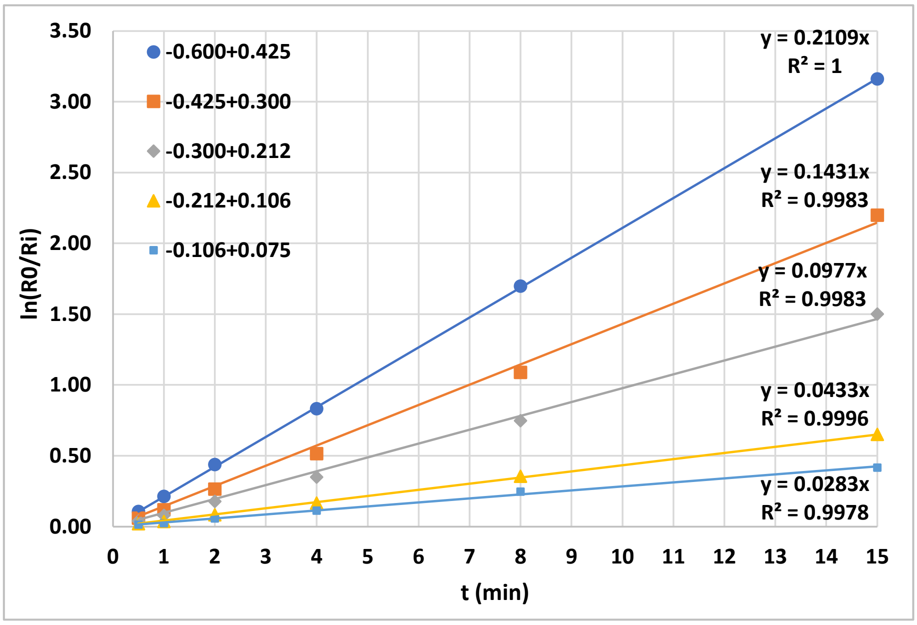

Figure 7 Quartz grinding kinetics with 10 mm ball diameter in charge

It can be noticed that the grinding rate with all three ball diameter in charge decreases with the reduction quartz sample size. The highest grinding rate constant was obtained at the largest size fraction -0.600+0.425 mm in all three cases.

Obtained correlation coefficients are bigger than the minimum value which is R^2_{min} = 0.569 from literature [6]. This confirms that the kinetics of grinding quartz narrow range of particle size in a laboratory ball mill can be described with an equation of the grinding kinetics law for the first order grinding.

For all conducted grinding tests, grinding rate constants has been determined and they are presented in Table 2. Figure 8 show relationship between grinding rate constant and ball diameter in charge. By comparing the results of grinding with 24 mm, 15 mm and 10 mm ball diameter in charge, the highest value of the grinding rate constant is obtained with 15 mm ball diameter in charge and the smallest with 10 mm ball diameter in charge, for each narrow size class.

Table 2 Grinding rate constant of narrow size classes with a different ball diameter in charge

Ball diameter in charge (mm)	Grinding rate constant				
	-0.600+0.425	-0.425+0.300	-0.300+0.212	-0.212+0.106	-0.106+0.075
10	0.2109	0.1431	0.0977	0.0433	0.0283
15	0.3977	0.2473	0.1572	0.0609	0.0380
24	0.3614	0.2218	0.1421	0.0573	0.0361

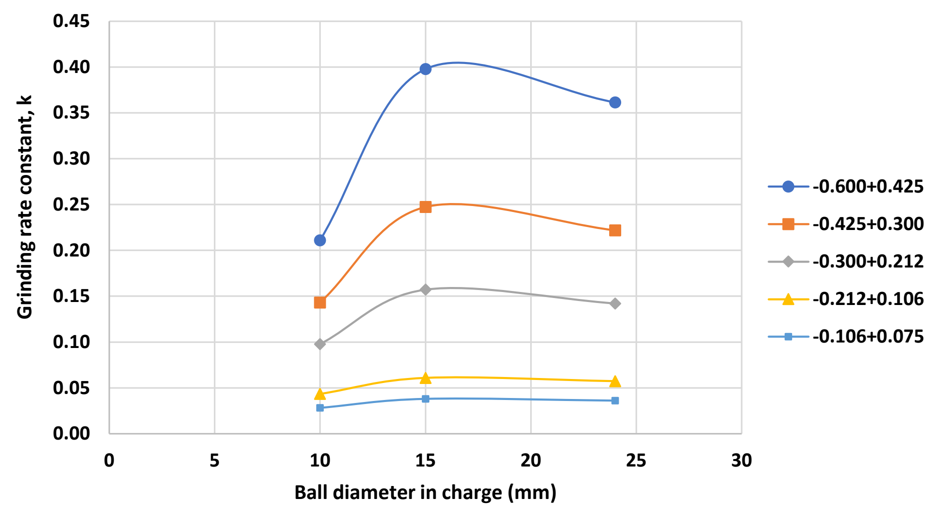

Figure 8 Grinding rate constant of narrow size classes with a different ball diameter in charge

CONCLUSION

This paper presents the results of an investigation into the effects of ball size on grinding kinetics in a ball mill. The experiments of quartz grinding were carried out in the laboratory ball mill with steel balls in dry environs. Degree of mill feed was maintained on 40% of mill volume in all experiments as well as mill revolution was constant at value 85% of mill critical speed.

Based on all obtained results it is concluded that the grinding rate constant, with different ball diameter in charge (24 mm, 15 mm and 10 mm), decreases with the reduction quartz sample size. The highest grinding rate constant, in all cases, was obtained at the largest size fraction -0.600+0.425 mm. For each narrow size distribution of quartz, there exists an optimal ball diameter that gives the highest grinding rate, and that is 15 mm diameter ball for this type of material.

ACKNOWLEDGEMENT

The research presented in this paper was done with the financial support of the Ministry of Education, Science and Technological Development of the Republic of Serbia, within the funding of the scientific research work at the University of Belgrade, Technical Faculty in Bor, according to the contract with registration number 451-03-9/2021-14/ 200131.

REFERENCES

1. Fuerstenau, D.W., Venkataraman, K.S. (1988) The comminution of multicomponent feeds under batch and locked-cycle conditions: Kinetics, simulation and energy distribution. International Journal of Mineral Processing, 22(1-4), 105-118.
2. Deniz, V. (2016) An investigation on the effects of the ball filling on the breakage parameters of natural amorphous silica. Advanced Powder Technology, 27(4), 1272-1279.
3. Kano, J., Mio, H., Saito, F. (2000) Correlation of grinding rate of gibbsite with impact energy of balls. American Institute of Chemical Engineers. AIChE Journal, 46(8), 1694.
4. Trumić, M., Magdalinović, N., Trumić, G. (2007) The model for optimal charge in the ball mill. Journal of Mining and Metallurgy A: Mining, 43(1), 19-31.
5. Magdalinović, N. (1999) Usitnjavanje i klasiranje, Nauka Beograd, pp.195-205.
6. Volk, W. (1965) Statystyka stosowana dla inżynierów. Wydawnictwa Naukowo-Techniczne.

XIV International Mineral Processing and Recycling Conference
Belgrade, Serbia, 12-14 May 2021

MONITORING THE GRINDING KINETICS IN BALL MILL WITH DIFFERENT SIZE BALL

Nemanja Bogdanović[1#], Milan Trumić[2]
[1] SERBIA ZIJIN COPPER BOR DOO, Bor, Serbia
[2] University of Belgrade, Technical Faculty in Bor, Bor, Serbia

ABSTRACT – The influence of different size ball charge in ball mill on grinding kinetics was investigated in this paper. The research was performed on quartz sand. For the grinding experiments, three different charges made of balls of the same diameter (10 mm, 15 mm, and 20 mm) were formed. The grinding was performed on a narrow size class at a constant rotation speed of the mill. The grinding kinetics was monitored via a grinding rate constant, a first-order kinetics model. The aim of the research was to determine the diameter of the balls that gave the highest grinding speed for the examined size classes, based on the kinetics of grinding quartz sand.

Keywords: Ball Mill, Grinding Rate Constant, Mill Loading.

INTRODUCTION

The final operation in the crushing process is the grinding process where the raw material is crushed to the size required by the concentration process, further technological processing, or direct use of the raw material. The grinding process is performed in one, two, less often in three stages, and the number of stages depends on the size of the input raw material and the final grinding product. In order to understand the grinding process and the operation of the mill, extensive research has been conducted. Different influencing factors have been investigated, which depended on the characteristics of the raw material to be ground, the operating conditions of the mills, and the construction of the mills. In the balls mills, steel balls are used and in the process of grinding, the balls wear out, so it is necessary to make additions with new balls in order to maintain the level of the charge of balls in order to efficiently grind. Raw material characteristics such as size and hardness affect grinding. In previous research, it has been found that each grain size corresponds to a certain diameter of grinding charge. The grinding charges used are rods, steel balls, or large pieces of raw material that are ground. For the process of preparation of mineral raw materials where the grinding process is the most expensive, it is necessary to choose the most favorable conditions for the operation of the mill, and to know how the grinding process takes place over time, i.e., the grinding kinetics.

The shape of the grinding kinetics curve is hyperbolic, which indicates a stable relation between the mass of unground coarse class (R) and grinding time (t) and depends on the

---

[#] corresponding author: nbogdanovi13@yahoo.com characteristics of the raw materials to be ground, grinding conditions, and the size of the control sieve opening (d) [1].

The differential form of the first order grinding kinetics equation is [1]:

$$\frac{dR}{dt} = -kR^n \tag{1}$$

where:

$\frac{dR}{dt}$ – grinding speed of a large class,

R – the content of the wide class in the mill at the moment (t),

t – grinding time,

k – grinding rate constant,

n - order of grinding kinetics.

The integral form of equation (1) is:

$$R = R_0 \cdot e^{-kt} \tag{2}$$

Equation (2) can be written in the form:

$$ln\, R_0 - ln\, R = kt \tag{3}$$

Or otherwise:

$$ln \frac{R_0}{R} = kt \tag{4}$$

$$k = tg\, \alpha = \frac{Y}{X} = \frac{ln\frac{R_0}{R_2} - ln\frac{R_0}{R_1}}{t_2 - t_1} \tag{5}$$

MATERIALS AND METHODS

The test was carried out on a samples of quartz sand (99.2% SiO_2). For research purposes, grinding kinetics in a ball mill narrow size class (-0.85 + 0.6 mm) was formed. Six experiments with samples of 200 g were performed and grinding kinetics was monitored. The intervals were 0.5 min, 1 min, 2 min, 4 min, 8 min, and 15 min and the charge of balls of the same size of diameter (10 mm, 15 mm, and 20 mm) were formed for grinding. Two size classes (-0.300 + 0.212 mm) and (-0.212 + 0.106 mm) were monitored in the grinding product. Grinding experiments were carried out in a laboratory ball mill with the following characteristics: D=158 mm, L=198 mm, V=3.880 dm^3, ribbed inside surface of cylinder mill, dry grinding, coefficient of ball mill loading 35% and 45%, and relative rotational rate of mil 0.85 of the critical.

Figure 1 Quartz sand, ball mill and charge of balls

RESULTS AND DISCUSSION

The results of the grinding kinetics of quartz sand samples are shown in Figures 2 and 3. Tables 1 and 2 show the values of the grinding rate constant and correlation coefficients with different values of ball charges and mill loading 35% and 45%.

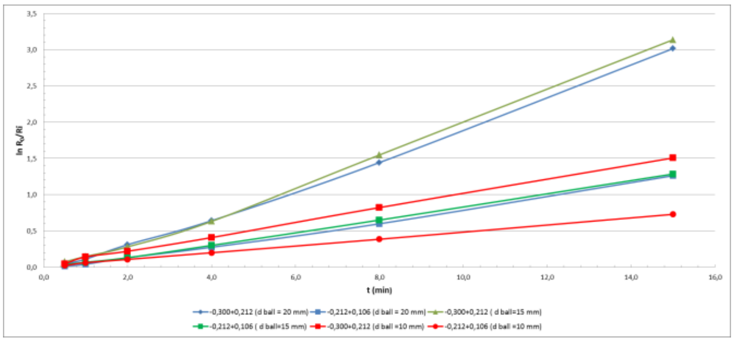

Figure 2 Kinetics of grinding quartz sand with a charge of balls with a diameter of 10 mm, 15 mm, and 20 mm at a coefficient of ball mill loading 45%

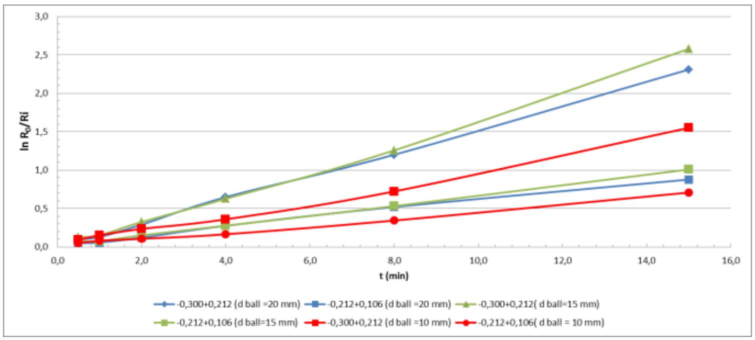

Figure 3 Kinetics of grinding quartz sand with a charge of balls with a diameter of 10 mm, 15 mm, and 20 mm at a coefficient of ball mill loading 35%

Figures 2 and 3 show that the kinetics of quartz sand grinding with a charge of balls with diameters of 10 mm, 15 mm, and 20 mm describe the model of first order grinding kinetics adequately, because the correlation coefficients were R^2> 0.99 for both tested size classes (Table 1 and 2).

Table 1 Grinding rate constants and correlation coefficients obtained by grinding quartz sand at a ball mill loading of 45%

Size class d (mm)	Coefficient of ball mill loading 45%					
	20 mm		15 mm		10 mm	
	R^2	k	R^2	k	R^2	k
-0.300+0.212	0.9912	0.1936	0.9905	0.2021	0.9986	0.1012
-0.300+0.212	0.9975	0.0859	0.9964	0.0838	0.9992	0.0486

Table 2 Grinding rate constants and correlation coefficients obtained by grinding quartz sand at a ball mill loading of 35%

Size class d (mm)	Coefficient of ball mill loading 35%					
	20 mm		15 mm		10 mm	
	R	k	R	k	R	k
-0.300+0.212	0.9991	0.1535	0.9966	0.1680	0.9897	0.1005
-0.300+0.212	0.9927	0.0606	0.9963	0.0675	0.9884	0.0464

The value of the grinding rate constant decreased with decreasing raw material size class. The obtained results were in agreement with the results of other researchers who showed that the value of the grinding constant was the highest in larger classes of raw material size and that there was an optimal ball diameter for each size class [2].

At the same value for the coefficient of ball mill loading the grinding quartz sand with a charge of balls with a diameter of 10 mm, the lowest value of the grinding rate constant in relation to the previous two charges of balls was obtained.

Comparing the obtained results of grinding quartz sand with a charge of balls of the same diameter, it is concluded that a higher grinding speed was obtained when the mill was more loaded. The obtained results were in accordance with the research of the authors Petrakis and et. al. (2017) who changed the value of ball mill loading during quartz grinding and showed that higher ball mill loading had a positive effect on grinding efficiency. Figure 4 shows the comparative results of the obtained values of the grinding rate constants for ball mill loading of 35% and 45%, and in Table 3 the optimal diameters of the balls determined by the grinding rate constant on the quartz sand sample are presented.

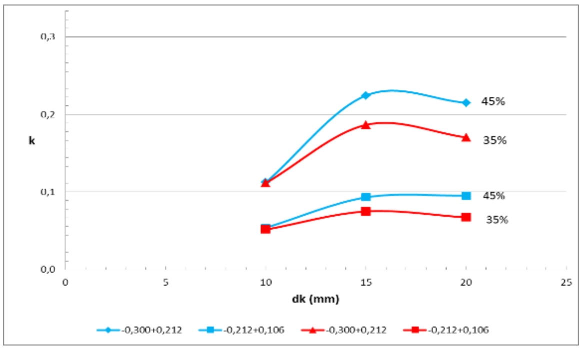

Figure 4 Change of the grinding rate constant of a narrow class of quartz sand coarseness as a function of the diameter of the balls in the charge, at a ball mill loading of 35% and 45%

Table 3 Optimal ball diameters determined by the grinding rate constant on a quartz sand sample

Size class d (mm)	Medium diameter narrow size fraction (mm)	Quartz sand	
		The optimal ball diameter (mm)	
		45%	35%
-0.300+0.212	0.256	16	15.9
-0.212+0.106	0.159	/	15.6

The analysis of the obtained results of quartz sand grinding results clearly showed the influence of the size of the ball diameter in the charge and the ball mill loading on the grinding speed [4]. Also, the results obtained in this paper showed that the values of the grinding speed constants increased with increasing ball mill loading and positively affected the grinding efficiency, which was in accordance with the results of the authors Petrakis et.al. (2017).

CONCLUSION

Analyzing the grinding kinetics quartz sand in a ball mill when changing the size of the balls, the following conclusions can be reached:

- In all grinding experiments of the narrow size class (-0.85 + 0.6 mm), the grinding kinetics took place according to the model of first-order grinding kinetics with a high correlation coefficient (R^2=0.98 ÷ 0.99).
- The value of the grinding rate constant decreased with decreasing size class and with the ball mill loading grinding charges in all experiments.
- When grinding quartz sand of size class (-0.300 + 0.212 mm), the optimal diameter of the balls was 16 mm (φ=45%), or 15.9 mm (φ=35%). For the size class (-0.212 + 0.106 mm, at φ=45%) it was not possible to determine the optimal diameter of the balls because based on the graphs it could be seen that the values of the grinding rate constant increased with the diameter of the ball in the charge. For the same class at φ = 35%, the optimal diameter of the ball was 15.6 mm.

REFERENCES

1. Magdalinović, N. (1999) Comminution and classification, Science, Belgrade, (In Serbian).
2. Trumić, M., Magdalinović, N., Trumić, G. (2007) The model for optimal charge in the ball mill, Journal of Mining and Metallurgy, 43 A, 19-31.
3. Petrakis, E., Stamboliadis, E., Komnitsas, K. (2017) Identification of Optimal Mill Operating Parameters during Grinding of Quartz with the Use of Population Balance Modeling, Kona Powder and Particle Journal, 34, 213-223.
4. Bogdanović, N. (2020) Monitoring the grinding kinetics in ball mill with different size ball, Bachelor Thesis, Technical faculty in Bor, (In Serbian).

XIV International Mineral Processing
and Recycling Conference
Belgrade, Serbia, 12-14 May 2021

INFLUENCE OF GRAIN DENSITY AND SHAPE ON THE SCREENING RATE CONSTANT VALUE

Maja Trumić[#], Milan Trumić, Grozdanka Bogdanović, Ljubiša Andrić
University of Belgrade, Technical Faculty in Bor, Bor, Serbia

ABSTRACT – Screening kinetics were performed on samples of PVC (polyvinyl chloride) insulation, magnesite ore and copper wire. Screening experiments were done on a sieve shaker with a 1.7 mm sieve. The used samples have different characteristics and during screening they filled the entire sieve area in two layers.

Based on the obtained data, it can be said that PVC sample and Cu sample have approximately the same efficiency value for the observed time of screening, while the ore sample has a significantly higher efficiency. Given that the ore sample has a cubic grain shape and the remaining two samples have a needle grain shape, it can be said that the influence of the grain shape is not negligible. The influence of material density proved to be a negligible parameter under the given screening conditions.

Keywords: PVC Insulation, Copper Wire, Magnesite Ore, Screening Kinetic, Grain Shape.

INTRODUCTION

Screening or sieving is an important unit operation to separate particles on the basis of size by a screening or sieving surface which will either accept or reject particles. [1]

Screening plays a significant role in many industries, because separates valuable minerals and non-valuable materials from waste rock and other elements that are not needed for further processing. This process mainly occurs in industries such as mining, mineral processing, agriculture, pharmacy, recycling and etc.

The efficiency of the screening process relies on several factors: vibration, g force, density and grain shape of material and so on. Screening process is modelled by reaction kinetics and usually a some mathematical model is used to determine screening rate constant. For mathematical interpolation of screening kinetics, several models are proposed in literature. [1, 2] The model used in this paper is the modified screening model Magdalinović-Trumić. [2].

$$\frac{E}{1-E} = kt \tag{1}$$

$$E = 1 - \frac{m}{m_0} \tag{2}$$

where, k is screening rate constant, E is screening efficiency, m is the mass of particles of size (-a + 0) on the screening at time t, a is the aperture size, m_0 is the initial mass of a particle (-a + 0).

[#] corresponding author: majatrumic@tfbor.bg.ac.rs

MATERIALS AND METHODS

Experiments were carried out on three materials: PVC insulation, magnesite ore and copper wire. The density and grains shape of materials were differ (Table 1). Experiments were performed using a sieve and sieve shaker Retsch at a constant amplitude value (A=1). The sieving surface used in the experiments was square with openings of 1.7 mm. Experiments were performed with samples that filled the entire surface of the sieve in two (2L) characteristic layers.

Table 1 Characteristic of samples

Samples	Density (kg/m^3)	Grains shape
PVC insulation	1350	needle
Magnesite ore	3280	cubical
Copper wire	8920	needle

Table 2 Grain size distribution of samples

d (mm)	Sample 1 PVC insulation	Sample 2 Magnesite ore	Sample 3 Copper wire
-3.35 +2.36	10	10	10
-2.36 +1.7	10	10	10
-1.7 +1.18	50	50	50
-1.18 +0.850	20	20	20
-0.850 +0.600	10	10	10
∑	100%	100%	100%

*Screening was done in (2L) two layers.

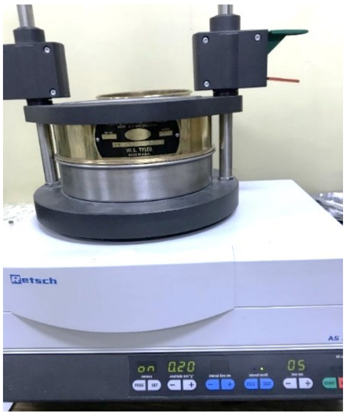

Figure 1 Sieve shaker Retsch

RESULTS AND DISCUSSIONS

The results of screening kinetics for PVC insulation, magnesite ore and copper wire are shown in Table 3.

Table 3 Screening kinetics of PVC insulation [3], magnesite ore and copper wire

	t(s)	10	20	30	45	60	90	120	180
PVC insulation	E	72.45	85.44	88.33	91.02	91.44	93.46	93.89	94.83
	$\frac{E}{1-E}$	2.63	5.87	7.57	10.14	10.68	14.29	15.37	18.34
Magnesite ore	E	92.87	95.84	96.57	97.07	97.74	98.14	98.41	98.63
	$\frac{E}{1-E}$	13.03	23.04	28.15	33.13	43.25	52.76	61.89	71.90
Copper wire	E	78.08	81.00	86.96	88.09	90.02	91.86	92.45	93.97
	$\frac{E}{1-E}$	3.56	4.26	6.67	7.40	9.02	11.29	12.25	15.58

Table 3 shows the screening kinetics results of used samples. Based on this data it can be said that Sample 1 (PVC insulation), and Sample 3 (Copper wire), achieved approximately the same efficiency value for the observed time of screening. Sample 2 (Magnesite ore), has a greater efficiency value for the same observed time of screening (efficiency value after the screening time of 20s reach 95%).

The results obtained by screening show that the Sample 2 (Magnesite ore), after 20s of screening achieved an efficiency value of 95%. For Sample 1 (PVC insulation), and Sample 3 (Copper wire), it is necessary to screened the secondary raw materials for a long time to achieve the same efficiency value (Sample 1~180s).

The Figure 2 shown the screening kinetics of samples with the different physical characteristics and the same grain size distribution in the same height of the layer on the sieve (two layers).

Since the minimum value of correlation coefficient is R^2_{min} =0.44 [4], it can be said that used model describes screening kinetics with high correlation coefficient (R^2>0.70 for Sample 1, R^2>0.75 for Sample 2, R^2>0.71 for Sample 3), and achieved value of correlation coefficient confirm previous research of testing modified model screening kinetics Magdalinović-Trumić [2-3, 5-9].

From the Figure 2 can be seen that the samples with the same grain shape (PVC insulation and copper wire have needle grain shape) and the different density (PVC insulation-1350 kg/m^3 and copper wire-8920 kg/m^3) have approximately the same values of screening rate constant. Raw material with the density value between these two samples cubical shape grains (magnesite ore-3280 kg/m^3) has a greater rate constant screening value k, compared to secondary raw material (PVC insulation and copper wire). It can be concluded that under the given conditions the influence of sample grain shape is greater than the influence of density values.

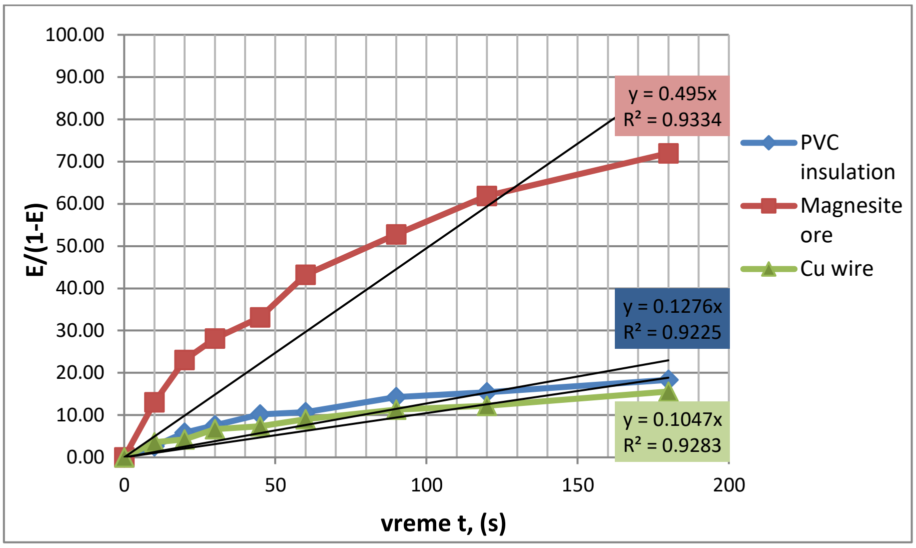

Figure 2 Screening kinetics of PVC insulation, magnesite ore and copper wire

Table 4 Values of constant screening rate

Sample	k	R^2
PVC insulation	0.128	0.709
Magnesite ore	0.495	0.752
Cu wire	0.105	0.719

Correlation coefficient R^2 and screening rate constant k of tested samples are given in Table 4. The data show that PVC insulation with lower density and needle grain shape have the same value of k as the copper wire with high density and needle grain shape, which indicates that the influence of density is negligible. By screening the magnesite ore with cubical grain shape and a density value 3 times less than the Cu wire and 3 times higher than the PVC insulation, the 5 times higher value for k was obtained.

CONCLUSION

Based on the experimental data presented in this paper and the analysis of screening kinetics of PVC insolation, magnesite ore and copper wire samples for given grain size distribution, can be concluded:

- The influence of density for secondary raw materials with the same grain shape (PVC insulation and Cu wire) on k value is negligible.
- The influence of grain shape for materials on k value is not negligible. The samples with cubical grain shape have higher value for k.
- Since screening was performed at a constant amplitude value, these experiments should be repeated in order to determine the optimal amplitude value, and then to analyze whether the influence of grain shape is still the dominant factor.

ACKNOWLEDGEMENT

The research presented in this paper was done with the financial support of the Ministry of Education, Science and Technological Development of the Republic of Serbia, within the funding of the scientific research work at the University of Belgrade, Technical Faculty in Bor, according to the contract with registration number 451-03-9/2021-14/ 200131.

REFERENCES

1. Esfandiary, A.H. (2014) Simulation and modelling of screening processes. (Doctoral thesis), The University of New South Wales, Faculty of Science, Australia.
2. Trumic, M., Magdalinovic, N. (2011) New model of screening kinetics. Minerals Engineering, Volume 24 (1), 42–49.
3. Trumić, M.S., Marilović, D., Trumić, M., Bogdanović, G., Andrić, Lj. (2016) Influence of secondary raw materials density and grain shape on screening kinetics. XI international Symposium on Recycling technologies and Sustainable Development, Bor, Serbia, 171-176.
4. Volk, W. (1965) Statystyka stosowana dla inżynierów. Wydawnictwa Naukowo – Techniczne, Warszawa.
5. Stojanovic, A., Trumic, M.S., Trumic, M.Z., Andric, Lj. (2015) Screening kinetics analysis of PVC insulation and copper wire. X International Symposium on Recycling Technologies and Sustainable Development, Bor, Serbia, 80-85.
6. Stojanovic, A., Trumic, M.Z., Trumic, M.S. (2015) The influence of particle shape on screening kinetics. 47th International October Conference on Mining and Metallurgy, Bor, Serbia, 95-100.
7. Trumić, M.Ž., Marilović, D., Trumić, M.S., Bogdanović, G. (2016) The influence of particle size distribution and height layer of raw material on screening kinetic, 48th International October Conference on Mining and Metallurgy, Bor, Serbia.
8. Janković, I. (2016) Testing the efficiency of the screening process of primary and secondary raw materials by changing the influential parameters, graduate thesis, University of Belgrade, Technical Faculty in Bor.
9. Vojinović, B. (2019) Monitoring the efficiency of screening of non-metallic mineral raw materials, graduate thesis, University of Belgrade, Technical Faculty in Bor.

XIV International Mineral Processing
and Recycling Conference
Belgrade, Serbia, 12-14 May 2021

THE IMPACT OF LIMESTONE FRAGMENTATION ON RAW MIX PRODUCTION IN CEMENT INDUSTRY

Nikola Đokić[1#], Lazar Kričak[2], Stefan Milanović[2], Marinko Pavlović[1], Stefan Krstić[1]
[1] Moravacem Ltd, Popovac, Serbia
[2] University of Belgrade, Faculty of Mining and Geology, Belgrade, Serbia

ABSTRACT – Raw mix design is one of crucial point in production of clinker. Cement industry use limestone, marl, clay in particular percent to provide the best quality in production of clinker. The quality of the material must be in line with the quality targets. Fragmentation is important element, because affect pre-blending design, economic norm from blasting to crusher. Blasting is an operation which affects all subsequent operations and costs. The Kuz-Ram model is possibly the most widely used approach to estimating fragmentation from blasting, and renewed interest in the field of blast control has brought increased focus on the model.

Keywords: Blasting, Fragmentation, Crusher, Kuz-Ram, Raw Mix.

INTRODUCTION

Optimum blasting just does not happen. It requires suitable planning, good blast design, accurate drilling, the correct choice of explosives and initiation system and methods, adequate supervision and considerable attention to detail. The primary purpose of blasting is to fragment rock, and there are significant rewards for delivering a fragmentation size range that is not only well suited to the mining system it feeds but also minimizes unsaleable fractions and enhances the value of what can be used in production. Over the past decades, significant progress has been made in the development for blast design and blast fragmentation size prediction. Rock fragmentation depends on many variables such as rock mass properties, site geology, in situ fracturing and blasting parameters and as such has no complete theoretical solution for its prediction. Empirical models for the estimation of size distribution of rock fragments have been developed such as those based on the Kuz–Ram fragmentation model. This method is able to predict the entire fragmentation size distribution, taking into account intact and joints rock properties, the type and properties of explosives and the drilling pattern. Element like fragmentation can affect electrical, diesel and explosives consumption. Marl in this case is not included, there is no blasting in marl quarry.

EXPERIMENTAL

Calculation started with finding particular size of limestone for hammer crusher type FLS EV 200x200 (Table 1). Optimal input sizes of limestone should satisfy the capacity of

---

[#] corresponding author: nikola.djokic@moravacem.rs the crusher, mixing ratios for pre-blending, output size that affects the capacity of the mill, as well as economic norms.

Table 1 Hammer crusher FLS EV 200x200, manufacturer characteristics

Hammer crusher	Inlet roller			Hammer rotor		Max. feed size		Weight
Type	Nos.	Peripheral speed (m/s)	Speed (rpm)	Peripheral speed (m/s)	Speed (rpm)	Max. size (mm)	Max. weight (kg)	Total weight (ton)
EV 200x200	1	1	19	30-39	290-375	1,400	2,000	95

The requirement of the ball mill, in order to satisfy the capacity is that the size of the material be around 30mm. In relation to the requirements of the mill, and in order to satisfy the capacity of the crusher, the optimal size of the input on the crusher can be calculated:

$$Dopt = \frac{Di-Do}{2} \tag{1}$$

Di = 1.4 (m) - Input size;
Do = 0.03 (m) - Output size;
Dopt = 0.685 ± 0.1 ≈ 0.5-0.7 (m).

The primary assumption of empirical fragmentation modelling is that increased energy levels result in reduced fragmentation across the whole range of sizes, from oversize to fines. This is generally valid, but not necessarily applicable to real situations. Some of the other factors that may override the expected relationship include:

- Rock properties and structure (variation, relationship to drilling pattern, dominance of jointing);
- Blast dimensions (number of holes per row and number of rows);
- Bench dimensions (bench height versus stemming and subdrilling);
- Timing between holes, and precision of the timing;
- Detonation behaviour, in particular detonation velocity (VoD);
- Decking with air, water and stemming;
- Edge effects from the six borders of the blast, each conditioned by previous blasting or geological influences.

Table 2 show different input parameters for drilling and blasting by years.

Table 2 Drilling and blasting parameters

Parameters	2016.	2017.
Diameter of drill hole	90 mm	90 mm
Burden	3 m	2.6 m
Sub-drill	1.5m	1.5 m
Distance between rows	5 m	3 m
Distance between holes	5 m	4 m
Slope of the blasting hole	70°	70°
Stemming	3 m	2.5 m

RESULTS AND DISCUSSION

The major changes to the Kuz-Ram model, was developed as a result of the introduction of electronic delay detonators (EDs), since these have patiently transformed fragmentation. Both the effect of assigned timing and the effect of timing scatter are accommodated (Cunningham, 2005). The equation set includes changes in the uniformity and mean fragment size equations, which is as follows:

$$X_{50} = AA_T K^{-0.8} Q^{\frac{1}{6}} \left(\frac{115}{RWS}\right)^{\frac{19}{20}} C(A) \tag{2}$$

Where, A_t is timing factor, which is multiplier, and incorporates the effect of interhole delay on fragmentation, C(A) a correction factor for the rock factor, n_s is the uniformity factor governed by the scatter ratio. As with the rock factor A, it can happen that the uniformity index is just not what the algorithm suggests, in which case correction factor C(n) is provided to overlay the inputs and enable estimation of the effects of changes from a common base.

$$n = n_s \sqrt{\left(2 - \frac{30B}{d}\right)} \sqrt{\left(\frac{1+S/B}{2}\right)} \left(1 - \frac{W}{B}\right) \left(\frac{L}{H}\right)^{0.3} \mathrm{C(n)} \tag{3}$$

Where, B is burden (m), d is the hole diameter (mm), S is the spacing (m), W is the standard deviation of drilling accuracy (m), L is the total length of drilled hole (m), H is the bench height (m), C(n) is a correction factor for the uniformity index.

For data input, there is graphics for two years, 2016. (Figure 1) and 2017. (Figure 2) which show different size of material relative to percent passing by Kuz-Ram model based on drilling and blasting parameters for 2016. and 2017.

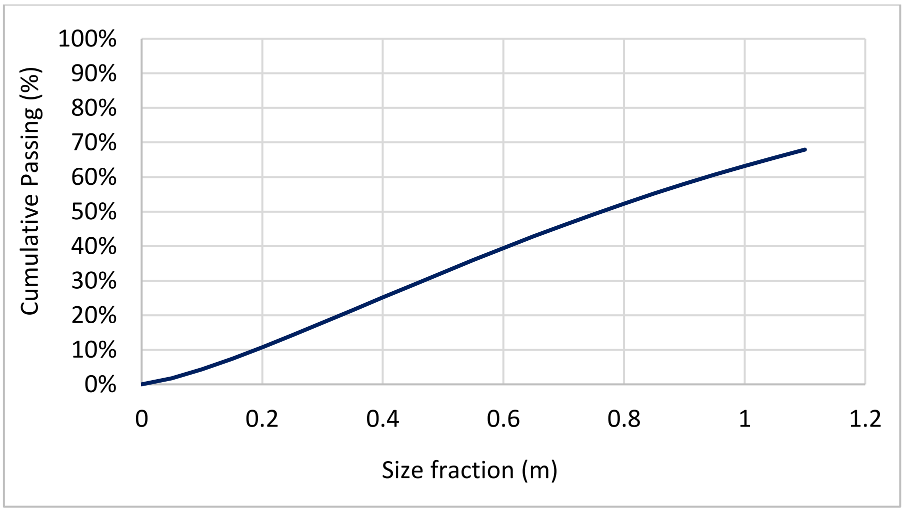

Figure 1 Kuz-Ram model base on drilling and blasting parameters for 2016

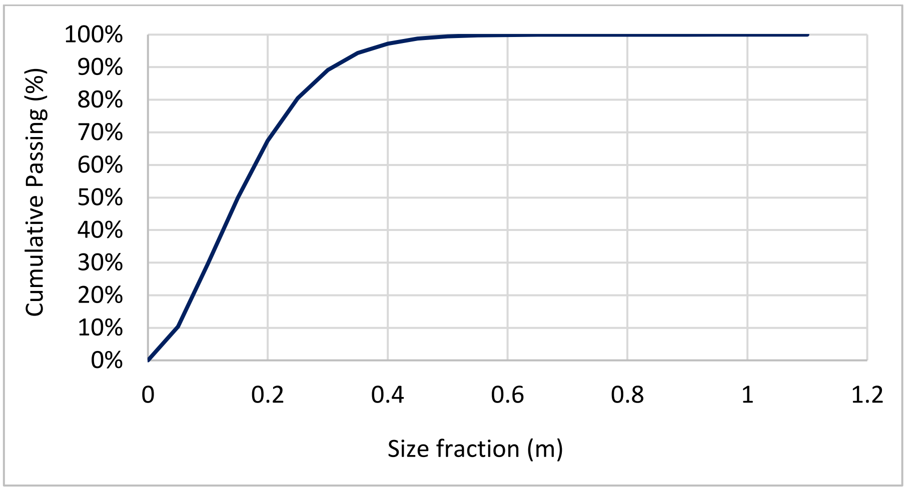

Figure 2 Kuz-Ram model base on drilling and blasting parameters for 2017

Predicted fragmentation base on Kuz-Ram model show different (Table 3) between percent passing of good materials which is affected from drilling and blasting parameters.

Table 3 Predicted fragmentation base on Kuz-Ram model

Percent	2016.	2017.
Oversize	20.7 %	10.9 %
In range	68.6 %	88.4 %
Undersize	10.7 %	0.7 %

Along with the results of the Kuz-Ram model, the consumption of electricity on the crusher can be predicted according to the formula by Kick:

$$E = Ck\,log\,\frac{Di}{Do} \tag{4}$$

E - Electrical energy (Kwh/t);
Ck = 10 * Wi - cons. of proportionality;
Wi = 12.77 Kwh/t (empirical value for limestone);
Di - Diameter of input material;
Do - Diameter of output material.

Applied Kick formula for electrical consumption on optimal and max. size of fragmentation give result (Table 4).

Table 4 Consumption of electrical power by Kick formula

Kick formula	Max. size (1.4 m)	Optimal size (0.8 m)
Electrical consumption	85.45 kWh	54.39 kWh

According to different sizes of fragmentation, differences in electricity power consumption can be seen as well as economic justification of using more explosives for drilling and blasting parameters from 2017. (Table 5).

Table 5 Electrical power consumption on hammer crusher

Year	2016.	2017.
Consumption of explosives (t)	82421	90757
Limestone production (t)	590176	632702
Electrical power (kWh)	385800	403500
Total (kWh/t)	0.56	0.49
Secondary blasting (times)	18	3

The benefit of increasing the consumption of explosives, and reducing fragmentation is the consumption of diesel and better utilization of machanization (Table 6). Machine can give more production, better cycle with less working hours and diesel consumption.

Table 6 Diesel consumption of different mechanization in quarry

Mechanization	Loader Caterpillar 988		Bulldozer Caterpillar D9R	Drilling rig AtlasCopco Roc F6	
Year	Fuel consumption (l)	Working hour (h)	Fuel consumption (l)	Working hour (h)	Drilled meter (m)
2016.	64151	2001	15785	1216	17340
2017.	63804	2106	9675	954	18563

When optimal fragmentation is good, it can avoid safety problems:

- Inequality on the lower part of banch;
- Irregular upper edges of the bench;
- Generating excessive mass on the edge of the bench;
- Increased number of boulders;
- Genarating cracks on bench;
- The distribution of materials in the truck basket.

CONCLUSION

Being an empirical model, which infers finer fragmentation from higher energy input, it is more about guidance rather than accuracy. The results obtained remain a starting point to give an overview of what is expected of an adjustment to a preexisting blast design. It can also serve as a basis for evaluating different designs, investigating the effect of changing certain variables and predicting the size distribution to be produced by the design. Results from calculated is near real value, so usage of Kuz-Ram model give positive benefits and good prediction what to expect. Safety and economically benefits are is another good indicator of the use of model and empiricism. The most important function of Kuz-Ram is to guide the blasting engineer in thinking through the effect of various parameters when attempting to improve blasting effects, leading to the final product, which is clinker in the cement industry.

ACKNOWLEDGEMENT

Gratitude goes to the management of Moravacem Ltd, the part of CRH cement company for granting us the permission to carry out this research and all data to work at quarry site and for considering the research work.

REFERENCES

1. Chung, S. H. Katsabanis, P.D. (2000) Fragmentation prediction using improved engineering formula.
2. FRAGBLAST – Int. J .Blast. Fragment. 4: pp 198-207.Author, D. (2011) Book title. No. Edition, Publisher, City.
3. Clark, G. B. (1987) Principles of Rock Fragmentation. John Wiley & Sons, New York. 432-442.
4. Cunningham, C.V.B. (2005) The Kuz-Ram Model-20 years on. Brighton Conference Proceedings. pp 201-210 Esen, S. & Bilgin, H.A. (2000) Effect of explosive on fragmentation. The 4th Drilling and Blasting Symposium. Faramarzi, F.; Mansouri, H.and Ebrahimi Farsangi, M.A (2013). A rock engineering systems based model to predict rock fragmentation by blasting, International Journal of Rock Mechanics & Mining Sciences 60, pp 82–94.
5. Rodgers, J. A. (1999) Measurement Technology in Mining, Proceeding MINEBLAST 99, Duluth, Minnesota, pp 17-23.
6. Magdalinović N. (1999) Usitnjavanje i klasiranje, 346.
7. Cunningham, C.V.B. (1987) Fragmentation estimations and the Kuz–Ram model – four years on. Proceedings of Second International Symposium on Rock Fragmentation by Blasting, Keystone, Colorado. pp 475-487.
8. Cunningham, C.V.B. (1983) The Kuz–Ram model for prediction of fragmentation from blasting. In R. Holmberg & A Rustan (eds), Proceedings of First International Symposium on Rock Fragmentation by Blasting, Lulea, pp 439-454.

XIV International Mineral Processing and Recycling Conference
Belgrade, Serbia, 12-14 May 2021

APPLICATION OF MECHANOCHEMICALLY ACTIVATED SODIUM CARBONATE IN ENVIRONMENTAL PROTECTION

Nataša Đorđević[1#], Slavica Mihajlović[1], Milica Vlahović[2], Sanja Martinović[2]
[1] Institute for Technology of Nuclear and Other Mineral Raw Materials, Belgrade, Serbia
[2] University of Belgrade, Institute of Chemistry, Technology and Metallurgy, Belgrade, Serbia

ABSTRACT – Sodium carbonate samples were mechanicaly activated in a vibro mill. The increase in the free surface area of the activated samples was monitored by the BET method, and the state of the crystal lattice by the diffraction method. The analysis of the results showed a significant increase in the free surface of the activated material as well as significant changes in the crystal structure of the samples due to grinding in a vibro mill. Such activation of sodium carbonate would enable a significant increase in the sorption properties of sodium carbonate and thus its application in environmental protection.

Keywords: Air Protection, Sodium Carbonate, Mechanochemical Activation.

INTRODUCTION

Due to the increasing pollution of the environment, there is a need for fast and efficient methods of prevention and solving the problem of ecological protection. Increasing the concentration of carbon dioxide in the atmosphere is one of the key parameters of nature pollution, which has multiple negative consequences for life on Earth. One of the most effective ways to maintain the concentration of CO_2 in the air is the natural absorption of carbon dioxide by plants. Unfortunately, deforestation in the world is in expanding, and the problem of greenhouses and rising temperatures worldwide contributes to the growing problem. The reduction of the Earth's green mantle, especially in Brazil and Argentina in order to increase livestock is one of the causes of the increase in the amount of CO_2 in the air.

Possibilities of improving CO_2 intake by polyethyleneamines were investigated, using zinc-silicate supports [1], as well as other methods [2-4]. It is known that different models have been tested in order to absorb carbon dioxide, either in industrial plants or directly exposed to air (since carbon dioxide is obtained as a by-product of many industrial plants, its release greatly affects environmental pollution). A special problem is the exhaust gases from cars, where carbon dioxide and water vapor are obtained as a product in the process of fuel combustion. All the carbon dioxide that goes into the atmosphere as a result of human activities has a great impact on environmental pollution, creating a greenhouse effect and raising the average temperature, which directly affects the climate. At least its partial elimination from industrial plants would already significantly

---

[#] corresponding author: n.djordjevic@itnms.ac.rs reduce its concentration and slow down the process of environmental pollution. It is of great importance to monitor the level of carbon dioxide in the air, whether it is natural disasters that contribute to disturbances of the atmosphere, water and soil, or human impact through heavy and automotive industry and life in big cities [5-14].

EXPERIMENTAL

In order to investigate the possibility of improving the absorption capacity of sodium carbonate, Na_2CO_3 was mechanochemically activated in a high-energy mill with torsion springs and ring working elements "KHD HUMBOLDT WEDAGAG". The mill consists of a housing in which there is a mechanism with a horizontally placed working vessel. The working vessel of the mill has a cylindrical shape of small height and is located on a specially constructed bearing with a cap. Under the working vessel of the mill, which has a vibrating oscillatory movement, there is a drive mechanism with an elastic shaft. The eccentric flywheel and torsion springs convert the circular motion of the elastic shaft into the vibrating oscillatory motion of the working vessel of the mill. The working vessel has two massive annular working elements of different diameters, with a total weight of 3 kg, which occupy one third of the working volume of the mill. The lid of the working vessel of the mill has a felt seal around the perimeter. The base of the working vessel of the mill is placed horizontally on the body of the mill.

The volume of the working vessel of the mill is 2 dm^3, and the mass of material that can be activated under optimal conditions is 200 g. Engine power is 0.8 kW. The device works discontinuously in an air atmosphere. Intense vibrating movement of the working vessel of the mill with massive rings, leads to heating of the vessel to a temperature of 80 °C.

A sample of Na_2CO_3, weighing 50 g, was activated by mechanochemical procedure for 1, 3, 5, 7, 14 and 28 minutes. The activated samples are then disposed of in order to absorb carbon dioxide. Exposure to activated sodium carbonate depends on the current needs of the environment in terms of carbon dioxide absorption (industrial plant, laboratory conditions, closed or open system, atmospheric conditions, already existing equipment using CO_2 absorbent). The standing time of the samples was from 1 to 85 days. The temperature at which the samples were deposited was room temperature. As a function of the activation time in the mechanochemical reactor, the residence time of the sample after activation and the atmosphere in which the sample is located (carbon dioxide content in the atmosphere), it is necessary to monitor changes in CO_2 in the atmosphere and activated sodium carbonate using different methods. was followed by the BET method. Crystallographic tests of activated Na_2CO_3 were performed. X-ray diffraction of polycrystalline samples was performed on a PHILIPS PW-1700, an automated diffractometer with a copper tube, which operates at 40 kV and 35 mA. The device is equipped with a graphite monochromator and a proportional counter filled with xenon. Shooting angle (2Θ) of 4-15 °.

The bond energy values represented in sodium carbonate are as follows [9]:

a) Na - O (364 kJ/mol)
b) C - O (1076.4 kJ/mol)
c) C = O (532.2 kJ/mol)

The decomposition temperature of sodium carbonate is 851 °C. Sodium carbonate has a monoclinic crystal lattice (a = 8.907; b = 5.239; c = 6.043), specific gravity 2500 kg/m3. The chemical composition of sodium carbonate according to the catalog MERCK index 11.8541, and the content of Na_2CO_3 was 99.5%. A chemical analysis was performed on a representative sample, which is in full agreement with MERCK's characterization.

RESULTS AND DISCUSSION

The increase in the specific surface area of Na_2CO_3 determined by the BET method as a function of the time of mechanochemical activation is shown in Figure 1. The highest degree of fragmentation and increase of free surface area was achieved in the first 40 minutes of activation, from 6.8 m^2/g of inactivated sample to 8.25 m^2/g. In the period from 40 to 100 minutes of activation, the free surface area continues to increase slightly, so that the free surface area of ground sodium carbonate for 28 minutes is 8.6 m^2/g. An increase in the free surface area of activated sodium carbonate indicates the possibility of a significant increase in the adsorption capacity of CO_2 from the air.

Mechanochemically activated Na_2CO_3 samples were submitted for X-ray diffraction analysis. The samples were isolated from the outside atmosphere, so that no additional influence on the already activated samples could occur. The aim of this analysis was to establish how the structure of sodium carbonate behaved as a function of the grinding time in the vibro mill. Table 1 shows the intensities of diffraction peaks of activated Na_2CO_3 depending on the activation time. Figure 2 shows the diffractograms of Na_2CO_3 activated for 1-21 min in a vibro mill.

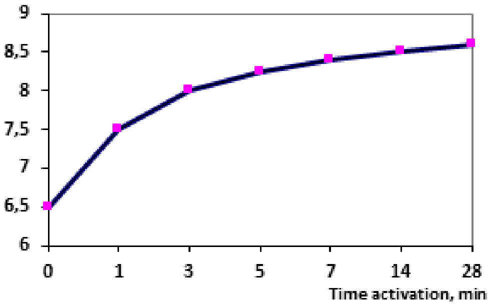

Figure 1 Change of specific surface of Na_2CO_3 as a function of time of mechanochemical activation by BET method

Table 1 Values of the intensity of diffraction maxima at a certain diffraction angle as a function of the activation time of Na_2CO_3 samples

	Peak intensities I (cts) depending on the activation time, min					
Diffraction angle, 2Θ	1 min	3 min	5 min	7 min	14 min	28 min
30	350	193	199	276	177	193
34.165	146	128	125	142	106	108
35.225	222	166	164	228	144	154
37.965	310	196	174	228	146	156
40	154	194	83	106	72	86
Middle value 35.471	236	155	149	196	158	139

As a function of the time of activation of sodium carbonate, the crystal lattice is disturbed at all diffraction angles and the free surface of the activated material is increased. During the first five minutes of activation, there is a sharp decrease in the value of the intensity of diffraction maxima. Between the fifth and seventh minutes of grinding, the values of the maximum intensity increase, also at all diffraction angles. The increase in the intensity of diffraction maxima can be explained by the fact that after five minutes of grinding, after the collapse of the crystal structure, the mechanical energy supplied to the system allows a certain recrystallization of the existing system, the partial arrangement of the destroyed structure. After the fifth minute, the intensities decrease again until the fourteenth minute of grinding, after which the change in the intensity of the maximum has a steady flow with a slight tendency to increase in function from the time of grinding. This stationary flow of the curve can be explained by the assumption that after the collapse of the newly formed structure, after 14 minutes of grinding, no changes in the structure of the activated sample occur. It can also be concluded that by further extending the grinding time after 28 minutes, no further change in the structure of the activated material would be achieved.

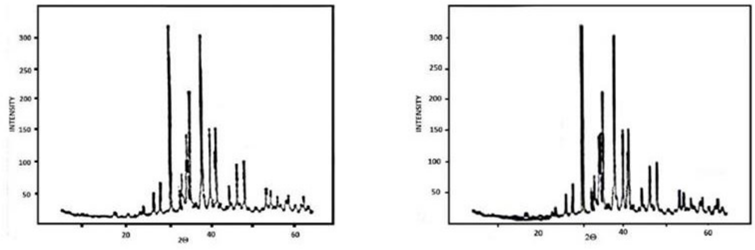

1 minute

3 minutes

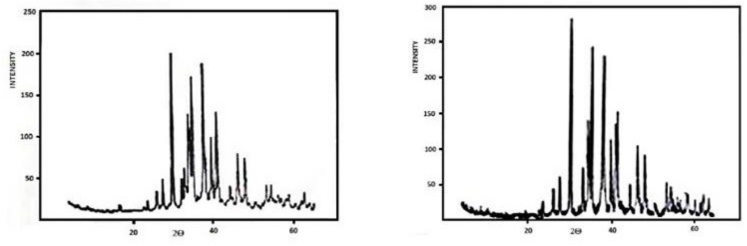

5 minutes

7 minutes

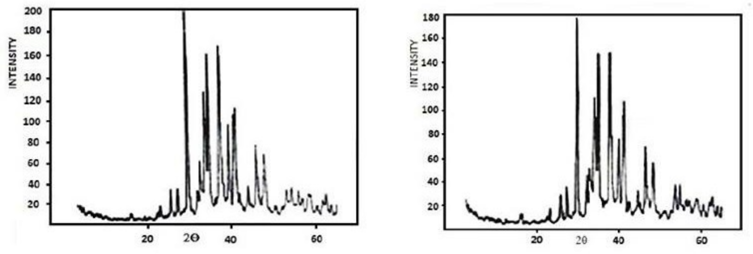

14 minutes

21 minutes

Figure 2 Diffractograms of Na_2CO_3 activated 1-21 min in a vibro mill

The results of the BET method after activation indicate the fact that due to grinding there was a significant increase in the free surface area of the activated sodium carbonate powder. As sodium carbonate is a known sorbent of carbon dioxide from the air, increasing the free surface area of the activated powder significantly increases the possibility of CO_2 sorption.

Comparing the results of the diffractograms of the activated samples in relation to the inactivated sample, it can be noticed that the grinding of sodium carbonate led to a disturbance of the crystal structure. In order to monitor the change in the intensity of diffraction maxima as a function of the activation time, five characteristic peaks at certain values of diffraction angles were selected from the data given with the diffractograms. Based on the analysis, it can be concluded that during 28 minutes of activation there is a sudden and significant decrease in the value of the intensity of diffraction maxima, ie the collapse of the crystal structure, at all angles of diffraction. This is due to the fact that the invested mechanical energy is spent on the comminution of existing grains of sodium carbonate, and then leads to the collapse of the internal structure of Na_2CO_3 crystals.

Based on the results, it can be seen that during the first five minutes of activation, there is a sharp decrease in the value of the intensity of diffraction maxima, the collapse of the crystal structure, at all angles of diffraction. This is a consequence of the fact that the invested mechanical energy is spent on crushing the existing grains of sodium carbonate, and then it leads to the destruction of the internal structure of the Na_2CO_3 crystal. Between the fifth and seventh minutes of grinding, the values of the maximum intensity increase at all diffraction angles. The increase in the intensity of diffraction maxima can be explained by the fact that after five minutes of grinding, after the collapse of the crystal structure, the mechanical energy supplied to the system allows a certain recrystallization of the existing system, partial arrangement of the destroyed structure.

As sodium carbonate is an effective carbon dioxide absorption agent, based on the attached research results, it can be concluded that mechanochemical activation can significantly contribute to an additional increase in the absorption capacity of sodium carbonate. In the next course of experiments, it is important to determine the increase in the degree of CO_2 absorption on sodium carbonate as a function of activation time, by monitoring the change in sample mass during relaxation in atmospheres with increased CO_2 concentration and humidity, and spectrophotometric analysis of activated samples after relaxation time.

CONCLUSION

Based on the results of the BET method of samples of sodium carbonate activated from 1 to 28 minutes, it can be concluded that grinding the samples leads to a significant increase in the free surface area of activated material, which increases the possibility of adsorption and absorption (sorption by surface area and volume) of CO_2. From the results obtained by diffractometric analysis, a significant destruction of the crystal lattice of the ground sample is observed, which enables not only the sorption of CO_2, but also the hemisorption of gas on the activated sample. The results of further tests will be presented in the next paper. Increasing the sorption capacity of CO_2 on sodium carbonate opens up great possibilities for its application in environmental protection, especially in industrial conditions.

ACKNOWLEDGEMENT

The authors are grateful to the Ministry of Education, Science and Technological Development of the Republic of Serbia for their support in the research whose results are presented in the paper (contract 451-03-68 / 2020-14 / 200023).

REFERENCES

1. Kuwahara, Y., Kang, D.Y., Copeland, J.R., Brunelli, N.A., Didas, S.A., Bollini, P., Sievers, C., Kamegawa, T., Yamashita, H., Jones, C.W. (2012) Diamine-functionalized metal–organic framework: exceptionally high CO_2 capacities from ambient air and flue gas, ultrafast CO_2 uptake rate, and adsorption mechanism. J. Am. Chem. Soc., 134, 10757–10760.
2. Borhani, T.N.G., Azarpour, A., Akbari, V., Alwi, S.R.W., Manan, Z.A. (2015) Effective Capture of Carbon Dioxide Using HydratedSodium Carbonate Powders. Int. J. Greenh. Gas Control., 41, 142–162.
3. Choi, S., Drese, J.H., Jones, C.W. (2009) Adsorbent Materials for Carbon Dioxide Capture from Large Anthropogenic Point Sources. Chem. Sus. Chem., 2, 796–854.
4. Xu, Y., Zhou, Y., Liu, J., Sun, L. (2017) Effective Capture of Carbon Dioxide Using HydratedSodium Carbonate Powders. J. Energy Chem., 26, 1026–1029.
5. Gilman, P., Benjamin, J. (1983) Mechanical alloying of brittle materials, Ann. Rev. Matterials. Sci. Paolo Alto, 13, 279.
6. Obradović, N., Fahrenholtz, W.G., Filipović, S., Corlett, C., Đorđević, P., Rogan, J., Vulić, P.J., Buljak, V., Pavlović, V. (2019) Characterization of MgAl2O4 Sintered Ceramics. Sci. Sinter., 51, 363-376.
7. Labus, N., Obradović, N., Srećković, T., Mitić, V., Ristić, M.M. (2005) Influence of mechanical activation on zinc metatitanate synthesis. Sci. Sint. 37, 115-122.
8. Filipovic, S., Obradovic, N., Petrovic, V. (2009) Influence of mechanical activation on structural and electrical properties of sintered MgTiO3 ceramics. Science of Sintering, vol. 41, no. 2, 117-123.
9. Đorđević, N. G., Obradović, N. N., Filipović, S. Ž. (2011) Kinetika mehanohemijske sinteze barijum-titanata. Tehnika-Novi materijali 20:3 367-371.
10. Đorđević, N., Obradović, N., Filipović, S., Živojinović, J., MItrić, M., Marković, S. (2012) Influence of Mechanical Activation on the Constituents of the MgO-Al2O3-SiO2-TiO2 System. Tehnika–Novi materijali 21 3, 329-333.
11. Liang, Y. (2003) Carbon dioxide capture from flue gas using regenerable sodium-based sorbents, Carbon dioxide capture from flue gas usingregenerable sodium-based sorbents. Master`s Thesis, Louisiana State University.
12. Dusek, M., Chapuis, G., Meyer, M., Petricek, V. (2003) Thermodynamic Aspect of Sodium Carbonate Mechanical Transformations under Different Environment. Acta Crystallog B 59 (3), 337–352.
13. Li, J., Hitch, M. (2017) Ultra-fine grinding and mechanical activation of mine waste rock using a planetary mill for mineral carbonation. International Journal of Mineral Processing 158:18-26.
14. Boldyrev, V. V. (1986) Mechanochemistry of inorganic solids. Proceedings of Indian National Science Academy, 52, A, 1 400-417.

XIV International Mineral Processing
and Recycling Conference
Belgrade, Serbia, 12-14 May 2021

DESTRUCTION OF CRYSTALLINE MINERAL COATINGS ON THE SURFACE OF DIAMONDS WITH THE USE OF THERMAL AND ELECTROCHEMICAL TREATMENT

Galina Dvoichenkova[1,2], Evgeny Kovalenko[2,3#], Valery Morozov[4], Yuri Podkamenny[2]

[1] Institute of Comprehensive Exploitation of Mineral Resources of Russian Academy of Sciences, Moscow, Russian Federation
[2] Mirny Polytechnic Institute (branch) of North-Eastern Federal University, Mirny, Russian Federation
[3] Institute YAKUTNIPROALMAZ PJSC “ALROSA”, Mirny, Russian Federation
[4] National University of Science and Technology “MISiS”, Moscow, Russian Federation

ABSTRACT – Coming on foam separation of kimberlites diamond crystals includes hydroxides and carbonates coats. A method of restore the hydrophobicity of diamonds using thermal and electrochemical destruction of crystalline mineral coatings has been proposed. The use of combine method of the conditioning in the foam separation it possible to decrease concentration of minerals coats on diamonds surface in 3-10 time. Technological research showed that using products of non-diaphragm electrolysis of circulating water, in time of thermals processing of input of foam separation enables increasing the recovery of diamonds into the concentrate of foam separation from 76.5% to 83.7%.

Keywords: Diamonds, Foam Separation, Heat Treatment, Circulating Water, Conditioning.

INTRODUCTION

The intensive hypergene processes in kimberlite lead to the formation of hydrophilic cover on crystal surfaces, which reduces hydrophobicity of diamonds and increase their losses in the processes of sticky and foam separation [1]. The most common types of these surface formations are crystalline minerals and thin films. These formations are hydrophilic and worsen the interaction of diamonds with collectors and air bubbles. This fact makes topical the issues of restoring the hydrophobic properties of diamonds for increasing their recovery in separation processes [2,3]. A task of the research is to study and choosing of combine technologies of renovation of diamond crystals surface, for example using thermal and electrochemical methods [4]. The use of thermal methods allows controlling the mineral properties and increasing their floatability. The mechanism of influence of the electrochemical conditioning consists in optimizing the ion composition of circulating water and effecting on the mineral surface and reagents [5].

[#] corresponding author: KovalenkoEG@alrosa.ru

METHODS OF ANALYSIS OF THE PHASE COMPOSITION OF THE SURFACE OF DIAMOND CRYSTALS AND TECHNOLOGICAL EXPERIENCE

Impurities on diamond surfaces are studied by using methods of optical microscopy, Auger and X-ray spectroscopy, infrared spectroscopy, UV-VIS spectroscopy and micro-X-ray spectroscopy. The chemical composition of mineral admixtures is determined by using a JXA-8800R microanalyzer.

The flotation activity of diamonds was determined in laboratory conditions by the methods of froth separation. Bench tests of the process of foam separation of the were carried out in the laboratory of the Institute "Yakutniproalmaz" on a pilot plant, which included sample preparation units, conditioning of circulating water, agitation of ore with reagents and subsequent foam separation. At the first stage of the research, the composition of impurities on the surface of diamonds and the regularities of the processes of their formation were studied under the conditions of processing of refractory kimberlites.

The assaying findings and preferential location of the surface mineral formations on the defects of the diamond crystals enabled, for analysis of the processes of their hypergene and technogenic hydrophilization, using the hypothesis of the formation and attachment of hypergene secondary minerals and salt-like substances on the diamond surface, with a broken crystal structure to be the most prone to the epitaxial growth.

THE DESTRUCTION COVERS ON THE SURFACE OF DIAMONDS WITH THE USE OF THERMAL TREATMENT

To substantiate the feasibility of and select optimum conditions for thermochemical decomposition of carbonate compounds when heating the pulp, tests on crystallization of salts from supersaturated model solutions simulating in composition circulating waters of Processing Plant No. 3 were carried out. Soda was added to the initial solution with preset ion-molecular composition to provide precipitation of carbonate compounds from the supersaturated solution. The formed precipitates were dried and assayed by spectrophotometric technique using the IR-75 instrument.

Review of the IR spectra of the precipitates showed that in the common foam separation temperature area (14 ˚C), the precipitates include carbonate and carbonate hydroxide compounds of calcium and magnesium. At 80 ˚C, the amount of purely carbonate substances decreases, while the amount of hydroxide compounds remains stable or even possibly increases. Comparison of the test results with the calculated data allows concluding that the thermal conditioning leads to partial dissolution and decomposition of calcium and magnesium carbonate minerals and transformation of magnesium carbonate into magnesium carbonate hydroxide. In both cases, decomposition of the minerals occurs, and their mechanical or thermomechanical removal is facilitated. The calculations show that maintaining the calcium carbonate dissolution conditions or preventing its crystallization on the surface of diamonds in the course of the pulp heat treatment requires maintaining weakly acid solution conditions (pH = 6-6.5). To experimentally check the solution pH effect on the efficiency of thermal removal of the minerals from the surface of diamonds, laboratory tests were carried out on diamonds from the “Internatsionalnaya” kimberlite pipe. The diamonds were treated at the solution working temperature of 60-90 °C. After the treatment, the diamond surface was studied using JEOL JIB-Z4500 scanning electron microscope.

The study of the diamond crystal surface electron microscopic images showed that the 120 sec. heat treatment provides removing more than 90% of the mineral impurities from the diamond surface, and the surface concentration of calcium, magnesium, silicon, and iron decreases several times (Table 1).

Table 1 Change in the surface composition of diamonds heat treatment (at 80 °C)

Chemical element	Mass fractions of elements, %			
	Before treatment	*After* 30 s *treatment*	*After* 60 s *treatment*	*After* 120 s *treatment*
C	88.08	90.9	92.70	94.50
O_2	7.10	5.95	4.33	2.33
Ca	0.42	0.36	0.19	0.09
Fe	0.30	0.22	0.11	0.07
Si	0.58	0.33	0.23	0.18
Mg	0.24	0.21	0.13	0.07
Al	0.20	0.17	0.09	0.05

THE DESTRUCTION FILMS ON THE SURFACE OF DIAMONDS WITH THE USE OF ELECTROCHEMICALLY TREATED WATER PRODUCTS

In the previous studies, we have shown the possibility of using water electrolysis products for desorption of surface films on diamond crystals [4,5]. Taking into account the findings of the present studies, testing of the products of the non-diaphragm electrolysis of circulating water for removing the hydrophilic mineral formations from the diamond surface was performed. The recycled water of the foam separation cycle accumulates various substances, including calcium and magnesium carbonate salts, which crystallize on the surface of diamonds and cause their technogenic hydrophilization. The reason for the change in the hydrophobicity of diamonds is the cleaning of their surface in an aqueous medium that has passed the stage of electrochemical conditioning (table 2). It was experimentally determined that the crystal surface, washed by the water electrolysis products, is characterised by low content of the impurity elements (< 5 %) and oxygen content of less than 15% (Table 2).

Table 2 Change in the surface composition of diamonds after interaction with the products of electrolysis of mineralized water in a non-diaphragm electrolyser

Chemical element	Mass fractions of elements, %			
	Before treatment	*After treatment at power consumption, kWh/m³*		
		0.5	*1*	*1.5*
C	78.0	87.5	91.2	94.0
O_2	9.4	6.8	4.3	3.3
Ca	1.4	1.06	0.39	0.19
Fe	1.3	1.12	0.61	0.37
Si	2.5	1.7	1.2	0.8
Mg	0.65	0.4	0.33	0.17
Al	0.4	0.27	0.19	0.1

EXPERIMENTS ON FLOTATION OF DIAMOND CRYSTALS BY USING OF THERMAL AND ELECTROCHEMICAL NON-DIAPHRAGM PROCESSING

To evaluate the efficiency and select the best mode of thermal and electrochemical conditioning of recycling water in order to give them the ability to activate the surface of diamonds in conditions close to industrial, a series of experiments on flotation of the studied diamond crystals in mineralized water and products of its non-diaphragm processing was conducted. Bench tests of the process of foam separation of the studied mineral objects were carried out in the laboratory of the Institute "Yakutniproalmaz" on a pilot plant, which included sample preparation units, conditioning of circulating water, agitation of ore with reagents and subsequent foam separation.

In the laboratory tests, an artificial diamond-kimberlite mixture was used. Preparation of the rough diamonds (size of +1-1.5 mm) included preliminary purification of their surface for each individual test. The diamonds recovered from the foam separation concentrate were washed in carbon tetrachloride, alcohol, distilled water and treated with concentrated solution of hydrochloric acid, which removed mineral films. For the diamond surface hydrophilization, the diamonds were aged in circulating water at pH 8.5 exposed to air for 4 hours. After the preparation, the diamonds were mixed with a kimberlite sample of grain size of +0.5-1 mm and floated in a foam separation facility.

The laboratory tests confirmed the theoretical physicochemical study outcomes and showed that maximizing the benefit from the heat treatment of the diamond foam separation feed is achieved when heated to 80-85 ^{o}C. Application of the solution pH electrochemical regulation technique enabled achieving additional increasing the diamond recovery by 7.2-7.6% (Figure 1).

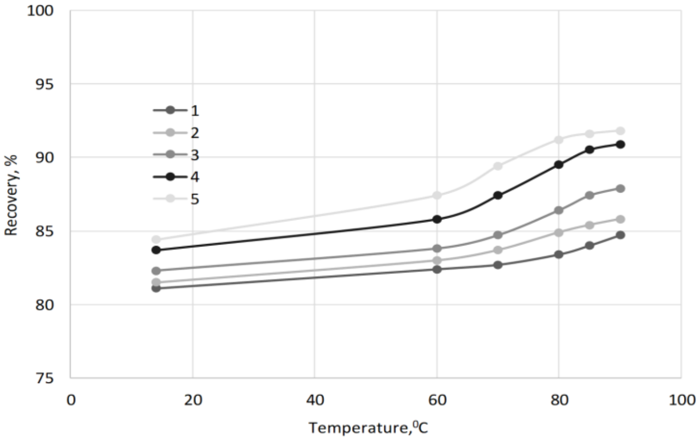

Figure 1 Diamond recovery into foam separation concentrate when using heat treatment of initial feed: 1 — with no electrochemical treatment of circulating water; 2-4 — with using of nondiaphragm conditioning of circulating water: 2 – Q = 0.2 kWh/t, pH = 8; 3 – Q = 0.5 kWh/t, pH = 7.6; 4 – Q = 1.0 kWh/t, pH = 6.7; 5 — Q = 0.2 kWh/t, pH = 6.2

The research outcomes showed the feasibility of applying electrochemical treatment of the pulp aqueous phase for increasing the efficiency of diamond surface purification in the foam separation cycle and determined the optimum treatment conditions (Q = 1.0-2.0, pH = 6.2-6.7), at which maximum increasing the floatability of diamonds was achievable.

Industrial tests of the developed technology were carried out at the processing plant No. 3 of the "Mirninsky" mining and processing combine. During the tests, the capacity of the foam separation unit was 18.3 tons/hour. The scheme included a main, cleaning and control operations. During the testing period, the following reagent costs were maintained: fleet fuel oil F-5 - 980 g/t; Aeroflot butyl - 2.2 g/t; foaming agent OPSB - 80 g/t.

Technological scheme involved the heat treatment of foam separator PFM-10 superheated steam to a temperature of 80-85 ^{0}C and electrochemical processing of water held in the cell EKWB-50 at a current density of 200 A/m^2 and a power consumption of 1.4 - 1.6 kWh/m^3). The tests of the developed mode of preparation for foam separation confirmed the possibility of increasing the extraction of diamonds from the +0.5–2 mm class from 76.5% to 83.7% (Table 3).

Table 3 Indicators of semi-industrial tests of foam separation when using a combined technology for preparing the input stream and circulating water

№	Mode of the process of foam separation	The temperature of the input stream of foam separation,^{0}C	Current density in the electrolyzer, A/m^2	Recovery of diamonds (class +0.5–2 mm), %
0	Control testing (without processing the input stream)	11-14	-	76.5
1	With heat treatment the input stream	80-85	-	77.5
2	With heat treatment the input stream and electrochemical conditioning of circulating water	80-86	200	83.7

CONCLUSIONS

The results of the technological research showed that the heat treatment of input feeding of foam separation by superheated steam at temperature of 80-85 ^{0}C and electrochemical processing of circulating water at a current density of 200 A/m^2 and a power consumption of 1.4-1.6 kWh/m^3 made the possibility of increasing the recovery of diamonds from the +0.5–2 mm class from 76.5% to 83.7%.

REFERENCES

1. Chanturiya, V.A., Dvoichenkova, G.P., Bunin, I.Zh., Minenko, V.G. (2017) Combination processes of diamond recovery from metasomatically altered kimberlite rocks. J. of Mining Science, 2, 317-322.
2. Westhyzen, P., Bouwer, W.; Jakins, A. (2014) Current trends in the development of new or optimization of existing diamond processing plants, with the focus on beneficiation. J of the Southern African Institute of Mining and Metallurgy, 114, 7, 539–545.

3. Zhang, J. Kouznetsov, D.L., Yu, M., Rylatt, M., Yoon, R.H. (2012) Improving the separation of diamond from gangue minerals. Minerals Engineering, 36–38, 168–171.
4. Chanturia, V.A., Dvoichenkova, G.P., Kovalchuk, O.E., Timofeev, A.S. (2015) Surface composition and role of hydrophilic diamonds in foam separation. J of Mining Science, 6, 1235–1241.
5. Dvoichenkova, G.P. (2014) Mineral formations on the surface of natural diamonds and the method of their destruction on the basis of electrochemically modified mineralized waters. J of Mining Science, 4, 159-165.

XIV International Mineral Processing and Recycling Conference
Belgrade, Serbia, 12-14 May 2021

THE ALTERATIONS OF THE CALCIFEROUS MINERALS SURFACE AND DIRECTED AJUSTMENT OF THE FLOATABILITY THROUGH THE APPLICATION OF HIGH - POWER ELECTROMAGNETIC PULSES

Valentine Chanturiya, Igor Bunin, Maria Ryazantseva[#]
Mel'nikov' Institute of Comprehensive Exploitation of Mineral Resources
Russian Academy of Sciences ICEMR RAS, Moscow, Russia

ABSTRACT – The treatment of calciferous minerals by high-power electromagnetic pulses (HPEMP - treatment) leads to the transformation of the surface structural heterogeneity. It involve the formation, annihilation and transformation of intrinsic and impurity structural defects, cause a change in the energy state and acid-base properties. It leads to a change in the sorption activity of the surface and flotation properties of minerals.

Single mineral flotation tests with use of sodium oleate and silicate has allowed to determine that HPEMP - treatment results to the cocurrent improvement of the calciferous minerals floatability. The rising of the scheelite recovery was 10 - 12%, for fluorite it was 5 - 6%, for calcite – 7 - 8%.

The combined application of HPEMP with special reagent regime allows find the condition for the selective separation of the minerals with very close flotation properties: the recovery of scheelite rise from 41.2% (untreated sample) to 58.5 (sample treated at 10^3 pulses). On opposite the floatability of calcite and fluorite decrees significant: the recovery of calcite drop from 74.7% (untreated sample) to 41.1% (sample treated at 10^3 pulses); the recovery of fluorite was dropped from 73.6% (untreated sample) to 41.1 (treated at 10^3 pulses).

Keywords: Calcite, Fluorite, Scheelite, Floatability, High - Power Electromagnetic Pulses, Selective Separation.

INTRODUCTION

Flotation is the main concentration process for the great majority of ores. Flotation process improving and optimizing is the key opportunity for recovery improving and the promoting of the mineral resources comprehensive processing. It makes possible to produce tens and hundreds of thousands of metals tons without incurring major capital costs and keeping operating costs low.

The problems of calciferous minerals selective flotation are actual for the majority of mineral processing plants that process scheelite, apatite, fluorite, and other ores. The key principle of calciferous minerals flotation separation process is using carboxylic acid-based collectors in an alkaline environment, which form insoluble compounds with Ca^{2+} cation by attaching themselves to the mineral surfaces and provide a long-lasting collector action.

However, in the presence of two or three calciferous minerals in the ore, in order to avoid collective flotation, sophisticated processing technology becomes necessary. To

---

[#] corresponding author: ryzanceva@mail.ru achieve effective separation of calcium minerals, the Petrov' method is used, where the mineral pulp undergoes a high-temperature treatment at 85 - 90° C and depressants, mainly liquid glass, are added at high feed rates. This process is complex and energy intensive. The research aimed at enhancing of calcium minerals flotation properties continues despite the existence of a reliable, proven method for the selective recovery of scheelite from bulk concentrates containing other calcium minerals. It is be highlighted the directions aimed to the improvement of existing reagent scheme and the development of new selective reagents [1-5].

This paper presents the findings of the high-power electromagnetic pulses (HPEMP) parameters effects on the structural and chemical state of the surfaces of calcite, fluorite, and scheelite and their sorption and flotation properties. The HPEMP – treatment is suggested for the consideration as an effective tool for the regulation of the calciferous minerals floatability regulation.

MATERIALS AND METHODS

In this study, natural calciferous minerals were used – calcite ($CaCO_3$ > 98%), scheelite ($CaWO_4$ > 98%),) and fluorite (CaF_2 > 98%), size fraction -80 + 50 µm. Distilled water (MeS / H_2O = 10 / 1) was added to the samples before they were treated with high – power electromagnetic pulses (HPEMP - treatment).

HPEMP - treatment HPEMP - treatment of the samples was performed on a lab scale unit in air by a series of nanosecond pulses with pulse duration from 5 to 10 ns. The pulse amplitude was 30 kV, a pulse repetition rate frequency of 100 Hz. The pulse energy was approximately 0.1 J and the integral treatment pulse number varied from $5 \cdot 10^2$ to $1.5 \cdot 10^4$ pulses. Pulse parameters were kept constant and the number of pulses was controlled by varying the treatment duration between 5 s and 150 s.

To identify and study the acid - base properties of the mineral surfaces, the Hammett indicator adsorption method from aqueous media was adopted [6, 7].

X–ray photoelectron spectra were obtained with an Axis UltraDLD (Kratos) spectrometer irradiating the samples at an operating pressure of 10^{-8} Torr with monochromatized AlKα radiation (1486.6 eV) at 150 W. The pass energy was equal to 160 eV for survey spectrum recording and 20 eV for multiregion spectrum recording. Spectrometer energy scale was preliminary calibrated using Au 4 f $_{5/2}$, Cu 2 p $_{3/2}$, Ag 3d $_{5/2}$ photoelectron lines at 83.96, 932.62, and 368.21 eV, respectively, using metal film pre-treated with an ion gun.

Survey and multiregion spectra were recorded of W 4 f photoelectron peaks. The survey spectra were recorded with an increment of 1.0 eV, and the spectra of the individual lines were recorded with an increment of 0.05 eV. The calibration of the spectrometer energy scale corresponded to the following peaks of standards (purified by ion sputtering of metal surfaces): Au 4 f 5 / 2 - 83.96 eV, Cu 2p3 / 2 - 932.62 eV, Ag 3d5 / 2 - 368.21 eV with an accuracy is 0.05 eV. To eliminate the samples charging effect, spectra were recorded using a neutralizer. The obtained spectra were calibrated by the binding energy of the low-energy component in the C 1 s line of adsorbed hydrocarbons (BE = 284.8 eV). Casa XPS software suite was used for data collection and analysis. Atomic concentrations were calculated from photoelectron peak areas using Shirley background subtraction, and sensitivity factors were provided by the spectrometer manufacturer.

***Infrared spectra** were* obtained with a Fourier transform infrared spectrometer IR Affinity (Shimadzu) equipped by the diffuse reflectance attachment from spectrometer supplier (DiffuzIR, Pike). Samples preparation involved the dilution of the mineral in KBr (1:10). The spectra were recorded in the range 400 - 4000 cm^{-1} with the resolution of 1 cm^{-1} using a mixture of mineral and KBr (1 : 10) as background.

X - ray luminescence studies were carried out on unit consisting of an X-ray generator based on "Iris - 3m" (NPP "Burevestnik", Russia) and an X - ray tube 5 BHV7 (NPP "Svetlana – X - ray", Russia), anode voltage of 35 kV, anode current of 30 mA. The MDR 23 monochromator (NPP "LOMO", Russia) with computer control and a registration system based on the "photon counting" was used.

The adsorption of oleate was determined using UV spectroscopy according to the residual concentration of oleate ion in the pulp filtrate after contact of the mineral sample with the reagent solution (SU 1322130). Sorption of sodium silicate was determined by the residual concentration of silicon (C_{Si}) in the pulp filtrate by the method (PND 14.1: 2.215 - 06), based on the interaction of silicic acid with ammonium molybdate in an acidic medium.

Flotation test conditions for bulk flotation recovery improvement: monomineral sample fraction ($CaCO_3$, CaF_2, $CaWO_4$) sized -80 +50 µm, 1.00 g; pH = 10.5; contact time of the mineral with water (S:L = 1:6) 1 min, with sodium silicate (100 g/t) 3 min, sodium oleate (300 g/t) 3 min, flotation time - 1.0 min.

Flotation test conditions for the selective separation: monomineral sample fraction ($CaCO_3$, $CaWO_4$) sized -80 +50 µm, 1.00 g; pH = 10.5; contact time of the mineral with water (S:L = 1:6) 1 min, with sodium silicate and aluminum sulphate (200 g/t) 3 min, ethereramin (500 g/t) 3 min and sodium oleate (150 g/t) 3 min, flotation time - 1 min.

Reagent treatment was defined to achieve the highest possible recovery in the flotation of untreated scheelite sample.

RESULTS AND DISCUSSION

Acid - base properties of the surface: The modification of structural chemical properties of natural fluorite, scheelite and calcite under the impact of high – power electromagnetic pulses (HPEMP - treatment) were studied with help of adsorption of acid – base indicators. It was determined that the HPEMP - treatment during the of 30 seconds (3×10^3 pulses) resulted in the intensification of fluorite surface 'electron – donating ability and acceptor properties of calcite and scheelite surfaces [7].

The sorption activity of calcium minerals (bulk flotation): The sorption activity of calcium minerals towards oleate was investigated by UV - spectroscopy based on the residual concentration of oleic acid in the pulp after the contact of the mineral with the reagent solution. The obtained results are presented in Figure 1 a, as it can be seen the preliminary HPEMP - treatment activated the collector sorption o at the surface of calciferous minerals.

For scheelite samples HEMP – treatment results to the increasing of the adsorbed oleate quantity (µg / g) by a factor of 1.2-1.3 times: from 139 µg / g (the mineral in the initial state) to 173 - 185 µg / g (the sample after the HPEMP – treatment, $N_{pules} = 3 \times 10^3$-$10^4$). For fluorite and calcite, the increasing of the adsorbed reagent quantity is 10 - 17%: the reagent adsorption for fluorite increased from 209 µg / g (initial state) to 238 - 244 µg / g ($N_{\text{pules}} = 3 \times 10^3$-$10^4$). For calcite samples, the rising of the sorption quantity was about 15%: from 229 µg / g (initial sample) to 260 - 269 µg / g for the mineral after HPEMP - treatment ($N_{\text{pules}} = 3 \times 10^3$-$10^4$).

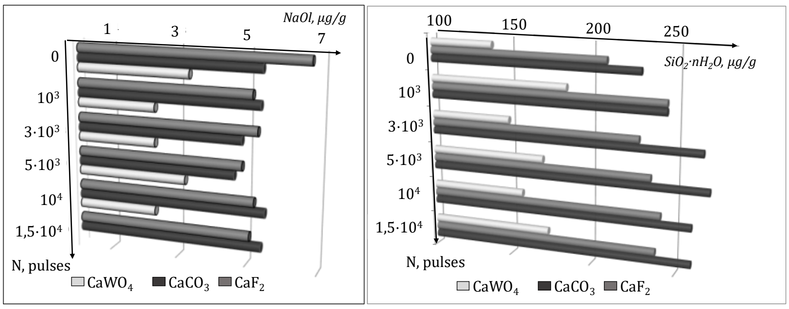

a b

Figure 1 The influence of HPEMP - treatment ($N_{\text{imp.}} = 10^3$ - $1{,}5\times10^4$) on the quantity (mg / g) of oleic acid adsorbed on the surface of calcite, fluorite and scheelite (a); the influence of the HPEMP – treatment on the sodium silicate sorption at the surface of shelite, fluorite and calcite (b)

The study of the HPEMP – treatment influence on adsorption of sodium silicate at the minerals surface demonstrates the decreasng in the quantity (mg / g) of the adsorbed reagent by 10-25% (Figure 1 b). In the case of scheelite and fluorite, the decreasing in the amount of adsorbed sodium silicate quantity was 10 - 14%: for scheelite - 3.2 mg / g (mineral in the initial state), 2.1 - 2.2 mg / g for samples after the HPEMP - treatment ($N_{\text{pulses}} = 10^3$ - 3×10^3). The influence is more effective for calcite: the decreasing in the quantity of adsorbed sodium silicate was ~ 20 - 25% as compared to the sample in the initial state (6.7 mg / g) and 4.8 - 5.1 mg / g for the sample after the HPEMP - treatment ($N_{\text{pulses}} = (3 - 5) \times 10^3$)).

The UV spectroscopy method was used to study the sorption activity of calcite and scheelite towards sodium oleate in a selective separation process (in the presence of sodium silicate, aluminum sulfate, and etheramine) before and after electromagnetic pulse treatment. It was found that HPEMP treatment does not significantly affect the adsorption of sodium oleate by the mineral surface: in calcite samples, the amount of adsorbed reagent was 225 - 228 µg/g of mineral mass, in scheelite 149 - 157 µg/g of mineral mass.

DRIFT results The IR spectroscopy method was applied to study the sorption activity of the mineral surface towards etheramine in a selective separation process (in the presence of sodium silicate, aluminum sulfate, and sodium oleate). The experiment was carried out in such a way as to simulate the conditions of flotation experiments. The results are presented in Fig. 2.

A bands (1375 cm^{-1}, 1460 cm^{-1}, 1650 cm^{-1}, 2890 cm^{-1}, 2950 cm^{-1}) is observed in the original scheelite sample spectrum, characterizing the adsorption of amine on the mineral surface. The presence of band at 2500 cm^{-1} at the spectra of the treated samples indicates that collector sorption occurs through the formation of the hydrogen bonding of the protonated collector molecule with oxygen atom of tungstate ion (Figure 2).

The predominant collector adsorption form for the initial (untreated) sample is the physical sorption.

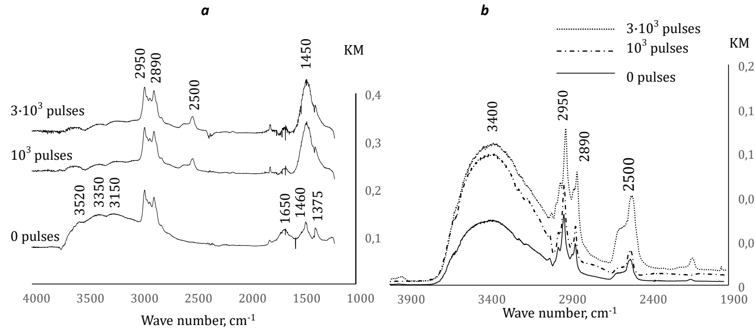

Figure2 IR spectra of scheelite (a) and calcite (b) non – treated (initial) samples and samples treated at 10^3 and $3 \cdot 10^3$ pulses

In addition, it is important to note that, as can be clearly seen in Figure 2 *a*, in the case of the original (not treated) sample, in the region of stretching vibrations H – O – H (3100 - 3600 cm^{-1}) a wide, medium-intensity band is observed. While for the samples after the HPEMP - treatment, the absorption intensity in that range is much less intensive, that indicates a less hydrated surface of the samples after HPEMP treatment.

IR spectra of calcite before and after HPEMP treatment are shown in Figure 2 *b*. In this case, the fact of amine adsorption on the mineral surface is proved by the presence in the spectra of bands characterizing the stretching vibrations of the C – H bond of the collector molecule hydrocarbon skeleton (2890 + 2950 cm^{-1}). As was mentioned above, the presence of the band at 2500 cm^{-1}indicates that the collector molecule forms ion – associates with the mineral surface. There is an increase in the integrated band intensity in the region of O – H band stretching vibrations (3100 – 3600 cm^{-1}) for the treated samples. It indicates the hydration of the mineral surface because of the electromagnetic pulse treatment.

Thus, in terms of IR spectroscopy, two opposite trends are observed: the hydration of calcite and dehydration of scheelite surface. In addition, the HPEMP - treatment, obviously, contributes to an increase in the sorption activity of the scheelite surface towardhps etheramine (an increase in the integrated intensity of the 1460 cm^{-1} band). Additionally, the HPEMP – treatment causes a change in the sorption form of the reagent: for the untreated sample the reagent was adsorbed through the physical sorption, for the treated one it was adsorbed as an ion – associates.

XPS Based on the XPS data, HPEMP treatment of fluorite for 10 seconds (10^3 imp) causes hydroxylation (BE = 531.7 eV) of the mineral surface due to the adsorption of the radical decomposition products of physically sorbed water (BE = 533.13 eV) on the active sites of the surface. The concentration of oxygen atoms associated with surface water decreases from 17.3 at% to 10.3 at%, and the concentration of oxygen associated with hydroxyl groups increases from 12.07 at% to 14.12 at%.

Deconvolution into individual components of the fluorine 1s level showed that electromagnetic pulse treatment with 10^3 imp leads to an increase in the surface concentration of interstitial fluorine (F_i^-) from 5.36% to 8.12%. At $3\cdot10^3$ imp, the atomic concentration (F_i^-) was 6.37 at%, at $5\cdot10^3$ imp 1.47 at%, at 10^4 imp 3.97 at%.

Using XPS, the effect of electromagnetic pulse treatment was studied on the surface of scheelite samples after contact with etheramine in the presence of sodium silicate and aluminum sulfate (Fig. 3 a, b).

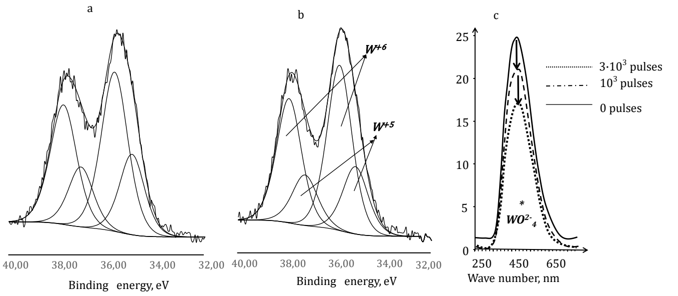

Figure 3 Scheeite W (4 f) spectra of non – treated (initial) sample (a), sample treated at 10^3 pulses (b) and X – ray luminescrnce spectra of sheelite samples

XPS spectrum of tungsten photoelectrons emitted from the 4 f $_{7/2}$ level is satisfactorily described using two components with a BE of 35.0 eV and 35.7 eV. The former belongs to W^{+5} state, the latter to W^{+6} state [8]. It can be seen that electromagnetic pulse treatment of scheelite for 10 seconds (10^3 pulses) leads to a decrease in the component associated with the W^{+5} state and a proportional increase in the component describing the W^{+6} state. It can be good confirmation of the amine adsorption in the form of ion – associates.

XPS data is consistent with the ***X-ray fluorescence studies*** of scheelite (Fig. 3 *c*). For instance, in the X-ray luminescence spectrum of ***scheelite,*** a broad band was identified with a maximum at 480 nm associated with the emission of at least four types of centers ($\{[W^{5+}O_4]_2V_A^{\cdot\cdot}\}^x$; $\{[W^{5+}O_4]'V_A^{\cdot\cdot}\}'$;$[W^{5+}O_4]'$; $[W^{5+}O_4]'''V_A^{\cdot\cdot}$). Under HPEMP - treatment, the band intensity is collapse. The integrated band intensity is reduced by a factor of 1.3 to 1.4, which indicates the destruction of the luminescence centers of this type. The reason for the destruction of these centers in the presence of amine might be the attachment of the amine on the scheelite surface as a result of the interaction of the active form of etheramine ($(R_1 - O - R_2 - NH_3)^+OH^-$ with the centers ($\{[W^{5+}O_4]_2V_A^{\cdot\cdot}\}^x$; $\{[W^{5+}O_4]'V_A^{\cdot\cdot}\}'$; $[W^{5+}O_4]'$; $[W^{5+}O_4]'''V_A^{\cdot\cdot}$).

The X-ray fluorescence dates of calcite and fluorite are presented in Figure 4. In the X-ray fluorescence spectrum of fluorite (Figure 4 a), a series of bands is observed with peaks at 4.25 eV (V_k center), 3.62 eV (Ce^{3+}), 2.88 eV (Eu^{2+}), 2.7 eV (Dy^{3+}), 2.18 eV ($Dy^{3+}\cdot OH$), 1.8 eV, 1.6 eV ($Dy^{3+}\cdot F_i$).

It was found that ***fluorite*** HPEMP - treatment leads to a general increase in the luminescence intensity without altering the individual bands symmetry and the spectral curve profile. The maximum increase (by a factor of 2.1 to 2.2) of the integrated band intensities is achieved by a HPEMP - treatment of 10 seconds (10^3 pulses). A further increase in the treatment duration (30 seconds) leads to a slight decrease in the area of the bands, but at the same time, their numerical values exceed the initial ones (untreated sample) by a factor of 1.5 to 1.7. An analysis of the obtained data suggests that the effect of the HPEMP - treatment include the formation (at 10^3 imp) and subsequent ($t_{tr} > 30$ s) partial annihilation of self-trapped holes (V_k site). Simultaneously a symbatic change in the number of sites associated with the luminescence of the Ce^{3+}; Eu^{2+}; Dy^{3+}; $Dy^{3+}·OH^-$, and $Dy^{3+}·F_i^-$ sites take place.

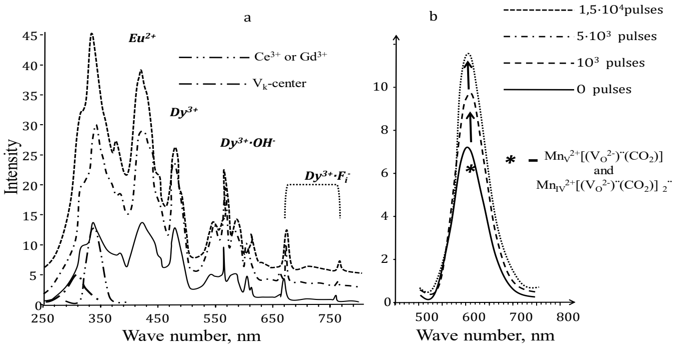

Figure 4 X – ray luminescrnce spectra of fluorite (a) and calcite (b) samples

The calcite HPEMP - treatment causes an increase in the band intensity at 600 nm (Figure 4 b). This band represents the luminescence of the impurity ions Mn^{2+} isomorphically substituting Ca^{2+}, Ca^{2+} located in the internodes and variously coordinated with oxygen vacancies. It indicates the deformation of the crystalline structure, associated in this case with the accumulation of defects ($(Mn_V^{2+}[(V_O^{2-})^{¨}(CO_2)]^{¨}$; $Mn_{IV}^{2+}[(V_{O2})^{¨}(CO_2)]^{¨}$).

Flotation test results Figure 5 illustrates the relationship between the floatability of monomineral fractions of calcite, fluorite, and scheelite and the duration of HPEMP – treatment at the different flotation conditions.

Single mineral flotation tests with use of sodium oleate (300g / t) and silicate (100 g /t) has allowed to determine that HPEMP - treatment results in the cocurrent improvement of the calciferous minerals floatability. The rising of the scheelite recovery was 10 – 12%, for fluorite it was 5 – 6%, for calcite – 7 – 8% [7].

Flotation experiments with a mixture of pure minerals (Σ m = 3 g, ratio of calcite: fluorite: scheelite = 1: 1: 1) were carried out to confirm the obtained results with the single mineral flotation tests. The results showed that HPEMP - treatment of the mineral mixture allows to improve the recovery of tungsten: at a consumption of sodium oleate of 200 g / t and sodium silicate of 100 g / t, the rising in W recovery is 6.1 - 7.2%: 44.4% (0 pulses – initial sample), 51.5% (3000 pulses) and 50.6% (5000 pulses). The quantity of W in the concentrate, at the same time, increases by 1.9 - 2.5%. The increase in the consumption of sodium oleate up to 250 g / t eliminates the effect of HPEMP - treatment: W recovery increases by 3.0 - 3.3% from 95.5% (0 pulses) to 98.5 - 98.8% (3 000 pulses and 5 000 pulses), the quantity of the concentrate improves by 1.5 - 2.0%.

Under selective separation conditions (Figure 5 b), recovery of $CaCO_3$ before the HPEMP was 74.7%, fluorite recovery was 73.6%, and scheelite rcovery was 41.2%. After HPEMP treatment (10 seconds, 10^3 imp), the floatability of calcite and fluorite samples decreased sharply to ~41.1%, i.e. by a factor of 1.8, while scheelite yield increased significantly from 41.1% to 58.8%.

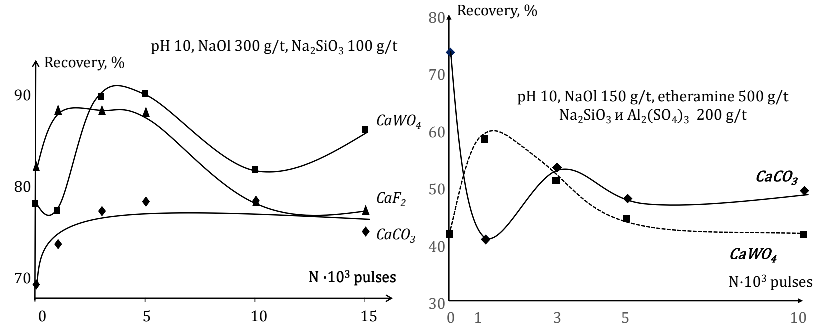

Figuer 5 Floatability of calcite, fluorite and scheelite as function of the number of pulses: a – bulk flotation and b-slective separation.

CONCLUSION

Thus, the HPEMP – treatment of calciferous minerals (calcite, fluorite, scheelite) leads to the transformation of the surface structural heterogeneity. It involve the formation, annihilation and transformation of intrinsic and impurity structural defects, which cause a change in the energy state and acid-base properties. This leads to a change in the sorption activity of the surface and flotation properties of minerals.

1. It was determined that HPEMP – treatment of calciferous minerals causes the evolution of the acid-base sites in calcium mineral surfaces and as consequence of this the increasing in their sorption activity towards a fatty acid collector (sodium oleate) and a decrease in the quantity (mg / g) of adsorbed depressor (sodium silicate). The increasing of adsorbed sodium oleate quantity for scheelite was 20 –30% as compared with the initial sample; for calcite and fluorite, the increasing of the adsorbed reagent quantity was about 10 – 20%. The decreasing in the quantity of adsorbed sodium silicate (mg / g) was 10 – 15% for scheelite and fluorite and 20–25% for calcite.

2. The possibility of bulk flotation features improving was shown. In monomineral flotation tests the optimal parameters of the HPEMP - treatment were identified ($t_{\text{treatment}}$~ 10 - 50 sec) and reagent scheme (sodium oleate 300g / t and sodium silicate 100 g /t) were determined. This flotation parameters allows to increase the recovery of calcite (8%), fluorite (6%) and scheelite (. 10-12%).

Flotation experiments with a mixture of pure minerals (Σ m = 3 g, ratio of calcite: fluorite: scheelite = 1: 1: 1) confirmed the efficiency of the HPEMP – treatment: the improvement of the tungsten recovery was 6.1 - 7.2%: 44.4% (0 pulses – initial sample), 51.5% (3000 pulses) and 50.6% (5000 pulses). The quantity of W in the concentrate, at the same time, increases by 1.9 - 2.5%.

3. The possibility of the selectivity enhancing were determined. It was achieved through the application of etheramine, sodium oleate, sodium silicate and aluminum sulfate. The optimal flotation conditions (pH 10.5, etheramine 500 g/t, sodium oleate 150 g/t, sodium silicate and aluminum sulfate 200 g/t) and HPEMP – treatment

($t_{treatment}$ = 10 s, 10^3 imp) allows to get the selectivity of the minerals flotation. The recovery of scheelite into the flotation froth increased by 17.7% (from 41.1% to 58.8%), the recovery of calcite and fluorite decreased by ~30% (from ~74% to 40%).

REFERENCES

1. Arsentiev, A.V., Gorlovsky, S.I., Ustinov I.D. (1992) Combained effect of floation regents. Nedra, Moscow.
2. Ustinov, I.D., Ryaboi, V.I., Koroleva, E.G., Petrova, L.N. (1995) Development of molybdoscheelite ores flotation with application of new flotation reagents In: Processing of oxidized ores. Nauka, Moscow.
3. Ryaboi, V.I. (1995) Development in work on flotation reagents in “Mekhanobr” institute. Obogashenie rud. 15, 22-25.
4. Wei, Z., Hu, Y., Han, H., Sun, W., Wang, R., Sun, W., Wang, J., Gao, Z., Wang, L., Zhang, Ch., Sun, L., Liu R. (2019) Selective Separation of Scheelite from Calcite by Self-Assembly of H_2SiO_3 Polymer Using Al^{3+} in Pb-BHA Flotation. Minerals, 9-43.
5. Gao, Y., Gao, Z., Sun, W., Hu Y. (2016) Selective flotation of scheelite from calcite: A novel reagent scheme International. International Journal of Mineral Processing, 10-15.
6. Nechiporenko, A. P. et. al. (1985) Indicative method of the solid surface acidity investigation. Russian journal of general chemistry, 9, 1907-1912.
7. Chanturiya V.A., Bunin I.Zh., Ryazantseva M.V. (2019) The impact of high - power electromagnetic pulses on the surface state and technological properties of the calciferous minerals. Journal of Mining and Metallurgy, 55 A (1), 45-52.
8. Liu, Y., Li, J., Tang, H., Li, W., Yang, Y., Li, Y., Chen, Q. (2016) Enhanced photoelectrochemical performance of plate-like WO_3 induced by surface oxygen vacancies. Electrochemistry Communications, 68, 81-85.

XIV International Mineral Processing
and Recycling Conference
Belgrade, Serbia, 12-14 May 2021

EFFECT OF GAS RATE AND PRESSURE IN THE GAS HOLDUP IN A LABORATORY FLOTATION COLUMN

Kyriakos Syrmakezis#, Konstantinos Tsakalakis
National Technical University of Athens (NTUA), Athens, Greece

ABSTRACT – For column flotation processes, gas holdup is considered to be a critical flotation kinetics parameter. Its prediction, in a typical column flotation operation, is considered a challenge. Using a Laboratory-scale Flotation Column, it was investigated the dependency of gas holdup with the rate and pressure of the supplied gas. A strong dependence relationship has been proved. Based on this dependency, a numerical model for the prediction of the gas holdup at the column basis has been elaborated and applied to real measurements, with reliable obtained results.

Keywords: Gas Hold Up, Column Flotation, Gas Rate, Gas Pressure.

INTRODUCTION

In case of column flotation processes, gas holdup (εg) is considered a critical flotation kinetics parameter since it affects directly the quantity of bubble surface available for particle attachment [1,2]. Since the first steps of column flotation process, Shah et al. [3] highlighted the significance of gas hold up, reporting that defines the flow regime together with air superficial velocity. Despite that, the accurate measurement of gas holdup, in a typical flotation column operation, is quite difficult [4]. As Moaveni [5] mentions mineral processing industry was considering gas holdup as an unmeasured variable until 2001. For this reason, significant initiatives have been developed with the aim to study and determine accurately the gas holdup incorporated in a flotation column.

As part of the development of a laboratory scale Flotation Column for research purposes, in the Laboratory of Mineral Processing (NTUA), its hydrodynamic characteristics were extensively studied. Following a predetermined research methodology, the gas holdup was determined for twelve different combinations of gas pressure and flowrate. The results of this study were statistically analyzed, resulting in significant findings about gas holdup dependency on air flowrate and pressure.

In the following paragraphs, the research methodology, results and conclusions of this investigation are presented, highlighting the strong relationship among the pressure and the rate of the air and its holdup in the main part of the column apparatus.

EXPERIMENTAL PROCEDURE

The aim of the present research is to define the fluctuations of gas holdup of water within a flotation column, under different air flow regimes. For the needs of the present

---

corresponding author: kcs@metal.ntua.gr

investigation, a 0.5 m lab-scale column was used. The range of gas flowrate ranged from 0.5 to 2 Nl/min, while the pressure of the supplied air was between 0.5 and 2 bar.

For each test, 1L of water was used in the main vertical column. In each case from a predetermined point, a photo camera was utilized to depict the situation in the basis of the column. As shown in Figures 1 and 2, it was clearly observed that the number, as well as, the size of the bubbles was changing, under different gas pressure and flowrate. For each applied flow regime, the photos were used for the determination of gas holdup. In specific, each photo was used to predict the number and the dimensions of the bubbles projected in it.

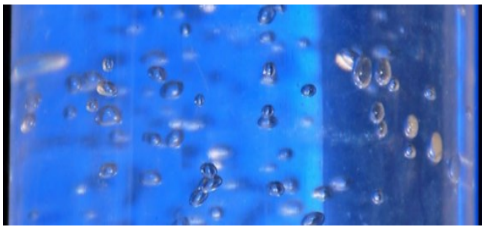

Figure 1 Bubble flow obtained with gas pressure 1.00 bar and rate 0.25 Nl/min

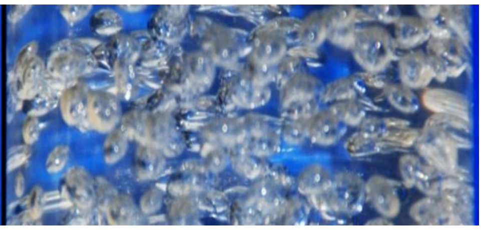

Figure 2 Bubble flow obtained with gas pressure 1.00 bar and rate 2 Nl/min

Macroscopically, it was clearly realized that for low level pressure and air rate values, the bubbles are distinct, with a normal and quite uniform shape, obtaining an almost “perfect bubbly flow”, as suggested by Bouaifi et al. [6]. On the contrary increased air flowrate and pressures result in the enlargement of bubbles and they create “churn-turbulent” flow, which burdens its visual clear distinction. For the illustration of the phenomenon, two cases were selected, showing clearly the difference among different upward bubble flows, under different flow regimes. The difference in the flow characteristics of the air bubbles, between the two different flow regimes, become obvious through the observation of Figures 1 and 2. Both these photos correspond to flows for experiments performed with air pressure of 1.00 bar. The first case, shown in Figure 1, presents the bubble flow obtained at 0.25 Nl/min, while the second case, shown in Figure 2, is the bubble flow obtained at 2.00 Nl/min.

The computational methodology, which was developed and applied, considered the needs and the expectations of the present research and seeks to calculate the gas hold up as a sum of bubbles’ volume within the region of the transparent column under consideration. The estimation of actual dimensions of the bubbles was obtained from the photos, with proportional estimation of their lengths, based on the known actual diameter of the transparent column, equal to 60 mm. Based on the calculated dimensions, gas holdup was determined. Totally, twelve different combinations of gas flowrate and pressure were selected, as shown in Table 1. For each one of the twelve cases, the designed research approach was deployed in six stages, as presented in the following paragraphs. All the stages were deployed for each test.

The results of each case were used and statistically analyzed with the aim to define and asses the effects of gas flowrate and pressure in the gas holdup in the selected zone of the flotation column.

Stage 1. Determination of the Selected Zone

Given that gas holdup presented variations through the column, it was decided that a selected zone of the column to be used for the determination of gas holdup. For the determination of gas holdup (ε_g), as well as, for the comparison of different cases, a specific horizontal zone of the transparent column on the photos available, was used. This zone remained fixed for all the tests. Its height is 20 mm and it starts 60 mm above the interface of the visible and the invisible part of the column.

Stage 2. Calculation of the Length Reduction Coefficient (ϕ)

Knowing the exact diameter of the column, length reduction coefficient was calculated. According to the proportionality rule, it was defined the length reduction coefficient (ϕ), which was unique for each photo or projection. After systematic observations, it was identified that in cases of bubbly flows, the shape of the generated bubbles can be simulated with the geometry of a rotating triaxial ellipsoid. Considering length reduction coefficient, in each case, semi-axes and the volume of each bubble projected in each photo were measured.

Stage 3. Determination of the average diffraction factor (μ)

But, the observation of the photos resulted in the conclusion that the accuracy of the measured dimensions and volumes should consider the diffraction of the water. For the needs of the present study, an approximate estimation of the diffraction factor μ for the bubbles was required. To determine the diffraction factor (μ), a common wooden meter was placed in five different points of the column. Analyzing the different diffraction factors, it can be concluded that the diffraction factor μ decreases from the face of the pipe to its depth, obviously due to the increase of the intervening water mass, up to a percentage of up to 35%. Moreover, it was noticed that the diffraction factors at the edges (right – left) of the column are almost equal, with an average value μ = 0.70, while a small deviation (≃8%) is noticed in the factor calculated for the center of the column.

Stage 4. Calculation of visible bubble dimensions and total volume of visible bubbles

Having defined the Length Reduction Coefficient (ϕ) and the average diffraction factor (μ), the dimensions of the bubbles, projected in each photo, were calculated. For each one of the visible bubbles, its two (visible) semi-axes are measured graphically (on the screen or on the paper) and are recorded. Based on the records, the actual dimensions of the bubbles are calculated, taking into consideration Length Reduction Coefficient (ϕ) and average diffraction factor (μ). All the collected data were used for the calculation of the total number of bubbles and their total volume.

Stage 5. Determination of visible zone of the column

Through the research, it was noticed that there are bubbles in the selected zone, which are not visible. It was observed that the depth of the visible zone is depended on bubbles density, within the upward bubble flow; the denser the flow, the smaller the visible zone of the column in a photo. For this reason, it was studied the visibility zone of the noticed bubbles, which was considered for the calculation of the gas holdup, for each case. This area is enclosed between the cyclic perimeter of the column and an ideal trapezoid with the large base to be the longitudinal diameter AB of the column, and the small base to be the line ΔE, parallel to AB, dividing the triangle ABΓ at a distance x from the center K of the circle, as shown in Figure 3.

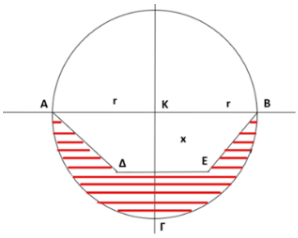

Figure 3 Visibility area of the generated bubbles

The area of the field of bubbles' view AΓBEΔA is equal to:

$$E_{\Pi} = (\pi r^2 - 4rx + 2x^2)/2 \tag{1}$$

Thus, the ratio ε of the considered area EΠ to the total area of the column cross section $E_Z = \pi r^2$ results in the equation:

$$\varepsilon = E_{\Pi}/E_Z = \{\pi + 2\,(x/r)^2 - 4\,(x/r)\}/2\pi \tag{2}$$

Moreover, based on the fact that the height of the zone considered is constant it is also:

$$V_{\Pi}/V_Z = E_{\Pi}/E_Z = \varepsilon \tag{3}$$

Considering a uniform distribution of bubbles within the whole volume of the considered zone, if V_{ϕ} is the total volume of the bubbles in the zone considered of volume V_z and $V_{\phi\pi}$ the total volume of the bubbles in the visible area V_{π} it is:

$$\varepsilon = V_{\Pi}\,/\,V_Z = V_{\phi\pi}\,/\,V_{\phi} \tag{4}$$

Under different flow regimes, the vertical distance of visible zone (x value) changes. This change affects, in extent, the x/r ratio. When x decreases, the visible zone increases and vice versa. Therefore, a key issue that was faced during the execution of the present study, was the selection of the appropriate value of x/r ratio.

The selection of the values was made by attentive notices, during the realization of the tests, considering the previously mentioned conclusion that the depth of the visible zone depends on bubbles density, within the upward bubble flow; the denser the flow, the smaller the visible zone of the column in a photo. The final values of x/r ratios that were selected are given in Table 1.

Stage 6. Determination of gas holdup in the selected zone.

Knowing the actual volume of the bubbles, for the determination of the gas holdup, the volume of the selected zone was required. The measured and calculated values, for the twelve cases considered for the present research, are presented in the next paragraph of the present paper in a table format.

EXPERIMENTAL RESULTS

In Table 1 are shown the measured and calculated values referred to the previous stages of the research.

Table 1 Results and Calculations for various experimental conditions

Air Press. P (bar)	**Air Flow Q (Nl/sec):**	**Q=0.50**	**Q=1.00**	**Q=1.50**	**Q=2.00**
P=0.50	Number of bubbles (N)	83	91	102	120
	Mean value of Radius a (mm)	1.34	1.52	1.64	1.69
	Standard Deviation σ_a	0.41	0.45	0.51	0.53
	Mean value of Radius b (mm)	0.68	0.77	0.79	0.83
	Standard Deviation σ_b	0.17	0.23	0.25	0.26
	Mean value of ratio a/b	1.92	1.99	2.08	2.15
	Standard Deviation $\sigma_{a/b}$	0.51	0.59	0.72	0.82
	M.V. bubbles’ volume V (mm^3)	3.02	4.46	5.22	5.85
	Standard Deviation σ_V	2.37	3.65	4.75	5.18
	Total bubbles’ volume V_ϕ (mm^3)	1004	1904	2663	2925
	Gas Holdup (εg) = V_ϕ / V_Z (%)	2.19	4.16	5.25	5.80
P=1.00	Number of bubbles (N)	83	98	129	136
	Mean value of Radius a (mm)	1.43	1.70	1.72	1.73
	Standard Deviation σ_a	0.48	0.51	0.54	0.55
	Mean value of Radius b (mm)	0.74	0.81	0.83	0.84
	Standard Deviationσ_b	0.18	0.27	0.27	0.29
	Mean value of ratio a/b	1.97	2.03	2.19	2.23
	Standard Deviation $\sigma_{a/b}$	0.57	0.63	0.76	0.89
	M.V. bubbles’ volume V (mm^3)	3.74	5.91	6.10	6.22
	Standard Deviation σ_V	2.93	5.65	5.85	6.06
	Total bubbles’ volume V_ϕ (mm^3)	1263	2918	3569	4024
	Gas Holdup (εg) = V_ϕ / V_Z (%)	2.76	6.37	7.80	8.78
P=2.00	Number of bubbles (N)	83	109	137	149
	Mean value of Radius a (mm)	1.72	1.86	1.92	1.98
	Standard Deviation σ_a	0.57	0.86	0.88	0.92
	Mean value of Radius b (mm)	0.93	0.94	0.95	0.97
	Standard Deviationσ_b	0.38	0.39	0.40	0.41
	Mean value of ratio a/b	2.08	2.12	2.21	2.33
	Standard Deviation $\sigma_{a/b}$	0.84	0.94	1.06	1.11
	M.V. bubbles’ volume V (mm^3)	8.83	10.08	11.12	11.95
	Standard Deviation σ_V	8.29	9.44	10.06	11.02
	Total bubbles’ volume V_ϕ (mm^3)	3639	5654	7219	8090
	Gas Holdup (εg) = V_ϕ / V_Z (%)	7.95	12.35	15.77	17.67

ANALYSIS OF EXPERIMENTAL RESULTS

For the determination of the gas holdup, through the control of air flow rate and pressure, the findings of the research, as presented in Table 1, were analyzed. Applying regression analysis, it was investigated the relationship of gas holdup (dependent variable) with the pressure (independent variable) and different flowrates of provided gas. Regression analysis, as presented in Figure 4, resulted in the development of statistical models, which describe the effect of different gas pressures, under four different gas flowrates into gas holdup. The high value of R-squared observed in all the investigated cases verifies the accuracy of the deployed research approach, as well as, the adequacy of proposed models.

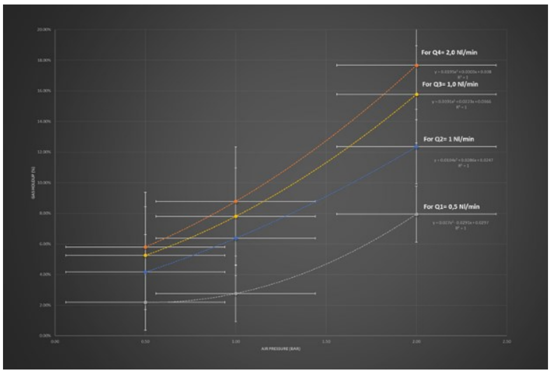

Figure 4 Gas Holdup, under different gas pressure and flowrate

CONCLUSION

Gas holdup (εg) is considered a critical flotation kinetics parameter for all column flotation processes. Various studies have shown that gas holdup is a function of numerous variables in flotation and dependent to the bubble size, which is also the result of a multivariable process function [5]. As part of the development of a laboratory scale Flotation Column for research purposes, in the Laboratory of Mineral Processing (NTUA), its hydrodynamic characteristics were studied. Following a predetermined research methodology, the gas holdup was determined for the twelve different combinations of gas pressure and flowrate. The results of this study were analyzed statistically, resulting in high accurate statistical regression models, which reveal the dependence of obtained gas holdup and gas pressure, under different flowrates. The development of these models contributes in the ongoing study of gas holdup, as column flotation kinetic parameter, proving the strong relationship of gas holdup, primarily, with gas pressure, and the gas flow rates, for the lab-scale column developed in the Laboratory of Mineral Processing (NTUA).

REFERENCES

1. Jameson, G. J., Nam, S., Young, M. M. (1977) Physical factors affecting recovery rates in flotation. Miner. Sci. Eng, 9 (3), 103-118.

2. Sastri, S. R. S. (1996) Carrying capacity in flotation columns. Minerals Engineering, 9 (4), 465-468.
3. Shah, Y. T., Kelkar, B. G., Godbole, S. P., Deckwer, W. D. (1982) Design parameters estimations for bubble column reactors. AIChE Journal, 28 (3), 353-379.
4. Sastri, S. R. S. (1998) Column flotation: theory and practice
5. Moaveni, A. K. (2015) Design, Construction and Performance Test of a Laboratory Column Flotation Apparatus, p. 17, 2015.
6. Bouaifi, M., Hebrard, G., Bastoul, D., & Roustan, M. (2001) A comparative study of gas hold-up, bubble size, interfacial area and mass transfer coefficients in stirred gas–liquid reactors and bubble columns. Chemical engineering and processing: Process intensification, 40 (2), 97-111.

XIV International Mineral Processing and Recycling Conference
Belgrade, Serbia, 12-14 May 2021

OPTIMIZING THE FLOTATION OF COPPER-MOLYBDENUM ORES USING THE ABSORPTION CAPACITY OF ORE TO THE COLLECTOR

Valeriy Morozov[1#], Irina Pestriak[1], Erdenezul Jargalsaikhan[2]
[1] National University of Science and Technology "MISIS", Moscow, Russia
[2] Erdenet Mining Corporation, Erdenet, Mongolia

ABSTRACT – As a parameter of flotation process optimization proposed to use the absorption capacity of the ore in relation to the collector. It is determined, a significant reason for the decrease in the residual concentration of the collector is its absorption by some rock-forming minerals. The value of the absorption capacity of the ore relative to the collector was used as a parameter of the grade of the ore. The developed technique was applied to calculate the optimal parameters of grinding and flotation of copper-molybdenum ore at the ore processing plant of Erdenet Mining Corporation.

Keywords: Collector, Concentration, Absorption Capacity, Ore Grade, Optimization.

INTRODUCTION

A promising way for improving the systems for automated control of enrichment processes is the use of methods and algorithms of automatic control of reagent consumption based on the operational analysis of the collector concentration in the aqueous phase of the pulp [1]. For water-soluble collectors such as xanthate standardized methods have been developed and applied, involving direct UV spectrophotometry of the reagents in the filtrates of the liquid phase of the flotation pulp [2]. However, it is difficult for water-insoluble flotation reagents, the application of direct UV spectral analysis of residual concentration. Previously, a technique was previously developed involving the extraction of the allyl ether of butyl xanthate acid into acetone and the measurement of the optical density of the solution at a wavelength of 355-358 nm [3]. However, this technique had not found application in processing plants due to low sensitivity. In the flotation of copper-molybdenum ores, automatic control systems are successfully applied here according to process indicators: metal recovery and the quality of the concentrates obtained [4]. A further increase in the efficiency of automatic control systems and optimization of flotation processes is possible when measuring the residual concentration of a non-ionic collector.

EXPERIMENTAL AND MATERIALS

The spectral-active fraction of the collector AeroMX-5140 is characterized by three bright and distinct absorption peaks: at 220, 255 and 273 nm. According to published data the wavelengths of electronic transitions responsible esters alkyl xanthate acid [5].

[#] corresponding author: dchmggu@mail.ru

The extraction method allows to measure the concentration of non-ionic esters of xanthogenic acids. The absorption bands of UV radiation of allyl ether of amyl xanthate acid do not coincide with the absorption bands of unsaturated alcohols and disulfides partially extracted into the extract, which are components and products of oxidation of frother and ionogenic collectors. Measurement of concentration of the main spectral – active component of the extracted organic phase is possible using absorption peaks at 220 and 273 nm. Analysis of calibration graphs for the collector extractant shows that in the concentration range from 0 to 1.5 mg/l there is a rectilinear dependence of the optical density on the concentration. The interval of reliable measurement of the residual concentration of the collector - from 0.2 to 1.5 mg/l with a measurement error of not more than 2.5-7.5%. By varying the ratio of the extragent - aliquot solution, the reliably determined concentration interval is from 0.1 to 15 mg/l.

RESULTS AND DISCUSSION OF THE RESULTS

The determining of the absorption capacity of the pulp in relation to xanthate was proposed in research [6]. It was also noted that in flotation of oxidized ores characterized by significant absorption of the collector by copper ions, the use of this parameter makes it possible to quantify the required consumption of the collector [7]. A significant reason for the decrease in the residual concentration of the collector is its absorption by some rock-forming minerals, in particular sericite. To establish the value of the absorption capacity of the mineral, experiments were made on the interaction of the collector with some rock-forming minerals. In the experiment, a sample of minerals or rock weighing 100 g with a size of 62% class -74 microns was kept for 10 minutes at room temperature in a collector solution (100 ml) with an initial concentration of 10 mg/l at different pH of the medium. The sericite that has the highest absorption capacity in relation to the collector (table 1). The lowest absorption capacity is characterized by porphyry minerals.

The analysis of table 1 data showed the regularity of the decrease in the absorption capacity of rock-forming minerals with increasing pH. The increasing pH from 10.1 to 10.35 reduces the absorption capacity of rock-forming minerals by 7-12% (table 1).

Table 1 Absorption capacity of rock-forming minerals in relation to the collector at a concentration of 10 mg/l

Minerals	pH	Collector absorption mg/kg
Porfires	10.1	0.45
	10.35	0.41
Quartzite	10.1	0.55
	10.35	0.50
Metamorphically quartz	10.1	1.77
	10.35	1.52
Sericite	10.1	4.42
	10.35	4.10

The general algorithm for controlling the processes of grinding and flotation, involves the consistent implementation of methods for assessing the grade of processed ores and optimization of technological processes. The layout of the control algorithms of the flotation process is carried out on the principle of dual control, when calculation of optimal parameters of processes of grinding and flotation is based on advance estimates grade of ores, and the definition of the basic parameters for typical ores produced [8].

Grade assessment is performed according to the algorithm proposed in the research and involves determining its similarity with the main technological types of ores [8]. In this algorithm, the final task of determining the grade of ore is to determine its composition as a share in it of the main technological types of ores. As the primary information system analysis used the testimony of the material composition analyzers and sensors, video-image analysis of the mineral composition of the ore.

Calculation of ore grade was carried out using a multi-criteria method of calculating the belonging. The area of finding the desired solution in our problem is represented by the images of five typical ores, and the proportion of each ore type is determined in the ore. The mathematical part of the system calculates the grade of the incoming ore by six or more significant ore parameters (for example, the content of copper, molybdenum and iron in the ore, the mass fraction of oxidized copper minerals, secondary sulfide minerals of copper in the ore, primary minerals of copper and sericite).

In determining the grade of ore, the parameters of typical ores, addition to the absorption capacity, presented in table 2. Analysis of the results of measuring in collective copper-molybdenum flotation carried out with the use of the collector AeroMX-5140, showed that the greatest tendency to exhibit absorption of the mixed oxide ore and mixed seritized ore.

Table 2 Typical ore Parameters, used to determine the grade of the processed ore

Parameters	Types of ore				
	MPO	MSSO	LPO	MOO	MSO
Ratio of mass fractions of primary and secondary copper sulfides	2.1	0.50	0.45	0.75	0.57
Ratio of mass fractions of primary and oxidized copper minerals	18.5	15.4	21.4	10.4	17.6
Ratio of mass fractions of chalcopyrite and pyrite	0.77	1.5	0.45	0.86	0.67
Mass fraction of copper in ore, %	0.44	0.57	0.39	0.55	0.52
Mass fraction of sericite in ore, %	0.12	0.15	0.1	0.17	0.34
The absorption capacity of ore to the collector, %	66.7	76.9	63.5	80.1	84.1

*Massive Primary Ore (MPO); - Mixed Secondary Sulphidised Ore (MSSO); - Lean Pyritised Ore (LPO); - Mixed Seriticitised Ore (MSO) and Mixed Oxidised Ore (MOO).

Therefore, the value of the absorption capacity of the ore relative to the collector can be used as a parameter of the grade of the ore.

The essence of calculating the proportion of ore belonging to a certain type is to determine the degree of "similarity" to each of the known 5 types of ore, and in proportion to this degree to establish the proportion that each of the 5 types of ore is received for processing ore [8]. To do this, first determine the distance from the point whose coordinates correspond to the parameters of ore taken for processing, to each of the points, coordinates of which correspond to types, ores, dedicated technologists as a base.

Figure 1 explains the ore grade recognition algorithm by the example of the two - parameter system "copper content" - "collector absorption". In practice, a system of 8 parameters is used: the contents of three metals, the contents of five minerals. When the system is equipped with a sensor of the absorption capacity of the pulp relative to the collector, the ore grade recognition system becomes more accurate.

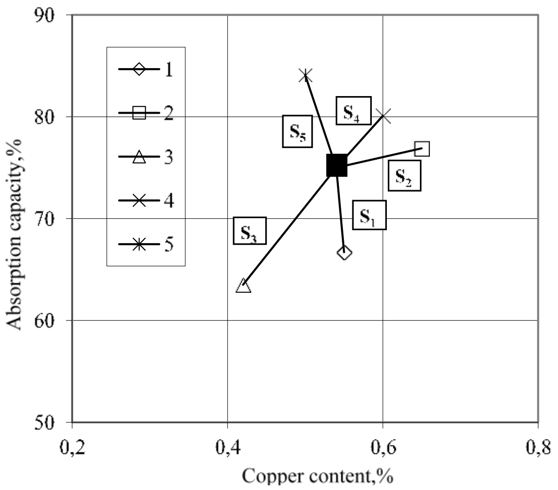

Figure 1 The example of estimating the ore in two-dimensional space 1, 2, 3, 4, 5 – the types of ores; 6 (■) - current ore production; S_1, S_2, S_3, S_4, S_5 – the deviation of parameters of ore from current production parameters ore types 1, 2, 3, 4, 5

Then, calculation equations with the help the values of mass fractions of typical ores in the ore entering the processing are determined after the normalization operations and evaluation of the significance of the parameters.

The normalized value of the deviation (S_i) of the parameters of the ore mixture (Z_n) from the parameters of typical ores (Z_{ni}) is calculated by the formula:

$S_i = (|Z_n - Z_{ni}|/Z_{ni})$, when i=1-5. (1)

Normalized values of similarity of ore mixture parameters with typical ore parameters are calculated by the formula:

$D_1 = 1/S_i$, when i=1-5, (2)

where: S_i is the normalized deviation of ore mixture parameters from typical ore parameters. The calculation of the mass fraction of a single ore type (γ_i) in a mixture of ores is carried out by the formula:

$\gamma_i = kD_i/\sum(kD_i)$, when i=1-5, (3) where: k is the significance coefficients of the individual measured ore parameters.

To confirm the appropriateness of the use as additional criteria the grade of the ore the adsorption capacity of the pulp used in the calculation of the residual variance in the original dataset relative to the result function when determining the grade of the incoming ore.

To assess the accuracy of the determination, five model types of ore were mixed in pre-known ratios. Then, using radiometric and x-ray fluorescence analysis, as well as measuring the residual concentration of the collector, the grade of the ore was evaluated. The accuracy of the analysis was determined by the criteria of coefficient of determination R^2 and the residual dispersion.

The results of calculations showed that the inclusion of this parameter reduces the relative variance for individual dependencies from 0.26-0.28 to 0.21-0.23. This reduction allows us to conclude that the adequacy of the model and improve the accuracy of determining the grade of processed ore.

The value of the target function SF for each process parameter was calculated as the weighted average of these parameters for each standard grade of ore (SF_i) considering the contribution of this grade (γ_i) to the ore mixture, calculated by equation 4:

$$SF = \sum \gamma_i SF_i, \tag{4}$$

where: relative mass fraction of ore i type into the input for processing the mixture of ores.

The calculated data set includes the fineness of grinding, pulp pH, and reagent costs for ore types (table 3).

Table 3 Target functions of the main parameters in control systems for grinding and collective flotation processes

№	Process of parameters	MPO	MSSO	LPO	MOO	MSO
1	Fineness of grinding – the output of the class – 74 microns, %	67.5	64.5	67.0	66.0	66.0
2	pH of the pulp in the main flotation	10.36	10.59	10.50	10.31	10.55
3	AeroMX 5140 collector consumption, g/t	10.0	12.0	10.0	13.0	17.5
4	The consumption of the foaming agent, g/t	13.0	16.0	13.0	16.0	19.0

*Massive Primary Ore (MPO); - Mixed Secondary Sulphidised Ore (MSSO); - Lean Pyritised Ore (LPO); - Mixed Seriticitised Ore (MSO) and Mixed Oxidised Ore (MOO).

The preset functions of the main technological parameters were used as a base level in local automatic control systems for the grinding and flotation process during the enrichment of copper-molybdenum ores. Using the procedure for determining the grade of ore using the value of the absorption capacity relative to the collector as the grade parameter increases the efficiency of automatic control. The use of an upgraded method for evaluating the grade of ore provides an increase in the productivity of the grinding cycle by 1.5% and an increase the recovery of copper and molybdenum into concentrates by 0.5-0.8%.

CONCLUSION

It was used spectral method of measuring is developed concentration of non-ionic collector AeroMX-5140. The method used the UV-measuring the concentration of the spectral active fraction of non-ionic collector – allyl ether amyl xanthate acid in the aqueous phase. The dependences of the residual concentration of the nonionic collector AeroMX-5140 in the collective copper-molybdenum flotation pulp were determined. A method is proposed for determining the grade of copper-molybdenum ore, using the adsorptions capacity to of the pulp to the collector as a parameter. The developed technique was applied to calculate the optimal parameters of grinding and flotation of copper-molybdenum ore at the ore processing plant of Erdenet Mining Corporation. The use of method provides an increase in the productivity of the grinding cycle by 1.5% and an increase the recovery of copper and molybdenum into concentrates by 0.5-0.8%.

REFERENCES

1. Abramov, A. (2010) Flotation. Physico-chemical modeling of the processes. Moscow, Mir gornoy krnigi, 672 p.
2. Hao, F., Davey, K.J., Bruckard, W.J., Woodcock, J.T. (2008) Online analysis for xanthate in laboratory flotation pulps with a UV monitor. International Journal of Mineral Processing, 89, 1–4, 71–75.
3. Sivkova, P.I., Voronina, L.V. & Molodtsova, V.I. (1980) Method of quantitative determination of xanthogenic acid esters. USSR Patent No. 726472. Appl. 27.10.75 in Bulletin 13.
4. Ganbaatar, Z., Zimin, A.V., Soloveva L.M., Nazarov, Y.P. (2010) Improving the technology of enrichment of copper-molybdenum ore deposits Erdenetiin-Ovoo. Gornyi Zhurnal, 10, 34-36.
5. Morozov, V.V., Pestryak, I.V., Erdenezuul, J. (2018) Influence of concentration of nonionic collector-allyl ether of amylxanthogenic acid on flotation of copper-molybdenum ores. Non-Ferrous metals, 11, 14-20.
6. Zhong, H., Huang, Z., Zhao, G. at al. (2015) The collecting performance and interaction mechanism of sodium diisobutyl dithiophosphinate in sulfide minerals flotation. Journal of Materials Research and Technology, 4, (2), 151-161.
7. Seifelnasr, Ahmed A.S., Zain, Ghorashi Z. Abouzeid, Abdel-Zaher M. (2017) Flotation of an Oxidized Copper Sulfide Ore. Journal of Mining World Express, 6, 1-9.
8. Morozov, V.V., Ganbaatar, Zorigt, Delgerbat, Lodoy, Morozov, Y.P. (2018) Modern method and systems of optical ore grade analysis by processing of copper-molybdenum ores. Canadian Institute of Mining, Metallurgy and Petroleum (Ed), Proceedings of IMPC 2018, Moscow, Russia, 52-60.

2021 IMPRC INTERNATIONAL MINERAL PROCESSING & RECYCLING CONFERENCE

XIV International Mineral Processing
and Recycling Conference
Belgrade, Serbia, 12-14 May 2021

NEW REAGENT AND METHOD FOR SELECTIVE FLOATING OF CLAYS IN THE CONCENTRATION PROCESS OF NON-FERROUS MINERALS

Zoran Petkovic#
Petkom Chile ltd., Santiago, Chile

ABSTRACT – I have presented laboratory reagent tests and methods for selective floating of clays in the concentration process of non-ferrous minerals that have been proved in DMH mine floating of clays in the tailings in Chile, and selective floating clay - gold in mineral gold of Delta plant, in Chile.

Flotation of tailings (DMH) was recover a 28.8% clays, to use collector P-342Ar, dose 80 g/t and increased the sedimentation until 3.4 cm/h (RT), to about 8 cm/h.

Results of gold recover (Delta) in concentrates for standard and selective flotation for Petkom -70 increased by 39.14%. When used Petkom - 4635 increased by 23.62%.

Key words: Clays, Reagents, Flotation, Gold, Tailings.

INTRODUCTION

Clays, due to their high surface area, chemical and mechanical stability, laminar structure and high cation exchange capacity, are an excellent absorbent material, but due to these very same characteristics, serious problems arise at different stages of the mineral concentration process, that is, grinding, flotation, thickening and filtration of the ore, affecting its efficiency and negatively impacting the recovery and the law of the resulting concentrate. In this context, various actions have been taken in the industry, whose purpose is to minimize the negative impact.

In 2015, Zoran Petkovic presented his method of flotation and reagents by flotation clays in non-ferrous minerals containing clays and in 2016 reagent group for flotation clays in deposits of non-ferrous metals.

The presence of high concentrations of fines and/or clays in the current DMH flotation circuit has caused negative impacts on the recovery of copper, reaching recoveries around 83%.

These experiments are carried out in order to improve the rheological properties and sedimentation rate of the floating tail, by removing a significant fraction of fine particles and clay through the concentrate from being achieved and thereby the required level of clean water.

The clays present in the Delta plant deposits in Chile, decrease the recovery of gold minerals and gold law in concentrate. In this document we present results of selective float test of clay-gold in laboratory using Petkom 721Ar reagents, Petkom 70 and Petkom 4635.

---

corresponding author: zpetkovic789@gmail.com

LABORATORY EXAM

The DRX analysis were performed using a Bruker® D4 Endeavor device, operated with Cu radiation and Kß Ni filter.

The measurements were made in Haake RS6000 model rheometer.

Microtrac S3500 laser equipment used to perform granulometric analysis.

The study considers the evaluation of the effectiveness of the Petkom-342Ar and Petkom -721Ar collectors for the flotation no metals minerals and particularly, for clay.

The Petkom342Ar®and Petkom 721Ar collectors is highly selective for the flotation of clays and corresponds to a mixture of chemical compounds of the type aril alkylamines.

Likewise, the behavior of the Magnafloc 7793 LT coagulant is evaluated, in combination with the selected flocculant Nalco 8173, and Kemira SFE 4833.

A) Exam floating clay in tailings DMH

The DRX analyzes were performed using a Bruker® D4 device.

Table 1 Minerals of clays

Sample	Quantitative mineralogy				
	Esmectita	Caolinita	Clorita	Illita/Mica*	Pirofilita
Tailings received	Not detected	Minority phase	Not detected	Very abundant phase	Abundant phase
Clay concentrate	Not detected	Minority phase	Not detected	Very abundant phase	Minority phase
Floated tail	Not detected	Minority phase	Not detected	Very abundant phase	Minority phase

*Note: In total rock DRX analysis, performed in a complementary way, muscovite is identified

The most abundant phase it is Illita/Mica followed by pyrophyllite and kaolinite to a lesser extent. The analyzes reported 5 minerals belonging to this family: muscovite, biotite, clorite and pyrophyllite.

Table 2 Tailings characteristic diameters

Sample	Diameter (µm)		
	D10	D50	D80
Complex received tailings	3.3	50.4	218.8
Floated tailings	3.8	70.7	244.8

*Average of 2 measurements, CV D10=5%; D50=3%; D80=5%; Microtrac S3500

The parameters of fixed variables used in these experiments are found in table 3. The design of experiments, in terms of reagent doses is indicated in table 4.

Table 3 Fixed variables for floating with collector Petkom 342Ar

Variable	Unit	Value
Percentage of solids	%	35
Mineral mass	g	1,164
Rotational speed during conditioning	rpm	600
Rotational speed on floating	rpm	800
Conditioning time	min	10
Air flow	$Lmin^{-1}$	10

Table 4 Parameters for the preliminary flotation of clays with Petkom-342Ar collector

Sample	P342Ar Collector (gt^-1)	Nalco flocculant (gt^-1)	Magnafloc coagulant (gt^-1)	rotational kinetics (min)	Dry concentrate mass (g)
C 100-3M	75	8	23	3	253.96
C 100-5M				5	0.73
C 100-10M				10	0.48
C 300-3M	226	15	23	3	505.78
C 300-5M				5	30.24
C 300-10M				10	8.82
C 500-3M	376	8	23	3	356.44
C 500-5M				5	67.38
C 500-10M				10	34.22

As previously indicated the Petkom-342Ar collector dosing experiments are performed around the dose 75 g/t, 226 g/t, 376 g/t.

The flotation kinetics carried out in these three experiments allows obtaining partial concenters at 3, 5, 10 minutes of flotation for each collector dosages can be seen in table 4 in figure 4 more than 90% of the feeder tailings floats for the first three minutes. Note tan for the lowest concentration of Petkom -342Ar collector 75 g/t the recovery in weight of clays is constant over time.

Figure 1 shows that for a float time of 3 minutes it is possible to extract the order of 22% of clays with the lowest collector dosage value of 75 g/t. On the other hand, the best recovery in weight is achieved with the collector dose 226 g/t. However, the optimal flotation time not only depends on the recovery in weight of clays increase in the sedimentation rate that facilitates normal operation of the tailings thickener and clear water level increase. Due to the fast kinetics in the preliminary experiments, it was determined to adjust the flotation kinetics to 5 minutes for next experiments.

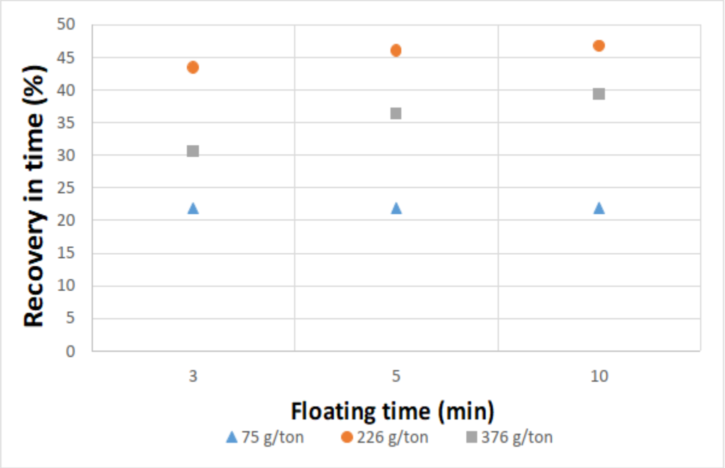

Figure 1 Flotation kinetics at different doses collector P342Ar with coagulant, flocculants

Table 5 Fixed variables for floating with collector, flocculants, coagulant

Variable	Unit	Value
Percentage of solids	%	40
Rotational speed during conditioning	rpm	600
Rotational speed on floating	rpm	800
Conditioning time	min	10
Floating time	min	5
Air flow	$Lmin^{-1}$	10

Table 6 Flotation test design with P342Ar collector

Sample	Pulp volume (mL)	Mineral mass (g)	Dry concentrate mass (g)	P342Ar Collector (gt^{-1})	Nalco flocculant (gt^{-1})	SF E 4833 Kemira flocculant (gt^{-1})	Magnafloc coagulant (gt^{-1})	Clear water recovery (%)
C 19-5M	2,700	1,436	30.18	19	0	38	0	56.0
C 23-5M	2,700	1,436	24.71	23	0	38	0	57.3
C 30-5M	2,600	1,383	198.71	30	0	30	8	54.2
C 38-5M	2,600	1,383	150.65	38	15	0	23	53.8
C 45-5M	2,600	1,383	272.06	45	0	38	8	52.0
C 60-5M	2,600	1,383	350.97	60	15	0	23	52.2
C 75-5M	2,600	1,383	185.63	75	15	0	23	48.3
C 80-5M	2,700	1,436	414.5	80	0	50	0	52.4

The last column of table 6 show the calculation of the fraction of water recovered in percent, which represent the water recovered in floats tail versus the water recovered in tailings received under equal conditions of coagulant and flocculants.

The highest recovery in weight of clays is achieved with a collector dose 60 g/t although the highest sedimentation rate (7.7 cm/h) corresponds to a dose 80 g/t in this answer as the main objective is the recovery of clear water and the improvement of the sedimentation conditions in the tailings thickener it can be indicated that the optimum point between recovery and sedimentation is adding 80 g/t is convenient to highlight that the sedimentation of the received tailings (RT) which is the order of 3.4 cm/h, is lower at all speeds.

It should be noted that under the different flotation conditions tested the recovery of clear water does not exceed the range 48 to 57%.

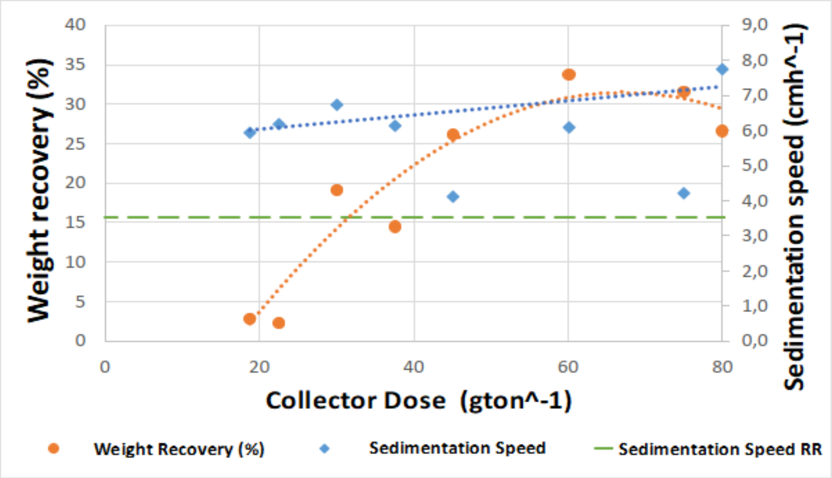

Figure 2 Results of flotation of tailings with different doses of petkom-342Ar collector and their respective sedimentation rate in the presence of flocculants and/or coagulant

B) Selective flotation of clays and gold in the ore of the Delta plant Chile

Analytical equipment; Atomic emission spectrophotometer in flame Perkin Elmer; Chemical analysis of mineral; Au (g/t) = 1.92; Sale of selective flotation clays, gold.

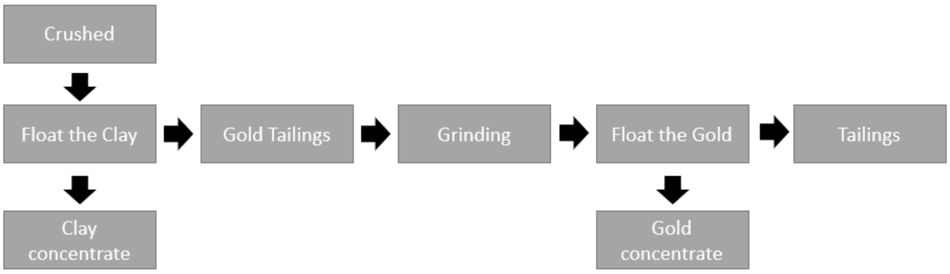

Figure 3 Block diagram of the process selective flotation clay -gold mineral

Table 7 General conditions for two flotation tests

b-1 Gold rougher standard float	
Granulometry after grinding	P80 120 microns
Pulp density	30% solid
T conditioning	10 min
Rpm	1200 º/min
T flotation	12 min
pH	9.5
Reagents	Petkom 70 120g/t (Petkom 4,635 120 g/t second float)
Foaming	MIBC 20 g/t

Gold rouger standard float was done with two experiments (reagents Petkom-70 and Petkom 4635) so that we could make a compare results between the standard float of gold mineral and selective flotation of clay-gold.

Table 8 General conditions for selective clay-gold flotation test

Selective flotation of clays after crushing		Selective flotation the gold	
Granulometry	100$ under 10# Mash	Granulometry	P80 120 microns
Pulp density	40% solid	Pulp density	30% solid
T conditioning	10 min	T conditioning	5 min
Rpm	1200 º/min	Rpm	1200 º/min
T flotation	12 min	T flotation	12 min
pH	natural 7,5	pH	9,5
Reagents	petkom 721Ar 200 g/t	Reagents	petkom 70 80 g/t
Flocculant	SFE kemira 50 g/t	Flocculant	petkom 4635 80 g/t second the float
Foaming	MIBC 50 g/t	Foaming	20 g/t

Concentrates obtained by classic rouger flotation with Petkom-70 and Petkom-4635 collectors with optimal doses of 120 g/t. Higher doses did not give increased recuperations and reduced gold contents due to increased presence of clay.

Table 9 Classic rouger flotation results for gold

Reagents	Fiding (gr)	Tailings (gr)	Gold concentrate	Rm Au (%)	Golden Law (g/t)
Petkom -70	918.1	877.4	40.7	48.55	22.38
Petkom -4635	918.4	868.9	51.4	61.6	19.33

Table 10 Selective flotation clays – gold

Selective Flotation	Reagents	Fiding (gr)	Clay concentrate	Tailings (gr)	Gold concentrate	Rm Au (%)	Golden Law (g/t)
Clay´s selective flotation	Petkom 721Ar	914.9	236.6	678.3			
	Petkom 721	916.6	247.5	669.1			
Gold´s selective flotation	Petkom - 70	678.3		640.2	33.22	78.69	35.81
	Petkom-3645	669.6		619.7	37.4	84.72	39.45

By selective flotation of clay care very pure in the first selective flotation of clays 25.86% of weight clays are concentrated and in the second flotation of clays with Petkom-721, 27% of weight clays are concentrated in tailings other minerals mainly quartz with gold minerals and other minerals.

From the obtained results in tables 9 and 10 for Gold minerals concentred we see that the recovery for Petkom-70 (table 9) and the recovery for Petkom-70 (table 10) after flotation clay jumped significantly from 48.55% to 78.69% and the gold content in the concentrate from 22.35% to 35.81% respectively content obtained with Petkom -4635 recuperation standar 61.6% a selective flotation 84.72% gold content in the concentrate from 19.33% to 39.45%.

CONCLUSION

The optimal PETKOM -342Ar reagent formula for the selective flotation of the tailings is: 80 g/t, 50 g/t SF e 4833b Kemira flocculant, Without coagulant, Without sparkling.

The laser granulometric distribution of the products of the selective flotation shows that the D50 of the tailings received, increases from 52.9 to 67.8 microns (Petkom 342Ar), in the flotation tails, facilitating the sedimentation of particles in the thickening.

The addition of flocculant and/or coagulant in the formulation of the flotation reagent plays an important role in the recovery of clay and in the behavior of the sedimentation rate of the flotation tailings.

The kinetics of selective flotation of clay, contained in the tailings, is extremely fast, achieving maximum recovery at 3 minutes of flotation. For industrial scaling it is recommended to use a scale factor equal to 2, that is, a float time of 6 minutes.

The reagent the Petkom 342Ar collector, in the absence of coagulant, using the formula indicated above, increases the sedimentation rate from 3.4 cm/h to about 8.0 cm/h.

The fraction of clear or recovered water in the float tailings sedimentation tests is increased in the order of 55%, due to a higher sedimentation rate of the solids and characteristics of the pulp particles more favorable to the sedimentation process.

By the method of selective flotation of clay -gold with or a high content of clay, has been successfully applied to the mineral clay-gold reagent Petkom-721Ar for clays and reagents for gold minerals Petkom-70 and Petkom-4635 optimal doses 80 g/t.

Reagent Petkom-721Ar at an optimal dose of 200 g/t made clay concentrate respectively for two laboratory tests 25.86% and 27% weight, residual clay negligible for further process.

The obtained results of gold recover in concentrates for standard rouger and selective flotation g for reagent Petkom -70 increased by 39.14% for reagent Petkom -4635 increased by 23.62%.

The obtained results for standard rouger flotation and selective flotation of gold reagent Petkom-70 increased by 1323 g/t and for Petkom 4635 increased by 22.13 g/t.

REFERENCES

1. Devenport, W.G., King, M., Shlesinger, M., Biswas, A.K. (2002) Extractive metallurgy of cooper. Fourth edition, Pergamon.
2. Magdalinovic, N., Trumic, M., Ignjatovic, R., Petkovic, Z., Rajic, V. (2001) The influence of the new BZ-2000 reagent on the use of balls and technological results in the flotation of non-ferrous metals ore. In: 9th BMPC, Istanbul, Turkey, Proceedings, 227-233.
3. Petkovic, Z. (2015) Flotacion de arcillas en concentración de minerales no ferrosos. Clase maestra Universidad Santa María, Santiago de Chile.
4. Andrić, Lj. (2017) Preparation of non-metals in Serbia. Institut za tehnologiju nuklearnih i drugih mineralnih sirovina ITNMS Beograd.
5. Velde, B., ed., (1995) Composition and mineralogy of clay minerals. Origin and mineralogy of clays: New York, Springer-Verlag, 8–42.
6. Valderrama, L., Chamorro, J., Zazzali. B., Rodríguez, A., Díaz, A. (2012) Estudios de reactivos para la flotación de silicato contenidos en concentrados de hierro. Uda revista dela facultad de ingeneria 28, 27-34.
7. Petkovic, Z. (2014) Colectores Selectivos e inhibidorres de corrosion y método de flotacion. Clase maestra en Facultad Nacional de Ingeniería, Oruro Bolivia, mayo.

XIV International Mineral Processing
and Recycling Conference
Belgrade, Serbia, 12-14 May 2021

APPLICATIONS OF A NEW THIOAMIDE GROUP COLLECTOR IN SULFIDE ORE FLOTATION

Vladimir Riaboy[1#], Vitaly Kretov[2], Sergei Levkovets[2], Ilia Riaboy[1], Ekaterina Smirnova[2]
[1] Mekhanobr-Orgsintez-Reagent, Saint-Petersburg, Russia
[2] KvadratPlus, Togliatty, Russia

ABSTRACT – The study investigates the performance of a new thioamide group collector Reaflot-3790 in the flotation of copper, copper-molybdenum, and gold pyrite-arsenopyrite ores. We have shown that this collector performs best in two- and three-component compositions with other collectors such as xanthates, dialkyldithiophosphates, etc. In most cases, adding Reaflot-3790 alone or in combination with other collectors makes it possible to increase the recovery of copper, molybdenum, gold, and silver by 1-3% compared to standard treatments. We have proposed a hypothesis explaining the action of the new collector, including in combination with other collectors. Our research indicates the prospects of using Reaflot-3790 in the flotation of sulfide ores.

Keywords: Flotation, Collectors, Thioamide group, Sulfide ores.

INTRODUCTION

The practical application of reagents containing a thioamide group in the flotation of sulfide ores has its origins back in the 1950s when American researchers proposed to use the reagent Z-200, which is an O-isopropyl-N-ethylthionocarbamate, as a collector.

After the publication in the 1970s of theoretical studies on the action mechanism of nonionic collectors, including those containing a thioamide group [2, 10], a number of new collectors containing a thioamide group belonging to thionocarbamates and thiourea [1, 3, 4, 9] were developed and proposed for industrial applications.

Among thionocarbamates, O-isobutyl (butyl)-N-allylthionocarbamate is currently widespread. This reagent was proposed as a collector at the Mekhanobr Institute (USSR) in the late 1970s [11].

In furtherance of those studies, a thioamide group reagent was developed belonging to the class of thiourea derivatives with the general chemical formula R_1R_2NC (S) NH-$CH_2CH = CH_2$ [8]. The reagent with the above formula, where $R_1 – C_6H_5$, $R_2 – CH_3$ (1-phenyl-1-methyl-3-allylthiomocenine), was named Reaflot-3790.

EXPERIMENTAL

Flotation tests in the flotation of sulfide ores were conducted in the following conditions. Flotation of copper sandstone ores: ore grinding time to achieve a particle size of 65% passing -0.071 mm was 21 minutes, flotation included rougher (7 minutes)

[#] corresponding author: mekhanobror@gmail.com and scavenger (10 minutes) circuits. Reagent feed rate in the rougher and scavenger flotation was as follows, g/ton: potassium butyl xanthate (PBX) 45 + 30, sodium sulphide 36 + 0, machine oil 40 + 20, foaming agent OPSB 25 + 0.

Flotation of copper-pyrite ores: ore grinding time to achieve a particle class of 85% passing 0.071 mm was 20 minutes with addition of lime at 3.5 kg/ton with an activity of 56%. Grinding pH was 10.5, flotation pH was 10.3. Free CaO content was 120 g/m^3. Solids content was 27.5%. The flotation included rougher (2 min) and scavenger (2 min) circuits. Collector feed rate in rougher flotation was 36 g/ton and 16 g/ton in scavenger flotation.

Flotation of copper-molybdenum ores: ore grinding time to achieve a particle size of 80% passing -180 microns was 5 minutes 35 seconds. Spindle oil was fed into the mill at 2.5 g/ton. The flotation included rougher (2 min) and scavenger (10 min) circuits. The collector was fed to the rougher and scavenger flotation (see Table 3), the foaming agent was also fed to the rougher at 15 g/ton and scavenger at 9 g/ton. The flotation pH of 9.5 was regulated by the addition of lime.

Flotation of gold-bearing pyrite-arsenopyrite ores: ore grinding time to achieve a particle size of 80% passing 0.071 mm was 15 min. Coal flotation was carried out for 10 minutes, rougher flotation 7 minutes and scavenger flotation 14 minutes. The following reagents were used: collectors potassium butyl xanthate at 160 g/ton and Aero-8045 at 60 g/ton, as modifiers soda at 900 g/ton, liquid glass at 50 g/ton, copper sulfate at 200 g/ton, depressor A636 at 100 g/ton (standard experiment, Table 4). In the tests, Aero-8045 was replaced by Reaflot-3790 at a feed rate of 60 g/ton.

RESULTS AND DISCUSSION

In this study, we attempted to apply the existing industry experience when using thioamide group reagents, which include Reaflot-3790, both independently and in combination with other collectors, mainly in the flotation of copper ores.

Table 1 shows the flotation performance of commercially processed copper sandstone ores.

Table 1 The flotation performance of commercially processed copper sandstone ores

№ Experiment	Product	Mass Yield, Cu, %	Grade Cu, %	Recovery Cu, %
Standard, PBX 45+30 g/ton				
1	Bulk concentrate	9.3	9.01	87.3
Reaflot-3790, 45+30 g/ton				
2	Bulk concentrate	8.6	19.94	88.0
PBX 32+21 g/ton, Reaflot-3790 7+5 g/ton, sodium diisobutyldithiophosphate (SDTP) 6+4 g/ton				
3	Bulk concentrate	9.4	9.34	88.7
PBX 40+26 g/ton, Reaflot-3790 7+5 g/ton, SDTP 6+4 g/ton				
4	Bulk concentrate	8.6	10.34	89.5
PBX 32+21 g/ton, Reaflot-3790 13+9 g/ton				
5	Bulk concentrate	8.5	10.16	88.2

From Table 1, it follows that Reaflot-3790, at a similar feed rate, provides a slightly higher recovery of copper in comparison with xanthate and results in a copper concentrate with a higher copper grade (experiments 1 and 5). When replacing about 30% of the xanthate feed by Reaflot-3790 (experiment 2), the copper recovery slightly increases at a noticeably higher copper grade of the concentrate. When a small amount of sodium diisobutyldithiophosphate was introduced into the composition (experiment 3), the recovery of copper increased by almost 1.5%. Since in this composition, xanthate, being a strong collector, has a greater effect on the collecting performance of the composition, an increase in copper recovery could be expected with an increase in xanthate feed rate. Indeed, by increasing the feed rate of xanthate to 66 g/ton from 53 g/ton, an increase in copper recovery of over 2% was obtained (experiment 4).

A more detailed study of the effect of the feed rate of xanthate, Reaflot-3790, and sodium diisobutyldithiophosphate on this ore sample showed that the optimal recovery of copper and silver was achieved at a xanthate feed rate of 67 g/ton (or 88% of the optimal feed rate of xanthate at 76 g/ton), a Reaflot-3790 feed rate of 16 g/ton (21% of the xanthate feed rate), and a sodium diisobutyldithiophosphate feed rate of 7 g/ton (9% of the xanthate feed rate).

The results of Reaflot-3790 tests on copper-pyrite ore are shown in Table 2.

Table 2 The results of Reaflot-3790 tests on copper-pyrite ore

№ Experiment	Product	Mass Yield, Cu, %	Grade Cu, %	Recovery Cu, %	Collector
1	Bulk concentrate	3.48	7.58	90.10	PBX
2	Bulk concentrate	3.47	7.57	93.16	Reaflot-3790
3	Bulk concentrate	3.96	6.89	87.66	$C_4H_9OC(S)NHCH=CH_2$

From the data in Table 2, it follows that in the flotation of copper-pyrite ore, Reaflot-3790 floats copper minerals much better than butyl xanthate when producing a rougher copper concentrate of equal grade. For comparison, the flotation performance of the same ore using O-isobutyl-N-allylthionocarbamate is presented. In the flotation of this ore type, this reagent is a poorer collector compared to with xanthate and Reaflot-3790.

In the flotation of copper-molybdenum ores, based on the results of preliminary tests, it was decided to add as a collector a composition consisting of isobutyl xanthate 60% and Reaflot-3790 40% fed to the rougher and scavenger flotation. The use of this composition made it possible to significantly increase the recovery of copper and molybdenum into a rougher copper-molybdenum concentrate at a higher grade. At the same time, the recovery of gold, of which the ore contains a noticeable amount, improved (Table 3).

Currently, multiple gold deposits of the pyrite-arsenopyrite type are in operation in Russia and Kazakhstan. The most refractory are deposits of this type, containing carbonaceous inclusions. It was considered relevant to test Reaflot-3790 at one of such deposits in Kazakhstan. The ore has gold-pyrite-arsenopyrite associations of the vein-disseminated type and contains 1.5-22% pyrite and 3-15% arsenopyrite. The total content of carbon in the host rocks ranges from 0.3 to 26.5% and 2.5-6% in the ore zones. Carbon is represented by oxidized (carbonates) and reduced forms (graphite, bitumoids, shungite). The presence of carbon-containing impurities complicates both the flotation process and the subsequent upgrading of the gold concentrate (by cyanidation).

Table 3 Flotation of copper-molybdenum ores

Product	Yield, %	Grade			Recovery		
		Cu, %	Mo, %	Au, g/ton	Cu, %	Mo, %	Au, g/ton
Standard, PBX 4+2 g/ton							
Bulk concentrate	10.07	3.80	0.03	2.42	72.10	54.42	65.85
PBX 2.4+1.2 g/ton, Reaflot-3790 1.6+0.8 g/ton							
Bulk concentrate	10.79	4.4	0.04	2.41	76.94	64.73	70.74

The test results of a composition consisting of 73% xanthate and 27% Reaflot-3790 in the flotation of the specified ore are presented in Table 4.

Table 4 Flotation of gold-bearing pyrite-arsenopyrite ore

Product	Yield, %	Grade Au, g/ton	Grade C, %	Recovery		Effective concentration, %
				Au, %	C, %	
Standard test						
Carbon flotation concentrate	9.67	3.30	7.27	31.90	70.24	63.24
Rougher concentrate	7.81	16.75	6.12	51.68	19.8	
Bulk concentrate	19.50	16.62	4.54	80.12	36.59	
Scavenger tails	70.83	0.68	1.17	11.92	34.4	
Ore	100.0	4.04	2.42	100.0	100.0	
Reaflot 3790 test						
Carbon flotation concentrate	19.68	2.80	7.33	13.35	57.6	69.79
Rougher concentrate	8.43	36.55	2.05	74.69	6.0	
Bulk concentrate	15.66	21.76	2.29	82.58	14.29	
Scavenger tails	64.66	0.26	1.09	4.07	18.1	
Ore	100.0	4.13	2.51	100.0	100.0	

*Bulk concentrate = rougher concentrate + scavenger concentrate.

From Table 4, it follows that when using the composition of Reaflot-3790 and xanthate, not only the recovery of gold increases and the concentrate grade improves, but there is also a noticeable reduction in the recovery of carbon-containing impurities.

The experimental results obtained make it possible to explain the action of Reaflot-3790 both as a thioamide group reagent and in combination with xanthates and dialkyldithiophosphates as follows:

Reaflot-3790 attaches itself to the electrophilic surfaces of a copper mineral as an NH-acid due to the coordination by the mineral surface of lone electron pairs of sulfur and nitrogen in molecular or ionic form, hydrophobizing the mineral surface and, accordingly, improving its floatability.

According to our measurements, the protolytic dissociation constant of the reagent is $Ka = 1.82 \times 10^{-11}$ ($pKa = 10.74$). Thus, in a pH range of 9.74-10.74, it is dissociated and represented by the ionic form by 10% and 50%, which should actively bind to the surface of the mineral. In addition, the formation of an ionic form on the surface of the copper mineral is favored by the presence in the Reaflot-3790 molecule of an electron-accepting substituent $–CH_2CH=CH_2$, which polarizes the N–H bond, strengthening the acidic properties of the group.

The ionic form of this reagent on the mineral surface is more conducive to hydrophobization of the mineral surface than the molecular form.

The peculiarity of the action of this reagent in a combination with xanthates and dialkyldithiophosphates, which make a predominant contribution to the process of hydrophobization of the mineral surface, is manifested as follows. In addition to the ionic form, which competes with xanthogenates and dialkyldithiophosphates, Reaflot-3790 can bind to the electrophilic areas of the copper mineral surface also in its molecular form without counterion displacement even by the weak electrophilic centers of the copper mineral surface [2]. Xanthogenates and dialkyldithiophosphates cannot bind to such centers, since the necessary prerequisite for this is the displacement of the counterion. Consequently, this collector, when interacting with the surface of a copper mineral, employs additional adsorption centers in comparison with the action of ionic collectors. The action of dialkyldithiophosphate deserves a separate discussion. Dialkyldithiophosphate, by hydrophobizing the mineral surface, unlike xanthate and thioamide group reagents, has a noticeable surface activity at the liquid-gas interface. As a result, when an air bubble collides with a mineral particle containing dialkyldithiophosphate on its surface, some of the reagent can migrate from the surface of the mineral to the surface of the bubble. This causes a decrease in the surface tension at the liquid-gas interface over the entire area of the bubble, which strengthens the bubble-particle contact [5-7]. On the other hand, the surface-active properties of dialkydithiophosphates contribute to an increase in the rate of convergence of an air bubble with a mineral particle, which leads to an improvement in the flotation performance of fine particles – this is well-known from the practice of using these reagents – and in some cases contributes to an increase in the flotation rate [7].

CONCLUSIONS

A new thioamide group collector was proposed, which, either alone or in combination with other collectors, makes it possible to increase the recovery of copper, molybdenum, and gold in the flotation of sulfide ores.

REFERENCES

1. Ackerman, P.K., Harris, G.H., Klimpel, R.R. et al. (1984) Effect of alkyl substituents on performance of thionocarbamates as copper sulphide and pyrite collectors. Reagents Miner. Ind. Pap. Conf., Rome, 18-21 Sept., London.
2. Bogdanov, O.S., Podnek, A.K., Ryaboi, V.I. et al. (1977) Reagents chemisorption on minerals as a process of formation of surface compounds with a coordination bond. Proceeding of the XII International Minerals Congress, Sao Paulo, Brazil.
3. Nagaraj, D. R. (1985) Process for the flotation of base metal sulfide minerals in acid, neutral or mildly alkaline circuits. U.S. Patent№US4556482A.
4. Fairthorne, G., Fornasiero, D., Ralston, J. (1996) Solution properties of thionocarbamate collectors. Int. Miner. Process, 46 (1-2), 137-153.
5. Kondratyev, S.A. (2010) Estimation of Reagents-Collectors Flotation Activity. [In Russian]. Obogashenie rud, №4, 24-30.
6. Kondratyev, S.A., Moshkin, N.P. Assessment of the Collective Force of Flotation Reagents. Journal of Mining Science, 51, 150-156.
7. Kondratyev, S.A., Ryaboy, V.I. (2016) Influence of Desorbed Species of Xanthates and Dialkyldithiophosphates on their Collecting Ability. XXVIII International Minerals Processing Congress, Quebec, Canada, 133.
8. Kretov, V.P., Levkovets, S.E., Ryaboy, V.I., Ryaboy, I.V. (2019) The collector reagent composition for the flotation of sulfide ores. Eurasian Patent №. 031517. [In Russian].
9. Liu, G., Zhong, H., Dai, T., Xia, L. (2008) Investigation of the effect of N-substituents on performance of thionocarbamates as selective collectors for copper sulfides by ab inito calculations. Min. Eng., 21, 1050-1054.
10. Ryaboi, V.I. (1981) About the possibility of dative π- link in interoperation of thionocarbamates with copper and chalcopyrite [In Russian]. Physical Chemistry Journal, Volume LV, № 4, 982-985.
11. Uryev, G.G., Ryaboy, V.I., Starovoitov, M.K. (1979) Sulfide ore flotation collector. USSR inventor certificate no. 83326, issued February 2, 1981, priority date October 25. [In Russian].

XIV International Mineral Processing and Recycling Conference
Belgrade, Serbia, 12-14 May 2021

EFFECT OF SULPHATE IN MINING-PROCESS WATER ON SULPHIDE FLOTATION

Maria Sinche-Gonzalez[1#], Daniel Fornasiero[2]
[1] University of Oulu, Oulu Mining School, Oulu, Finland
[2] University of South Australia, Future Industries Institute, Australia

ABSTRACT – A high concentration of sulphate ions is usually found in mining-process waters, their effect on the flotation of copper, molybdenum and zinc sulphides were investigated in single minerals and complex ores experiments with complementary mineral surface analysis (XPS) and particle-bubble detachment force studies.

The negative effect of sulphate in water is attributed to the change in the characteristics of the pulp solution, decrement of the strength of adhesion, adsorption of sulphate ions or formed saturated sulphate-complexes and/or hydrophilic species (such as MoO_2 and SO_3^{2-}) onto the mineral surface competing with or inhibiting collector adsorption, and diminish the effect of depressants reagents.

Keywords: Sulphate Ions, Sulphides Flotation, Mining-Process Water.

INTRODUCTION

Water quality is important in mineral processing operations as it may impact on mineral recovery and separation and the discharge of used water into the environment [1-6]. Water used in processing plants comes from various sources such as fresh water, bore and surface waters, waters from industrial wastewaters but also from recycled waters from tailing dam, which all affect water quality [7-9]. Recycled waters contain sulphur-ions mostly those are in the form of sulphate and thiosulphate [2,10]. At difference of other ions present in water, sulphate content accumulates and can reach appreciable concentration >1,500-12,000 mg/L [8,9]. The use reagents in mineral processing plant also contribute to the sulphate content in water [1].

The sulphate concentration can build up to high levels that may have an important harmful bearing on the mineral beneficiation altering for example, froth stability and surface chemistry of minerals [11] and/or considerable change in the pulp solution [12]. Furthermore, different ions react differently with sulphate, forming soluble and insoluble complexes [13] and may cause various kinds of problems in mineral treatment depending on concentration and associated species such as adsorption, depression, activation, others [14]. Also, sulphate ion is particularly the main contributor to so-called 'water mineralization'; thereby it increases the conductivity [13], decrease the pH [15], increase in dissolution of mineral [16,17]. Also, when the solution is saturated with sulphate ions depending on other conditions may happen both, (i) increase of the potential leading to increase in the collector uptake [18] or (ii) decrease the pulp potential lower than the potential of the adsorption of xanthate imposing the electrochemical mechanism

---

[#] corresponding author: maria.sinchegonzalez@oulu.fi collector-particle and depression effect on sulphide minerals such as in a Cu-Pb-Zn ore [2].

Strong evidence of increased sulphide mineral oxidation, formation/precipitation of metal sulphate and replacement of collectors by sulphate ions at the mineral surface, which all result in decreased surface hydrophobicity [19,20] and therefore depression of mineral flotation at high sulphate ion concentrations.

EXPERIMENTAL

Materials

Two single minerals, chalcopyrite (Cp) and molybdenite (MoS_2), and two complex ores (Cu-Mo and Cu-Zn) were used for testing. The chalcopyrite ($CuFeS_2$) sample contains Cu 30.1%, Fe 29.4%, and S 32.1% and particles +38-75 µm were used in kinetic flotation tests. The molybdenite sample contains Mo 56.9% and MoS_2 > 95% it was cleaned (with n-propyl bromide >93%) and sieved to retain only the coarse particles >150 µm. The Cu-Mo ore contains $CuFeS_2$ 2.27% and MoS_2 0.02% (0.7% Cu, 0.01% Mo). The Cu-Zn ore contains $CuFeS_2$ 1.75% and sphalerite (ZnS) 3.247% as main valuable minerals (Cu 0.79%, Zn 2.19%).

Flotation tests with single minerals of Cu and Mo

Five grams of sample was floated using sodium isopropyl xanthate (SIPX) or diesel oil used as collectors (7 g/t) for chalcopyrite and molybdenite, respectively. Methyl isopropyl carbinol (MIBC 15 g/t) was used as a frother, prepared as a dilute solution (1%) conditioning times were 2 and 1 min respectively. Sulphates of potassium and calcium (K_2SO_4; $CaSO_4$) were used in flotation experiments at a concentration of 10^{-4}, 10^{-3}, 10^{-2} molar (M). All reagents were analytical grade. The pH 10 of the pulp was controlled with NaOH. Four concentrates were collected at times of 1, 3, 5 and 8 min (cumulative). Flotation tests were carried out in duplicate and averaged recoveries were calculated. A 1st order rate equation was used to fit the recovery versus flotation time data to extract the parameters of maximum recovery, R_{max}, and flotation rate constant, k.

Flotation of a complex Cu-Mo and Cu-Zn ores

Kinetic flotation tests were conducted following the standard flotation procedures of source plant operations and using water with sulphate concentrations of 10^{-2} M (960 mg/L) and $2.1\cdot10^{-2}$ M (2,000 mg/L). Three concentrates were collected at flotation times of 2, 6 and 15 min.

The Cu-Mo ore a rougher bulk Cu-Mo was floated and with the ore Cu-Zn, rougher Cu kinetic flotation tests were conducted (with Zn depression) testing also tap water with sulphate $0.4\cdot10^{-2}$ M (250 mg/L).

X-ray photoelectron spectroscopy (XPS)

The surface chemical composition of Cp and MoS_2 samples was determined by XPS using an X-ray photoelectron spectrometer (Kratos Axis Ultra DLD) at Al Kα source (1486.6 eV) operated at 130 W. The XPS spectra curve was fitted with CasaXPS program.

Detachment force measurement

Samples of chalcopyrite and molybdenite with size fraction 350-425 µm were used. The critical amplitude of vibration for the detachment of particles from a 2 mm bubble was measured with a loudspeaker apparatus connected to an audio signal generator and the program Sine 30 following the procedure of Xu et al. [21], at a fixed frequency of 50 Hz. The experiment was repeated ten times for the same particle and with five different particles. The force required for particle-bubble detachment ($F_{det,\ max}$) can be calculated using Eq. 1 [22].

$$F_{det,\ max} = F_{v,\ max} + F_g \qquad (1)$$

where: $F_{v,\ max}$ is the maximum vibrational force for the detachment of particles and F_g is the particle immersed gravity force.

$$F_{v,\ max} = A \cdot m \cdot (2\pi \cdot f)^2 \qquad (2)$$

where: m is the particle mass, A the amplitude and f the frequency of vibration.

RESULTS AND DISCUSSION

Results of flotation tests with increasing concentration of K_2SO_4 (0, 10^{-4}, 10^{-3}, 10^{-2} M) are showed in Figure 1 for chalcopyrite and molybdenite. The recovery of molybdenite is more affected by sulphate addition than recovery of chalcopyrite. It is only at 10^{-2} M K_2SO_4 that a decrease in chalcopyrite recovery is observed, although there is a constant decrease in the flotation rate constant (k) from 0.7 min^{-1} (no K_2SO_4) to 0.3 min^{-1} (10^{-2} M K_2SO_4) as shown in Table 1. Molybdenite flotation is more sensitive to the presence of K_2SO_4 as both its flotation recovery (after 8 min) and k decrease gradually from 71% and 0.6 min^{-1}, respectively with no K_2SO_4 down to 45% and 0.2 min^{-1} at 10^{-2} M K_2SO_4. These flotation results confirm a previous observation that the flotation of molybdenite is more affected by changes in water quality than chalcopyrite [5].

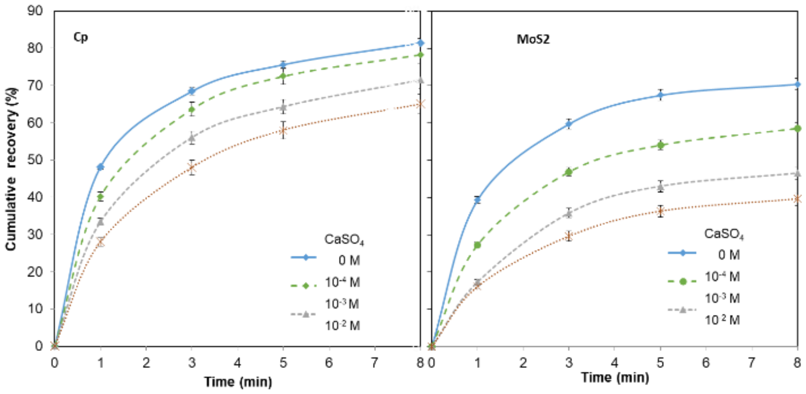

Figure 1 Effect of potassium sulphate concentration on chalcopyrite (SIPX = 7 g/t) and molybdenite recovery (diesel oil = 7 g/t) at pH=9.3 ($[KNO_3]$ = 10^{-2} M)

A larger decrease in flotation recoveries was observed when potassium sulphate was replaced with calcium sulphate in Table 1; calcium sulphate ($CaSO_4$) is generally found in recycled process water when lime is added to increase the pH. Similar results were found by Li et al. [23] for molybdenite as they reported that addition of sodium sulphate, potassium sulphate or calcium sulphate all depressed molybdenite flotation in alkaline pH conditions. However, it was reported that sodium sulphate (0-10^{-2} M) had no or little effect on chalcopyrite flotation [4].

Calcium sulphate has the same mechanism of depression of flotation than metal hydroxides that reduce hydrophobicity of the mineral due to their precipitation as a thin layer (slime coating) and adsorption on the mineral surface, which also affects xanthate adsorption [24].

Table 1 Effect of K_2SO_4 and $CaSO_4$ on chalcopyrite and molybdenite recovery at 8 min and flotation rate constant (k)

K_2SO_4	Chalcopyrite		Molybdenite		$CaSO_4$	Chalcopyrite		Molybdenite	
(M)	Rec (%)	k (min^{-1})	Rec (%)	k (min^{-1})	(M)	Rec (%)	k (min^{-1})	Rec (%)	k (min^{-1})
0	82 ± 1	0.7	70 ± 2	0.6	0	82 ± 1	0.7	70 ± 2	0.6
10^{-4}	82 ± 2	0.6	64 ± 3	0.5	10^{-4}	78± 2	0.5	59 ± 2	0.3
10^{-5}	81 ± 2	0.4	53 ± 3	0.4	10^{-5}	71± 2	0.4	47 ± 2	0.2
10^{-6}	75 ± 4	0.3	45 ± 5	0.2	10^{-6}	65 ± 2	0.3	40 ± 2	0.2

Particle-bubble adhesion force

Results of the particle-bubble detachment force experiments are shown in Figure 2 for (a) chalcopyrite and (b) molybdenite particles (350-425 µm), respectively.

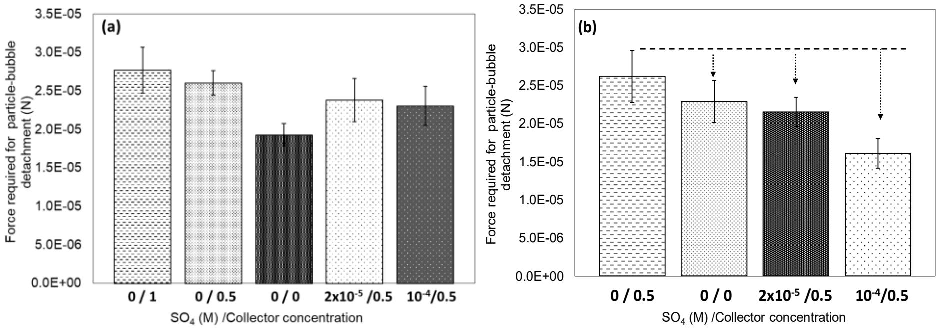

Figure 2 Force required for the detachment of (a) chalcopyrite and (b) molybdenite particles from bubbles as a function of collector and sulphate ion concentration at pH 9.3 (for Cp ‘0.5’ and ‘1’ refer to 3.5 and 7 g/t SIPX, and for MoS_2 ‘0.5’ refers to 3.5 g/t diesel oil)

It was found that the force required for particle-bubble detachment increases with increasing collector concentration, which indicates that the particle-bubble adhesion is stronger when the particle surface is made more hydrophobic after collector adsorption.

On the contrary, the addition of 10^{-4} M K_2SO_4 decreases substantially the force required to detach the molybdenite particles, which indicates that the particle-bubble adhesion is weaker as a result of the molybdenite surface becoming less hydrophobic. As for chalcopyrite, K_2SO_4 addition has no effect (within experimental error) on the force required for its detachment from the bubble, in agreement with the trends observed in the flotation results in Figure 1.

XPS study of molybdenite and chalcopyrite in the presence of K_2SO_4

X-ray photoelectron spectroscopy (XPS) identified species responsible for the decrease in surface hydrophobicity after K_2SO_4 addition and explain the flotation results. The proportions of elements (C, O, Mo and S) on the surface of molybdenite particles collected just before frother addition are shown in Table 2. The results indicate that the proportion of carbon (contribution from hydrocarbon contamination and collector) at the surface remains almost constant, within experimental error, after K_2SO_4 addition but that of oxygen increases while that of molybdenum and sulphur decreases. This is not the case for chalcopyrite where the proportion of these elements on the chalcopyrite surface remains almost constant after K_2SO_4 addition within experimental error.

Table 2 Concentration (atomic %) of the elements measured on the chalcopyrite and molybdenite surface by XPS without and with 10^{-4} M K_2SO_4 addition

Element	Chalcopyrite		Molybdenite	
	no K_2SO_4	with K_2SO_4	no K_2SO_4	with K_2SO_4
C 1s	27	26	27	29
O 1s	31	31	23	30
S 2p	24	25	29	24
Mo 3d			21	17
Cu 2p	11	12		
Fe 2p	6	6		

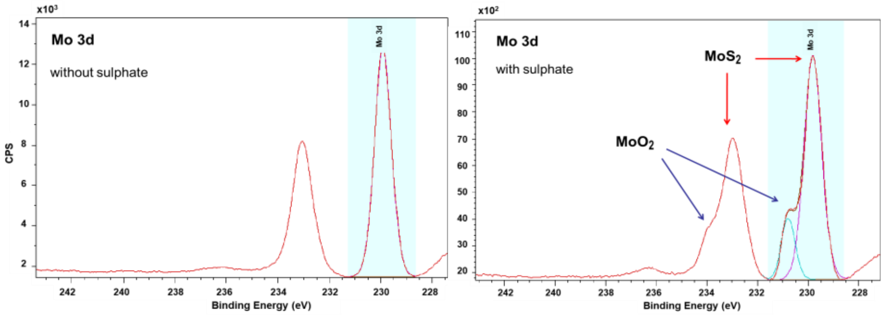

Figure 3 Mo 2p XPS spectra of molybdenite conditioned at pH 9.3 without (left) and with (right) 10^{-4} M K_2SO_4

Detailed information on the type of surface species can be extracted from the XPS spectra by deconvoluting each spectrum into components [25]. The most significant results are shown in the Mo 3d spectrum of molybdenite in Figure 3 presents two peaks, the main peak (Mo 3d5/2) at 229.9 eV and the other (Mo 3d3/2) of lower intensity at 233 eV. They are both attributed to MoS_2. In the presence of potassium sulphate, two new peaks/shoulders appear at 230.57 eV and 234 eV on the high energy side of the two Mo 3d peaks; they are attributed to MoO_2 [26].

The S 2p spectrum of molybdenite in Figure 4 is typical of that for metal sulphide and is composed of two peaks (doublet) separated by around 1.2 eV and with the intensity of the low binding energy peak (S 2p5/2) double that of the high binding energy peak (S 2p1/2) [27]. The position of the peak for sulphide (S^{2-}) in MoS_2 at 162.7 eV agrees with literature values for molybdenite at 162.0-162.8 eV (Gerson and Bredow, 2000; Von Oertzen et al., 2006). In the presence of potassium sulphate, two new doublets appear at higher binding energies; they are attributed to polysulphide, Sn^{2-} (163-164 eV) and sulphite, SO_3^{2-} (~166 eV). No sulphate peak at 169 eV was observed in the S 2p spectra in Figure 6 [26].

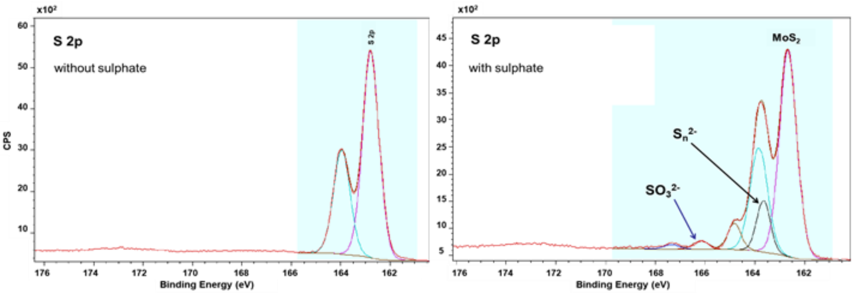

Figure 4 S 2p XPS spectra of molybdenite conditioned at pH 9.3 without (left) and with (right) 10^{-4} M K_2SO_4

Potassium sulphate addition didn't produce significant changes in the surface of chalcopyrite. The XPS analysis of molybdenite (Table 2 and Figures 3 and 4) indicates that its surface becomes oxidised after addition of potassium sulphate, with the formation of polysulphide (Sn^{2-}) and more oxygen species on its surface as MoO_2 and sulphite, SO_3^{2-}.

These surface oxidation species detected on the molybdenite surface confirm that sulphate ions promote the oxidation of molybdenite [20] and can explain the decrease in particle-bubble adhesion and recovery of molybdenite observed in Figure 2 and Figure 1, respectively after potassium sulphate addition. These oxidation species may also prevent collector adsorption on molybdenite. Indeed, an infrared study has shown that less xanthate collector is observed on the galena surface in the presence of sulphate in water [19].

Effect of sulphate on the flotation of Cu-Mo ore

Results in Table 3 show that the flotation of Cu minerals is not affected by the presence of sulphate as its recovery remains high and constant (94%). This is not the case for molybdenite which recovery decreased. The grade of these elements all decreased, other minerals (pyrite, quartz, clays) reported to the concentrate (as mass recovery increases with sulphate concentration) by entrainment or/and because of copper activation. Results corroborated the negative effect of sulphate mainly in molybdenite in single mineral experiments.

Table 3 Effect of sulphate concentration in Cu-Mo ore, pH 10.5

SO_4 concentration (M)	Grade			Recovery %			Mass recovery %		
	Cu %	Mo ppm	Fe %	Cu	Mo	Fe	2 min	6 min	15 min
0	3.4	521	7.8	94	75	40	6.6	11.8	19.5
10^{-2} (960 mg/L)	3.1	439	6.6	94	74	43	6.5	11.9	22.1
$2.1 \cdot 10^{-2}$ (2,000 mg/L)	2.9	319	6.5	94	72	48	6	11.3	22.7

Effect of sulphate on the flotation of Cu-Zn ore

Figure 5 depicts the cumulative recoveries and grades for Cu which is decreased with an increasing amount of sulphate in water (after 3, 8 and 15 minutes of flotation). There is a gradual decrease in recovery and grade of Cu (from left to right) with increasing sulphate concentration. The right figure shows the increment of grade and recovery of Zn (that should be depressed) with increasing sulphate concentration (left to right). It evidences that the depressant effect of the $ZnSO_4$ for Zn has been blinded and there is activation of sphalerite and gangue minerals diluting the concentrate affecting the selectivity and those increased the mass recovery.

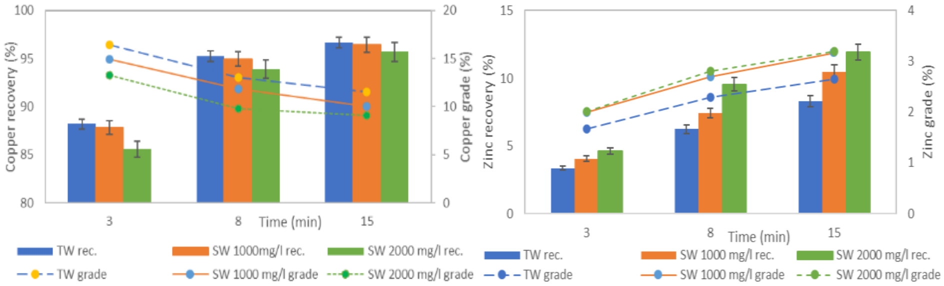

Figure 5 Recovery and grade of Cu (left) and Zn (right) with sulphate $2.6 \cdot 10^{-4}$ M, 10^{-2} M and $2.1 \cdot 10^{-2}$ M in water, pH 11

Results indicate that depression of sphalerite is prevented by sulphate and possibly reactions with Cu-ions increasing collector adsorption.

Table 4 shows the natural pH of water with sulphate ~250 mg/L, 1,000 mg/L and 2,000 mg/L and the amount of lime added to increase the pH from the natural value to pH 11.8, the pH used in the flotation experiments. Results show that increasing sulphate concentration causes acidification of the pulp solution and therefore more lime was required to reach the required pH.

As it was mentioned earlier, sulphate addition promotes the dissolution/oxidation of sulphide minerals [20], which may explain this acidification of the solution. Furthermore, dissolution/oxidation of chalcopyrite (Eq. 3) may promote the copper-activation of sphalerite, pyrite and quartz resulting in the increased recovery of these three minerals [30–32].

$$CuFeS_2 + \frac{17}{4}O_2 + \frac{9}{2}H_2O \leftrightarrow Cu(OH)_2 + Fe(OH)_3 + 2H_2OSO_4 \qquad (3)$$

Table 4 Total amount of lime for each flotation test

Test	250 mg/L SO_4	1,000 mg/L SO_4	2,000 mg/L SO_4
pH natural	8.6	6.1	5.85
Total lime g/t	4,142	5,110	5,193

CONCLUSIONS

Sulphate ions are found in high concentrations (> 1,500 mg/L) in mining-process water and have specific effect on the flotation of sulphide minerals.

Increasing concentration of sulphate negatively affects the recovery and grade of Mo. It may decrease those of Cu. It activates the flotation of Zn and gangues.

Detachment test confirmed the negative effect of sulphate by the decrement of adhesion of the particles-bubbles aggregates.

XPS analysis confirms that even a small concentration of sulphate (10^{-4} M) can promote the formation of more oxidized species

Sulphate ions easily attach to some ions such as calcium (from the use of lime) forming calcium sulphate which will precipitate on the mineral surface reducing hydrophobicity of the mineral due to thin layer coating and adsorption on the mineral surface, which also affects xanthate adsorption.

The effect in depressor reagents such as $ZnSO_4$ for Zn could be blinded when sulphate concentration increase.

Gangue minerals recovery increase at higher SO_4 concentration (2,000 mg/L), diluting the concentrate affecting the selectivity.

The effect of sulphate in flotation of sulphide minerals indicates the necessity to treat high sulphate containing waters (> 1,500 mg/L) particularly if the water is recycled to the process plant. Results also indicated that possible sulphate limit (> 1,000 mg/L) can be found where certain recoveries and grades are more influenced by sulphate.

The negative effect of sulphate is when water is more saturated and the effects of its increasing concentration could be summarized (i) sulphate may react with the mineral surface decreasing hydrophobicity, (ii) a strong bond is generated between sulphate ions and the mineral surfaces, inhibiting collector adsorption, (iii) sulphate and complex with species in the water and acts as an inorganic ligand (iv) it may be in the form of localized particle colloids precipitating or continuous reacting (v) sulphate may adsorb in valuable sulphides, (vi) it diminishes the effect of depressants such as $ZnSO_4$ (vii) it has depressing capability in alkaline condition via chemical adsorption of an ionic bond.

The action of sulphate is sensitive to the type of the sulphide mineral and type of used collector and cannot be generalized its effect. Complex ores and associated gangue minerals make the evaluation of sulphate more difficult, and therefore, further research is needed for specific sulphide minerals.

ACKNOWLEDGEMENT

The authors thank the funds provided by K. H. Renlund Foundation.

REFERENCES

1. Broman, P.G. (1980) Water reuse at sulphide ore concentrators in Sweden: practice,

experience and current developments. In Complex Sulphide Ores. 28-39.

2. Biçak, Ö., Ekmekçi, Z., Can, M., Öztürk, Y. (2012) The effect of water chemistry on froth stability and surface chemistry of the flotation of a Cu-Zn sulfide ore. Int. J. Miner. Process., 102–103, 32-37.
3. Chen, J.M., Liu, R.Q., Sun, W., Qiu G.Z. (2009) Effect of mineral processing wastewater on flotation of sulfide minerals. Trans. Nonferrous Met. Soc. China (English Ed., 19 (2), 454-457.
4. Ikumapayi, F., Rao, K.H. (2015) Recycling process water in complex sulfide ore flotation: Effect of calcium and sulfate on sulfide minerals recovery. Miner. Process. Extr. Metall. Rev.
5. Sinche-Gonzalez, M., Fornasiero, D., Zanin, M. (2016) Flotation of chalcopyrite and molybdenite in the presence of organics in water. Minerals, 6 (4).
6. Castro, S. (2018) Physico-chemical factors in flotation of Cu-Mo-Fe ores with seawater: A critical review. Physicochem. Probl. Miner. Process.
7. Fisher, W., Rudy, S. (1976) Municipal waste water utilization for froth flotation of copper and molybdenum sulfides. Soc. Min. Eng. AIME, 264, 698-1702.
8. Levay, G., Smart, R.S.C., Skinner, W.M. (2001) The impact of water quality on flotation performance. J. South African Inst. Min. Metall., 101 (2), 69-75.
9. Levay, G., Schumann, R. (2006) A systematic approach to water quality management in the minerals processing industry. . In Australasian Institute of Mining and Metallurgy Publication Series. 277-287.
10. Barskii, L.A., Rybas, V. V., Fat'yanova, M.A., Ponomarev, G.P. (1986) Influence of sulfur-containing ions on selective flotation of copper-nickel ores. Sov. Min. Sci.
11. Sinche-Gonzalez, M. (2014) The influence of recycled process water quality on the flotation of copper and molybdenum sulphide flotation. Available at: https://find.library.unisa.edu.au/.
12. Glembotskii, V.A., Klassen, V.I., Plaksin, I.N. (1963) Flotation. Tsvetnye Metally, New York.
13. Silva, R., Cadorin, L., Rubio, J. (2010) Sulphate ions removal from an aqueous solution: I. Co-precipitation with hydrolysed aluminum-bearing salts. Miner. Eng.
14. Morris, M.E., Levy, G. (1983) Absorption of sulfate from orally administered magnesium sulfate in man. Clin. Toxicol.
15. Sinche-Gonzalez, M., Mollehuara-Canales, R. (2020) Sulphate removal from mining-process water by capacitive deionization. Inżynieria Miner., 2 (1), 189-194.
16. Eric, Forssberg, K.S., Subrahmanyam, T. V., Nilsson, L.K. (1993) Influence of grinding method on complex sulphide ore flotation: a pilot plant study. Int. J. Miner. Process.
17. Kirjavainen, V., Schreithofer, N., Heiskanen, K. (2002) Effect of calcium and thiosulfate ions on flotation selectivity of nickel-copper ores. Miner. Eng., 15 (1-2), 1-5.
18. Barskii, L.A., Rybas, V., Fat'yanova, M., Ponomarev, G.P. (1985) Influence of sulfur-containg ions on selective flotation of copper-nickel ores. Sov. Min., 22 (4), 310-316.
19. Ikumapayi, F., Makitalo, M., Johansson, B., Rao, K.H. (2012) Recycling of process water in sulphide flotation: Effect of calcium and sulphate ions on flotation of galena. Miner. Eng., 39, 77-88.
20. Li, Y., Lartey, C., Song, S., Li, Y., Gerson, A.R. (2018) The fundamental roles of monovalent and divalent cations with sulfates on molybdenite flotation in the

absence of flotation reagents. RSC Adv.

21. Xu, D., Wang, W., Ametov, I., Fornasiero, D., Grano, S. (2010) The detachment of coarse, composite particles from bubbles. In XXV International Mineral Processing Congress 2010, IMPC 2010.
22. Cheng, T.W., Holtham, P.N. (1995) The particle detachment process in flotation. Miner. Eng.
23. Li, M.Y., Wei, D.Z., Shen, Y.B., Liu, W.G., Gao, S.L., Liang, G.Q. (2015) Selective depression effect in flotation separation of copper-molybdenum sulfides using 2,3-disulfanylbutanedioic acid. Trans. Nonferrous Met. Soc. China (English Ed., 25 (9), 3126–3132.
24. Wu, C.H., Kuo, C.Y., Lin, C.F., Lo, S.L. (2002) Modeling competitive adsorption of molybdate, sulfate, selenate, and selenite using a Freundlich-type multi-component isotherm. Chemosphere.
25. Fairthorne, G., Fornasiero, D., Ralston, J. (1997) Effect of oxidation on the collectorless flotation of chalcopyrite. Int. J. Miner. Process., 49, 31-48.
26. Wagner, C.D. (1990) Photoelectron and Auger energies and the Auger parameter: a data set. . In Practical Surface Analysis (C. Wiley, ed)., 595-634.
27. Buckley, A.N., & Woods, R. (1984) An X-Ray photoelectron spectroscopic study of the oxidation of chalcopyrite. Aust. J. Chem. doi:10.1071/CH9842403.
28. Gerson, A.R., & Bredow, T. (2000) Interpretation of sulphur 2p XPS spectra in sulfide minerals by means of ab initio calculations. Surf. Interface Anal. doi:10.1002/(SICI)1096-9918(200002)29:2<145::AID-SIA727>3.0.CO;2-N.
29. Oertzen, G.U., Von, Harmer, S.L., & Skinner, W.M. (2006) XPS and ab initio calculation of surface states of sulfide minerals: pyrite, chalcopyrite and molybdenite. Mol. Simul., 32 (15), 1207–1212. doi:10.1080/08927020601081616.
30. Bushell, C.H., & Krauss, C.J. (1962) Copper activation of Pyrite. Bull. Can. Inst. Min. Met., (55), 314–318.
31. Voigt, S., Szargan, R., & Suoninen, E. (1994) Interaction of copper(II) ions with pyrite and its influence on ethyl xanthate adsorption. Surf. Interface Anal. doi:10.1002/sia.740210804.
32. Fornasiero, D., & Ralston, J. (2005) Cu(II) and Ni(II) activation in the flotation of quartz, lizardite and chlorite. Int. J. Miner. Process. doi:10.1016/j.minpro.2004.12.002.

XIV International Mineral Processing and Recycling Conference
Belgrade, Serbia, 12-14 May 2021

FROTH FLOTATION STUDIES FOR BENEFICIATION OF ESTONIAN PHOSPHATE ROCK

Kadriann Tamm[1,2#], Zeinab Arab Zadeh[1], Xiaosheng Yang[3]
[1] Tallinn University of Technology, Laboratory of Inorganic Materials, Tallinn, Estonia
[2] Geological Survey of Estonia, Department of Geological Resources, Rakvere, Estonia
[3] GTK Mintec, Outokumpu, Finland

ABSTRACT – Estonia holds the largest phosphate rock reserves in the EU. Estonian deposit is a sandstone that holds the remains of phosphatic brachiopod shells and compared to other sedimentary rocks contains low Cd (up to 5 ppm), low trace of U (~50 ppm), and a valuable amount of REEs. The distribution of the main minerals between slimes, tailings and concentrates was obtained and the relationships between the grades and recovery was calculated. The best result in the concentrates with 35.56wt.% of P_2O_5 and 86.46% recovery rate was obtained by using the reverse flotation process with Custamine 1205 as the collector.

Keywords: Flotation and Surface Chemistry Processes, Flotation Reagents, Flotation Technology.

INTRODUCTION

Estonian phosphate rock is a typical shelly phosphorite that occurs at the Upper Cambrian/Lower Ordovician boundary (Kallavere Formation). The basic rock-forming minerals are quartz and biogenic phosphate (Francolite apatite following formula is a common way to present the chemical formula: Ca10-x-yNaxMgy(PO$_4$)6-z(CO$_3$)zF0.4zF) originated from remnants of brachiopods in association of calcite, gypsum, potassium feldspar, glauconite, and ferrous hydroxides) which occur in insignificant amounts. To a lesser extent, Estonian phosphorite also contains pyrite and dolomite. These matrix sandstones often show a well-developed, small scale, randomly oriented cross bedding with individual bed sets about 20-30 cm thickness [1]. The proportion of these minerals varies with layers and deposits.

The available data indicate that the main phosphorus-bearing layers are sand and shellfish, which contain 9-13 wt.% P_2O_5, 13-18 wt.% CaO, 55-62 wt.% SiO_2, 1-2 wt.% pyrite, 1-2 wt.% iron oxides, 1.3-1.7 wt.% CO_2, 0.36-1.01 wt.% F, 20-28 ppm uranium, and about 0.2 wt.% organic carbon [2].

The shell contains between 33.67-35.45% and 46.16-51.5% of P_2O_5 and CaO, respectively. At the same time, the CO_2 content increases to 2.22-4.70% and the silicon content decreases to 0.50-2.0% [3].

Cadmium (Cd) is one of the trace elements highly enriched in phosphate rocks. Sedimentary phosphate rocks that were under the investigation from various locations

---

[#] corresponding author: kadriann.tamm@taltech.ee in the world show that generally the content of the Cd is between 3-150 mg/kg. While igneous deposits are typically less in Cd content [4].

One of the most important advantages of Estonian phosphate rock is its remarkable low content of Cd which is up to 5 mg/kg. The Cd content in phosphate rocks in the United States, Morocco, Russia, and China (Yunam deposit) is up to 185, 165, 13, and 4 respectively [5]. The Cd concentration is reduced by use of sulfide salt which results in the precipitation of Cd following by the separation of the solid phase in filtration stage [6].

Cd concentration plays a vital role in determining the quality of phosphate resources which does not have any critical limit, because the maximum allowable concentration depends largely on soil characteristics, water quality, crop type, etc. [5].

Uranium (U) is one of the strategic elements in phosphate rock. Israel, Morocco, and Egypt deposits contain 120, 97, and 90 mg/kg of U. The content of the U in Estonian phosphate rock is up to 50 mg/kg which can be a source of nuclear energy in the European Union [7].

Currently, the beneficiation process along with wet process for Estonian phosphate rock is mainly conducted in laboratory scale. Considering at least 30 years gap, research in this field needs to recommence to re-assess the economic, technological, and environmental challenges for processing Estonian phosphorite. In 2018, with the governmental support for further scoping studies, innovative thermal process has been evaluated to produce high-grade phosphoric. Among the technological challenges, preliminary beneficiation from low level (5-20%) to the marketable grade (28-32%) is the critical one. Reverse flotation was found to be the most efficient processes to upgrade the phosphate level in Estonian phosphorite [8] which is currently under investigation.

This study investigates the experimental and functional information by studying the mineral characteristics of the Ülgase deposit-northern Estonia phosphate rock and its performance under two variables in flotation processes, namely flotation time and collector dosage. The flotation experiments were conducted in GTK Mintec Laboratory in Finland and chemical characterization and data analysis were done in Tallinn University of Technology, Estonia.

The focus is mainly on the chemical characteristics of products; recovery and grade, as well as particle size analysis to find an optimum flotation process for Estonian phosphate rock enrichment that can be used for further studies and the process simulation and modelling of the beneficiation of Estonian phosphate rock.

To achieve the above-mentioned aims the following objectives were examined: (i) investigation on the effect of flotation rate and collector's dosage in liberation of the main minerals (quartz and apatite); (ii) screening of the tailings and concentrates into three distinct fractions followed by particle size distribution measurement; (ii) analysis of the samples by XRF, chemical analysis, and XRD; (iv) data processing and visualization that can be utilized to identify the suitable and optimized condition of modelling the flotation of the Estonian phosphate rock.

MATERIALS AND METHODS

10 different flotation tests from 6 to 14 minutes as the flotation time, and 400 to 800 g/t Custamine 1205 (developed by ArrMaz as a part of Arkema, FL, USA) [9] as the

collector dosage, using LabCell (TM) flotation equipment with the cell volume of 1.5 liters in 4 minutes and 200 g/t increments, respectively. Thus, three dosages of collectors were used as minimum (400 g/t), optimum (600 g/t), and maximum (800 g/t); with each collector three tests with different flotation time were conducted, firstly in 6 minutes, secondly in 10 minutes and thirdly in 14 minutes in a total of 9 main tests and test 0 as a preparatory test. Wet grinding, de-sliming and flotation process was identical in all the tests. The ores first were ground in a rod mill to the size of 400 µm (P80 in which 80% of the particles pass through the screening step), then de-slimed by hydrodynamic settling method in order to remove the extra fine particles (-20 µm) using tap water at room temperature. The collected samples labeled as Slimes in this study. In the next step 150 g/t of Custamine 1205 and Na_2CO_3 were added and the situation was kept for 1 minute. Then each test was divided into 4 various segments characterized by a distinct flotation time and collector dosage.

Each flotation product was screened into three fractions of -45 µm, +45-200 µm and +200 µm by applying 15 minutes vibration. The mesh size was 45 and 200. The amount on the mesh was weighted, bagged and the data collected on the corresponding dataset. Consequently, particle size distribution measurement was conducted to obtain the mean size of each fraction using Horiba Laser Scattering Particle Size distribution analyzer LA-950V2. All the sieved samples were analyzed by XRF at Geological Institute in Tallinn University of Technology using melting method for macro components and powder method for sulfur, fluoride and REEs. XRD was also conducted using Rietveld method. Chemical analysis was done in Geological Survey of Estonia using weight analysis method for quartz, titration for Al_2O_3 and CaO content, AAS flame for MgO and Fe_2O_3 detection, Spectrophotometry for P_2O_5, and AAS graphite for Cd content. Another requirement to evaluate the quality of the beneficiated phosphate rock is the ratio of CaO/P_2O_5 which is recommended to be up to 1.6. This parameter is also calculated to identify the best flotation process for the beneficiation of Estonian phosphate rock.

RESULTS AND DISCUSSION

From the screening it was observed that tailings' samples particle size distribution was mainly between 45 and 200 µm with the average mean size of 165.5 µm. As the flotation time increases, the proportion of the coarser particles increases, and more particles were remaining on the mesh number 200 with the average mean size of 246.97 µm. This proportion in test 8 and 9 becomes approximately equal with 50% to 49% and 51 to 48%, respectively. Also, the percentage of the fine particles (-45 µm) is significantly lower compared to two other groups regardless of the flotation time and collector dosage with the average mean particle size of 27.77 µm. This phenomenon can be explained by the fact that coarser particles have a higher chance to collide with the bubbles and therefore collected as tailings and finer particles are mainly collected as slimes before flotation process.

In contrast, in concentrates (RT) the overall distribution of the particles is in favour of coarser particles (>200 µm) with the average mean size of 436.93 µm compared to tailings particle size distribution explaining that an optimum particle size can be calculated for an efficient flotation.

Chemical Analysis of the slimes revealed that they contain significant amount of P_2O_5 between 26.4 to 35.6 wt.% which is originated from brachiopods detritus which were liberated during the wet grinding. Similarly, in the fine particle fractions of the tailings with less than 45 µm there was considerable amount of phosphate between 16.38 and 34.88 wt.%. However, the main component in the concentrates was apatite which was successfully depressed in the beneficiation process. Here, the same pattern can be seen that fine particles (<45 µm) contain more phosphate than coarser particles with almost 30 wt.% although this number in tests 8 and 9 is almost equal in all the three fractions. Also, the content of the CaO is almost stable in the all the flotation products presenting dominantly in fine particles and to a lesser extent in coarse particles. However, in concentrates the content of the CaO is approximately 50% of the product. The separation of the CaO is usually associated with the separation of MgO (as dolomite) which is harmful to the fertilizer production. Although the content of the MgO was remarkably low (usually below 0.30%), from the CaO content, it can be perceived that the higher the amount of the CaO, the higher the MgO content.

XRF analysis revealed a considerable amount of REEs in the samples. The distribution of the REEs is almost similar in all the samples, in that strontium content is the highest in concentrates and slimes with more than 3,100 and 2,700 ppm, respectively, followed by yttrium (Y), cerium (Ce), neodymium (Nd), and lanthanum (La). Similarly, in flotation products, strontium (Sr) is of the highest amount with almost 1,200 ppm. From XRF analysis a quite comprehensive outlook can be seen showing Estonian phosphate rock as a valuable REEs source of which currently technological and economic values are well understood (Figure 1).

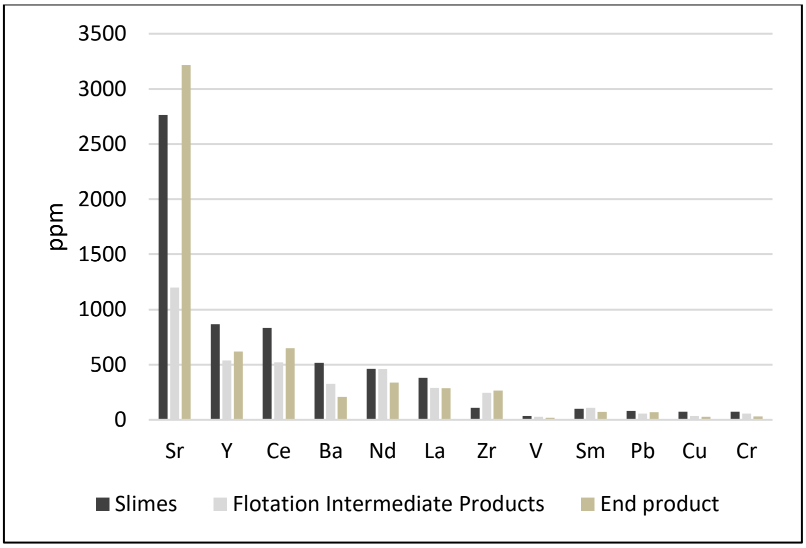

Figure 1 REEs content in beneficiated Estonian phosphate rock

Analysis of the products shows that in limited time duration (6 minutes), adding more collector may increase the phosphate grade, however, high amount of silicate which remained in the concentrates decrease the efficiency of the process. This shortage of time cannot be compensated by increasing the collector dosage. When the flotation process is conducted in 10 minutes time, lower dosages of the collector does not deliver a high-quality concentrate because the content of the quartz is still high and the grade of the phosphate is lower than the required level.

Table 1 Chemical Composition, phosphate grade, and recovery of conducted tests for beneficiation of Estonian phosphate rock

Test No.	**Rec %**	**Chemical Composition**					
		P_2O_5	**CaO**	**SiO_2**	**Fe_2O_3**	**MgO**	**Al_2O_3**
1	91.07	20.77	27.56	41.62	1.15	0.15	0.78
2	90.48	20.34	29.63	39.36	1.15	1.15	0.18
3	88.25	18.63	33.53	0	0.87	<LOD	<LOD
4	88.25	27.71	40.7	18.79	1.52	0.22	0.65
5	91.05	31.99	44.91	11.39	1.78	0.38	0.17
6	73.15	19.69	52.61	0.01	1	<LOD	<LOD
7	87.16	29.9	42.84	16.25	1.67	0.38	0.16
8	86.46	35.56	47.65	4.62	1.65	0.28	0.13
9	84.67	32.13	43.87	5.37	1.53	0.22	0.49

However, by adding the collector dosage, particles would have more chances to adhere to the air-bubbles and ascend in the suspension and concentrate delivered phosphate grade and recovery of almost 32.00 and 91.05% in test 5 and 35.56 and 86.46% in test 8, respectively. Moreover, allocating an extra time to the flotation process with a low dosage of the collector as in test 3 and 6 do not deliver a high-quality concentrate whereas in test 9 a high grade and recovery rate of phosphate with 32.13 and 84.76%, respectively were obtained. (Table 1)

CONCLUSION

From 2018, by the governmental support a comprehensive research has been commenced to employ the high-tech techniques and processes for Estonian phosphate rock beneficiation. This paper is an analysis on the conducted flotation processes in various time and collector's dosage to obtain the optimum beneficiation system parameters for this mineral. Thus, the tailings, slimes, and the concentrates of the 10 designed experiments were analyzed by screening, particle size distribution analysis, XRF, and chemical assays. From the above-mentioned analytical methods, it was observed that after screening and particle size distribution measurement of the samples, majority of the floated particles are between 45 and 200 µm with the average mean size of 165.5 µm, while in concentrates most of the particles size belongs to coarse-grain fraction with more than 200 µm with the average mean size of 436.93 µm. This data can be used in pre-processing in the grinding stage of the ore before the flotation method to obtain the most efficient particle size in the feedstock. The quality of the flotation products was investigated by XRF, XRD, and chemical analysis of the samples and it was observed that quartz content in the flotation products was higher while in concentrates, slimes, and fine particles flotation fraction P_2O_5 content was the dominant element. The beneficiation of the Estonian phosphorite was investigated as a function of collector dosage indicating that although at limited time (6 minutes) increasing the collector dosage will produce a relatively high-grade concentrate, the silicate content is also the highest. By maintaining the flotation time in 10 minutes and increasing the collector dosage, the highest quality of the concentrates was obtained. According to 14 minutes of flotation time, only in higher dosage of the collector, acceptable result was achieved.

Given the increase in phosphate rock consumption due to increased demand for the fertilizers, the present work offers an overview for the further studies on mathematical modeling of the Estonian phosphate rock beneficiation. In addition, further studies can utilize the presented data to extract REEs from tailings and final products.

ACKNOWLEDGEMENT

This work was financially supported by the Estonian Research Council grant (PUTJD705 and IUT33-19)) and the Geological Survey of Estonia, which are gratefully acknowledged.

REFERENCES

1. Ilyin, A.V., Heinsalu, H.N. (1990) Early Ordovician shelly phosphorites of the Baltic Phosphate Basin. In: Notholt, A.J.G. & Jarvis, I. (eds.) Phosphorite Research and Development. Geological Society Special Publication, 52, 253 – 259.
2. Bauert H., Alvar Soesoo, A., Hade, S. (2015) Strategic raw materials of Estonia. Conference volume-2015; Rakvere, 16-17.
3. Baturin, A.I.G.N. (2020) Comparative Geochemistry of Shell Phosphorites and Dictyonema Shales of the Baltic, Geochemistry International, 51, 1, 23-32.
4. Altschuler, Z.S. (1980) The geochemistry of trace elements in marine phosphorites. Part I. Characteristic abundances and enrichment, in: Y.K. Bentor (Ed.), Marine phosphorites, SEPM Spec. Publ.
5. Aydin, I., Aydin, F., Saydut, A., Bakirdere, E. G., Hamamci, C. (2010, Hazardous metal geochemistry of sedimentary phosphate rock used for fertilizer, Microchemical Journal 96, 247-251.
6. Roselli, C., Desideri, D., Meli, M.A. (2009) Radiological characterization of phosphate fertilizers: comparison between alpha and gamma spectrometry, Microchemical Journal 91, 181-186.
7. U.S. Department of Energy Office of Energy Efficiency and Renewable Energy, (2002), Energy and Environmental Profile of the U.S. Mining Industry.
8. Tamm, K., Zadeh, Z.A, Kuusik, R, Kallas, J., Yang, J., Tõnsuaadu, K., Trikkel, A. (2021) Effect of Flotation Time and Collector Dosage on Estonian Phosphorite Beneficiation Minerals, 11, 114, 1-18.
9. Parker, T., Wang, G. (2018) Solving Global Phosphate Challenges; ArrMaz: ArrMaz Solving Global Phosphate Challenges World Fertilizer March2018 (accessed on the 8 January 2021).

XIV International Mineral Processing
and Recycling Conference
Belgrade, Serbia, 12-14 May 2021

SELECTION OF COPPER-PYRITE FLOTATION CIRCUIT DESIGN BY APPLYING THE PREFERENCE SELECTION INDEX METHOD

Nedeljko Magdalinović, Zoran Štirbanović, Dragiša Stanujkić[#],
Jovica Sokolović
University of Belgrade, Technical Faculty in Bor, Bor, Serbia

ABSTRACT – Ores with lower content of useful components, as well as complex ores are being exploited in recent years, which makes it difficult to select the most appropriate technology for their processing. Multi-criteria decision making (MCDM) methods provide assistance in various kinds of decision making and selection problems, in all areas of life, industry and science.

Evaluation and selection of the most appropriate flotation circuit for processing of complex copper-pyrite ore by Performance Selection Index method is presented in this paper. Three flotation circuit designs were evaluated by using eight criteria and according to the results of the analysis sequential selective flotation circuit was found to be the most appropriate alternative for this type of ore.

Keywords: PCI Method, MCDM, Copper-pyrite Ore, Flotation Circuit.

INTRODUCTION

It is evident that ores with a significant content of useful and valuable metals are becoming rarer, which is why there is a need for exploitation of ores with a lower metal content, as well as complex ores. In order to better utilize useful minerals, as well as more efficient and cheaper ore processing, numerous technologies for its processing have been developed.

On the other hand, the application of multiple criteria decision making (MCDM) methods began at the end of the last century and so far these methods have been applied for solving numerous decision-making problems in various fields, and as a result, numerous MCDM methods have been proposed.

As some examples of the use of MCDM for solving problems in the field of mining and extractive metallurgy the following can be mentioned: equipment selection [1], flotation machine selection [2], mineral processing plant site selection [3,4], and flotation collector selection [5]. In their article, "Zadavskas *et al*. [6]" evaluated three lead-zinc flotation circuit designs using WASPAS method and single-valued neutrosophic set.

The Preference Selection Index (PCI) method was proposed by "Maniya and Bhatt [7]" in 2010. So far, the PCI method has been used to solve a number of decision problems, of which only a few will be listed here, such as: material selection [7], flexible manufacturing system selection [8], human resource management [9], laser cutting process conditions [10], and solving matching problem [11].

[#] corresponding author: dstanujkic@tfbor.bg.ac.rs

Therefore, the use of PCI method for selection of copper-pyrite flotation circuit design is presented in this article. Some characteristic copper-pyrite flotation circuit designs and PCI method are presented in Materials and methods section. An illustrative example is given in the Results and discussion section and concluding remarks are given in the Conclusion section.

EXPERIMENTAL MATERIALS AND METHODS

In this section three characteristic copper-pyrite flotation circuit designs and PCI method are presented.

Three characteristic copper-pyrite flotation circuit designs

In some copper ore deposits, copper minerals are found in association with Pyrite (FeS_2). Before a pyro-metallurgical treatment of copper concentrate it is necessary to increase the concentration of copper minerals in concentrate, which is usually carried out by froth flotation. On the other hand, the presence of pyrite in copper concentrate can cause lower quality of copper concentrate [12,13] and also production of slag that could deposit on walls of the smelter reducing throughput capacity [14].

During the flotation process it is necessary to achieve some requirements such as: the highest recovery of valuable minerals, the best possible separation of Cu minerals and FeS_2, a larger amount of concentrate, lover investment and processing costs, etc. In order to achieve such conflicting requirements various flotation circuit designs have been proposed, of which as frequently used can be mentioned the following:

- the Sequential Selective Cu-FeS_2 Flotation (SSF),
- the Collective-Sequential Selective Cu-FeS_2 Flotation (CSF), and
- the Collective Cu-FeS_2 Flotation (CF).

The above mentioned flotation circuit designs are shown in Figures 1 to 3.

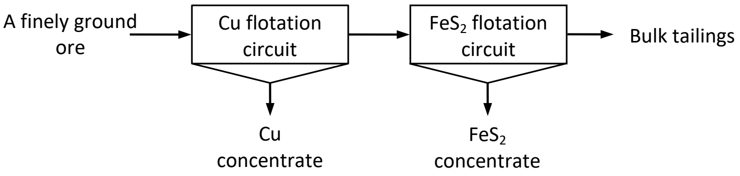

Figure 1 The Sequential Selective Cu-FeS_2 flotation

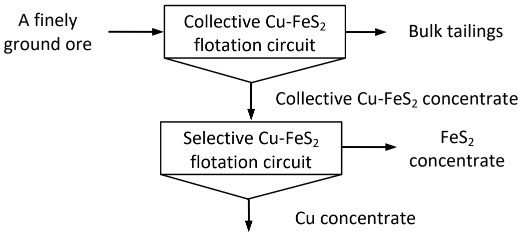

Figure 2 The Collective-Sequential Selective Cu-FeS_2 flotation

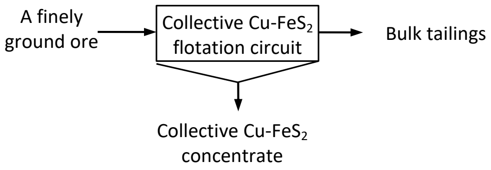

Figure 3 The Collective Cu-FeS_2 flotation

From the above, it is evident that selection of the most adequate Cu-FeS_2 flotation circuit design can be identified as multi-criteria decision making problem.

Due to the complexity of the froth flotation process, and based on the opinions of domain experts, the following criteria are proposed for evaluation and selection the most appropriate circuit design for copper-pyrite flotation circuit:

- Milling Costs - MiC,
- Capital Investment Costs - CIC,
- Flotation Reagents Costs - FRC,
- Maintenance Costs - MaC,
- Utilization of Copper - UCu,
- Utilization of Pyrite - UPy,
- Content of Copper in Concentrate - CuC,
- Content of Pyrite in Concentrate - PyC.

The Preference Selection Index (PCI) method

Based on "Maniya and Bhatt [7]" the computational procedure of PCI method for solving an MCDM problem containing *m* alternatives that are evaluated based on *n* criteria can be represented using the following seven steps:

Step 1: Evaluate the alternatives and construct initial decision making matrix *D*, as follows:

$$D = \left[x_{ij}\right]_{m\times n}, \tag{1}$$

where x_{ij} denotes ratings of the alternative *i* in relation to criterion *j*.

Step 2: Construct the normalized decision matrix in which the elements of the matrix are calculated as follows:

$$r_{ij} = \begin{cases} \frac{x_{ij}}{max_i x_{ij}}; & for\ beneficial\ criteria \\ \frac{max_i x_{ij}}{x_{ij}}; & for\ non-beneficial\ criteria \end{cases}, \tag{2}$$

where r_{ij} denotes normalized ratings of the alternative *i* in relation to criterion *j*.

Step 3: Calculate preference variation χ_j value in the relation to each criterion as follows:

$$\chi_j = \sum_{i=1}^{m}\left(r_{ij} - \bar{r}_j\right)^2 \quad , \tag{3}$$

where $\bar{r}_j$ denotes the mean value of normalized ratings of criterion j and it is determined as follows:

$$\bar{r}_j = \frac{1}{m}\sum_{i=1}^{m} r_{ij}. \tag{4}$$

Step 4: Calculate deviation in the preference variation value Ω_j as follows:

$$\Omega_j = 1 - \frac{\chi_j}{m-1}. \tag{5}$$

Step 5: Determine the criteria weights w_j as follows:

$$w_j = \frac{\Omega_j}{\sum_{j=1}^{n}\Omega_j}. \tag{6}$$

Step 6: Calculate the preference selection index of alternatives S_i as follows:

$$S_i = \sum_{j=1}^{n} \mathrm{r}_j w_j. \tag{7}$$

Step 7: Based on the preference selection index values of the alternatives, determine the complete ranking order of alternatives. The alternative which has the largest preference selection index represents the best ranked alternative.

RESULTS AND DISCUSSION

Based on the results of some studies that could not be shown in this paper due to data confidentiality, three above presented flotation circuit designs SSF, CSF, and CF were evaluated by PCI method. The ratings of considered alternatives, denoted as A1, A2 and A3, obtained from an expert are shown in Table 1.

Table 1 Initial decision-making matrix

	C_1	C_3	C_3	C_4	C_5	C_6	C_7	C_8
	MiC	CIC	FRC	MaC	UCu	UPy	CuC	PyC
	min	min	min	min	max	max	min	min
A_1	1.00	1.00	1.00	1.00	0.93	0.93	0.90	0.90
A_2	0.90	1.00	1.00	1.00	0.96	0.96	1.00	1.00
A_2	0.90	0.90	0.85	0.95	0.95	0.95	1.30	1.10

Normalized ratings, calculated using Eq. (2), are shown in Table 2, while preference variation values, deviation in the preference variation values, and the criteria weights, calculated using Eqs. (3), (5) and (6), are shown in Table 3.

Table 2 Normalized decision-making matrix

	C_1	C_3	C_3	C_4	C_5	C_6	C_7	C_8
A_1	0.90	0.90	0.85	0.95	0.97	0.97	1.00	1.00
A_2	1.00	0.90	0.85	0.95	1.00	1.00	0.90	0.90
A_2	1.00	1.00	1.00	1.00	0.99	0.99	0.69	0.82

Table 3 Calculation details of PCI method

	C_1	C_3	C_3	C_4	C_5	C_6	C_7	C_8
χ_j	0.007	0.007	0.015	0.002	0.001	0.001	0.049	0.017
Ω_j	0.997	0.997	0.993	0.999	1.000	1.000	0.975	0.992
w_j	0.125	0.125	0.125	0.126	0.126	0.126	0.123	0.125

The final results of the evaluation of the three flotation circuit designs, achieved using Eq. (7), are shown in Table 4.

Table 4 The final ranking order of three evaluated circuit designs

	S_i.	*Rank*
A_1	0.942	1
A_2	0.938	2
A_2	0.937	3

As can be concluded from Table 4, in this case the alternative denoted as A_1, i.e. sequential selective flotation (SSF) is the most suitable for studied copper-pyrite ore. Also it can be noted that the difference between the alternatives are very little and small variations in performance ratings of alternatives or criteria weights could result in different ranking order of alternatives.

CONCLUSION

The Preference Selection Index method is characterized by a relatively simple calculation procedure, as well as an integrated procedure for determining the significance of the criteria. Therefore, this method can be applied for the purpose of conducting preliminary selections or rankings, which can be verified later by applying other procedures or by applying proven MCDM methods.

Evaluation and selection of the most appropriate flotation circuit for processing complex copper-pyrite ore are shown in this paper. Three flotation circuits: sequential selective flotation (SSF), collective-sequential selective flotation (CSF), and collective flotation (CF), were evaluated by using eight criteria and according to the results of the analysis sequential selective flotation circuit was found to be the most appropriate alternative for this type of ore.

ACKNOWLEDGEMENT

The research presented in this paper was done with the financial support of the Ministry of Education, Science and Technological Development of the Republic of Serbia, within the funding of *the scientific research work at the University of Belgrade, Technical Faculty in Bor, according to the contract with registration number 451-03-9/2021-14/200131.*

REFERENCES

1. Sitorus, F., & Brito-Parada, P. R. (2020) Equipment selection in mineral processing-a sensitivity analysis approach for a fuzzy multiple criteria decision making model. Minerals Engineering, 150, 106261.
2. Štirbanović, Z., Stanujkić, D., Miljanović, I., & Milanović, D. (2019) Application of MCDM methods for flotation machine selection. Min. Engineering, 137, 140-146.
3. Sitorus, F., Cilliers, J. J., & Brito-Parada, P. R. (2019) Multi-criteria decision making for the choice problem in mining and mineral processing: Applications and trends. Expert systems with applications, 121, 393-417.
4. Bakhtavar, E., & Lotfian, R. (2017) Applying an integrated fuzzy gray MCDM approach: A case study on mineral processing plant site selection. International Journal of Mining and Geo-Engineering, 51 (2), 177-183.
5. Kostović, M., & Gligorić, Z. (2015) Multi-criteria decision making for collector selection in the flotation of lead–zinc sulfide ore. Minerals Engineering, 74, 142-149.
6. Zavadskas, E. K., Baušys, R., Stanujkic, D., & Magdalinovic-Kalinovic, M. (2016) Selection of lead-zinc flotation circuit design by applying WASPAS method with single-valued neutrosophic set. Acta Montanistica Slovaca 21 (2), 85-92.
7. Maniya, K., & Bhatt, M. G. (2010) A selection of material using a novel type decision-making method: Preference selection index method. Materials & Design, 31 (4), 1785-1789.
8. Maniya, K. D., & Bhatt, M. G. (2011) The selection of flexible manufacturing system using preference selection index method. International Journal of Industrial and Systems Engineering, 9 (3), 330-349.
9. Vahdani, B., Mousavi, S. M., & Ebrahimnejad, S. (2014) Soft computing-based preference selection index method for human resource management. Journal of Intelligent & Fuzzy Systems, 26 (1), 393-403.
10. Madić, M., Antucheviciene, J., Radovanović, M., & Petković, D. (2017) Determination of laser cutting process conditions using the preference selection index method. Optics & Laser Technology, 89, 214-220.
11. Petković, D., Madić, M., Radovanović, M., & Gečevska, V. (2017) Application of the performance selection index method for solving machining MCDM problems. Facta Universitatis, Series: Mechanical Engineering, 15 (1), 97-106.
12. Agheli, S., Hassanzadeh, A., Hassas, B. V., Hasanzadh, M. (2018) Effect of Pyrite Content of Feed and Configuration of Locked Particles on Rougher Flotation of Copper in Low and High Pyritic Ore Types. Int. J. Mineral Sci. Technol., 28 (2), 167. DOI: 10.1016/j.ijmst.2017.12.002.
13. Chandra, A. P., Gerson, A. R. (2009) A Review of the Fundamental Studies of the Copper Activation Mechanisms for Selective Flotation of the Sulfide Minerals, Sphalerite and Pyrite. Adv. Colloid Interfaces., 145 (1–2), 97. DOI: 10.1016/j.cis.2008.09.001.
14. Cadwell, E. P.; Upgrading of Copper Concentrates from Flotation. United States Patent Office, US3386572A, 1968. 10.1055/s-0028-1105114.

XIV International Mineral Processing
and Recycling Conference
Belgrade, Serbia, 12-14 May 2021

VALORIZATION OF COPPER FROM LOW-GRADE ORE BY LEACHING: INFLUENCE OF SULPHURIC ACID CONCENTRATION

Grozdanka Bogdanović[1#], Maja Trumić[1], Zoran Stevanović[2]
[1] University of Belgrade, Technical faculty in Bor, Bor, Serbia
[2] Mining and Metallurgy Institute Bor, Bor, Serbia

ABSTRACT – This paper presents an investigation of low-grade copper ore leaching using sulphuric acid where dissolved oxygen and iron(III) ions play a role of oxidant**.** The influence of initial acid concentration on copper and iron extraction was examined. The copper concentration in the leach solution ranged from 0.78 to 1.25 g/dm^3, whereas the iron concentration ranged from 1.89 -2.32 g/dm^3. It was found that the metal extraction increases with increasing acid concentration. The total copper extraction of 38% was attained with 0.5 M H_2SO_4 after 180 min of reaction.

Keywords: Acid Leaching, Copper, Low-Grade Ores.

INTRODUCTION

Hydrometallurgical processes are very often used for extraction of metals from ores (especially for oxide and polymetallic ores), industrial process residues, production scrap, and urban waste [1-4]. These methods use water as a solvent and were originally developed for the extraction of copper and gold, as well as for the extraction of uranium from low-grade ores [5].

Processing of mineral raw materials by hydrometallurgical processes is conducted by the following processes: grinding, chemical or biological leaching; separation of the residue; purification of the leach solution by solvent extraction or ion exchange; and metal recovery by precipitation or electrolysis. Currently, about 25% of the copper worldwide is produced by means of leaching in combination with the solvent extraction and electrolysis. Heap, dump and "in situ" leaching are technologies preferred for the processing of low-grade ores containing copper oxides or secondary copper sulfides [2].

Copper oxide minerals readily leach in any acidic solutions and the sulphuric acid has the greatest industrial application. In the case of leaching secondary copper sulfide minerals, such as chalcocite and covellite, oxidation is necessary (iron (III) ions, oxygen, etc.) and an important role in this is played by bioleaching, with the help of bacteria. The bacteria oxidize Fe (II) ions to Fe (III) ions, which improves the copper extraction rate [1]. Oxidative leaching of secondary copper sulfide minerals in an acidic medium is based on the stoichiometric reactions (1-4) and copper oxide minerals according to the stoichiometric reactions (5 -7) [2]:

[#] corresponding author: gbogdanovic@tfbor.bg.ac.rs

Chalcocite

$$Cu_2S + 1/2O_2 + H_2SO_4 \rightarrow CuS + CuSO_4 + H_2O \tag{1}$$

$$Cu_2S + Fe_2(SO_4)_3 \rightarrow CuS + CuSO_4 + 2FeSO_4 \tag{2}$$

Covellite

$$CuS + 2O_2 \rightarrow CuSO_4 \tag{3}$$

$$CuS + Fe_2(SO_4)_3 \rightarrow CuSO_4 + 2FeSO_4 + S \tag{4}$$

Malachite

$$Cu_2(OH)_2CO_3 + 2H_2SO_4 \rightarrow 2CuSO_4 + 3H_2O + CO_2 \tag{5}$$

Azurite

$$Cu_3(OH)_2(CO_3)_2 + 3H_2SO_4 \rightarrow 3CuSO_4 + 4H_2O + 2CO_2 \tag{6}$$

Cuprite

$$Cu_2O + 1/2O_2 + 2H_2SO_4 \rightarrow 2CuSO_4 + 2H_2O \tag{7}$$

The aim of this paper is to investigate the leaching of low - grade sulfide ore using sulphuric acid in order to obtain enriched solutions that would be suitable for the use of solvent extraction or ion exchange techniques for further treatment.

EXPERIMENTAL

A sample of low-grade copper ore was used for this study. Particle size distribution in a sample of ore was determined by the sieve analysis on the standard Tyler sieve series as shown in Table 1.

Table 1 Particle size distributions of ore

Particle size (mm)	Percent (%)	D (%)
+2.36	9.89	100
-2.36 +1.7	5.65	90.11
-1.7 +1.18	6.01	84.46
-1.18 +0.85	3.12	78.45
-0.85 +0.6	7.36	75.33
-0.6 +0.425	5.75	67.97
-0.425 +0.3	6.38	62.22
-0.3 +0.212	6.53	55.84
-0.212 +0.15	4.69	49.31
-0.15 +0.106	5.1	44.62
-0.106 +0.075	4.71	39.52
-0.075 +0.00	34.81	34.81
	100	

The chemical composition of the sample is presented in Table 2. It can be concluded that the sample represents a low-grade ore with a high content of copper oxide minerals (30%). It was estimated that, by the use of mineralogical and X-ray analysis, the most present copper minerals were chalcocite and chalcopyrite. Malachite, cuprite and azurite were found from copper oxide minerals. The most abundant sulphide mineral was pyrite.

Table 2 Chemical composition of ore

Component	Cu_{-total}	$Cu_{-sulfide}$	Cu_{-oxide}	S	Fe	Fe_2O_3	C_aO	M_gO
(%)	0.33	0.23	0.098	2.12	2.35	3.36	0.33	0.83
Component	SiO_2	K_2O	Al_2O_3	Na_2O	Zn	Ni	Mn	
(%)	63.18	3.07	21.58	0.24	0.009	<0.007	0.019	

The experiments were conducted in a 400 mL glass reactor with a magnetic stirrer. At the room temperature, 50 g sample was added to 50 ml leaching solution of desired concentrations and stirring was started. After different time period from 5 to 180 minutes, the suspension was filtered and the filtrate was analyzed by Optical emission spectrometers with inductively coupled plasma using the instrument PerkinElmer Optima 8300 (PerkinElmer, USA). The experiments were monitored as a function of time and acid concentrations. All solutions used were prepared using analytical grade chemicals and distilled water.

RESULTS AND DISCUSSION

The effect of acid concentrations (0.01 M, 0.03 M, 0.1 M, 0,5 M, 1 M H_2SO_4) on the copper and iron dissolution was investigated at solid /liquid ratio 1:1 and stirring speed of 400 rpm. The results are shown in Figures 1-3. During the experiments, the change of the pH and electrode potential of leach solutions was monitored over time as shown in Figures 4 and 5.

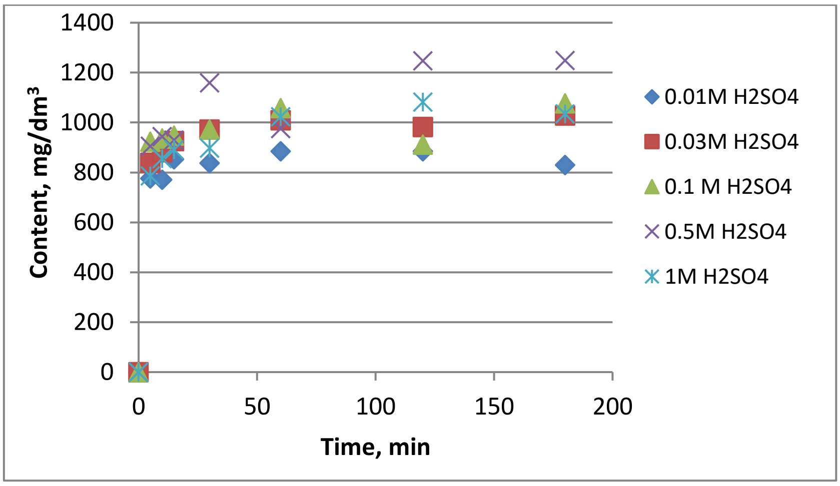

Figure 1 Effect of the sulphuric acid concentration on copper content in the leachate vs. time

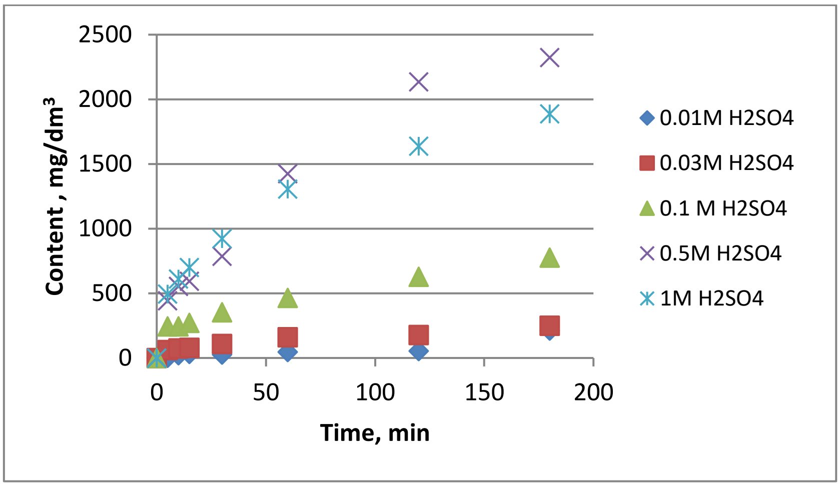

Figure 2 Effect of the sulphuric acid concentration on iron content in the leachate vs. time

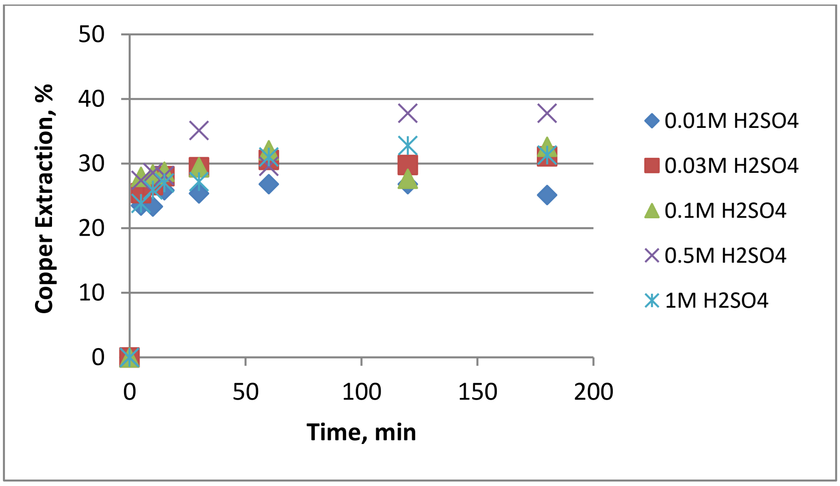

Figure 3 Effect of sulphuric acid concentration on copper extraction

The presented results (Figures 1 and 2) show that the copper and iron ions concentration increase with time. Also, the metal extraction increases with an increase in the acid concentration. Concentration of copper (II) in solutions, after 180 minutes of leaching, is in the range of 0.78 g/dm^3 (0.01 M H_2SO_4) to 1.25 g/dm^3 (0.5 M H_2SO_4). The results (Figure 2) showed that iron concentration increased slightly with increasing acid concentration from 0.01 to 0.1 M H_2SO_4. Higher acid concentration (0.5-1 M) had a significant effect on the reaction rate and final iron concentration was in the range of 1.89-2.32 g/ dm^3.

Final copper extractions in the 0.01 M H_2SO_4 and 0.5 M H_2SO_4 solution were 24% and 38%, respectively. At lower sulphuric acid concentration (0.01 M H_2SO_4), the lowest copper extraction value was found, which was the result of the lack of leaching agents.

The highest copper extraction rate (30 min leaching) at all tested acid concentrations indicated a high solubility of copper oxide minerals. Simultaneously with leaching of oxide minerals, a process of oxidation of sulfide copper minerals takes place due to the presence of Fe (III) ions and atmospheric oxygen in the solution. The sulfide mineral oxidation rate depends on the oxygen concentration, temperature, particle size, type of sulfide minerals, pH of the solution, Eh solution, presence of indigenous species of bacteria, etc.

Change in the potential and pH value of leach solutions with time is shown in Figures 4 and 5. It can be seen in Figure 4 that the potential is in a range of 255 to 367 mV which indicates that Fe (II) is dominant in the obtained solutions regarding Fe (III) ion. Due to this, oxidation processes of sulfide minerals are slower, resulting in low copper extractions in the solution.

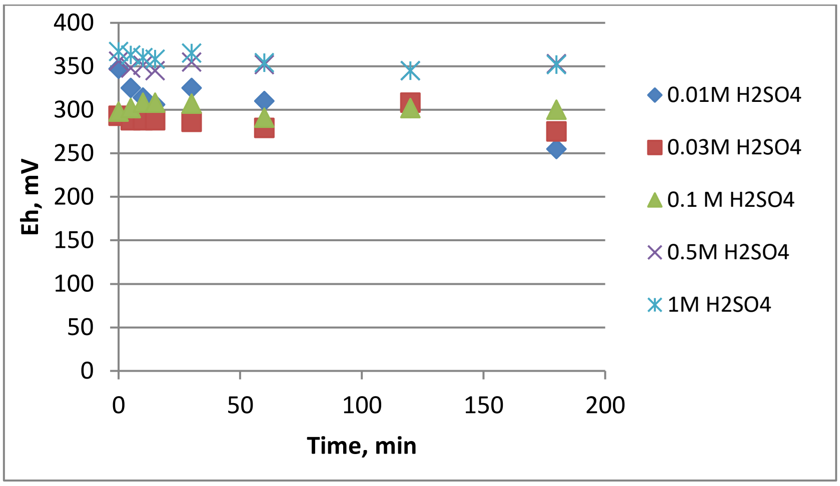

Figure 4 The change of the Eh of the leaching solution vs. time

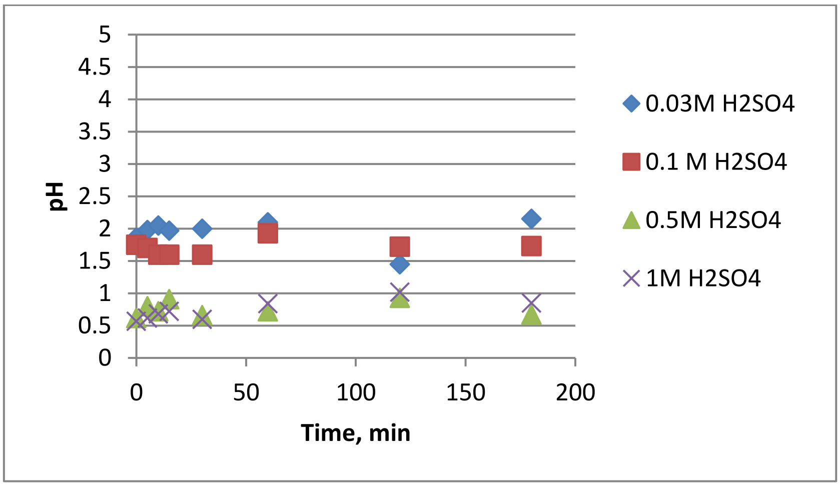

Figure 5 The change of the pH of the leaching solution vs. time

Figure 5 shows that the pH value increases in the initial period of the leaching process (up to 10 minutes), after which it remains constant throughout all experiments. During the leaching process, sulphuric acid is consumed due to reactions with copper minerals, but also due to reactions with iron oxide minerals and by other gangue minerals in the ore (carbonates and siliceous minerals). However, the oxidative reaction rate of iron sulfide minerals (e.g. pyrite) is responsible for the generation of acid, which contributes to the overall reduction of sulphuric acid consumption [6, 7].

CONCLUSION

It was found out that the majority of present copper and iron oxide minerals are dissolved during ore leaching by the use of sulphuric acid solutions, which was shown a significant concentration of copper and iron ions in obtained solutions. With increased leaching time and sulphuric acid concentration, copper and iron content in the solution increases, as well as extraction rate of these metals. At higher acid concentrations, copper sulfide minerals are more easily oxidized by oxygen and iron (III) present in leaching solutions. The total copper extraction was in the range of 24% to 38% and quite high concentration of copper ions was achieved (0.78 to 1.25 g/dm^3), suitable for further processing in the course of copper production.

ACKNOWLEDGEMENT

The research presented in this paper was done with the financial support of the Ministry of Education, Science and Technological Development of the Republic of Serbia, within the funding of the scientific research work at the University of Belgrade, Technical Faculty in Bor, according to the contract with registration number 451-03-9/2021-14/ 200131.

REFERENCES

1. Dreisinger, D. (2006) Copper leaching from primary sulfides: Options for biological and chemical extraction of copper. Hydrometallurgy, 83, 10-20.
2. Bogdanović, G.B., Stanković, V.D., Trumić, M.S., Antić, D.V., Trumić, M.Ž. (2016) Leaching of Low-Grade Copper Ores: A Case Study For „Kraku Bugaresku-Cementacija" Deposits (Eastern Serbia). Journal of Mining and Metallurgy, 52 A (1) 45-56
3. Luo, H., Cheng, Y., He, D., Yang, E. (2021) Review of leaching behavior of municipal solid waste incineration (MSWI) ash. Science of The Total Environment, 668, 90-10.
4. Wang, N., Sunb, X., Zhao, Q., Yang, Y., Wang, P. (2020) Leachability and adverse effects of coal fly ash: A review. Journal of Hazardous Materials, 396, 122725.
5. Binnemans, K., Jones,P.T. (2017) Solvometallurgy: An Emerging Branch of Extractive Metallurgy. J. Sustain. Metall. 3, 570-600.
6. Stevanović, Z.P., Antonijević, M.M., Bogdanović, G.D., Trujić, V. K., Bugarin, M.M. (2011) Influence of the chemical and mineralogical composition on the acidity of an abandoned copper mine in the Bor river valley (eastern Serbia). Chemistry and Ecology, 27 (5), 401-414.
7. Antonijević, M.M., Bogdanović,G.D. (2004) Investigation of the leaching of chalcopyritic ore in acidic solutions. Hydrometallurgy 73, 245-256.

KINETIC STUDY OF COPPER IONS BIOSORPTION ONTO BARLEY STRAW

Miljan Marković[1#], Milan Gorgievski[1], Nada Štrbac[1], Dragana Božić[2], Velizar Stanković[1], Vesna Grekulović[1], Milica Zdravković[1]
[1] University of Belgrade, Technical faculty in Bor, Bor, Serbia
[2] Mining and Metallurgy Institute Bor, Bor, Serbia

ABSTRACT – In this paper, the kinetic study of the copper ions biosorption onto barley straw is presented. The obtained experimental data were modeled using three kinetic models: pseudo-first order kinetic model, pseudo-second order kinetic model, and the intraparticle diffusion kinetic model (Weber-Morris model). Change in the adsorption capacity with process time was also monitored. Analyzing the obtained results, it can be concluded that the pseudo-second order kinetic model shows the best agreement with the analyzed data, which leads to a conclusion that chemisorption is a possible mechanism of binding the copper ions onto the surface of the barley straw.

Keywords: Kinetic Study, Copper Ions, Barley Straw, Biosorption, Chemisorption.

INTRODUCTION

Heavy metals can be removed from wastewaters by conventional methods, such as: coagulation and flocculation, flotation, aeration, oxidation, adsorption, ion exchange, membrane processes, and electrochemical methods [1].

These conventional methods don't always give satisfactory results. Due to the tendency of every industrial process to be more economical and efficient, different possible methods of wastewater treatment are being investigated. Biosorption is one of the possible alternative method to conventional technologies for wastewater treatment, especially those with low heavy metal ions content [2].

Many biological waste materials, such as fungi, algae, peat, yeasts, and different agricultural wastes are being tested as potential adsorbents for heavy metal ions adsorption from water solutions [3].

Kinetic models are often used for analyzing the experimental data in order to determine the rate of the adsorption, its mechanism, as well to determine the step that dictates the rate of the process [4].

There are a large number of kinetic models that are used to describe the adsorption processes. Models that are most often used in relevant literature are: pseudo-first model, pseudo-second order model, and the intraparticle diffusion kinetic model [5].

In this paper, the three above mentioned kinetic models were used for modeling the experimental results of Cu^{2+} ions biosorption onto barley straw.

[#] corresponding author: mmarkovic@tfbor.bg.ac.rs

EXPERIMENTAL

The change in the adsorption capacity with process time was determined by performing the following experiment: 0.5 g of barley straw was brought into contact with 50 mL of synthetic copper solutions of initial concentration 0.2 g dm^{-3}, for different contact time, ranging from 1 to 90 minutes, considering it a process time long enough to reach the equilibrium between phases [2].

RESULTS AND DISCUSSION

Change in the adsorption capacity with process time

The change in the adsorption capacity with a process time for copper ions biosorption onto barley straw is shown on Fig. 1. As can be seen from Fig. 1, the adsorption capacity rises rapidly in the first 10 minutes, as a result of a large number of available active sites in the structure of the adsorbent. After this period, the adsorption capacity further changes slowly over time, reaching its maximum value after 90 minutes.

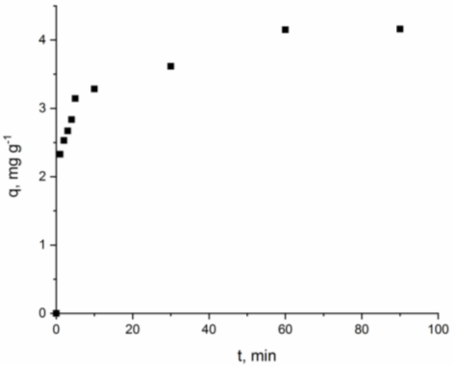

Figure 1 The change in the adsorption capacity with process time for copper ions biosorption onto barley straw

Pseudo-first order kinetic model

Pseudo-first order kinetic model was determined by Lagergren, and its often-named in literature as Lagergren's model. This model assumes that adsorption is a reversible process [6].

The pseudo-first order model is given as:

$$\frac{dq_{(t)}}{dt} = k_1\left(q_e - q_{(t)}\right) \tag{1}$$

where: $q_{(t)}$ - is the adsorbent capacity defined as the mass of the adsorbed metal per unit mass of the adsorbent (mg g^{-1}) at time t; q_e – is the adsorption capacity defined as mass of the adsorbed metal per unit mass of the adsorbent (mg g^{-1}) at equilibrium; k_1 - is the adsorption rate constant for the pseudo-first order kinetic model (min^{-1}).

By integrating the equation (1) for the boundary conditions: t = 0 to t = t and $q_{(t)} = 0$ to $q_{(t)} = q_{(t)}$ the following equation can be obtain:

$$log(\frac{q_e}{q_e - q_{(t)}}) = \frac{k_1}{2{,}303} \cdot t \qquad (2)$$

For practical use, this equation can be modified into:

$$log(q_e - q_{(t)}) = log(q_e) - \frac{k_1}{2{,}303} \cdot t \qquad (3)$$

Plotting log(q_e-$q_{(t)}$) vs. t gives a linear dependence where the constant k_1 and the equilibrium adsorption capacity q_e can be determined from the slope and the intercept, respectively (Fig. 2). The obtained model data is given in Table 1.

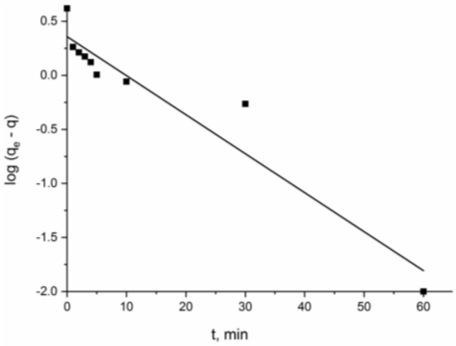

Figure 2 Pseudo-first order kinetic model for copper ions biosorption onto barley straw

Pseudo-second order kinetic model

The pseudo-second order kinetic model is based on the assumption that the rate of the adsorption is controlled by chemisorption [7].

A nonlinear form of the pseudo-second order kinetic model can be represented by the following equation:

$$\frac{dq_{(t)}}{dt} = k_2\left(q_e - q_{(t)}\right)^2 \qquad (4)$$

where: $q_{(t)}$ - is the adsorbent capacity defined as the mass of the adsorbed metal per unit mass of the adsorbent (mg g^{-1}) at time t; q_e - is the adsorption capacity defined as mass of the adsorbed metal per unit mass of the adsorbent (mg g^{-1}) at equilibrium; k_2 - is the adsorption rate constant for the pseudo-second order kinetic model (g mg^{-1} min^{-1}).

Rearranging Eq. (4) to obtain its linear form, leads to the following equation:

$$\frac{1}{(q_e - q_{(t)})} = \frac{1}{q_e} + k_2 t \qquad (5)$$

For practical use, the equation (5) is modified into:

$$\frac{t}{q_{(t)}} = \frac{1}{k_2 {q_e}^2} + \frac{t}{q_e} \qquad (6)$$

By plotting $t/q_{(t)}$ vs t (Fig.3), the pseudo-second order kinetic model parameters can be determined. The obtained model data is given in Table 1.

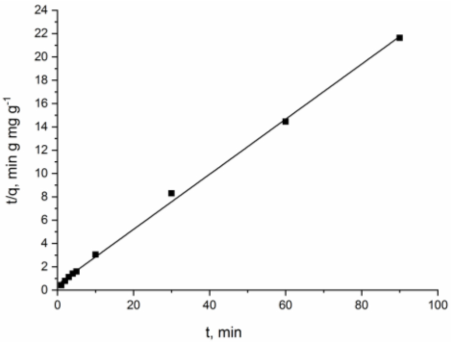

Figure 3 Pseudo-second order kinetic model for copper ions biosorption onto barley straw

Intraparticle diffusion kinetic model (Weber-Morris model)

The intraparticle diffusion kinetic model assumes that adsorption does not take place only on the surface of the adsorbent, but also includes diffusion and adsorption inside the adsorbent structure [8].

Linear form of this model is given by [9]:

$$q_{(t)} = k_i t^{1/2} + C_i \tag{7}$$

where: $q_{(t)}$ - is the adsorption capacity defined as the mass of the adsorbed metal per unit mass of the adsorbent (mg g^{-1}) at time t; k_i - is the internal particle diffusion rate constant (mg g^{-1} min$^{-0,5}$); C_i - is a constant that provides insight into the thickness of the boundary layer. If the C_i value is higher, the boundary layer effect is greater, so the effect of surface adsorption in controlling the process rate is higher (mg g^{-1}). The obtained model data is given in Table 1.

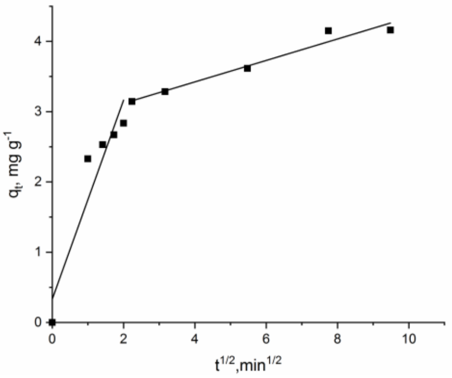

Figure 4 Intraparticle diffusion kinetic model (Weber-Morris model) for copper ions biosorption onto barley straw

The obtained experimental data, shown on Fig. 1, was fitted using the pseudo first-order kinetic model, pseudo-second order kinetic model, and the intraparticle diffusion kinetic model. Equilibrium parameters for the considered models were determined using the Eqs. (3), (6), and (7), and, along with the correlation coefficients R^2, are given in Table 1.

Table 1 Obtained parameters for the pseudo first-order model, pseudo-second kinetic model, intraparticle diffusion model, and the Elovich model for copper ions biosorption onto barley straw

Model	Parameters	Values
Pseudo-first order kinetic model	k_1 (min^{-1})	0.083
	$q_{e,exp}$ (mg g^{-1})	4.16
	$q_{e,cal}$ (mg g^{-1})	2.28
	R^2	0.917
Pseudo-second order kinetic model	k_2 (g mg^{-1} min^{-1})	0.116
	$q_{e,exp}$ (mg g^{-1})	4.16
	$q_{e,cal}$ (mg g^{-1})	4.23
	R^2	0.998
Intraparticle diffusion kinetic model	k_{i1} (g mg^{-1} min$^{-0,5}$)	1.415
	C_{i1} (mg g^{-1})	0.332
	R_1^2	0.889
	k_{i2} (g mg^{-1} min$^{-0,5}$)	0.152
	C_{i2} (mg g^{-1})	2.812
	R_2^2	0.960

CONCLUSION

In this paper, a kinetic study of copper ions biosorption onto barley straw was performed. Four kinetic models were used for modeling the experimental data: pseudo-first order kinetic model, pseudo-second order kinetic model, and the intraparticle diffusion kinetic model (Weber-Morris model). The obtained results showed that the pseudo-second order kinetic model gives the best fit for the analyzed experimental data, indicating that chemisorption is a possible mechanism of binding the copper ions onto the surface of the barley straw.

ACKNOWLEDGEMENT

The research presented in this paper was done with the financial support of the Ministry of Education, Science and Technological Development of the Republic of Serbia, within the funding of the scientific research work according to the contracts at the University of Belgrade, Technical

Faculty in Bor with registration number 451-03-68/2020-14/ 200131, and the Mining and Metallurgy Institute Bor with registration number 451-03-68/2020-14/200052.

REFERENCES

1. Šećerov Sokolović, R., Sokolović, S. (2002) Inženjerstvo u zaštiti okoline, Univerzitet u Novom Sadu Tehnološki fakultet, Novi Sad, 1-299.
2. Gorgievski, M., Božić, D., Stanković, V., Štrbac, N., Šerbula, S. (2013) Kinetics, equilibrium and mechanism of Cu^{2+}, Ni^{2+} and Zn^{2+} ions biosorption using wheat straw, Ecological Engineering, 58, 113-122.
3. Nemes, L. N., Bulgariu, L. (2016) Optimization of process parameters for heavy metals biosorption onto mustard waste biomass, Open Chemistry, 14, 175-187.
4. Guša, A., Đolić, M., Lekić, B., Rajaković-Ognjanović, V. (2015) Komparativna sorpcija jona teških metala na različitim tipovima sorbenata, Originalan naučni rad, Građevinski fakultet Univerziteta u Beogradu, Beograd, Srbija, Institut za nuklearne nauke Vinča, Univerzitet u Beogradu, Beograd, Srbija, 67-77.
5. Pap, S. (2017) Novi adsorpcioni medijumi za separaciju neorganskih polutanata otpadnih voda bazirani na termohemijskoj konverziji biomase (Doktrorska disertacija), Univerzitet u Novom Sadu, Fakultet tehničkih nauka, Departman za inženjerstvo zaštite životne sredine i zaštite na radu, Novi Sad, 1-211.
6. Lagergren, S. (1898) About the theory of so-called adsorption of soluble substances, Kungliga Suensk Vetenskapsakademiens Handlingar, 241, 1–39.
7. Lu, N., Hu, T., Zhai, Y., Qin, H., Aliyeva, J., Zhang, H. (2020) Fungal cell with artificial metal container for heavy metals biosorption: Equilibrium, kinetics study and mechanisms analysis,Environmental Research, 182, 1-10.
8. Cheung, W. H., Szeto, Y. S., McKay, G. (2007) Intraparticle diffusion processes during acid dye adsorption onto chitosan, Bioresource Technology, 98, 2897-2904.
9. Weber, W.J., Morris, J.C. (1963) Kinetics of adsorption on carbon from solution, Journal of the Sanitary Engineering Division, 89(2), 31–59.

XIV International Mineral Processing and Recycling Conference
Belgrade, Serbia, 12-14 May 2021

SYNTHESIS AND CHARACTERIZATION OF COBALT FERRITE/EXPANDED VERMICULITE AS A SORBENT OF NICKEL IONS

Mladen Bugarčić[1#], Dragana Milošević[2], Miroslav Sokić[1], Gvozden Jovanović[1], Zorica Lopičić[1], Aleksandar Marinković[3], Milan Milivojević[3]
[1] Institute for Technology of Nuclear and Other Mineral Raw Materials (ITNMS), Belgrade, Serbia
[2] Institute of Chemistry, Technology and Metallurgy; National Institute, Department of Ecology and Technoeconomic, Belgrade, Serbia
[3] University of Belgrade, Faculty of Technology and Metallurgy, Belgrade, Serbia

ABSTRACT – The minerals with unique properties such as mica minerals have promising approach in environmental and industrial sphere. In this study, cobalt ferrite/expanded vermiculite ($CoFe_2O_4$/EV) composite was prepared by in-situ method. Both composite and base materials are characterized by FTIR, XRD and SEM techniques, while the CEC and point of zero charge (pH_{PZC}) was also determined. The adsorption properties of $CoFe_2O_4$/EV and EV have been investigated in a batch system, for the Ni (II) sorption from water. Adsorption experimental results were fitted by kinetic and adsorption models, and resulted in ionic exchange mechanism with maximum adsorption capacity of 23.2mg g^{-1} (298 K).

Keywords: Mica Composite, Nickel Sorption, Solvothermal Deposition, Cation Exchange.

INTRODUCTION

Mineral resources already abundant in nature, such as micas possess quite interesting properties. Vermiculite, together with smectites is expandable mica mineral, intensive heating of vermiculite particles from ambient conditions up to 300 °C is method generally used for producing expanded vermiculite (EV) [1]. This, commercial readily-available material is already used as heat insulator, radiation shield [1, 2] as germination medium [3] as a matrix for phase change materials [4, 5]. Also, this material may be used as heavy metal sorbent [6, 7].

Sorption is one of the most promising methods that can be used in wastewater management. This process is simple, inexpensive and widely applicable. However, sorbent preparation and sorption management are more challenging task, since it is recommended to lead the water purification on optimal conditions with paying attention on techno economical parameters.

Sorption properties of EV towards cation species come from its moderate cation exchange capacity (CEC) from 25 to 250 $cmol_{eq}$/kg [8]. To utilize this material as a sorbent it is needed to improve its mechanical properties for EV is soft and brittle (longitudinal and transverse failure stress less than 30 MPa [9]).

[#] corresponding author: migognr@gmail.com

Such mechanical and sorption improvements could be provided decorating the surface of EV 2:1 sheets with harder minerals which would also provide its surface as a support for sorption such is cobalt ferrite.

In this study, deposition of cobalt ferrite on EV surface was done by solvothermal co-precipitation reaction. Thus, prepared composite was characterized in the manner of its sorption and physicochemical properties (pH_{PZC}, CEC, FTIR and XRD). Scanning Electron Microscopy is used to provide micro photographs of the obtained composites.

EXPERIMENTAL

Preparing this composite is done as further described: In first step 5.0000 g of EV is measured, in order to depose 0.5000 g of cobalt ferrite on the surface of EV as it was planned. So, stoichiometric amount of cobalt sulfate heptahydrate and iron (III) sulfate monohydrate plus 10 % excess of each compound are measured. These two salts were dissolved in 5000 µl ethanol - water mixture (volume ratio 3:1, respectively). Solution of these two salts is inserted in glass tube together with EV particles and this system is left for 1 hour on simultaneous sonicating and vacuuming with jet vacuum pump for 1 hour. After that, this system is left for 8 hours to cool down and stabilize. Stabilized sample was shut into autoclave and treated by following regime:

1 hour of preheating from ambient temperature to 180 °C
12 hours was held at 180 °C
And for 12 hours sample was cooling from 180 °C to ambient temperature

Reaction that takes place in autoclave reactor have further form (1):

$$CoSO_4 + Fe_2(SO_4)_3 + 2C_2H_5OH \rightarrow CoFe_2O_4 + 4SO_2 + 2CH_3COOH + 2H_2O \qquad (1)$$

Lastly sample is rinsed with ethanol and DW, after the rinsing sample is dried on atmosphere pressure on 50 °C for 4 hours. Dried sample is stored in plastic container covered with plastic caps.

Characterization of both EV and its modification included: cation exchange capacity (CEC) [10], point of zero charge (pH_{PZC}) [11], Scanning Electron Microscopy (SEM) (MIRA3 TESCAN), specific surface area (SSA) by Brunauer–Emmett–Teller (BET) technique, XRD analysis and Fourier Transform Infra-Red spectroscopy (FTIR).

Adsorption experiments were performed according to Taguchi method [12] in order to minimize the number of experiments.

RESULTS AND DISCUSSION

Summary of the CEC, pH_{PZC} and SSA results obtained from BET isotherm are given in Table 1. Values of CEC of $CoFe_2O_4$ modification and native EV sample is comparable, however $CoFe_2O_4$/EV has a little higher CEC. This is due to contribution of Co^{2+} ions which sustained in interlayer due to low yield of $CoFe_2O_4$ particles.

Table 1 CEC, pH$_{PZC}$ and SSA of EV and EV based adsorbents

	CEC*/cmol$_c$ kg^{-1}	pH$_{PZC}$	SSA/ m^2 g
EV	40.9	6.42	3.28
$CoFe_2O_4$/EV	42.7	6.30	8.47

*CEC values were determined measuring ion-exchange equilibrium concentrations of Na^+, K^+, Mg^{2+}, Ca^{2+} and Fe^{3+} ions for both samples, however Co^{2+} contribution to CEC is measured only for $CoFe_2O_4$/EV sample

Such low yield may be explained with low temperature applied in autoclave reactor (only 180 °C). However, presence of these particles increased SSA more than double. $CoFe_2O_4$ nanoparticles can be observed on the SEM images. On the Figure 1 are shown appropriate SEM images of start material (EV) and its modification with cobalt ferrite.

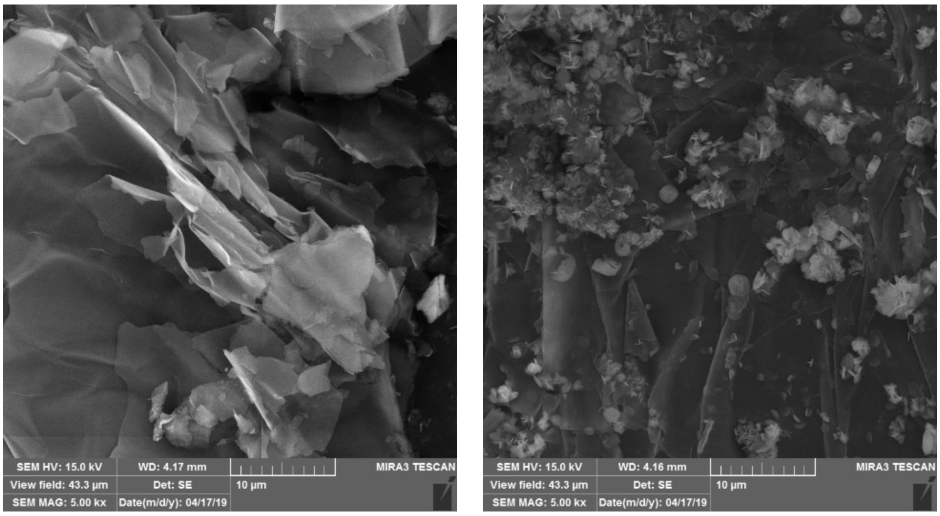

Figure 1 SEM images of EV (a) and $CoFe_2O_4$/EV (b)

At the Figure 1a can be seen sheet structure of vermiculite, at the Figure 1b can be seen $CoFe_2O_4$ nanoparticles on these sheets, dimensions of $CoFe_2O_4$ agglomerates are less than 3 μm while single particle is less than 0.3 μm.

Diffractogram of $CoFe_2O_4$/EV didn't have peaks corresponding to $CoFe_2O_4$ due to low content of these particles with regard to mass of EV carrier. However, modified mica composite ($CoFe_2O_4$/EV) possess peaks of both biotite vermiculite and vermiculite due to solvothermal action. At Figure 2 are shown diffractograms of both EV and its modification. Intensity of diffracted rays are arbitrary, for that reason, are not shown on y-axis label.

FTIR spectra of EV and $CoFe_2O_4$/EV are given at Figure 3, while the interpretations of the spectra are given within Figure itself.

Adsorption experiments results provided enough data to determine various parameters correlated to adsorption phenomena. Results of equilibrium adsorption were fitted by adsorption isotherms (Langmuir and Freundlich) and corresponding isotherm parameters were obtained (Table 2).

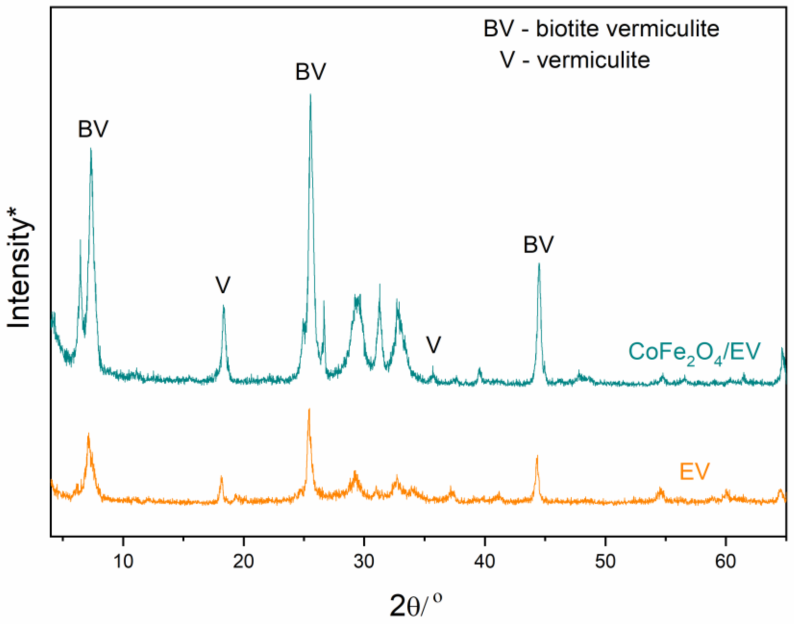

Figure 2 XRD of EV and its modification with $CoFe_2O_4$

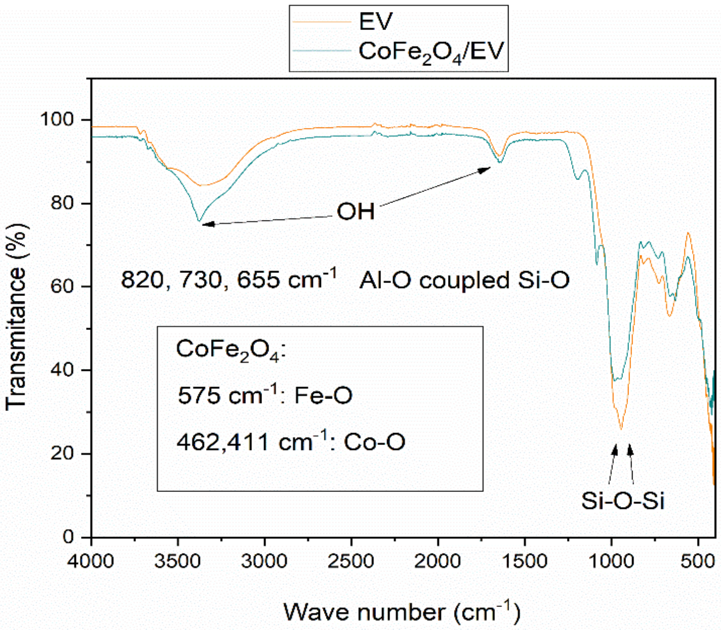

Figure 3 FTIR spectra of EV and $CoFe_2O_4$/EV with most important peaks position

Table 2 Results of nickel adsorption on EV and its modification with $CoFe_2O_4$ fitted with Langmuir and Freundlich isotherm models

			Temperature/ K		
			298	308	318
EV	Langmuir	q_m/ mg g^{-1}	18.89	21.95	24.82
		K_L/ L mg^{-1}	0.734	0.738	0.762
	Freundlich	K_F/ mg g^{-1} (Lmg^{-1})$^{1/n}$	8.372	9.397	10.547
		1/n	0.358	0.375	0.385
$CoFe_2O_4$/EV	Langmuir	q_m/ mg g^{-1}	23.20	27.08	29.53
		K_L/ L mg^{-1}	0.434	0.547	0.741
	Freundlich	K_F/ mg g^{-1} (Lmg^{-1})$^{1/n}$	7.097	9.243	11.804
		1/n	0.467	0.442	0.408

From the Table 2 it can be observed that the samples modified with $CoFe_2O_4$ possess higher maximum adsorption capacity as well as 1/n values, which means that presence of ferrite particles improves overall adsorption properties of EV surface.

Function between contact time and adsorption capacity towards nickel ions of the EV samples and $CoFe_2O_4$/EV samples were fitted by both kinetic and diffusion models. The best fitting goodness were obtained for pseudo second order (PSO) kinetic model and for Webber – Morris diffusion model. Determined parameters are presented in Table 3.

Table 3 Kinetic parameters for adsorption of Ni ions on EV and $CoFe_2O_4$/EV

Sample	Webber-Morris diffusion model			PSO	
	k_{id1}/ mg g^{-1} min$^{-0.5}$	C/ mg g^{-1}	k_{id2}/ mg g^{-1} min$^{-0.5}$	q_{max}/ mg g^{-1}	k_2/ g (min mg)$^{-1}$
EV	1.70	5.98	0.18	19.280	0.008162
$CoFe_2O_4$/EV	2.21	2.68	0.26	20.588	0.008324

From the results given in Table 3 can be concluded that both diffusion rates are increased (see k_{id1} and k_{id2} values) for modified mica sample. Although, intercept capacity is lowered, overall positive effect of $CoFe_2O_4$ nanoparticle presence can be noticed from both PSO parameters. These particles give extra surface for Ni ions adsorption, as well as solvothermal action offered an increase in CEC value of mica composite (Table 1).

CONCLUSION

Deposition of cobalt ferrite on the surface of EV, via or hydrothermal co-precipitation method, had induced certain changes in EV which have reflected on its properties, CEC and SSA in the first place. These particles support the adsorption process as they provide extra surface for adsorption of Ni ions and impact the rates of diffusion through adsorbent particles. Composites based on these types of minerals should be considered as adsorbents of heavy metals present as cation species.

ACKNOWLEDGEMENT

This work was supported by the Ministry of Education, Science and Technological Development of the Republic of Serbia (Contract Nos. 451-03-9/2021-14/200023)

REFERENCES

1. Suvorov, S.A., Skurikhin, V.V. (2003) Vermiculite - A promising material for high-temperature heat insulators. Refractories and Industrial Ceramics, 44, 186-193.
2. Kaur, S., Singh, S., Singh, L. (2019) Opto-electric and physio-chemical changes in oxygen ion irradiated natural Vermiculite mineral. Applied Radiation and Isotopes, 148, 7-12.
3. Martins, C.C., MacHado, C.G., De Santana, D.G., Zucareli, C. (2012) Vermiculita como substrato para o teste de germinação de sementes de ipê-amarelo. Semina: Ciencias Agrarias, 33, 533-540.
4. Zhou, W., Zhang, H., Li, K., Liu, F., Zhu, J. (2018) Synthesis and thermal properties of a capric acid-modified expanded vermiculite phase change material. Journal of Materials Science, 54, 2231-2240.
5. Deng, Y., He, M., Li, J. (2019) Non-isothermal crystallization behavior of polyethylene glycol/expanded vermiculite form-stable composite phase change material. Materials Letters, 234, 17-20.
6. Malandrino, M., Abollino, O., Giacomino, A., Aceto, M., Mentasti, E. (2006) Adsorption of heavy metals on vermiculite: Influence of pH and organic ligands. Journal of Colloid and Interface Science, 299, 537-546.
7. Rente, A.F.S., Moraes, D.S., Lamarão, C.N., Rodrigues, E.M.S., Marques, G.T. (2018) New sodium activated vermiculite process. Testing on Cu2+ removal from tailing dam waters. Journal of Hazardous Materials, 366, 34-38.
8. Weiss, A., Koch, G., Hofmann, U. (1955) Zur Kenntnis von Saponite. Berichte der Deutsche Keramische Gesellschaft, 22, 12-17.
9. Belhouideg, S., Lagache, M. (2014) The Effect of Moisture on the Mechanical Properties of Compacted Exfoliated Vermiculite. Engineering Structures and Technologies, 6, 124-130.
10. Daković, A., Tomašević-Čanović, M., Dondur, V., Rottinghaus, G.E., Medaković, V., Zarić S. (2005) Adsorption of mycotoxins by organozeolites. Colloids Surfaces B: Biointerfaces, 46, 20-25.
11. Milonjić, S.K., Ruvarac, A.L., Šušić, M. V. (1975) The heat of immersion of natural magnetite in aqueous solutions. Thermochimica Acta, 11, 261-266.
12. Mori, T., Tsai, S.-C. (2011) Taguchi Methods Benefits, Impacts, Mathematics, Statistics, and Applications, ASME Press, New York, 800.

XIV International Mineral Processing and Recycling Conference
Belgrade, Serbia, 12-14 May 2021

INFLUENCE OF pH VALUE OF LEACH SOLUTIONS ON EFFICIENCY OF ELECTROLYTIC DEPOSITION OF COBALT

Dragana Medić[1#], Snežana Milić[1], Slađana Alagić[1], Silvana Dimitrijević[2], Stefan Đorđievski[2], Maja Nujkić[1], Aleksandra Papludis[1]
[1] University of Belgrade, Technical Faculty in Bor, Bor, Serbia
[2] Mining and Metallurgy Institute Bor, Bor, Serbia

ABSTRACT – $LiCoO_2$ belongs to the first generation of cathode materials and is a component with the greatest potential for recycling. In order to recover cobalt from spent lithium-ion batteries, the cathode material was dissolved in sulfuric acid in an atmosphere of nitrogen and oxygen. As a result, a leach solution with a low pH value was obtained. In this paper, the influence of the initial pH value of leach solutions on the efficiency of electrolytic precipitation of cobalt was investigated. Recorded cyclic voltammogram indicated that the obtained leach solutions were not suitable for electrolytic precipitation of cobalt. However, 93% of cobalt was recovered by increasing the electrical conductivity and pH value of leach solutions.

Keywords: Lithium-ion batteries, Recycling, Leaching, Valorisation, Cobalt.

INTRODUCTION

Cobalt is a ferromagnetic metal and, thanks to its magnetic properties, cobalt alloys are widely used [1]. About 70% of world cobalt production is based on the hydrometallurgical process, in which the last phase is the electrolytic deposition of cobalt. Sulfate solutions are most often used in the process of electrolytic deposition of cobalt [2,3].

In this paper, the influence of the initial pH value of leach solutions on the current efficiency during electrolytic deposition of cobalt was investigated. Leach solutions were obtained by dissolving $LiCoO_2$ from spent lithium-ion batteries in sulfuric acid in the presence of oxygen and nitrogen. In order to increase the quality of the obtained product, sodium sulfate and boric acid were added to the leach solution.

EXPERIMENTAL

Electrolytic precipitation of cobalt was performed from a sulfuric acid solution. Due to the pronounced ferromagnetic properties of $LiCoO_2$, oxygen and nitrogen were used to mix the solution during the leaching of the cathode material. Leach solutions that were obtained after dissolution of the cathode material in sulfuric acid in an atmosphere of nitrogen and oxygen had almost identical composition. Because of that, these two solutions were mixed and further considered as one system (leaching system $H_2SO_4 + O_2 + N_2$). The initial pH of the leach solution was 0.9. In order to examine the possibility of

---

[#] corresponding author: dmedic@tfbor.bg.ac.rs valorization of cobalt from solutions obtained after the process of leaching of the cathode material, a cyclic voltamogram was recorded. The cyclic voltamogram was recorded in the potential range of -1.0 - 0.4 V and at a potential change rate of 20 mV/s. In order to examine the efficiency of the cobalt deposition process, an apparatus for electrolytic metal deposition was assembled. Before starting the process of cobalt deposition, the copper plates were cleaned with abrasive papers, in order to remove the products of corrosion and other impurities. The samples were then degreased by immersion in 96% ethyl alcohol, washed with distilled water and dried at room temperature. After drying, the dimensions of the samples as well as their mass were measured. The copper cathode and the platinum anode were connected in an electrical circuit. During the process, the electric current was constantly controlled. After 60 minutes, the power supply was switched off, the cathode was washed with 96% ethyl alcohol and distilled water, air-dried and its mass was measured.

During the electrolytic deposition of cobalt, in addition to the basic process, secondary chemical and electrochemical processes took place, which lead to a decrease in the degree of current efficiency.

In order to calculate the current efficiency, defined by the ratio of the actual mass of metal extracted at the cathode to the theoretically possible one, the following equations were used:

$$\eta = \frac{m_s}{m_t} 100\ (\%) \tag{1}$$

$$m_t = \frac{I \cdot t \cdot k}{26.8}\ (g) \tag{2}$$

where is:

η - current efficiency (%);

m_s - measured weight of the metal deposited on the cathode (g);

m_t - theoretical weight of the metal deposited on the cathode (g);

I - electrical current that flows through the electrolyte (A);

t - time of the process (h);

k - electrochemical equivalent.

RESULTS AND DISCUSSION

On the cyclic voltammogram shown in Fig. 1, it can be noticed that during the electrolytic precipitation of cobalt from the obtained solution, the following reactions took place [3,4,5]:

On the cathode:

$Co^{2+}_{(aq)} + 2e^- \rightarrow Co_{(s)}$ E° = - 0.227 V (3)

$2H^+_{(aq)} + 2e^- \rightarrow H_{2(g)}$ E° = 0.000 V (4)

On the anode:

$2H_2O \rightarrow O_2 + 4H^+ + 4e^-$ E° = 1.229 V (5)

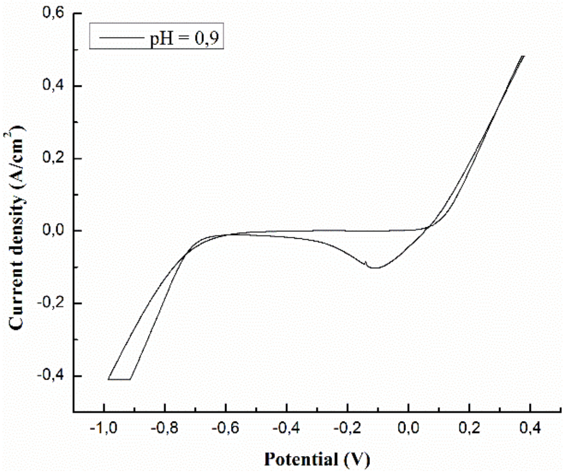

Figure 1 Cyclic voltammogram of cobalt deposition from leaching system H_2SO_4+N_2+O_2

In the cathode part of the voltamogram, the cobalt reduction reaction is observed at a potential of -0.68 V. The shift of the cobalt separation potential to more negative values, as well as the sudden increase in the cathode current density is probably a consequence of the side reaction of hydrogen ion reduction [3,6]. In addition to the side reaction of hydrogen ion reduction, the reaction of water oxidation is also noticeable in the system during electrolytic precipitation of cobalt. The present side reactions during the electrolytic deposition of cobalt cause a decrease in the current efficiency and can lead to a change in the morphological and structural properties of the electrolysis product [7].

The cyclic voltamogram in Fig. 1 indicates that the leach solutions obtained under optimal conditions of dissolution of the cathode material in sulfuric acid (2 mol/dm^3 H_2SO_4, solid phase concentration 33 g/dm^3, gas volume flow 2 dm^3/min, temperature 85 °C and time 100 min) are not suitable for electrolytic precipitation of cobalt, and that for a higher degree of process efficiency it is necessary to increase the pH and electrical conductivity of the solution.

Table 1 shows the operating conditions for electrolytic precipitation of cobalt from solutions obtained under optimal conditions of leaching of cathode material in the tested leaching systems. Due to the low initial pH of the leach solutions, the pH of the solution was adjusted to 4.5 using saturated NaOH solution and concentrated sulfuric acid. In addition to the already present components in the bath for electrolytic precipitation of cobalt ($CoSO_4$ and Li_2SO_4), sodium sulfate and boric acid were added to the acid-sulfate bath. The introduction of sodium sulfate into the acid sulfate bath was necessary to ensure an increase in the electrical conductivity of the solution. The presence of boric acid should inhibit the formation of hydroxyl ions. Santos *et al.* [8] also reported about the phenomenon of adding boric acid to a leach solution and its buffering role in the process of electrolytic precipitation of cobalt.

The dependence of the current efficiency on the pH value of leach solutions and the time of cobalt deposition is shown in Fig. 2. The results of experimental studies given in Fig. 2 show that with increasing duration of the electrolysis process there is a sharp decrease in pH value of the solution. After 15 minutes from the beginning of the process of cobalt deposition on copper electrodes, the pH of the solution decreased to 2.89. The sharp drop in the initial pH value of the solution is probably a consequence of the mixing of the catholyte and anolyte solutions due to the absence of an ion-exchange membrane. Also, during the process of cobalt deposition, electrolyte depletion by cobalt ions occurs. If only reactions 3, 4 and 5 are present in the system for electrolytic precipitation of cobalt from leach solutions, then the decrease in the pH value of the solution is directly proportional to the amount of precipitated cobalt [3].

Table 1 Operating conditions for electrolytic precipitation of cobalt from leach solutions

Leaching system $H_2SO_4 + O_2 + N_2$						
Cathode	Anode	Electrolyte composition (mol/dm^3)	Current density (A/m^2)	Temp. (°C)	pH value	Stirring rate (rpm)
Cu (plate)	Pt (spyral wire)	$CoSO_4$ (0.037) Li_2SO_4 (0.068) Na_2SO_4 (0.018) H_3BO_3 (0.018)	200	25	4.5	200

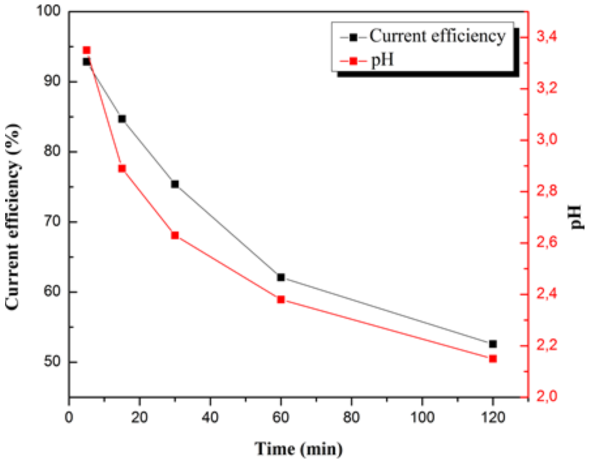

Figure 2 Dependence of the current efficiency on the pH value of leach solutions and the duration of the process of electrolytic deposition of cobalt

During the experiments, it was noticed that after 5 minutes from the beginning of the process of electrolytic deposition of cobalt the solution becomes turbid throughout the volume, and that along with the reaction of cobalt separation on the copper electrode, the platinum anode is coated with a black coating.

SEM microphotography of electrochemically precipitated cobalt is shown in Fig. 3. The presented cauliflower-shaped agglomerates are formed under the conditions of the secondary reaction of hydrogen ion reduction [9], which is also characteristic for the process of electrolytic deposition of cobalt. The results of SEM and EDS analysis of the electrodeposited layer of the product on the platinum electrode are shown in Fig. 4.

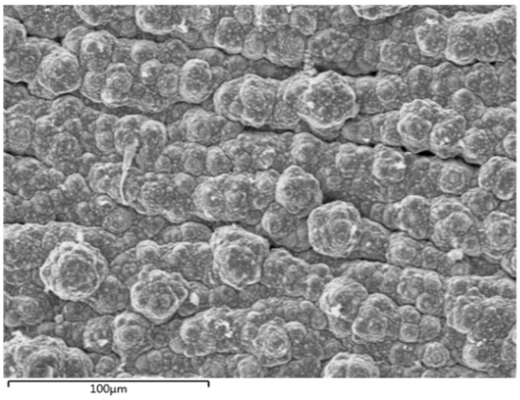

Figure 3 Morphology of cobalt particles obtained in the process of electrochemical precipitation from leach solutions in the presence of boric acid (magnification 500 times)

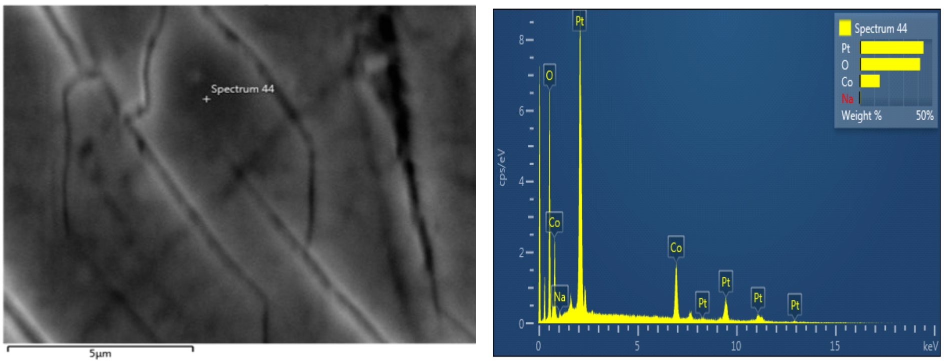

Figure 4 SEM and EDS analysis of the electrodeposited layer of the product on the platinum electrode

The results of SEM and EDS analysis indicated that during the electrolytic deposition of cobalt at the copper cathode, the formation of cobalt oxide at the platinum anode probably also occurred. EDS analysis revealed the presence of a small amount of sodium, which probably originated from the sodium hydroxide used to adjust the pH of the leach solutions. The presence of platinum indicates that a very thin layer of product has formed, which does not cover the entire surface of the platinum electrode.

CONCLUSION

Based on the presented results of experimental research, it can be concluded that leach solutions with a pH value of 0.9 are not suitable for electrolytic precipitation of cobalt. Also, the obtained results indicate that with the increase of the duration of the electrolysis process, there is a sharp decrease in the pH value of the solution. To achieve a high degree of process efficiency, it is necessary to maintain the pH value of the solution above 3, which can be achieved by using an ion-exchange membrane between the cathode and anode space, as well as by providing an additional source of cobalt ions.

ACKNOWLEDGEMENT

The research presented in this paper was done with the financial support of the Ministry of Education, Science and Technological Development of the Republic of Serbia, within the funding of the scientific research work at the University of Belgrade, Technical Faculty in Bor, according to the contract with registration number 451-03-9/2021-14/ 200131, and within the funding of the scientific research work at the Mining and Metallurgy Institute Bor, according to the contract with registration number 451-03-9/2021-14/ 200052.

REFERENCES

1. Li, M., Wang, Z., Reddy, R.G. (2014) Cobalt electrodeposition using urea and choline chloride. Electrochimica Acta, 123, 325-331.
2. Patnaik, P., Padhy, S.K., Tripathy, B.C., Bhattacharya, I.N., Paramguru, R.K. (2015) Electrodeposition of cobalt from aqueous sulphate solutions in the presence of tetra ethyl ammonium bromide. Trans. Nonferrous Met. Soc. China, 25, 2047-2053.
3. Sharma, I.G., Alex Pamela, Bidaye, A.C., Suri, A.K. (2005) Electrowinning of cobalt from sulphate solutions. Hydrometallurgy, 80, 132-138.
4. Elsherief, A.E. (2003) Effects of cobalt, temperature and certain impurities upon cobalt electrowinning from sulfate solutions. Journal of Applied Electrochemistry, 33, 43-49.
5. Zhou, J., Wang, S-F., Song, X-S. (2016) Electrodeposition of cobalt in double-membrane three compartment electrolytic reactor. Transactions of Nonferrous Metals Society of China, 26, 1706-1713.
6. Schiavi, P.G., Altimari, P., Zanoni, R., Pagnanelli, F. (2016) Morphology-controlled synthesis of cobalt nanostructures by facile electrodeposition: transition from hexagonal nanoplatelets to nanoflakes. Electrochimica Acta, 220, 405-416.
7. Santos, J.S., Matos, R., Trivinho-Strixino, F., Pereira, E.C. (2007) Effect of temperature on Co electrodepositionin the presence of boric acid. Electrochimica Acta, 53, 644-649.
8. Santos, J.S., Trivinho-Strixino, F., Pereira, E.C. (2010) Investigation of $Co(OH)_2$ formation during cobalt electrodeposition using a chemometric procedure. Surface & Coatings Technology, 205, 2585-2589.
9. Avramović, Lj., Maksimović, V.M., Baščarević, Z., Ignjatović, N., Bugarin, M., Marković, R., Nikolić, N.D. (2019) Influence of the Shape of Copper Powder Particles on the Crystal Structure and Some Decisive Characteristics of the Metal Powders. Metals, 9, 56.

XIV International Mineral Processing
and Recycling Conference
Belgrade, Serbia, 12-14 May 2021

DISSOLUTION OF RARE EARTH ELEMENTS FROM PHOSPHATE ORE IN HYDROCHLORIC ACID

Gizem Hacialioglu[#], Kaia Tõnsuaadu, Kristjan Urtson, Toivo Kallaste, Andres Trikkel
Tallinn University of Technology, Department of Materials and Environmental Technology and Institute of Geology, Tallinn, Estonia

ABSTRACT – Phosphate rock (PR) reserves in Estonia are about 700 mln t of P_2O_5 containing also valuable rare earth elements (REEs), which both are classified as the Critical Raw Materials. The main goal of the study was to evaluate the impact of HCl concentration and content of phosphorus in the formed solution on the solubility of REEs at PR (from Ülgase – Estonia) HCl dissolution process. The composition of the liquid and solid residues was determined using spectroscopic, AAS, ICPM and XRD methods. The data obtained enables to estimate the dissolution rate of apatite and REEs and clarify the precipitation of new solid phases.

Keywords: REE, HCl leaching, Phosphate ore, Sustainable processing.

INTRODUCTION

In the periodic table, fifteen lanthanides and two IIIB elements (scandium and yttrium) are called rare earth elements (REEs). Usage of REEs is common in automotive industry (catalysts, batteries), optics (glasses), health care, electronics (cell phones, televisions), and defense technology (precision-guided weapons, night-vision goggles) industries.

As a flag holder of technology production, China is the biggest consumer of REEs [1]. According to the U.S. Geological Survey, China is producing 63% of the REEs to be used in these industries [2]. As the biggest producer and consumer, China is controlling the REE market prices. To be more independent to use REEs, scientists are looking for other sources and new sustainable methods to produce REEs.

Among all secondary resources to recovery REEs, phosphate rocks are considered the most reliable ones according to their abundant reserves. Estonia has the largest phosphate rock reserves in Europe (approximately 3 billion metric tons) with an average 1200 – 1500 ppm content of total REEs [3].

General processing of phosphate rock is performed via decomposition with acids. The most common acid to perform the leaching process is sulfuric acid (H_2SO_4) but the recovery of REE is complicated in this case [4]. Possibilities to use other mineral acids (HCl, HNO_3, H_3PO_4) for REE leaching from phosphate ore are studied, followed by REE separation from the liquid phase. Previous studies show us that the leaching efficiencies of REEs in HCl are higher compared to those in H_3PO_4 and more

---

[#] corresponding author: gihaci@taltech.ee environmental friendly than HNO_3 (vaporization and NOx emissions) [5,6].

The decomposition of apatite mineral in acids is a fast process [4] and depends mainly on the solid/liquid ratio and acid concentration [7]. Temperature and mixing intensity have lower impact on phosphorus solubility.

Our aim is to use hydrochloric acid (HCl) as relatively cheaper than nitric acid and phosphoric acid [7] to recover the phosphorus and REE in the same technological step but in different phases. Additional to the economic aspect of this method, we wanted to perform this study to increase the sustainability of the process to waste less sources.

The main goal of the study was to evaluate the impact of HCl concentration, time of mixing, and content of phosphorus in the formed solution on the solubility of REEs at PR hydrochloric acid dissolution process.

EXPERIMENTAL

Materials

The phosphate rock sample was collected from Ülgase deposit, Estonia. The chemical composition of the sample is presented in Table 1. The main minerals determined by X-ray diffraction (XRD) are francolite, quartz sand, pyrite and bassanite.

Table 1 Chemical composition of the phosphate rock sample from Ülgase, Estonia

Chemical characteristics (%wt)							
P_2O_5	CaO	MgO	Fe_2O_3	K_2O	Na_2O	SiO_2	F
18.78	27.31	0.21	1.24	0.07	0.51	47.35	1.21
REEs (ppm)							
Ce	Pb	Pr	Nd	Dy	Y	U	La
124.14	14.36	15.90	70.65	15.04	123.38	8.75	56.25

The parameters for the experiments were chosen on the basis of preliminary studies and apatite dissolution reaction where 10 moles of acid are needed for one mole of $Ca_5(PO_4)_3F$. The parameters varied were: acid concentration (2.5, 5, 7.5% and 10%), to keep the HCl/Ca mole ratio around 1.5 – 2.8 the solid-liquid ratio was according to the acid concentration 0.05, 0.07, 0.11, 0.15, 0.25, and mixing time (10, 20, 30, 60 min).

Leaching process was carried out with different sample masses in 100 mL of HCl with various stirring time using magnetic stirrer. Thereafter, the mixture was at first filtered for separation of coarse fraction (>200 µm), and then the suspension was centrifuged for separation of fine solid particles (5-200 µm). The solid residues were washed with distilled water. Solid part was dried and separated to different particle size ranges.

Methods

The macrocomponents in the solution were determined by standard analytical methods. Content of Ca was determined by AAS (Varian SpectrAA 55B Flame AAS) and phosphorus by photocolorimetry method as phosphomolybdate yellow complex (Biochrom Libras 70PC UV/Visible Spectrophotometer).

Microcomponents (REE) were determined in a solution by ICP-MS (Thermo X- series II quadrupole) and in solid material by X-ray fluorescence (XRF), the mineral composition by X-Ray diffractometer (Bruker AXS GmbH, model D8 Advance, Fe-filtered Co radiation, Lynxeye detector). TOPAS software was used for quantitative analysis (Rietveld refinement method).

RESULTS AND DISCUSSION

The results of analysis of the products, mainly of the solutions, show that all the parameters followed have an impact on the apatite dissolution, more detailed on P and REE solubility. As the dissolution of fluorapatite is a fast reaction [5] the impact of mixing time more than 10 minutes on P solubility is relatively small (Fig. 1).

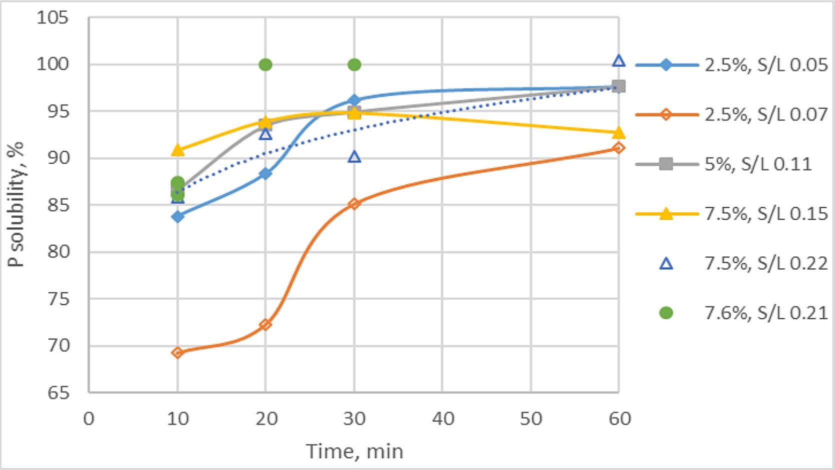

Figure 1 Solubility of P versus HCl concentration and S/L ratio in different mixing times

Phosphorus solubility increases by 5 to 15%, with increase in HCl/Ca ratio up to 30 min. Increasing the mixing time up to 60 min increases the solubility additionally 5%.

The impact of HCl concentration and HCl/Ca ratio on P solubility is seen in Fig.2. where the results of the experiments at 30 min are presented. The P solubility increases with the increase of acid concentration if the dose of HCl is lower or stoichiometric (HCl/Ca=2), when at higher acid dose above 2.4 the solubility decreases in 2.5, 7.5 and 10% acids at about 5%.

The solubility of REEs is different from phosphorus (Fig. 3). It varied from 5 to 85% depending strongly on acid concentration and dose. The solubility value started to decrease almost at all acid concentrations when the acid dose was below stoichiometric value, except with HCl 2.5% and dose 2.8 with the longer mixing time. This can be explained by the lower solubility of REEs at higher P content in a solution [4], which also explains the decrease in P solubility at higher acid doses. At the same time the REE solubility increases with the increase in HCl dose for all acid concentrations (Fig. 3b) that indicates the visible effect of acidity of the solution on REE dissolution.

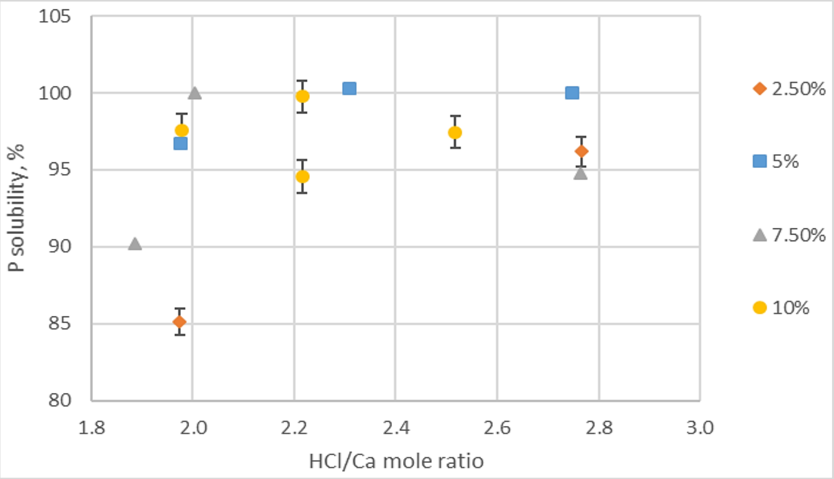

Figure 2 Phosphorus solubility depending on HCl/Ca mole ratio and acid concentration at 30 min mixing duration

XRD analysis of the solid residue revealed that the coarse fraction contains 75-90% of quartz. The fine residue consists mainly of pyrite, CaF_2, orthoclase, $CaSO_4$, rutile, and some unrecognized phases. The content of REE oxides in summary varied from 0.4 – 4.1%.

Therefore, the equilibrium in the solutions of acidic dissolution of phosphate rock is complex and depends on many factors, mainly, on the HCl concentration and acid dose, less on mixing time. There is a good possibility to estimate optimal conditions for phosphorus solubility keeping REEs insoluble that leads to their high concentration in the solid residue, similar to the treatment of PR with phosphoric acid.

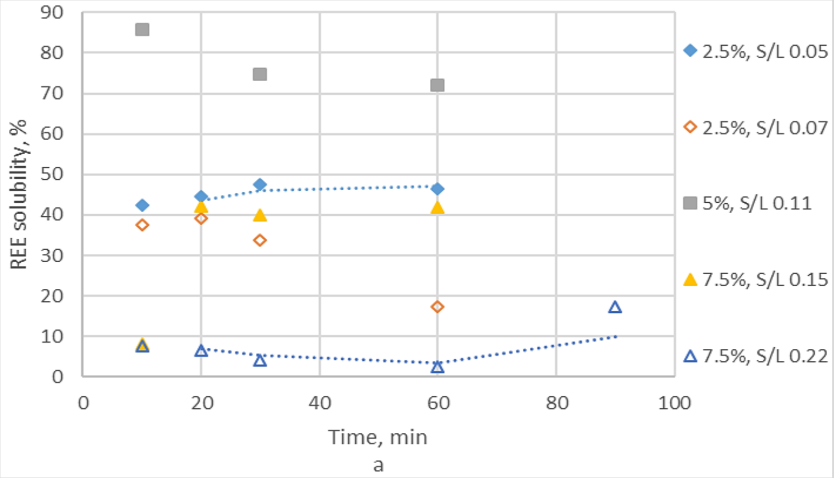

Figure 3 (a) REE solubility depending on mixing time and acid concentration (a) and on HCl/Ca mole ratio at 30 min mixing duration (b)

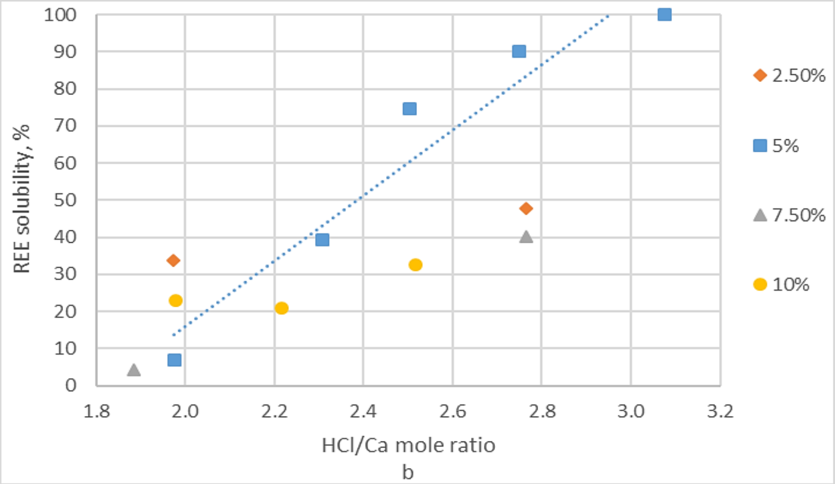

Figure 3 (b) REE solubility depending on mixing time and acid concentration (a) and on HCl/Ca mole ratio at 30 min mixing duration (b)

CONCLUSION

The results of this study indicate that solubility of REEs depends on acid concentration and dose and these were found to be less soluble at low HCl/Ca mole ratios. The data obtained shows that the optimal HCl concentration range is around of 5% at which the solubility of P is the highest (86.7%–100%) after 30 minutes of leaching. Further studies are needed to collect more data and expand the number of samples to determine the most favorable conditions for sustainable processing of different phosphate rocks.

ACKNOWLEDGEMENT

The authors would like to acknowledge the great help of chemical engineer Marve Einard for laboratory work and support of Tallinn University of Technology, Department of Materials and Environmental Technology and Institute of Geology.

This study was supported by ERDF and Estonian Research Council via project RESTA23.

REFERENCES

1. King, H.M. (2013) REE–rare earth elements and their uses, https://geology.com/articles/rare-earth-elements/ (accessed date 2018).
2. Gambogi, J. (2020) U.S. Geological Survey, Mineral Commodity Summaries, January 2020, https://pubs.usgs.gov/periodicals/mcs2020/mcs2020-rare-earths.pdf (accessed date 2020).
3. Soesoo, A., Vind, J., Hade, S. (2020) Uranium and Thorium Resources of Estonia, Minerals, 5-14.
4. Wu, S., Zhao, L., Wang, L., Huang, X., Zhang, Y., Feng, Z., Cui, D. (2019) Simultaneous recovery of rare earth elements and phosphorus from phosphate rock by

phosphoric acid leaching and selective precipitation: Towards green process. Journal of Rare Earths, 37 (6), 652-658.

5. Bandara, A. M. T. S., Senanayake, G. (2019) Dissolution of calcium, phosphate, fluoride and rare earth elements (REEs) from a disc of natural fluorapatite mineral (FAP) in perchloric, hydrochloric, nitric, sulphuric and phosphoric acid solutions: A kinetic model and comparative batch leaching of major and minor elements from FAP and RE- FAP concentrate. Hydrometallurgy, 184, 218-236.
6. Amine, M., Asafar, F., Bilali, L., Nadifiyine, M. (2019) Hydrochloric Acid Leaching Study of Rare Earth Elements from Moroccan Phosphate, 5-9.
7. Wu, S. X., Wang, L. S., Zhao, L. S., Zhang, P., El-Shall, H., Moudgil, B., Huang, X. W., Zhang, L. F. (2018) Recovery of rare earth elements from phosphate rock by hydrometallurgical processes - A critical review. Chemical Engineering Journal, 335, 774-800.

XIV International Mineral Processing and Recycling Conference
Belgrade, Serbia, 12-14 May 2021

POSSIBILITIES OF EOLIAN SANDS GRAVITY UPGRADING FROM THE ŠAJDÍKOVE HUMENCE DEPOSIT (WEST SLOVAKIA)

Slavomir Hredzák[#], Marek Matik, Oľga Šestinová, Anton Zubrik, Daniel Kupka, Silvia Dolinská, Ingrid Znamenáčková
Institute of Geotechnics of the Slovak Academy of Science, Košice, Slovakia

ABSTRACT – The contribution deals with gravity upgrading test of quartz sand under laboratory condition. Thus, quartz sand of quality 96.32% SiO_2, 1.55% Al_2O_3, 0.32% Fe_2O_3, 0.04% TiO_2 and 0.01% MnO was subjected to sink-float analyses in bromoform. It was shown that float product at a mass yield of 99% and quality of 96.94% SiO_2, 1.27% Al_2O_3, and 0.13% Fe_2O_3 at SiO_2 recovery 99.70% can be won. As to main impurities, 60% Fe, 82% Mn, and 21% Ti were removed into sink product, wherein mainly garnets, staurolite and amphiboles were identified.

Keywords: Quartz Sand, Gravity Pre-concentration, Iron Removal.

INTRODUCTION

Quartz sands are significant industrials applied in various industrial branches such as glassmaking, foundry, hydraulic-fracturing, whole grain fillers, ceramics, recreational, abrasives, chemicals, fillers, filtration sand, metallurgical flux, etc. [8].

In 2020 an estimated annual production in the world attained 265 Mt, so it means fall by 60 Mt comparing to production 325 Mt in 2019. It was caused above all by steep decrease in USA from 114 Mt in 2019 to 71 Mt in 2020. Furthermore, Netherlands 51 Mt, Spain 34 Mt, Italy 13 Mt and India 11 Mt belong to the biggest sand producers [4].

In Slovakia the annual production of industrial sands 749.1 kt is reported in 2019. Thus, the exploitation of foundry and glass sands in individual mine fields was as follows: Šajdíkove Humence 251.8 kt, Bažantnica 217.5 kt, Šaštín 150.0 kt and Borský Peter 129.8 kt [17].

Despite of the fact that Slovak sand producers hold their market, they also consider about their products diversification and/or about higher value-added products. So for this reason the research of quartz sand products from Šajdíkove Humence (Kerkosand, Ltd., a member of Quarzwerke Group) was performed. Special attention was paid to sand product SH30 in which the highest iron content (0.31% Fe_2O_3) was detected.

EXPERIMENTAL

The sample SH30 with grain size of 0.3–1.4 mm and mean grain d_{50}=0.6 mm was subjected to float-sink analysis or gravity pre-concentration to remove heavy minerals.

The test was performed in measuring cylinder using bromoform as heavy medium, grade p.a. 99%, stabilized by ethanol, a density of 2.89 g.cm^{-3}, delivered by mikroCHEM,

---

[#] corresponding author: hredzak@saske.sk

Ltd. Pezinok (Slovakia). An amount of ca 2.5 kg of SH30 sample was processed. The both products, i.e. float and sink ones were filtered and decanted by methanol and water to remove rest of bromoform, and dried. Consequently, these separation products were weighed to determine mass yields, and assayed using available techniques.

Loss on ignition (LOI) at 900 ºC and SiO_2 content was assayed gravimetrically (GA). Mg, Ca, Mn, Al, Fe, K a Na have been analyzed by AAS using the device VARIAN AA240FS (Australia). Ti, Cr, Zn a Mn were assayed by ICP-MS using the device Agilent 7700 (Agilent Technologies, Inc. Wilmington, USA).

XRD study was performed using D8 Advance diffractometer (Bruker, Germany), working with Cu Kα radiation at voltage 40 kV and current 40 mA. The data were collected over the angular range $5° < 2\theta < 80°$ with measuring steps 0.03° and a counting time 5s. Measured diffractograms were processed using programs Diffracplus Basic and Excel. The databases such as webmineral, handbookofmineralogy and the Arizona library were also used at mineral phases identification [2, 3].

Optical observations were performed by monocular microscope LEVENHUK (magnification max. ca 30x).

RESULTS

The results are introduced in Tables 1-2. XRD patterns of float and sink products are presented in Figs. 1-2. Similarly, the examples are documented in Figs. 3-4 [8, 12].

Table 1 Quality of products obtained by gravity upgrading (contents of analytes in %)

product	mass yield [%]	[ab]SiO_2	Fe_2O_3	K_2O	Na_2O	CaO	MgO	Al_2O_3	TiO_2	Cr_2O_3	MnO	ZnO
Float	99.06	[a]96.94	0.13	0.54	0.34	0.42	0.32	1.27	0.0308	0.0007	0.0027	0.0017
Sink	0.94	[b]30.20	20.45	0.08	4.54	2.66	3.76	31.50	0.8656	0.1106	1.2684	0.0349
[c]Feed	100.00	96.32	0.32	0.54	0.40	0.44	0.35	1.55	0.0387	0.0017	0.0146	0.0019

[a]calculated as difference to 100%, [b]determined by GA, [c]calculated quality of feed based on obtained products.

Table 2 Recoveries of observed components into separation products vs. mass yields

product	mass yield [%]	recovery / distribution ε [%]										
		SiO_2	Fe_2O_3	K_2O	Na_2O	CaO	MgO	Al_2O_3	TiO_2	Cr_2O_3	MnO	ZnO
Float	99.06	99.70	40.08	99.86	88.74	94.32	89.95	80.92	78.94	38.99	18.21	83.51
Sink	0.94	0.30	**59.92**	0.14	11.26	5.68	10.05	19.08	**21.06**	**61.01**	**81.79**	16.49
Feed	100	100	100	100	100	100	100	100	100	100	100	100

As it is shown in Table 1 a reduction of Fe content can be attained, namely from 0.32% Fe_2O_3 in feed to 0.13% Fe_2O_3 in float product. A mass yield into light product was of about 99%. The recovery of SiO_2 into light product attained almost 97%, so losses of SiO_2 in heavy product are not observable. Rest of SiO_2 is most probably bonded in so called heavy minerals. Thus, gravitational upgrading resulted in removal 60% of iron, 82% of manganese, 61% of chromium and 21% of titanium as introduced in Table 2 (all oxides of these metals are considered to be glass colouring).

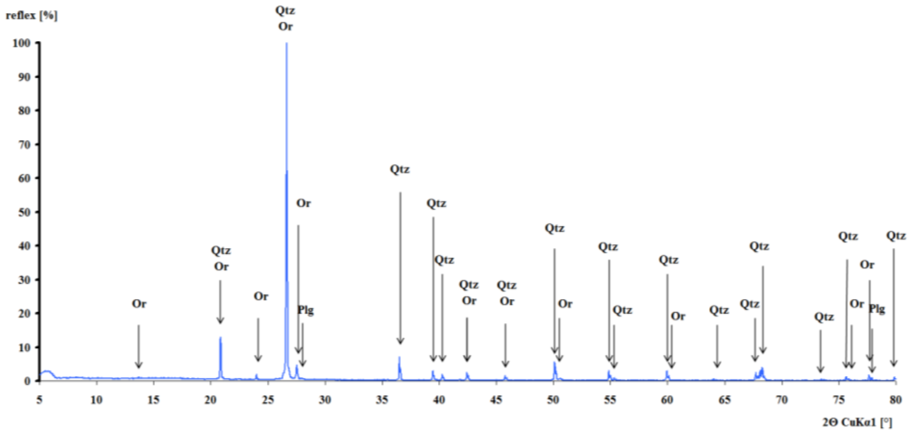

Figure 1 XRD pattern of float (light) product:
Qtz – quartz, Or – orthoclase, Plg – Plagioclase [8, 12, 14, 16]

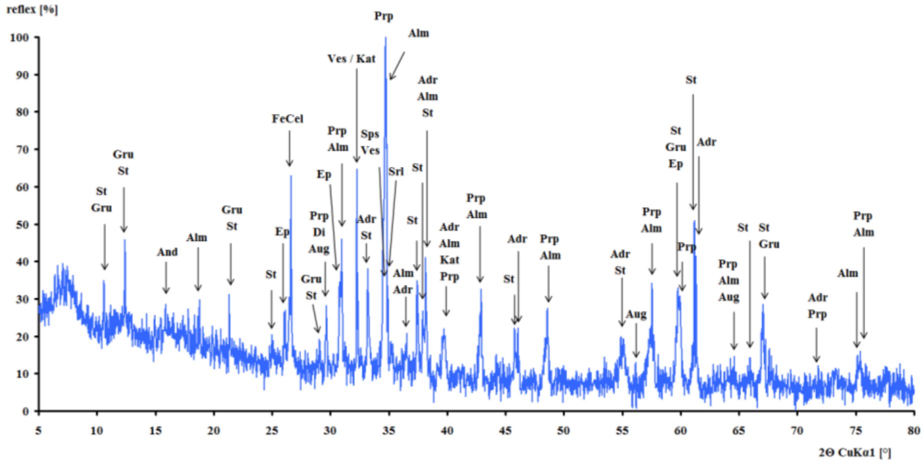

Figure 2 XRD pattern of sink (heavy) product:
Prp – pyrope, Alm – Almandine, Sps – Spessartine, Adr – Andradite, Kat – Katoite (all garnet group),
St – Staurolite, Gru – Grunerite (amphibole group), Srl – Schorl (here probably Oxy-Schorl, tourmaline group),
Ves – Vesuvianite, FeCel – Ferroceladonite, Ep – Epidote, And – Andalusite, and pyroxenes: Aug – Augite,
Di - Diopside [8, 12, 14, 16]

As to float product, quartz is dominant mineral, which is accompanied by orthoclase and plagioclase. Naturally, peaks of orthoclase are overlapped by quartz peaks. Taking into consideration chemical composition of this product it can contain maximally about 3% of orthoclase and 4.8% of plagioclase, probably andesine, or mixture of plagioclases (Fig. 1). On the surface of grains ochreous coatings of iron (oxy)hydroxides are visible (Fig. 3).

Concerning sink product, very complicated diffractogram was obtained by measuring (Fig. 2). Despite of this fact, it seems that dominant minerals are represented by pyrope, almandine, amphibole, most probably grunerite, and staurolite.

The main peaks of katoite and vesuvianite are overlapped. Furthermore, ferroceladonite can also occur as accompanying mineral. The other peaks point to an occurrence of spessartine, andradite, oxy-schorl, epidote, andalusite and from pyroxenes: augite, diopside and hedenbergite. The grains are rounded shape, but also elongato-oval and elongated grains, and angular fragments can be observed (Fig. 4).

Figure 3 Float product

Figure 4 Sink product

DISCUSSION

Naturally, intensive research has been performed after the establishment of mining and processing plant of the Czechoslovak Ceramic Works in 1970 to verify the possibilities of value added sand products preparation. Eolian sands of the Záhorská lowland were originally utilized in construction industry. Since 1972 after installation of countercurrent hydraulic classifiers a part of raw material is processed to several types of foundry sands for gray cast iron and colored container glass [11].

Gašparík (1971) [5] introduces that light fraction contains 95% of quartz, rest is represent by feldspars. The content of heavy minerals never overruns 1% wherein garnets, amphibole, metalliferous minerals, staurolite, epidote and apatite occur.

Špaldon et al. (1972) [18] referred that besides dominant quartz, sands contain 6-7% of orthoclase and about 3% of plagioclase. As to heavy minerals, garnets, staurolite, tourmaline, amphibole, ilmenite, rock detritus, zircon, rutile, etc. are presented.

Hredzák et al. (1996) [6] studied magnetic fractions of sands prepared at inductions 1.0T and 1.3T, respectively. The product containing mainly pyrope and almandine, less ortoclase, further amphibole, ilmenite, staurolite and titanite (?) was obtained at 1.0T. Fraction extracted at 1.3T contained quartz, orthoclase, oligoclase (?) and pyrope.

Ábelová & Maglay (2008) [1] refer that sands are composed of rounded grains of quartz (75–90 %), a rest is represented by rock detritus and feldspars. Garnets (about 40%), accompanied by amphibole and staurolite, is the most abundant in heavy fraction.

Špaldon et al. (1972) [18] dealt with sand upgrading using scrubbing, flotation and magnetic separation. Finally, sand product with 0.053% Fe_2O_3 was prepared using magnetic separation at 1.4T.

Klusák et al. (1973-74) [10] performed research on flotation of feldspar and they achieved 76% of feldspar in froth product.

Hredzák et al. (1996) [6] inter alia prepared a non-magnetic product containing 0.047 % Fe_2O_3, at Fe recovery of 32.90% by dry way at 1.3T from the feed of 0.143% Fe_2O_3.

Hredzák et al. (1998) [7] using ultrasound scrubbing and magnetic separation at 1.6T attained final product with 0.040% Fe_2O_3 from the feed with 0.120% Fe_2O_3.

Štyriaková et al. (2006) [19] studied bioleaching with subsequent leaching in oxalic acid. Final product after leaching and magnetic separation contained 0.024% Fe_2O_3.

Thus, a suitable combination of (bio)chemical and physical techniques ecologically and economically acceptable at given place and time seems to be the most passable way to obtain more value-added products from Slovak eolian sands.

Regarding garnets content in sink product, this mixture of minerals could be used as low grade abrasive. Price of industrial garnet is ca 270 USD/t after [13] comparing to 45 USD/t of industrial sands [4]. Despite of very low mass yield, i.e. 1%, at taking account annual production of ca 250,000 tons (Šajdíkové Humence 251.8 kt in 2019 [17], an amount of this product can attain 2,500 tons per year, so it is not negligible tonnage. Moreover, a presence of staurolite is welcome, it can be also applied as an abrasive as it is referred in [15].

Thus, the Humphrey spiral concentrators would be applied in pre-treatment of sand (partial 60% Fe removal) or sink product winning under industrial scale, moreover the mining plant already uses several these spirals in plant operation.

CONCLUSION

A gravity pre-concentration test showed that it is possible to remove 60% Fe, 82% Mn, and 21% Ti from raw sand at reduction of iron content from 0.32% to 0.13% Fe_2O_3. In such way the float heavy-minerals-free product suitable for bioleaching was prepared.

Thus, after removal heavy minerals the activity of microorganisms/bacteria can be aimed only at iron-bearing coats of quartz and feldspar grains. The microorganisms / bacteria will not unnecessarily employed by dissolving of Fe-bearing minerals like garnets, amphiboles, staurolite, etc. and this fact can finally result in cost saving on organic nutrient requirement for microorganisms and better control of bioleaching process.

ACKNOWLEDGEMENT

This work was supported by the Slovak Scientific Grant Agency for the projects VEGA2/0156/19 and VEGA2/0167/21.

This study has received funding from the European Institute of Innovation and Technology (EIT), a body of the European Union, under the Horizon 2020, the EU Framework Programme for Research and Innovation (Project BioLeach: Innovative Bio-treatment of RM, grant number: 18259).

REFERENCES

1. Ábelová, M. & Maglay, J. (2008) Aeolian sands of Záhorská lowland. Enviromagazín, vol. 13, No. 5, 26-27. (in Slovak)
2. Anthony, J.W., Bideaux, R.A., Bladh, K.W., Nichols, M.C. (eds.) (2004-2020) Handbook of Mineralogy, Mineralogical Society of America, Chantilly, VA 20151-1110, USA. http://www.handbookofmineralogy.org/. 2004-2020.
3. Barthelmy, D. (1997-2014). www.webmineral.com.
4. Dolley, T.P. (2021) Sand and Gravel (Industrial), 142-143. U.S. Geological Survey, Mineral Commodity Summaries, January 2021, 200 p., https://doi.org/10.3133/mcs2021.
5. Gašparík, J. (1971) Arenaceous Sediments and Their Utilization in Glass and Foundry Industry. In: Proceeding on Industrial Minerals in Slovakia. Mineralia Slovaca, vol. III., No. 12-13, 587-595. (in Slovak).
6. Hredzák, S., Jakabský, Š., Lovás, M., Mockovčiaková, A., Boldižárová, E., Bálintová, M. (1996) Deferrization of Eolic Sands from Šajdíkove Humence Deposit. The 2nd International Mineral Processing Conference „Modern Technologies and Devices for Mineral and Waste Processing“, Ustroń, 5-8.11.1996, Poland, Scientific Papers of Silesian University of Technology, MINING (GÓRNICTWO), Vol. 231, No. 1349, Gliwice 1996, 227-235. https://delibra.bg.polsl.pl/dlibra/publication/76434#structure.
7. Hredzák, S., Jakabský, Š., Lovás, M., Mockovčiaková, A., Bálintová, M., Gešperová, D. (1998) Properties and upgrading possibilities of eolian sands. Particulate Solids 98 – conference proceedings (ed. Fečko, P.), VŠB-TU Ostrava, Czech Republic, 50-55. (in Slovak).
8. Hredzák, S., Matik, M., Šestinová, O., Zubrik, A., Kupka, D., Dolinská, S., Znamenáčková, I. (2020) Eolian Sands from Šajdíkove Humence and possibilities of their upgrading using physical techniques. Geochémia 2020: Conference Proceedings (eds. Jurkovič, Ľ., Kordík, J., Slaninka, I., Hiller, E., Koděra, P.), Bratislava: State Geological Institute of Dionýz Štúr, 2020, 47-50. (in Slovak).
9. Jakabský, Š., Hredzák, S., Lovás, M. (1996) Research on Applicability of Magnetic Separation in Upgrading of Eolian Sand from the Šajdíkove Humence deposit. Expert opinion, Institute of Geotechnics of the Slovak Academy of Sciences, Košice, 14 pages. (in Slovak).
10. Klusák, J. et al. (1973-74) Research on Treatment of Sand from Šajdikove Humence. Report of the Research Institute of Ceramics in Horní Bříza, workplace Karlovy Vary-Rybáře, 204 pages. (in Czech).
11. Kraus, I., Kužvart, M. (1987) Deposits of Industrial Minerals. SNTL/ALFA, Prague/Bratislava, 232 pages. (in Czech and Slovak).

12. Kupka, D., Hredzák, S. et al. (2021) Report EITRM106357 WP3.1 on collection and laboratory works on raw materials samples with spectographic analyzes - KAVA: 18259-BioLeach. BioLeach: Innovative Bio-treatment of RM. Institute of Geotechnics SAS, Research Report, 36 pages.
13. Olson, D.W. (2021) Garnet (Industrial), 64-65, U.S. Geological Survey, Mineral Commodity Summaries, 200 p., https://doi.org/10.3133/mcs2021.
14. Ozdín, D. (2004) Symbols of minerals approved by IMA. Mineralia Slovaca 36, 367-370. (in Slovak).
15. Poltoratskiy, V., Leshchenko, O. (2019) Abrasive Ability of Staurolite Mineral Concentrate Produced by Vilnohirsk Mining and Metallurgical Combine. Aspects in Mining & Mineral Science, Vol. 2, Issue 5, 333-335. DOI: 10.31031/AMMA.2019.02.000547.
16. Siivola, J., Schmid, R. (2007) 0B12. List of Mineral Abbreviations. Recommendations by the IUGS Subcommission on the Systematics of Metamorphic Rocks. Recommendations, web version of 01.02.2007. http://www.bgs.ac.uk/scmr/products.html.
17. Slovak Main Bureau of Mines (2020) Annual report on activities of the Main Bureau of Mines and regional mining offices of the Slovak Republic in the year 2019. Banská Štiavnica, April 28th, 2020, 139 pages. (in Slovak).
18. Špaldon, F., Tarhanič, L., Michalíková, F. (1972) Research on Washability of Sand for Glass Industry. Report, Dept. of Mineral Processing, Mining Faculty, Institute of Technology in Košice, Košice, 42 pages. (in Slovak).
19. Štyriaková, I., Hredzák, S., Lovás, M. (2006) A combination of bioleaching and electromagnetic separation in the treatment of quartz sand. Acta Montanistica Slovaca, Vol. 11, Special Issue 2, 384–387. (in Slovak).

XIV International Mineral Processing
and Recycling Conference
Belgrade, Serbia, 12-14 May 2021

POSSIBILITY OF CLEANING OF BURNING COAL FROM SURFACE MINING

Milena Kostović[1#], Nina Pantelić[2]
[1] University of Belgrade, Faculty of Mining and Geology, Belgrade, Serbia
[2] RB Kolubara, Tamnava - Zapadno polje, Kalenić, Serbia

ABSTRACT – The paper presents the results of laboratory tests aimed to establish the possibility of cleaning of burning coal from surface mining before combustion in thermal power plants in Serbia. It has been confirmed that by simple coal cleaning process can be removed about 30-35% of tailings from burning coal, which mostly consist from mineral impurities. Final products obtained from the cleaning process have satisfactory quality (lower contents of ash and higher calorific values) than feed, i.e. burning coal. In addition, the paper highlighted the problem of combustion of lower quality coals in thermal power plants and considering this problem from the aspect of mineral processing.

Keywords: Burning Coal, Cleaning, Mineral Impurities, Surface Mining, Thermal Power Plants.

INTRODUCTION

Coal plays a vital role in electricity generation worldwide. Coal-fired power plants currently fuel 37% of global electricity and data from IEA show that coal will still generate 22% of the world's electricity in 2040, retaining coal's position as the single largest source of electricity worldwide [12]. Coal produced in mining basin Kolubara in Serbia provides about 53% of electricity in EPS, but coal from Kostolac open pit provides 17% of electricity production. Total coal production of coal in EPS in 2020 amounted to 39.1 million tons [3]. From 9 underground mines that operate within the JP PEU Resavica is produced about 500.000 tons of high quality coal per year. However, this coal participates with about 1.3% in total electricity production [6].

Based on all the above mentioned, it is obviously that coal from surface mining will be the main source of energy in Serbia in the future.

All coals contain noncombustible mineral matter. The residue from these minerals after coal has been burned is called ash. Minerals vary widely in coal seams with respect to kind, abundance and distribution. From the standpoint of coal cleaning, impurities occurring in coal may be classified as ash-forming and the sulfur-containing impurities, which both can be subdivided into inherent impurities and extraneous impurities. The inherent impurities are inseparably combined with the coal, while the extraneous impurities are segregated. Ash-forming material organically combined with the coal is considered inherent mineral matter. Extraneous mineral matter is ash-forming material from detrial matter and consists usually of slate, shale, sandstone, limestone or clay or other extraneous mineral matter from the roof and floor of the mine. All extraneous matter can be removed, i.e. separated physically with various method [5].

The ultimate goal of coal preparation is to maximaze the value of the coal material by

---

[#] corresponding author: milena.kostovic@rgf.bg.ac.rs separating the coal from the waste impurities to shipment to the end consumer [9].

The processes of coal preparation include coarse and intermediate coal cleaning (in dense medium vessels and dense medium cyclones) and fine and ultrafine coal cleaning (in spirals, water-only-cyclones, teeter-bed separators, conventional and column flotation cells). For coarse and intermediate size classes, crushing and screening is efficient methods for size reduction and classification. Grizzlies, inclined vibratory screens, high frequency screens and banana screens are often utilized for screening, while hammer mills, sizers and jaw crushers are the most popular machines for crushing [1, 9, 11].

Coals from mines in Serbia, both from underground and surface mining, in the aim to obtain final products are treated by simple processes (crushing and screening) or complex cleaning processes (usually by gravity concentration in a suspension of magnetite or quartz sand or by Parnaby process in autogeneous suspension) [7]. The selection of the applied process depends on the type of coal and its quality, exploitation capacity, purpose and quality of the obtained final products (ash content, calorific value, moisture, size fraction, etc.) and other factors. Coals from underground and surface mining, especially from surface mining, intended for combustion in thermal power plants, are not cleaned often. These coals are treated only by simple processes such as crushing and screening, reducing to the appropriate size fraction and, then, sent to the thermal power plant. In addition to required size fraction, these coals must also satisfy the requirements of thermal power plants for calorific values, ash and moisture contents.

Thermal power plants have the capacities of boilers designed for a certain quality of coals. It is generally known, and confirmed through the paper of other authors, that combustion of coal with higher calorific values, lower ash and moisture contents, enables high boiler efficiency [2, 4, 10, 11]. The lower quality of coal, in addition to reducing the efficiency of boiler in thermal power plants, imposes other problems: complex disposal requirements of ash and slag, transport of large quantities of materials, environmental problem (air quality, soil, etc.). This problem is often viewed one-sided, i.e. from the aspect of coal recovery from the deposit, without considering the consequences that lower quality coal has in the combustion process. A serious analysis of this problem is necessary, especially from the aspect of mineral processing. The aim of this paper is to consider the needs for cleaning of burning coal and to point out the advantages and importance of cleaning of our coals, or individual parts of the coal deposits before combustion in thermal power plants.

In eastern part of the Kolubara coal basin, there are three exploitation fields: Tamnava – East field, whose exploitation has been finished, Tamnava – West field and the Radljevo field. According to data from the exploration works, almost 21% of the coal in the Tamnava – West field does not satisfy the required quality in relation to lower calorific value (LCV) by the thermal power plants in Obrenovac. The situation is especially interesting in certain parts of the deposit where there are significant reserves of coal finely impregnated with tailings. Reserves of this coal are estimated at 10 million tons, and lower calorific value (LCV) is below 6000 kJ/kg, which is significantly lower than the requirements of thermal power plants.

The Tamnava coal preparation plant aims to prepare raw coal from surface mining for combustion in thermal power plants. Due to the nature of the deposit and the structure of the coal layer, selective coal mining at the Tamnava surface mine is difficult. Burning coal from mass coal mining sent to the Nikola Tesla thermal power plants in Obrenovac. This coal has lower quality because of presence of high content of clay, quartz sand and other mineral impurities. The new crushing line was introduced aimed at increasing the capacity and obtaining coal of satisfactory size fraction, while the homogenization process was introduced with the aim of making uniform the quality of coal. However, although the process of homogenization makes uniform the quality of coal, the problem is not solved, because the impurities presented in the coal for combustion to the thermal power plant are not removed on this way.

MATERIALS AND METHODS

The sample for these tests [8] was taken at the conveyor belt on line 2 (after the hammer crushers) in the Tamnava coal preparation plant. This sample represents burning coal, size fraction -40+0 mm, which is sent to the thermal power plant in Obrenovac.

Particle size distribution of the coal sample was determined by wet screening on a series of laboratory screens with 60, 40, 30, 20, 10 and 5 mm openings. The sample of coal, size fraction -40+0 mm, was screen by dry and wet procedure on laboratory screens with 5 mm opening. Products of screening (oversize fraction -40+5 mm and undersize fraction -5+0 mm) were dried, measured and prepared for analysis. The samples were analysed to: ash (%), lower calorific value (LCV, %), higher calorific value (HCV, %) and moisture (W, %).

RESULTS AND DISCUSSION

Particle size distribution showed that coal sample have d_{50}=16.2 mm and d_{95}=55 mm. The mass of the size fractions -40+0 mm and -5+0 mm were 83.68% and 31.86%, respectively.

Results of dry and wet screening are shown in Tables 1 and 2. Table 3 shows the distribution of ash and HCV in screening products.

Table 1 Results of dry screening of burning coal (size fraction -40+0 mm)

Products Size fraction (mm)	with moisture				without moisture		
	Mass %	W %	Ash %	LCV kJ/kg	Mass %	Ash %	HCV kJ/kg
-40+0 mm	100.0	39.30	17.18	9853.6	100.00	28.30	13850.6
-40+5 mm	70.4	35.00	14.33	12307.0	77.33	22.05	15913.0
-5+0 mm	29.6	49.00	25.30	4987.2	22.67	49.61	6816.0

Table 2 Results of wet screening of burning coal (size fraction -40+0 mm)

Products Size fraction (mm)	with moisture				without moisture		
	Mass %	W %	Ash %	LCV kJ/kg	Mass %	Ash %	HCV kJ/kg
-40+0 mm	100.0	41.10	17.01	9741.0	100.00	28.88	14392.3
-40+5 mm	65.1	40.00	10.19	12084.5	71.32	16.99	17674.0
-5+0 mm	34.9	48.80	29.92	3675.0	28.68	58.43	6233.0

Table 3 Distribution of ash and HCV in screening products

Products Size fraction (mm)	Dry screening		Wet screening	
	Ash %	HCV %	Ash %	HCV %
-40+0 mm	100.0	100.00	100.0	100.00
-40+5 mm	60.24	88.84	41.96	87.58
-5+0 mm	39.74	11.16	58.04	12.42

It can be seen from Table 1 and 2 that oversize products, size fraction -40+5 mm, obtained by dry and wet screening have higher calorific values (LCV about 12000 kJ/kg) than raw coal, which has LCV about 9800 kJ/kg. Also, the contents of HCV are increased in both products (about 16000 kJ/kg by dry screening and about 17600 kJ/kg by wet screening) in relation to raw coal (about 13800 kJ/kg and 14400 kJ/kg). The products, i.e. oversize fractions, have lower ash contents: 10-14% of ash (with moisture) and 17-22% of ash (without moisture) compared to raw coal (17% of ash with moisture and about 28% of ash without moisture). Beside this, by dry, and especially wet screening, lower ash contents are obtained in products and, also, higher both calorific values (LCV and HCV) in relation to the feed coal. According to the results presented in Table 3, about 88% of the heat (calorific value) will be separated in the oversize fractions. About 60% of ash and 42% of ash (according to distrubution) are separated in the oversize fractions by dry and wet screening, respectively. The presence of tailings is evident in undersize fractions (-5+0 mm) due to the higher ash content and significantly less calorific values in relation to raw coal. It is possible to remove by screening about 30-35% mass of coal (in undersize fractions) with increasing presence of tailings.

CONCLUSION

Experimental tests have shown that it is possible to successfully clean burning coal of size fraction -40+0 mm from the Tamnava West field in Mining basin Kolubara. Cleaning of burning coal is performed by screening as simple process. By both dry and wet screening processes, it is possible to obtain products (oversize fraction -40+5 mm) with higher calorific values (both LCV and HCV), as well as with lower ash contents in relation to raw coal. According to the distribution, about 88% of heat and about 40% and 60% of ashes will be separated in these products. In this way, it is possible to remove by mass about 30-35% of coal (in undersize fraction) with increasing presence of tailings. Taking into consideration that tailings in lignite are consisted of mineral impurities, mainly quartz sand and clays, these impurities could be removed in industrial conditions by simple and cheap processes: quartz sand by previous dry screening on vibratory screen, and clays by wet processes (disintegration, desliming and washing). Removal of these impurities can be done in the process of coal preparation and before the crushing. In industrial conditions, it is not realistic to expect that all amount of coal could be cleaned, but individual parts of coal layers in deposit where it is not possible to selectively excavate tailings, could certainly be subjected to some cleaning process, i.e. coal could be planned for cleaning. Considering the results of these tests, it is obviously that cleaning of coal from the surface mining is becoming a necessity, and not just one of the possibilities.

REFERENCES

1. Bethell, P. J., Luttrell G. H. (2004) Coal preparation. In: Encyclopedia of energy, 1st edition (Cleveland C. J. Editor), Elsevier, Boston, 507-528.
2. Bureska, L. J. (2017) Influence of coal quality to the boiler efficiency and opportunity for its improvement. Tehnika, 43 (1-4), 59-65.
3. EPS (2021) Production Capacities. http://www.eps.rs/eng/Poslovanje-ugalj/Pages/Kapaciteti-Ugalj.aspx (accessed on the 24th February 2021).
4. Harikrishnan, S. Pillai, Seshadri P. S., Balasubramanian K. R. (2016) Effect on performance of utility boiler with variation in fuel properties. International Journal of Applied Engineering Research, 11 (6), 3786-3790.
5. Hower, J. C., Parekh, B. K. (1991) Chemical/physical properties and marketing. In: Coal preparation (Leonard, J. W., III and Hardinge, B. C. Editors), Society for Mining, Metallurgy and Exploration, Inc., Littleton, Colorado, 1-94.
6. JP PEU Resavica (2021). https://www.jppeu.rs/index.html.
7. Kostović, M., Kostović, N., Tokalić, R. (2018) Coal mining and preparation in Serbia. Underground Mining Engineering, 33, 69-77.
8. Pantelić, N. (2018) Possibility of washing of energetic coal size fraction -40+0 mm from Tamnava for use in Thermal power plant, Master's thesis, University of Belgrade, Faculty of mining and geology, Belgrade.
9. Noble, A., Luttrell G. H. (2015) A review of state-of-the art processing operations in coal preparation. International Journal of Mining Science and Technology, 25 (4), 511-521.
10. Saxena P. (2013) Impact of coal quality variation on power plants, Power Line, 56-57 https://npti.gov.in/sites/default/files/download-document/impact-of_coal_quality_variation_on_power_plant.pdf (accessed on the 24th February 2021).
11. Waymel, E. B., Hatt, R. M. (1988) Improving coal quality: An impact on plant performance, In: Joint Power Generation Conference, Coal Quality, Control Fact V.2. Philadelpia, Pensylvania, Proceddings, 1-7. http://www.coalcombustion.com/Webpage%20PDF%20Files/Presentations%20and%20Papers%20pdf%20files/Improving%20Coal%20Quality.pdf (accessed on the 24th February 2021).
12. Word Coal Association. Coal & electricity. https://www.worldcoal.org/coal-facts/coal-electricity/ (accessed on the 24th February 2021).

XIV International Mineral Processing
and Recycling Conference
Belgrade, Serbia, 12-14 May 2021

BENEFICIATION OF NON COKING COAL FROM OPEN CAST MINES OF WESTERN COALFIELD AREA FOR VALUABLE UTILIZATION

Sanjay Chaudhuri[#], Uday Sankar Chattopadhyay, Subash Maji,
Thonangi Gouri Charan
Coal Mineral Processing Division, CSIR-Central Institute of Mining and Fuel
Research, Digwadih Campus, Dhanbad, India

ABSTRACT – The non-coking coal constitutes about 85% of the Indian coal reserves and the depositions remained mostly as low rank sub-bituminous and non-coking types. The vast reserves of the non-coking coal are usually high moisture, high ash, high volatile and sub-bituminous types (Ro % ranging between 0.4 to 0.65). Beneficiation of Indian non-coking coals is gaining importance due to varied reasons. A recent study was carried out on a sample from open Cast Mines of Western Coalfield area to find out the possibility for the better utilization of these coals for different end uses. In the initial characterization it is observed that ash, moisture, VM, fixed carbon, GCV and HGI are 36.8%, 7.1%, 24.9%, 31.2%, 4,025 Kcal/kg and 62 respectively. The detailed studies carried out on these coals, showed that the coal poses easy washability characteristics and if it is judiciously beneficiated, the product may be used for the sponge industry and power sector.

Keywords: Open Cast Coal Samples, Proximate Analysis, Ultimate Analysis, Petrographic Analysis, AFT Studies and Washability Investigation.

INTRODUCTION

India's energy sector is primarily dependent on coal which is the abundant indigenous resources. Presently about 70 percent of primary commercial energy supply and 70 percent of the power generation is through coal. Such dependence on coal is going to continue in the foreseeable future. Almost 70% of the Indian non-coking coal produced in India has high ash content (40-45% on average) and the users, especially the power sector are unhappy with the quality of the coal being supplied by the coal producer. The average calorific value of the coal produced from the coalfields have reduced significantly from an average of 5000 kcal/kg in 1970 to an average of 2500-3000 kcal/kg in 2015. The problem is further aggravated because of the multiplicity of coal fed to the power plants.

The tests carried out by various Government agencies proved beyond doubt that the use of washed coal in power stations will improve the overall efficiency of the boiler and reduce environmental pollution. With the advent of more and more open cast, mechanized mining (accounts for 85-90% of total production of power grade coal); the quality of the coals being supplied to the power stations is deteriorating. Quality control of coal fed to the power plants being one of the most important ingredients for improvement in the present energy situation; there is an absolute need for

---

[#] corresponding author: sanjaycfri@yahoo.co.in beneficiation of Indian non-coking coals to the extent to meet the qualities required. The coal washing capacity from all the 52 washing plants is 131 Mtpa, indicating that around 30% of the coal is being washed before it is used in power stations.

Govt. of India has promulgated a Gazette Notification (GSR 560(E) & 378 (E), dated September 19,1997 and June 30,1998 respectively) on use of beneficiated/blended coal containing ash not more than 34 percent w.e.f. June 2001 and the distance was further reduced to less than 500 kms w.e.f. January'2016. The committed linkage by Coal India Limited to the thermal plants located beyond 500 km distance away from pit heads is 236 million tons in 2015-16 which is likely to increase to 271 million tons by 2016-20. All these coals will have to be beneficiated for improvement in the quality.

Coal continues to be a major source of power generation through many new sources of electricity that have emerged in the past few decades. The relative abundance of coal in India makes it a natural choice as the primary source of power generation. As on today, the total reserves of coal in India are 310 billion tones, out of which about 83% constitute non-coking coal. For more than a century, the backbone of the power sector in India has been the thermal generation plants (coal-fired thermal plants, in particular). Of the installed base of 330 GW in 2017, coal-based power plants contribute almost 60 percent (194 GW).

In the present study an attempt has been made to beneficiate two non-coking coals supplied from Open Cast Mines of Western Coalfield area to find out the possibility for the better utilization of these coals after blending into single coal in a suitable proportions as desired by the sponsor.

EXPERIMENTAL

Rom sample

Two ROM coal samples were blended in the proportion as desired by the sponsorer after each of the samples was thoroughly mixed.

Crushing

The ROM sample was first screened at 100 mm and the + 100 mm was crushed in a pilot plant single roll crusher to below 100 mm. The crushed material was blended with the below natural 100 mm fraction and a total sample was prepared for characterization, screen analysis, float and sink tests, cleans generation, reserve.

Characterization of raw coal

The characterization results of the raw coal with respect to proximate, GCV and HGI are shown in Table 1, Tables 2, 3 and 4 depicts the ultimate, ash fusion and petrographic analysis of the raw coal.

Screen analysis of raw coal (x100mm)

Screen analysis was carried at sizes 100, 75, 50, 25, 13, 6, 3 and 0.5 mm. The size fractions were weighed and analyzed for ash and moisture percent. The screen analysis data is shown in Table 5.

Washability investigations

The individual size fractions 100–75 mm, 75–50 mm, 50–25 mm, 25–13 mm, 13–6 mm, 6–3 mm and 3–0.5 mm were subjected to float & sink tests, the specific gravity range being 1.40–1.90. The combined washability data (100–0.5 mm) are shown in Table 6. The washability data of the combined fraction (100–0.5 mm) was generated and used for plotting various washability curves for 100–0.5 mm coals to establish the washability characteristics. The minus 0.5 mm coal fractions were not subjected to float & sink tests. The washability and Mayers curve are shown in Fig 1.

Generation of cleans and characterization

It was noticed from the size analysis data (Table 5), that by crushing the ROM coal at 100 mm followed by stage wise screening at 0.5 mm, the desired clean coal having ash <34% may be achieved. Hence, the size fraction (100–0.5mm) was treated as clean coal and was reduced in size to desire specifications as per the Standard and samples were prepared for characterization.

RESULTS AND DISCUSSIONS

Characterization of raw coal

Table 1 Characterization of Raw Coal

Sample	Moisture %	Ash %	Volatile Matter %	Fixed Carbon %	GCV, kcal/kg	HGI
Proximate (AD basis)	7.1	36.8	24.9	31.2	4025	62

Table 2 Ultimate Analysis of Raw Coal

Carbon %	Hydrogen %	Nitrogen %	Sulphur %
42.3	2.4	1.1	0.4

Table 3 Ash fusion temperature of Raw Coal

a) Initial Deformation Temperature, ^{O}C	1353
b) Spherical Temperature, ^{O}C	>1400
c) Hemi-Spherical Temperature, ^{O}C	>1400
c) Flow Temperature, ^{O}C	>1400

Table 4 Petrographic data of raw coal

Maceral (Vol %)					Ro %
Vitrinite	Semi-vitrinite	Liptinite	Inertinite	Mineral Matter	0.62
31.3	-	18.6	34.5	15.6	
(37.1)		(22.0)	(40.9)		

*Figures in parenthesis are on mineral matter free basis.

On the basis of characterization study it was found that coal possessed moderately high ash value (36.8%) with GCV 4,025 kcal/kg. Ash fusion temperature study indicated that the coal was suitable for power industries. The petrographic analysis showed that the coal contained low vitrinite with low maturity whereas the ultimate analysis reflected the low contribution of carbon contain (42.3%) in the coal.

Table 5 Screen analysis of raw coal crushed to 100 mm

Size(mm)	Wt %	Ash %	Moist %
+100	4.1	29.0	13.4
100-75	21.4	28.2	12.5
75-50	20.0	26.6	12.6
50-25	18.9	28.3	11.9
25-13	6.9	30.8	11.3
13-6	7.6	35.6	6.3
6-3	4.6	49.9	4.4
3-0.5	7.8	74.0	2.4
-0.5	8.6	76.1	2.6
	100.0	37.4	9.9

Table 5.1 Size analysis of coal fines (-0.5mm)

Size (mesh)	Wt %	Ash %	Mois %
+72	65.0	81.6	2.2
-72+100	4.9	83.7	2.0
-100+200	8.1	73.0	2.8
-200+300	2.8	67.4	3.0
-300	19.1	58.3	4.1
	100.0	76.1	2.6

It was observed from size analysis data of raw coal crushed to 100mm that ash percent was increasing with the decreasing the size of coal and the ash% was found highest as 76.1% at the size range of below 0.5mm. The wet size analysis data of -0.5mm fraction indicated the major contributory fraction was -30 to 72 mesh of wt % as 65% with the highest ash value 81.6%.

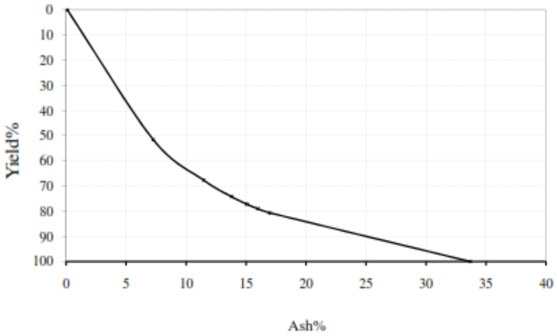

Figure 1 Mayer's curve size tested 100-0.5 mm

Table 6 Composite Washability data (Size: 100-0.5mm)

Sp.Gr	Wt %	Ash %	Cum. Float		Cum. Sink		Ch. Wt %	Mayer's pt.value
			Wt. %	Ash %	Wt. %	Ash %		
<1.40	51.6	14.1	51.6	14.1	48.4	54.6	25.8	7.3
1.40-1.50	16.1	26.2	67.7	17.0	32.3	68.7	59.6	11.5
1.50-1.55	6.6	35.2	74.2	18.6	25.8	77.3	71.0	13.8
1.60-1.70	2.9	42.9	77.2	19.5	22.8	81.7	75.7	15.1
1.70-1.80	1.8	50.8	79.0	20.2	21.0	84.4	78.1	16.0
1.80-1.90	1.6	60.2	80.6	21.0	19.4	86.4	79.8	17.0
>1.90	19.4	86.4	100.0	33.7			90.3	33.7
	100.0							

It was found from the washability investigation that the coal was easy to wash. No washing is required to achieve the clean coal of 34% ash range. Only screening is to be performed at 3 mm or 0.5 mm size to get clean coal of yield >90% at 34% ash level. At 20% ash level the recovery of clean coal is about 79% and that can be done by simple washing through Jigging. The cumulative yield of clean coal was found above 80.0% for the <1.90 specific gravity fraction of an ash value 21.0%. The rejects (>1.90) ash was 86.4% with the yield 19.4.

Characterization of cleans (100-0.5mm)

The clean coals (100–0.5 mm, wt%=91.4%) were characterized for proximate analysis, GCV and HGI respectively. The proximate analysis, GCV and HGI results of the clean coal are shown in Table 7, Tables 8, 9 and 10 depicts the ultimate, ash fusion and petrographic analysis, of the clean coal.

Table 7 Characterization of Clean Coal

Sample	Moisture %	Ash %	Volatile Matter %	Fixed Carbon %	GCV, kcal/kg	HGI
Proximate (AD basis)	9.7	33.0	23.2	34.1	4325	54

Table 8 Ultimate Analysis of Raw Coal

Carbon %	Hydrogen %	Nitrogen %	Sulphur %
50.96	3.07	1.04	0.48

Table 9 Ash fusion temperature of Raw Coal

a) Initial Deformation Temperature, ^{O}C	1320
b) Spherical Temperature, ^{O}C	>1400
c) Hemi-Spherical Temperature, ^{O}C	>1400
c) Flow Temperature, ^{O}C	>1400

Table 10 Petrographic data of raw coal

Maceral (Vol %)					Ro %
Vitrinite	Semi-vitrinite	Liptinite	Inertinite	Mineral Matter	
38.7	0.1	11.9	32.4	16.9	0.71
(46.5)	(0.2)	(14.4)	(38.9)		

*Figures in parenthesis are on mineral matter free basis.

The characterization of clean coal at 33.0% ash level indicated that the gross calorific value has increased to 4,300 kcal /kg and the ultimate results showed the improvement of carbon content 50.96% whereas petrographic test reflected the improvement of vitrinite concentration in clean coal (38.7%).

CONCLUSION

- The washability characteristics of coal tested is easy to wash.
- The ash content of the fine coal and coal fines are very high compared to that of the coarse coal.
- The ROM coal may be crushed at 100 mm and by either single stage dry screening with 13 mm or two stage screening at 13 and 0.5 mm, the target ash may be achieved. At 100-0.5mm size coal of 91.4% may be achieved at 33.8% ash level. No beneficiation is required, only coal handling, crushing and screening is sufficient.
- At 20% ash level the recovery of clean coal is about 79% and that can be done simple washing by Jigging. Hence this coal is suitable for corex process. As the cumulative yield of clean coal was found above 80.0% for the <1.90 specific gravity fraction of an ash value 21.0% so this coal may also be utilized for Cement and Sponge Iron Industries.

ACKNOWLEDGEMENT

The author is thankful to the Director CIMFR, Dhanbad for giving his consent to publish this paper in the journal. The authors are also thankful to all the staff members of the division for providing valuable support at various stages of this work.

REFERENCES

1. Provisional Coal Statistics 2016-17, Coal Controller Organization Office, Kolkata, Govt. of India.
2. Gouricharan, G.T., Jha, G.S., Chattopadhyay, P.C., Haldar, D.D., Sen, K. (2007) Cleaning potential of Samleshwari noncoking coal by washability investigation. Coal Preparation, 27 (1-3), 138-148.
3. Sen, K., Das, N.S. (2002) Economic washing of Indian power coal & availability of indigenous technology. Seminar on 'Challenges Facing Indian coal'. Coal Consumers Association of India, 21 Feb, 2002, Kolkata.
4. Gouricharan, T.G., Chaudhuri, S., Majhi, S.C., Prasad, P.S., Singh, P.K. (2018) Studies on the cleaning potentialities of high ash Indian non-coking coals for meeing the MOEF's stipulations. Journal of Mines, Metals & Fuels, 66 (7), 370-374.

XIV International Mineral Processing
and Recycling Conference
Belgrade, Serbia, 12-14 May 2021

CORRELATION BETWEEN IMAGE ANALYSIS AND CALORIFIC VALUES OF COALS

Mehmet Bilen#
Bülent Ecevit University, Faculty of Engineering, Department of Mining Engineering, Zonguldak, Turkey

ABSTRACT – In this study, image analysis were carried out for a total of 40 samples collected. In terms of their image analysis, RGB and HSV values (color space) were evaluated. In addition to that, corresponding calorific values for each sample were determined. Samples, latterly described more in detail, are collected from coal preparation plants of various locations of coal production, i.e. Zonguldak Region for hardcoal, Kütahya Region for lignites. Although correlations obtained were not that successful for the initial estimates, still they can be considered as first attempts for the calorific value determination based on the image analysis.

Keywords: Image Analysis, RGB&HSV, Calorific Value, Turkish Coal, Coal Preparation Plant.

INTRODUCTION

Image analysis is widely employed in terms of characterization purposes in ore preparation and it is addressed as a way to digitize the images. For example, Moolman et al. (1994) [4] has investigated bubbles of floatation in terms of image analysis. Sgarbossa et al. (2014) [6] have investigated wood pellets and they tried to observe the effect of color differences on quality and energy parameters. Referring to the same study of Sgarbossa et al. (2014) [6], significant correlations between ash content of these above mentioned samples and their corresponding RGB&HSV values were obtained. As opposed to the context of this study, higher heating values were observed in lighter color samples, while it is known that hardcoal samples (darker color) have higher heating values compared to lignites (lighter color), respectively. Corresponding representation by Sgarbossa et al. (2014) [6] is provided in Figure 1.

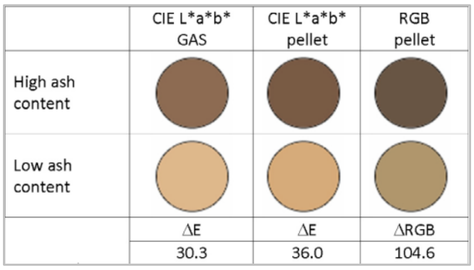

	CIE L*a*b* GAS	CIE L*a*b* pellet	RGB pellet
High ash content	●	●	●
Low ash content	●	●	●
	ΔE	ΔE	ΔRGB
	30.3	36.0	104.6

Figure 1 Classification of low and high ash content wood pellets with RGB [6]

---

corresponding author: mehmetubilen@yandex.com

$$Gray = 0.2989 \cdot R + 0.5870 \cdot G + 0.1140 \cdot B \tag{1}$$

Referring back and forth to the study of Zelin et al. (2012) [8], they have provided representations of coal particles in gray scale, and the corresponding images are provided in Figure 2. However in this regard, some techniques should be employed in order to have better representation of images and in the order of particle size prediction. Zelin et al. (2012) [8] have employed EHPF (exponential high pass filter) on the images (Refer to Figure 2 (c)).

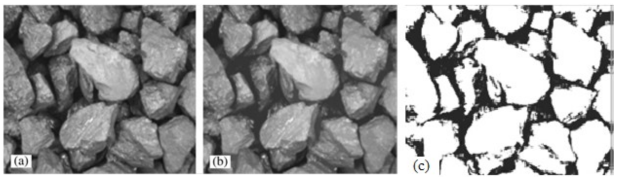

Figure 2 Images of coal particles, a) image at gray scale, b) improved image of coal particles at gray scale, c) employment of exponential high pass filter [8]

Zelin et al. (2012) [8] have employed some methods to process the coal particles' images in two dimensions and later they have tried to obtain size orientations of the samples under investigation.

In a similar methodology, Gokay and Gundogdu (2001) [3] have developed a software based on the color differentiations of marble samples. As Gokay and Gundogdu (2001) [3] proposed, marbles can be better described with their RGB values instead of just only color orientations. Wang and Liang (2011) [7] study have aimed to determine valuable and unvaluable coal samples in terms of their mineral composition and they simply employed image processing methods for this abovementioned purpose. The authors [7] have compared the gray scale values of each revised images [7]. With the method proposed in abovementioned study of Wang and Liang (2011) [7], the authors have determined the unvaluable coal stocks. Rathod and Soni (2015) [5] have implemented image processing to determine the coal quality parameters. Referring back to Zelin et al. (2012) [8], authors have claimed the fact that "no clear relationships among pellet characteristics and its color have been proved". In addition to the study of Zelin et al. (2012) [8] about wood pellets, there is very little literature as regards to coal quality parameters and their color.

In the scope of this study, 40 samples from 5 various location (8 sample from each) were collected. The samples abovementioned are representative samples of coal preparation plant feed samples from the locations of coal productions, i.e. "Amasra", "Kozlu", "Çatalağzı", "Üzülmez" for hardcoal samples, and "Omerler" for lignite samples.

EXPERIMENTAL

Samples were collected from 5 different location namely "Amasra", "Kozlu", "Çatalağzı", "Üzülmez" and "Omerler". The first 4 locations ("Amasra", "Kozlu", "Çatalağzı", "Üzülmez") correspond to hardcoal while the last one ("Omerler") corresponds to lignite samples. Samples are the representative samples collected from the feed to the coal preparation plant operating at that location of coal production. So, sampling places are the coal preparation plants located nearby the coal production sites. “Amasra”, “Kozlu”, “Çatalağzı”, “Üzülmez” are organizations that produce hardcoal in Zonguldak under the rule of TTK (Turkish Hardcoal Enterprise). “Omerler” is an organization under the rule of TKI (Turkish Coal Enterprise) likewise. Collected coal samples have coarse size distribution in the beginning and they were about 20 kg initially. The representative samples were taken from the collected samples after size reduction was realized. Accordingly, samples were prepared for calorific value measurements. Samples were dehumidified at an oven (105 °C) and they were ground as an initial requirements. Calorific value measurements were realized with Parr 6100 calorimeter equipment and the standard [1] testing procedure was employed.

RESULTS AND DISCUSSION

In this study, samples (a total of 40) were analyzed in terms of their calorific values and the corresponding images were evaluated in terms of their RGB & HSV orientations. Results are tabulated and provided in Table 1.

Table 1 Results of the images processing (Average R, G, B, H, S, V values) and calorific values for each sample

	Sample No	Average R	Average G	Average B	Average H	Average S	Average V	Calorific Value kcal/kg
Omerler	1	94	97	99	202	5	39	4447
	2	103	107	107	175	5	42	4454
	3	106	109	110	188	4	43	4321
	4	108	112	120	218	10	47	4300
	5	107	110	119	221	10	47	4232
	6	115	115	119	236	4	47	4356
	7	129	133	146	210	18	57	4231
	8	125	123	122	6	4	49	4223
	Sample No	Average R	Average G	Average B	Average H	Average S	Average V	Calorific Value kcal/kg
Amasra	1	119	132	146	212	19	57	2231
	2	119	132	145	210	18	57	2545
	3	110	114	122	218	10	48	4050
	4	121	119	125	262	5	49	3014
	5	130	137	151	219	14	59	2050
	6	115	128	141	209	19	55	2054
	7	124	129	141	224	12	55	2075
	8	119	124	135	224	12	53	3254
	Sample No	Average R	Average G	Average B	Average H	Average S	Average V	Calorific Value kcal/kg
Kozlu	1	132	130	131	350	4	53	4768
	2	124	122	121	5	4	49	4556
	3	107	108	112	232	4	44	5443
	4	100	107	114	209	13	45	5025
	5	98	107	111	193	12	44	4798
	6	126	131	142	224	11	56	4579
	7	126	133	145	217	13	57	4535
	8	87	103	106	187	18	42	4451
	Sample No	Average R	Average G	Average B	Average H	Average S	Average V	Calorific Value kcal/kg
Çatalağzı	1	124	123	123	345	3	49	3486
	2	130	136	148	222	12	58	2025
	3	97	111	119	201	19	47	3547
	4	104	112	115	193	10	45	3754
	5	95	98	100	201	5	39	3994
	6	118	124	134	219	12	53	3545
	7	105	122	133	204	22	52	4112
	8	133	134	149	236	11	58	2892
	Sample No	Average R	Average G	Average B	Average H	Average S	Average V	Calorific Value kcal/kg
Üzülmez	1	97	99	98	148	4	39	6259
	2	99	106	121	220	19	47	6650
	3	94	105	107	188	13	42	5235
	4	133	131	129	28	4	53	6635
	5	93	108	111	188	17	44	5034
	6	91	102	102	172	11	41	5343
	7	93	103	103	178	11	41	5632
	8	100	104	103	163	4	41	4923

As regards to Table 1, calorific values are lowest for Çatalagzı and Amasra samples while they are highest for Uzulmez and Kozlu. However, not a distinct interpretation can be made regarding to average R, G, B and H, S, V values, respectively. However at this stage, it is rather meaningful to compare each image processing parameter with calorific value. Once, calorific value is plotted against an average parameter of image processing (For example Average "R" versus "calorific value", see Figure 3(a)), correlation coefficients of each could be determined. Refer to Figure 3 (a, b, c, d, e and f) for the correlations between image processing parameter and calorific value.

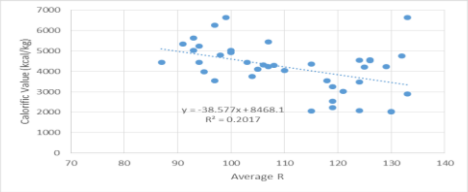

Figure 3 (a) Average "R" versus Calorific value

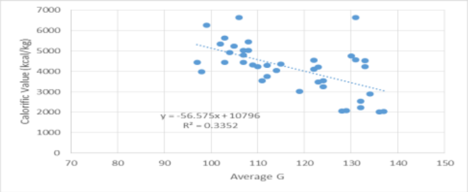

Figure 3 (b) Average "G" versus calorific value

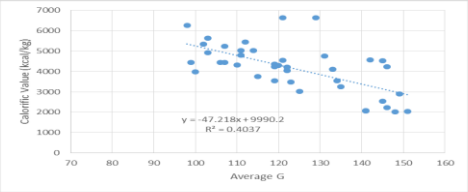

Figure 3 (c) Average "B" versus calorific value

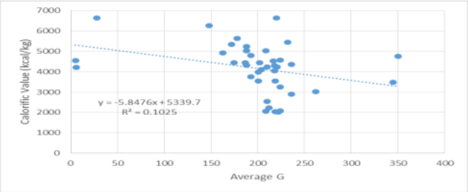

Figure 3 (d) Average "H" versus calorific value

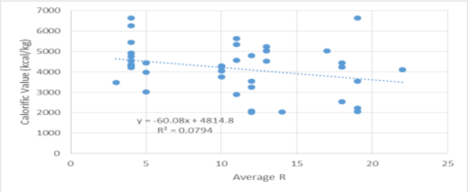

Figure 3 (e) Average "S" versus calorific value

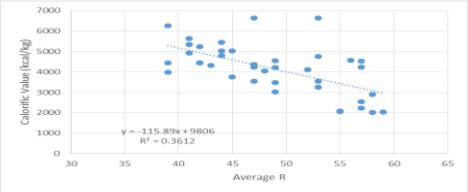

Figure 3 (f) Average "V" versus calorific value

Obtained correlation coefficients, (R^2) are tabulated in Table 2. According to the results (Figure 3 (a)(b)(c)(d)(e)(f)), correlation coefficients are between 0.08 and 0.36, respectively. Proposed model (evaluated on XLSTAT) is provided in Equation 2 and corresponding correlation (predicted vs measured calorific values) is provided in Figure 4.

Table 2 Image processing parameter versus calorific values and corresponding R^2

Image Procesing Parameter vs Calorific Values	R^2
Average "R" vs Calorific Values	0.20
Average "G" vs Calorific Values	0.34
Average "B" vs Calorific Values	0.40
Average "H" vs Calorific Values	0.10
Average "S" vs Calorific Values	0.08
Average "V" vs Calorific Values	0.36

$$Calorific\ Value = 13014 + (154 \cdot R) - (241 \cdot G) - (437 \cdot B) - (0.6 \cdot H) + (157 \cdot S) + (1120 \cdot V) \qquad (2)$$

Having calculated the calorific values based on Eq. (2), the following graphical representation of predicted (calculated) vs measured calorific values can be established (See Figure 4).

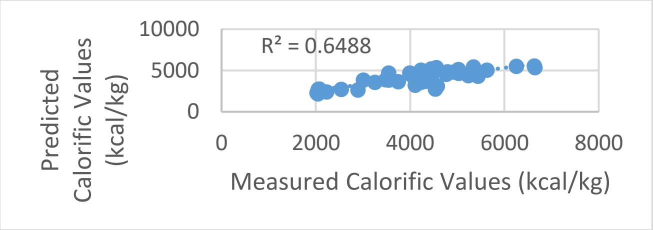

Figure 4 Model (Equation 2) predicted calorific values with respect to measured calorific values

As regards to the correlation between predicted and measured calorific values (Figure 4), it can be claimed that calorific value can be predicted based on the image analysis results to some extent. The correlation coefficient obtained is not as significant as it is desired. However, still the correlation coefficient obtained (Figure 4) is one of the highest among others. Based on this equation (Eq. 2), one can predict calorific value of an unknown sample to some degree. Heterogen structure of coal is one of the main reason for this respectively low correlation coefficient. Along with heterogeneity of coal samples, number of samples could be another issue which should be under evaluation. Coal formation on the other hand might not be as significant as the constraints abovementioned. Image analysis is not regarded as an alternative way for petrographical analysis and petrography either alone or with coal formation has the key role on calorific value differentiation. However, Chelgani et al. (2010) [2] have tried to relate petrographical analysis results with calorific values and they have only obtained a correlation coefficient (R^2=0.83) with a second order equation. Considering these findings of Chelgani et al. (2010) [2], method proposed (Eq. 2) is more user friendly with only employing image analysis parameters and it is first order equation. As regards to gray scale values in addition, possible relation was investigated likewise. Initially gray scale values for each sample were calculated based on the equation provided by Zelin et al. (2012) [8], Eqn. (1). And calculated gray scale values were compared to measured calorific values (See Figure 5). However, as regards to Figure 5, not really a significant relation between gray scale values and calorific values was observed. Instead, the model (Equation 2) can be better employed in terms of calorific value estimations.

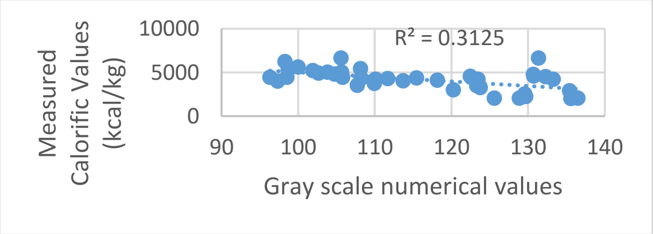

Figure 5 Gray scale values with respect to measured calorific values

Although in the context of this study, there is no distinct relationship observed between color space orientation and quality parameters of coal, still this study can be regarded as an initial step in terms of coal quality determination through an image analysis based applications.

CONCLUSION

In this study, coal samples collected from various locations (in Turkey) have been tested in terms of their calorific values. In addition, images taken (under specific environments) were analyzed in terms of their color space orientations. In this context, having evaluated all coal types RGB and HSV values (with image processing), coals can be better classified, i.e. a definite range of RGB & HSV values for each coal type. This proposed method of classification would lead no misunderstanding and it would enable more clear definition of each coal. All in all, this study aims to find out any possible relationship between image analysis and calorific values of coal samples. Although, no distinct relationship between any image analysis parameter and calorific value was observed, still multiple regression of the data resulted in a significant correlation coefficient (R^2=0.66).

REFERENCES

1. ASTM D5865-13 Standard Test Method for Gross Calorific Value of Coal and Coke, ASTM International, West Conshohocken, PA, 2013, https://doi.org/10.1520/D5865-13
2. Chelgani, S., Chehreh, B.H, William, C.G., James C.H. (2011) Study Relationship between Inorganic and Organic Coal Analysis with Gross Calorific Value by Multiple Regression and ANFIS. International Journal of Coal Preparation and Utilization, 31 (1), 9-19.
3. Gokay, M.K., Gundoğdu, I.B. (2001) Mermer Renklerinin Sayisal Analiz Yoluyla Siniflandirilmasi Ve Mermer Işleme Tesislerindeki Kullanilabilirliği. MADENCİLİK/Haziran-Eylül-Aralık.
4. Moolman, D.W., Aldrich, C., Van Deventer, J.S.J., Stange, W.W. (1994) Digital image processing as a tool for on-line monitoring of froth in floatation plants. Mineral Engineering, 7, 1149-1164.
5. Rathod, S.P., Soni, A.H. (2015) An Approach on Determination on Coal Quality using Digital Image Processing. International Journal of Engineering Research and Applications, 1 (5), 38-41.
6. Sgarbossa, A., Costa, C., Menesatti, P., Antonucci, F., Pallottino, F., Zanetti M., Grigolato, S., Cavalli, R. (2014) Colorimetric patterns of wood pellets and their relations with quality and energy parameters. Fuel, 137, 70-76.
7. Wang, R., Liang, Z. (2011) Automatic separation system of coal gangue based on DSP and digital image processing. IEEE 2011 Symposium on Photonics and Optoelectronics (SOPO 2011), Wuhan, China, 1-3.
8. Zelin, Z., Jianguo, Y., Lihua, D., Yuemin, Z. (2012) Estimation of coal particle size distribution by image segmentation. International Journal of Mining Science and Technology, 22, 739-744.

XIV International Mineral Processing
and Recycling Conference
Belgrade, Serbia, 12-14 May 2021

PREDICTION OF CALORIFIC VALUE FOR SOME TURKISH LIGNITES BASED ON MOISTURE AND ASH CONTENT

Serdar Yilmaz[1#], İhsan Toroglu[1], Dilek Cuhadaroglu[1], Anna Rasskazova[2]
[1] Bülent Ecevit University, Faculty of Engineering, Department of Mining Engineering, Zonguldak, Turkey
[2] Mining Institute of Far Eastern branch of Russian Academy of Sciences, Khabarovsk, Russia

ABSTRACT – In this study, ash and moisture content data of Turkish lignites from various locations were evaluated and their corresponding calorific values were scrutinized. Turkey has significant underground treasure in terms of lignites and substantial amount of energy supply is met at the end of combustion of these lignite coals in power plants. In this context, suitability of calorific values of lignite coals for combustion in power plants is the most important parameter. On the other hand, coal samples can have fluctuated calorific values does not matter if they are produced from a specific location. Calorific values of coals can be said to be directly proportional to carbon content basically while they are indirectly proportional to ash or moisture content. Studying the data under consideration, it was observed the fact that lower the ash and/or moisture content of the coal samples higher the calorific values are. This observation was taken as a basis of this research in fact. In the body of this study, ash content, moisture content and calorific values data obtained from various power plants are investigated and a calorific value prediction tool for the Turkish lignites on the basis of statistical methods was proposed. Statistical evaluations were carried out either with single linear regression or multiple linear regression and effect of each parameter was aimed to understand. Finally, statistically obtained results were considered in detail and a calorific value prediction tool for Turkish lignites was proposed.

Keywords: Turkish lignites, Moisture, Ash, Calorific value.

INTRODUCTION

Turkish lignites, when considered together with energy demand of Turkey and better technological achievements in terms of clean coal utilization, have an increasing significance along with increasing demand for the time being and for the close future. According to Akkaya [1], in order to meet the challenge of sustainable development and increasing energy demand, coal consumption would be approximately twice by the year 2030 [2]. In terms of utilization of coals specifically lignites in a power plant, calorific value is one of the most addressed concern. According to Majumder *et al*. [3] for example, common practices to assess the quality of coal is summarized as calorific value, proximate analysis and ultimate analysis. Akkaya [1] has pointed out this fact as “heating value of the used coal is a critical parameter for the proper design and operation process of the coal fueled systems”. Akkaya [1] has referred to one of the previous study of their selves [4] and claimed the fact that measurement of heating value of coal is time consuming and expensive.

[#] corresponding author: s_yilmaz67@hotmail.com

Rather referring to its complexity of coal calorific value measurement, the quick assessment of coal quality is a pre-requisite to run the boilers of power plants [3]. Due to availability of various types of coals from suppliers and due to the limitations in terms of boiler design and operational parameters, prediction requirements of calorific values gets more significant day by day. Not only because of the reasons abovementioned but also calorific value fluctuations either in a specific pit of coal mine or in a coal stock, calorific value determination/prediction in the shortest time is one of the greatest obstacle to understand the boiler efficiency. In this context many researchers [3-19] have tried to predict coal calorific value based on the proximate analysis data (See Akkaya 2020 for detail [1]).

In terms of calorific value prediction of Turkish lignites in specific, there is not a study after Kucukbayrak *et al*. [20]. Kucukbayrak *et al*. [20] have proposed a new formula for the estimation of calorific values of Turkish lignites by employing the proximate analysis data. They [20] have analyzed 24 Turkish lignites in terms of calorific value and proximate analysis. The data of 26 other lignite sample (Turkish Lignite) was also employed in their [20] own formulization. Unlike Kucukbayrak *et al*. [20], many researchers [1, 6, 10, 11, 13, 14, 15, 16, 19] have studied with the large number of samples (mostly obtained from literature).

In the context of this study, Turkish lignites data (ash, moisture and calorific value) were obtained from 8 different power plants. A prediction tool for the calorific value was proposed by employing ash content and moisture content data.

DATA COLLECTION AND INITIAL EVALUATIONS

The data of each individual power plant includes a list of ash content, moisture content and calorific value for different times (years). In this context, this list of data can be regarded as lots of samples (data) from a specific region of power plant, i.e. the coal mine itself. The data addressed in this study is actually the corresponding data of coals of power plants (lignite fired) from the study of Elevli [21]. Elevli [21] have investigated the coal prices of power plants and tried to develop pricing models. Although the main concern of Elevli [21] is the coal pricing models, she has tabulated the corresponding calorific values, ash content and moisture content along with their prices in their study. Data set provided by Elevli [21] for the aim of coal pricing can be attributed and employed in this study for the aim of calorific value prediction. The data of corresponding coals of different power plants for different times can be regarded as an individual sample data of each coal collected from that specific region. In the study of Elevli [21], a total of 521 lignite coal sample data, 43 out of which belongs to “Orhaneli”, 45 out of which belongs to “Afşin-Elbistan”, 94 out of which belongs to “Kangal”, 47 out of which belongs to “Seyitömer”, 174 out of which belongs to “Soma”, 48 out of which belongs to “Tunçbilek”, 34 out of which belongs to “Yatağan”, 36 out of which belongs to “Yeniköy” was evaluated.

RESULTS AND DISCUSSION

As presented earlier, it was aimed to find out successful prediction method for calorific values of Turkish lignites. For this purpose Multiple Linear Regression was employed and resulting from this employment an empirical equation (based on ash and moisture content) was proposed.

Initially at this stage, it is rather helpful to analyze the whole data. In order to perform this initial analysis, corresponding graphs of ash content vs calorific values and moisture content vs calorific values were plotted (See Figure 1 and Figure 2, respectively).

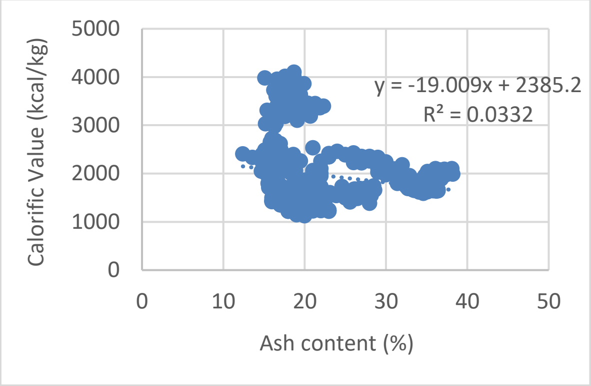

Figure 1 Ash content (%) of the samples versus the corresponding calorific values (kcal/kg) (corresponding data of calorific values and moisture content of Turkish lignites was adapted from the study of Elevli [21])

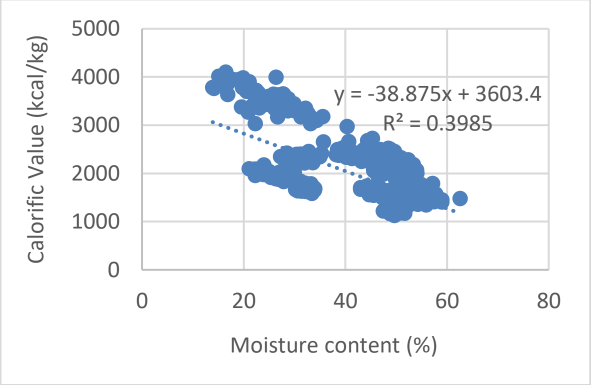

Figure 2 Moisture content (%) of the samples versus the corresponding calorific values (kcal/kg) (corresponding data of calorific values and moisture content of Turkish lignites was adapted from the study of Elevli [21])

Referring to Figure 1 and Figure 2, moisture content of Turkish lignites have better relationship with the calorific values. Kumari *et al*. [17] have employed ash and moisture content data to predict calorific values of Indian coals. If calorific value prediction methodology of Kumari *et al*. [17] is applicable to the data evaluated in this paper, then it would be no need to develop one another. Figure 3 briefly is the plot of calculated calorific values of Turkish lignites with the method suggested by Kumari *et al*. [17] and real calorific values.

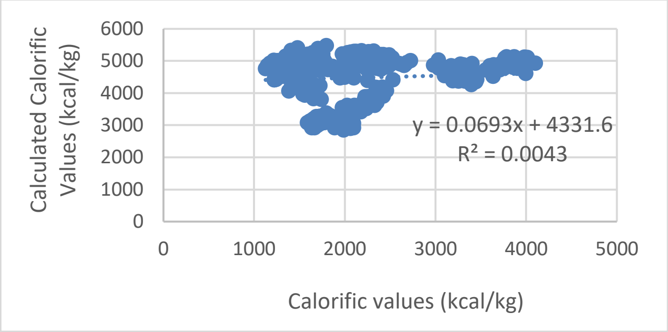

Figure 3 Graphical representation of calculated calorific values of Turkish lignites with the method suggested by Kumari *et al*. [17] and data of calorific values of Turkish lignites (adapted from the study of Elevli [21])

As regards to the graphical representation (Figure 3), Kumari *et al*. [17] study was not even considerable for Turkish lignites in this case. It is obvious the fact that there is a need for calorific value prediction for Turkish lignites in specific because of the low degree of correlation, i.e. R^2. Employment of multiple linear regressions was carried out with the help of statistical software (XLSTAT). Multiple linear regressions resulted with an empirical formula (Eqn. 1).

$$CV = -65.174x[AC(\%) + MC(\%)] + 6171.7 \quad (1)$$

where CV is for calorific value, AC is for ash content and MC is for moisture content, respectively. The method proposed is not only user friendly but it was achieved with a reasonable R^2 (Figure 4).

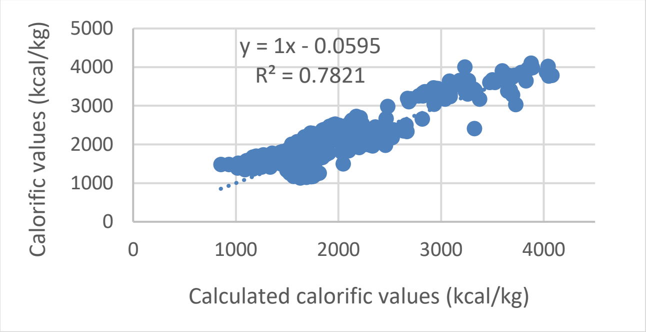

Figure 4 Graphical representation of calculated (with Eqn.1) calorific values of Turkish lignites and the data of calorific values of Turkish lignites (adapted from the study of Elevli [21])

Referring to Figure 4, in terms of calorific value prediction for Turkish lignites one can easily refer to the method provided in Eqn.1. As it is seen from the graphical representation and the corresponding R^2 (R^2=0.78), prediction method could be employed for Turkish lignites in specific.

CONCLUSION

In this study, employing the data of coal ash and moisture content, a new method for the prediction of Turkish lignites' calorific values was proposed. A literature data of Turkish lignites was reviewed and ash content, moisture content and calorific values were adapted in this context. Calorific values of Turkish lignites was found out to be in relation with ash content (%) and moisture content (%). However this relations abovementioned are not that meaningful as for the initial observations. Rather meaningful one is moisture content in term of calorific value interrelations. The proposed method in this study is a linear function, consists of slope and intercept. The main function proposed takes the sum of ash content and moisture content into account and it yielded a R^2 about 0.8 (R^2=0.78). The abovementioned methodology is proposed by employing a total of 8 Turkish lignites. This study is not only novel in terms of the considering the fluctuated data of same coal mine, but also it includes a comparison of literature and current methodology, and it emphasizes the necessity of region specific prediction methods/models.

REFERENCES

1. Akkaya, A.V. (2020) Coal higher heating value prediction using constituents of proximate analysis: Gaussian process regression model. International Journal of Coal Preparation and Utilization, 1-16.
2. Seervi, K. (2015) Prediction of calorific value of Indian coals by artificial neural network. BSc Thesis, Department of mining engineering national institute of technology, Rourkela, 50.
3. Majumder, A., Jain, R., Banerjee, P., Barnwal, J. (2008) Development of a new proximate analysis based correlation to predict calorific value of coal. Fuel 87 (13-14), 3077–3081.
4. Akkaya, A.V. (2013) Predicting coal heating values using proximate analysis via a neural network approach. Energy Sources, Part A: Recovery, Utilization, and Environmental Effects 35 (3), 253–260.
5. Patel, S.U., Kumar, B.J., Badhe, Y.P., Sharma, B.K., Saha, S., Biswas, S., Chaudhury, A., Tambe, S.S., Kulkarni, B.D. (2007) Estimation of gross calorific value of coals using artificial neural networks. Fuel 86 (3), 334–344.
6. Mesroghli, Sh., Jorjani, E., Chelgani, S.C. (2009) Estimation of gross calorific value based on coal analysis using regression and artificial neural networks. International Journal of Coal Geology, 79 (1-2), 49–54.
7. Erik, N.Y., Yilmaz, I. (2011) On the use of conventional and soft computing models for prediction of gross calorific value (GCV) of coal. International Journal of Coal Preparation and Utilization 31, 32–59.
8. Kavšek, D., Bednárová, A., Biro, M., Kranvogl, R., Vončina, D., Beinrohr, E. (2013) Characterization of Slovenian coal and estimation of coal heating value based on proximate analysis using regression and artificial neural networks. Central European Journal of Chemistry, 11 (9), 1481–1491.
9. Feng, Q., Zhang, J., Zhang, X., Wen, S. (2015) Proximate analysis based prediction of gross calorific value of coals: A comparison of support vector machine, alternating

conditional expectation and artificial neural network. Fuel Process Technology 129, 120–129.

10. Tan, P., Zhang, C., Xia, J., Fang, Q.Y., Chen, G. (2015) Estimation of higher heating value of coal based on proximate analysis using support vector regression. Fuel Process Technology, 138, 298–304.
11. Ghugare, S.B., Tambe, S.S. (2017) Genetic programming based high performing correlations for prediction of higher heating value of coals of different ranks and from diverse geographies. Journal of the Energy Institute 90, 476–84.
12. Akhtar, J., Sheikh, N., Munir, S. (2017) Linear regression based correlations for estimation of high heating values of Pakistani lignite coals. Energy Sources, Part A: Recovery, Utilization, and Environmental Effects, 39 (10), 1063–70.
13. Wen, X., Jian, S., Wang, J. (2017) Prediction models of calorific value of coal based on wavelet neural networks. Fuel, 199, 512–22.
14. Acikkar, M., Sivrikaya, O. (2018) Prediction of gross calorific value of coal based on proximate analysis using multiple linear regression and artificial neural networks. Turkish Journal of Electrical Engineering & Computer Sciences, 26, 2541–52.
15. Bui, H.B., Nguyen, H., Choi, Y., Bui, X.N., Nguyen-Thoi, T., Zandi, Y. (2019) A novel artificial intelligence technique to estimate the gross calorific value of coal based on meta-heuristic and support vector regression algorithms. Applied Science, 9 (22), 4868.
16. Go, A.W., Agapay, R.C., Ju, Y.H., Conag, A.T. (2019). Unified semi-Empirical models for predicting or estimating the heating value of coal and related properties – Theoretical basis and thermochemical implications. Combustion Science and Technology 1–26.
17. Kumari, P., Singh, A.K., Wood, D.A., Hazra, B. (2019) Predictions of gross calorific value of Indian coals from their moisture and ash content. Journal Geological Society of India 93, 437–42.
18. Onifadea, M., Lawal, A. I., Aladejare, A. E., Bada, S., Idris M. A. (2019) Prediction of gross calorific value of solid fuels from their proximate analysis using soft computing and regression analysis. International Journal of Coal Preparation and Utilization, 1–15.
19. Qi, M., Luo, H., Weib, P., Fu, Z. (2019) Estimation of low calorific value of blended coals based on support vector regression and sensitivity analysis in coal-fired power plants. Fuel, 236, 1400–1407.
20. Kucukbayrak, S., Durus, B., Mericboyu, A.E., Kadioglu, E. (1991) Estimation of calorific values of Turkish lignites. Fuel, 70 (8), 979-981.
21. Elevli, S. (2003) Analysis of coal prices in thermal power plants and development of pricing models. PhD. Thesis, Department of Mining Engineering, Graduate School of Natural and Applied Sciences, Cumhuriyet University, Sivas, Turkey.

A COMPARISON OF SEPARATION EFFICIENCY OF RAW AND WASTE COALS IN A COAL SEPARATION PLANT IN THE ANTHRACITE COAL MINE "VRSKA CUKA"

Jovica Sokolović[1#], Slobodan Mitić[2], Ivana Ilić[1]
[1] University of Belgrade, Technical Faculty in Bor, Bor, Serbia
[2] JPPEU, Resavica, Serbia

ABSTRACT – Anthracite coal mine “Vrska Cuka” Avramica is located near Zajecar (about 10 km) in eastern Serbia. High quality raw anthracite coal is exploited and processed in the coal separation plant. This plant was designed in the late 1980s, and construction was completed during 1994. The separation process includes gravity and flotation concentration. The process of the gravity concentration of coal is carried out in a dense-medium separator "BSRI-1200". The flotation process is not operating. The Vrska Cuka anthracite coal mine, besides of the well-known reserve of high-quality raw coal, also has significant quantities of low-quality waste coal which has been deposited on tailings. Valorization of coal from old tailings ponds has great significance from both economic and environmental aspects of coal processing.

This paper presents the comparative results of studying the efficiency of separation of raw and waste coal in the coal separation plant in the anthracite coal mine "Vrska Cuka".

Keywords: Vrska Cuka, Separation, Raw, Waste, Coal.

INTRODUCTION

Anthracite coal mine "Vrska Cuka" Avramica is located about 10 km from Zajecar in eastern Serbia.

The industrial plant was built 1992 and it comprises of a complex technological process for gravity and flotation concentration of raw coal [1]. Size fractions over 0.5 mm are treated by dense-medium processes, whereas flotation has been proposed for sizes finer than 0.5 mm.

The gravitational concentration of coal is performed in a two - part separator "BSRI - 1200" with a spiral and a solenoid valve for separating the sinking fraction. The two-part trough separator for coal separation belongs to the group of separators with medium depth and static operating conditions. It can be treated simultaneously in this separator, namely: (- 25 + 5) and (- 5 + 0.5) mm [1].

Anthracite coal mine "Vrska Cuka" besides of known reserve of high-quality raw coal, has about 2 million tons of coal waste. There are several small and three large tailing ponds as follows: tailing pond Avramica in Avramica stream, tailing pond Planir in Avramica stream and tailing pond Vrska Cuka in Bukovo stream [2-4].

[#] corresponding author: jsokolovic@tfbor.bg.ac.rs

EXPERIMENTAL

Materials

The representative sample of raw coal and waste coal samples, as well as the products of separation of both coal samples collected manually from separation process in the anthracite coal mine Vrska Cuka in Serbia.

Float-Sink analyses

The laboratory float-sink analysis was performed on the raw coal sample of size fraction - 25 + 0.5 mm [4] and waste coal sample of size fraction - 20 + 0.5 mm [2] as well as products of separation process (clean coal as float fraction and tailing as sink fraction).

The float-sink analysis was performed using a mixture of organic heavy liquid (solutions of $CHBr_3$, CCl_4 and whitespirit of density ranging from 1.3 to 2.0 g/cm^3) of increasing density [6]. The fractions obtained by the densimetric analysis are subjected to chemical analysis of the ash.

RESULTS AND DISCUSSION

The results of float-sink analysis of the size fractions - 25 + 0.5 mm of a raw coal as well as products of separation (separation coal as float fraction and tailing as sink fraction) by the fraction density are shown in Table 1.

Table 1 Sink-float analysis of a raw coal, clean coal and tailing, size fraction -25+0.5 mm

Specific gravity	Raw coal (feed) (%)		Clean coal (float) (%)		Tailing (sink) (%)	
kg/m^3	Mass %	Ash %	Mass %	kg/m^3	Mass %	Ash %
-1300	13.45	4.39	19.25	5.24	2.54	3.13
-1400	30.38	4.26	40.11	3.66	7.31	3.48
-1500	8.54	13.67	17.83	10.65	6.20	13.10
-1600	4.25	23.10	7.23	23.14	2.26	19.66
-1700	2.35	30.04	5.27	25.62	2.32	33.38
-1800	1.54	43.44	3.51	35.46	3.60	38.10
-1900	1.19	45.98	1.15	49.21	4.73	59.11
-2000	3.84	67.91	0.48	56.63	7.64	71.46
+2000	33.87	82.34	5.17	80.68	63.40	84.27
∑	100.00		100.00		100.00	

By separation of raw coal, it can be noticed that depending on the quality, in the zone of separation densities, the mass yield of the float fraction is about 60%. It can be seen that the separation would be easily carried out over a wide range of operating densities. For instance, the separation of raw coal on the density 1700 kg/m^3, it can be achieved mass recovery of coal, Im = 59.56% with average ash content, p = 7.93%. The average ash content in the clean coal is about 14%.

The results of float-sink analysis of the size fractions - 20 + 0.5 mm of a waste coal as well as products of separation (separation coal as float fraction and tailing as sink fraction) by the fraction density are shown in Table 2.

Table 2 Sink-float analysis of a waste coal, clean coal and tailing, size fraction -20+0.5 mm

Specific gravity	Feed waste coal (%)		Clean coal (float) (%)		Tailing (sink) (%)	
kg/m^3	Mass %	Ash %	Mass %	Ash %	Mass %	Mass %
-1300	1.77	5.89	10.91	3.96	0.44	5.08
-1400	12.22	4.63	42.41	4.17	2.43	3.80
-1500	5.75	13.01	14.20	13.86	0.82	13.78
-1600	2.25	24.42	9.82	32.03	0.29	25.35
-1700	2.10	30.82	2.75	34.63	0.40	34.11
-1800	4.33	58.39	2.10	44.08	1.82	59.68
-2000	4.48	58.84	1.62	55.70	3.41	62.17
+2000	67.10	86.19	16.19	83.67	90.39	86.99
∑	100.00		100.00		100.00	

The data from the float-sink analysis of waste coal indicates that it can be obtained under ideal operating conditions. The separation of waste coal on the density 1700 kg/m^3, it can be achieved mass yield of clean coal, Im = 24.09% with average ash content in the final float product 10.85%.

Determination of separation efficiency of raw and waste coals

The partition or distribution curve is useful in assessing the efficiency or sharpness of the coal separation [7]. The partition curve or Tromp curve (introduced by Tromp in 1937) is obtained by plotting the partition coefficient against the mean of its density range [8]. The gradient of the curve is a measure of the sharpness of separation and to indicate the accuracy of the separation [7]. From the partition curve the probable error of separation (EP) and the separation density or cut point (ρ_{50}) can be determined.

The probable error of separation (EP) is defined as half the difference between the S.G. where 75% is recovered in the sinks and the S.G. at which 25% is recovered in the sinks [7]. The Grumbrecht method was used to determine the mass recovery. The results are shown in Table 3 and Figure 1.

Table 3 Calculation of mass recovery of Grumbercht methods – raw coal

Specific gravity	Feed raw coal (%)	Separation coal (float) (%)	Tailing (sink) (%)				
kg/m^3	U	K	J	U - J	K - J	(U – J) (K – J)	(K – J)^2
-1300	13.45	19.25	2.54	11.00	16.71	138.810	279.224
-1400	30.38	40.11	7.31	23.57	32.83	773.096	1075.840
-1500	8.54	17.83	6.20	2.34	11.63	27.214	135.257
-1600	4.25	7.23	2.26	1.99	4.97	9.890	24.701
-1700	2.35	5.27	2.32	0.03	2.95	0.099	8.703
-1800	1.54	3.51	3.60	-2.06	-0.09	0.185	0.008
-1900	1.19	1.15	4.73	-3.45	-3.58	12.673	12.816
-2000	3.84	0.48	7.64	-3.80	-7.16	27.208	51.266
+2000	33.87	5.17	63.40	-29.53	-58.23	1719.532	3390.773
∑						2753.397	4978.548

$$Im = \frac{2753.697}{4978.548} \cdot 100 = 55.31\% \qquad (1)$$

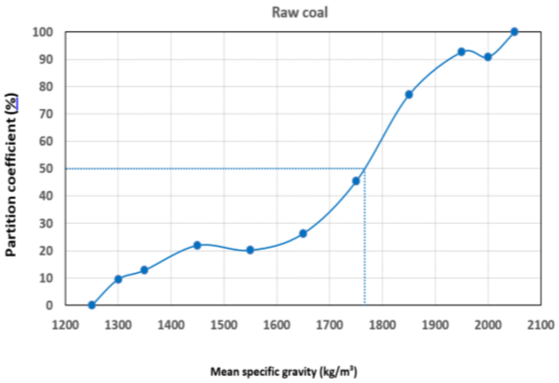

Figure 1 Partition curve for gravity separation of raw coal

From the partition curve, the separation density or ρ_{50} is 1775 kg/m^3.
The probable error of separation is expressed as:

$$E_p = \frac{\rho_{75}-\rho_{25}}{2} = \frac{1850-1650}{2} = 100\ kg/m^3 \qquad (2)$$

Compared theoretic and industrial values for gravity separation of raw is given in table 4.

Table 4 Compared theoretic and industrial values for gravity separation of raw coal

	Theoretic values	Industrial values
Mass yield (wt. %)	60.71	55.31
Average ash (%)	8.61	13.65
ρ_p (kg/m^3)	1775	1775
E_p (kg/m^3)	0	100

The results of the calculation of mass recovery of Grumbercht methods as well as partition curve for gravity separation of waste coal are shown in Table 5 and Figure 2.

Table 5 Calculation of mass recovery of Grumbercht methods – waste coal

Specific gravity	Feed waste coal (%)	Separation coal (float) (%)	Tailing (sink) (%)				
kg/m^3	U	K	J	U - J	K - J	(U – J) (K – J)	(K – J)^2
-1300	1.77	10.91	0.44	1.33	10.47	13.93	109.62
-1400	12.22	42.41	2.43	9.79	39.98	391.40	1598.40
-1500	5.75	14.20	0.82	4.93	13.38	65.96	179.02
-1600	2.25	9.82	0.29	1.96	9.53	18.68	90.82
-1700	2.10	2.75	0.40	1.70	2.35	4.00	5.52
-1800	4.33	2.10	1.82	2.51	0.28	0.70	0.08
-2000	4.48	1.62	3.41	1.07	-1.79	-1.92	3.20
+2000	67.10	16.19	90.39	-23.29	-74.20	1728.12	5505.64
∑						2220.87	7492.31

$$Im = \frac{2220.87}{7492.31} \cdot 100 = 29.64\% \tag{3}$$

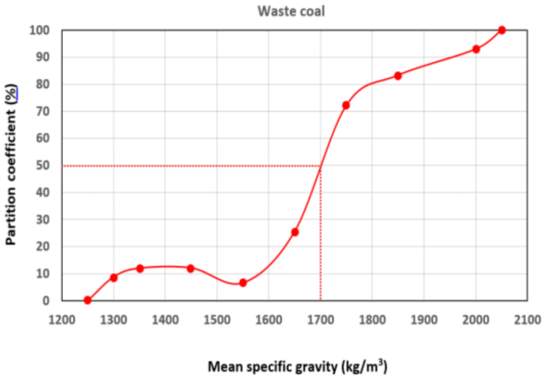

Figure 2 Partition curve for gravity separation of waste coal

From the partition curve, the separation density or ρ_{50} is 1700 kg/m^3.

The area between the ideal and real curves is called the "error area" and is a measure of the degree of misplacement of particles to the wrong product.

The probable error of separation is expressed as:

$$E_p = \frac{\rho_{75}-\rho_{25}}{2} = \frac{1770-1650}{2} = 62.5\ kg/m^3 \tag{4}$$

Compared theoretic and industrial values for gravity separation of waste coal is given in table 6.

Table 6 Compared theoretic and industrial values for gravity separation of waste coal

	Theoretic values	Industrial values
Mass yield (wt. %)	24.09	29.64
Average ash (%)	10.85	23.64
ρ_p (kg/m^3)	1700	1700
E_p (kg/m^3)	0	100

CONCLUSION

The control of the efficiency of the gravity separation process is reflected in the determination of the deviation of the obtained industrially results in relation to the laboratory results. The separation density (ρ_{50}) and the probable error of separation (Ep) are the basic indicators for assessing the separation efficiency that are determined from the partition curve.

The partition curves for gravity separation of raw and waste coals are shown in Figures 1 and 2. It can be used to indicate the operating parameters of separation. The following conclusions can be drawn from this paper.

The separation density for raw and waste coals are 1775 kg/m^3 (Figure 1) and 1700 kg/m^3 (Figure 2). The probable error of separation for raw coal and waste coal are 100 kg/m^3 and 62.5 kg/m^3, respectively.

By comparing the obtained values, it can be conclude that the process of waste coal separation takes place with a higher separation sharpness because the value of the probable deviation is lower.

Mass yield for raw coal obtained in industrial conditions (55.31%) is lower than the theoretical value (60.71%). Mass yield of waste coal in industrial process (29.64%) is approximately the theoretical value (29.04%). The ash content obtained in the industrial conditions with operating parameters is in both cases higher than theoretical.

Different of industrial from theoretical results are a consequence of inefficiency of operation of concentration devices, as well as increased probability of wandering of lighter particles to the sink product.

ACKNOWLEDGEMENT

"The research presented in this paper was done with the financial support of the Ministry of Education, Science and Technological Development of the Republic of Serbia, within the funding of the scientific research work at the University of Belgrade, Technical Faculty in Bor, according to the contract with registration number 451-03-9/2021-14/ 200131".

REFERENCES

1. The Main Mining Project of separation for concentration of coal from the anthracite mines "Vrška Cuka" - Avramica, Book I, Technology and mechanical project, Institute for Copper, Bor. (In Serbian)
2. Stanojlovic, R., Markovic, Z.S., Milanovic, D., Trumic, G. (1995) The technology for valorization of coal from old discard of antracite mine "Vrška Čuka", Proceedings of the 6th Balkan Conference on Mineral Processing. Ohrid, Macedonia, pp. 418-421.
3. Mitić, S. (1994). Technological possibilities of obtaining coal from the old tailings of coal mine „Vrška Čuka“, Graduated thesis, University of Belgrade, Technical Faculty in Bor, Bor. (In Serbian)
4. Sokolovic, J. (2012) The study of phenomenon of coal activation in the flotation process by attrition, Ph.D. thesis, University of Belgrade, Technical faculty in Bor, Serbia.
5. Sokolović, J. (2000) Consideration of the possibility of improving the existing technological process of separation of raw coal mine "Vrška Cuka" Avramica, Graduated thesis, University of Belgrade, Technical Faculty in Bor, Bor. (In Serbian)
6. Sokolović, J. (2020) Practicum in physical methods of concentration, Technical Faculty in Bor, Bor. (In Serbian)
7. Gupta, A., Denis Yan, D. (2016) Chapter 16 - Gravity Separation. In: Mineral Processing Design and Operations (Second Edition), Elsevier, 563-628.
8. Tromp, K. F. (1937). New methods of computing the washability of coals. Glückauf, 37, 125-131.

XIV International Mineral Processing and Recycling Conference
Belgrade, Serbia, 12-14 May 2021

COMPARISON OF THE INFLUENCE OF POLYACRYLAMIDE AND SODIUM OLEATE ON SELECTIVE FLOCULATION OF GETITE FROM SLUDGE

Ljiljana Tankosić[#], Svjetlana Sredić
University of Banja Luka, Faculty of Mining Prijedor, Bosnia and Herzegovina

ABSTRACT – The paper is part of the research conducted with the aim of examining the possibility of applying selective flocculation of goethite from sludge that occurs in the process of iron ore production. Selective flocculation is one of the methods that can be applied to separate iron minerals from useless and harmful impurities. The aim of this study was to compare the influence of polyacrylamide and sodium oleate as a flocculant on the rate of deposition of goethite under different conditions. For the purpose of sample characterization, chemical and mineralogical analysis and determination of granulometric composition were performed. Mineralogical analysis was performed using the methods of X-ray structural analysis and polarization microscopy. Granulometric analysis of the sample was performed by sieve analysis (wet and dry) on the goethite sample. The paper examines the influence of the type and concentration of flocculants based on polyacrylamide and sodium oleate and pH values on the deposition rate of a goethite sample. The results showed that the rate of deposition of goethite is influenced by the type of flocculant and pH value, while the concentration of flocculant does not significantly affect the rate of deposition.

Keywords: Selective Flocculation, Goethite, Flocculants, Deposition Rate.

INTRODUCTION

In recent years, generation of fines and slimes during mining and mineral processing has become an important problem, both economically and ecologically. The large quantity of these fines/slimes are often discarged as waste into tailing ponds. Fine iron ores most often contain clay, silica and other minerals as gangue material along with iron minerals. For these reasons, a number of new approaches to recover the fine and ultrafine particles have been investigated, including selective flocculation [1, 2].

Processing of iron ore in Omarska mine is carried out by following methods: washing, sieving, grading and magnetic concentration. The large quantity of fine sized sludge disposed as final waste in the beneficiation plants of the Omarska mine (Republic of Srpska, Bosnia and Herzegovina) is an important economically and ecologically problem. That sludge samples are composed of major goethite -FeO(OH) and quartz, less clay minerals (mostly illite-sericite), and minor magnetite and todorokite [3].

Selective flocculation studies of iron ore were carried out using different flocculants, such as starch, polyacrylamide, oleate [4-6], etc., but mostly on hematite. The characteristics of ores/slimes from different localities differ substantially and the knowledge about fine goethite ore processing is still relatively poor. The reason for this

---

[#] corresponding author: ljiljana.tankosic@rf.unibl.org research is that the selectivity of anionic polyacrylamide has not been achieved in the flocculation of waste sludge from the Omarska mine [7]. These results suggest that it is necessary to further examine the individual components and their behavior in a complex system such as sludge, in order to determine the best parameters (conditions, reagents, etc.) for selective flocculation.

This paper presents a part of the research of individual components of waste sludge from the Omarska mine. The polyacrylamide and sodium oleate eficiency in goethite removal from aqueous solutions was investigated on a sample of natural goethite from Omarska mine. In order to compare of the two flocculants, a study of the flocculation goethite suspensions using anionic poliacrylamyde and sodium oleate as flocculants was made by determining the settling rates of the suspensions and the amount of suspended solids. All experiments were performed as a function of the pH value and flocculant dosage.

MATERIALS AND METHODS

Materials

Goethite

Representative iron ore from Omarska mine, labeled as “limonite ore” was handpicked. The “limonite ore” samples are composed of major goethite -FeO(OH) which dominate over hematite (Fe_2O_3), and with minor contents of magnetite (Fe_3O_4), quartz (SiO_2) and clay minerals. XRPD, FTIR and SEM-EDS analyses were recently performed for obtaining more precise mineral determination [8]. The density of the sample is also determined: 3.940 g/cm^3. Chemical composition obtained by wet analysis of natural goethite from Omarska mine is given in the Table 1.

Table 1 Chemical composition of the goethite from Omarska mine

Sample	**Chemical compositions (in mass %)**											
	Fe	**SiO_2**	**Al_2O_3**	**CaO**	**MgO**	**TiO_2**	**P**	**Mn**	**S**	**Na_2O**	**K_2O**	**LOI**
Goethite	57.16	4.44	0.59	0.03	0.22	<0.01	0.078	1.18	0.007	0.009	0.033	10.86

The results of particle size distribution analyzes of the goethite sample showed that 80% of the sample belongs to the classes bellow 25 µm, and the highest mass percentage (about 50%) belongs to the finest classes, i.e. to those bellow 10 µm. This confirms that the limonite ore from Omarska is fine-grained, which is one of the reasons for the large amount of waste sludge.

Flocculants

All reagents used were of analytical grade, and they were prepared as solutions in distilled water. The 1% sodium oleate were used as first flocculant and 0.1% PAM A100 (Kemira) as second flocculant. Preparation of flocculant for all experiments was carried out in the same way according to the instructions provided by the manufacturer of reagents. As pH modifier, 0.1M NaOH and 0.1M HCl was used.

Methods

The natural settling, and settling with the addition of sodium oleate and polyacrylamide as flocculant, were determined. The flocculation experiments were performed at a pulp density with 13.8% of solid, which is adequate to the simulation of natural industrial conditions. To examine the effect of flocculant dosage it was used: (i) Beaker of 100 ml volume, (ii) 13.8 g of dry sample in 100 ml of distilled water for the experiment; (iii) 250 g/t, 500 g/t, 1000 g/t of sodium oleate and (iv) 50 g/t, 100 g/t, 250 g/t of PAM. All of the tests were performed at the pH=4, pH=7 and pH=10.5. For flocculation tests, sample was mixed for two minutes. After adjusting pH value, the suspension continued to mix for two minutes. After addition of flocculant, sample was mixed for five minutes, and left to settle for one minute, separated float from sink, dried both of them at 105 °C in oven and weighed the sediment material.

RESULTS AND DISCUSSION

Influence of the type and dosage of flocculants on settling rates

The effect of two flocculants was studied by comparing critical rates. The critical rate (V_{av}) in this paper is calculated as: $V_{av} = H/t_{cr}$ (mm/min); where H is height of the clear zone during critical time (in mm), and t_{cr} is deposition time required to achieve a critical deposition point (in minutes).

The usual doses for each flocculant were used, taking into account the maximum doses recommended for each of them. The effect of different flocculants was studied by conducting settling tests at pH 7, which is an average pH value in real conditions.

Settling rates of the goethite suspensions depending on the dosage of two different flocculants are shown in Figure 1. It is obvious that the addition of flocculant causes an increase in settling rates in both of cases. The maximum settling rate achieved with dosages of 1000 g/t for the sodium oleate and 250 g/t for PAM A100. Also, Figure 2 shows that anionic polyacrylamide has a significantly greater effect on the rate of settlement of goethite than sodium oleate even in the case of the maximum dosage of sodium oleate.

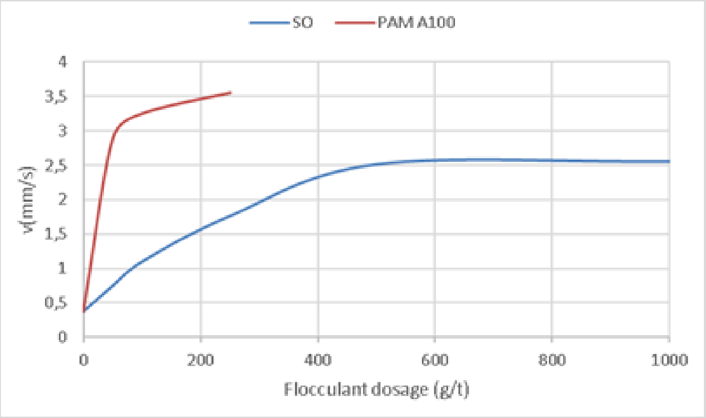

Figure 1 Settling rates of the goethite suspensions for two flocculants comparatively

Influence of pH

Generally, the stability of the metal oxide suspension strongly depends on the pH value, because their surface charge becomes increasingly positive as the pH decreases and becomes increasingly negative as the pH increases. The charge on most oxides in aqueous systems is controlled by the acid-base chemistry of surface oxide and hydroxide species. The stability of the goethite suspension without flocculants strongly depends on the pH value. This is clearly seen in Figure 2, in which they are shown natural settling curves of goethite at different pH values. There is not settling at either pH 4 or pH 10, because of increasing of surface charge causing the repulsive forces.

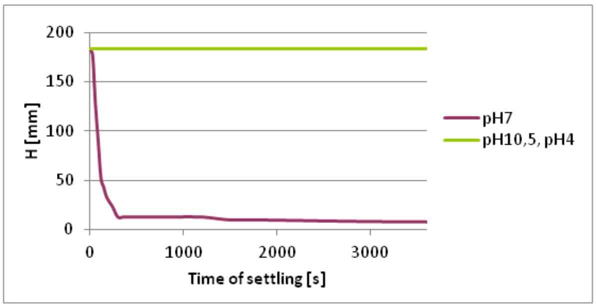

Figure 2 Natural settling of goethite at different pH values

Influence of the type of flocculants on settling behavior of goethite depending on pH is also investigated.

The effect of flocculants is also highly dependent on pH (Figure 3 - 4), but there is no difference in the behavior of the suspension, regardless of used flocculant. Settling tests with additional different flocculants at different pH shows that none of the sample is precipitated at pH=4 and pH=10.5.

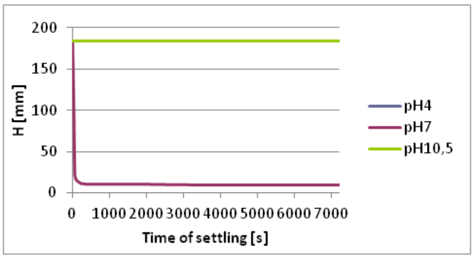

Figure 3 Flocculation settling of goethite with sodium-oleate (250 g/t) at different pH values

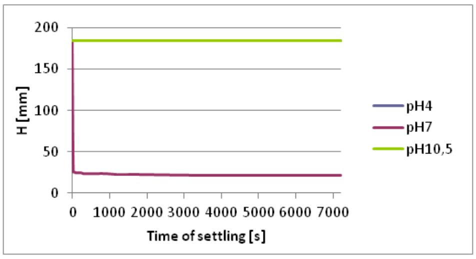

Figure 4 Flocculation settling of goethite with PAM A100 (250 g/t) at different pH values

Since the positive charge of the goethite decreases with increasing of pH value, the occurrence of inefficient action of both flocculants in an alkaline medium is understandable. From the other side dependence of flocculation on pH can be due to the effect of pH on the surface characteristics of goethite in water as well as that on the anionic poliacrylamyde and sodium oleate solution chemistry. Namely, for anionic polyacrylamide and sodium oleate, in the base medium, anionic spices are predominate as well as for goethite. The settling in a neutral medium occurs because in the neutral pH (range of about 5-8) neutral surfaces predominate, both in goethite and in both flocculants (the un-dissociated oleic acid and weakly dissociated polyacrylamide).

A comparison of the amounts of suspended solids as a function of pH shows that the highest amounts are expected at pH=7 in both cases (Figure 5).

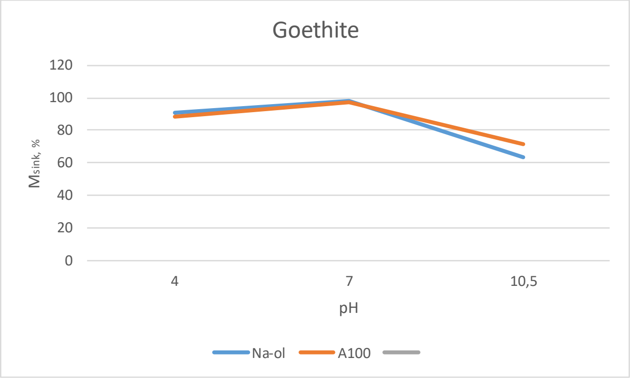

Figure 5 Amount of suspended solids with dosage of 250 g/t with sodium-oleate and PAM A100

CONCLUSION

The polyacrylamide and sodium oleate efficiency in goethite removal from aqueous solutions was investigated on a sample of natural goethite from Omarska mine.

Comparison of the critical rates has shown that the addition of the flocculant increases critical rates in both cases, but more significant in the case of using PAM A100.

The natural settling behavior of the goethite without flocculant strongly depends on the pH value, because their surface charge in aqueous systems is controlled by the acid-base chemistry of surface oxide and hydroxide species. There is not settling at either pH=4 or pH=10, because of increasing of surface charge causing the repulsive forces.

The settling behavior of the goethite with additional flocculant is influenced more by the type of flocculant and pH value, than by the dosage of the flocculant.

The effect of anionic polyacrylamide and oleate as a flocculants is highly dependent on pH. Effect of anionic poliacrylamyde and sodium oleate on the flocculation of goethite is noticeable at pH=7 only. A comparison of the amounts of suspended solids as a function of pH shows that the highest amounts are expected at pH= 7 in both cases regardless of the dosage of flocculants.

The highest settling rate of goethite and the highest amount of suspended solids are achieved under the following conditions: at pH=7 and the addition of anionic polyacrylamide with dosage of 250 g/t.

In relation to selectivity, our unpublished results indicate greater selectivity of oleates, but the conclusion can be made only when all research with anionic polyacrylamide on other components of sludge (quartz and clay sample from Omarska mine) is completed.

REFERENCES

1. Somasundaran, P., Runkana, V. (2000) Selective flocculation of fines. Trans. Nonferrous Met. Soc.China, 10, 8-11.
2. Weissenborn, P.K., Warren, L.J., Dunn, J.G. (1994) Optimisation of selective flocculation of ultrafine iron ore. Int. J. Miner. Process., 42, 191-213.
3. Tankosić, Lj., Tančić, P., Sredić, S., Nedić, Z. (2017) Characterization of the sludge generated during the processing of iron ore in Omarska mine, 6th International Symposium "Mining and Environmental Protection" Vrdnik, 21th-24th June 2017, Book of Proceedings, 255-262.
4. Severov, V.V., Filippova, I.V. (2013) Mechanism of starch adsorption on Fe–Mg–Al-bearing amphiboles, International Journal of Mineral Processing, 123, 120-128.
5. Khangaonkar, P.R., Bala Subramani, K.J. (1993) Flocculation of hematite fines by anionic polyacrylamide polymers, Minerals Engineering, 6 (7), 765-774.
6. Shibata, J., Fuerstenau, D.W. (2003) Flocculation and flotation characteristics of fine hematite with sodium oleate, International J. of Mineral Processing, 72 (1-4), 25-32.
7. Tankosić, Lj., Tančić, P., Sredić, S., Nedić, Z. (2018) Comparative Study of the Mineral Composition and Its Connection with Some Properties Important for the Sludge Flocculation Process-Examples from Omarska Mine, Minerals, 8 (3), 119.
8. Tankosić, Lj., Tančić, P., Sredić, S., Nedić, Z., Malbašić, V. (2017) Characterization of natural raw materials in the processing of iron ore from Omarska mine, Proceedings of International Symposium "Mining and Geology Today", Belgrade, Serbia, 316-330.

XIV International Mineral Processing
and Recycling Conference
Belgrade, Serbia, 12-14 May 2021

RESEARCH ON REGIMES OF LIMONITE ORE HYDROTRANSPORT FOR THE CONDITIONS OF PERDO SOTO ALBA PLANT

Aleksandr Nikolaev[1#], Sergey Avksentiev[1], Raul Izquierdo Pupo[2],
Alberto Turro Breff[2]
[1] Saint-Petersburg Mining University, Saint Petersburg, Russia
[2] Institute of Mining and Metallurgy, Moa, Republic of Cuba

ABSTRACT – The paper examines regular flow patterns of high-concentrated limonite pulp with significant content of finest grains. Engineering procedures have been developed to calculate basic parameters of limonite ore hydrotransport in turbulent and structured regimes. Trustworthiness of scientific statements, conclusions and recommendations is justified by theoretical research, establishment of analytical dependences, results of laboratory and industrial experiments. Practical regularities of behavior have been identified for the coefficient of hydraulic resistance, depending on pulp density in the range 35-45% in case of pulp flow in structured regime, as well as regularity of pressure losses in case of pulp flow in horizontal and inclined pipelines in turbulent regime.

Keywords: Hydrotransport, Flow Regimes, Limonite Ore, Pulp, Rheological Properties.

INTRODUCTION

Increase in production of nickel and cobalt due to opening of new nickel plants in Punta Gorda and Las Camariocas and further improvement of technological processes and equipment, used by operating enterprises, is one of the key development objectives for nickel-cobalt industry of Cuba. For 50 years the haulage of limonite ore from the quarry to Pedro Soto Alba plant has been performed by hydrotransport. However, the quarry reserves will have been depleted by 2025. Therefore today various projects are being designed to organize transportation from the new deposit Moa-East to the plant. Existing difference of geodesic altitudes (65 m) between the deposit and the point where pulp is loaded into hydroseparators is an important condition, emphasizing the possibility to use gravity transfer, as it does not consume any energy. Pedro Soto Alba plant is the only enterprise in Cuba that applies hydrotransport of limonite ore. In the pulp processing station, limonite ore is watered down to the mass concentration 25-30%. Under the gravity particles of the size –0.833 mm are fed into the hydroseparator, using concrete and cast iron pipelines 610 mm in diameter and 5129 m in length. The pipeline is divided into 54 sections, in-between which there are wells, where velocity of the pulp decreases. The flow velocity varies in the range 1-1.4 m/s. Results of experiments have shown that settling velocity of the pulp is higher on the exit from processing station than on the entry to hydroseparator.

After hydroseparators, thickened pulp (45-48% of solid mass) is transported with the help of centrifugal pumps; the pipeline is 460 m long and 508 mm in diameter; average

---

[#] corresponding author: aleknikol@mail.ru flow velocity varies from 0.3 to 0.57 m/s. Apart from limonite ore, the pulp contains solid serpentine fraction (up to 5%), which crusts at the bottom of a pipeline, reducing its useful section and causing pressure losses. Hence, when designing a new pulp processing facility, it is necessary to introduce technical measures preventing serpentine fraction from entering hydroseparators.

Preliminary estimations and practical data by other researchers suggest the presence of viscoplastic properties in the limonite pulp.

Analysis of related publications and operation of hydrotransport facilities has shown that, despite its wide application and abundance of experimental research on hydrotransport, there is still no theory and analytical model that would describe the flow structure of viscoplastic pulp. Enormous diversity of physical and mechanical properties of viscoplastic pulp and conditions of its hydrotransportation limits applicability of proposed calculation formulas, therefore in most cases it is impossible to define transportation parameters with the precision, necessary for practical purposes.

Efficiency of hydrotransport is determined by flow velocity, concentration and pressure losses. Proposed methods of calculating these parameters are based on Shvedov-Bingham law of viscoplastic flow, derived using continuum dynamics, and require relevant adjustments, relying on experimental research of specific pulp flow.

Research methods included: analysis of literature sources, experience of operating hydrotransport facilities of limonite pulp in Cuba and scientific integration of research on fine-grain suspension-carrying flows; theoretical and experimental investigations of rheological properties and transportation parameters of limonite pulps; planning of experiments and processing of experimental data using methods of mathematical statistics and regression analysis. A procedure has been developed to calculate parameters of limonite pulp hydrotransport facility in structured and turbulent regimes [5].

Recommendations have been elaborated for the design of a new hydrotransportation line MoaEast in Pedro Soto Alba plant. Fig.1 shows distribution of flow velocity and stress in the pipeline, and Fig.2 contains a generalized rheological curve of limonite pulp [5, 9].

Results of preliminary estimations of rheological properties of limonite pulp, performed on capillary viscosimeter, demonstrate that rheological curves can be described using BulkleyHerschel model [5].

$$\tau = \tau_0 + k\gamma^n \tag{1}$$

To describe deformational behavior of concentrated suspensions, showing signs of viscosity anomaly, Yu. K. Safronov proposed the following dependence [6]:

$$\frac{\varphi}{\varphi_m} = k \cdot \left(\frac{\tau - \tau_0}{\tau_k - \tau_0}\right)^n \tag{2}$$

where τ_0 – yield stress; τ_k – stress, associated with total disintegration of the structure; n – flow index; k – concentration ratio; ϕ – fluidity. Taking into account that:

$$\varphi = \frac{1}{\eta} \tag{3}$$

we obtain:

$$dr = \frac{2 \cdot l}{\Delta P} \cdot d\tau \qquad (4)$$

Plugging expressions (3) and (4) into Newton equation, we get:

$$\tau = -\eta^{\gamma} = -\eta \cdot \frac{dU}{dr} \qquad (5)$$

1. Under stress $\tau_0 < \tau < \tau_a$ the flow occurs in structured regime with practically intact structure.
2. In stress range between τ_a and τ_k the flow occurs in transition regime with continuously disintegrating structure.
3. Under stress $\tau > \tau_k$ the flow occurs in turbulent regime.

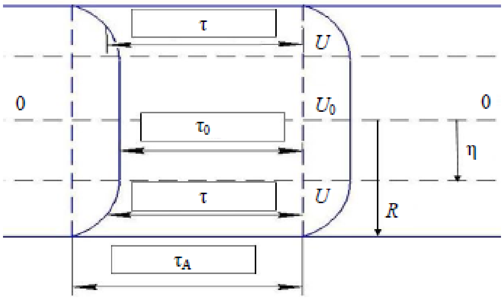

Figure 1 Distribution of flow velocity and stress in the pipeline

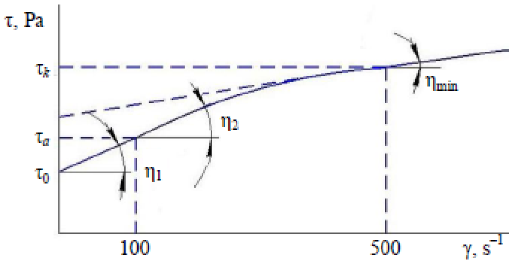

Figure 2 Generalized rheological curve of limonite pulp

$$dU = \frac{k \cdot \varphi_m}{(\tau_k - \tau_0)^n \cdot (n+1)} \cdot \left[R \cdot (\tau_R - \tau_0)^{n+1} - r \cdot (\tau - \tau_0)^{n+1}\right] \qquad (6)$$

$$U = \frac{k \cdot \varphi_m}{(\tau_k - \tau)^n \cdot (n+1)} \cdot \left[R \cdot (\tau_R - \tau_0)^{n+1} - r \cdot (\tau - \tau_0)^{n+1}\right] \qquad (7)$$

Equation (7) is correct for values $r_0 < R_0$, $r = r_0$, $\tau = \tau_0$, $U = U_0$. Velocity of the flow core equals:

$$U_0 = \frac{k \cdot \varphi_m}{(\tau_k - \tau)^n \cdot (n+1)} \cdot R \cdot (\tau_R - \tau_0)^{n+1} \qquad (8)$$

Pulp flow rate is expressed as follows:

$$Q = Q_1 + Q_0 \tag{9}$$

$$Q_0 = \pi {r_0}^2 U_0 \tag{10}$$

$$dQ_1 = 2\pi r U dr \tag{11}$$

Plugging into equation (11) the value of velocity, calculated using formula (7), and integrating, we get the flow rate equation for annular zone Q_1. From this, overall flow rate equals:

$$Q = \frac{4\pi l k(\Delta P - \tau_0)^{n+2}}{\Delta P \eta m(\tau_k - \tau_0)^n (n+1)} \left[R r_0 + R l(\Delta P - \tau_0)^{n+1} - \frac{{r_0}^2}{n+2} \cdot \frac{2 r_0 l(\Delta P - \tau_0)^{n+1}}{\Delta P(n+3)} - \frac{\Delta l^2 (\Delta P - \tau_0)^{n+1}}{\Delta P^2 (n+3)} \right] + \frac{\pi {r_0}^2 k R(\Delta P - \tau_0)^{n+1}}{\eta m(\tau_k - \tau_0)^n (n+1)} \tag{12}$$

Obtained equation (12) allows to compute the flow rate of limonite pulp in the pipeline, depending on rheological properties of the pulp and hydraulic parameters of the flow, which can be identified by experiment.

Performed research on geologic properties of limonite pulp indicated that, when deformation gradient exceeds 500 s^{-1}, there is a direct proportion between internal shear and velocity gradient. Experiments on capillary viscosimeter showed that, when velocity gradient is lower than 100 s^{-1}, experimental dependence is graphically represented as a straight line.

Basing on the analysis carried out, it has been proposed to describe limonite pulp flow with a rheological curve, containing three sections [4, 5].

According to suggested model, limonite pulp flow is determined by a set of equations:

$$\begin{gathered} \tau = \tau_0 + \eta\gamma; \quad \tau \in [\tau_0,\ \tau_a], n = 1; \\ \tau = \tau_0 + k\gamma^n; \quad \tau \in [\tau_a,\ \tau_k]; \\ \tau = \eta_{min\gamma}; \quad \tau > \ \tau_k, n = 1. \end{gathered} \tag{13}$$

Pressure losses of the pulp flow can be expressed by the following dependence:

$$i = F_1\left(Re, Y, \frac{\Delta}{D}\right) + F_2\left(F_1, \frac{\Delta}{D}, \pi\right) \tag{14}$$

The first function F_1 in expression (14) operates with viscosity forces, the second function F_2 – with gravitational ones.

Viscosity forces are critical for the flow of viscoplastic suspensions. Thus, processing of experimental results has been performed using Reynolds (Re) and Ilyushin (I) criteria as similarity parameters for structured regime (function Δ/D). For turbulent regime viscosity forces are of secondary importance, and sometimes a dimensionless group (function F_2) is used as similarity parameter [2].

Most researchers (V.V. Traynis, A.B. Smoldyrev, Yu.K. Safonov, V.B. Filatov and others) use simplified Buckingham equation to calculate pressure losses of viscoplastic pulp flow. From this equation after some manipulations Z. Lanzhinov and V.B. Filatov have obtained the following expression, defining coefficient of hydraulic resistance:

$$\lambda = \frac{64\left(I+\frac{I}{N}\right)}{Re} \tag{15}$$

where N = 8. To calculate λ for limonite pulp flow it is necessary to obtain the value of N by experiment.

Pressure losses of suspension-carrying flow in turbulent regime can be retrieved from the expression:

$$i_r = i_0(l + ack_i) \tag{16}$$

where a, c, k – densities of water, solid phase and pulp; i_0 – specific pressure losses of the water flow.

For pulp transportation in inclined pipelines hydraulic slope can be defined from the formula:

$$i_H = i_r(i_r - i_0)\cos \alpha k_2 \tag{17}$$

where α– slope angle of the pipeline.

Values of coefficients K_1 and K_2 in the course of limonite pulp flow should also be estimated experimentally.

Grain size analysis of limonite ore has shown that it contains predominantly fine grains (–0.045 mm, 86.87%), average density of the solid matter is 3400 kg/m^3.

Rheological parameters of the pulp have been measured by rotary viscosimeter RV [4-6, 9]. The method of experimental data processing is presented in the form of dependence between average velocity gradient in the gap γ and shear stress τ. Experimental rheological curves, shown in Fig.3, can be described by Shvedov-Bingham equation:

$$\tau = \tau_0 + \eta_{CT}\gamma \tag{18}$$

where τ_0 – initial shear stress.

Examination of dependences τ=Fγ demonstrates that limonite pulps with concentration S > 30% form spatial structures [7].

Results of processing experimental data:

Concentrations	0.30	0.35	0.40	0.45
Regression equation	$\tau = 0.131\gamma$	$\tau = 0.58 + 0.152\gamma$	$\tau = 2 + 0.170\gamma$	$\tau = 5.57 + 0.194\gamma$

Investigations of hydrotransport parameters of limonite pulp have been carried out for concentrations 25, 30, 35, 40, 45% of solid mass. After the processing of data, i(U) dependences have been retrieved for pulp flow along the pipelines 100 and 150 mm in diameter (Fig.4).

It can be seen from graphs in Fig.4 that, from the position of concentration and flow velocity, hydrotransport of limonite pulp can occur in three regimes: structured, transitional and turbulent. Thus, experimental data confirm results of earlier tests on viscosimeters and a proposed physicomathematical model.

Executed experimental tests allowed to estimate values of coefficients k1, k2 and N: k1 = 3.31; k2 = 4.53; N = 2.3.

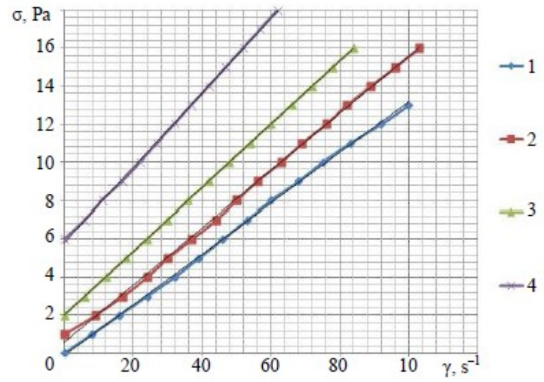

Figure 3 Rheological curves of limonite pulp for mass concentrations 30% (1); 35% (2); 40% (3); 45% (4)

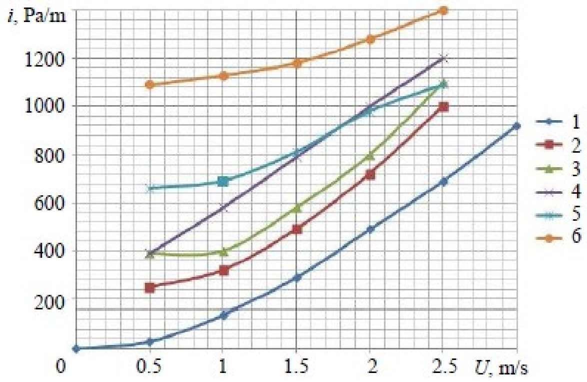

Figure 4 *i(U)* dependence for limonite pulp flow along the pipeline 100 mm in diameter with mass concentrations: 1 - water; 2 - 25%; 3 - 30; 4 - 35; 5 - 40; 6 – 45

Basing on performed theoretical and experimental research, a procedure to calculate hydrotransport parameters of limonite pulp has been developed. The idea behind engineering calculation of transportation parameters, taking into account input properties of the fine-grain limonite pulp (production capacity, transportation distance, density), is in estimating operational characteristics of the pipeline and pumps, which guarantee transportation of required volumes of solid material with minimal economic costs and stable performance of the technological system [3].

Calculation procedure is the following. First, the transportation regime of limonite pulp is determined, which is defined by technological specifics of Pedro Soto Alba plant and depends on concentration of the solid ore, the content of which is determined by processing technology and varies from 25 to 48% in mass [5].

Depending on solid ore concentration, pulp transportation from the processing station to the plant occurs either in structured, or in turbulent regime.

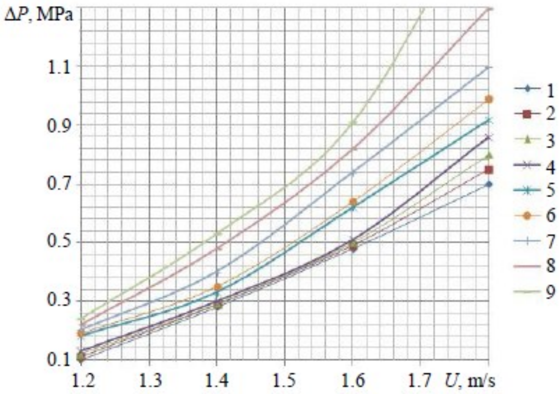

Figure 5 Pressure losses in the pipeline depending on velocity, diameter (D = 0.438; 0.415; 0.366; 0.317; 0.266 m) and pulp concentration: (25% - curves 1-5; 30% - 6-9)

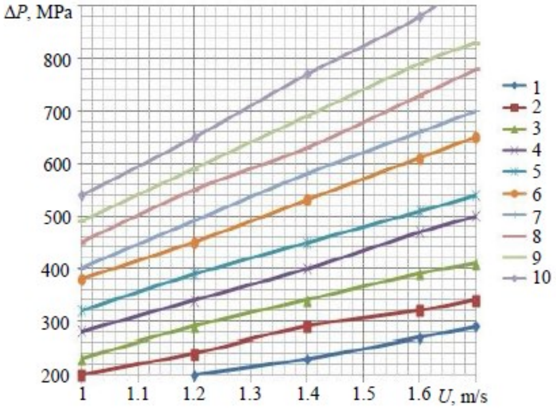

Figure 6 Capacity of solid ore production depending on velocity, diameter and pulp concentration: (25% - curves 1-5; 30% - 6-10)

In structured regime, specific pressure losses are defined as follows:

$$i = \frac{\lambda U^2 \rho_{st}}{2D} \tag{19}$$

where λ – coefficient of hydraulic resistance; U – velocity of pulp flow; ρ_{st} – pulp density; D – pipeline diameter.

Coefficient of hydraulic resistance λ is calculated using formula (15), depending on Re and I criteria:

$$R_e = \frac{UD\rho_{st}}{\eta_{st}}; \quad I = \frac{\tau_0 D}{\eta_{st} U} \tag{20}$$

Rheological parameters τ_0 and η_{st}, obtained with rotary viscosimeter, are estimated using the graph in Fig.5.

In turbulent regime, hydraulic resistance is computed by formulas (16) and (17), taking into account coefficients k_1 and k_2, obtained by experiment.

Obtained values of specific pressure losses are used to calculate required pump head and to choose its type, providing established parameters. Flow rate of the pulp is calculated and compared to the estimated value [1, 8].

To perform calculations for designed hydrotransportation line Moa-East, a computer program has been developed, aimed at estimating pressure losses ΔP for different pipeline diameters and concentrations. Results of calculations are presented in Fig.6. Graphs in Fig.6 allow to estimate capacity of solid ore production facility depending on the velocity, pipeline diameter and solid mass concentration.

As an alternative option, a combination of gravity and pressurized hydrotransportation is proposed, where the pulp is fed to the final height of the route (58 m) using elevation difference [4, 5]. Hence, the feed station has to be 32 m (2 m as a reserve) higher than the end of the pipeline, i.e. at the level of 90 m. In the initial section of the route, 300 m in length and elevation difference of 33 m, cascading system has to be installed [1]. Slope angle of the chutes should not exceed 1.5%.

CONCLUSION

Currently there is no universally accepted, sufficiently justified and experimentally confirmed procedure to calculate hydraulic resistances, associated with viscoplastic pulp flows.

Suggested procedure of calculation, based on Shvedov-Bingham rheological equation, requires relevant adjustments, relying on experimental research.

The main approach to estimating hydraulic resistance is to replace the actual rheological dependency by an empirical formula, close to the experimental flow curve of a specific pulp.

Basing on performed investigations of rheological properties of limonite pulp, a working hypothesis has been proposed, according to which, from the position of concentration and velocity, three zones can be distinguished in the current, characterized by the following flow regimes: structured, transition and turbulent. Basing on this hypothesis, a physical model of limonite fine-grain pulp flow has been developed and its mathematical description prepared.

Performed investigations allowed:

- to establish a dependence in order to estimate coefficient of hydraulic resistance for pulp flow in structured regime;
- to obtain formulas to compute pressure losses for viscoplastic pulp flow in turbulent regime in horizontal pipeline;
- to define the greatest slope angle of pipelines, applicable for limonite pulp transportation, which equals 25 degrees.

Practical recommendations consist in developed procedure to calculate parameters of limonite pulp hydrotransportation facility in turbulent and structured regimes, which allow to obtain better justified and more precise results.

REFERENCES

1. Dmitriev, G.P., Maharadze, L.I., Gogitashvili, T.Sh. (1991) Pressurized Hydrotransport Systems. Moscow: Nedra, 304 (in Russian).
2. Dzhunusov, I. (2001) Research on Processes of Mixing and Hydrotransportation of Structured Pulps of Mine Refuses: Avtoref. dis…kand. tehn. nauk. SPGGU. St. Petersburg, 20, (in Russian).
3. Dokukin, V.P. (2005) Improvement of Operational Performance of Pipeline Transport Systems. SPGGI (TU). St. Petersburg, 84, (in Russian).
4. Manujel' Vega Al'mager. (2006) Justification of Technological Scheme and Parameters of the Transportation Complex for High Concentration Pulp in Laterite Quarries (Republic of Cuba): Avtoref. dis…kand. tehn. nauk. SPGGI(TU). St. Petersburg, 220, (in Russian).
5. Raul' Isk'erdo Pupo, (1989) Investigation of Parameters and Development of Optimal Regimes of Laterite Hydrotransportation for the Conditions of Pedro Soto Alba Plant: Avtoref. dis…kand. tehn. nauk. Leningradskij gornyj institut im. G.V.Plehanova. Leningrad, 18, (in Russian).
6. Smoldyrev, A.E., Safonov, Ju.K. (1989) Pipeline Transport of Concentrated Pulps. Moscow: Mashinostroenie, 255, (in Russian).
7. Frisman, M.L. (1980) Rheology of Alkali-Sulphate Mixtures. Moscow: Nauka, 182, (in Russian).
8. Jaltanec, I.M., Egorov, V.K. (1999) Hydromechanization. Moscow: Izd-vo MGU, 335, (in Russian).
9. Izquiedo, P.R. (1989) Comportamiento Geologico de la Pulpa Lateritica a Bajos Gradients de Velocidad. Revista. Mineria y Geologia. N 2, 5-20.

XIV International Mineral Processing and Recycling Conference
Belgrade, Serbia, 12-14 May 2021

PROCESSING OF SULFIDE COPPER-NICKEL RAW MATERIALS BY LOW-TEMPERATURE ROASTING WITH AMMONIUM SULFATE

Andrey Goryachev#
Institute of Industrial North Ecology Problems of the Kola Science Centre of RAS, Apatity, Russia

ABSTRACT – A method of sulfide copper-nickel ores processing by the low-temperature roasting with ammonium sulfate is considered. The regularities of the thermal transformation of sulfides during low-temperature roasting were established. The use of ammonium sulfate made it possible to recover over 80% of copper and nickel. The ratio of concentrate:$(NH_4)_2SO_4$=1:7, grinding of the concentrate to a fraction -0.04 mm and temperature=400 °C were selected as optimal technological parameters during roasting, rotation 230 rpm, temperature 80 °C – during water leaching.

Keywords: Sulfide Ores, Non-ferrous Metals, Low-temperature Roasting, Ammonium Sulfate, Water Leaching.

INTRODUCTION

More than 400 deposits of copper-nickel ores have been discovered in the world, including 235 sulfide and 155 silicate. The total reserves of copper and nickel in the world are currently estimated at 1.6 billion tons and 210 million tons, respectively. Sulfide copper-nickel ore deposits account for about 65% of global nickel production, amounting to approximately 1.35 million tones/year. At the same time, the growth rates of production and consumption of copper and nickel in the 21st century are steadily increasing, which is associated with the leading role of these metals in the development of basic industries in many countries [1].

Despite such significant reserves of copper and nickel, the quality of raw materials supplied for enrichment is gradually decreasing and enterprises are forced to involve refractory raw materials in processing. Off-balance ores and dressing wastes are characterized by a low content of useful components, the presence of oxidized forms, a significant amount of fine sulfide dissemination [2]. For instance, the currently processed copper-nickel ore from the Pechenga ore field is characterized by the following metal content: 0.5-0.6% nickel and 0.2% copper.

Physical methods of beneficiation – flotation, gravity and magnetic separation, which are the most economical ones, are ineffective for processing mixed composition ores due to low selectivity [3]. In this regard, in order to expand the resource base of the mining and processing industry and minimize damage to the environment, it is necessary to search for an economically and environmentally sound method for non-ferrous metals recovery from refractory ores. One of the ways promising from an ecological and

---

corresponding author: a.goryachev@ksc.ru

economic point of view is low-temperature roasting of copper-nickel raw materials with ammonium sulfate with the formation of water-soluble compounds. Ammonium sulfate is a technologically efficient ammonium compound due to its high solubility. The studies carried out on the roasting of copper-nickel raw materials with ammonium sulfate $(NH_4)_2SO_4$ made it possible to establish that metal oxides are capable of reacting with the formation of water-soluble sulfates. This process is characterized by a high degree of metal recovery, reaction selectivity, energy efficiency, and low cost [4,5].

EXPERIMENTAL

To establish the features of thermal transformation of sulfide raw materials, sulfide minerals were synthesized – pentlandite $Fe_{4.5}Ni_{4.5}S_8$ and chalcopyrite $CuFeS_2$. The synthesis was carried out by the Kullerud method using quartz ampoules. To establish the possibility of processing sulfide copper-nickel raw materials of the Murmansk region, the ore of the Allarechensky technogenic deposit (TD), which is a dump of rocks, was taken as an object of research. The dump occupies an area of 33.29 hectares, the total volume of its species is about 6700 thousand m^3 (Figure 1).

Among the ores in the dumps, almost all the main groups and types characteristic of the primary Allarechensk deposit have been identified. The main ore-forming minerals are pyrrhotite Fe_7S_8, pentlandite, chalcopyrite and magnetite Fe_3O_4. All types of ores are characterized by approximately the same composition of ore minerals and differ only in their quantitative ratio. The dominant nickel concentrator in the ore is pentlandite.

A relatively small proportion of nickel is included in pyrrhotite and ubiquitous violarite $(Fe,Ni,Co)_3S_4$, which replaces pentlandite and indicates the development of hypergene processes in ores. Copper is concentrated mainly in tetragonal chalcopyrite.

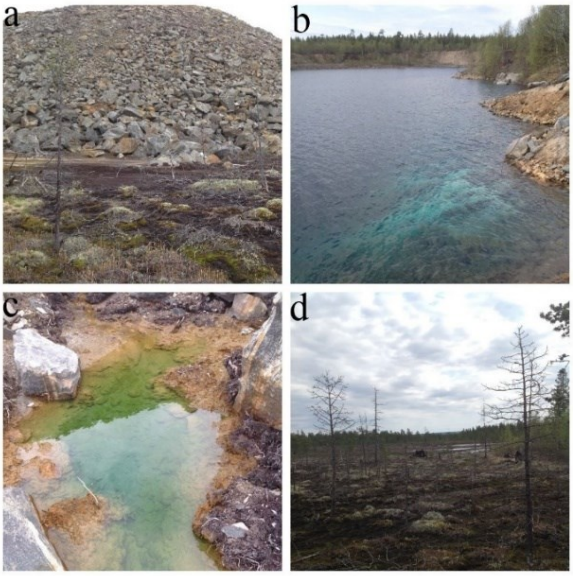

Figure 1 Allarechensk technogenic deposit. a – waste dumps; b – flooded quarry; c – result of sulfides natural leaching; d – disrupted ecosystems

In laboratory experiments, the sulfide feed was mechanically mixed with ammonium sulfate. The resulting mixture was loaded into an alundum crucible and fired in a muffle furnace for 4 hours on air atmosphere. After roasting, the clinker was cooled in the open air for one hour. The clinker was then leached in distilled water at 80 °C for 40 minutes with constant stirring at 230 rpm. The concentration of nickel and copper in the leach solution was measured by atomic absorption spectrometry (Shimadzu-AA7000G) with electrothermal atomization.

The initial ore, clinker and the leach residue were examined by powder X-ray diffraction (XRD) analysis using a DRON-2.0 instrument and copper K-alpha (CuKα) radiation with a wavelength of 0.154184 Å. X-ray phase analysis makes it possible to diagnose phases (minerals, mineral species) of polymineral samples, provided that the sample contains at least 5 wt. % of the determined mineral.

The measurement of the specific surface area of ore particles was carried out using a specific surface area and porosity analyzer TriStar 3000. Surface morphology analysis was performed using the scanning electron microscopy (SEM) method on an SEM LEO-420 microscope.

RESULTS AND DISCUSSION

After roasting the synthesized pentlandite at a temperature of 400 °C, reflections of the following sulfides were recorded – pyrrhotite, pyrite FeS_2, crowningshieldite NiS. The sample also contains pentlandite.

It is known that the dominant process during the roasting of pentlandite is its transformation into monosulfide. This reaction is accompanied by the formation of a small amount of iron oxides in the form of Fe_3O_4, as well as the oxidation of excess S to SO_2. It was established by XRD that these processes begin to occur already at a temperature of 400 °C.

When roasting a mixture of pentlandite with ammonium sulfate (a natural analogue - the mineral maskagnite $(NH_4)_2SO_4$) in a ratio of 1:2, reflections of the following minerals are recorded - sabiite $NH_4Fe(SO_4)_2$, polymidite Ni_3S_4, nickelhexahydrite $(Ni,Mg,Fe)SO_4*6H_2O$, crowningschildite. SEM-images of the particle surface after roasting indicate a sufficiently intensive course of the roasting process, a needle-like sulfate build-up is noted on the surface (Figure 2a). It should be noted that mascagnite reflexes are not recorded in the clinker. Probably, at such a ratio of pentlandite:ammonium sulfate, mascagnite is completely decomposed.

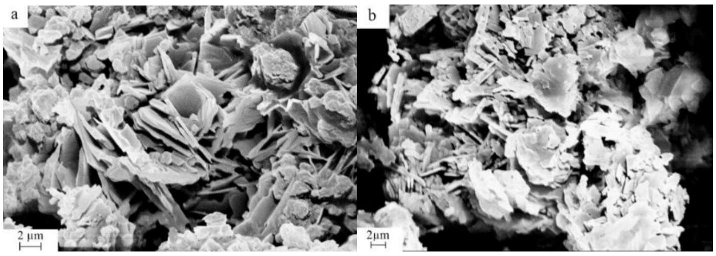

Figure 2 Particle morphology of synthesized pentlandite and ammonium sulfate (a); synthesized chalcopyrite and ammonium sulfate (b) mixtures after roasting

It should be noted that mascagnite reflexes are not recorded in the clinker. Probably, with such a ratio of pentlandite: ammonium sulfate, mascagnite is completely decomposed. The following mineral phases were recorded in the residue after leaching - crowningshieldite, violarite, pentlandite, and pyrite.

A significant sulfide residue in the residue indicates the need to increase the consumption of ammonium sulfate. With an increase in the pentlandite: ammonium sulfate ratio to 1:7, the following minerals are fixed in the clinker – nukundamite $Cu_{3.4}Fe_{0.6}S_4$, pyracmonite $(NH_4)_3Fe(SO_4)_3$. In addition, an increase in the consumption of ammonium sulfate led to the formation of nickel sulfates. Reflexes of nickelbussengotite $(NH_4)_2(Ni,Mg)(SO_4)_2*6H_2O$ are noted. In the residue, as well as at a lower consumption of ammonium sulfate, reflexes of violarite and crowningshildite appear. It is characteristic that reflections of pentlandite and pyrite are not found in the sediment at a given flow rate.

Thus, studies of low-temperature roasting of pentlandite and its mixture with ammonium sulfate showed that this mineral is capable of actively reacting with the formation of nickel sulfates. However, it should be taking into account that the composition of natural pentlandites varies widely and differs from stoichiometric Me_9S_8 in the ratio of metals to sulfur, the most common isomorphism Ni ← Fe. Copper can also be included in their composition as an isomorphic impurity. Deviation from stoichiometry can lead to a change in the optimal parameters of low-temperature roasting of natural ore. Therefore, to select the most effective roasting parameters, it is necessary to take into account the peculiarities of natural minerals.

The behavior of chalcopyrite during low-temperature roasting requires special consideration. This is due to the fact that this mineral, being the main concentrator of copper in ores, is resistant enough to be opened by various acid and alkaline reagents.

It was found that the oxidation of chalcopyrite does not occur as a result of its decomposition into simple copper and iron sulfides, but as a result of the stage of bornite Cu_5FeS_4 formation. After roasting synthetic chalcopyrite by XRD, reflexes of sulfides – chalcopyrite and bornite – were recorded. Iron ions removed from the chalcopyrite crystal lattice led to the formation of sulfates. Thus, in the sample after firing, reflections of melanterite $FeSO_4*7H_2O$ were recorded.

During the roasting process, copper is concentrated in the core of the grain, and the shell consists of iron oxide. Accordingly, the change in the structure of the chalcopyrite grain depends mainly on the oxidation time. After roasting chalcopyrite in a mixture with ammonium sulfate at a ratio of 1:2, large agglomerates (Figure 2b) are observed, consisting mainly of the following minerals – chalcopyrite, digenite Cu_9S_5, chalcocite Cu_2S, melanterite $FeSO_4$, goethite α-FeO(OH). Among the sulfate minerals, poatvenite $CuSO_4*H_2O$, chalcantite $CuSO_4$, sabiite $NH_4Fe(SO_4)_2$ are noted.

With an increase in the consumption of ammonium sulfate in the clinker, the reflexes of chalcopyrite are no longer recorded. A new mineral appears – mohrite $(NH_4)_2Fe_2(SO_4)_2*6H_2O$. After leaching, chalcopyrite reflections were again recorded in the sediment. In addition, the following minerals were diagnosed – fucuchilite Cu_3FeS_8, nukundamite $Cu_{3.39}Fe_{0.61}S_4$, elemental sulfur S. Thereby, when chalcopyrite is heated in an air atmosphere, oxygen freely flows to the surface of mineral particles. However, due to the difficult diffusion of oxygen, its deficiency can be observed in the inner layers and the core of the particle. This uneven oxygen distribution explains the formation of both oxidation products – melanterite, and products of an inert atmosphere – bornite.

Studies carried out with synthetic minerals have shown the promise of processing copper-nickel raw materials using ammonium sulfate. It has been established that the processes of formation of sulfates of target metals occur in the temperature range up to 500 °C.

In the original ore sample of the Allarechensk TD, reflections of the following minerals were recorded – chalcopyrite, pyrrhotite, pentlandite, cristobalite SiO_2. After roasting the ore with ammonium sulfate at a ratio of 1:7, only chalcopyrite is reliably diagnosed among sulfides. New phases appear – sabiite, pyracmonite, goethite. After water leaching, reflexes of sulfides were still found – chalcopyrite, pyrite and fukuchilite Cu_3FeS_8. In addition, ammonioyarosite $(NH_4)Fe_3(SO_4)_2(OH)_6$, marcasite FeS_2, magnetite are recorded.

The rate of metals recovery from the Allarechensk TD ore in the process of leaching indicates the need to search for ways to intensify the process. An increase in metals recovery was noted with a decrease in the size of the raw material to a fraction of <50 µm (Figure 3a). The level of metal recovery is directly related to the specific surface area of ore particles (Figure 3b). Thus, when ore is ground to a particle size of <50 µm, the specific surface area reaches 2.88 m^2/g, while for a fraction <71 µm it is equal to 1.60 m^2/g. It was possible to recovery 84.8% nickel and 77.6% copper from ore with fraction <40 µm.

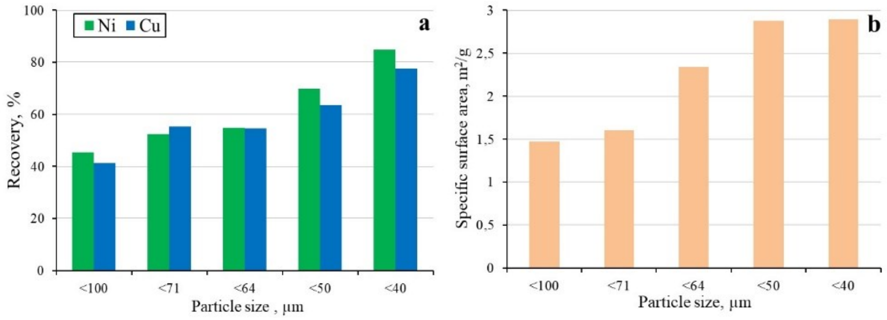

Figure 3 Metals recovery depending on particle size (a) and specific area surface of Allarechensk ore particles (b)

The kinetics of metal recovery into solution is confirmed by the method of chemical analysis (table 1). In addition, cobalt is intensively extracted into the solution, which is also of practical interest due to the constant growth of market demand for this metal.

Table 1 Ore samples chemical composition

	Content, wt %*												
	SiO_2	**TiO_2**	**Al_2O_3**	**Fe_{com}**	**Fe_2O_3**	**FeO**	**MnO**	**CaO**	**MgO**	**Ni**	**Cu**	**Co**	**S**
A	17.04	0.34	1.05	27.52	39.62	31.09	0.096	1.29	13.64	6.42	5.12	0.10	18.35
B	8.09	0.15	0.52	12.00	17.28	4.28	0.043	0.74	6.06	2.79	2.34	0.037	23.48
C	33.03	0.60	0.96	19.56	28.16	11.02	0.093	1.39	12.10	2.58	1.35	0.051	6.01

*A – ore sample; B – sample after roasting (ore:ammonium sulfate = 1:7); C – sample after leaching.

CONCLUSION

On the example of the ore from the dump of the Allarechensk technogenic deposit, the prospects of the technology for roasting fine fractions of sulfide ores with ammonium sulfate were shown. Roasting at 400 °C with a ratio of ore and ammonium sulfate = 1:7 make it possible to recovery more than 80% of the non-ferrous metals into the solution. Measurement of the specific surface area of ore particles showed that it is advisable to grind raw materials to a fraction of <0.05 mm, which is confirmed by the kinetics of metal recovery in the process of leaching. It must be taken into account that the temperature of 400 °C is lower than the temperature of traditional pyrometallurgical processes. In addition, it is possible to regenerate the reagent by capturing off-gases – SO_3 and NH_3. Low-temperature roasting of sulfide raw materials with ammonium sulfate, provided the process is optimized, can also be considered promising for processing low-grade ores due to high selectivity, relatively low energy consumption and low cost. Varying such parameters as the size of the original ore, the consumption of ammonium sulfate, the roasting temperature, the leaching time, will effectively involve sulphide ores that are not in demand at the moment.

ACKNOWLEDGEMENT

The author is grateful to Potapov S.S., Parshina N.V., Krasavtseva E.A., Belyaevsky A.T.
This research was funded by Russian government grant nos. 0226-2019-0011.

REFERENCES

1. Mantsevich, M.I., Malinsky, R.A., Khersonsky, M.I., Lapshina, G.A. (2008) Search for methods to improve the grade of copper-nickel concentrates. Min. Inf. Anal. Bull., 7, 359–363. (In Russian).
2. Likhacheva, S.V., Neradovskiy, Y.N. (2013) Decreasing of losses of nickel with flotation tailings of Pechenga copper-nickel ores. Tsvetnye Met., 10, 37–40. (In Russian).
3. Goryachev, A.A., Makarov, D.V., Belyaevsky, A.T. (2020) Low-temperature roasting of copper-nickel ores with ammonium sulphate as a perspective method for processing such raw materials. Mineralogy of Technogenesis, 21, 144–151. (In Russian).
4. Mu, W., Cui, F., Huang, Z., Zhai, Y., Xu, Q., Luo, S. (2018) Synchronous extraction of nickel and copper from a mixed oxide-sulfide nickel ore in a low-temperature roasting system. Journal of cleaner production, 177, 371–377.
5. Sukla, L.B., Panda, S.C., Jena, P.K. (1986) Recovery of cobalt, nickel and copper from converter slag through roasting with ammonium sulphate and sulphuric acid. Hydrometalllurgy, 16, 153–165.

XIV International Mineral Processing
and Recycling Conference
Belgrade, Serbia, 12-14 May 2021

A CRITICAL ASSESSMENT OF URANIUM RESOURCES OF TURKEY

Sibel Gezer[#]
Middle East Technical University, Ankara, Turkey

ABSTRACT – Uranium is the primary fuel for nuclear reactors and must be managed properly, in a safe and sustainable manner. Recent annual production of natural uranium worldwide has been nearly 60,000 tons. Global uranium resources as total identified recoverable resources increased by only 1% since 2017. Turkey has distinctly progressing its nuclear energy program in nuclear milestones. As being aware of that uranium mining and activities would be a significant role in the nuclear power plant projects. This paper wholly investigated the recent uranium exploration activities, drilling efforts, identified conventional resources, environmental activities and regulatory regime of Turkey with the details.

Keywords: Uranium Deposit, Nuclear Power, Energy, Fuel.

INTRODUCTION

Background: uranium for nuclear power

Uranium resources are an integral part of the nuclear fuel cycle. To increase the capability of interested Member States for planning and policy making on uranium production, the IAEA works together with the OECD Nuclear Energy Agency (NEA) to collect and provide information on uranium resources, production and demand.

With uranium production ready to expand to new countries, efforts are being made to develop transparent and well-regulated operations similar to those used elsewhere to minimise potential environmental and local health impacts [1].

The general energy policy of Turkey focuses on the supply of secure, sustainable and affordable energy by diversifying energy supply routes and source countries, promoting usage of domestic resources and increasing the energy efficiency and renewable energy usage to decrease the energy intensity of production. Nuclear energy is considered for diversification of electricity generation and also for mitigation of GHG emissions from energy sector.

The Akkuyu NPP project started with the IGA between Turkey and Russia for construction and operation of 4 VVER-1200 reactors in Akkuyu site situated on the Mediterranean coast of Turkey. A comprehensive EIA report had been prepared by the PC taking into consideration the requests from a wide range of stakeholders which was approved in December 2014. EMRA had granted electricity generation licence in June 2016 which will form the basis of the PPA. The revised site parameters report was approved by TAEK on February 2017 and granted limited work permit for construction of non-nuclear safety related facilities in October 2017. The full construction of the first unit

---

[#] corresponding author: sgezer@metu.edu.tr is planned to start in the first quarter of 2018 with the grant of construction licence by TAEK.

The other nuclear power plant project IGA which includes construction and operation of 4 ATMEA1 reactors in Sinop site and development of nuclear industry in Turkey was signed between Turkey and Japan in 2013 and ratified in 2015. EÜAŞ ICC established in November 2015 will participate to the project as shareholder of the project company which will be established based on the results of the feasibility study. The feasibility study started in July 2015 and the further support from Japanese government was provided with the MoU signed between MENR and METI in September 2016. The feasibility study is expected to be completed in the first quarter of 2018.

The strategic goal of nuclear energy usage is mentioned in the strategic plan of MENR under the goal for optimum energy resource diversity. Turkey has a high energy import and fossil fuel dependency which makes it vulnerable to external shocks in global markets. Nuclear energy is considered as one of the options together with local resources and renewable energy to strengthen the energy sector in Turkey. Radioactive minerals have been historically explored in Turkey which requires further studies for their feasibilities to start production [2].

As a result, the strategic plan includes the target for reserve determination of radioactive minerals together with their respective feasibility studies for usage in the nuclear energy sector [3].

MATERIALS AND METHODS

General Directorate of Mineral Research and Exploration (MTA)

Uranium exploration in Turkey began in 1956-1957 and was directed towards the discovery of vein-type deposits in crystalline terrain, such as acidic igneous and metamorphic rocks. As a result of these activities, some pitchblende mineralisation was found but these occurrences was not accepted as economic deposits. Since 1960, studies have been conducted in sedimentary rocks which surround the crystalline rock and some small orebodies containing autunite and torbernite mineralization have been found in different parts of the country. In the mid-1970s, the first hidden uranium deposit with black ore, below the water table, was found in the Koprubaşı area of Manisa. As a result of these exploration activities, a total of 9,129 tonnes U_3O_8 (7,740 tU) in situ resources were identified in the Manisa-Köprübaşı (2,852 tonnes U_3O_8; 2,419 tU), Uşak-Eşme (490 tonnes U_3O_8; 415 tU), Aydın-Koçarlı (208 tonnes U_3O_8; 176 tU), Aydın-Söke (1,729 tonnes U_3O_8; 1,466 tU) and Yozgat-Sorgun (3,850 tonnes U_3O_8; 3,265 tU) regions.

Eti Mine Works General Management (Eti Maden)

State-owned organization Eti Maden is responsible for a total of six uranium mine sites with uranium resources. Geological exploration has been performed by MTA at these sites in the past. Between 1960-1980 uranium exploration was performed by aerial prospecting, general and detailed prospecting on-site, geologic mapping studies and drilling activities. These uranium sites were transferred to Eti Maden as possible mines which can be operated by the state under law number 2,840 on the "Operation of Boron Salts, Trona and Asphaltite Mines and Nuclear Energy Raw Materials" (10 June 1983).

Recent and ongoing uranium exploration and mine development activities

General Directorate of Mineral Research and Exploration (MTA)

In 2012, granite, acidic igneous and sedimentary rocks around Manisa, Denizli and Aydın (an area of approximately 5,000 km^2) were explored for radioactive raw materials. Exploration for radioactive raw materials was also performed in sites licenced by MTA inside Manisa, Uşak and Nevşehir.

In 2013, granite, acidic igneous and sedimentary rocks around Aydın and Denizli (an area of approximately 5,000 km^2) will be explored for radioactive raw materials. Exploration for radioactive raw materials was also performed in sites licenced by MTA inside Manisa, Uşak and Nevşehir.

In 2014, Exploration for radioactive raw materials was conducted in sites licenced by MTA inside Manisa, Uşak and Nevşehir.

In 2015, Exploration for radioactive raw materials will be conducted in sites licensed by MTA inside Manisa and Nevşehir [4].

Private sector exploration

Adur, a wholly owned subsidiary of Anatolia Energy, a Turkish uranium exploration company with current and active drill programmes at the Temrezli and Şefaatli uranium sites, has carried out exploration and resource evaluation drilling with a total of 206 drill holes completed for a total drill advance of over 26,000 m since 2011 in both Şefaatli and Temrezli projects. Over 16,000 m of drilling was in Temrezli region. Until now, 112 holes have been completed in Temrezli project. The drilling in Temrezli, mostly twinning the earlier MTA drill holes but also in-fill and step-out holes, confirmed work conducted in the 1980s and extended the uranium mineralisation to the north-east over a strike length of more than 3,000 m.

In 2011, CSA Global Pty Ltd prepared a JORC compliant mineral resource estimate for the Temrezli deposit of 13.282 Mlb U_3O_8 (6,025 tU) (measured, indicated and inferred) in situ uranium at an average grade of 1,157 ppm (0.117% U_3O_8).

Preliminary metallurgical bottle-roll leach test work confirmed MTA's earlier work and returned 93% and 90% uranium recovery was obtained by using an acid or alkali leach method, respectively.

Several hydrological test wells were constructed at Temrezli since 2012 in order to assess the regional groundwater conditions and to conduct hydraulic testing of the mineralised horizons at a scale typically seen at in-situ recovery (ISR) operations. Test work was performed by HydroSolutions, a US-based hydrogeologist with considerable experience in ground water conditions relating to uranium ISR operations throughout western United States. The test confirmed the aquifer has sufficient flow rate for ISR mining.

Regional exploration identified new areas of mineralization, at West Sorgun and Akoluk. The rotary and diamond drill programme tested a number of regional sites that are considered prospective for Eocene-aged sediment-hosted uranium mineralisation, similar to what is seen at the Temrezli uranium deposit.

Since early stage studies indicate that the Temrezli uranium deposit will be amenable to ISL mining, a preliminary economic assessment (PEA) contract was awarded to US based WWC Engineering of Sheridan, Wyoming. The PEA is completed and followed by PFS study which was awarded to Tetra Tech, US origin company PFS was completed and issued in early 2015 which indicated that the project is economically feasible to proceed, with a total expected recovery of 9.7 m lbs. over 12 years, with operating costs of less than USD17 per lb U_3O_8 (USD44.2 per kg U). Adur initiated the Environmental Impact Assessment (EIA) process by preparing and submitting a Project Description to the Ministry of Environment and Urban Planning in 2015. Adur will also initiate the permitting process with Turkish Atomic Energy Commission regarding licensing Temrezli site as a nuclear facility since ISR operations are considered as nuclear facilities. In 2015, the permits and licenses will be obtained prior to initiating the construction in early 2016.

RESULTS AND DISCUSSION

Identified conventional resources (reasonably assured and inferred resources)

Identified conventional uranium resources in Turkey determined from exploration activities performed by MTA in the past are listed below, with the addition of JORC compliant resources identified through recent work by Adur exploration, described in more detail:

- Manisa-Köprübaşı: 3 011 tU in ten orebodies and at grades of 0.04-0.05% U_3O_8 (0.034 0.042% U) in fluvial Neogene sediments;
- Uşak-Eşme: 415 tU at 0.05% U_3O_8 (0.042% U) in Neogene lacustrine sediments;
- Aydın-Koçarlı: 176 tU at 0.05% U_3O_8 (0.042% U) in Neogene sediments;
- Aydın-Söke: 1,466 tU at 0.08% U_3O_8 (0.068% U) in gneiss fracture zones;
- Yozgat-Sorgun: 5,109 tU at 0.117% U_3O_8 in Eocene deltaic lagoon sediments;
- Avanos-Gülşehir: 1,085 tU at 0.05% U_3O_8 (0.012% U) Paleozoic sediments.

Temrezli (Yozgat / Sorgun) uranium deposit is one of Turkey's largest and highest grade uranium deposits, with a JORC compliant Mineral Resource estimate of 13,282 Mlb of contained uranium at an average grade of 1,157 ppm (0.117%) U_3O_8 with an average depth of 120 m.

Undiscovered conventional resources (prognosticated and speculative resources)

- Temrezli Project: The ongoing exploration and development drillings is to be continued and is expected to increase the resource by a potential of 1-3 Mlb U_3O_8.
- Şefaatli Prospect: exploration and development drillings is being conducted in 2015 and is expected to increase the known uranium resource values by approximately 5-6Mlb U_3O_8. The recent drill results include 1,10m at grade 2,150 ppm e U_3O_8 from 39m [4].

Unconventional resources and other materials

None reported, but grassroots exploration is in place.

Table 1 Identified conventional resources (reasonably assured and inferred resources)

Site	Grade (ppm U)	Resource (tonnes U)	U_3O_8 (%)
Manisa-Köprübaşı	340-420	3.011	0.04-0.05
Uşak-Eşme	370	415	0.044
Aydın-Koçarlı	420	176	0.05
Aydın-Söke	680	1.466	0.08
Yozgat-Sorgun	1,170	5.109	0.117
Avanos-Gülşehir	1,280	1.085	0.05
Total		**11.263**	

CONCLUSION

- Although growth in nuclear power production slows down, it will continue;
- Uranium demand will increase in the future;
- Resources under the cost of $ 130/kg U can meet the high demand projection for 2035;
- Delays in mine development: The release of resources depends on the market situation;
- Excess supply and inventories put pressure on price;
- Due to the increasing demand, the sustainability of occupational safety and environmental protection should be emphasized.

REFERENCES

1. The Red Book - Uranium (2020) Resources, Production and Demand A Joint Report by the OECD Nuclear Energy Agency and the International Atomic Energy Agency/Turkey Updated Chapter 2020.
2. Presidency of the Republic of Turkey, Strategy and Budget Presidency: “The Eleventh Development Plan (2019-2023)”.
3. Republic of Turkey, Ministry of Energy and Natural Resources Strategic Energy Plan 2015 – 2019.
4. Alkan, M., Gülmez, A., Ulusoy, M. A (2016) Review of Uranium and Thorium Studies in Turkey, IMMC 2016: 18. International Metallurgy and Materials Congress.

XIV International Mineral Processing
and Recycling Conference
Belgrade, Serbia, 12-14 May 2021

POTENTIAL MINERAL RESOURCES OF ANTHRACITE MINE VRSKA CUKA AVRAMICA

Branislav Stakić[#], Bojana Maksimović, Dejan Ćirić
JPPEU, RA "Vrška Čuka" Avramica, Grljan, Serbia

ABSTRACT –Coal basin Vrska Cuka is located on north side of Stara planina approximately 10 km south east from Zajecar. In coal basin Vrska Cuka the most important deposit is "Mala Cuka". Deposit "Mala Cuka" contains economic resources of anthracite, with a high calorific value. In coal deposit "Mala Cuka" also have quartz sandstone a footwall of anthracite bearing layers. Quartz sandstone have mineral characteristic with 91% SiO_2; 0.88% Fe_2O_3; 4.06% Al_2O_3 thus said represents a huge potential as a raw material for silicon carbide production. Mala Cuka deposit also contains limestone with more than 95% $CaCO_3$, which can be used for quicklime (Calcium oxide) and rejects with less mineral content have a significant potential as construction material.

Keywords: Anthracite, Quartz Sandstone, Limestone, Vrska Cuka.

INTRODUCTION

Coal basin Vrska Cuka is located on north side of Stara planina, approximately 10 km southeast from Zajecar. Area is bordering with Bulgaria from the East, with Timok valley from the West, and with Velikoizvorski plato from northeast. Precise location is determined by streams around Vrska Cuka. Area is bordered by Bujkov potok from NE, Avramcki potok from SE and with Priltski potok from NW.

Exploitation in coal seam "Mala Cuka", the only active mine in the vicinity of Vrska Cuka, started in 1959, and by the end of 2013 produced 1,465,430 tonnes. Extraction ratio from the mine Mala Cuka is around 95% with a production loss not exceeding 5%.

GEOLOGY

Lias sediments are identifying three coal seams with various thickness ranging from 0.5m up to 3.5m. Up to date data collected by exploration, mine development and production gives geological data identifying all three seams as non-liable nor in horizontal nor in vertical direction.

That inconsistency manifest with seam irregularities ranging from seam pinch out to up to 5m in seam thickness. Vertical manifestations of the seams are splitting the seam in from single layer to up to three seams. Coal seams are irregular horizontally as well, those seams can be exploited, as they are generally thicker than homogenous layer, but in lateral direction they are short in the length as they are pinching out and forms a coal lens [1].

[#] corresponding author: stakicbranislav1@gmail.com

TYPE, QUALITY AND COAL RESOURCES

Coal from “Mala Cuka” deposit is black-grey in colour, glassy metal shiny, and depending on metamorphosis it can look alike graphite. Its brittleness makes exploitation hard, and it is not possible to produce lumps. It is soft, and lumps are easily broken to grain size or dust, and makes fingers dirty. Scratch marks are black. Broken sides are shale shaped, with a multiply sharp edges. The coal can be found in two different modifications, characterised by mechanical influence. Faulty zones are bearing an amorphous type, while crystalline type is beaded in tectonic blocks.

Coal characteristics in “Mala Cuka” deposit:

Moisture	0.96%
Ash	13.19%
S total	2.26%
Combustible	86.06%
Volatile	8.82%
Coke	90.36%
Cfix	79.68%
GTE	30,605 kJ/kg
DTE	29,730 kJ/kg.

RESOURCES AND RESERVES

Total reserves and resources (A+B+C1) in “Mala Cuka” deposit is shown in Table 1.

Table 1 Resources and Reserves [1]

Category	Geological (t)	Mineable (t)
Category A	9,580	9,101
Category B	685,703	651,418
Category C_1	774,042	735,340
Total:	**1,469,325**	**1,395,859**

USE OF ANTHRACITE AS FILTRATION MATERIAL FOR WATER PURIFICATION

Filter anthracite is produced from crystalline type of coal produced from Anthracite Mine “Vrska Cuka” Avramica with a high carbonisation level, processed via separation and other treatments yet not treated chemically nor thermally, still not activated [2, 3].

This product is used for water purification originated from different water sources (rivers, lakes or wells) to potable water for human consumption [3, 4]. Filter antracit is efficient in removing organic impurities, as well as oil and grease from industrial water, so it is used for treatment waste waters from industry and mining [2, 5]. It is suitable for removal of heavy metals from waste waters originated from mining and industry [6].

Geology map of deposit “Mala Cuka” is shown on Figure 1 [1].

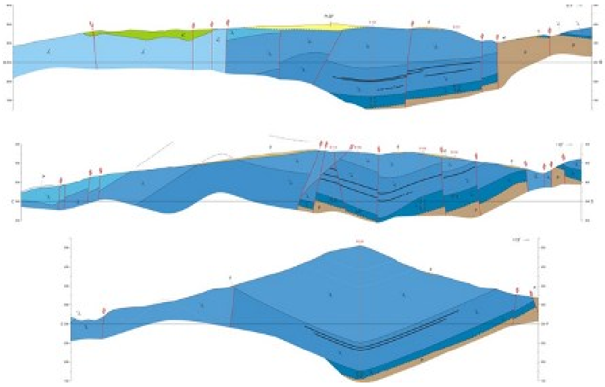

Figure 1 Geology map “Mala Cuka”

QUARTZ SANDSTONE

Historical geological exploration and mining works in coal deposit “Vrska Cuka” are dating from the last quarter in 19th century. According to geological exploration data in the Mining licence of Vrska Cuka area surrounding “Mala Cuka” have substantial resources of quartz sandstone where some portion was exploited in 70’s for the needs of Smelter in RTB Bor.

Morphology of Mala Cuka is represented by hill bordered by Bonin potok from South, Avramicki potok from SouthWest. Great Severni rased splits Krecnjacki plato from Mala Cuka looking North West and East. Severni rased stretches toward South looking from the road Avramica-Velika Cuka, where from SouthEast and East is naturally split by Burdeljski and Bujkov potok. (Figure 2).

Figure 2 Quartz sandstone deposit “Mala Cuka”

REGIONAL GEOLOGY OF DEPOSIT

Area around coal basin “Vrska Cuka” is represented by dozen stratigraphic columns:

- Rift Cambrian crystalline shales, Perm Carbon sandstones, coaly clays and clay,
- Perm based conglomerates, clayey shales, and red sandstone,
- Triassic colourful sandstones,

- Lias based basal conglomerate, coal, clay and shales, clay shales, with coal intrusion, quartz sandstone, clayey iron sandstones, sandy limestones,
- Dogger based quartz, clayey and iron sandstones and sandy limestones,
- Lower Cretaceous sandstone, marl and marl sandstones,
- Upper Cretaceous breccia, conglomerates, sandstones, marl and limestones,
- Tertiary (Miocene)-clay, sand, lajtovacki limestone,
- Quartz conglomerate, sand, clay,
- Magmatic formations-quartz porphyry, diabase, and granite.

GEOLOGY OF DEPOSIT

Dogger clasts

The biggest area cover in line of Jurassic units sediments from Dogger split in two super positioned units. Lower area is developed concordant from coal bearing sediments. Footwall is dogger carboniferous layers partially touching base with Upper Jurassic limestones and Albian marl. Lithological replacement of this unit in lower is dark grey clayey alevrolytes rich in fauna originated from lower dogger. Those sediments are changing to grey alevrolytes and fine grinded sands. Above them are grey fine grain limy sandstones- calcarenites. According to the rule of thumb above them is thick interchangeable layer of quartz yellowish and lightgrey sandstones and micro conglomerates. Those clasts are developed in Mala Cuka. Sandstones and conglomerates are various thickness from layers to banks.

Total thickness those units is ranging from 150 meters in North part of ore body to over 200 meters in ahe area of Vrska Cuka. Quartz sandstone deposit is located in upper part (crown) of Mala Cuka (Figure 2), and is structured from coarse yellow and light grey quartz sandstones. Those sandstones are indicating fossil association from Bajocian-Lower Callovian era. Total sandstone thickness is up to 120 meters. Footwall quartz sandstones represents limy sandstones- calcarenites [1].

QUARTZ SANDSTONE QUALITY AND RESOURCES

In historical mining area operational from 1970 to 1980 few trenches were dig out in order to collect samples for chemical analysis. Also, some samples were taken from historical drill holes drilled for anthracite exploration. Results of chemical analysis from collected samples are presented in Table 2.

Table 2 Chemical analysis results for quartz sandstone from “Mala Cuka” deposit

Mark	SiO_2	Al_2O_3	Fe_2O_3	CaO	MgO	H_2O
R-1, U-1	83.42	7.80	3.20	0.500	0.720	3.39
R-1, U-2	89.83	4.01	1.23	0.300	0.120	0.96
R-1, U-3	91.31	3.82	1.18	0.043	0.120	0.48
R-4, U-1	92.54	3.10	0.46	0.190	0.049	0.29
B-139	90.32	4.06	0.88	0.400	0.110	0.15
B-1KP	89.83	4.00	2.15	0.500	0.360	0.27

According to data present it can be stated that quartz sandstone deposit averaging with 90% of quartz mineral. This type of quartz sandstone is in use by cement manufacturers (CRH Popovac is requesting supply of 40,000 t/year), in smelters, and rejects are used for gravelling.

Mining of higher quality of quartz sandstone with 90% of mineral could be designated as selective. Up to date exploration estimates resources of 20,000,000 t.

This deposit produces anthracite as a primary product of the mine, and coal footwall is represented by quartz sandstone. Those raw materials could be used as a source for production of silicon carbide, which have a wide use [6].

LIMESTONE

Late Jurassic-Early Cretaceous are capturing wide area in the vicinity of Vrska Cuka. They are developed in northern part of deposit (Krecnjacki plato) on Velika Cuka and western part of anticline (Grljanski venac and Kantarijsko brdo).

There are numerous historical quarries where production was for local supply for construction, quick lime production, and for gravelling. Laboratory testing of the samples are showing that limestone from this area meets requirements to be used as construction material and gravelling.

Limestones are represented in wide area and significantly are dipping down in the vicinity of Vrska Cuka. Results from chemical testing are presenting high value of calcium carbonate up 95%. The impurities in rock are inside predetermined boundaries. According to those results, this limestone can be used in for sugar production, additive for cattle feeding, and as construction material [1].

CONCLUSION

In Mala Cuka deposit three mineral resources can be identified, anthracite with average calorific values of 30,000 kJ/kg, quartz sandstone with average 90% of Quartz and limestone with average $CaCO_3$ of 95 percent. Anthracite and Quartz sandstone are row materials for silicon carbide production with high demand in country and outside of country borders. Silicon Carbide is used in nuclear plants, automotive industry, burners, military industry, as abrasive material etc. Just technological developed countries are producing silicon carbide, and according to that it is fair to say that anthracite and quartz sunstone are technological raw materials. Limestone within this quality is widely used in road construction industry.

REFERENCES

1. Stakić, B. et al. (2006) Reserve classification in “Mala Cuka” Avramica.
2. Jovisic, D., (1997) Investigation of the adsorption properties of activated carbons produced from Vrska Cuka anthracite, Faculty of Science, Novi Sad, Serbia.
3. Simonović, B. (2002) Final Report “Filtration agents for drinking water purification”. Belgrade.
4. Ciric, D., Stakic, B., Perendic, S., Usage of anthracite in drinking and wastewater purification, Proceedings of XXII International Scientific and Professional Meeting

„Ecological Truth", Eco-Ist '14, 10 - 13 June 2014, Bor Lake, Bor, Serbia, (2014), 414-419.

5. Simonović, B. (2003) Use of anthracite as filtration/sorption agent in purification of oil/mazut waste waters, Belgrade.
6. Sokolović, J., Stakić, B., Perendić, S., (2017) Sustainable use of resources in the coal mine Vrska Cuka: Application of anthracite coal for water treatment, Plenary lectures, Proceedings of VIII Symposium with international participation "Mining 2017", 16 - 18 May 2017., Palic, Serbia, 72-84.

XIV International Mineral Processing
and Recycling Conference
Belgrade, Serbia, 12-14 May 2021

UTILIZATION POTENTIAL OF A SERPENTINE-RICH SAMPLE AS A REFRACTORY RAW MATERIAL

Ilker Acar[#]
Atatürk University, Faculty of Engineering, Department of Environmental Engineering, Erzurum, Turkey

ABSTRACT – In this study, a serpentine-rich sample obtained as tailing from a chromite enrichment plant was examined for its utilization potential as a refractory raw material. Within this scope, various characterization analyses such as XRF, particle size distribution, XRD and some thermo-analytical methods were accomplished. According to the results, the sample has a relatively high MgO content, 35.96%, and a suitable size distribution. In addition, the sample exhibited only 6.39% weight reduction up to 1000 °C. On the other hand, 9.71% Fe_2O_3 and 5.48% Al_2O_3 contents and the formation of clinoenstatite phase during calcination limit its usage for the refractory purpose. Overall results have indicated that the serpentine-rich sample cannot be used as a refractory raw material mainly due to the high amounts of reactive iron and aluminum oxide contents.

Keywords: Serpentine, Utilization, Refractory Raw Material, Thermo-Analytical Methods.

INTRODUCTION

Serpentine minerals are naturally derived from the exothermic hydro-thermal alteration of ultramafic rocks, peridotites like olivine. They are 1:1 layered hydrated magnesium silicates which crystallize in the monoclinic system. They consist of alternating silica-like tetrahedral and brucite-like octahedral sheets. There are three principal serpentine polymorphs, namely antigorite, chrysotile and lizardite which differ in structural stacking arrangements [1, 2].

Chemically, serpentine minerals are mainly composed of MgO, SiO_2 and structural water, and they also have some oxides of iron, aluminum, calcium, chromium, nickel and cobalt elements. Their colors vary from green to grayish green depending on the chemical composition. Serpentine minerals have densities in the range of 2.5-2.6 g/cm^3, which are lower than their parent olivine (3.22 to 4.39 g/cm^3 based on its fayalite content) due to the volume increase during the hydration. Accessory minerals commonly found in serpentinite rocks are olivine, enstatite, brucite, carbonates and some spinel-like phases such as magnetite and chromite [1-4].

Although there are various application areas such as raw materials in the ceramic and refractory industries, extraction of amorphous silicate and pure magnesium compounds, CO_2 sequestration, fertilizer production and soil amelioration, beneficial bulk utilization of serpentine is only limited to some engineering applications such as a flux in iron and steel making and as a filler for road reclamation [2, 4]. For most of the above application

---

[#] corresponding author: ilker.acar@atauni.edu.tr areas especially for the ceramic and refractory industries, serpentine should be calcined in order to remove from its structural water and obtain sintered angular shaped aggregates [4].

In this study, a chromite enrichment tailing serpentine-rich sample was characterized in detail to determine its suitability as a raw material for the refractory industry.

EXPERIMENTAL

Materials

The serpentine-rich sample used was obtained from the chromite enrichment plant of ETI KROM INC., located in Kovancılar, Elazığ, Turkey. In this plant, serpentine with lower specific gravity is separated from heavier chromite and olivine minerals by shaking table and stored in a tailings dam.

Methods

The major chemical constituents of the sample were determined via a Spectro IQ X-ray fluorescence (XRF) instrument. The particle size distribution was determined by wet sieving method. The mineralogical inclusions were examined by a PANalytical Empyrean X-ray diffractometer (XRD) which operates with Cu-Kα radiation (λ = 1.54060 Å) at 40 kV and 40 mA over 10-90°. Thermogravimetric (TGA) and differential thermal (DTA) analyses were conducted by a TGA 1,500 instrument from ambient up to 1,000 °C in nitrogen atmosphere (20 ml/min) with the heating rate of 10 °C/min.

RESULTS AND DISCUSSION

The main chemical composition of the sample is given in Table 1. As seen in Table 1, 35.96% MgO, 25.69% SiO_2 and about 6% loss on ignition (LOI) contents show the hydrated magnesium-silicate structure of the serpentine-rich sample. Table 1 also indicates high amounts of Cr_2O_3, Fe_2O_3 and Al_2O_3 contents, determined as 16.34, 9.71 and 5.48%, respectively.

Table 1 Chemical composition of the sample

Constituents	**(%)**
MgO	35.96
SiO_2	25.69
Cr_2O_3	16.34
Fe_2O_3	9.71
Al_2O_3	5.48
CaO	0.41
NiO	0.27
TiO_2	0.14
Loss on ignition (LOI)	6.00*

*Calculated by the subtraction of total from 100.

The wet sieving analysis results are illustrated in Figure 1. According to Figure 1, more than 80% of the particles are distributed within the range of 106-425 µm. From the particle size distribution curve, 80% (P_{80}) and 50% (P_{50}) cumulative passing sizes by weight were determined to be approximately 326 µm and 210 µm, respectively.

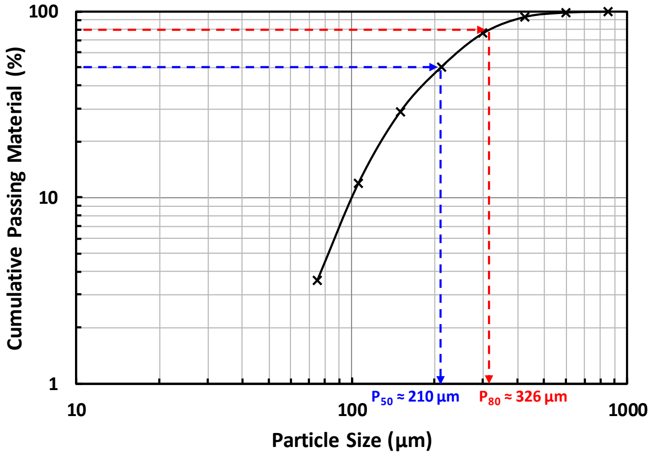

Figure 1 Particle size distribution of the sample

The XRD pattern and the detailed mineralogical analysis of the sample are given in Figure 2. The diffraction peaks were analyzed via a software program using ICSD (Inorganic Crystal Structure Database) database.

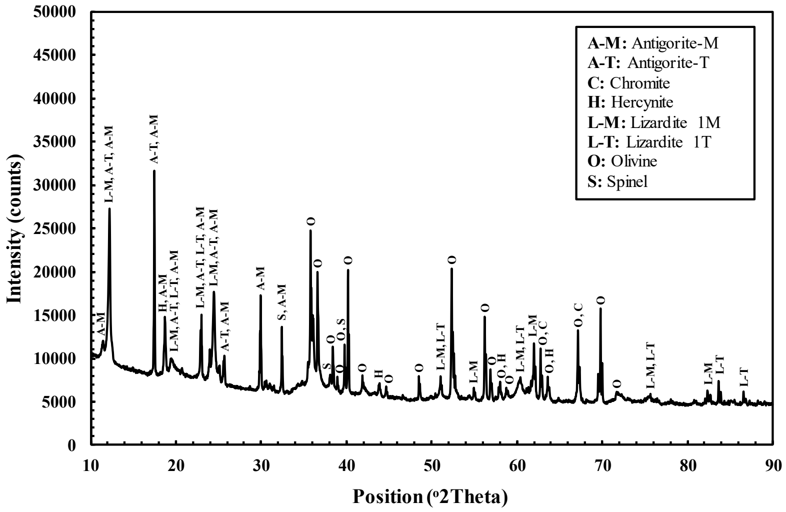

Figure 2 Mineralogical composition of the sample

As seen from Figure 2, the sample mainly consists of magnesium silicate minerals and also includes some spinel group minerals. Specifically, two different types of serpentine minerals, lizardite (1M and 1T) ($Mg_3Si_2O_9H_4$, 98-003-8534 and 98-002-8257) and antigorite (T and M) ($Mg_{48}Si_{34}O_{147}H_{62}$ and $Mg_{2.823}Si_2O_{8.639}H_{3.639}$, 98-006-7729 and 98-007-9872), olivine ($Mg_{1.8}Fe_{0.2}SiO_4$, 98-001-3459), hercynite ($AlFe_2O_4$, 98-005-5043), spinel (Al_2MgO_4, 98-007-6252) and chromite (Cr_2FeO_4, 98-004-8793) were determined from the detailed XRD analysis.

When chemical and mineralogical analysis of the sample are taken into consideration together, it can be said that the results obtained are quite consistent and compatible with the literature investigations [1, 4-6].

Figure 3 displays the DTA/TGA patterns of the serpentine-rich sample. As seen in Figure 3, the sample exhibited only 6.39% weight reduction up to approximately 1,000 °C. Large part of this reduction, 4.13%, is due to the dehydroxylation stage occurred in the range of 514-818 °C. These low weight loss values can be attributed to the high Cr_2O_3, Fe_2O_3 and Al_2O_3 contents and the antigorite polymorph of the serpentine, which was determined from the XRD analysis. Low structural water content of antigorite was also reported in the literature [1].

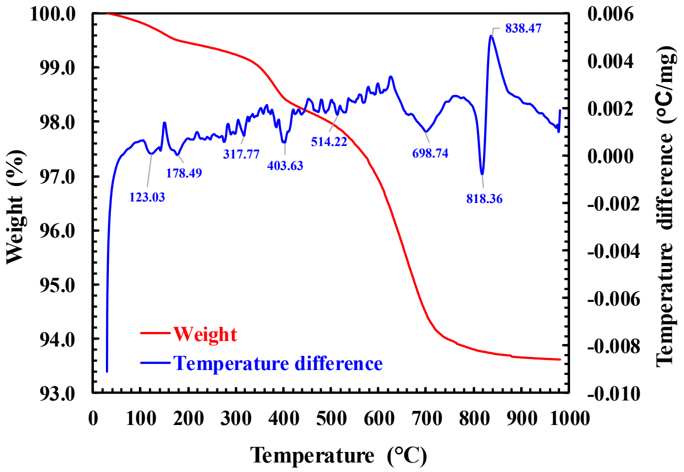

Figure 3 DTA/TGA patterns of the sample

Small endothermic peaks appeared up to 317.77 °C can be attributed to the release of physical water, corresponding to only 0.82% weight loss [2, 6]. A relatively large endothermic peak appeared at 403.63 °C is probably resulted from the dehydroxylation of brucite and the heat effect of other impurities [6, 7]. The highest weight reduction observed between 514.22 and 818.36 °C is quite possibly due to the release of structural water from the antigorite and lizardite phases [2, 4, 6-8]. A large endothermic peak seen at 698.74 °C also confirms this inference. A large exothermic peak appeared at 838.47 °C represents the destruction of antigorite and lizardite crystalline structure and the formation of forsterite and enstatite phases [2]. In particular, this large peak especially points out the transformation of enstatite to clinoenstatite, indicating that the structure of the serpentine phases is not perfect and have some structural misfits most probably due to the antigorite phase [1, 2].

As a final discussion, the serpentine-rich sample used in this study has a relatively high MgO content, appropriate particle size distribution and a low LOI content, all of which are advantageous for the purpose of refractory usage. On the other hand, the sample also contain high amounts of undesirable iron and aluminum oxides due to the reactivity of these phases at high temperatures. Unlike aluminum oxide, iron-bearing phases may be partially reduced by magnetic separation. However, in this case, an additional cost limits the usage. Furthermore, the formation of clinoenstatite, determined from the DTA/TGA analysis, is another undesirable phase because of its low melting point [4, 8]. When all of these analyses are taken into consideration, it can be said that the serpentine-rich sample examined cannot be used as a refractory raw material.

CONCLUSION

Overall results have shown that despite its promising MgO content, particle size distribution and LOI content, the serpentine-rich sample used in this study is not suitable for the refractory usage mainly due to the high amounts of undesirable iron and aluminum oxide inclusions.

ACKNOWLEDGEMENT

The technical supports by East Anatolia High Technology Application and Research Center (DAYTAM) and ETI KROM INC. are gratefully acknowledged.

REFERENCES

1. Dlugogorski, B.Z., Balucan, R.D. (2014) Dehydroxylation of serpentine minerals: Implications for mineral carbonation. Renewable and sustainable energy reviews, 31, 353-367.
2. Emrullahoglu Abi, C.B., Gürel, S.B., Kılınç, D., Emrullahoglu, Ö.F. (2015) Production of forsterite from serpentine – Effects of magnesium chloride hexahydrate addition. Advanced powder technology, 26 (3), 947-953.
3. Acar, I. (2021) Olivinin refrakter hammaddesi olarak kullanımı için demir içeriğinin manyetik ayırma ile azaltılması. Bilimsel madencilik dergisi, 60 (1), 41-49.
4. Nemat, S., Ramezani, A., Emami, S.M. (2016) Possible use of waste serpentine from Abdasht chromite mines into the refractory and ceramic industries. Ceramics international, 42 (16), 18479-18483.
5. Emami, S.M., Ramezani, A., Nemat, S. (2017) Sintering behavior of waste serpentine from abdasht chromite mines Abdasht chromite mines and kaolin blends. Ceramics international, 43 (17), 15189-15193.
6. Lafay, R., Montes-Hernandez, G., Janots, E., Munoz, M., Auzende, A.L., Gehin A., Chiriac, R., Proux, O. (2016) Experimental investigation of As, Sb and Cs behavior during olivine serpentinization in hydrothermal alkaline systems. Geochimica et cosmochimica acta, 179, 177-202.
7. Cheng, T.W., Ding, Y.C., Chiu, J.P. (2002) A study of synthetic forsterite refractory materials using waste serpentine cutting. Minerals engineering, 15 (4), 271-275.
8. Acar, İ. (2020) Sintering properties of olivine and its utilization potential as a refractory raw material: Mineralogical and microstructural investigations. Ceramics international, 46 (18, Part A), 28025-28034.

XIV International Mineral Processing
and Recycling Conference
Belgrade, Serbia, 12-14 May 2021

HEXAVALENT CHROMIUM ANALYSIS OF A FERROCHROME SLAG

Ilker Acar#
Atatürk University, Faculty of Engineering, Department of Environmental
Engineering, Erzurum, Turkey

ABSTRACT – In this study, a slag sample resulted from a ferrochrome production process was analyzed for its hexavalent chromium content. Within this scope, in addition to the main material characterization, X-ray photoelectron spectroscopy (XPS) analysis was conducted. According to the results, the sample contains 3.11% Cr_2O_3 as spinel phases. The detailed XPS analysis indicates that chromium exists as two forms, hexavalent chromate (VI) and trivalent chromite (III) in almost equal amounts. Overall results have shown that hazardous hexavalent chromate content of the slag sample must be immobilized as much as possible prior to disposed in landfills.

Keywords: Ferrochrome Slag, Hexavalent Chromium, X-ray Photoelectron Spectroscopy.

INTRODUCTION

Ferrochromium is a commonly used alloy for the manufacturing of stainless steel. It consists mainly of chromium, 45-80%, and also includes various amounts of iron, carbon and other elements [1-3]. Ferrochromium is pyrometallurgically produced in electric-arc furnaces by carbothermic reduction of chromite ($FeO.Cr_2O_3$) with coke at the temperature of about 1700 °C [1, 4].

Two by-products are generated as a result of the ferrochrome production, namely ferrochrome slag (FS) and electric-arc furnace dust (EAFD). From these wastes, while EAFD is only generated approximately 1% of the ferrochrome produced, on the other hand, for FS, this ratio is at least more than hundred times higher, varying in the range of 110-160% [1, 5-7]. Accordingly, the annual production of FS is estimated around 11.8 million tons [2]. A small percentage of this finds applications in construction industry as mostly aggregate but the vast majority is held in dumps [1, 4].

In addition to the loss of landfill area and lack of aesthetics, dumping of FS in huge quantities can cause adverse environmental effects especially on nearby water sources due to its high levels of toxic elements [1, 2, 7]. One of these elements is chromium which contaminates to land and surface water [2]. Although chromium has several oxidation states from 0 to +6, the two most common and stable forms are hexavalent chromate (VI) and trivalent chromite (III). However, both these forms possess different chemical, epidemiological and toxicological properties. Unlike chromite (III), hexavalent chromate is highly mobile, extremely toxic (10-100 times) and carcinogenic to living organisms, causing a potential health hazard. Therefore, the reduction of hazardous hexavalent chromate to immobile trivalent chromite constitutes the main mechanism of detoxification and immobilization processes [1, 8].

---

corresponding author: ilker.acar@atauni.edu.tr

In this study, a ferrochrome slag sample was examined for its hexavalent chromium inclusion by X-ray photoelectron spectroscopy (XPS) analysis.

EXPERIMENTAL

Materials

The slag sample used was resulted as the main bulk waste from the production of ferrochromium metal in the electric-arc furnace of ETI KROM INC., located in Kovancılar, Elazığ, Turkey. In this plant, after the removal of high-carbon ferrochromium metal from the slag in liquid state, the molten slag is slowly cooled in air. This results in a highly crystalline irregularly-shaped lumpy material with approximately 4-5 cm in size [3, 4, 7]. Therefore, prior to the instrumental analyses, the slag sample was crushed and ground to particle sizes finer than 100 µm.

Methods

The major chemical constituents of the sample were determined via a Spectro IQ X-ray fluorescence (XRF) instrument. The mineralogical inclusions were examined by a PANalytical Empyrean X-ray diffractometer (XRD) which operates with Cu-Kα radiation ($\lambda = 1.54060$ Å) at 40 kV and 40 mA over 10-90°. Thermogravimetric analysis (TGA/DTGA) was conducted by a TGA 1500 instrument from ambient up to 1000 °C in nitrogen atmosphere (20 ml/min) with the heating rate of 10 °C/min. X-ray photoelectron spectroscopy (XPS) analysis of the slag sample was carried out with a Specs-Flex instrument. General survey spectra were taken for the binding energy of 0-1387 eV at 100 eV pass energy while narrow range spectra for chromium were acquired in the range of 564-604 eV at the pass energy of 40 eV.

RESULTS AND DISCUSSION

The main chemical composition of the sample is given in Table 1. As seen in Table 1, MgO, SiO_2 and Al_2O_3 constitute the main chemical composition. The slag sample also includes 3.11% Cr_2O_3 and low amounts of Fe_2O_3 and CaO contents. Similar chemical compositions with varying Cr_2O_3 contents were reported in the literature [2-4].

Table 1 Chemical composition of the sample

Constituents	**(%)**
MgO	38.31
SiO_2	32.56
Al_2O_3	23.01
Cr_2O_3	3.11
Fe_2O_3	1.29
CaO	1.22

The XRD pattern of the slag sample is illustrated in Figure 1. The diffraction peaks were analyzed via a software program. As seen from Figure 1, the sample mainly consists of magnesium-silicate and magnesium-aluminate minerals as expected, and also includes amorphous glassy phase. Specifically, forsterite ($(Mg,Fe)_2SiO_4$), Fe-Mg-Cr-Al-spinels ($MgAl_2O_4$) and enstatite ($MgSiO_3$) phases were determined from the XRD analysis, which is quite consistent and compatible with the literature investigations [3, 4, 7, 9].

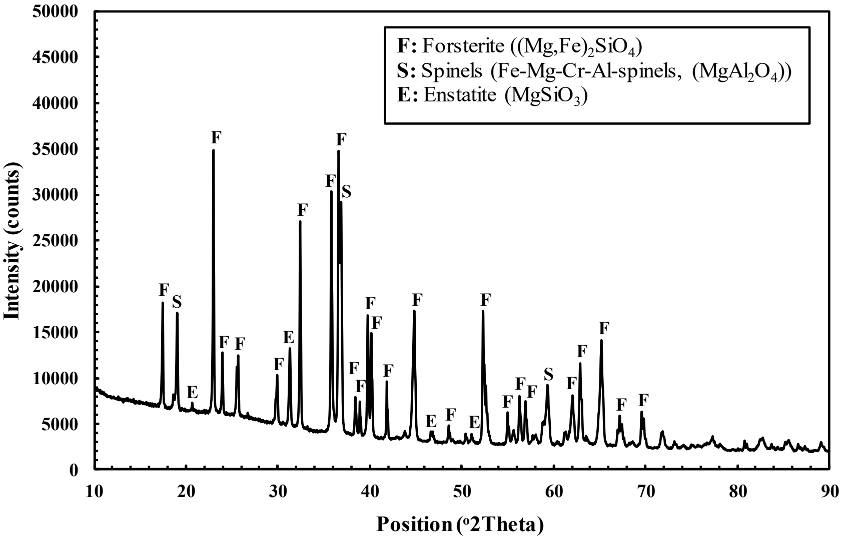

Figure 1 Mineralogical composition of the sample

Figure 2 displays the TGA/DTGA patterns of the slag sample. As seen in Figure 2, the sample exhibited almost no weight reduction, only 0.065% up to the highest temperature tested [4].

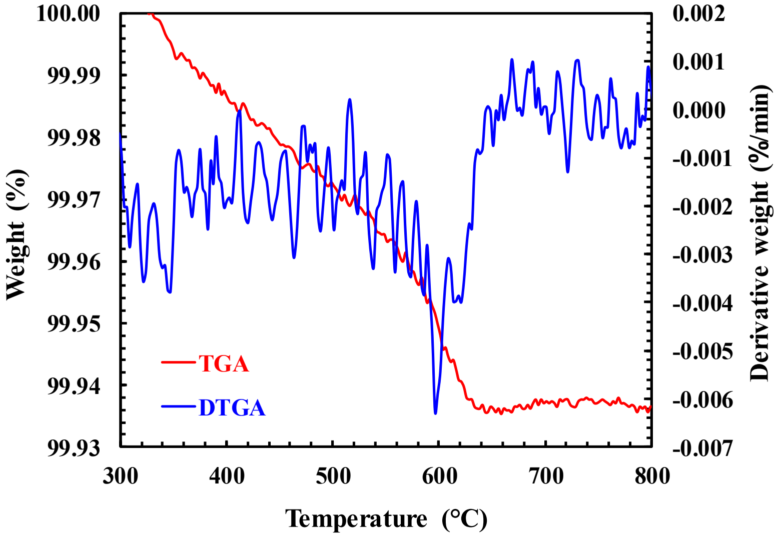

Figure 2 TGA/DTGA patterns of the slag sample

Figure 3 and Table 2 show the general XPS spectra and atomic ratio of the sample, respectively. In line with the chemical and mineralogical analyses, the main peaks for O, Mg, Si and Al can be clearly seen in Figure 3. In addition, a small peak appeared at 575 eV confirms chromium inclusion of the slag sample.

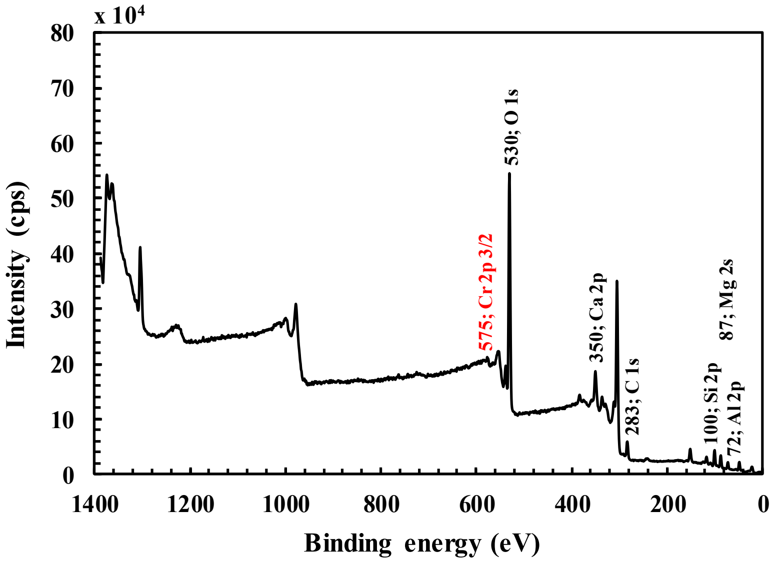

Figure 3 General XPS spectra of the sample

Table 2 XPS atomic ratio of the sample

Elements	Orbitals	Positions (eV)	Atomic ratio (%)
O	1s	530	56.200
Mg	2s	87	10.888
Si	2p	100	9.212
Al	2p	72	5.595
Ca	2p	350	7.321
Cr	***2p 3/2***	***575***	***0.505***
C	1s	283	10.142

Figure 4 illustrates the detailed narrow range spectra for chromium. As seen in Figure 4, two oxidation states, trivalent chromite and hexavalent chromate were determined at $2p_{3/2}$ orbitals. Specifically, trivalent chromite (Cr_2O_3) and hexavalent chromate (CrO_3) were assigned at 576.4 and 578.2 eV, respectively. Similar binding energy values were also reported in the literature [10, 11]. By comparing the Cr peaks observed, the relative proportions of Cr (III) and Cr (VI) were sequentially calculated as 50.65 and 49.35%. In other words, almost half of the chromium content is present as hazardous hexavalent chromate which must be reduced to immobile trivalent chromite form prior to disposed in landfills.

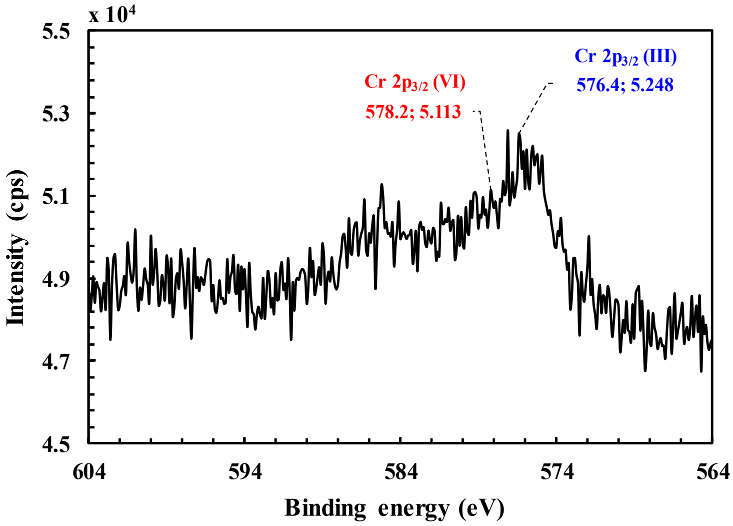

Figure 4 Narrow range XPS analysis for chromium

CONCLUSION

Overall results have shown that the ferrochrome slag sample examined in this study has a considerable amount of hexavalent chromate content. Due to its hazardous properties such as high mobility and extreme toxicity, the hexavalent (VI) chromate must be first reduced to much less dangerous trivalent (III) form and then carefully disposed in landfills.

ACKNOWLEDGEMENT

The technical supports by East Anatolia High Technology Application and Research Center (DAYTAM) and ETI KROM INC. are gratefully acknowledged.

REFERENCES

1. Bulut, U., Ozverdi, A., Erdem, M. (2009) Leaching behavior of pollutants in ferrochrome arc furnace dust and its stabilization/solidification using ferrous sulphate and Portland cement. Journal of hazardous materials, 162 (2-3), 893-898.
2. Jena, S., Panigrahi, R. (2021) Feasibility study of the properties of geopolymer concrete with ferrochrome slag and silica fume. Materials today: Proceedings, 38, 2476-2480.
3. Erdoğan, S.T. (2011) Öğütülmüş ferrokrom cürufu kullanılarak jeopolimer üretimi. In: 9th National congress on concrete. İzmir, Turkey, Proceedings.
4. Gencel, O., Sutcu, M., Erdogmus, E., Koc, V., Cay, V.V., Gok, M.S. (2013) Properties of bricks with waste ferrochromium slag and zeolite. Journal of cleaner production, 59: p. 111-119.
5. Arnold, M.C., de Vargas, A.S., Bianchini, L. (2017) Study of electric-arc furnace dust (EAFD) in fly ash and rice husk ash-based geopolymers. Advanced powder technology, 28 (9), 2023-2034.

6. Karakoç, M.B., Türkmen, İ., Maraş, M.M., Kantarci, F., Demirboğa, R., Toprak M.U. (2014) Mechanical properties and setting time of ferrochrome slag based geopolymer paste and mortar. Construction and building materials, 72, 283-292.
7. Nath, S.K. (2018) Geopolymerization behavior of ferrochrome slag and fly ash blends. Construction and building materials, 181, 487-494.
8. Shahid, M., Shamshad, S., Rafiq, M., Khalid, S., Bibi, I., Niazi, N.K., Dumat, C., Rashid, M.I. (2017) Chromium speciation, bioavailability, uptake, toxicity and detoxification in soil-plant system: A review. Chemosphere, 178, 513-533.
9. Acar, İ. (2020) Sintering properties of olivine and its utilization potential as a refractory raw material: Mineralogical and microstructural investigations. Ceramics international, 46 (18, Part A), 28025-28034.
10. Greunz, T., Steinberger, R., Strauß, B., Stifter, D. (2018) Reduction of hexavalent chromium embedded in organic insulation and corrosion inhibition layers during X-ray photoelectron spectroscopy (XPS) measurements. Corrosion science, 143, 39-45.
11. Murphy, V., Tofail, S.A.M., Hughes, H., McLoughlin, P. (2009) A novel study of hexavalent chromium detoxification by selected seaweed species using SEM-EDX and XPS analysis. Chemical engineering journal, 148 (2-3), 425-433.

XIV International Mineral Processing and Recycling Conference
Belgrade, Serbia, 12-14 May 2021

THERMAL PROPERTIES OF LITHIUM GERMANATE PHOSPHATE GLASS STUDIED BY DTA

Vladimir Topalović[1#], Srđan Matijašević[1], Snežana Grujić[2], Veljko Savić[1], Jelena Nikolić[1], Sonja Smiljanić[2,3], Snežana Zildžović[1]
[1] Institute for Technology of Nuclear and Other Mineral Raw Materials (ITNMS), Belgrade, Serbia
[2] Faculty of Technology and Metallurgy, University of Belgrade, Belgrade, Serbia
[3]Institute "Jožef Stefan", Ljubljana, Slovenia

ABSTRACT - The DTA data collected for $22.5Li_2O{\cdot}10Al_2O_3{\cdot}30GeO_2{\cdot}37.5P_2O_5$ (mol%) glass sample was reported and discussed. The ease of glass formation has been studied. It was determined that the DTA exothermal temperature peaks revealed the crystallization of $LiGe_2(PO_4)_3$ and GeO_2 phases. The activation energy of crystallization and viscous flow was determined. The value of the Avrami exponent and reduced glass transition temperature indicates that the $LiGe_2(PO_4)_3$ phase has three-dimensional growth.

Keywords: Glass, DTA, Thermal Properties.

INTRODUCTION

Glass is a unique state of matter that combines features of both liquids and solids and also exhibits its unique characteristics [1]. Glass is a nonequilibrium, noncrystalline condensed state of matter that exhibits a glass transition [2]. Lithium germanate phosphate glasses have recently emerged as multipurpose materials and have been drawn great attention because of their potential applications in various solid-state devices [3]. By crystallization of some glasses from the system Li_2O-Al_2O_3-GeO_2-P_2O_5, the $LiGe_2(PO_4)_3$ phase which belongs to the solid solutions with the general formula of $Li_{1+x}M_xGe_{2-x}(PO_4)_3$ (M=Al, V or Cr) is formed. This family of crystalline phosphates is often referred to as NASICON-type materials [4]. For this investigation, the glass composition $22.5Li_2O{\cdot}10Al_2O_3{\cdot}30GeO_2{\cdot}37.5P_2O_5$ (moll %) was selected.

EXPERIMENTAL

The glass was prepared by melting a homogeneous mixture of reagent-grade Li_2CO_3, A_2O_3, $GeO_{2,}$ and $(NH_4)_2HPO_4$ in a covered platinum crucible. The chemical analysis was performed using spectrophotometer AAS PERKIN ELMER Analyst 703. The melting was performed in an electric furnace BLF 17/3 at T=1400 °C during t=0.5 h. The melts were cast on a steel plate and cooled in the air. The experiments under non-isothermal conditions were performed using a Netzsch STA 409 EP device and Al_2O_3 powder as the reference material. In the experiments, a constant weight (100 mg) of the samples were

---

[#] corresponding author: v.topalovic@itnms.ac.rs heated at different rates (*β*) of 5, 10, 15 and 20 °C min^{-1} from T = 20 °C to 1120 °C. The density of the sample was determined by the pycnometric method with a measurement accuracy of ± 0.50%. The experimental error was estimated after 3 parallel measurements. All the measurements have been recorded at room temperature (20 °C).

RESULTS AND DISCUSSION

The obtained glass samples were transparent, without visible residual gas bubbles. The results of the chemical analysis show that a glass composition of $22.5Li_2O·10Al_2O_3·30GeO_2·37.5P_2O_5$ (mol%) was obtained. The density of obtained glass is ρ= (3.61±0.02) g·cm^{-3} determined by the standard pycnometric method.

DTA provides an overview of the possible transformations that the glasses undergo at different temperatures, such as the glass transition T_g (manifested by the first inflection in the trace), onset crystallization temperature T_x, crystallization temperature T_p (characterized by exothermic peak), and melting temperature T_m (characterized by endothermic peak). In Fig.1 DTA curves recorded at heating rates β of 5, 10, 15 and 20 °Cmin^{-1} from T = 20 °C to 1120 °C are shown.

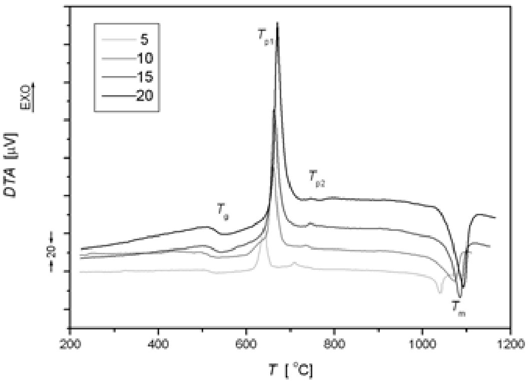

Figure 1 DTA curves for glass powder sample particle sizes 0.50-0.65 mm, recorded at different heating rates 5-20 °C/min

Two exothermal peaks T_{p1} and T_{p2} were registered at DTA curves. As determined previously by XRD analysis of the crystallized glass sample, the peak T_{p1} depicts the crystallization of primary $LiGe_2(PO_4)_3$ phase (rhombohedral crystal system, space group R3c) and T_{p2} the crystallization of secondary α-GeO_2 phase which appeared in traces (2.4 vol%) [5]. In Table 1, characteristic DTA temperatures were summarized.

Table 1 DTA temperatures and the parameters calculated for glass powder sample particle sizes 0.50-0.65 mm, heated at different heating rates

β	T_g	T_x	T_{p1}	T_m	T_{rg}
5	512	615	640	1040	0.49
10	516	640	661	1074	0.48
15	521	646	665	1085	0.48
20	524	651	670	1092	0.48

Also, the reduced glass transition temperatures $T_{rg}=T_g/T_m$ is shown [6]. The value of reduced glass transition temperature $T_{rg}<0.58$ suggests that this glass has volume (homogeneous) nucleation [7,8]. Glass forming ability (GFA), as related to the ease of vitrification, is vital for understanding the origin of glass formation and is important for designing glasses. The glass transition temperature represents the strength or rigidity of the glassy structure. The value of reduced glass transition temperature T_{rg} indicates a modern glass-forming tendency of this glass and also volume crystallization. Also, according to the temperature difference between (T_x-T_g) >100 °C the process of sintering could be independent of crystallization.

Following the method for analysis of non-isothermal crystallization data suggested by Matusita and Sakka (eq. 1), the Avrami parameter n and the activation energy for crystallization E_a can be calculated [9].

$$ln\frac{\beta^n}{{T_p}^2} = -\frac{m \cdot E_{a,m}}{R \cdot T_p} + const. \tag{1}$$

where R is the gas constant. The values of the parameters n and m depend on the rate-controlling mechanism of the crystallization kinetics, while the value of E_a is obtained from the ratio $\ln(\beta^n/T_p^2)$ *vs.* $1/T_p$ using the corresponding values for n and m.

In Fig.2, the plot of log [−ln(1 − χ)] versus log (β) where χ is the degree of glass - crystal transformation at an arbitrary fixed temperature T=665 °C is shown. The fraction of crystals, χ was obtained from the ratio $\chi = A/A_o$ where A designates the peak area at the chosen temperature, while A_o is the total area of the corresponding DTA peak. The positions of the crystallization peak on the DTA curves of this sample recorded at heating rates of 5, 10, 15, and 20 °C min^{-1} enabled the determination of four values of χ at the selected temperature T=665 °C to be determined (Fig.1). The value of the Avrami parameter n = 3.9 was determined from the slope of the straight line [10]. From the mean value of n, it is possible to postulate a crystallization mechanism [11]. This high value of the Avrami exponent (n ~ 4) indicates a very high nucleation rate and three-dimensional growth of crystals [12].

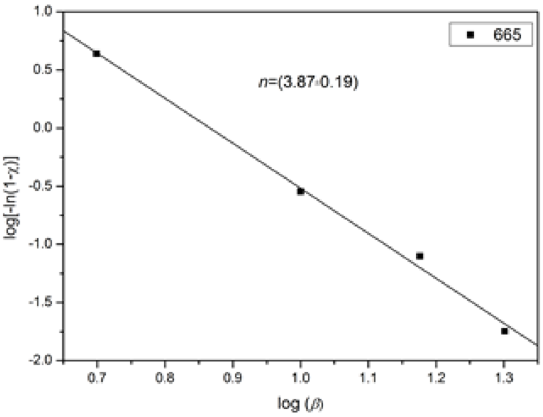

Figure 2 log[−ln(1 − χ)] against log (β) for the test glass at T=665 °C

Also, the Ozawa method [10] can be applied for E_a calculation using the relationship:

$$ln\,\beta = -\frac{m\cdot E_{a,oz}}{n\cdot RT_p} + const. \tag{2}$$

By introducing the parameters n and m ($m = n$ -1) in the Matusita and Sakka equation (627 kJ mol^{-1}) and also from the Ozawa method (635 kJ mol^{-1}) the average value for activation energy for crystallization were calculated $E_{a,moz}$ = (632 ± 7) kJ mol^{-1}.

Viscosity is one of the fundamental properties of glass. By knowing the viscosity of glass, it is possible to determine when the glass is in solid form, when it is in the melting phase, and when it is in the transformation region (the temperature region between the cooled melting and the solid phase in the unbalanced state is called the transition region or glass transformation region).

Also, based on viscosity, the area of glass processing can be determined. One of the most important factors in the production of glass articles is the variation of glass viscosity under changing temperature. All glasses can be arbitrarily classified as “short” i.e., fast-solidifying glasses, and “long” ones that solidify slowly.

It is generally accepted that the limiting values of viscosity in making glass articles are 10^2 and 10^8 Pa·s. Therefore, the temperature interval of glass manufacture is restricted by the specified viscosity values and lies within a range from a few tens to a few hundred degrees. According to the temperature interval of 370 °C for glass viscosity 10^2-10^8 Pa·s this glass belongs to long therm glasses, Figure 3 [13].

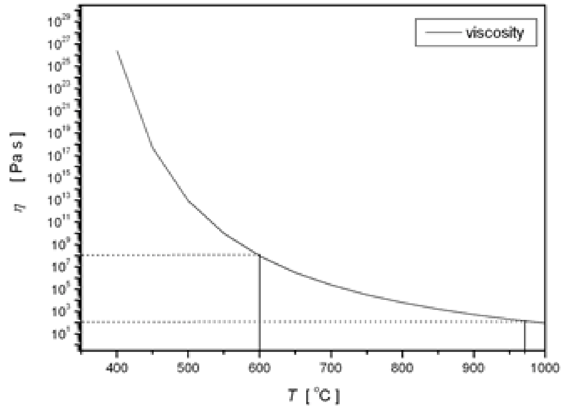

Figure 3 The viscosity of test glass between 600-970 °C [14]

Based on the obtained temperature dependence of the viscosity was calculated activation energy of viscous flow E_{η} = ΔG_{η} [11] from the slope of the line log (η) = f (1 / T), shown in Figure 4 [15].

The activation energy of viscous flow around glass transition temperature was calculated E_{η} = (671 ± 16) kJ mol^{-1} and are in good agreement with Ozawa and Matusita methods.

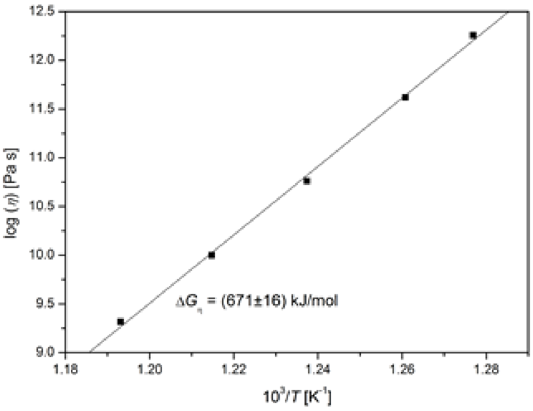

Figure 4 The activation energy of viscous flow between 500-570 °C for test glass

CONCLUSION

Test glass $22.5Li_2O{\cdot}10Al_2O_3{\cdot}30GeO_2{\cdot}37.5P_2O_5$ (moll %) has been obtained from the good glass-forming liquid. Small glass forming tendencies for test glass have been found using the DTA method. High crystallization ability was determined for this glass during heating. Due to the *m*, *n* parameters of crystallization calculated it was concluded that a three-dimensional growth of the $LiGe_2(PO_4)_3$ phase in glass matrix appeared. The activation energy for crystallization E_a = (632 ±7) kJ mol^{-1} and viscous flow E_η = (671± 16) kJ mol^{-1} were determined. Based on the thermal properties obtained glass is suitable for manufacturing.

ACKNOWLEDGEMENT

The authors are grateful to the Ministry of Education and Science, Republic of Serbia for financial support (grant contract No.: 451-03-68/2020-14/200023).

REFERENCES

1. Zheng, Q., Zhang, Y., Montazerian, M., Gulbiten, O., Mauro, J.C., Zanotto, E.D., Yue, Y. (2019) Understanding glass through differential scanning Calorimetry. Chem.Rev., 119, 7848-7939.
2. Zanotto, E.D., Mauro, J. C. (2017) The Glassy State of Matter: Its Definition and Ultimate Fate. J. Non-Cryst. Solids 471, 490-495.
3. Masquelier, C. (2011) Solid electrolytes: Lithium ions on the fast track. Nat. Mater., 10, 649-650.
4. Anantharamulu, N., Rao, K.K., Rambabu, G., Kumar, B.V., Radha, V., Vithal, M. (2011) A Wide-Ranging Review on Nasicon Type Materials. J. Mater. Sci., 46 2821-2837.
5. Nikolić, J.D., Smiljanjić, S.V., Matijašević, S.D., Živanović, V.D., Tošić, M.B., Grujić, S.R., Stojanović, J.N. (2013) Preparation of glass-ceramic in $Li_2O{\cdot}Al_2O_3{\cdot}GeO_2{\cdot}P_2O_5$ system. Processing and Application of Ceramics, 7 [4], 147-151.
6. Augis, J.A., Bennett, J.E. (1978) Calculation of Avrami parameters for heterogeneous solid-state reactions using a Modified Kissinger's method. J.Therm.Anal., 13, 283-292.

7. Zanotto, E.D., Fokin, V.M. (2003) Recent studies of internal and surface nucleation in silicate glasses. Phil. Trans. R. Soc. Lond. A 361, 591-613.
8. Matijašević, S.D., Grujić, S.R., Topalović, V.S., Nikolić, J.D., Smiljanić, S.V., Labus, N.J., Savić, V.V. (2018) Non-Isothermal crystallization of lithium germanophosphate glass studied by different kinetic methods, Sci. Sinter, 50 (2), 193-203.
9. Matusita, K., Sakka, S. (1980) Kinetic study of crystallization of glass by differential thermal analysis-criterion on application of Kissinger plot. J. Non-Cryst. Solids, 38-39, 741-746.
10. Ozawa, T. (1976) A modified method for kinetic analysis of thermoanalytical data. J. Therm. Anal., 9, 369-373.
11. Macfarlane, D.R., Matecki, M., Poulan,M. (1984) Crystallization in fluoride glasses: I. Devitrification on reheating. J. Non-Cryst. Solids, 64, 351-362.
12. Živanović, V., Grujić, S., Tošić, M., Blagojević, N., Nikolić, J. (2009) Non-isothermal crystallization of K2O·TiO2·3GeO2 glass. J. Therm. Anal., 96, 427-432.
13. Bessmertnyi, V.S., Krokhin, V.P., Panasenko, V., Drizhd, N., Dyumina, P., Kolchina, O. (2001) Plasma rod decorating of household glass. Glass and Ceramics, 58, 176-179.
14. Matijašević, S. (2012) Crystallization behavior of multicomponent germanate glasses, Doctoral dissertation, TMF, University of Belgrade, 134.
15. Hlavač, J. (1983) The Technology of Glass and Ceramics, Elsevier Sci. Pub. Comp., Inc., New York. 431.

XIV International Mineral Processing
and Recycling Conference
Belgrade, Serbia, 12-14 May 2021

ANALYZE OF MUNICIPAL WASTE MORPHOLOGY

Džafer Dautbegović[1#], Mirsada Hasanbašić[2]
[1] University of Zenica, Zenica, Bosnia and Herzegovina
[2] Student at university of Zenica, Zenica, Bosnia and Herzegovina

ABSTRACT – This paper provides results on municipal waste morphology analysis in city of Zenica in Bosnia and Herzegovina, that will help improvement of waste collecting system but also in planning of recycling plant. The process of municipal waste sampling included five trucks from rural areas, and seven trucks from urban areas over twelve-day period in August 2020. Methodology for the analysis of Solid Waste (SWA-Tool) was used for 3.32 t weighed samples, and 38 waste types were separated by six sieves of different size. According to the results, the dominant fractions were organic waste, followed by plastics. It was also revealed that there were hazardous wastes in the composition of solid municipal waste in small quantities (<1%).

Keywords: Waste Morphology, Municipal Waste, Raw Materials.

INTRODUCTION

Waste management and recycling company "ALBA Zenica" d.o.o. Zenica is a company for waste collection in Zenica, Bosnia and Herzegovina. It was founded in 1999. by its majority owner ALBA Group AG from Berlin, which is today one of the three leading European companies for the provision of utility services, and is the leading recycling concern in Europe.

According to the final results of 2013 population census in B&H, the Zenica area of 500 km^2 is inhabited with about 130,000 inhabitants.

The object of disposal in households is a usable and unusable household waste, a compact material that is not filled with liquid or air in a clearly visible and tangible form, predominantly generated in consumption. These materials represent the mentioned municipal (household) waste in the existing Waste management act and the Waste catalog in the FBiH [1,2].

For the establishment of a system of organized waste disposal of municipal waste, data on expected waste are needed, as well as waste generators, i.e., the population and the area in which waste will be collected. The most important parameters for the analysis are:

a) quantity of produced waste on a daily, weekly and monthly basis,
b) composition of municipal waste,
c) number and arrangement of users of the municipal waste collection system,
d) location, distance and capacity of the facility for processing/receiving municipal waste,

---

[#] corresponding author: dautbegovic@alba.ba

e) settlement structure (rural/urban, density, type of construction),
f) network and traffic conditions,
g) climatic conditions (hygiene requirements),
h) collection budgets. [3]

Morphological analysis of municipal waste in Zenica resulted with relevant data on the composition of waste collected in Zenica and disposed at the Regional landfill “Mošćanica”.

Determining amount and composition of waste is of great importance for improvement of future waste collecting system, but also for planning the waste management center.

EXPERIMENTAL (MATHERIALS AND METHODS)

Determining the categories of waste that are selected is done on the basis of waste categories according to the Rulebook on waste categories with lists (Official Gazette of Federation of Bosnia and Herzegovina No. 9/05) according to the potential of their recyclability and reuse.

The following equipment was used for the process of sorting and determining the morphological composition of waste:

- Electronic scale (measuring range 150 kg, platform width 400x500 mm, with LED display and the possibility of working on a rechargeable battery),
- Sampling waste container,
- Waste bins into which waste is classified by category,
- The screens for sorting and separating larger waste components. First screen contains three sieves of 250 mm, 150 mm, 100 mm, and the second screen contains sieves of 60 mm, 40 mm and 15 mm,
- Auxiliary tools and implements (shovels, nylon, scissors, bag cutting knives, etc.).

The method of sampling and analysis of waste can be described as follows:

- When the truck from specific area arrives, it is been weighed;
- Waste samples for analysis are taken after the truck from specific area unloads the waste,
- For the purposes of morphology, 3 waste containers of volume 1110 l from each truck were analyzed, and they are considered as a waste sample for specific area,
- When filled, each container with waste is weighed,
- Waste sample from the first waste container is dumped on a waste sorting screen where the waste is sorted manually, sifted through first three sieves, then the rest is transfered to the second sorting screen and then sorted and sifted through other three sieves again, until finally a fine sifted residue remains.
- After sorting, each obtained fraction is weighed separately and as a result of the analysis the amount of waste by categories is obtained,
- The obtained results are written in a special form containing: date of sampling, origin of waste (area from which the waste was brought), total amount of waste brought in the truck, data on the net weight of each waste fraction.
- The same procedure is repeated for waste from the remaining two containers, and the sum of the obtained results from all the containers represent the waste composition for the specific area.

RESULTS AND DISCUSSION

Table 1 Absolute and percentage shares of individual components in observed sample

No.	WASTE		Absolute shares (kg)	Percentage shares (%)	Absolute shares (kg)	Percentage shares (%)
1	biodegradable waste	kitchen waste	834.11	25.44	1697.98	48.13
2		garden waste	692.48	20.58		
3		treated wood	20.56	0.62		
4		untreated wood	37.73	1.13		
5		packaging wood	13.10	0.36		
6	paper and cardboard	office paper	24.73	0.74	253	8.16
7		paper and cardboard packaging	228.58	7.04		
8	multilayer materials	composite packaging	36.88	1.12	38.33	1.16
9		composite materials	1.45	0.04		
10	plastic	hard plastics	173	5.13	568.33	16.93
11		packaging plastic and foil and bags	307.97	9.15		
12		packaging plastic PET transparent	48.85	1.47		
13		packaging plastic PET mixed	38.51	1.18		
14	glass	glass	21.65	0.66	95.37	2.91
15		packaging glass transparent	42.40	1.33		
16		packaging glass mixed	31.32	0.93		
17	textile	textile	181.22	5.62	203.50	6.27
18		footwear	22.28	0.66		
19	metal	iron packaging	1.84	0.05	44.12	1.33
20		other metals packaging	27.82	0.84		
21		iron	8.59	0.26		
22		other metals	5.87	0.18		
23	hazardous waste	paints and varnishes	2.48	0.07	22.18	0.69
24		hazardous substances packaging	4.58	0.15		
25		medications	1.28	0.04		
26		batteries	1.16	0.04		
27		car batteries	0.00	0.00		
28		large household appliances	4.04	0.14		
29		WEEE–IT devices	2.48	0.07		
30		WEEE– other	6.16	0.18		
31	mineral waste	construction waste	68.46	1.97	100.08	2.88
32		construction debris	13.24	0.40		
33		bulky waste	7.90	0.20		
34		land and stone	10.48	0.31		
35	rest	hygiene supplies	270.96	8.08	385.53	11.50
36		leather	15.89	0.48		
37		gum	3.53	0.11		
38		fine fractions <15 mm	95.15	2.84		
	non-municipal waste	animal waste	8.82	1.81	12.38	2.26
		medical waste	2.28	0.23		
		car filters	1.28	0.21		

The waste morpholphology analysis was performed during twelve−days period from 03.08. to 21.08.2020., and process of separation and sampling of municipal waste included five trucks from rural areas, and seven trucks from urban area. In the process of sampling and analysis, 38 waste types were separated, and percentage share of each component in overall waste was provided.

The total amount of municipal waste for these twelve days is 76.15 t and the total weight of all samples is 3,321 t, or 4.36% of the total amount.

The results of morphology analysis from Table 1 show that the largest share of waste belong to biodegradable waste. Large amounts of valuable components which can be used as a secondary raw materials were found in municipal waste, especially paper and PET packagings. Smaller amounts of metal components can be explained by the fact that this component has recognizable market value and often is removed from waste bins. The smallest quantities in municipal waste has hazardous waste with 0.69%. We can see that in the samples, taken during twelve days, only accumulators (car batteries) of 38 selected waste types, were not found.

Unfortunately, municipal waste also contains waste that does not belong there, such as animal waste, medical waste and car waste.

It is important to say that, in average, there is more hygiene supplies than paper and cardboard, and all other types, besides the biodegradable waste and plastics.

It is interesting that waste composition in rural and urban area is pretty much similar, with the highest quantities of biodegradable waste and plastics in both areas, and the lowest quantities of hazardous waste, as shown in Figure 1.

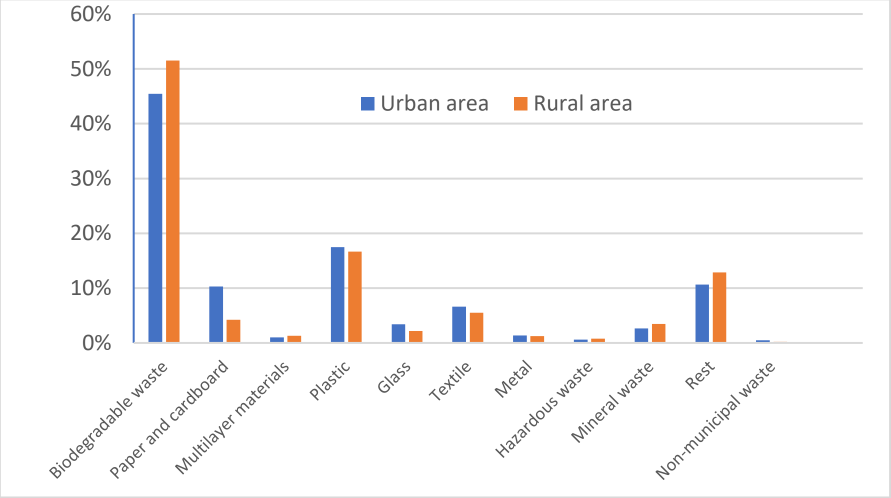

Figure 1 Comparation of waste morphology in urban and rural area

The main difference between waste composition in rural and urban area is that there is above two times more paper in urban areas. In urban areas, there is more waste that must not be in municipal waste.

What is also interesting from the waste analysis is which waste fraction size is most common. Based on the size of the openings on the sieves, we can get data on the amount of secondary materials that can used in the recycling process. From the Figure 2, we can see that in average, the most common waste fraction size is over 150 mm, followed by more than 100 mm, and the smallest quantites are waste fractions size of less than 15 mm, that is fine fraction. Share of fine fraction, from 0 to 40 mm, which is not very usable for material recycling in simple plants, is below 15%, which leaves us a lot of secondary raw materials for recycling.

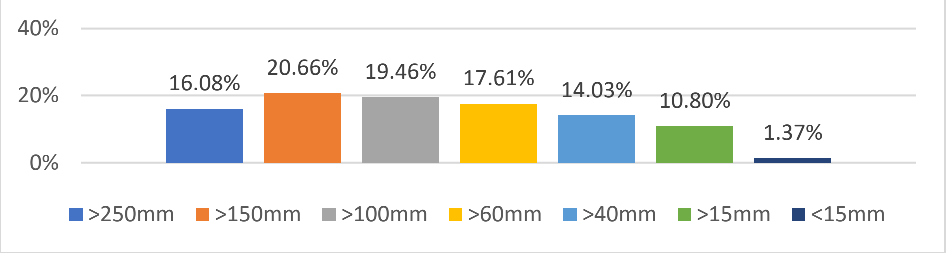

Figure 2 Waste analysis by fraction size

When taken in account biggest quantites and most common sizes of waste fractions, we can conclude that municipal waste mainly consist of larger food fractions, big diapers and plastic bottles. Also, we could see a lot of big cardboards.

From the Figure 3, we can see there is about 30% of waste materials bigger than 80 mm, which are very usable in recycling plants, biodegradable waste not counted, and only diapers can not be used as secondary raw materials. Besides that, in municipal waste, there is about 23% waste fractions between 40–80 mm and big part of these materials are also secondary raw materials.

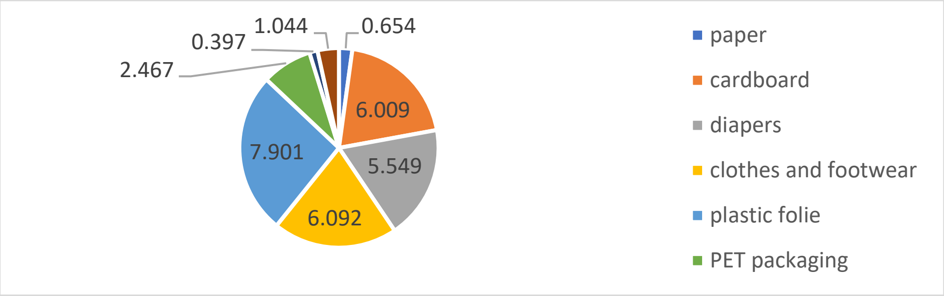

Figure 3 Percentage share of waste materials >80 mm

Based on collected data, we calculated the confidence interval, which showed us once more that the waste composition is variable and depends on many factors, such as number of people in household, type of area (rural, urban), season of the year, population habits, infrastructure, etc. We also concluded we need more samples for more accurate results.

$$C.I. = \bar{x} \pm \frac{t_{\alpha;n-1} \cdot varcoeff(x_i)}{\sqrt{n}} = \bar{x} \pm \left(t_{\alpha;n-1} \cdot varcoeff\left(\hat{X}\right)\right) \tag{1}$$

Intervals constructed in this manner will contain the true value of μ, 95% of the time.

Table 2 gives the values of confidence intervals for six waste categories that can be used as secondary raw materials and their usable weight for recycling.

Table 2 Confidence intervals

Waste	Weight (kg)	C.I. (%)
kitchen waste	834.11	24.05
garden waste	692.48	27.07
paper and cardboard packaging	228.58	24.92
plastic bags	307.97	25.06
textile	181.22	40.32
hygiene supplies	270.96	32.86

CONCLUSION

The main aim of morphological analysis of the municipal waste composition in Zenica was to improve future planning of the organisation of waste collection system and also of Centre for waste management.

The results of the analysis indicate large amounts of organic substances in waste that is being transported to Regional landfill Mošćanica for final disposal. With regard to the European Union regulations, maximum amount of organic waste that can be disposed to the landfill cannot exceed 5% [4]. In accordance with these regulations, it is necessary to carry out actions to reduce the amount of biodegradable waste disposed, primarily by educating the population how to use appropriate components of organic waste to make compost.

Significant amounts of usable components that can be used as raw materials (PET bottles, paper and cardboard) were found in municipal waste stream. Considering the fact, that in Zenica the system at separate collection on source exists, this shows us that it needs improvement, and that the waste management centre is needed. Also, the size of these components is mostly over 100 mm, so they could easily be separated manually, if there was a sorting line.

The ecological effect of separating useful components from waste is reflected in extending the life of the landfill and preserving natural resources. On the other hand, secondary raw materials from waste can be placed on the market, which provides a financial benefit from their sale.

REFERENCES

1. Zakon o upravljanju otpadom FBiH (Sl.nov. FBiH 33/03), Article. 15 , page 4.
2. Pravilnik o kategorijama otpada sa listama (Sl.nov.FBiH 09/05).
3. Džafer, D., Šefket, G., Darko, P., Muvedet, Š. (2018) Appendix to logistics of municipal waste disposal. in: EMFM 2018, Zenica, Bosnia and Herzegovina.
4. Jovan, S. (2003) Obrada i deponije otpada. Mašinski fakultet u Zenici, Univerzitet u Sarajevu, Zenica.

MATERIAL FLOW ANALYSIS OF GLASS PACKAGING WASTE IN THE REPUBLIC OF SERBIA

Angelina Pavlović#, Goran Bošković, Nebojša Jovičić
University of Kragujevac, Faculty of Engineering, Kragujevac, Serbia

ABSTRACT – Accelerated population growth and economic development cause an increase in the consumption of material goods and an increase in the generated amount of municipal waste. Glass amounts to 5% of total generated waste worldwide. Millions of glass waste pose serious environmental problems every year, which primarily arise due to unharmonized glass waste flows. This paper aims to quantitatively and qualitatively investigate the system of glass packaging waste management in the Republic of Serbia, using the material flow analysis (abbr. MFA) since glass packaging makes up to 85% of the total generated glass waste.

Keywords: MFA, Glass Packaging, Waste, Environment Protection.

INTRODUCTION

Every year, world glass production grows, which is proved by the fact that the global glass manufacturing market size was valued at USD 127.1 billion in 2019 [1]. Following a global trend, the production and consumption of glass in the Republic of Serbia has continuously risen over the past decades. That leads to the generation of large quantities of glass waste that have caused problems related to the environment. In 2019, 2.35 million tons of municipal solid waste (abbr. MSW) were generated in the Republic of Serbia, and glass waste amounts to 4% [2,3]. Globally, most waste is currently dumped or disposed of in some form of a landfill [4]. However, glass can be recycled countless times in 100% [5]. The landfilled glass will never decompose, so disposed glass represents the loss of raw materials.

Glass is a material that is used in numerous applications in daily human lives. In particular, glass represents one of the safest and most suitable materials for packaging [6]. Management of glass packaging and glass packaging waste has a very pronounced environmental, social and economic significance. Today, the largest percentage of total used glass packaging is used for a single-use and the purpose of packaging products for further distribution (food, beverages, pharmaceuticals, etc.), so that is the reason because 85% [7] of the glass in MSW is glass packaging. According to that, the importance of minimizing and recycling glass packaging waste disposal has long been recognized. To improve the glass packaging waste management system, it is essential to identify flows of glass packaging waste that can be easy to improve. Forecasting material flows is essential for sound policymaking on issues relating to waste management [8]. In this paper, the MFA approach was used to assess the flows and stocks of glass waste packaging to understand and quantify sources, pathways and sinks of the analyzed material.

---

corresponding author: angelina.pavlovic@uni.kg.ac.rs

Considering that this topic is important for improving the quality of the environment, both in the world and in the Republic of Serbia, this paper aims to define measures to improve the system of monitoring the flow of glass packaging waste, based on analysis of inappropriate software – STAN 2.6.

EXPERIMENTAL

A large number of methods have been developed in the world, which are used during decision-making in the field of resource management and environmental protection. One of the methods, which has a wide application and can be said that is the basis for other methods, but also, can be used independently of other methods, is the MFA. During the developing of the MFA method, it was started from the fact that materials behave following the fundamental laws of conservation of mass. MFA is based on the material balance, which means - matter cannot disappear; it can only transform and leave the system in the form of emissions or other by-products [9,10].

In order to create an MFA model, it is necessary to follow the next steps [10,11]:

- analysis of the system and the involved processes and materials (model building stage),
- measurement of the material or mass flows (data collection),
- calculation of material or mass flows, and
- interpretation of the results.

The focus of this paper is the analysis of glass packaging waste flows in the Republic of Serbia, and it is essential to note that by balancing the inputs and outputs of waste streams in one system, the environmental footprint becomes more noticeable, and the sources of environmental pollution are possible to locate. Appropriate measures to improve the current state of the glass packaging waste management system in the Republic of Serbia can be taken based on identifying depletion or accumulation of material stocks in the complete system.

Packaging quickly becomes waste, so data about packaging placed on the market are generally taken as data on the generated amount of glass packaging waste in one year. In this case, MFA can locate material flows, i.e. processes during the life cycle of glass packaging that can be improved by simultaneously reducing the extraction of new raw materials and the total generated amount of packaging glass waste.

In the MFA system building stage, it is necessary to define the analysis's boundaries, which are defined in time and space. Frequently, the MFA's spatial system boundary coincided with the politically defined region (intended as administrative regions such as states) [12]. In this paper, the geographical border is defined by the territory of the Republic of Serbia. The time interval determines processes within the MFA, i.e. the year from which the data were taken. During the analysis, data from 2019 was used; in the case where data are not available for the mentioned year, the last available data was used. The number of flows and processes during one MFA model depends on the analysis's goal and its complexity. For the analysis of glass packaging flows, ten processes are shown by the model that is composed of four phases:

- the first phase comprises two processes: manufactures and industries that use glass packaging (food and beverage industry, the pharmaceutical industry, etc.),

- the second phase includes the only process of glass packaging consumption in households and small businesses,
- the third phase implies four processes that are connected to a different way of collection and treatment of glass waste packaging (collection and transport of MSW by public utility companies, informal waste collection, secondary waste separation and glass packaging recycling), and
- the fourth phase covers three processes that refer to landfilling of glass waste packaging on unregulated (illegal) landfills, controlled landfills and sanitary landfills. All processes in this phase are considered as processes with stocks of materials.

Processes are connected by flows (mass of material per unit time) that can be observed as input and output flows from one process. Flows can be internal and external, depending on whether it exceeds the defined boundary of the system. In the analysis, twenty flows were defined, of which four were defined as external input flows – imported flows, and three were defined as external output flows – exported flows. The remaining flows are internal flows, i.e. input/output flows from defined processes. In the analyzed model, imported flows represent raw materials for production of glass packaging products, imported secondary raw materials, imported glass packaging and imported material goods (products packed in glass packaging). The exported flows represent the export of secondary raw materials, export of products in glass packaging as well as export of glass packaging.

The choice of substances depends on the type of system to be analyzed. In this paper, material goods will be defined without defining substances.

Since there is no record of the amount of glass packaging produced in the Republic of Serbia, it is possible to use different approaches to obtain the necessary data to measure the glass packaging flows.

According to the Environmental Protection Agency data, 2.35 million tons of waste were generated in Serbia in 2019, of which 4% is glass waste [2]. Based on the above, it is concluded that 94,000 tons of glass waste were generated in Serbia during the same year. Since it is known that 85% of glass in municipal waste is glass packaging, it is known that 79,900 t of glass packaging can be identified in the total amount of municipal waste [7].

The total amount of glass packaging placed on the Republic of Serbia market is 61,979.8 [13]. Imported material goods, i.e. products packed in glass packaging used by households and small enterprises, are unknown. However, the data on the differences between glass packaging distributed to the industries that use it and the amount of packaging placed on the RS market is adopted since MFA analyzes material flows on that way, everything that enters one system must leave the same, and that is 17,920 t.

Based on the Glass Alliance Europe's statistical report, it was found that in 2019, 74,743 tons of glass packaging were exported from Serbia, while 16,928 tons were imported [14].

In the Republic of Serbia, concerning the amount of glass produced and in general in circulation, there are few accredited collectors, especially recyclers of this secondary raw material. Of the total amount of glass packaging placed on the market, 27,743.7 t was recycled [13], while 21,691 tons of secondary raw materials from packaging glass were exported, and 0 tons of secondary raw materials were imported [2]. The amount of secondary raw materials used in glass packaging production is determined as the difference between the total recycled amount of glass packaging waste and the secondary raw material that is exported.

On the other hand, significant amounts of glass packaging waste are irretrievably disposed of in landfills and dumps. Based on data from the Statistical Office of the Republic of Serbia, the amount of generated industrial waste that the processing industry sends to the controlled landfill is 10,437 tons [15]. The quantities of generated glass packaging waste disposed of in unregulated landfills were adopted according to the average MSW collection rates. Therefore, 86.2% is disposed of in controlled and sanitary landfills, while 13.8% is disposed of in illegal landfills [2]. Of the total amount of glass packaging waste generated, about 30% is collected by informal collectors [16].

It is estimated that about 60% of glass packaging waste collected by the public utility company is disposed of in controlled landfills. During 2019, out of the total amount of generated waste, 500,897 t of the generated waste was disposed of at sanitary landfills [2]. That amount represents 21% of total generated municipal solid waste, so the same percentage was adopted to determine the amount of waste sent to sanitary landfills collected by public utility companies. The specific target for recycling glass packaging waste for 2019 was 43%, so the stated coefficient was adopted for the amount of waste that undergoes the process of secondary separation [13].

Based on analyzing collected and assumed data, calculation of glass packaging waste as possible, and interpretation of the results.

It is possible to find much-developed software on the market that are used in the analysis of material flows. The use of appropriate software for the formation of MFA models has various advantages, the most important of which are:

- possibility of graphic modelling with automatic translation into a mathematical model,
- creating a database of collected data, including source documentation,
- calculation of unknown flows and stocks,
- interpretation of the obtained results using SANKEY diagrams and others.

To simulate the flow of glass packaging waste in the Republic of Serbia, software STAN 2.6 was used in this paper. STAN (subSTance flow Analysis) is freely available software (www.stan2web.net) that helps to perform analysis of material flows following the Austrian standard ÖNORM S 2096 [17], which relates to the application of MFA in the field of waste management. After creating a graphical model with predefined elements (processes, flows, system boundaries, text fields), it is possible to enter or import data using STAN software, after which software calculates unknown quantities of material flows according to a predefined mass balance algorithm [17].

RESULTS AND DISCUSSION

Based on the analysis conducted in the STAN software, the amount of imported raw materials for obtaining glass packaging products is estimated at 159,027 tons, while the amount of exports of products in glass packaging is 34,848 tons. The second phase of the model formed in the STAN software includes waste primary glass packaging from households and small businesses collected and transported by the public utility company, which amounts to 44,904 tons per year, while 11,026 tons are disposed of in uncontrolled (illegal) landfills. Of the total amount of mixed waste collected by the public utility company, 43% is used for secondary separation - 19,309 tons. 3,774 tons of secondary separated fractions are recycled. 21% of total input glass packaging waste in the process of collection and transport of MSW by the public utility company is disposed of in sanitary landfills, i.e. 9,430 tons per year and the remaining amount of 16,165 tons is disposed of in controlled landfills. 30% of the total amount of glass packaging waste generated in households and small business is informally collected, representing 23,970 tons per year, from where the same amount passes into the recycling process. From the secondary separation process, 21% of packaging residues are disposed of in the sanitary landfill, which is 4,055 tons per year, and 11,480 tons in the controlled landfill. In the last phase of the model, the amount of waste deposed in controlled landfills is 38,082 tons per year, while 13,485 tons are disposed of in sanitary landfills. The MFA model of glass packaging waste in the Republic of Serbia for 2019 is shown in Figure 1.

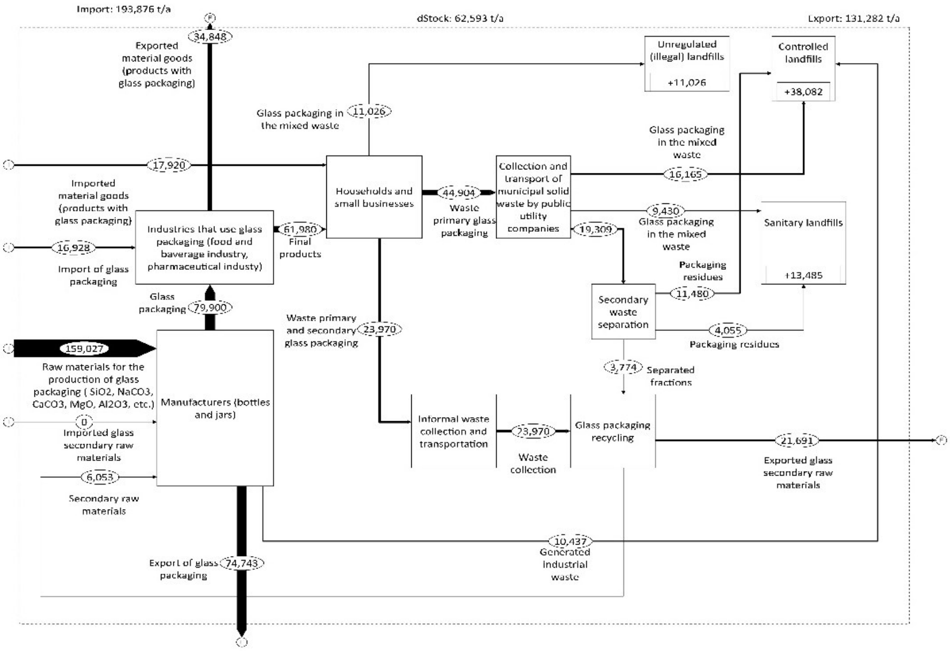

Figure 1 Material flow analysis of glass packaging waste in the Republic of Serbia

The model results are interpreted using diagrams created according to the Sankey principle, where the width of the arrows is proportional to the flow rate.

Based on the above data, which is imported in STAN 2.6, it is concluded that the largest share of glass packaging is disposed of in landfills in Serbia. In order to solve this problem, it is necessary to increase the reuse and recycling of glass. Glass is a material in which products for human consumption can be stored most safely, it can be completely recycled, and the reuse process saves a significant amount of energy and natural resources, reduces disposal costs and saves landfill space. Organized collection for recycling and reuse of glass can be the only answer to the situation shown by created scenario. Currently, glass recycling in Serbia is unprofitable, which is explained through the price of one kilogram of waste packaging glass from 0.5 to 2.2 Serbian dinars [18], transportation costs are high, and there are insufficient registered recyclers.

CONCLUSION

Since glass was introduced into mass production, and with the exponential growth of its consumption until today, there have been significant problems related to glass packaging waste. The negative consequences caused by glass waste mainly occur due to the long-term decomposition of its components in a natural way. Most of the problems are caused by single-use glass packaging, which has a short lifecycle and it is disposed of immediately after the use phase.

In the recent past, Serbia has witnessed substantial growth in glass packaging consumption and increased glass waste production. So, the Republic of Serbia, as a candidate for EU membership, has to ensure that all packaging on the market will be reusable or recyclable in an economically viable way by 2030 [19] because for the Republic of Serbia, it is necessary to harmonize its legislation with European, which includes the adoption of regulations on waste reduction, utilization, reuse, treatment and disposal of waste in a way which is safe for the human environment.

To analyze the current situation of glass packaging waste management in the Republic of Serbia, the MFA model was formed. An adequately defined MFA model characterizes input, output, and stocks following a system's controlled material balance. The system analyzed in this paper is created from 10 processes, and 20 material flows that are created in the software STAN 2.6. Based on the analysis of the flows of glass packaging, obtained data shows that the most considerable amount of glass packaging waste is currently dumped or disposed of in some form of a landfill – 62,593 tons per year. This amount needs to be reduced as well as the number of raw materials for the production of glass packaging such as SiO_2, $NaCO_3$, $CaCO_3$, MgO, Al_2O_3, etc., for which it is determined that their mass approximates 159,027 tons.

Based on the conducted MFA of glass packaging materials in the Republic of Serbia, in order to improve the complete system, it can be proposed:

- financial investment in domestic glass factories, state assistance to meet the capacity of the factories themselves,
- increase in the number of unique containers and bins for the collection of glass packaging, thereby increasing the citizens awareness about the benefits of recycling as well as reducing the disposal of glass waste in unregulated landfills,
- introduction of separate collection of packaging waste and its use to obtain new raw materials,
- reduction of the imported raw materials for glass products, encourage national recycling,
- investment in better sorting infrastructure,
- definition by law for the working conditions and obligation of authorized collectors and recyclers.

The created MFA model shows that in the Republic of Serbia, it is necessary to decrease the amount of used raw materials used for the glass packaging production process as well as a share of glass packaging waste disposal and increase the share of recycling glass packaging through a new system of technical, organizational and economic arrangements for carrying out stated requirements.

ACKNOWLEDGEMENT

This research has been supported by the Ministry of Education, Science and Technological Development, Republic of Serbia (Project III 42013).

REFERENCES

1. Grand View Research. (2020) Glass Manufacturing Market Size, Share, Growth, Trends, Consumption, Production, Segment Forecasts, Regional Outlook 2020 – 2027: https://www.grandviewresearch.com/industry/specialty-glass-ceramic-and-fiber (14th January 2021).
2. Environmental Protection Agency of the Republic of Serbia. (2020) Waste management report for the period 2011 – 2019 [in Serbian language]. Environmental Protection Agency, Ministry of Environmental Protection, Belgrade, Republic of Serbia.
3. Environmental Protection Agency of the Republic of Serbia. (2020) Report on the state of the environment in the Republic of Serbia – 2019 [in Serbian language]. Environmental Protection Agency, Ministry of Environmental Protection, Belgrade, Republic of Serbia.
4. Kaza, S., Yao, L., Bhada-Tata, P., Van Woerden, F. (2018) What a Waste 2.0: A Global Snapshot of Solid Waste Management to 2050. Urban Development Series. Washington, DC: World Bank. DOI:10.1596/978-1-4648 -1329-0. License: Creative Commons Attribution CC BY 3.0 IGO.
5. Environmental Protection Agency of the Republic of Serbia. (2012) Package and packaging waste management report, 2011 [in Serbian language]. Environmental Protection Agency, Ministry of Environmental Protection, Belgrade, Republic of Serbia.
6. Gallucci, T., Lagioia, G., Piccinno, P., Lacalamita, A., Pontrandolfo, A., Paiano, A. (2020) Environmental performance scenarios in the production of hollow glass containers for food packaging: an LCA approach. Int J Life Cycle Assess (2020). https://doi.org/10.1007/s11367-020-01797-7.
7. Energy portal. (2020) Waste glass imagined in a completely different way: https://www.energetskiportal.rs/otpadno-staklo-u-sasvim-drugacijem-svetlu/ [in Serbian language] (16th January 2021).
8. Mutha, N. H., Patel, M., Premnath, V. (2006) Plastics materials flow analysis for India. Resources, Conservation and Recycling, 47 (3), 222-244.
9. Neškovic-Markić, D. (2016) Modeling and optimization of municipal solid waste management by using material flow analysis and life cycle assessment - PhD Thesis [in Serbian language]. University Educons – Sremska Kamenica, Republic of Serbia, 165.

10. Steubing, B., Böni, H., Schluep, M., Silva, U., Ludwig, C. (2010) Assessing computer waste generation in Chile using material flow analysis. Waste Management, 30 (3), 473-482.
11. Brunner, P.H., Rechberger, H. (2003) Practical Handbook of Material Flow Analysis. Lewis Publishers, Boca Raton, FL, USA. pp. 35-68.
12. Regional Activity Centre for Sustainable Consumption and Production - SCP/RAC. (2019) Priority areas of intervention to curb marine litter from food and beverage plastic packaging in Albania, Bosnia and Herzegovina, and Montenegro: Phase 1 Findings - Executive Summary. Barcelona, Catalunya, Spain, 52.
13. Environmental Protection Agency of the Republic of Serbia. (2020) Package and packaging waste management report in 2019 [in Serbian language]. Environmental Protection Agency, Ministry of Environmental Protection, Belgrade, Republic of Serbia.
14. Glass Alliance Europe. (2020) Statistical Report 2019-2020. Brussels, Belgium, 15.
15. Statistical Office of the Republic of Serbia. (2020). Generated and treated waste, 2019 [in Serbian language]. Department of Environmental Statistics and Accounts, Belgrade, Serbia. ISSN 0353-9555.
16. Serbian factory for recycling “Grejač”. (2020) Glass Imports and Exports: https://sfr.rs/staklice-i-uvozimo-i-izvozimo/, [in Serbian language] (1st February 2021).
17. Cenčić, O. (2017) STAN Software for substance flow analysis: Version 2.6 – User manual. Tu Wien, Vienna, Austria.
18. Pubilc Utility Company Čistoća Sombo. (2021) Packaging glass: http://www.cistoca.co.rs/aktuelnosti/385/galerija-23-sekretari-mz-u-poseti-jkp-.html, [in Serbian language] (16th February 2021).
19. European Commission. (2020) A new Circular Economy Action Plan: For a cleaner and more competitive Europe. COM (2020) 98 final. Brussels, Belgium.

XIV International Mineral Processing
and Recycling Conference
Belgrade, Serbia, 12-14 May 2021

IMPACT OF THE CIRCULAR ECONOMY AND EXTENDED PRODUCER RESPONSIBILITY (EPR) ON REDUCTION OF PACKAGING WASTE

Višnja Mihajlović[1#], Jovanka Milićević[2]
[1] University of Novi Sad, Technical Faculty "Mihajlo Pupin" Zrenjanin, Serbia
[2] Cenex, Zemun, Serbia

ABSTRACT – In 2018 European Union adopted a circular economy package, and the latest documents adopted in 2020 are Circular Economy Action plan and Green Deal. Circular economy legal framework aims to move society and industry towards circular economy, from production and consumption, to waste management and the market for secondary raw materials. In October 2020 Serbia adopted Roadmap for Circular Economy to encourage manufacturing sector and industry to use circular business models, by finding innovative and sustainable solutions for the market. Due the great importance of circular economy for future development of the market, aim of this paper is to analyze the impact of circular economy and EPR on reduction of packaging waste in Serbia.

Keywords: Circular Economy, Packaging Waste, Waste Management.

INTRODUCTION

The amount of materials used for packaging is growing continuously and in 2017 packaging waste in Europe reached a record – 173 kg per inhabitant, the highest level ever [1].

In latest Circular Economy Action plan and Green Deal to increase uptake of recycled plastics and contribute to the more sustainable use of plastics, the Commission propose mandatory requirements for recycled content and waste reduction measures for key products such as packaging, construction materials and vehicles [2]. In order to ensure that all packaging on the EU market is reusable or recyclable in an economically viable way by 2030, the Commission will consider new measures, with a focus on reducing (over)packaging and packaging waste, driving design for re-use and recyclability of packaging and considering reducing the complexity of packaging materials.

The development of Extended Producer Responsibility (EPR) in Europe has contributed to improvements in waste prevention, reuse and recycling, and in 2018, recovery rate in EU-27 was 80.9% and recycling rate was 66.3% [1]. EPR may be considered as a policy approach that can contribute to increasing plastics circularity [3]. The transition to a circular economy offers potential to pursue global plastic waste objectives and to identify the policies which can best contribute to this aim [4].

In Serbia there is a legal framework regulating packaging waste management and EPR [5]. In addition, in 2020 Serbia has adopted Circular Economy Road Map, as an initial document towards establishment of circular economy business model in Serbia [6]. The

---

[#] corresponding author: visnjamihajlovic@uns.ac.rs document is guidance for transition to a model of circular economy focusing, apart from the profit, to the protection of the environment and preservation of resources.

According to Serbian National Environmental Protection Agency (SEPA) in 2019 Serbia met the recycling goals [7]. However, there is gradually increase in reuse of packaging waste compared to packaging waste put in the market from 2011 to 2019, but it can be further increased and developed.

Unfortunately, Serbia is also exporting waste which can be processed (used) in Serbia, namely paper and metals [7]. In addition, Serbia is importing the waste from the country where waste is previously exported.

Circular economy will be one the main driver for reduction and reuse of packaging waste, and use of secondary raw materials. EPR is well established mechanism which can support the goals set by circular economy, in terms of reuse, reduce of packaging waste, and use of secondary raw materials.

Aim of this paper is to analyze the impact of circular economy and EPR on reduction of packaging waste in Serbia. The impact will be analyzed on example of company which is s an importer and distributor of consumer goods at Serbian market.

MATERIALS AND METHODS

In the Republic of Serbia, the area of waste management is regulated by the Law on Waste Management [5], the Law on Packaging and Packaging Waste [8] and bylaws such as ordinances and regulations. The guideline for achieving the goals of the circular economy is the Regulation on the establishment of a plan for the reduction of packaging waste, which is adopted for a period of 5 years. The current Regulation is the third published. Figure 1 shows the objectives under the regulations from the first one that was valid for the period 2010-2014, 2015-2019 and from 2020 – 2024.

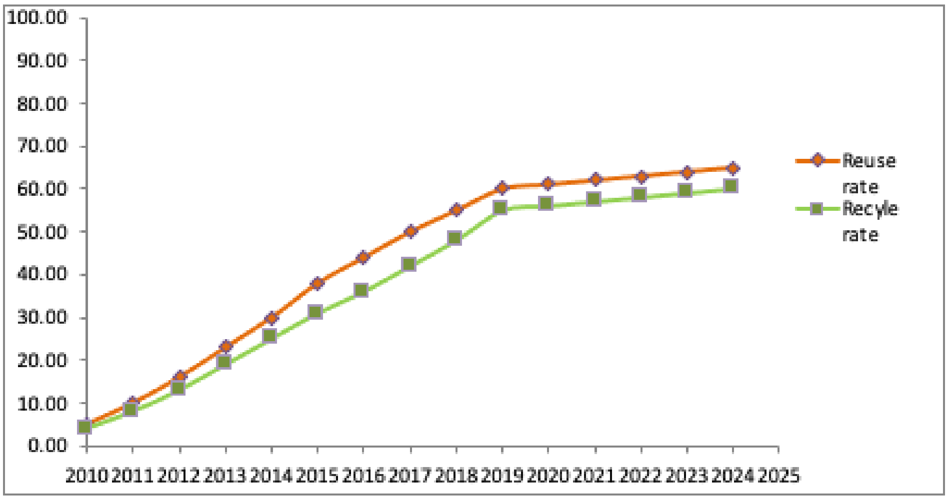

Figure 1 Development of national and specific goals for the period 2010 - 2024 by years

In order to achieve all these goals, it is necessary that the applicable laws and by-laws are followed/forced and implemented in practice. This implies certain investments in the system of organized sorting, collection, transport and handing over of such waste for recycling.

The analysis of the impact of circular economy and EPR on reduction of packaging waste in Serbia, was performed on the company which operates throughout Serbia, is an importer of food and other consumer goods e.g., soft drinks, bottled water and which has distribution centers in major cities in Serbia, Belgrade, Novi Sad, Cacak and Nis.

RESULTS AND DISCUSSION

Through the import of its product range, the company placed a total of 3,670 ton of packaging waste on the market of the Republic of Serbia in the period from 2016-2020 and handed over 530 t of packaging waste for recycling in the same period. Table 1 shows the quantities of packaging that the company placed on the market of the Republic of Serbia in the period 2016-2020 by year through the import of its product range, and a diagram of the growth of sales and recycling for the same period.

Table 1 Quantities of packaging placed on the market of the Republic of Serbia from 2016-2020

	Placed on the market (ton)	***Collected and recycled (ton)***	***Recycling rate***
2016	165.00	65.00	39.39
2017	625.00	102.00	16.32
2018	1,220.00	108.00	8.85
2019	900.00	103.00	11.44
2020	760.00	152.00	20.00
Total	***3,670.00***	***530.00***	***14.44***

In Table 1, it can be seen that the company has significantly contributed to reducing the disposal of generated packaging waste in municipal waste by investing in equipment and training of employees to manipulate it (unpacking, repacking and preparation for further transport and distribution) disposed of in appropriate containers such as mesh containers, jumbo bags, abroll and press containers. At the location where most of the waste is generated, the installation of a baling press for waste packaging cardboard and foil has proven to be a sustainable solution, which achieves lower costs of transporting baled waste, easier handling on site and safety of employees in waste preparation.

Considering that an integrated packaging and packaging waste management system has been established in Serbia, in which one of the basic principles is "polluter pays", the company must pay a fee for placement to the operator or to the budget of the Republic of Serbia for each kilogram of packaging waste. Part of the money that company pays as compensation, is returned through the sale of packaging waste from its distribution centers. For every kilogram of cardboard and foil that he sells to the operator for which he has a license for storage and treatment of non-hazardous waste, our company earns and thus returns part of the money invested in the system to its budget.

Following the legal obligations, the principles of circular economy, the company has about 15% recycling rate, if only cardboard and foil are taking into account, for the collection of generated waste. If one see the structure of packaging waste placed on the market and handed over for recycling generated waste by fractions, it is certain that the results would be different and for that it is necessary to do a detailed analysis. We have followed cardboard and foil here as the most common types of packaging waste generated at the location of the company

CONCLUSION

Recycling rate of the company is very low if we take into account that this company is very responsible in managing waste in its organization. It is certain that the average is far below 15% and that increased subsidies to polluters, collectors and recyclers could increase the circular economy. For example, the fund which collect market placement fees should be further invested in the collection and recycling sector. It would also be extremely important to encourage domestic collectors / recyclers, public utility companies as well as individual / informal collectors so that less packaging waste as possible ends up in landfills and so that after its life the packaging has its value as a raw material and is valorized through production of the same or similar materials.

REFERENCES

1. Eurostat (2020) Waste Statistics explained. Packaging waste statistics Available at https://ec.europa.eu/eurostat/statistics-explained/index.php/Packaging_waste_statistics.
2. EC (2020) European Commission, COMMUNICATION FROM THE COMMISSION TO THE EUROPEAN PARLIAMENT, THE COUNCIL, THE EUROPEAN ECONOMIC AND SOCIAL COMMITTEE AND THE COMMITTEE OF THE REGIONS. A new Circular Economy Action Plan, COM (2020) 98 final, Brussel.
3. Bourguignon, D. (2017) Plastics in a circular economy -Opportunities and challenges. European Parliamentary Research Service, Brussels.
4. van den Oever, M., Molenveld, K., van der Zee, M. and Bos, H. L. (2017) Bio-based and biodegradable plastics -Facts and Figures: Focus on food packaging in the Netherlands. Wageningen Food & Biobased Research, The Netherlands.
5. OG (2019) Law on Waste Management., Republic of Serbia, Official Gazette 36/2009, 88/2010, 14/2016 and 95/2018.
6. UNPD (2020) A Roadmap for circular economy in Serbia.
7. SEPA, Report on waste management in Serbia from 2011-2019. Serbian Environmental Protection Agency.
8. OG (2009) Law on Package and Packaging Waste, Republic of Serbia, Official Gazette 36/2009 and 95/2018.

REACTIVITY ASSESSMENT OF SEASONAL COMPOST OF MUNICIPAL SOLID WASTES (MSW) AND THEIR CO-COMBUSTION WITH LIGNITE VIA ACTIVATION ENERGY

Agapi Vasileiadou[1,2#], Stamatis Zoras[1], Andreas Iordanidis[2]
[1] Democritus University of Thrace, Faculty of Engineering, Department of Environmental Engineering, Xanthi, Greece
[2] University of Western Macedonia, Department of Mineral Resources Engineering, Kozani, Greece

ABSTRACT – The reactivity of compost like-outputs of MSW was evaluated in this study in order to assess their combustibility for potential energy recovery. Four seasonal MSW compost (fall, summer, spring, winter) samples, and a lignite sample were collected from northern Greece. Calorific Value determination, Thermogravimetric and Derivative Thermogravimetric Analysis (TG/DTG) were performed. Kinetic Modelling of TG/DTG data were performed in order to determine the Activation Energy and Pre-exponential Factor of analyzed samples and their blends with lignite. All blends with lignite reveal lower activation energy than raw samples due to synergy effect in blends. Compost could be a promising alternative biofuel.

Keywords: Activation Energy, Compost of MSW, Lignite, Reactivity, Thermogravimetric Analysis.

INTRODUCTION

Due to post-lignite era, energy supply and security in Greece constitutes a crucial problem. From the other hand, the management of Municipal Solid Waste (MSW) is mainly based on landfilling, composting and incineration. The annual rate of production of MSW is more than 2 billion tonnes and will increase to 4 billion in the next years [1]. MSW consist mainly of organic fraction (approx. 50%) which could be used as an alternative energy source [2].

Several studies were performed about co-combustion of biomass and fossil fuels yielding promising results for alternative mixed fuels with reducing the cost of the power production [3].

There are different thermochemical approaches in order to study the thermal decomposition and kinetic parameters of a fuel, which are important in order to describe different thermal phenomena and properties of a fuel [4]. Thermal analysis provides the fingerprint of a fuel [5].

The aim of this work is to study the combustion and the co-combustion (50 wt.%) of the seasonal compost (CLO) of the MSW with lignite (LIGA) via thermogravimetric analysis (TG/DTG). Kinetic parameters like Activation Energy (E) and pre-exponential factor (A), were determined.

[#] corresponding author: agvasileiadou@gmail.com

MATERIALS AND METHODS

MSW Compost were collected from Greece, from four different seasons of a year (Fall-CLOF, Spring-CLOSP, Winter-CLOW and summer-CLOSM). All samples were air-dried for 2 weeks and then, dried at an oven (80 °C) for 24 hours. Furthermore, the samples were grounded to grain size less than 1 mm. Thermal (Thermogravimetric and derivative thermogravimetric) analysis (TG/DTG) was performed using TGA 701 (leco). About 1000 mg of every sample was heated from 25 °C to 1000 °C, under air atmosphere with a flow rate of 3.5 l/min and heating rate 10 °C/min [6].

Activation Energy (E) and pre-exponential factor (A) were determined using kinetic modelling analysis. Data from Thermogravimetric analysis and Arrhenius equation [7](Eq. 1) were used for this reason. The combustion kinetics can be described by first order kinetics. Kinetic modelling was applied for the stage after dehydration and until there is the peak temperature (T_{max}) at which there is the maximum rate of weight loss (R_{max}).

$$K = A \cdot e^{\left(-\frac{E}{RT}\right)} \tag{1}$$

where K is the reaction rate, A is the pre-exponential factor (1/s), R is the constant 8.314 J/Kmol), T is the absolute temperature (K) and K=-(dW/dt) · W where dW/dt is the instantaneous rate of weight loss (%/min) and W is the unburn combustible.

RESULTS AND DISCUSSION

The total weight loss of the analyzed samples is presented in Figure 1. Compost of summer, raw sample, revealed the highest total weight loss of all raw samples (approx. 80 wt.%) whilst the compost raw sample of spring revealed the lowest value (approx. 60 wt.%) of all raw samples. In blends with lignite, the compost of spring revealed the lowest value (<65 wt.%) of blends with lignite, while the compost of summer revealed a value more than 70 wt.%. Samples with high total weight loss, reveal low ash content and in consequence lower ash related problems (e.g. slagging, fouling, agglomeration etc.).

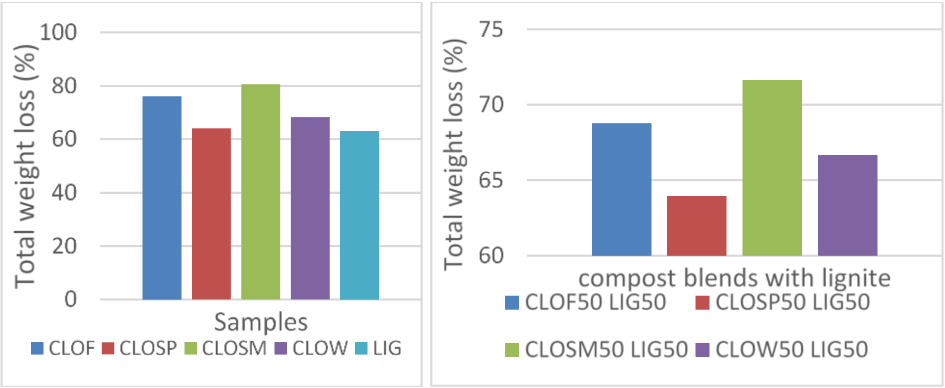

a) b)

Figure 1 Total weight loss of the analyzed samples, in wt.%.
a) raw samples, **b)** blends with lignite

The results of the maximum rate of weight loss R_{max} (%/min) and the maximum temperature T_{max} (^oC) at which there is the maximum rate of weight loss, of the analyzed samples and blends with lignite, are illustrated in Figure 2.

In raw materials, the highest value of maximum temperature is exhibited by the compost of spring with a low maximum rate of weight loss (304 ^oC, 3.2%/min) whilst the lowest maximum temperature (277 ^oC, 4.7%/min) leveled in compost of summer having a high rate of weight loss.

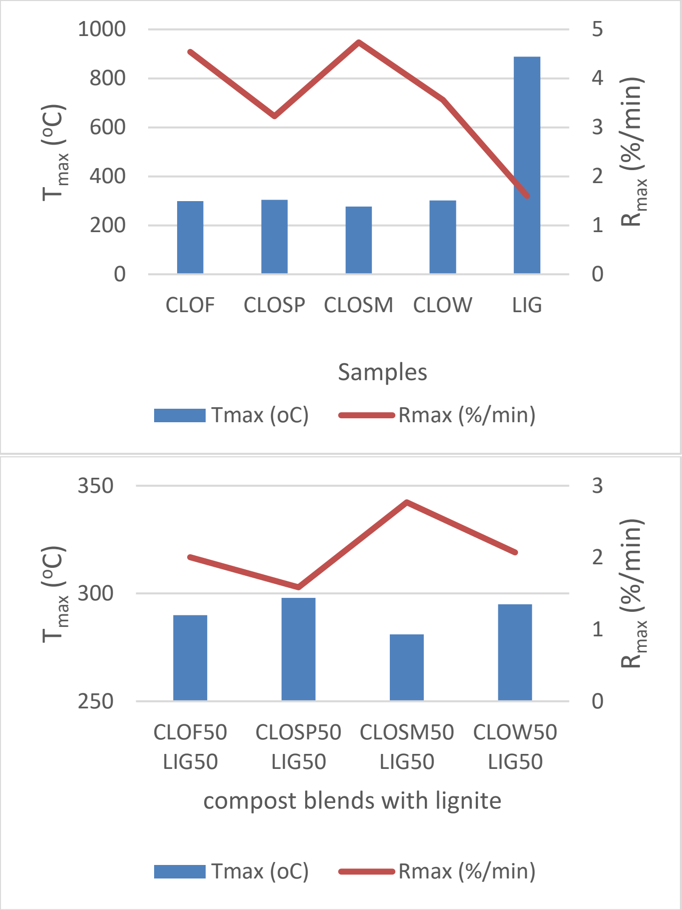

Figure 2 Maximum temperature and maximum rate of weight loss of analyzed samples and blends with lignite

TG and DTG profiles of raw seasonal MSW compost and their blends with lignite are illustrated in Figure 3. TG/DTG profiles are a precise mapping of thermal decomposition of a fuel. The first stage (<200 ^oC) refers to moisture release. Then, occurs the release of volatiles and then the combustion of fixed carbon. Raw samples, in DTG curves, reveal one exothermic peak while blends reveal two. Lignite revealed slow weight loss compared to MSW compost samples. CLO samples showed high weight loss between approx. 200 °C to 390 °C whereas lignite weight loss is between 690 °C to 960 °C. The slow weight loss in lignite sample maybe is related to low volatiles and high ash content [8]. This is why the decomposition process in lignite occurs in higher temperature. This results is in accordance with [9].

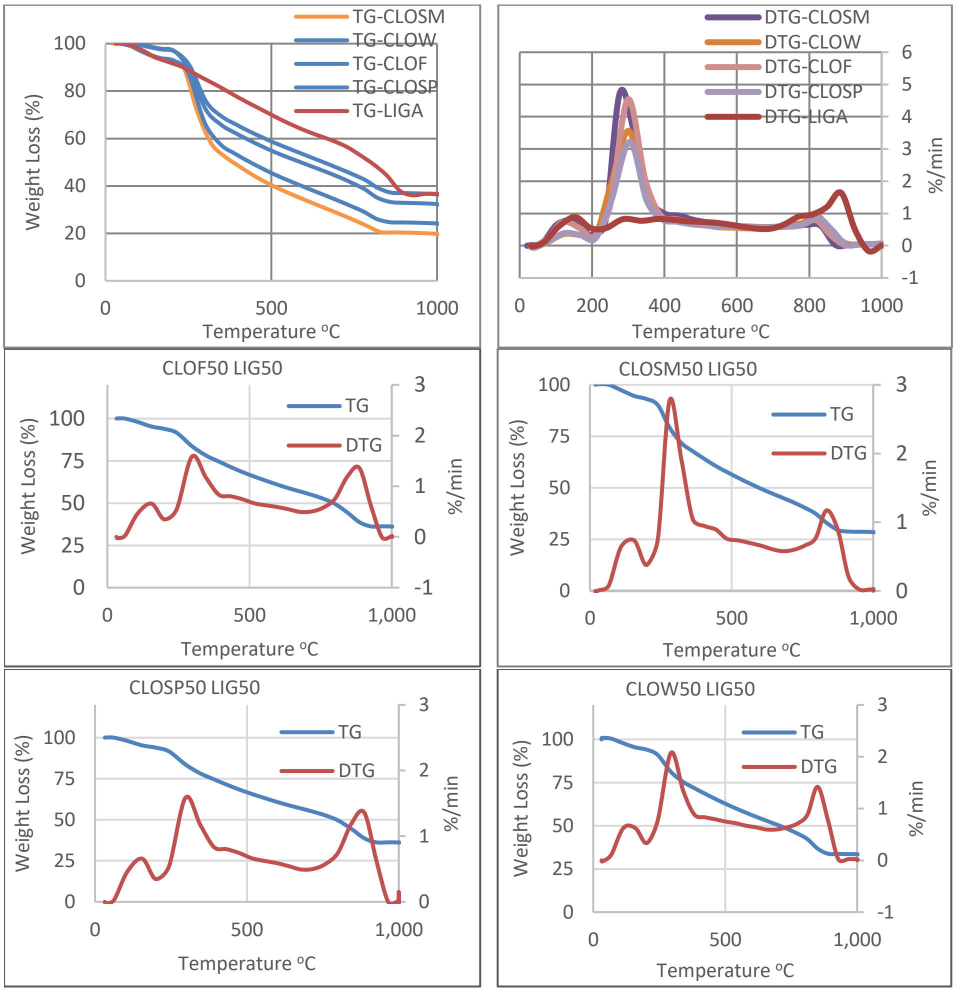

Figure 3 TG/DTG graphs of the raw analyzed samples and their blends with lignite

Activation energy and pre-exponential factor are presented in Figure 4. Compost CLOSM reveal the highest activation energy of all samples and blends with lignite. Compost blends with lignite (CLOF50 LIG50 and CLOSP50 LIG50) reveal the lowest activation energy of all analyzed samples. Low activation energy of blends arises from synergy effect. High values of E mean a less reactive solid (the reaction will be slower) [5]. Pre-exponential factor of the analyzed samples varied from 94000 1/s (CLOSM) to 0.001 1/s (LIGA). Pre-exponential factor is about the frequency of collision between reactant molecules.

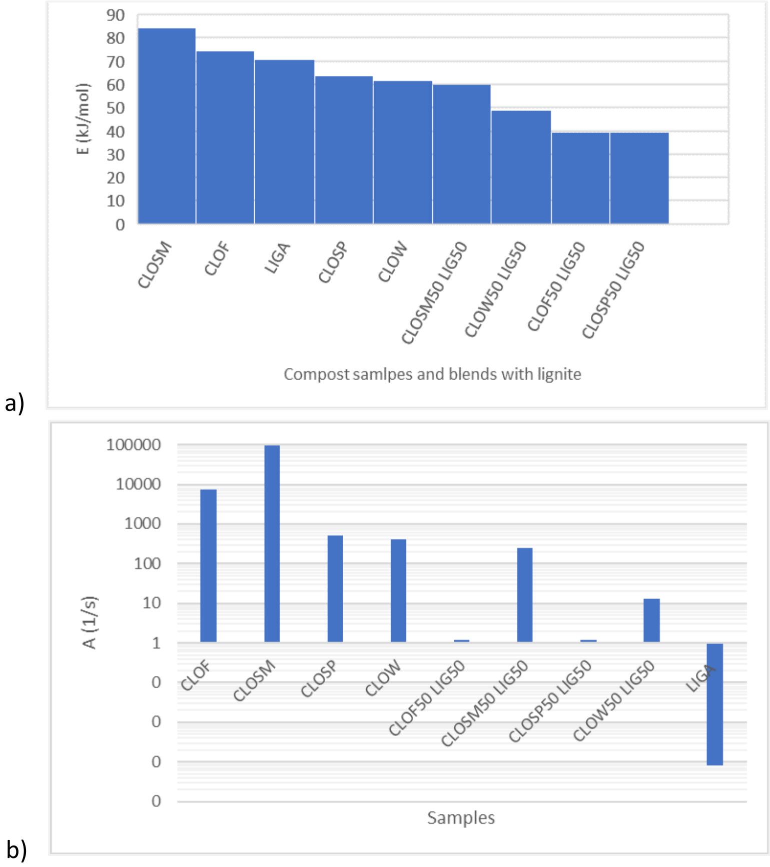

Figure 4 a) Activation energy and, **b)** Pre-exponential factor of the analyzed samples and blends

CONCLUSION

In this work, combustion characteristics and kinetic parameters of four seasonal MSW compost and their (four) blends with lignite (50 wt.%) were investigated using thermogravimetric analysis at heating rate of 10 °C/min. This study suggests that combustion of MSW compost and their co-combustion with lignite could be a promising alternative energy source. Furthermore, thermogravimetric data could be used in order to predict kinetic characteristics of a sustainable fuels (MSW compost, biomass residues, etc.) to meet the challenges of energy and waste management in Greece and worldwide.

ACKNOWLEDGEMENT

This research is co-financed by Greece and the European Union (European Social Fund- ESF) through the Operational Programme «Human Resources Development. Education and Lifelong Learning» in the context of the project "Strengthening Human Resources Research Potential via Doctorate Research" (MIS-5000432), implemented by the State Scholarships Foundation (IKY).

REFERENCES

1. Lu, J.S., Chang, Y., Poon, C.S., Lee, D.J. (2020) Slow pyrolysis of municipal solid waste (MSW): A review. Bioresource Technology, 312, 123615.
2. Katakojwala, R., Kopperi, H., Kumar, S., Venkata, M.S. (2020) Hydrothermal liquefaction of biogenic municipal solid waste under reduced H2 atmosphere in biorefinery format, Bioresource Technology, 310, 123369.
3. Bhuiyan, A.A., Blicblau, A.S., Islam, A. K.M. S., Naser, J. (2018) A review on thermo-chemical characteristics of coal/biomass co-firing in industrial furnace, Journal of the Energy Institute, 91 (1) 1-18.
4. Smith, S.E., Neavel, R.C., Hippo, E.J., Miller, R.N. (1981) DTGA combustion of coals in the Exxon coal library. Fuel, 60 (6), 458-62.
5. Biagini, E., Fantei, A., Tognotti, L. (2008) Effect of the heating rate on the devolatilization of biomass residues. Thermochimica Acta, 472 (1), 55-63.
6. Iordanidis, A., Asvesta, A., Vasileiadou, A. (2018) Combustion behaviour of different types of solid wastes and their blends with lignite. Thermal Science, 22 (2), 1077-88.
7. Cumming, J.W. (1984) Reactivity assessment of coals via a weighted mean activation energy, Fuel, 63 (10), 1436-40.
8. Vasileiadou, A., Zoras, S., Dimoudi, A., Iordanidis, A., Evagelopoulos, V. (2020) Compost of Biodegradable Municipal Solid Waste as a Fuel in Lignite Co-combustion. Environmental Research, Engineering and Management, 76 (4), 60–7.
9. Azam, M., Jahromy, S.S., Raza, W., Jordan, C., Harasek, M., Winter, F. (2019) Comparison of the combustion characteristics and kinetic study of coal, municipal solid waste, and refuse-derived fuel: Model-fitting methods, Energy Science & Engineering, 7 (6), 2646-57.

XIV International Mineral Processing
and Recycling Conference
Belgrade, Serbia, 12-14 May 2021

COMPARISON OF WEEE RECYCLING PRACTICE IN ITALY AND SERBIA

Isidora Berežni[1], Bojan Batinić[1#], Nemanja Stanisavljević[1],
Francine Duarte Castro[2], Mentore Vaccari[2]
[1] University of Novi Sad, Faculty of Technical Sciences, Department of Environmental Engineering, Novi Sad, Serbia
[2] University of Brescia, Department of Civil, Environmental, Architectural Engineering and Mathematics, Brescia, Italy

ABSTRACT – Waste electrical and electronic equipment (WEEE) represent one of the fastest growing waste streams in Europe, whose content of hazardous substances as well as valuable materials put a focus on how it is handled. Disposal of this waste stream at landfills represent extremely dangerous activity due to its limited biodegradability of polymers, high metal losses and toxicity of certain part of electronic equipment. In terms of applied e-waste management practice, there is difference between countries in Europe. This paper presents the overview of current state of the electrical and electronic waste management system in two countries, Italy and Serbia, considering legal regulations, collection schemes and existing treatment technologies. The focus of the paper is on comparison of WEEE pre-treatment processes in the plants in Niš and Verona with the insight of mass flows of different materials, using material flow analysis (MFA). Finally, based on comparison and analysis, recommendations for improving the current waste management system in the Republic of Serbia are addressed.

Key words: WEEE, Pre-treatment, Recycling, MFA, Italy, Serbia.

INTRODUCTION

Rapid advances in material science, manufacturing processes and electronic product have created a global marketplace with the rapid spread of technology to consumers. Electrical and electronic equipment (EEE) has become necessary part of modern societies and is improving living standards, but its production combined with their affordability has created challenges in e-waste management since massive consumption creates an increasing amount of this waste stream. The challenges that arise with a managing of e-waste are not only the consequences of the growing amounts, but also its complexity. While hazardous substances found in some electronic products require specific treatment, in order to avoid environmental damage, precious and other valuable materials can be used in the production of new products after the processing.

According to Global e-waste monitor, the world has generated 53.6 Mt of e-waste (an average of 7.3 kg per capita) in 2019. Since 2014. the generation of e-waste grew by 9.2 Mt and it is projected to grow to 74.7 Mt until the 2030. which is almost double in 16 years. [1]

Observing the composition of e-waste, its disposal on the landfills presents extremely dangerous activity given the limited biodegradability of polymers, high metal losses and

---

[#] corresponding author: bojanbatinic@uns.ac.rs toxicity of certain parts of electronic equipment, such as batteries and other storage units. The European Union, through the Directives such as 2012/19/EU and RoHS 2002/95/EC, as well as extended producer responsibility (EPR), has emphasized the need to improve the system management of e-waste. However, number of challenges have arisen with the implementation of these regulations, such as problems in collection, waste categorization, sorting procedures, information management, etc. To solve these problems, the support of relevant institutions at the state level is needed, as well as new innovations in technology. The situation is not much different in countries outside the EU, such as Serbia, where similar challenges in waste management also occur, even more complex in some cases, due to the weaker economic development of the country itself and insufficient support for the system.

In this study, e-waste system management is analyzed in two country, from collection systems, legal regulations, existing treatment technologies to final disposition. Italy has been chosen as an example for a country that largely implements defined EU directives and has experience in WEEE management to follow and Serbia as an EU candidate aiming to adopt all WEEE Directive requirements. Therefore, comparing the situations in both countries and using the Italian expririence of organizing WEEE management, reccomedations for improving Serbian system can be made.

MATERIALS AND METHODS

Within this work, to present the current state of e-waste management system in both countries, the following aspects were analyzed via available literature research: legislation framework together with EU Directive goals in terms of e-waste; collection system and technologies and capacities for treatment. Focus of the paper was put on pre-treatment processes in the plants in Niš and Verona where material flow analysis (MFA) is used to model mass balance of products within the plants. MFA is tool consist of the flows of materials, stocks and processes, where balancing of the system is based on the law of mass conservation. Model assume the assesment of the overall mass of all inputs and outputs of the system, as well as the mass that remains stocked for the year for which the analysis is carried out. [2] Therefore, by comparing available data and current management situations, possible steps for improving the WEEE management system in Serbia is outlined.

Current state of WEEE system management in Italy

Through Law Decree 49/14 in Italy is implemented the WEEE Directive 2012/19/EU which regulated the management of electronic waste by promoting recycling, recovery and reuse and limiting the use of certain hazardous substances contained in electronic equipment. “Clearing house” model is adopted as national system, while producers are grouped into the so-called Collective system which is responsible for the entire e-waste management system. Stakeholders of this collective system cooperate with different operators and organizations (logistics centers, recycling centers, collection systems, etc.) to provide electronic waste management services in its entirety. The government monitors the operation of these systems through the Coordination Centre. [3] In this way, it is ensured that there are equal conditions for all the actors and that whole national territory is adequately served in order to achieve collection targets and fully implement the producer responsibility principles. Targets defined by Decree 49/14 are the same as the ones defined by European Directive 2012/19. (Table 1)

Table 1 Recovery/Reuse and recycling rates for WEEE categories defined by Directive 2012/19/EU

WEEE category	Recovery/Reuse and recycling rates (%)
1. Heat exchange equipment	85/80
2. Screens and monitors	80/70
3. Lamps	-/80
4. Big appliances	85/80
5. Small appliances	75/55
6. Small IT and telecommunication devices	75/55

The body responsible for monitoring the achievements of the targets in Italy is ISPRA (Higher Institute for Environmental Protection and Research). The owners of the facilities must communicate annually the data relating to the quantities of WEEE managed. Commerce chambers communicate the data relating to WEEE collected and ISPRA monitors the achievement of the targets and reports annually to the Ministry of the Environment and the protection of the territory and the sea (MATTM) the information acquired.

As regards to WEEE collection system, there are two channels; one that includes fixed collection points managed by local municipalities where citizens can bring e-waste for free and the other one which collects waste from customers through one-to-one or one-to-zero models and is carried out directly by EEE retailers. In Italian legislative five groups of WEEE are defined: R1 – cooling and freezing appliances; R2 – large appliances; R3 – TV and monitors; R4 – small household appliances; R5 – lighting equipment. To increase the disposal of end-of-life EEE by different end users, collection of WEEE is carried out via different types of waste recycling centers, i.e. sites: Designated collection facilities (DCF) open for all the citizens; Distributors collection sites (DCS) for “One for one” and “One for Zero” take back schemes; Large users (LU) registered by public or private entities; Individual collection sites (ICS) set up by producers through collective systems; Installers (INST) managed by the installers of lighting equipment (R5). The number of so-called “sites” in Italy in 2018 was 4883 and during this year, the total amount of WEEE collected was 310,610 tons. [4]

Current state of WEEE system management in Serbia

Serbia harmonized and adopted most of the requirements from WEEE Directive 2012/19 through national legislation, but with certain targets postponed regarding the legislation currently valid for EU member states, such as the target of 4 kg/capita of collected WEEE that need to be achieved until the end of 2019., while in EU countries collection this target was set up to 45% of EEE placed on the market in the previous three years starting from 2016. [5] Ministry of Environmental protection (MEP) and Serbian Environmental Protection Agency (SEPA) are the crucial institutions for monitoring and controlling the WEEE flows and collecting the required data. Beside those two, producers or importers of electrical and electronic products which became waste after use, waste owner, i.e., waste producers and operators who perform collection, transport and treatment of waste are the other acters in this system. The obligation for producers and importers of products that after use became special waste streams to keep daily records on the quantity and type of produced and imported products and in the form of annual reports submit it to SEPA are defined within The Law of Waste Management (Official Gazette of the RS, No 36/09, 88/10 and 14/16) and by-laws. [6]

The current collection system is based on the extended producer responsibility, where producers and importers of electronic and electrical equipment are obliged to pay a certain fee (depending on the type of product), for ensuring adequate management of e-waste. Recycling and other companies are then subsidised by the Ministry of Environmental Protection from 108 to 900 e-t of treated e-waste. Therefore, companies involved in recycling and treatment of e-waste also have the role of collectors. [7] There are four main operators in Serbia that carry out organized collection and recycling of electronic waste. According to recent estimates between 15 and 20 thousand tons of WEEE are recycled per year which represents 20% of the total amount of generated waste. This amount, at the same time, represents the total amount of e-waste collected. [8]

MFA and pre-treatment in Italy and Serbia

In pre-treatment plants, components that are manually extracted, such as batteries, cathode ray tubes and other, depending on existing technology are either sent to secondary treatment plants in the country or exported for further processing. Mechanical treatment consists of shredding, milling, magnetic and other types of separators, while refrigerator treatment plants have also a line for Freon separation.

In order to compare the situation with one in Serbia, a pre-treatment plant in Verona was chosen as a case study for Italy. Activities carried out in the facility complex include treatment lines: R1 – cooling and freezing appliances; R2 – large appliances; R3 – TV and monitors; R4 – small household appliances; R5 – lighting equipment; Battery and toner separation line; Separation lines by gridding, granulation, aeraulic and wet separation in order to concentrate the most used fractions into homogeneous and clearly defined classes. As a case study in Serbia, recycling company from Niš was selected as a leading operator for collection and treatment of e-waste in Serbia.

In terms of pre-treatment technology, the approach is similar in both plants, based primarily on the manual separation of valuable components, followed by the mechanical treatment of individual devices. The main percentage of collected and treated quantities of waste in both plants makes cooling devices, large and small household appliances and TVs with around 80% of total WEEE collected.

Datas about the inputs and outputs in the plants from the year of 2018. was taken in order to model the MFA, where main processes and e-waste flows are identified and quantified. Schemes of the processes are given further in Figures. Figure 1 present the MFA of e-waste treated in Serbian plant in 2018. and because of the lack of the data it was possible to present MFA only for the entire plant, but not for each process line, while Figures 2, 3, 4 and 5 present the materials flow analysis for each process line in Italian plant.

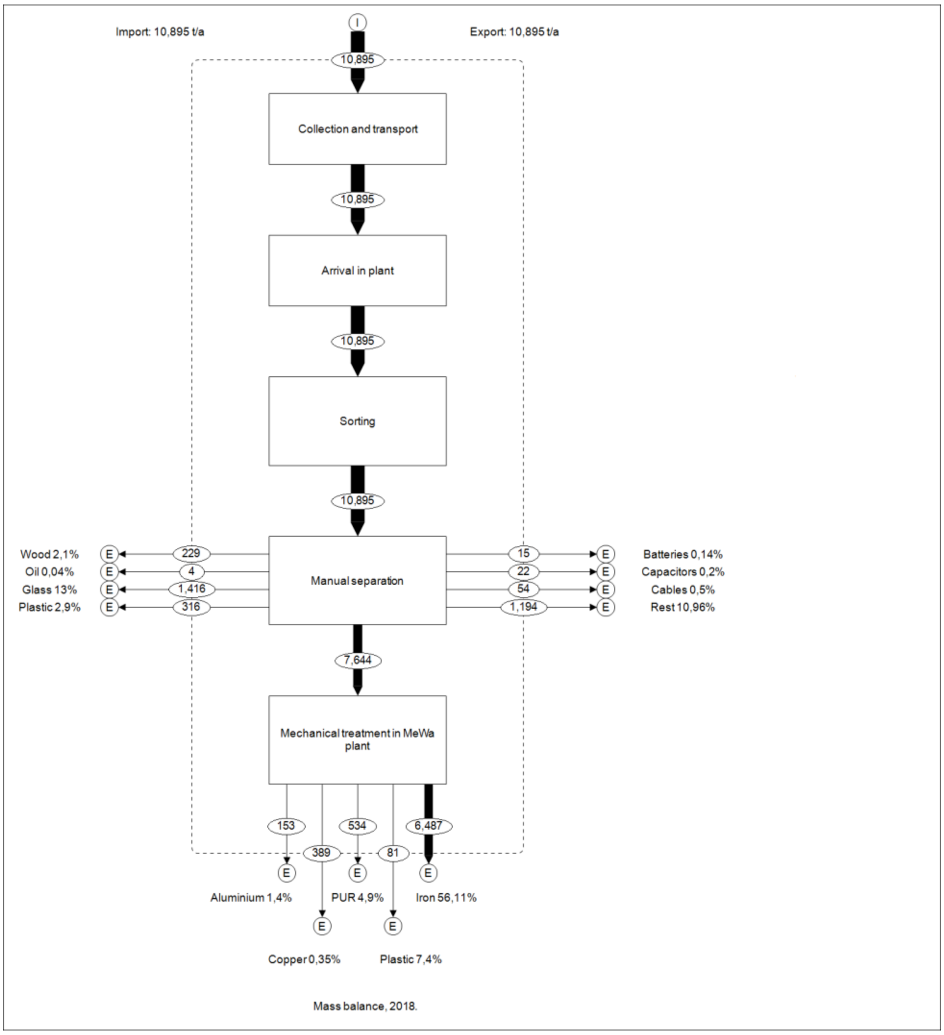

Figure 1 Mass balance of treated e-waste in Serbia plant, 2018

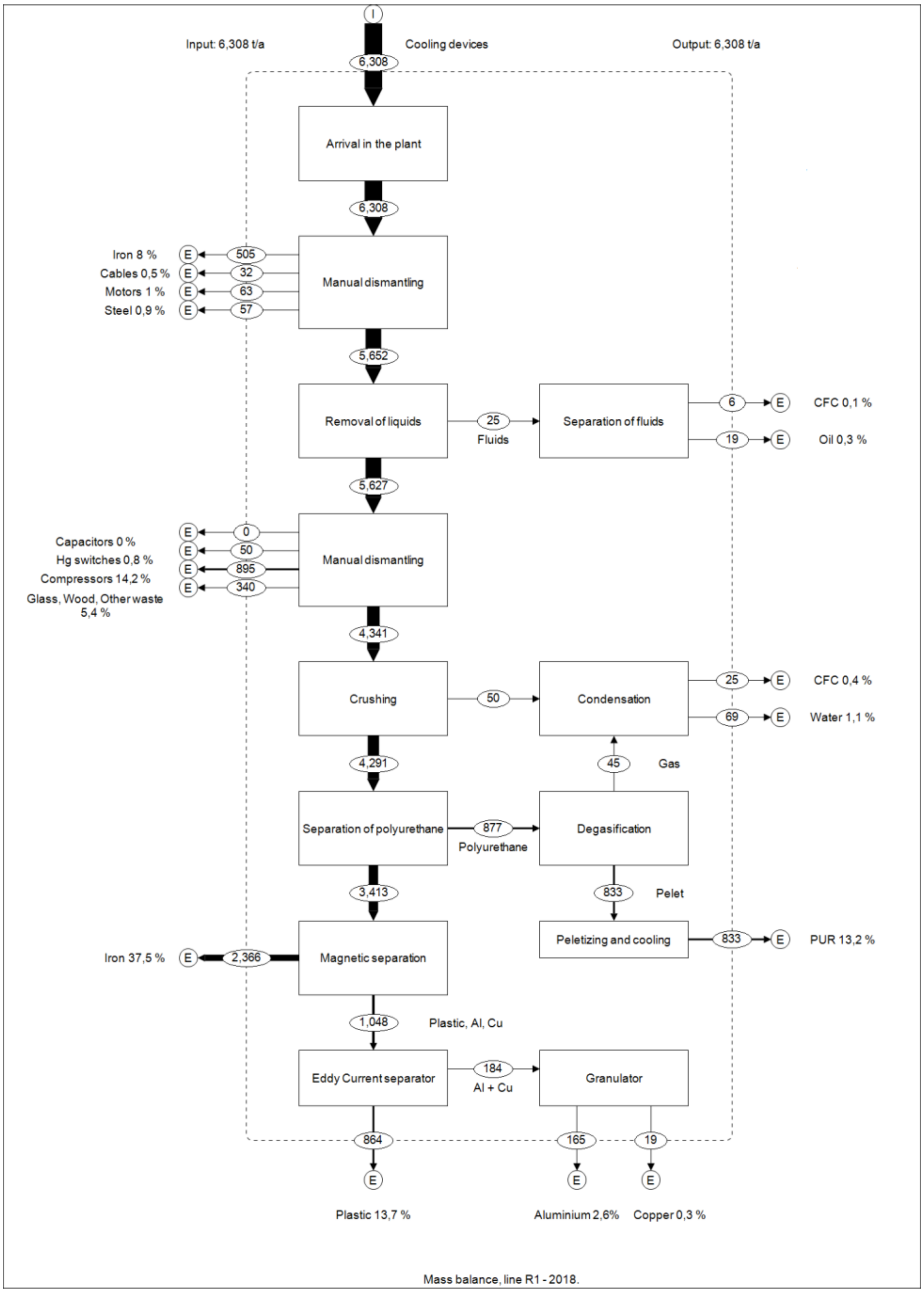

Figure 2 Mass balance of R1 category of e-waste in Italian plant, 2018

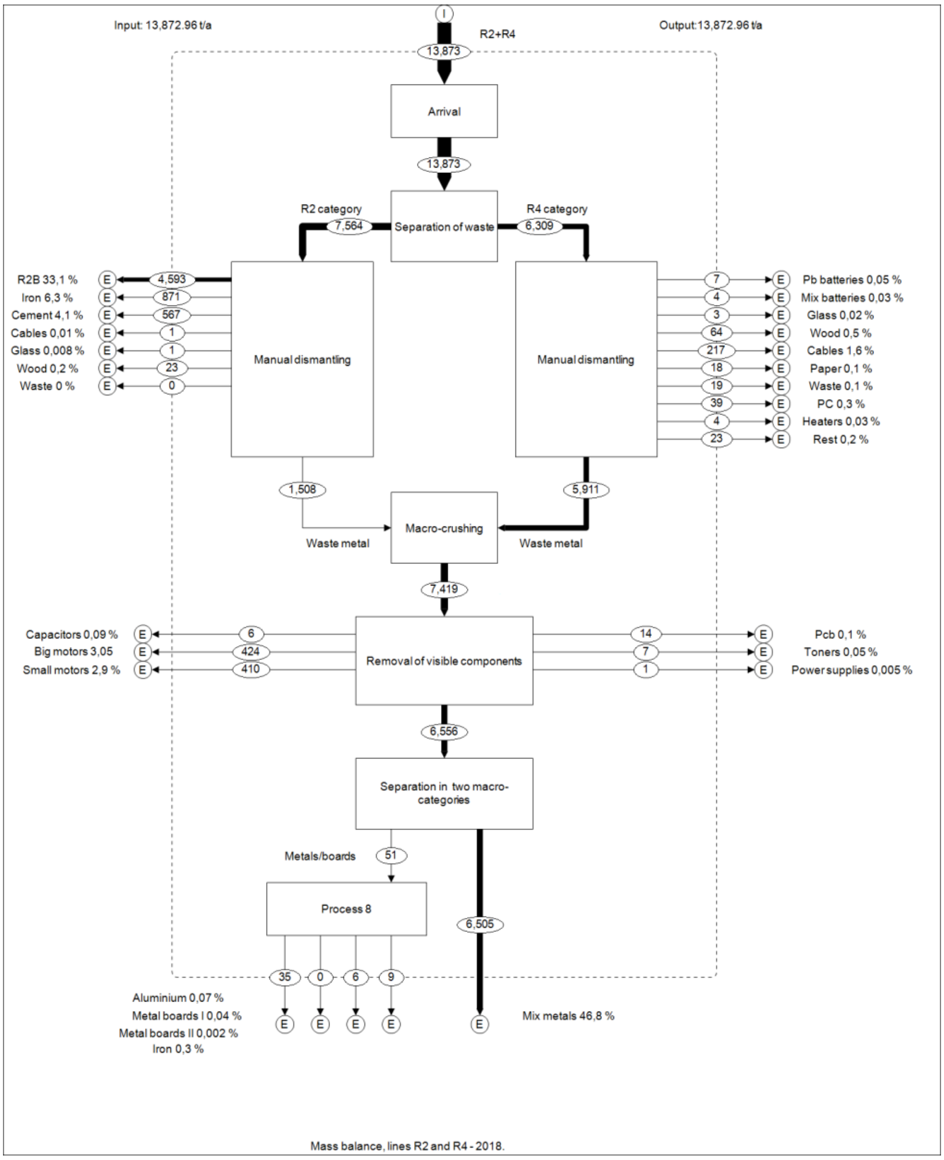

Figure 2 Mass balance of R2 and R4 categories of e-waste in Italian plant, 2018

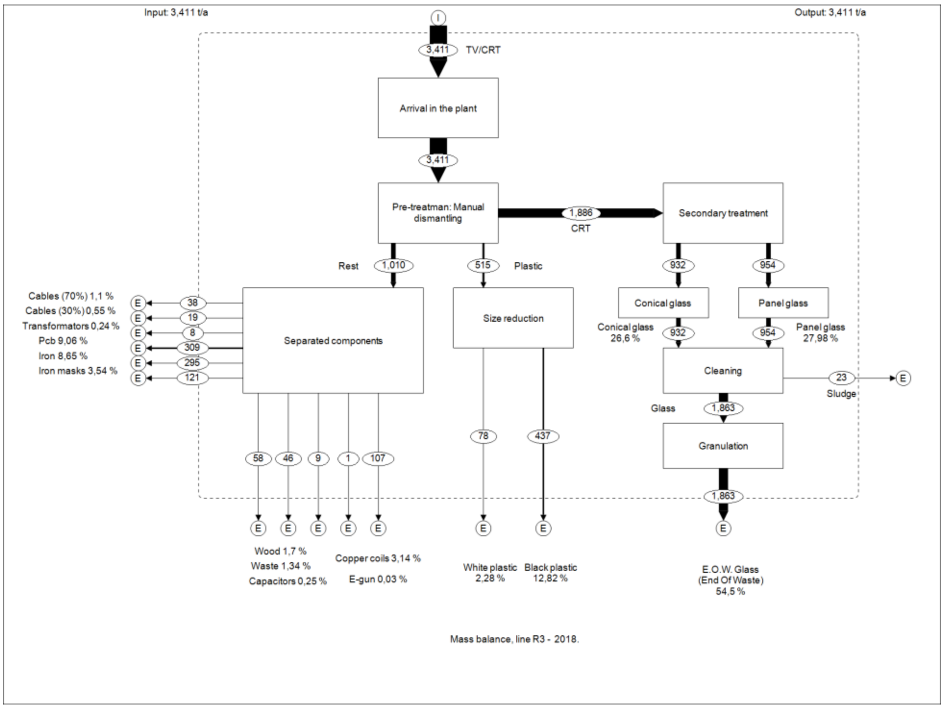

Figure 3 Mass balance of R3 category of e-waste in Italian plant, 2018

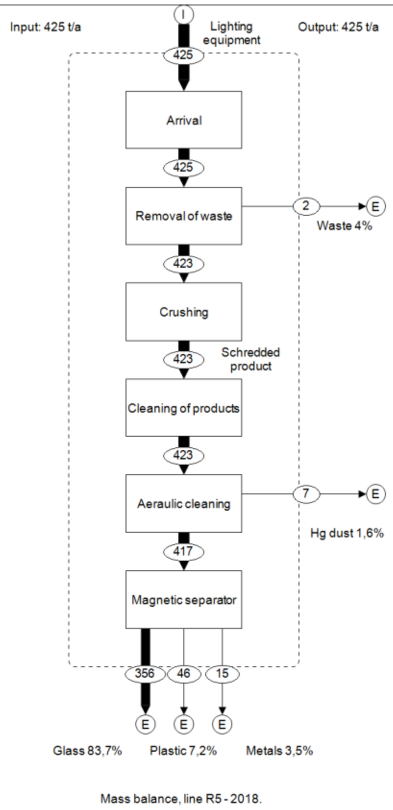

Figure 4 Mass balance of R5 category of e-waste in Italian plant, 2018

RESULTS AND DISCUSSION

The problems identified as major in the WEEE management system in Serbia can be divided into those related to the system infrastructure, legal framework and reporting and data collection system.

The shortcomings related to infrastructure are primarily undeveloped waste collection schemes, then insufficient number of recycling yards, e-waste collection centers, as well as treatment plants. Consumers, even in places where they exist, do not dispose their e-waste in an adequate way and it mostly ends up mixed and disposed of with municipal waste. If compare with situation in Italy, a great advantage of their system is the presence of fixed collection points managed by local municipalities. There are no fixed collection points carried out by local municipalities, where citizens can bring their e-waste any time, like the points for municipal waste or recycling yards for other recyclable waste (plastic, paper, etc.). For this purpose, four leading companies have deployed 14 location across Serbia, or 1 recycling site per 513,347 inhabitants, which is 36 times less compared with DCFs in Italy. (Table 2)

Table 2 Data regarding WEEE collection and treatment capacities in Italy and Serbia for 2018

	Italy	**Serbia**
Population[1]	60,431,238	7,186,862
Population density (/km^2)[1]	205	80
WEEE generated (kg/cap/year)	19[2]	11.8[2]
No. of WEEE collection points	4,212[3]	Unknown
No. of WEEE treatment facilities	59[3]	4
Total WEEE collected	310,610[3]	15,000-20,000[4]
Collection (kg/cap)	5.14[3] (27% of WEEE generated)	2.78[4] (24% of WEEE generated)

[1] http://www.worldbank.org
[2] estimated
[3] CDCRAEE – Italian WEEE coordination center, 2018. Collection and processing of WEEE in Italy (Ritiro e trattamento dei rifiuti da apparecchiature Elettriche ed elettroniche in Italia
[4] SEPA, 2019

As regards to legal framework, the main problem is the lack of a national coordinating body that would be responsible to ensure fulfilling of targets stipulated in legislative and fully implement producer responsibility principles. A significant number of importers and manufacturers of electronic and electrical equipment do not comply with the obligations to report on the quantities of equipment placed on the market or do not report adequate quantities, which makes it difficult to monitor and plan the management system. Information from companies that treat this waste stream is too general and often inconsistent, and data on pre-treatment, recycling, and outflows are also lacking.

If we look the numbers in Table 2, it can be noticed that Italy is ahead of the situation in Serbia, not only with collection point, but also with treatment capacities. The four treatment facilities in Serbia are only for pre-treatment of e-waste, so all the secondary raw materials are sent abroad for further treatment. The only exceptions are metals such as copper, lead and aluminum which can be used directly, therefore are sold to companies in the country itself for use as a secondary resourse. E-waste pre-treatment facilities in Serbia face the problem of profitability and lack of capacity for treatment of hazardous waste. Eco-tax, i.e., fee which producers and importers of EEE pay, goes to Ministry of Finance instead of a defined fund (e.g Green Fund) for establishing of appropriate WEEE management. In this way, the fee is used for various finance applications in the country and the development of the WEEE management system is disabled.

In order to improve the situation in the electronic waste collection system, it is primarily necessary to define clear local and national investment strategies for the establishment of collective centers in urban areas at the municipal level.

In a shorter timeframe, an appropriate number of containers should be provided for different categories of electronic waste in commercial places, such as supermarkets, public institutions and the like.

In order to lead consumers to adequate disposal, it is necessary to develop incentive schemes for citizens by companies responsible for e-waste management in the form of rewards or clearly define penal policies for inadequate disposal.

Operators recycling e-waste should be subsidized for the treatment of hazardous substances and other recovered components from waste, in order to encourage the application of more advanced treatment technologies. In addition to the Agency and the Ministry of Environmental Protection, it is necessary to introduce a national operator, such as a coordination center that exists in Italy, which will control all e-waste management activities related to extended producer responsibility and achieving the goals set by Directive 2012/19.

Manufacturers and importers should be subject to more effective control mechanisms regarding their data reporting responsibilities, such as stricter penal policies and data reliability controls. It is also of great importance to design a special data monitoring system that will apply only to electronic and electrical waste and that will include all information about its flow during all phases, from collection to final processing and to develop a national open access platform, on which data related to e-waste will be available to the public, such as information on the location of disposal containers, recycling centers, etc.

REFERENCES

1. Forti, V., Baldé, C.P., Kuehr, R., Bel, G. (2020) The Global E-waste Monitor. Quantities, flows and the circular economy potential, 13-15.
2. Vujić, V.G., Jovičić, M.N., Babić, J.M., Stanisavljević, S.N., Batinić, J.B., Pavlović R.A. (2010) Assessment of plastic flows and stocks in Serbia using material flow analysis. Thermal Science, 14, 89-95.
3. Isernia, R., Passaro, R., Quinto, I., Thomas, A. (2019) The Reverse Supply Chain of the E-Waste Management Processes in a Circular Economy Framework: Evidence from Italy. Sustainability, 11 (8), 2430.
4. CDCRAEE - Italian WEEE coordination center, (2018) Collection and processing of WEEE in Italy (Ritiro e trattamento dei rifiuti da apparecchiature Elettriche ed elettroniche in Italia.
5. Diedler, S., Hobohm, J., Batinić, B., Kalverkamp, M., Kuchta, K. (2018) WEEE data management in Germany and Serbia. Global NEST journal 20, 751-757.
6. Law on Waste Management, Official Gazette of the Republic of Serbia, No 36/09, 88/10 and 14/16)
7. Batinić, B., Berežni, I., Marinković, T., Stanisavljević, N. (2019) Current state and challenges in WEEE recycling industry in Serbia. 16th International Conference on Environmental Science and Technology (CEST 2019) , 4-7 September, 2019 Rhodes, Greece.
8. Marinkovic, T., Batinic, B., Stanisavljevic, N. (2017) Analysis of WEEE management in Republic of Serbia (in Serbian). Proceedings of Conference "Wastewaters, municipal waste and hazardous waste", April, 2017, Pirot, Serbia.

XIV International Mineral Processing
and Recycling Conference
Belgrade, Serbia, 12-14 May 2021

LEGISLATION ASPECTS ON ENVIRONMENTAL PROTECTION AND WASTE MANAGEMENT ON THE EXAMPLE OF THE REPUBLIC OF SERBIA

Vladan Joldžić[#]
Institute for Criminological and Sociological Research, Belgrade, Serbia

ABSTRACT – Bearing in mind environmental protection and waste management as topic, we point that we have to form adequate orientation toward: mines, minerals, their solutions and wastes, as well as treatment of wastes from factories. This also means that we need adequate legislative approach to the observed and mentioned problems, based on law-logical principles and methods (for example: analyzes, comparisons, and syntheses) moving in our perception from the general to the specific questions and observations and from the highest to the lowest legislative categories.

Keywords: Waste management, Environmental protection, Legislative approach.

INTRODUCTION

Our text is oriented toward legislative aspects of the environmental protection and waste management, and is based especially on perception of the: environmental engineering, sustainable development, from such reason a plant and process design, mineral and coal threatening (mechanical, biological, chemical, thermal, and other), also their waste processing and its' dewatering. Of course for our theme also is of importance recycling of wastes. Orienting our attention to the treatment of mining and industrial waste, we are obliged to base it on a comprehensive legal approach. It must be multi-layered, based on the Constitution [7, p. 113-115] and by it oriented and demarcated by the most general laws. Then elaborated with specialized legal texts, supplemented and specified by the elements of necessary by-laws [7, p. 109-128]. This especially due to possible negative technogenic influences of mining as well of many industries.

LAW WAYS AND LEVELS OF ENVIRONMENTAL PROTECTION FROM MINERAL PROCESSING AND RECYCLING

The highest level of environmental protection is provided by modern constitutions that directly establish human right on healthy environment. This also means right to be protected from any environmental danger or consequences. This can be seen, for example, from the Constitution of: Germany [1], France [8], Switzerland [2], Grèce [18], Republic of Serbia [3], that directly oblige states to form legal and sub-legal texts to protect environmental values, rights, obligations and duties, thus also providing basic protection of negative technogenic impacts [7, p. 97/107], while such protection is elaborated by specialized laws and bylaws.

[#] corresponding author: joldzicvladan2@gmail.com; vladanj@eunet.rs

ENVIRONMENTAL PROTECTION FROM MINERAL PROCESSING AND RECYCLING AT THE LEVEL OF THE REPUBLIC OF SERBIA LEGISLATURE

Law on environmental protection, its elements of general importance for the protection from mining and waste management which also lead to specialized laws

Environmental protection of importance at the levels of mineral processing and recycling, basically is formed by the Law on environmental protection [9], which obliges to use any resource (mineral also) in accordance with the: principle of sustainable use (Art. 11, par. 1), adequate control and protection (Art. 14), officially approved projects for protection and remediation (Art. 15) and to do such remediation (Art. 16). All mentioned obligations arise from the duty to protect: soil (Art. 22), water (Art. 23), and air (Art. 24). This also leads to general obligations to perform adequate: planning and construction (Art. 33), assessment of possible environmental impacts (Art. 35 and 36) and integrated control and prevention of pollution (Art. 37), while not violating the limited values of various emissions (Art. 39). Hence, it is necessary to define conditions of concrete mining (Art. 40) and provide reduction or elimination of pollutants (Art. 41). Law on Environmental Protection established the obligation of pollution monitoring (Art. 60d and art 70/72). All the previously distilled requirements lead toward their deeper and more precise approach through the specialized laws and their bylaws, text that regulate fields of: planning and construction [11], mining [10], and water and soil use.

Importance of the Law on Planning and Construction

Law on Planning and Construction has norms at the same time important for mining and the environment. For example Art. 3 protects natural and created environmental values while articles: 15, 18 and 19 provide guidelines for the prevention of negative impacts on the natural and cultural environmental values. This law also established many other obligations, between them to prepare: Preliminary feasibility study (Art. 113), respecting environmental requirements, Feasibility study itself (Art. 114), General project, avoiding negative environmental impacts (Ar. 117), satisfying the requirements to formulate conceptual solutions (Art. 117a) and conceptual design (Art. 118). Construction permit project (Art. 118a), which is necessary for the construction of a tailings and ash dumps and have to be done according to the requirements of the specialized Rulebook [14]. This law also oblige the economic entity to: execute all works of environmental importance on the concrete construction (Art. 123), environmentally adequate reconstruction, if it wants to make some change in the approved technology or in the facility with which it operates (Art. 124), and to act in accordance with the requirements of importance how to treat mining ash and tailings (Art. 133, par. 2, under 1, 6, 8, 10 and 11).

Importance of the Law on Mining and geological researching

Law on Mining and geological researches established obligation for rehabilitation and remediation of explored and used terrarians (Art. 1). Also, with the Art. 3 par. 1, item 7, defines so cold “technogenic resources”: mineral resources created through the process of exploitation, preparation and processing of raw mineral materials, as well as “secondary raw materials”. The law is clear. Geological research, exploitation of reserves and maintenance of mining facilities, have to be performed in accordance with modern professional achievements and regulations of importance for safety work and environmental protection (Art. 5). In specially protected natural and historical areas mining may be performed exceptionally, on the basis of special approvals (Art. 6). The observed law also obliges on so-called applied geological researching having in mind the elements of importance for the protection of environment, as well as for rehabilitation of used terrain (Art. 21, par. 1). Each researching project is subject to control (Art. 25, par.1), which includes checking compliance with standards in the field of mining, nature and environmental protection, and even the protection of cultural heritage (Art. 25, par. 2). Such project must be approved by a special decision and can be carried out in accordance with the parameters determined by this decision (see Art.: 30, 37, 38, 41 and 45). Project contractor is obliged to implement the prescribed measures of importance for: safety and health at work, human health and the environment (Art. 50, par. 1, item 8). Permit to mine can be issued if mining facility, or its’ part, was build in accordance with prescribed requirements and conditions of approved project (Art. 109, par 1 and 2), having in mind the protection of humans and the environment. Law on Mining and Geological Research also regulates rules of importance for: action in the case of accidents (Art, 129), planning of measures to prevent endangerment of the environment (Art, 130, par. 1, item 1), especially waters (Art, 130, par, 1, item 3) and planning of remediation measures (Art. 130, par. 1, item 1). From the reason of environmental protection mining waste must be managed on the basis of a specific Permit for mining waste management (Art. 144). Also the holder of exploitation is obliged to take all measures for the protection of mining treasures and the environment after its permanent cessation (Art. 151, par. 1) on the basis of the approved Mine closure program (see Art. 152), which includes its rehabilitation and reclamation (Art. 153).

Environmental protection from waste management

Waste, including waste produced during mining and its subsequent recycling, are expressed as strong factors of negative impact on environmental rights and values. From this reason, in the Republic of Serbia, the basic and most general elements are incorporated into the Law on Environmental Protection, and elaborated in a specialized legislative text: Law on Waste Management [12], as well as a number of bylaws. The Law on Environmental Protection prescribes that all subjects of law are responsible for any activity that can change conditions of the environment (Art. 5, par. 1). Also oblige all subjects to take necessary measures to protect the environment (Art. 5, par. 2). This law prescribes (with the Art. 10, par. 1, items: 2, 3, 4, 5 and 6) obligation for State to form special laws which have to regulate: integrated prevention and pollution control; protection of nature; protection of air, water, land, forests, geological resources; chemical management; and, which is of particular importance for our topic, waste management. Waste disposal is correct (according to the Art. 19 -Use of space) only if the specific subject acts legally correct through the: construction of facilities important for waste management, temporary waste disposal, or permanent disposal, providing the protection from degradation and contamination to the soil (Art. 22) and water (Art. 23, par. 2). The Law on Environmental Protection also established obligations for subjects to remediate concrete space according to the mandatory remediation project (Art. 16, par. 1) approved by the Ministry (Art. 16, par. 2). This law also obliges that: “Waste management is carried out… according to the prescribed conditions and measures for waste management within the system of collection, transport, storage, preparation for reuse, i.e. again (Art. 30, pa.1)”, whereby (pursuant to Ar. 30, par. 2) “the owner and/or other waste holder is obliged to take waste management measures in order to secure: prevention or reduction of waste generation, reuse and recycling, separation of secondary raw materials, use of waste as an energy source, i.e. temporary and final disposal of waste (Art. 30, par. 2)”. For more detailed implementation of these obligations, the Law on Waste Management must be respected.

Subject of regulation of the Law on Waste Management is: determination of types and classification of waste; waste management planning; identification of waste management entities; waste management obligations; and the management of special waste streams (Art.1, par.1); all this, on the base of Art. 2, in order to treats waste in a way that does not endanger human health and the environment. Law prohibits disposal and incineration of waste which is in collision with prescribed standards (Art. 38 - Reuse and exploatation, par. 7). What surprises us is that the observed law does not regulate the adequate treatment of garbage - the type of waste that has no use value and cannot be used as a source of secondary raw materials, except that it prescribes the control of garbage distribution (Art. 16, para. 6.). We also point out that the this law does not treat radioactive waste (Art. 4, par. 1, item 4) and that cannot be applied to: gases emitted into the atmosphere (Art. 4, par. 1, item 1), wastewater (Art. 4, par. 2, item 1).), mining waste generated by exploration, excavation, processing and storage of mineral raw materials, as well as tailings from mines and quarries (Art. 4, par. 2, item 4). This is understandable given that the issues in question are regulated by a series of special conventions and accompanying annexes to international law, and that the documents in question have been ratified and thus become an integral specialized part of the current legislation of the Republic of Serbia. The Law on Waste Management distinguishes hazardous waste (Art. 5, par. 1, item 18) and other types of wastes, requiring their classification according to the waste catalog (Art. 8, par. 1 and 6, item 1). It also prescribes that the classification of waste is generally performed according to the presence of hazardous or non-hazardous substances, and hazardous waste itself according to the concentration limit values of hazardous substances (Art. 8, par. 3) for treatment, i.e. reuse and disposal of waste (Art. 23, par. 1, item 2). Art. 25 strongly contribute to the prevention of ecologically negative technogenic impacts of any waste, while the Art. 26, with par. 1, item 6, obliges the waste producer to store it in a way that does not affect human health and the environment and not to mix different types of wastes nor waste with water. From this reason Art. 42 explicitly prohibits the disposal of waste in places that are not officially designated for such purpose, while Art. 44, with the paragraph 6, *in principium*, prohibits the disposal of hazardous and non-hazardous waste. Also is prohibited possible incineration outside specially designated and officially approved areas and plants (see: Art. 38 - Reuse of waste, par 1, Art. 41 - Thermal treatment, Art. 59 - Issuance and types of permits, par. 1, item 4 - Permit for waste treatment, and Ar. 60 - Competence for issuing permits), while the incineration of certain substances is completely prohibited. The observed law (with the Art. 71, par. 6) allows cros-border movement only to nonhazardous waste.

In addition to the observed Law on Waste Management, it is important to list a number of bylaws that are of exceptional importance for the topic we are dealing with, precisely because they supplement the observed law: Decision on establishing the Yugoslav standard for waste characterization [4], Rulebook on the manner of storage, packaging and marking of hazardous waste [16], Rulebook on the treatment of waste containing asbestos [17], Rulebook on the list of POPs substances [15], Decree on types of waste for which thermal treatment is performed [6], and Rulebook on permitted quantities of hazardous and waste materials in soil and water for irrigation and methods for their testing [13].

CONCLUSION

Our environmental law researching, between them researching connected with the techogenick problems of environmental importance indicate that main elements of environmental protection, between them also environmental protection connected with mining and waste management, at the example of the Republic of Serbia, are, for the most part, relatively new, not older than 10 or 15 years, or even less. Unfortunately, not all legal and sub-legal elements are relatively new and adequate. Some are more than 40 year old. For example such are Decree on the classification of waters of inter-republican watercourses, interstate waters and waters of the coastal sea of Yugoslavia [5] and Decree on the classification of waters of inter-republican watercourses, inter-state waters and waters of the coastal sea of Yugoslavia, , sub-legal text that are legally binding. Legally binding although, observing them through the actual knowledge of natural and legal sciences, such elements deserve to be replaced by new ones. Moreover, having in mind that such elements are numerous, it is obvious that is beter to replace this acts by newer and more adequate ones. It is our opinion that this should be approached and formed through the teamwork of people of natural sciences, medicine, ecology and law. That is why we suggest it here.

REFERENCES

1. Basic Law for the Federal Republic of Germany from 23 May 1949, last amended on 28 March 2019), articles: 87c-87f, 89, 90 and 91.
2. Constitution fédérale de la Confédération suisse du 18 april 1999, Articles: 73. – 80.
3. Constitution of the Republic of Serbia, Official Gazette of Republic of Serbia, No 83/2006), Art.: 13, 16 and 74.
4. Decision on establishing the Yugoslav standard for waste characterization, Official Gazette of Serbia and Montenegro, No. 6/2005.
5. Decree on the classification of waters of inter-republican watercourses, interstate waters and waters of the coastal sea of Yugoslavia, Official Gazette of SFRY, no. 6/1978.
6. Decree on types of waste for which thermal treatment is performed, conditions and criteria for determining the location, technical and technological conditions for design, construction, equipment and operation of thermal treatment plants, handling the residue after incineration, Official Gazette of the Republic of Serbia, No. 102/2010

and 50/2012.

7. Joldžić Vladan (2020): Environmental (Ecology) Law as Independent Law Science Discipline, IKSI, Belgrade, 2020.
8. La Constitution du 4 octobre 1958; Révisions constitutionnelles de mars 2005, Article 53-1, also its' Charter for the Environment, Article 1.
9. Law on environmental protection, Official Gazette of Republic of Serbia, No. 135/2004, 36/2009, 36/2009 72/, 43/2011, 14/2016, 76/2018, and 95/2018.
10. Law on Mining and Geological Research, Official Gazette of the Republic of Serbia, No. 101/2015 and 95/2018.
11. Law on Planning and Construction, Official Gazette of the Republic of Serbia, No.: 72/2009, 81/2009, 64/2010, 24/2011, 121/2012, 42/2013, 50 / 2013, 98/2013, 132/2014 and 145/2014.
12. Law on Waste Management, Official Gazette of the Republic of Serbia, No.: 36/2009, 88/2010 and 14/2016, formed through the project that properly used the elements of the European Union legislation, for example: Council Directive 75/442/EEC on waste, Hazardous waste Directive 91/689/EEC, Directive 2008/98/EC on Waste, Decision 2000/532/EC establishing a list of wastes and others.
13. Rulebook on permitted quantities of hazardous and waste materials in soil and water for irrigation and methods for their testing, Official Gazette of the Republic of Serbia, No. 23/1994.
14. Rulebook on the content of mining projects, Official Gazette of the Republic of Serbia, no. 27/1997.
15. Rulebook on the list of POPs substances, manner and procedure for management of pops waste and limit values of concentrations of POPs substances related to the disposal of waste containing or contaminated with POPs substances, Official Gazette of the Republic of Serbia, No. 65/2010.
16. Rulebook on the manner of storage, packaging and marking of hazardous waste, Official Gazette of the Republic of Serbia, No. 92/2010.
17. Rulebook on the treatment of waste containing asbestos, Official Gazette of the Republic of Serbia, No. 75/2010.
18. The Constitution of Grèce, Révision, April 2001, Art. 24.

XIV International Mineral Processing
and Recycling Conference
Belgrade, Serbia, 12-14 May 2021

EFFECT OF SODIUM DODECYL SULFATE IN DEINKING FLOTATION

Dragana Marilović[#], **Maja Trumić**
University of Belgrade, Technical Faculty in Bor, Bor, Serbia

ABSTRACT – Deinking flotation is a process that has been researched for decades. One of the most important items of this process is the correct selection of surfactant that would promote the utilization of waste paper. This is the reason why research is being done on the use of new surfactant and finding the best solution for application from a technological and environmental point of view. Sodium dodecyl sulfate (SDS) is an anionic surfactant that is widely used in industry. In deinking flotation it has application in waste paper purification printed with carbon based or iron based toner. This is a reviewed paper and presents some of the results of authors who did their research in flotation process using SDS as surfactant.

Keywords: Deinking flotation, SDS, Surfactant, Toner.

INTRODUCTION

Toner is a component in cartridges that is most commonly used in photocopiers, laser printers, fax machines, and combination devices. Over the years, with the advancement of technology, printing machines have become cheaper and more accessible, leading to higher toner consumption and the generation of large amounts of waste by individuals and industries. [1] As a raw material, toner is of great importance not only because it contains valuable metals that are important in the industry, but also because it negatively affects the environment. After use, cartridges still contain certain amounts of toner which, if not treated properly, can endanger the environment and have a negative impact on human health. In order to clean the used paper from toner particles, a flotation concentration, known as deinking flotation, the process has been applied which has been investigated for the past few decades. [2, 3, 4, 5] The chemical composition and characteristics of the toner particles are important parameters for this process. Toners generally contain styrene acrylate copolymer which serves as a binder. Other additives are pigment or charge control additives [6, 7]. Toner particles are not soluble in water, but they are soluble in many organic solvents.

APPLICATION OF SURFACTANT SODIUM DODECYL SULFATE IN FLOTATION CONCENTRATION

Ionic surfactants are organic compounds whose molecules are composed of a hydrophobic part (tail) and a hydrophilic part (head) shown in Figure 1. Sodium dodecyl sulfate (SDS) is a synthetic anionic surfactant that is often used in cleaning and hygiene products, but also in flotation concentration. The SDS molecule contains 12 saturated carbon alkyl chains attached to a negatively charged sulphonate head ($-OSO_3^-$). [8]

[#] corresponding author: dmarilovic@tfbor.bg.ac.rs

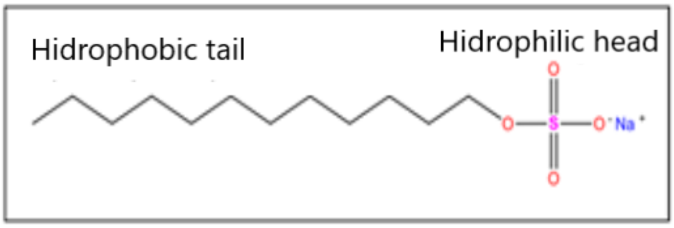

Figure 1 Chemical structure of sodium dodecyl sulfate (SDS) [8]

As the surfactant concentration increases, hemicell and then admicelles form on the surface of the particles with an increase in the surfactant concentration until the critical micellar concentration (CMC) above which the bilayer tends to be completely adsorbed on the surface making the particle surface hydrophobic. The formation of admicelles is significantly influenced by the concentration of surfactant, but also by the presence of electrolytes which can significantly reduce CMC due to electrostatic repulsive forces between charged ion heads. [9]

Scientists Jun and Meng [10] also came to these conclusions by examining the adsorption of SDS at different concentrations (from 2 mM-8.1 mM) to the steel surface. They hypothesized that the critical micellar concentration of SDS is 8.1 mM above which SDS is on the surface in the form of an admicells.

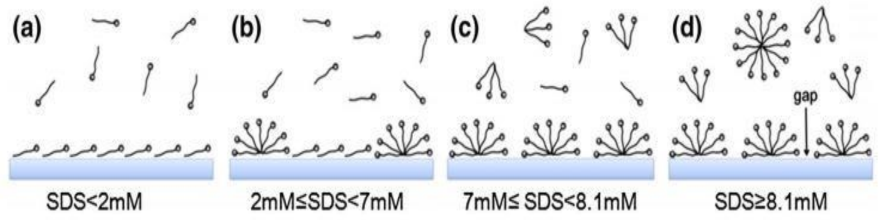

Figure 2 Schematic diagram of adsorption of different concentrations of SDS on the surface of stainless steel in four stages; sulfate groups are represented by circles, and carbon chains by curved lines [10]

Scientists Sritapunya *et al.* [11] examined the effect of anionic surfactant SDS on the surface of carbon-based toner particles in the presence of paper fibers (in the pulp) to show the real conditions in the industrial process. They concluded that SDS is adsorbed on the surface of toner particles through of a tail in a monolayer, forming hemicelles, while on the surface of cellulose fibers, it is adsorbed upside down, forming admicelles.

Calcium promotes the adsorption of surfactant on the carbon surface because it acts as a bridge between negatively charged fields on the surface and the anionic groups of the surfactant, especially at low surfactant concentrations while not improving the adsorption of surfactant on cellulose fibers. An increase in surfactant concentration can cause a decrease in calcium adsorption, probably due to the cover of negative fields on the toner particles.

Investigations of the adsorption mechanism of sodium dodecyl sulfate on toner particles were performed in the presence and absence of cations (Ca^{2+}, Mg^{2+} and Al^{3+}) which are most often present in industrial water. The graph shows the percentage fraction of non-floated toner particles as a function of pH in the presence of $5{\cdot}10^{-4}$ mol/L, $1{\cdot}10^{-4}$ mol/L and $5{\cdot}10^{-5}$ mol/L SDS. At the lowest examined surfactant concentration, there are no significant changes in the amount of non-floated particles. At the highest examined concentration, in an acidic medium at pH 2.2, a significantly smaller amount of non-floated particles was observed, which may indicate electrostatic adsorption of RSO_4^- ions on the positively charged surface of toner particles occurring in this pH range. [12]

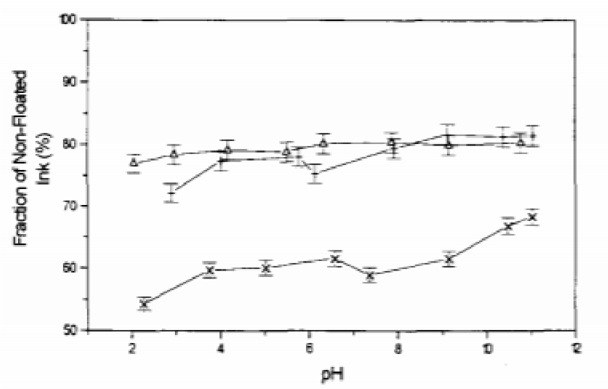

Figure 3 Fraction of non-floated ink as a function of pH with sodium dodecyl sulfate: (x) $5 \cdot 10^{-4}$ mol/L; (+) $1 \cdot 10^{-4}$ mol/L; (Δ) $5 \cdot 10^{-5}$ mol/L [12]

In the presence of calcium cation, an increase in floatability was verified, probably due to calcium/collector salt precipitation on the ink particle surface. In the presence of magnesium and aluminum species, an increase in floatability was noted for pH ranges related to the maximum concentration of their hydroxy complexes. [12]

The effect of calcium ions was observed in the pH range between 2.5 and 8.5 where the proportion of non-floated toner particles was reduced. The authors assume that the calcium ion Ca^{2+} previously adsorbed on the surface of the toner particles improves the adsorption of RSO_4^- collector ions.

The same conclusion was reached by the authors Sritapunya *et al.* [11] who examined the adsorption of SDS and sodium octanoate, C8 on the surface of carbon-based toner particles. Based on the distribution diagram in the form of hydroxide, magnesium is at a pH value of 6 to 11, and the increase in floatability was in the range of 8-11, so it is assumed that magnesium precipitated on the surface of toner particles in the form of $Mg(OH)_2$. In the presence of aluminum ions, toner particles are activated at pH values between 3.5 and 8.5, which, based on zeta potential results, can be associated with specific adsorption of aluminum hydroxy complexes $Al(OH)_2^+$ and $AlOH^{2+}$ and metal hydroxide $Al(OH)_3$ on the particle surface which is followed by adsorption of $RSO4^-$ collector ions.

It was also observed that above pH 7.5 the floatability of particles is reduced, which, as the authors concluded, is due to the negative value of the electrode potential of aluminum hydroxide. [12]

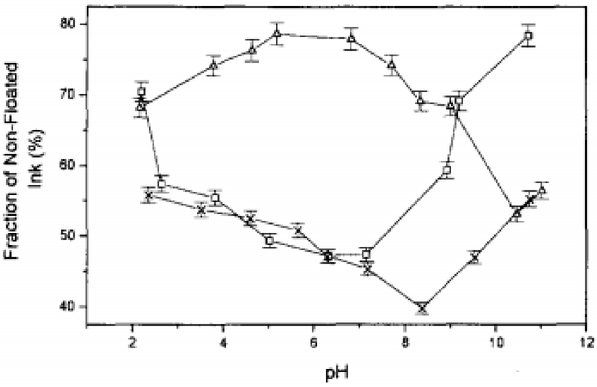

Figure 4 Fraction of non-floated ink as a function of pH with $1 \cdot 10^{-4}$ mol/L SDS in the presence of $1 \cdot 10^{-4}$ mol/L metallic cations: (x) $CaCl_2 \cdot 2H_2O$; (Δ) $MgCl_2 \cdot 6H_20$; (□) $AlCl_3 \cdot 6H_2O$ [12]

Electrostatic forces play a key role in determining the equilibrium in surfactant systems. The shape of the ionic surfactant aggregate in the solution is mostly influenced by the carbon-water interaction and the repulsive force between groups with the same charge. The balance of electrostatic forces can be disturbed by changes in intermolecular forces as a result of various conditions in the system such as changes in surfactant concentration, the addition of electrolytes, or changes in temperature. The presence of other ions prevents electrostatic repulsion between the groups, thus allowing the groups to attract each other. As a result, aggregates of different sizes are formed, and in some cases, the structure of particles can change [13].

Previous research has confirmed that ionic surfactants adsorbed from aqueous solutions on the hydrophobic surface of graphite form a vertical monolayer upon surface saturation of the solution. Based on the classical reorientation model [14, 15, 16, 17, 18] in the first stage of adsorption (at a concentration below the CMC) surfactant molecules are adsorbed on the surface graphite oriented horizontally, forming a densely packed monolayer where the hydrocarbon chains are distributed parallel to each other relative to the surface of the graphite, the binding mechanism occurs according to the arrangement of the tail-heads. In the second stage of adsorption (at concentrations close to the CMC), the adsorbed molecules gradually assume a vertical orientation with the polar heads directed towards the aqueous phase, facilitating vertical adsorption of molecules from the solution until the surface saturates near the CMC. The idea of this reorientation scheme relies mainly on molecule compaction analysis and adsorption isotherm.

AFM analyzes showed a two-step adsorption mechanism that differs significantly from the proposed classical reorientation model. In the first stage of adsorption, the surfactant molecules independently reorient themselves horizontally to the graphite surface, parallel to each other, but in a head-to-head and tail-tail arrangement. In the second stage, surface hemi-cylinders are formed as a result of hydrophobic interaction between free alkyl chains in the monolayer and molecules in the solution [19]. It is assumed that in the presence of a divalent ion, electrostatic interactions between charged groups change and lead to changes in the structure formed by monovalent ions.

However, AFM analyzes revealed that the adsorbed structures were long (1 µm) and thin (~5 nm) and its appearance is very similar to those which are formed only in the presence of monovalent counterion.

The scientist Parachuri *et al.* [20] examined the adsorption of SDS at the graphite-water interface using an AFM microscope and hypothesized that the functional groups of reagents have the ability to form a hydrogen bond with water. AFM analyzes shows the structures of the adsorbed surfactant as linearly parallel hemi-cylindrical micelles when the concentration is below the critical micellar concentration. The adsorbed hydrocarbon chains are bound to the surface by head-tail and act by creating nuclei for hemicell growth. If micellar structures are formed on the graphite surface at a concentration of 1 and 8 mM, then the zeta potential represents the zeta potential of the micelle surface. The values of the zeta potential in the reaction with SDS on the micelle surface are negative and amount to -75 mV at a higher surfactant concentration, and positive at a lower surfactant concentration and amount to 70 mV.

CONSLUSION

Based on the presented results, it can be concluded that the mechanism of sodium dodecyl sulfate in flotation processes has not been fully investigated. It can be assumed that in a strongly acidic environment electrostatic adsorption of RSO_4^- ions occurs on the positively charged surface of toner particles. It has also been proved that the critical micellar concentration of surfactant determines the way of adsorption and the orientation of molecules on the surface of the toner. The electrostatic forces between the adsorbed aggregates are dominant and determine the period of aggregation. What has been further proven in research is that electrolytes play an important role in flotation by acting as a bridge between negatively charged fields on the toner surface and the anionic groups of the surfactant.

REFERENCES

1. Salhofer, S. (2017) E-waste: An overview on generation, collection, legislation and recycling practices Resour. Conserv. Recy., 122, 32-42.
2. Borchardt, J. K. (1997) The use of surfactants in de-inking paper for paper recycling, Current Opinion in Colloid & Interface Science, 2 (4), 402-408.
3. Hu, Y., Wang, D., Millero, J.D. (2000) Interactions between the toner composites and cellulose and their implication to flotation deinking, 13, 20-26.
4. Subhashini, V., Bennington, C. P.J., Grace, J. R., Kerekes, R. J. (2011) Column Flotation Deinking: State-of-the-art and opportunities, Resources, Conservation and Recycling 55 (12), 1154-1177.
5. Trumić, M. S., Antonijević, M., Trumić, M. Ž., Bogdanović, G. (2016) The application of mineral processing technique for the printed paper recycling, Reciklaža i održivi

razvoj 9, 48-57.

6. Verma, N., Kumar, R., Sharma, V. (2018) Analysis of laser printer and photocopier toners by spectral properties and chemometrics, Spectrochimica Acta Part A: Molecular and Biomolecular Spectroscopy, 196, 40-48.
7. Kumar, R., Samkaria, A., Sharma, V. (2020) On the spectroscopic cum chemometric approach for differentiation and classification of inkjet, laser and photocopier printed documents, Science & Justice, 60 (4), 347-357.
8. Al-Karawi, D., Hussein, I. (2016) The investigation of the electrical control of hemimicelles and admicelles on gold for analyte preconcentration, dissertation, The Faculty of the Department of Chemistry, Western Kentucky University, 67.
9. Haigh, S. D. (1996) A review of the interaction of surfactants with organic contaminants in soil, Science of the Total Environment, 185, 1996, 161-170.
10. Jun, Z., Meng, Y. (2014) Stick–Slip Friction of Stainless Steel in Sodium Dodecyl Sulfate Aqueous Solution in the Boundary Lubrication Regime, Tribol Lett, 56, 543–552.
11. Sritapunya, T., Jairakdee, S., Kornprapakul, T., Somabutr, S., Siemanond, K., Bunyakiat, K., Kitiyanan, B., Scamehorn, J. F., Grady, B. P., Chavadej, S. (2011) Adsorption of surfactants on carbon black and paper fiber in the presence of calcium ions, Colloids and Surfaces A: Physicochem. Eng. Aspects 389, 206–212,
12. Oliveira, A.P., Torerm, M.L. (1996) The influence of some metallic cations on deinking flotation, Colloids and Surfaces A: Physicochemical and Engineering Aspects, 110, 75-85.
13. Wanless, EJ, Ducker, WA. (1997) Weak influence of divalent ions on anionic surfactant surface-aggregation. Langmuir, 13, 1463–1474.
14. Zettlemoyer, A.C., Skewis, J.D., Chessick, J.J. (1962) The adsorption of calcium ions to surfactant films on Graphon, Journal of Aericanm Oil Chemists Society, 39, 280–286.
15. Zettlemoyer, A. C. (1968) Hydrophobic surfaces, The Journal of Colloid and Interface Science, 28, 343-369.
16. Day, R. E., Greenwood, F. G., Parfitt, G. G. (1967) In Proceedings of the 4th International Congress on Surface Active Substances; Overbeek, J. Th. G., Ed.; Gordon and Beach: New York, 1005.
17. Greenwood, F. G., Parfitt G. D., Picton N. H., Wharton D. G. (1968) In Adsorption from Aqueous Solution; Weber, W. J., Matijevic, E., Eds.; American Chemical Society: Washington, DC, 135-144.
18. Hey, M. J., MacTaggart, J. W., Rochester, C. H. (1984) Enthalpies of adsorption of sodium dodecyl sulphate and O-n-octyltetraethylene glycol from aqueous solutions onto graphitized carbon, Journal of the Chemical Society, Faraday Trans, 1 (80), 699-707.
19. Manne, S., Cleveland, J. P., Gaub, H. E., Stucky, G. D., Hansma, P. K. (1994) Direct visualization of surfactant hemimicelles by force microscopy of the electrical double layer, Langmuir 10, 4409-4413.
20. Paruchuri, VK, Nguyen, A.V, Miller, J.D. (2004) Zeta-potentials of self-assembled surface micelles of ionic surfactants adsorbed at hydrophobic graphite surfaces. Colloids and Surfaces a Physicochemical and Engineering Aspects 250 (1–3), 519–526.

XIV International Mineral Processing
and Recycling Conference
Belgrade, Serbia, 12-14 May 2021

RESEARCH ON ACID LEACHING OF Cu, Zn AND In FROM JAROSITE WASTE

Vesna Conić[#], Dragana Božić, Suzana Dragulović, Ljiljana Avramović,
Radojka Jonović, Mile Bugarin
Mining and Metallurgy Institute Bor, Bor, Serbia

ABSTRACT – The paper presents the results of treatment of technogenic raw materials by the leaching process in order to valorize economically valuable metals and minimize the negative impact of leached residue on the environment. First, the sample was homogenized, and then granulometric, XRD and chemical analysis of the jarosite sample was done. The leaching agents used in experiments were HCl, HNO_3 and H_2SO_4. Investigations have shown that the most acceptable method for the treatment of jarosite is leaching of jarosite using sulfuric acid, where the best leaching of Cu, Zn and In was obtained, namely 93.76%, 91.64% and 97.59%, respectively.

Keywords: Hydrometallurgy, Acid Leaching, Jarosite Treatment, Indium Recovery.

INTRODUCTION

Zinc concentrates, beside zinc, also contain a number of commercially important metals such as copper, lead, silver, germanium, indium, gallium, etc. These metals do not create their own mineral deposits, but as zinc companions, in hydrometallurgical zinc production, by roasting, leaching and electrolytic extraction, they are concentrated in the output waste sludge's of so-called jarosites as by-products [1,2]. By processing by-products, a whole range of metals can be produced, which has a favorable effect on the overall economy of the basic process, because the prices of these metals are relatively high [3,4]. Jarosite, as a newly formed chemical structure, is very stable and poorly soluble in dilute acid [5]. Accompanying zinc metals from jarosite are usually obtained by the Waelz pyrometallurgical process. Pyrometallurgical processes of processing secondary raw materials of zinc and waste sludge from zinc hydrometallurgy are very efficient, but they involve expensive large-capacity industrial plants, in order to be economical. These processes release harmful gases that can have a serious impact on the environment. Some authors have shown that the application of pyrometallurgical processes such as the Waelz and Ausmelt methods consumes a huge amount of coal to provide the power required to achieve a high operating temperature (1100-1300 ^{0}C). These methods are not economically viable, so jarosites are usually deposited.

The aim of this work was to use the hydrometallurgical leaching process to valorize some of the accompanying metals such as Cu and In in addition to Zn. By hydrometallurgical processing of jarosite waste, beside additional recovery of Zn, also Cu and In would be valorized. This would support an integrated approach of metal production in zinc hydrometallurgy.

[#] corresponding author: vesna.conic@irmbor.co.rs

EXPERIMENTAL

Characterization of the jarosite

Granulometric composition of the sample

The obtained original jarosite sample was dried and homogenized and then granulometric analysis was done, which is shown in Table 1.

Table 1 Granulometric composition of jarosite sample

Particle size d (mm)	Mass participation m %	Cumulative participation by plus R %	Cumulative participation by minus D %
-0.150+0.106	0.50	0.50	100
-0.106+0.075	0.25	0.75	99.50
-0.075+0.053	0.30	1.05	99.25
-0.053+0.038	0.30	1.35	98.95
-0.038+0.020	0.15	1.50	98.65
-0.020+0.000	98.50	100	98.50

Granulometric analysis showed that the particle size below 38 µm was present in the amount of 98.65%. In order to better extract the metal, the sample was ground to a grain size of 98.50% -20 µm and homogenized again.

Mineralogical analysis of the sample

X-ray diffraction (XRD) analysis was performed on an instrument "Rigaku MiniFlex 600" with "D / teX Ultra 250" with high-speed detector and an X-ray tube with a copper anode. The detection limit of XRD analysis is about 1%. The diffractogram obtained by XRD analysis is shown in Figure 1. The following minerals were present in the jarosite sample: jarosite ($KFe_3(SO_4)_2(OH)_6$), magnetite (Fe_3O_4) and anglesite ($PbSO_4$). Jarosite and magnetite were the most abundant minerals in the sample, while anglesite was less represented.

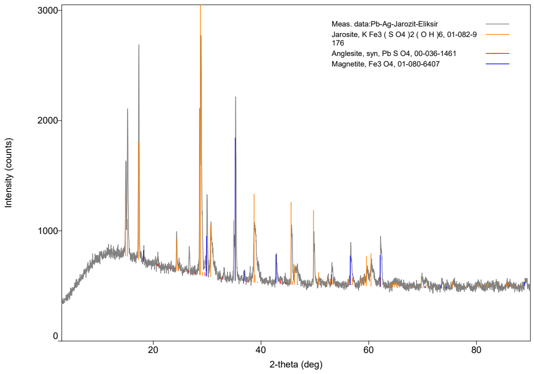

Figure 1 Diffractogram of a jarosite sample

Chemical characterization of jarosite sample

After homogenization, a representative sample was taken and chemical analysis was done. Chemical analysis of the sample is shown in Table 2.

Table 2 Chemical analysis of jarosite sample

Element	**Cu (%)**	**Zn (%)**	**In (ppm)**
Metal content	0.7	5.39	343.2

Preparation of jarosite sample for leaching experiments

Leaching of jarosites was performed in order metals extraction such as: Cu, Zn and In. Leaching was performed in glass beakers covered with watch glasses on a magnetic stirrer with stirring and heating with the introduction of air for the necessary processes, Figure 2. Three types of leaching were applied:

1. Chloride leaching-using HCl acid solution
2. Leaching in nitric acid solution
3. Leaching in a solution of sulfuric acid

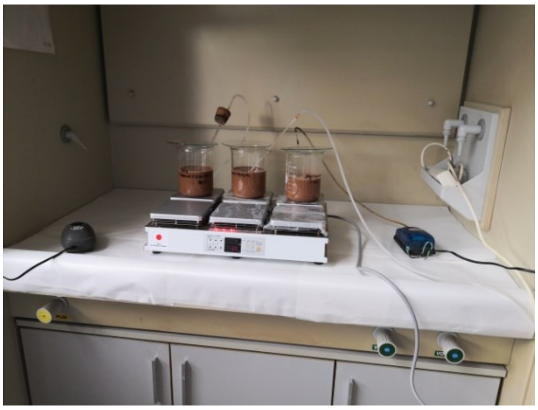

Figure 2 Leaching of jarosite on a magnetic stirrer

After leaching, each sample was filtered and washed. The volume of leach solution together with wash water was measured and 50 mL of the total volume of the solution was weighed in a normal vessel and given for chemical analysis.

RESULTS AND DISCUSSION

Chloride leaching in a solution of hydrochloric acid with air introduction

Leaching in hydrochloric acid was performed by changing the parameters: acid concentration, temperature and leaching time. The results of metals leaching are shown in Table 3.

Table 3 Recovery of metals by HCl leaching

HCl concentration	Temperature	Leaching time	Solid: Liquid ratio	Metals Recovery		
				Cu %	Zn %	In %
10%	room	1h	S:L = 1:4	19.70	14.83	17.02
10%	60 ^{0}C	1h	S:L = 1:4	43.99	35.06	64.03
10%	80 ^{0}C	1h	S:L = 1:4	56.00	52.86	95.06
20%	60 ^{0}C	1h	S:L = 1:4	70.25	92.12	98.00
20%	60 ^{0}C	2h	S:L = 1:4	68.83	57.60	99.12
20%	60 ^{0}C	4h	S:L = 1:4	78.34	70.88	99.01
20%	60 ^{0}C	6h	S:L = 1:4	87.24	95.20	98.50

It can be seen from the Table 3 that, using 20% HCl at a temperature of 60 ^{0}C, for the time of 1h, at a phase ratio of S:L = 1:4 can achieve over 70% recovery of Cu over 90% recovery of Zn and over 90% recovery of In.

Leaching in nitric acid solution

Leaching in nitric acid was performed under the following conditions:

- acid concentration of 20% HNO_3,
- temperature 60 ^{0}C,
- time 6h,
- phase ratio S:L = 1:5.

Metals recoveries are shown in Table 4.

Table 4 Recovery of metals by nitric acid leaching

HNO_3 concentration	Temperature	Leaching time	Solid: Liquid ratio	Metals Recovery		
				Cu %	Zn %	In %
10%	60 ^{0}C	6h	S:L = 1:5	40.25	39.50	63.33
15%	60 ^{0}C	6h	S:L = 1:5	47.39	44.22	68.10
20%	60 ^{0}C	6h	S:L = 1:5	50.79	47.41	71.20

Leaching in nitric acid showed relatively good leaching of Indium but also relatively low leaching of Cu and Zn.

Experimental laboratory tests of the leaching process in sulfuric acid solution with the introduction of air

Leaching with sulfuric acid was done using different acid concentrations of 2%-15%, under different conditions: temperature, leaching time and phase ratio. The results of metals recoveries are shown in Table 5.

Table 5 Recovery of metals by sulfuric acid leaching

Experiment No.	H_2SO_4 conc.	Temp.	Leaching time	Solid:Liquid ratio	Metals Recovery		
					Cu %	**Zn %**	**In %**
1.	2%	60 ^{0}C	6h	S:L = 1:4	7.87	13.22	6.50
2.	5%	60 ^{0}C	6h	S:L = 1:4	23.25	31.20	19.70
3.	10%	60 ^{0}C	6h	S:L = 1:4	46.98	47.49	42.70
4.	15%	60 ^{0}C	6h	S:L = 1:4	44.87	67.93	70.04
5.	2%	90 ^{0}C	6h	S:L = 1:4	10.15	17.81	5.13
6.	5%	90 ^{0}C	6h	S:L = 1:4	29.47	51.28	18.95
7.	10%	90 ^{0}C	6h	S:L = 1:4	54.15	82.97	37.10
8.	15%	90 ^{0}C	6h	S:L = 1:4	55.31	76.19	52.75
9.	2%	90 ^{0}C	1h	S:L = 1:4	12.10	22.02	6.63
10.	5%	90 ^{0}C	1h	S:L = 1:4	23.46	33.87	14.91
11.	10%	90 ^{0}C	1h	S:L = 1:4	44.09	30.19	37.80
12.	10%	90 ^{0}C	6h	S:L = 1:5	53.17	61.46	42.96
13.	10%	90 ^{0}C	6h	S:L = 1:10	75.80	84.96	77.50
14.	10%	90 ^{0}C	6h	S:L = 1:15	87.85	72.08	96.80
15.	15%	60 ^{0}C	1h	S:L = 1:4	54.54	51.18	59.90
16.	15%	90 ^{0}C	1h	S:L = 1:4	54.85	63.96	56.12
17.	15%	90 ^{0}C	6h	S:L = 1:5	68.68	73.02	68.50
18.	15%	90 ^{0}C	6h	S:L = 1:10	93.76	91.64	97.59
19.	15%	90 ^{0}C	6h	S:L = 1:15	93.48	80.04	98.74
20.	20%	90 ^{0}C	6h	S:L = 1:5	93.34	90.88	99.07
21.	30%	90 ^{0}C	6h	S:L = 1:5	93.39	88.36	98.80

Table 5 shows the different leaching conditions, under which different metal recovery occur. It can be seen from the table that using 15% H_2SO_4, at a temperature of 90 ^{0}C, leaching time 6h, with phase ratio S:L = 1:10, by introducing air, recovery of Cu and Zn were over 90% individually, and recovery of In was 97.59%. Under these conditions, one experiment was performed without the introduction of air. The results showed that the percentage of metal leaching is the same, which means that the process is possible without the introduction of air. Research by some authors has shown that by treating similar material under almost the same conditions (experiment no. 18), a high recovery of Zn and In can be achieved [6].

The solution obtained under the leaching conditions shown in experiment no.18 is acceptable for further treatment. Considering the price of sulfuric acid in relation to others that were used for leaching and working conditions that are not rigorous, it is considered that the choice of this acid is profitable. The resulting solution under these conditions can be further treated in order to selectively separations of the metals from the solution.

CONCLUSION

For the treatment of jarosite waste different kind of acids are used. The obtained metals recoveries under accepted leaching conditions are shown in order:

-20% HCl	(600C, 1h, S:L = 1:4)	70.25% Cu	92.12% Zn	98.00 %In,
-20% HNO_3	(600C, 6h, S:L = 1:5)	50.79% Cu	47.41% Zn	71.20 %In,
-15% H_2SO_4	(900C, 6h, S:L = 1:10)	93.76% Cu	91.64% Zn	97.59 %In.

It can be seen that leaching of jarosite using HCl acid under the most aggressive conditions results in high recovery of Cu, Zn and In, while leaching of jarosite in nitric acid yields relatively good recovery of In but also low recovery of Cu and Zn. Leaching in sulfuric acid yields the best recovery of all considered metals. Leaching with hydrochloric acid under selected conditions would not be safe due to the aggressive environment. Leaching with nitric acid releases a large amount of aggressive nitrogen oxides. Considering the price of sulfuric acid in relation to others that were used for leaching and working conditions that are not rigorous, it is considered that the choice of this acid is justified. The solution obtained using sulfuric acid would be further treated in order to selectively separations of the metals.

ACKNOWLEDGEMENT

This work was financially supported by the Ministry of Education, Science and Technological Development of the Republic of Serbia, Grant No. 451-03-9/2021-14/ 200052.

REFERENCES

1. Yong-xing, Z., Jin-fang, L.V., Wei, L., Wen-qing, Q., Shu-ming, W. (2016) An innovative technology for recovery of zinc, lead and silver from zinc leaching residue. Physicochem. Probl. Miner. Process., 52 (2) 943–954.
2. Yayun, W., Huifen, Y., Weihao, Z., Ronglong, S., Bo, J. (2018) Study on recovery of lead, zinc, iron from jarosite residues and simultaneous sulfur fixation by direct reduction. Physicochem. Probl. Miner. Process., 54 (2) 517-526.
3. Stanojević, D., Filipović-Petrović, L. (2014) Doprinos integrisanoj valorizaciji metala u hidrometalurgiji cink. Zaštita materijala, 55 (1) 25-35.
4. Stanojević, D., Todorović, M. (1998) Valorisation of useful metals from by-products of hydrometallurgical manufacturing of zinc. 1st International Conference of Chemical Societies of the South-East European Countries: “Chemical Sciences and Industry”, 1.-4. June, Solun, Greece, Vol II, PO 729.
5. Stanojevic, D., Rajkovic, M.B., Toskovic, D. (2006) Extraction of useful metals from lead-silver cake in the process of hydrometallurgical zinc production by leaching in calcium-chloride solution. Buletin of Electrochemistry, Karaikudi (India), 22, 337-341.
6. Deng, Z. (2016) Acid Leaching Zinc and Indium with Reduction Ferric Simultaneously From Marmatite and High Iron Neutral Leaching Residue. Rare metal technology, First published: 22 January, Chapter 6.

XIV International Mineral Processing
and Recycling Conference
Belgrade, Serbia, 12-14 May 2021

ANALYSIS OF THE EFFECTS OF THE VARIABLES IN THE PROCESS OF CADMIUM SEPARATION BY SEASHELL WASTE

Marija Šljivić-Ivanović[1#], Mihajlo Jović[1], Slavko Smiljanić[2], Ivana Smičiklas[1]
[1] "VINČA" Institute of Nuclear Sciences - National Institute of the Republic of Serbia, University of Belgrade, Belgrade, Serbia
[2] University of East Sarajevo, Faculty of Technology Zvornik, Zvornik, Republic of Srpska, Bosnia and Herzegovina

ABSTRACT – The full experimental design approach was utilized for the investigation of Cd separation by seashell waste. The effect of process factors (seashell type, particle size, and initial metal concentration) was determined and compared for process efficiency and final pH value as system responses. Only main effects were significant ($p<0.05$), while the effects of their interactions were not statistically significant. Obtained Cd sorption capacity of seashell waste was in the range of 0.3 mg/g-150 mg/g, depending on the conditions. The results point to the promising way of utilizing waste seashells as a material suitable for the separation of Cd.

Keywords: Seashell Waste, Water Purification, Cd, Experimental Design.

INTRODUCTION

The significant task facing contemporary society is to find out innovative solutions for the recycling of different waste types to produce new materials or energy. Seashells are an example of abundant waste potentially hazardous to the environment of coastal areas, especially near shellfish farms and pre-processing plants. On the other hand, the shells are a rich secondary source of $CaCO_3$ [1], with wide potential applicability in construction materials, rubber, plastics, paper, etc. Additionally, carbonates are commonly applied as neutralizing agents for acidic industrial wastewaters and acidic soil.

The research conducted so far point to the possibility of seashells' application as sorbent material for the removal of heavy metals and radionuclides [2-4]. The divalent cations removal is based on the ion exchange with calcium, chemisorption, and precipitation. The complexity of systems containing seashells and metal solutions was previously highlighted, as they are highly dependent on experimental conditions, chemical properties of the pollutant, as well as on their interactions [1]. Furthermore, the metal removal efficiency was found to be dependent on the seashell type due to the differences in the physicochemical properties, including the contribution of $CaCO_3$ polymorphs like calcite and aragonite [5].

Bearing in mind the large influence of process conditions on metal separation efficiency, this study aimed to investigate and compare the effect of chosen factors on

---

[#] corresponding author: marijasljivic@vin.bg.ac.rs

Cd separation. A full factorial design was used to identify significant factors and their interactions.

EXPERIMENTAL

The shells of *Mytilus galloprovincialis* (MG) and *Ostrea edulis* (OE) were sampled in Boka Kotorska Bay (Southeastern Adriatic Sea, Montenegro). About 10 kg of each seashell type were cleaned, washed, and dried in the oven at 60 °C for 48 h. The shells were subsequently milled and sieved into different particle size fractions (0.045–0.125 mm, 0.125–0.2 mm, and 0.2–1 mm).

Cadmium separation was investigated using solutions with initial Cd concentrations of 12.12 mg/L, 120.5 mg/L, and 1,150 mg/L, prepared from $Cd(NO_3)_2$. These simulated wastewater samples were equilibrated on a laboratory shaker with 0.1 g of MG or OE (solid/liquid ratio = 1:200 g/mL) for 24 h. The initial pH value of Cd solutions was 5±0.2.

Seashell type, initial metal concentration, and sorbent granulation were the selected process variables (Table 1). The experiments were conducted, and the data were analyzed according to the full factorial design matrix obtained by the MINITAB software (Table 2).

Table 1 Process variables and their levels

Symbol	Factor	Unit	Level 1	Level 2	Level 3
A	Cd concentration	mg/L	12.12	120.5	1,150
B	Particle size	mm	0.045-0.125	0.125-0.2	0.2-1
C	Seashell type	-	O.E	M.G	

After equilibration, the solid and liquid phases were separated by filtration, and the residual Cd concentrations were determined using Perkin Elmer 3100 Atomic Absorption Spectrometer. The pH values before and after the process were measured by WTW InoLab pH-meter, equipped with SenTix 81 glass electrode.

RESULTS AND DISCUSSION

The experimental results are presented with process conditions for each experimental run in Table 2.

The amounts of Cd removed by seashell waste varied in the wide range between 0.3 mg/g and 150.5 mg/g, demonstrating the significance of experimental factors and their levels (Table 2). The extreme values were observed when the most concentrated Cd solution was used in combination with the MG seashell type with different particle size fractions.

Furthermore, final pH values were in the range of 6.6 to 9.3 (Table 2). The values were commonly higher in respect to the initial pH due to the buffering properties of applied carbonate-based sorbents; however, they strongly depended on the experimental conditions.

In order to investigate the effects of process variables on system responses, the main effect plots were constructed. The main effect plot offers the information if the change of variable decreases or increases the selected system response. The mean for a given level of the variable is the average of all responses obtained for that level. In this plot, the means of responses for process variable levels are plotted and connected with the straight line. The overall mean response of the system for all levels of all factors is given with the horizontal line. Consequently, the strength of the effect of the chosen variable is indicated by the slope of the straight line in relation to the horizontal line.

Table 2 Experimental design matrix, and corresponding values of Cd sorption capacity, process efficiency and final pH values

	A	B	C	Sorption capacity (mg/g)	Final pH	Process efficiency (%)
1	1	2	1	2.4	9.2	99.7
2	2	2	2	22.4	8.4	96.1
3	2	1	1	21.3	7.6	88.9
4	2	2	1	16.7	7.3	69.4
5	1	2	2	2.1	9.1	93.9
6	2	1	2	22.9	8.6	98.3
7	1	1	1	2.4	9.3	99.7
8	3	2	1	23.4	6.6	10.2
9	3	3	1	3.6	6.5	1.6
10	3	2	2	70.4	6.6	33.3
11	1	3	1	2.4	9.1	98.4
12	2	3	2	13.6	7.3	58.5
13	1	1	2	2.2	9.3	98.5
14	3	1	1	19.4	6.6	8.5
15	1	3	2	2.2	9.1	96.5
16	2	3	1	5.4	7.1	22.6
17	3	3	2	0.3	6.5	0.2
18	3	1	2	150.5	6.9	71.3

The main effect plot (Figure 1,a) showed that the increase in solution final pH value was provoked both by the decrease in the initial metal concentration (Factor A), and by the decrease in the particle size fraction (Factor B), however, the effect of factor A was stronger. Furthermore, higher pH values were measured in the filtrates after contact with MG than OE.

The change in the levels of process variables had the same effect on Cd removal efficiency as on the final pH (Figure 1,c), which indicates a strong relationship between the final pH and the percentage of Cd removed from the solution.

The interaction plots for final pH (Figure 1,b) and for process efficiency (Figure 1,d) revealed that the interactions between process variables were negligible.

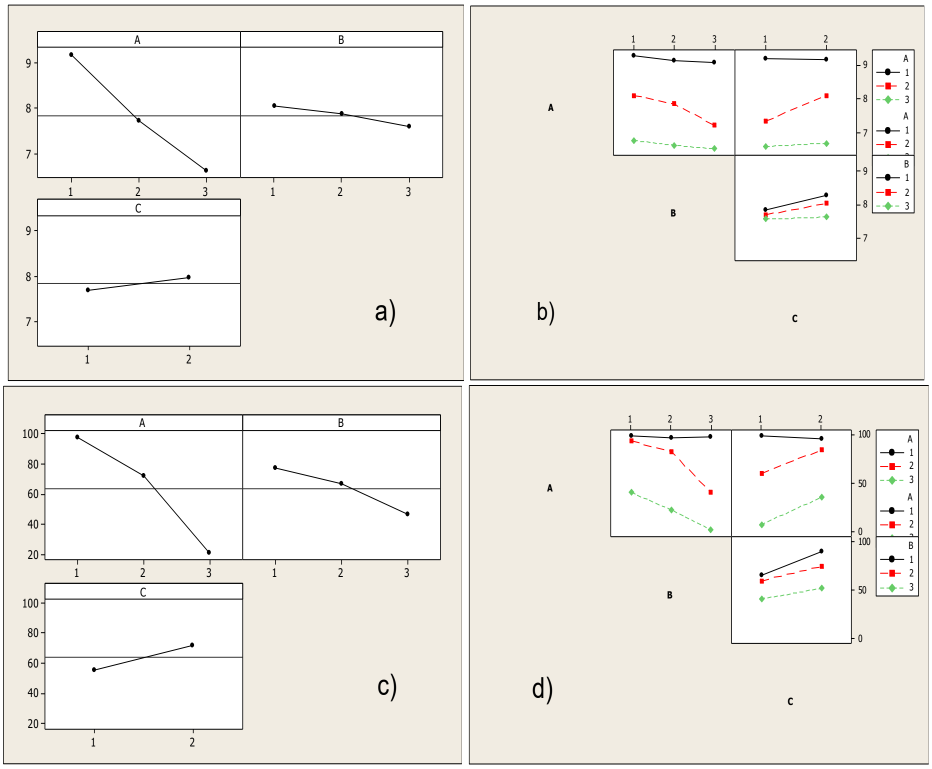

Figure 1 Main effect plots for a) final pH and c) process efficiency;
Interaction plots for b) final pH and d) process efficiency

STATISTICAL ANALYSIS

The behavior of the system can be expressed by multiple linear regression model given as:

$$Y_{predicted} = b_0 + \Sigma b_i x_i \qquad (1)$$

where Y is predicted response, b_0 is the value of fitted response at the center point of the design, b_i are regression coefficients, and x_i are variables that can be expressed as main effects (x_i=A, B, C…) or any of their interactions (x_i=A·B, A·B·C, …). This model is linear in the sense that the unknown regression coefficients appear in the linear form [6].

The adequacy of the proposed linear regression was tested using Analysis of variance (ANOVA). ANOVA test (Table 3) approved that only main effects were statistically significant ($p<0.05$). Considering final pH as system response, the statistically significant factors are A, B and C at $p<0.05$. Otherwise, only factor A significantly influences process efficiency. The interaction of initial solution concentration and sorbent type was significant at $p<0.1$, which may indicate that different sorption mechanisms dominant at lower and higher metal concentrations for different seashell types.

Table 3 ANOVA test

<table>
<tr><th colspan="7">Analysis of Variance for pH final</th></tr>
<tr><td>Source</td><td>DF</td><td>Seq SS</td><td>Adj SS</td><td>Adj MS</td><td>F</td><td>P</td></tr>
<tr><td>A</td><td>2</td><td>19.8978</td><td>19.8978</td><td>9.9489</td><td>235.63</td><td>0.000</td></tr>
<tr><td>B</td><td>2</td><td>0.6144</td><td>0.6144</td><td>0.3072</td><td>7.28</td><td>0.046</td></tr>
<tr><td>C</td><td>1</td><td>0.3472</td><td>0.3472</td><td>0.3472</td><td>8.22</td><td>0.046</td></tr>
<tr><td>A*B</td><td>4</td><td>0.3556</td><td>0.3556</td><td>0.0889</td><td>2.11</td><td>0.244</td></tr>
<tr><td>A*C</td><td>2</td><td>0.5511</td><td>0.5511</td><td>0.2756</td><td>6.53</td><td>0.055</td></tr>
<tr><td>B*C</td><td>2</td><td>0.1078</td><td>0.1078</td><td>0.0539</td><td>1.28</td><td>0.373</td></tr>
<tr><td>Error</td><td>4</td><td>0.1689</td><td>0.1689</td><td>0.0422</td><td></td><td></td></tr>
<tr><td>Total</td><td>17</td><td>22.0428</td><td></td><td></td><td></td><td></td></tr>
<tr><td colspan="7">S = 0.205480 R-Sq = 99.23% R-Sq(adj) = 96.74%</td></tr>
<tr><th colspan="7">Analysis of Variance for process efficiency</th></tr>
<tr><td>Source</td><td>DF</td><td>Seq SS</td><td>Adj SS</td><td>Adj MS</td><td>F</td><td>P</td></tr>
<tr><td>A</td><td>2</td><td>18,430.5</td><td>18,430.5</td><td>9,215.2</td><td>33.29</td><td>0.003</td></tr>
<tr><td>B</td><td>2</td><td>3,034.0</td><td>3,034.0</td><td>1,517.0</td><td>5.48</td><td>0.071</td></tr>
<tr><td>C</td><td>1</td><td>1,210.3</td><td>1,210.3</td><td>1,210.3</td><td>4.37</td><td>0.105</td></tr>
<tr><td>A*B</td><td>4</td><td>1,636.9</td><td>1,636.9</td><td>409.2</td><td>1.48</td><td>0.357</td></tr>
<tr><td>A*C</td><td>2</td><td>856.9</td><td>856.9</td><td>428.5</td><td>1.55</td><td>0.318</td></tr>
<tr><td>B*C</td><td>2</td><td>129.6</td><td>129.6</td><td>64.8</td><td>0.23</td><td>0.801</td></tr>
<tr><td>Error</td><td>4</td><td>1,107.2</td><td>1,107.2</td><td>276.8</td><td></td><td></td></tr>
<tr><td>Total</td><td>17</td><td>26,405.5</td><td></td><td></td><td></td><td></td></tr>
<tr><td colspan="7">S = 16.6373 R-Sq = 95.81% R-Sq(adj) = 82.18%</td></tr>
</table>

CONCLUSION

The applicability of seashell waste for Cd removal was tested. The effect of applied sorbent type (Mytilus galloprovincialis (MG) and *Ostrea edulis* (OE)), the particle size fraction, and initial metal concentration was investigated in terms of sorption capacity, process efficiency, and final pH of the solution. The initial metal concentration is the most significant factor influencing system responses. The increase in initial metal concentration and seashell particle size led to a decrease in both the final pH and the process efficiency. The addition of MG to simulated wastewaters provoked higher values of system responses, indicating that seashell composition affects the process. In the investigated range of experimental conditions, significant interactions of the factors were not found. The results point to the possible use of seashell waste in Cd separation, as high efficiencies of water purification can be achieved by optimizing the levels of the factors. Furthermore, the experimental design approach was found a suitable and useful tool for the investigation of the sorption processes.

ACKNOWLEDGEMENT

The authors would like to acknowledge the financial support of the Ministry of Education, Science and Technological Development of the Republic of Serbia.

REFERENCES

1. Egerić, M., Smičiklas, I., Mraković, A., Jović, M. Šljivić-Ivanović, M., Antanasijević, D., Ristić, M. (2018) Experimental and theoretical consideration of the factors influencing cationic pollutants retention by seashell waste. Journal of Chemical Technology and Biotechnology, 93, 1477–1487.
2. Du, Y., Lian, F., Zhu, L. (2011) Biosorption of divalent Pb, Cd and Zn on aragonite and calcite mollusk shells. Environmental Pollution, 159, 1763–1768.
3. Wu, Q., Chen, J., Clark, M., Yu, Y. (2014) Adsorption of copper to different biogenic oyster shell structures. Applied Surface Science, 311, 264–272.
4. Bozbas, S.K., Boz, Y., (2016) Low-cost biosorbent: *Anadara inaequivalvis* shells for removal of Pb(II) and Cu(II) from aqueous solution. Process Safety and Environmental Protection, 103, 144–152.
5. Janković, B., Smičiklas, I., Manić, N., Mraković, A., Mandić, M., Veljović, Đ., Jović, M. (2020) Thermo-oxidative evolution and physico-chemical characterization of seashell waste for application in commercial sectors. Thermochimica Acta, 686, 178568.
6. Yates, F. (1937.) *The Design and Analysis of Factorial Experiments*. Imperial Bureau of Soil Science, Harpenden.

XIV International Mineral Processing
and Recycling Conference
Belgrade, Serbia, 12-14 May 2021

DIFFERENT NEUTRALIZING AGENTS USED FOR TREATMENT OF ACID MINE WATER

Dragana Bozić[1#], Radmila Marković[1], Zoran Stevanović[1], Daniela Dascalu[2], Vulpe Bianca[2], Mariana Adina Matica[2]
[1] Mining and Metallurgy Institute Bor, Bor, Serbia
[2] West University of Timisoara, Department of Biology-Chemistry and Advanced Environmental Research Laboratories, Timisoara, Romania

ABSTRACT – Different neutralization agents are investigated for neutralization process of acid mine drainage from Robule Lake aim to precipitate the metal ions in a different sludge type. $Ca(OH)_2$ and $CaCO_3$ are used as neutralization agents and the neutralization process was done in several stages. After solution reached pH 3 or 4, each sample was filtered. AMD samples neutralized in the first neutralization step were used as start samples for second neutralization step to reached pH 7; 7.5 or 8. Metal ions concentrations at different pH values, as well as the consumption of the neutralizing agents were monitored.

Keywords: Neutralization, Acid Mine Drainage, Calcium Hydroxide, Calcium Carbonate.

INTRODUCTION

Acid mine drainage (AMD) as a consequence of the mining activities in the Eastern Serbia causes water systems pollution around the mine. Aim to protect water system around the mine, AMD require treatment through different treatment methods. Mine wastewater from the area of active or closed copper mines contains heavy metal ions where the concentrations of copper and iron ions are dominant [1]. The concentration of the other heavy metal ions (Mn, Cd, Zn, Pb, Ni, etc.) depends on the mineralization of an ore body but their concentration is much lower than the concentration of copper or iron ions. pH value of those water is, as a rule, mostly between 2.5 and 4 and those wastewaters have the acidic characteristics [2].

The neutralization method is a very effective for removal the dissolved metals from the wastewater due to the pH dependence of the metal solubility. However, removal of some metal ions, such as Ni and Mn, a higher pH value over the effluent standard is required. In this case, additional treatment methods are needed to decrease the pH value according the effluent standard. In Bor area in Serbia, all of the wastewater from the mine area is released out to natural environment and through the tributaries of Bor River and Timok River flowing in Danube River without any treatment, and has the negative environmental impact [3].

The aim of this work was to investigate the possibility of neutralization the AMD from Bor mine area by using various neutralizing agents. Also, the aim was to select the most suitable neutralizing agent for further use on the basis of the obtained chemical results

---

[#] corresponding author: dragana.bozic@irmbor.co.rs after the neutralization of water and the amount of consumed neutralizing agent.

EXPERIMENTAL

Real AMD sample from Robule Lake was used for neutralization. Start pH of this water was 2.67. As a neutralizing agent are used $Ca(OH)_2$, in a form of lame milk with concentration of 25 g/L, and $CaCO_3$ p.a. quality.

Neutralization of selected AMD with $Ca(OH)_2$ and $CaCO_3$ was done in several stages up to different pH values depending on chemical characterization of neutralized water, and depending on the legislation for surface water. Lime milk and $CaCO_3$ was used as a neutralizer to reached pH 3 or 4 in a first neutralization step. To AMD sample continually was added a certain amount of neutralization agent in a batch reactor. Stirring was performed with a magnetic stirrer, at a constant speed of 400 rpm/min, in order to avoid precipitation. After solution reached pH 3 or 4, each solution sample was filtered by vacuum filtration to separate solid from liquid phase. Dewatered sludge was dried to constant mass at 40 ^oC. Liquid sample was collected and given on chemical analyses according to the chemical characterization of the real sample. AMD samples neutralized in the first neutralization step up to pH 3 or 4 were used as start samples for second neutralization step to reached pH 7; 7.5 or 8. As in the first neutralization step, liquid and solid phase were separated by vacuum filtration. Liquid phase was used for the chemical analyses and solid phase was dried at 40 ^oC and measured after reaching the constant mass value

RESULTS AND DISCUSSION

In the Table 1 are given the results of chemical analyses of AMD from the site.

Table 1 Chemical analysis of real AMD samples

Neutralizing agent	Elements								
	Fe	**Mn**	**Cu**	**Zn**	**As**	**Ni**	**Pb**	**Cd**	**S**
	concentration, mg/L								
$Ca(OH)_2$	322.6	90.8	34.7	12.8	0.0042	0.413	0.007	0.04	2376
$CaCO_3$	506.2	86.1	51.0	19.5	<0.020	0.56	<0.020	0.11	3973

Neutralization with $Ca(OH)_2$

Neutralization process is carried out with 2000 ml of real AMD to reach pH 3 or 4. As a neutralizing agent is used $Ca(OH)_2$, as a lime milk with concentration of 25 g/L. After reached the pH 3 or 4, solution is filtered by vacuum filtration with aim to separate solid from liquid phase. Dewatered sludge was dried to constant mass. Results of the chemical analyses of solution are shown in the following Table 2.

From the Table 2, it can be seen that at pH 4 there is a significant drop in the concentration of iron ions while the concentrations of the other metal ions remained unchanged. It can be concluded that the iron ions precipitated in the sludge while the other metal ions remained in solution.

AMD neutralized up to pH 3 or pH 4 was used as start samples for neutralization up to 7, 7.5 and 8. As in the first neutralization stage, liquid and solid phase are separated by vacuum filtration. Liquid phase is used for the chemical analyses and solid phase is dried and measured after reaching the constant mass value. Chemical analyses of solution are shown in the following Table 3 and 4.

Table 2 Chemical analysis of solutions after neutralization

Neutralization from start pH value (2.67) to different pH values	**Elements**								
	Fe	**Mn**	**Cu**	**Zn**	**As**	**Ni**	**Pb**	**Cd**	**S**
	concentration, mg/L								
pH 3	274.1	62.1	31.6	12.6	0.004	0.4	0.017	0.04	2245
pH 4	0.98	62.7	31.4	12.4	0.001	0.4	0.003	0.04	2022

Table 3 Chemical analysis of solutions after neutralization from pH 3 to pH7, 7.5 or 8

Neutralization from pH 3 to different pH values	**Elements**								
	Fe	**Mn**	**Cu**	**Zn**	**As**	**Ni**	**Pb**	**Cd**	**S**
	concentration, mg/L								
to pH 7	0.14	38.2	0.06	0.44	0.0004	0.15	0.0007	0.01	1950
to pH 7.5	0.03	28.3	0.04	0.13	0.0004	0.08	0.0007	0.006	1976
to pH 8	0.09	20	0.03	0.03	0.0004	0.03	0.0007	0.002	1994

Table 4 Chemical analysis of solutions after neutralization from pH 4 to pH 7, 7.5 or 8

Neutralization from pH 4 to different pH values	**Elements**								
	Fe	**Mn**	**Cu**	**Zn**	**As**	**Ni**	**Pb**	**Cd**	**S**
	concentration, mg/L								
to pH 7	0.01	42.2	0.04	0.65	0.0009	0.21	0.001	0.02	1962
to pH 7.5	0.01	39.8	0.05	0.22	0.0008	0.14	0.0002	0.015	1949
to pH 8	0.01	36.8	0.03	0.11	0.0008	0.1	0.0004	0.009	1936

Table 5 Consumption of $Ca(OH)_2$ and sludge mass

Sample	**Consumption of 25 g/L $Ca(OH)_2$, ml/L**	**Sludge mass, g**
pH start to pH 3	3.5	0.7
from pH 3 to pH 7	65.4	2.9
from pH 3 to pH 7.5	67.2	3.3
from pH 3 to pH 8	70	3.7
pH start to pH 4	25	3.93
from pH 4 to pH 7	31.8	1.1
from pH 4 to pH 7.5	33.8	1.3
from pH 4 to pH 8	40.3	2.1

From the Tables 3 and 4, it can be seen that all the metals ions from the solution precipitated into a sludge. Only the concentration of manganese ions remained unchanged due to the fact that manganese precipitates at higher pH values, which is around 10. In the Table 5 is shown the lime consumption during the neutralization as well as the mass of the obtained sludge.

Neutralization with $CaCO_3$

Neutralization process is carried out with 2000 ml of real AMD to reach pH 3 or pH 4. $CaCO_3$ is used as a neutralizing agent. After reached the pH 3 or 4, solution is filtered by vacuum filtration with aim to separate solid from liquid phase. Dewatered sludge was dried to constant mass. Chemical analyses of solution are shown in the following Table 6.

Table 6 Chemical analysis of solutions after neutralization to pH 3 or 4

Neutralization from start pH 2.67	Elements								
	Fe	Mn	Cu	Zn	As	Ni	Pb	Cd	S
	concentration, mg/L								
to pH 3	39.9	79.4	47.3	18	<0.02	0.53	<0.02	0.06	3384
to pH 4	196	85.9	47.3	18.6	<0.02	0.58	<0.02	0.08	3163

AMD neutralized to pH 3 or 4 was used as start samples for neutralization to pH 7, 7.5 or 8. As in the first neutralization stage, liquid and solid phase are separated by vacuum filtration. Liquid phase is used for the chemical analyses and solid phase is dried and measured after reaching the constant mass value. Chemical analyses of solution are shown in the following Table 7 and 8.

Table 7 Chemical analysis of solutions after neutralization from pH 3 to pH 7, 7.5 or 8

Neutralization from pH 3 to different pH values	Elements								
	Fe	Mn	Cu	Zn	As	Ni	Pb	Cd	S
	concentration, mg/L								
to pH 7	<0.007	46.1	0.11	1.8	<0.02	0.24	<0.02	0.014	1772
to pH 7.5	<0.007	11.6	0.04	0.18	<0.02	0.16	<0.02	0.007	2622
to pH 8	<0.007	0.23	0.03	0.03	<0.02	<0.007	<0.02	0.012	2240

Table 8 Chemical analysis of solutions after neutralization from pH 4 to pH 7, 7.5 or 8

Neutralization from pH 4 to different pH values	Elements								
	Fe	Mn	Cu	Zn	As	Ni	Pb	Cd	S
	concentration, mg/L								
to pH 7	<0.007	32.1	0.05	1.1	<0.020	0.37	<0.020	<0.008	1962
to pH 7.5	<0.007	8.8	0.03	0.2	<0.020	0.16	<0.020	<0.008	1949
to pH 8	<0.007	8.4	0.03	0.21	<0.020	0.1	<0.020	<0.008	1936

From the Tables 7 and 8, it can be seen that all the metals ions from the solution precipitated into a sludge. Manganese concentration also decreased, which was not the case when $Ca(OH)_2$ is used as a neutralizing agent. The assumption is that a large amount of $CaCO_3$ consumption led to decreased manganese.

Table 9 shows the lime consumption during the neutralization process as well as the mass of the obtained sludge.

Table 9 Consumption of $CaCO_3$ and sludge mass

Sample	Consumption of $CaCO_3$, g	Sludge mass, g
start to pH 3	2	2.15
from pH 3 to pH 7	125	128.9
from pH 3 to pH 7.5	200	202.3
from pH 3 to pH 8	275	279.6
start to pH 4	4	4.15
from pH 4 to pH 7	101	103.7
from pH 4 to pH 7.5	175	175.3
from pH 4 to pH 8	250	254.6

From the Tables 5 and 9, it can be seen that the consumption of calcium carbonate is much higher than the consumption of calcium hydroxide. As chemical analyzes have shown almost the same results of changes in metal ions concentration, it can be concluded that it is better to use calcium hydroxide to neutralize acidic mine water.

CONCLUSION

The experiment results suggest that the two-step pH control neutralization method is effective and practical to recover iron and copper ions separately in the sludge generated along the process and are reliable in processing the water quality to the requited levels. The use of both neutralizing agents gave good results. however, since the consumption of calcium hydroxide is much lower compared to the consumption of calcium carbonate, the conclusion is that it is more justified to use calcium hydroxide to neutralize acidic mine wastewater.

ACKNOWLEDGEMENTS

We acknowledge the financial support of the Project RoRS 337- ROmania Serbia NETwork for assessing and disseminating the impact of copper mining activities on water quality in the cross-border area (RoS-NET2), implemented under the Interreg-IPA Cross-border Cooperation Romania-Serbia Programme that is financed by the European Union under the Instrument for Pre-accession Assistance (IPA II) and co-financed by the partner states in the Programme.

This work was also financially supported by the Ministry of Education, Science and Technological Development of the Republic of Serbia, Grant No. 451-03-9/2021-14/ 200052.

REFERENCES

1. Masuda, N., Marković, R., Bessho, M., Božić, D., Obradović, Lj., Marinković, V., Ishiyama, D., Stevanović, Z. (2017) A new approach to recover dissolved metals in AMD by two-step pH control on the neutralization method, 13th International Mine Water Association Congress – Mine Water & Circular Economy, 25-30 June 2017, Lappeenranta, Finland, proceedings, 1111-1118.
2. Markovic, R., Bessho, M., Masuda, N., Stevanovic, Z., Bozic, D., Apostolovski Trujic, T., and Gardic, V. (2020) New Approach of Metals Removal from Acid Mine Drainage,

Appl. Sci., 10, 5925.

3. Masuda, N., Marković, R., Božić, D., Bessho, M., Inoue, T., Hoshino, K., Ishiyama, D., Stevanović, Z. (2019), Experiment results of metal recovery by a two-step neutralization process from AMD from a copper mine in Serbia, IMWA 2019 Conference – Mine water: Technological and Ecological Challenges, 15-19 July 2019, Perm, Rusia, proceedings, 232-237.

XIV International Mineral Processing and Recycling Conference
Belgrade, Serbia, 12-14 May 2021

METAL RECOVERY FROM SLUDGE OBTAINED DURING THE NEUTRALIZATION PROCESSES OF AMD WATER

Ljiljana Avramović[1#], Radojka Jonović[1], Vanja Trifunović[1], Vojka Gardić[1], Mile Bugarin[1], Mariana Adina Matica[2], Gheorghița Menghiu[2]
[1] Mining and Metallurgy Institute, Bor, Republic of Serbia
[2] West University of Timisoara, Department of Biology-Chemistry and Advanced Environmental Research Laboratories, Timisoara, Romania

ABSTRACT – Investigations of the metal recovery process from the sludge formed during the neutralization of acid mine drainage (AMD) water at pH 8 were performed at the laboratory level. The metal recovery process included the following technological phases: sludge leaching, solvent extraction (SX) of pregnant leaching solution in order to selectively separate copper from the leaching solution, and obtaining zinc-based products from the solution after the SX process. Preliminary results indicate a high degree of separation of copper (about 91%) and zinc (about 98%) from sludge.

Keywords: AMD Waters, Metal Recovery, Leaching, SX-EW, Neutralization.

INTRODUCTION

Acid mine drainage waters (AMD) are waters formed by the oxidation of pyrite and other sulfide minerals under the action of air and water. Wastewater generated in ZiJin Bor's plants (either directly during current production or indirectly due to decomposition of delayed mine overburden and flotation tailings by formation of acidic drainage waters) pollutes the Borska and Krivelj rivers, which merge to form the Bela river which flows into the river Timok, and Timok into the Danube river. These pollutants are most often represented by low pH value, increased content of heavy metal ions, suspended particles and fine particles of flotation tailings deposited in the valleys of these rivers on an area of over 2000 hectares. Robule Lake, formed at the base of mining overburden Ostreljski plans (Copper mine Bor), was created as a result of mining activities. It is a typical example of acidic drainage water whose pH value is around 2.5 [1-5].

EXPERIMENTAL

The content of heavy metals in AMD water is: Cu=34 mg/l, Fe=320 mg/l, Mn=90 mg/l, Zn=12 mg/l, As=0.004 mg/l. Sludge formed during the neutralization of acid mine drainage (AMD) water at pH 8 with $Ca(OH)_2$ was treated in aim to recover valuable metals [6,7].

Chemical characterization of sludge used for leaching process is presented in Table 1.

[#] corresponding author: ljiljana.avramovic@irmbor.co.rs

Table 1 Chemical characterization of sludge obtained after neutralization with $Ca(OH)_2$ at pH 8

Element	Unit	Content	Element	Unit	Content
Al	%	7.58	Cr	ppm	4.60
Mg	%	3.19	Co	ppm	435.90
Mn	%	2.11	Ni	ppm	202.60
Fe	%	0.96	As	ppm	9.80
S	%	12.98	Cd	ppm	18.80
Zn	%	0.73	Cs	ppm	0.16
Cu	%	1.70	Pb	ppm	<10
Sr	%	0.0075	Mo	ppm	<10
Ca	%	14.88	-	-	-

Copper and zinc recovery process from neutralization sludge include four technological phases: sludge leaching, solvent extraction and electrowinning of copper (SX-EW), precipitation of zinc carbonate and obtaining zinc oxide.

Schematic representation of technological phases used for treatment of sludge are presented in Figure 1.

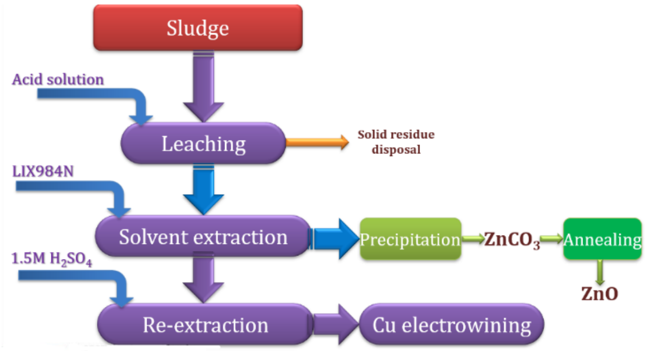

Figure 1 Schematic representation of the sludge treatment process

Leaching process

In aim of recovery of copper and zinc, sludge obtained after neutralization was leached at atmospheric pressure and temperature on following conditions: 1.2 M H_2SO_4 as leaching reagent, pulp density 20%, stirring speed 300 rpm, reaction time 60 min [8-11].

Solvent extraction process (SX)

The pregnant leaching solution (PLS) obtained after leaching process was treated in a solvent extraction process to selectively remove Cu from solution. Value of pH of solution was set from 0.94. at 1.49 using 10% solution of $Ca(OH)_2$, before starting of SX process. The influence of extractant type for the SX process was investigated. As solvent kerosene was used. For investigations of SX process four extractants were used: LIX984N, LIX622N, M5910 and M5640 with phase ratio org/aq=1:1, while re-extraction process was performed with 1.5 M H_2SO_4 with phase ratio org/aq=5:1. Experiments of solvent extraction and re-extraction were performed in two stages. The duration of each of the processes was 15 min [10-13].

Equipment used for all the experiments were glass separation funnels and shaker with regulated time and intensity of mixing the phases. At the end of two-step extraction and two-step re-extraction experiments, separated aqueous phase were analyzed by the ICP method in order to determine the metal concentration.

Precipitation of zinc

After solvent extraction of copper using LIX984N as extractant, from aqueous phase zinc was precipitated in the form of zinc carbonate by a two-stage neutralization process. The first stage of neutralization process was performed in order to remove iron from the solution, and the second stage in order to precipitate zinc in the form of zinc carbonate.

Two samples of obtained zinc carbonate were annealed in a chamber furnace at 450 °C, for 2 h and 4 h in aim to obtain zinc oxide. Samples of both zinc oxides were analyzed by the ICP method.

RESULTS AND DISCUSSION

Leaching process

Chemical composition of pregnant leaching solution (PLS), used for investigation of solvent extraction process, is given in Table 2.

Table 2 Concentrations of metals in PLS

Element	Fe	Mn	Cu	Mo	Zn	As	Ni	Pb	Cd	Cr	Se
Conc. (mg/l)	1549.7	1798.2	3104.4	1.2	1317.1	<0.02	22.7	<0.02	1.9	0.16	<0.033

Achieved leaching degree for Cu was 99.3%, and for Zn 99.4%.

Solvent extraction process

Figure 2 shows separating of phases in process extraction and re-extractions. In Table 3 are presented extraction and re-extraction degrees of Cu, Fe and Zn depending on the type of extractant.

Table 3 Extraction and re-extraction degrees od Cu, Fe and Zn

Extractant	Extraction degree 1st +2nd (%)			Re-extraction degree 1st +2nd (%)		
	Cu	Fe	Zn	Cu	Fe	Zn
LIX984N	98.55	14.38	15.69	73.31	13.98	10.99
LIX622N	99.30	19.03	30.41	68.65	10.62	1.44
M5910	98.17	17.95	18.21	65.87	7.43	6.44
M5640	98.89	69.29	40.00	73.01	5.19	1.22

1st EX 2nd EX

1st REX 2nd REX

Figure 2 Separating of phases in process extraction and re-extractions

Best selectivity for copper in relation to iron and zinc was achieved using LIX984N as extractant.

Solution obtained after re-extraction process is suitable for further investigations of electrowinning process in aim to obtain copper commercial quality.

Precipitation of zinc

After a two-stage process of neutralization and precipitation of zinc carbonate in the annealing process in the time of 2h (sample I ZnO) and 4 h (sample II ZnO), zinc oxides were obtained with contents of Zn 72% and 75% respectively.

CONCLUSION

After investigations of proposed technological processes of copper and zinc recovery from sludge obtained by neutralization of AMD water, following results were achieved:

- leaching degree of zinc was 99.4% and copper 99.3%;
- extraction degree of Cu using LIX984N was 98.55%,

- satisfactory degree of selective separation of copper in relation to zinc and iron has been achieved,
- zinc oxide with content of Zn 72-75% was obtained.

Advantage of the proposed procedure is the possibility to valorize copper from neutralization sludge, as well as valorize zinc to zinc oxide products.

ACKNOWLEDGEMENT

We acknowledge the financial support of the Project RoRS 337- ROmania Serbia NETwork for assessing and disseminating the impact of copper mining activities on water quality in the cross-border area (RoS-NET2), implemented under the Interreg-IPA Cross-border Cooperation Romania-Serbia Programme that is financed by the European Union under the Instrument for Pre-accession Assistance (IPA II) and co-financed by the partner states in the Programme. Also, this work was financially supported by the Ministry of Education, Science and Technological Development of the Republic of Serbia, Grant No. 451-03-9/2021-14/ 200052.

REFERENCES

1. Stevanović, Z., Obradović, Lj., Marković, R., Jonović, R., Avramović, Lj., Bugarin, M., Stevanović, J. (2014) Mine Waste Water Management in the Bor Municipality in Order to Protect the Bor River Water, https://www.researchgate.net/publication/268815386_Mine_Waste_Water_Management_in_the_Bor_Municipality_in_Order_to_Protect_the_Bor_River_Water.
2. Avramović, Lj., Stevanović, Z., Bugarin, M., Jonović, R., Marković, R., Gardić, V., Jonović, M., Đorđević, J. (2016) Characterization of Soil in the Coastal Area of the Bor River. Journal Materials Protection, 57 (3) 378–382.
3. Gardić, V., Marković, R., Masuda, N., Sokolović, J., Petrović, J., Đorđievski, S., Božić, D. (2017) The study of leachability and toxicity of sludge after neutralization of Saraka and Robule AMD wastewaters. Journal of Mining and Metallurgy, 17-29.
4. Dimitrijević, M. (2012) Acid mine drainage, Copper, 33-44.
5. Dimitrijević, M., Nujkić, M., Milić, S. (2012) The lime treatment of acid mine drainage, Copper, 45-56.
6. Iakovleva, E., Mäkilä, E., Salonen, J., Sitarz, M., Wang, S., Sillanpää, M., (2015) Acid mine drainage (AMD) treatment: Neutralization and toxic elements removal with unmodified and modified limestone. Ecological Engineering, 30-40.
7. Marković, R., Masuda, N., Bessho, M., Avramović, L., Gardić, V., Stanković, S., Sovrlić, Z. (2015) Neutralization of Artificial Acid Mine Drainage with Different Cu, Al and Fe Ions Content. In: 47th International October Conference on Mining and Metallurgy. Bor Lake, Serbia, 415-418.
8. Avramović, Lj., Jonović, R., Stevanović, Z., Shibayama, A., Haga, K., Takasaki, Y., Han, B., Urošević, D., Dimitrijević, S. (2018) Beaker Leaching and High Pressure Leaching of Flotation Tailings. In: International Satreps Conference Mining & Environment in Future. Bor Lake, Serbia, 39-44.
9. Avramović, Lj., Jonović, R., Trifunović, V., Gardić, V., Dimitrijević, S., Jonović, M., Haga, K. (2019) Treatment of flotation tailing using high pressure leaching and solvent extraction process. In: 51th International October Conference on Mining and Metallurgy. Bor Lake, Serbia, 175-178.

10. Haga, K., Godirilwe, L., Takasaki, Y., Ishiyama, D., Shibayama, A., Han, B., Avramović, Lj., Jonović, R., Dimitrijević, S., Stevanović, Z. (2019) Metal Recovery and Reducing of Environmental Loading of Copper Mine Tailings by High Pressure Leaching and SX-EW Process. In: 58th Annual Conference of Metallurgists (Com). Vancouver, Canada, 24-27.
11. Han, B., Altansukh, B., Haga, K., Stevanović, Z., Jonović, R., Avramović, Lj., Urosević, D., Takasaki, Y., Masuda, N., Ishiyama, D., Shibayama, A. (2018) Development of copper recovery process from flotation tailings by a combined method of high-pressure leaching solvent extraction. Journal Of Hazardous Materials, vol. 352, 192-203.
12. Conić, V., Avramović, Lj., Jonović, R., Marković, R., Bugarin, M. (2015) SX-EW Treatment of the Solution Obtained After Acid Leaching RTB Bor Flotation Tailing. In: XVI Balkan Mineral Processing Congress. Belgrade, Srbija, Proceedings, Volume II, 827-829.
13. Avramović, LJ., Jonović, R., Marković, R., Shibayama, A., Haga, K., Baisui, H., Urošević, D. (2017) Separation of copper and iron using LIX-984N by the solvent extraction. In: XII International Symposium on Recycling Technologies and Sustainable Development. Bor Lake, Bor, Serbia, 237-242.

XIV International Mineral Processing
and Recycling Conference
Belgrade, Serbia, 12-14 May 2021

STABILIZATION AND CHARACTERIZATION OF THE SOLID WASTE GENERATED IN NEUTRALIZATION SLUDGE LEACHING PROCESS

Vojka Gardić[1#], Zoran Stevanović[1], Radmila Marković[1], Ljiljana Avramović[1], Radojka Jonović[1], Dragana Bozić[1], Jelena Petrović[1], Renata Kovačević[1], Ljubiša Obradović[1], Vanja Trifunović[1], Bianca Boros[2], Adriana Isvoran[2], Vasile Ostafe[2]
[1] Mining and Metallurgy Institute Bor, Bor, Serbia
[2] West University of Timisoara, Department of Biology-Chemistry and Advanced Environmental Research Laboratories, Timisoara, Romania

ABSTRACT – Acid mine drainage from Robule Lake is treated by neutralization process. Generated sludge is reach in copper and because of that is treated by leaching process, during which generate new type of waste. Characterization of this type of waste shows that is non-hazardous waste with high mobility of sulphate ions in leachability test and high mobility of lead and cadmium ions in toxicity test. Developed stabilization process shows low influence on immobilization of sulfuric ions, but high influence on immobilization of cadmium and lead ions presents in solid waste.

Keywords: Characterization, Waste, Sludge, Stabilization, Leaching.

INTRODUCTION

The sulfidic minerals present in active or abounded tailing ponds during short or long disposal period, under oxidation condition, generates free acid. The leachate from this mine facilities are known as acid mine drainage (AMD). Simultaneous, under the acidic conditions trace metals became liberated from the tailings and reaches into solution causing acidification/heavy metals pollution of the surrounding soil, groundwater as well as rivers and streams that receiving such effluent. Further this phenomenon leads to the serious pollution of drinking water as well as loss of the agricultural land [1,2,3].

Low-cost treatment method for AMD is neutralization process. Neutralization sludge that is generated during the AMD neutralization treatment can be reach in some value elements. Aim to valorized present elements, leaching process is applying. During leaching process another type of sludge is generated.

The aim of this work is characterization and stabilization this type of waste.

EXPERIMENTAL

Experimental work consists of the following activities:

- Characterization of solid waste generated in neutralization sludge leaching process;

[#] Corresponding author: vojka.gardic@irmbor.co.rs

- Stabilization of solid waste generated in neutralization sludge leaching process;
- Characterization of stabilized solid waste.

Characterization of solid waste generated in neutralization sludge leaching process

Sludge generated in neutralization process of selected AMD – W1 is leached with sulfuric acid in controlled conditions (temperature and stirring).

Characterization of the solid waste generated in neutralization sludge leaching process was carried out in two phases:

- First - investigation of the waste leachability (LP procedure) by providing leaching test according to standard methods EN 12457-2 (Characterization of waste - Leaching - Compliance test for leaching of granular waste materials and sludges - Part 2: One stage batch test at a liquid-solid ratio of 10 l/kg for materials with a high content solids and particle size of less than 4 mm (with decreasing particle size, or without decreasing)) and
- Second - investigation of the waste toxicity (TCLP procedure) by providing Toxicity Characteristic Leaching Procedure according to standard method EPA 1311.

Stabilization of solid waste generated in neutralization sludge leaching process

Aim to ensure non-hazardous character of generated solid wastes after leaching for disposal on landfill for non-hazardous wastes, stabilization process is carried out.

Stabilization of the waste includes the following steps: determine the homogeneity of the waste; determine the moisture of the waste; determination the optimal ration lime and waste; determination of optimal contact time needed for stabilization process; confirmation defined parameters of stabilization by minimum five times repeated tests of leachability and toxicity of waste.

Characterization of the stabilized solid waste

Characterization of stabilized solid waste was carried out in two phases, same as for the solid waste generated in neutralization sludge leaching process.

RESULTS AND DISCUSSION

In the Table 1 are given the results of physicochemical testing waste (solid waste remaining after leaching) investigation of waste leachability according with SRPS EN 12457-2:2008. Moisture content in the sample is 45.44% and solid content is 54.56%.

Method SRPS EN ISO 11885 is used for As, Cu, Mo, Cd, Se, Ni, Hg, Pb, Cr, Zn, SO_4^{2-}, F^- and Cl^- determination, method SRPS EN 12506 for pH determination and EPA 120.1 for determination the conductivity.

In the Table 2 are given the results of physicochemical testing of toxic waste characteristics for disposal -TCLP test (EPA 1311).

Table 1 Results of physicochemical testing waste (solid waste remaining after leaching) leachability according with SRPS EN 12457-2:2008

Parameter	Unit	Measured value	The reference value for non-hazardous waste$^{2)}$	The reference value for non-hazardous waste$^{3)}$	The reference value for inert waste$^{4)}$
		Label of the sample			
		01.20.11 OR-10 L/kg			
Content in LP extract (neutral test, L/S = 10/1)					
Conductivity	µS/cm	2007	-	-	-
pH (25 °C)$^{1)}$	-	8.96	-	6-13	-
Arsenic, As	mg/kg dm	<0.020	25	2	0.5
Antimony, Sb	mg/kg dm	<0.5	5	0.7	0.06
Copper, Cu	mg/kg dm	0.096	100	50	2
Molybdenum, Mo	mg/kg dm	<0.007	30	10	0.5
Cadmium, Cd	mg/kg dm	<0.008	5	1	0.04
Selenium, Se	mg/kg dm	<0.033	7	0.5	0.1
Nickel, Ni	mg/kg dm	<0.007	40	10	0.4
Mercury, Hg	mg/kg dm	<0.005	2	0.2	0.01
Lead, Pb	mg/kg dm	0.44	50	10	0.5
Chromium, Cr	mg/kg dm	<0.020	70	10	0.5
Zinc, Zn	mg/kg dm	0.097	200	50	4
Sulphate, SO_4^{2-}	mg/kg dm	13 000	50000	20 000	1 000
Fluoride, F^-	mg/kg dm	10.4	500	150	10
Chloride, Cl^-	mg/kg dm	10	25000	15 000	800

$^{1)}$ Annex 7 of the Regulation on waste categories, testing, and classification (Official gazette RS 56/2010. and 93/2019), H15 waste characteristics.

$^{2), 3), 4)}$ Annex 10 of the Rules on categories, testing and classification of waste (Official Gazette RS 56/2010 and 93/2019), Article 2, Parameters for testing waste and process water from hazardous waste landfill$^{2)}$, non-hazardous waste landfill$^{3)}$ and inert waste$^{4)}$.

Based on the limit values given in Annex 10 of the Regulation on categories, testing and classification of waste (Office Gazete RS 56/2010.) for LP and TCLP procedure:

- concentration of sulfuric ions in LP test is near the limit value for disposal on landfill for non-hazardous waste and
- concentration of lead and cadmium in TCLP test is near the limit value for waste toxicity criteria.

Optimal parameters for solid waste stabilization process are defined based on the realized investigations. Homogeneity of the waste has to be high, moisture content has to be in range from 42 to 46%, optimal ratio of lime: waste has to be 1:10 (m/m) and optimal contact time is 12 h.

Efficiency of the stabilization process can be seen by the results of stabilized waste testing according to LP and TCLP procedure. Results of this testing are shown in table 3, and the results of the waste testing according to TCLP procedure are shown in table 4.

In the samples (residue after leaching) for LP and TCLP characterization, moisture content is 42.30% and solid content is 57.7%.

Table 2 Results of physicochemical testing of toxic waste characteristics for disposal - TCLP test (EPA 1311)

Parameter	Unit	Measured value	The reference value for non-hazardous waste[5]	Method
		Label of the sample		
		02.20.11 OR-TCLP		
Content in Eluate (TCLP test)				
Antimony, Sb	mg/L	<0.011	15	SRPS EN ISO 11885
Chromium, Cr	mg/L	0.018	5	SRPS EN ISO 11885
Molybdenum, Mo	mg/L	<0.007	350	SRPS EN ISO 11885
Nickel, Ni	mg/L	0.048	20	SRPS EN ISO 11885
Selenium, Se	mg/L	<0.033	1	SRPS EN ISO 11885
Zinc, Zn	mg/L	22.6	250	SRPS EN ISO 11885
Copper, Cu	mg/L	1.6	25	SRPS EN ISO 11885
Arsenic, As	mg/L	<0.020	5	SRPS EN ISO 11885
Cadmium, Cd	mg/L	0.77	1	SRPS EN ISO 11885
Lead, Pb	mg/L	4.6	5	SRPS EN ISO 11885
Mercury, Hg	mg/L	<0.0005	0.2	SRPS EN ISO 11885
Vanadium, V	mg/L	0.032	24	SRPS EN ISO 11885
Silver, Ag	mg/L	0.016	5	SRPS EN ISO 11885

[5] Annex 10 of the Role Book on the categories, testing and classification of waste (Official Gazette RS 56/2010), Article 1, Parameters for testing the toxic characteristics of waste intended for disposal.

Table 3 Results of physicochemical testing waste (residue after leaching) leachability according with SRPS EN 12457-2:2008

Parameter	Unit	Measured value	The reference value for non-hazardous waste[2]	The reference value for non-hazardous waste[3]	The reference value for inert waste[4]
		Label of the sample			
		01.20.11 ST-10 L/kg			
Content in LP extract (neutral test, L/S = 10/1)					
Conductivity	µS/cm	6658	-	-	-
pH (25 °C)[1]	-	12.34	-	6-13	-
Arsenic, As	mg/kg dm	<0.020	25	2	0.5
Antimony, Sb	mg/kg dm	<0.5	5	0.7	0.06
Copper, Cu	mg/kg dm	<0.005	100	50	2
Molybdenum, Mo	mg/kg dm	<0.007	30	10	0.5
Cadmium, Cd	mg/kg dm	<0.008	5	1	0.04
Selenium, Se	mg/kg dm	<0.033	7	0.5	0.1
Nickel, Ni	mg/kg dm	<0.007	40	10	0.4
Mercury, Hg	mg/kg dm	<0.005	2	0.2	0.01
Lead, Pb	mg/kg dm	0.012	50	10	0.5
Chromium, Cr	mg/kg dm	<0.020	70	10	0.5
Zinc, Zn	mg/kg dm	0.015	200	50	4
Sulphate, SO_4^{2-}	mg/kg dm	11400	50000	20 000	1 000
Fluoride, F^-	mg/kg dm	12.3	500	150	10
Chloride, Cl^-	mg/kg dm	10	25000	15 000	800

[1] Annex 7 of the Regulation on waste categories, testing, and classification (Official gazette RS 56/2010. and 93/2019), H15 waste characteristics.

[2], [3], [4] Annex 10 of the Rules on categories, testing and classification of waste (Official Gazette RS 56/2010 and 93/2019), Article 2, Parameters for testing waste and process water from hazardous waste landfill[2], non-hazardous waste landfill[3] and inert waste[4].

Method SRPS EN ISO 11885 is used for As, Cu, Mo, Cd, Se, Ni, Hg, Pb, Cr, Zn, SO_4^{2-}, F^- and Cl^- determination, method SRPS EN 12506 for pH determination and EPA 120.1 for determination the conductivity.

Table 4 Results of physicochemical testing of toxic waste characteristics for disposal - TCLP test (EPA 1311)

Parameter	Unit	Measured value Label of the sample 02.20.11 ST-TCLP	The reference value for non-hazardous waste[5]	Method
Content in Eluate (TCLP test)				
Antimony, Sb	mg/L	<0.011	15	SRPS EN ISO 11885
Chromium, Cr	mg/L	0.052	5	SRPS EN ISO 11885
Molybdenum, Mo	mg/L	<0.007	350	SRPS EN ISO 11885
Nickel, Ni	mg/L	0.035	20	SRPS EN ISO 11885
Selenium, Se	mg/L	<0.033	1	SRPS EN ISO 11885
Zinc, Zn	mg/L	0.60	250	SRPS EN ISO 11885
Copper, Cu	mg/L	0.35	25	SRPS EN ISO 11885
Arsenic, As	mg/L	<0.020	5	SRPS EN ISO 11885
Cadmium, Cd	mg/L	0.017	1	SRPS EN ISO 11885
Lead, Pb	mg/L	0.16	5	SRPS EN ISO 11885
Mercury, Hg	mg/L	<0.0005	0.2	SRPS EN ISO 11885
Vanadium, V	mg/L	0.045	24	SRPS EN ISO 11885
Silver, Ag	mg/L	0.010	5	SRPS EN ISO 11885

[5] Annex 10 of the Role Book on the categories, testing and classification of waste (Official Gazette RS 56/2010), Article 1, Parameters for testing the toxic characteristics of waste intended for disposal.

Based on comparison with the limits given in Annex 10 of the Regulation on categories, testing and classification of waste (Office Gazete RS 56/2010.) for LP and TCLP procedure comment are as follows:

- concentration of sulfuric ions in LP test of stabilized waste is lower than in unstabilized waste, but influence of stabilization process on immobilization of sulfuric ion is not high;
- concentration of lead and cadmium ions in TCLP test is lower than in unstabilized waste, and influence of stabilization process on immobilization of lead and cadmium ions is very high.

Proposed stabilization process is applicable for stabilization of solid waste generated in neutralization sludge leaching process.

CONCLUSION

The experiment results show that new type of waste generated after treatment process of AMD consists of neutralization process and leaching process is non-hazardous waste, but concentration of sulfuric ions in LP test is near the limit value for disposal on landfill for non-hazardous waste and concentration of lead and cadmium in TCLP test is near the limit value for waste toxicity criteria.

The efficiency of stabilization process is investigated. Results are shown that stabilization process doesn't have the significant influence on immobilization of sulfuric ions, but influence on immobilization of lead and cadmium ions is very high. Concentration of lead and cadmium ions in TCLP test is the lower than in unstabilized waste, and influence of stabilization process on immobilization of lead and cadmium ions is very high.

ACKNOWLEDGEMENTS

We acknowledge the financial support of the Project RoRS 337- ROmania Serbia NETwork for assessing and disseminating the impact of copper mining activities on water quality in the cross-border area (RoS-NET2), implemented under the Interreg-IPA Cross-border Cooperation Romania-Serbia Programme that is financed by the European Union under the Instrument for Pre-accession Assistance (IPA II) and co-financed by the partner states in the Programme. This work was also financially supported by the Ministry of Education, Science and Technological Development of the Republic of Serbia, Grant No. 451-03-9/2021-14/ 200052.

REFERENCES

1. Masuda, N., Marković, R., Bessho, M., Božić, D., Obradović, Lj., Marinković, V., Ishiyama, D., Stevanović, Z. (2017) A new approach to recover dissolved metals in AMD by two-step pH control on the neutralization method. 13th International Mine Water Association Congress – Mine Water & Circular Economy. Lappeenranta, Finland, proceedings, 1111-1118.
2. Markovic, R., Bessho, M., Masuda, N., Stevanovic, Z., Bozic, D., Apostolovski Trujic, T. and Gardic, V. (2020) New Approach of Metals Removal from Acid Mine Drainage, Appl. Sci., 10, 5925; doi:10.3390/app10175925.
3. Masuda, N., Marković, R., Božić, D., Bessho, M., Inoue, T., Hoshino, K., Ishiyama, D., Stevanović, Z. (2019) Experiment results of metal recovery by a two-step neutralization process from AMD from a copper mine in Serbia, IMWA 2019 Conference – Mine water: Technological and Ecological Challenges. Perm, Rusia, proceedings, 232-237.

XIV International Mineral Processing
and Recycling Conference
Belgrade, Serbia, 12-14 May 2021

PRODUCTION OF ELECTROLYTIC MANGANESE DIOXIDE (EMD) FOR Li ION BATTERY APPLICATIONS FROM SECONDARIES

V. Aishvarya[#], Barsha Marandi, Abdul Rauf Sheik, Indra Narayan Bhattacharya, Kali Sanjay
CSIR-Institute of Minerals and Materials Technology, Bhubaneswar, India

ABSTRACT – The demand for Lithium ion batteries has grown in the recent years due to immense surge of electric vehicles, and therefore, the need for high pure EMD which is a critical component in Lithium ion batteries has also grown. India is the 6th largest country in Mn ore reserves having an estimated 34 million tonnes of manganese metal, of which, the medium and high grade ores constituting a third of the total production are used for alloy making. Ferromanganese alloy industry is amongst the largest manganese ore based industry in the country. For every ton of ferro alloy produced, the industry generates nearly 1.2 to 1.5 tonnes of slag containing 10-20% Mn, which are being dumped as waste. Efforts have been made to produce Electrolytic Manganese Dioxide (EMD) from ferro alloy slag employing hydrometallurgical processing, for application in Li ion batteries. While, alkaline batteries require EMD with a certain specifications, the purity is more stringent with Li-ion batteries. The most efficient and widely used materials for Li ion battery cathodes are layered oxides in the $LiMO_2$ family, where 'M' is a combination of Co, Ni, Al, and Mn. The major challenge is to reduce the impurities in EMD to acceptable levels for Li ion battery application which is elucidated here through the processing of a ferro alloy slag. The process developed involves reductive acid leaching of the slag, purification steps to remove dissolved impurities such as Fe, Si, Al etc. and EMD preparation. The EMD produced is a battery grade material with applications in alkaline batteries and Li-ion batteries.

Keywords: EMD, Ferro Alloy Slag, Lithium Ion Batteries, Hydrometallurgy.

INTRODUCTION

Manganese is an essential metal for an industrial economy, with the major consumption being in the infrastructure industry for alloy preparation and in the energy industry for energy storage material (batteries) as chemical manganese dioxide (CMD) or Electrolytic manganese dioxide (EMD). For battery applications, gamma MnO_2 (γ-MnO_2) is much more active among the various polymorph of MnO_2 [1]. More than 80% of manganese produced is used in alloy industry and the Indian ferro alloy industry has a capacity of nearly 5.2 million tonnes which accounts for 10% of world ferro-alloy production [2]. The alloy making industry generates nearly 1.2 to 1.5 tonnes of slag per tonne of alloy [3]. FeMn slag contains typically 20-30% Mn as a mixture of MnO, Mn_2O_3 and Mn_3O_4 along with SiO_2, CaO, MgO, Al_2O_3 and Fe_2O_3 while SiMn slag typically contains 10-20% Mn along with CaO, MgO, Al_2O_3 etc. Attempts have been made to extract the residual Mn values from the slag, chiefly to address the environmental issues arising due to reactive soluble Mn resulting in health hazards. The general approach is to first recover the Mn in the soluble form by leaching [4] or roasting the slag with sulphuric acid at 300-

---

[#] corresponding author: aishvarya@immt.res.in

400 ^{0}C, followed by dissolution in water [5]. The current study presents research work wherein the Mn from SiMn slag is recovered by reductive acid leaching and used to produce electrolytic manganese dioxide (EMD) for applications in batteries. Reducing agents such as sucrose or SO_2 were chosen due to ease of availability. For EMD electrodeposition, different cathode materials were tested to produce an EMD having suitability for Lithium Ion Battery (LiB) application. The purity of EMD, morphology, phase and discharge capacity have been investigated.

EXPERIMENTAL

The silicomanganese slag was obtained from a ferroalloy plant (Steel Authority of India Ltd, Chandrapur). The slag sample was crushed, grinded and the size fraction less than 150 microns were used for the studies. Chemical analysis of the slag sample was carried out by wet chemical digestion in boiling aquaregia for determining the major elements. The powdered sample was also analyzed by X-ray fluorescence spectroscopy (PANalytical, Model Zetium, 4 kW) for obtaining overall quantitative analysis of the elements present in it. Phase determination was carried out using powder X-ray diffractometer (PANalytical, Model EMPYREAN) using Cu target having K-α 1.54 Å. Leaching was carried out in a stainless steel electrically heated reactor (Amar equipment Pvt Ltd) with provision for gas purging, sample addition, overhead stirring and temperature control using PID system (±0.1 ^{0}C). Typical leaching experiment was carried out by charging weighed amount of powdered slag to a spent liquor containing 25 g/L Mn as $MnSO_4$ and H_2SO_4 solution of desired concentration, with or without a reducing agent. Sucrose or gaseous SO_2 were used as reducing agent in the present work. Following leaching, purification was carried out by precipitation to remove impurities such as Al, Fe, Si etc. The dissolved metals were analyzed in ICP-OES or AAS (Perkin Elmer). The purified liquor was used to prepare EMD. The discharge capacity of EMD was tested using a BITRODE battery tester. Chemical analysis of EMD was carried out by digestion in hot aquaregia for determining the concentration of the impurities in EMD.

RESULTS & DISCUSSION

The silicomanganese slag used in the present work contained nearly 12.6% Mn, 0.56% Fe, 8.8% Al, 3.4% Mg and 8.3% Ca. The complete composition of slag as determined by XRF spectroscopy is shown in Table 1, nearly 45% SiO_2 was found to be present along with multiple impurities such as Na, K, Cr, P, Ba etc. in smaller quantities. The X-ray diffractogram of slag revealed that manganese in the slag was present as a mixture of Mn_2O_3 (JCPDS no: 98-023-6255) and Manganese oxide, MnO (JCPDS no: 98-026-2928). A part of the Mn was also found in the alumino silicate phase, Clinopyroxene (JCPDS no: 98-015-8033) with a complex composition of Al0.42 Ca0.646 Fe0.271 Mg0.69 Mn0.003 Na0.143 O6 Si1.783 Ti0.044.

Table 1 Composition of silicomanganese slag used in the study determined by XRF

Compound	**SiO_2**	**TiO_2**	**Al_2O_3**	**Fe_2O_3**	**MnO**
% Value	45.68	0.32	13.06	0.591	15.56
Compound	MgO	CaO	Na_2O	K_2O	BaO
% Value	5.06	11.30	1.0	2.42	2.89

Leaching and purification

Leaching recovery of Mn was proportional to acid concentration and more pronounced by the presence of a reducing agent such as sucrose or SO_2. However, impurities such as Fe, Al, small amounts of Si were also leached with Mn. Low acid concentration on the other hand, resulted in lower amount of impurities in solution but also lower Mn recovery of ~30-35%. Some typical leaching results with and without reducing agent at various leaching conditions is shown in Table 2.

Alternatively, leaching carried out in water following an acid pre-treatment step was also comparable with reductive leaching. Slag powder was pre-treated with sulphuric acid followed by water leaching at 80 °C and 10% pulp density. With a tradeoff between either time or pretreatment temperature, similar Mn recoveries can be obtained as seen from Table 3. Acid pretreatment at higher temperature i.e., roasting at 400 °C, which is a commonly reported slag treatment method [5], did not necessarily yield higher Mn recovery, making room temperature acid pretreatment sufficient.

Table 2 Leaching of SiMn slag with and without reductant *

Expt. No	**Pulp density (% w/v)**	**H_2SO_4 (g/L)**	**Temperature (°C)**	**Reducing agent**	**Mn extraction (%)**	**Fe extraction (%)**	**Al extraction (%)**
1	10	92	85	nil	36	53	29.8
2	10	92	85	0.1 g sucrose/g slag	76.3	54.3	68.2
3	20	184	85	0.1 g sucrose/g slag	74.6	81	70.6
4	10	35	85	nil	33.4	51	11.6
5	10	92	Ambient	0.1 LPM SO_2	45	26.7	NA

*All experiments were carried out for 4h duration; NA- not available.

Table 3 Water leaching of SiMn slag with pretreatment

Expt. No	**Slag: H_2SO_4 ratio**	**Temperature (°C)**	**Duration (h)**	**Mn extraction (%)**	**Fe extraction (%)**	**Al extraction (%)**
1	1:1	400	2	65.5	25.4	81
2	1:1	Ambient	24	73.8	39	58.2

A maximum of 76% Mn was recovered by reductive acid leaching while 74% was recovered by ambient acid pretreatment-water leaching method. It is likely that part of Mn which is present in silicate phase was not reduced or leached and remained unreactive, which may be safely discarded to landfill with the residue.

The leach liquor obtained from reductive acid leaching and by ambient acid pretreatment-water leaching method, was purified for the removal of major impurities namely iron and aluminium, by precipitation technique. Iron was removed by first treating with hydrogen peroxide, followed by MgO. Nearly all of Fe (>99%) was removed at pH 3.5- 4.0 with partial removal of Al. To remove the Al from liquor and traces of Si, solution pH was further raised using MgO and aged for 3-6 hours resulting in <100ppm Al and Si in final purified liquor. The resultant $MnSO_4$ bearing purified solution was used in EMD preparation. The composition of purified liquor is shown in Table 4.

Table 4 Composition of purified liquor

Element	**Mn**	**Fe**	**Al**	**Si**	**Cu**	**Pb**
Concentration	36 g/L	0.45ppm	98ppm	56 ppm	<1ppm	<1ppm

EMD preparation

Different cathode materials such as nickel, copper, zirconium, platinum coated titanium were tested for producing EMD. The EMD electrowinning studies were carried out at a current density of 200 A/m^2 for 4 hours duration. Titanium was used as the anode material for all the experiments. Table 5 represents the concentration of iron and respective cathode ion impurity in EMD while testing with different cathode material, along with the average cell voltage observed. Amongst the several cathode material tested, graphite cathode was found to be most suitable both in terms of iron impurity and cell voltage, eventually leading to minimal energy consumption. For platinum coated titanium cathode, though the average cell voltage was observed to be lowest, more than 50 ppm titanium and nearly 40 ppm platinum were found to be in the EMD. EMD obtained using graphite cathode and titanium anode was further analyzed for impurities such as Cu, Ni, Co, Pb, Al and Si, morphology and phase determination.

Table 5 Impurity analysis of EMD using different cathode materials

Cathode Material	Impurity conc. in EMD (ppm)		Cell voltage(V)
Nickel	Ni: 35	Fe: 42	2.1
Copper	Cu: 39	Fe: 48	2.21
Zirconium	Zr: 29	Fe: 43	2.5
Pt coated Titanium	Pt: 42; Ti: >50	Fe: 45	1.54
Graphite	Ni: 10; Co: 8; Cu: 5 Al: 25; Pb: 12; Si: 20	Fe: 40	1.72

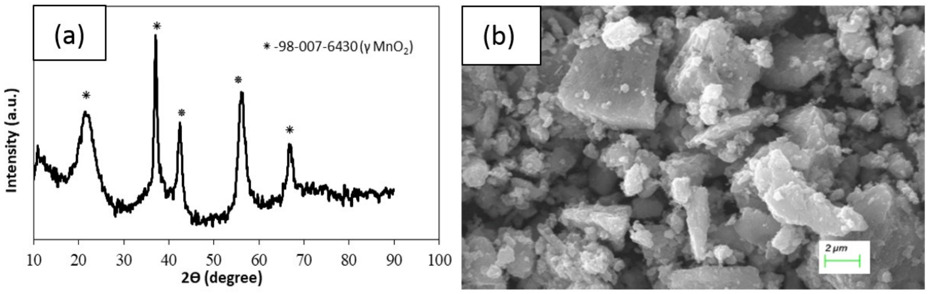

Figure 1 (a) X-ray diffractogram of EMD obtained using Graphite as cathode and Titanium as anode, showing γ-MnO_2 (JCPDS card no. 98-007-6430); **(b)** SEM image of EMD obtained using Graphite as cathode and Titanium as anode

Figure 1 (a) and (b) show the XRD and SEM micrograph of the EMD produced respectively. From the XRD pattern of EMD, it can be confirmed that the EMD obtained is of gamma phase. The discharge capacity of the EMD produced was found to be nearly 230 mAh/g.

CONCLUSION

Electrolytic manganese dioxide (EMD) of Li ion battery grade purity was prepared from silicomanganese slag following a reductive acid leaching and precipitation process. The EMD produced was found to be γ-MnO_2 with a discharge capacity of 230 mAh/g. The current simplified hydrometallurgical process will enable utilization and value addition of waste SiMn slag without the conventional high temperature pyrometallurgical operations to obtain a marketable material, EMD, for energy application.

ACKNOWLEDGEMENT

The authors thank SAIL, Chandrapur for providing the silicomanganese slag sample. The authors are thankful to the Director, CSIR-Institute of Minerals and Materials Technology, for his kind permission to present this work at XIV-IMPRC 2021.

REFERENCES

1. Biswal, A., Tripathy, B. C., Sanjay, K., Subbaiah, T., & Minakshi, M. (2015) Electrolytic manganese dioxide (EMD): a perspective on worldwide production, reserves and its role in electrochemistry. RSC Advances, 5 (72), 58255-58283.
2. GoI, Ministry of Mines, Indian Bureau of Mines. (2016) Indian minerals yearbook, (Part II: Metals and Alloys) Ferro-Alloys (Advance Release), http://ibm.nic.in/writereaddata/files/01162018134131Ferro%20Alloys%202016(AdvanceRelease).pdf, Jan 2018.
3. Ayala, J., & Fernández, B. (2015) Recovery of manganese from silicomanganese slag by means of a hydrometallurgical process. Hydrometallurgy, 158, 68-73.
4. McIntosh, S.N. and Baglin, E.G. (1992) Recovery of Manganese from steel plant slag by carbamate leaching, U.S. Bureau of Mines Report of Investigations, https://books.google.co.in/books?hl=en&lr=&id=EK8wH68NsoIC&oi=fnd&pg=PP8&dq=Recovery+of+Manganese+from+steel+plant+slag+by+carbamate+leaching&ots=SiYee7V0F6&sig=JXV-A1IpNL_fcYdpvvFNF8b9olo&redir_esc=y#v=onepage&q=Recovery%20of%20Manganese%20from%20steel%20plant%20slag%20by%20carbamate%20leaching&f=false.
5. Groot, D. R., Kazad, D. M., Pollmann, H., Villiers, J. P., Redtmann, T., & Steenkamp, J. (2013) The recovery of manganese and generation of a valuable residue from ferromanganese slags by a hydrometallurgical route. In: 13th International ferroalloys congress—efficient technologies in ferroalloy industry. Almaty, Kazakhstan, Recycling, 1051-1060.
6. Baumgartner, S. J., & Groot, D. R. (2014) The recovery of manganese products from ferromanganese slag using a hydrometallurgical route. Journal of the Southern African Institute of Mining and Metallurgy, 114 (4), 331-340.

CEMENTITIOUS WASTE MATERIALS UTILIZATION IN RADIONUCLIDE IMMOBILIZATION BY SORPTION

Marija Šljivić-Ivanović, Ivana Jelić#, Slavko Dimović
"VINČA" Institute of Nuclear Sciences - National Institute of the Republic of Serbia, University of Belgrade, Belgrade, Serbia

ABSTRACT – This paper represents an overview of the investigations of cementitious waste materials (CWM) utilization in Sr, Co, and Ni radionuclides immobilization by sorption. The highest Co^{2+} and Ni^{2+} ions removal efficiency was achieved using a wall-concrete sample, while the Sr^{2+} uptake was equal on all. The results agreed with the sorption capacity of investigated ions onto C-S-H (calcium silicate hydrate) as the main hardened cement-paste component. Studies showed that the use of CWM in the conditioning of liquid radioactive waste (LRW) could represent the efficient and economically viable alternatives for commonly used methods.

Keywords: Liquid Radioactive Waste, Concrete, Environment, Sustainable Development.

INTRODUCTION

The investigation trend of waste materials sorption characteristics has become more expressed in recent years. The utilization of waste-based materials as sorbents is highly acceptable from the aspects of environmental protection due to reduction of non-renewable resource usage, energy consumption, and generated end-waste disposal [1]. Further, the re-use of waste materials contributes to a reduction of possible environmental pollution, occupation of large surface area, and disposal costs. Among these, one of the essential things is that these materials are cost-effective and easily accessible. Likewise, the recommendation to the harmonization of all processes with the so-called 3R Criteria: reduce, recycle, and re-use, as well as the principles of the Circular economy, that implies efficient utilization of materials [2] are the main reasons for such researches. Also, high costs of immobilization (conditioning), temporary storage, and final disposal of liquid radioactive waste (LRW) encourage the application of waste materials, especially those that represent the end-waste [3]. Generally, the utilization of waste-based sorbents is widely accepted from the aspects of sustainable development.

Recent studies on cementitious waste materials (CWM) include a wide range of waste concrete, façade materials, mortar, and mixtures. The basis for these scientific researches represents the fact that these waste materials have substantial similarities with the common composite materials, i.e., solidification matrices for immobilization of LRW, such as concrete and mortar [4].

This paper presents an overview of the large part of the investigations during 2016 – 2020 of construction and demolition waste (C&DW) utilization in Sr, Co, and Ni

---

[#] corresponding author: ivana.jelic@vin.bg.ac.rs radionuclides immobilization [5-10]. Studies have been shown that the usage of CWM in the sorption process could be very efficient and economically viable alternatives for standardly used methods. Since radioactive isotopes of Sr, Co, and Ni are significant components of LRW, immobilization of their ions from aqueous solutions was studied in batch sorption systems.

EXPERIMENTAL METHOD

The CWM samples were collected from five demolition sites located in the residential area of Belgrade, Serbia. Three waste cement-based sample types from the 1970s debris were used [5,6]:

- C1 – Waste concrete (walls construction),
- C2 – Waste concrete (pathways parts), and
- F – Façade waste material (from residential buildings).

Collected samples of each type were mixed, and the total amount of 1 kg was crushed, homogenized, milled, and sieved to a particle size between 0.3 and 0.6 mm to obtain representative samples (Figure 1). Three mixtures were spread over the 1 m^2 area, and 50 g per each was taken randomly from different points. Prior to the experiments, samples were washed with distilled water and dried at 373 K.

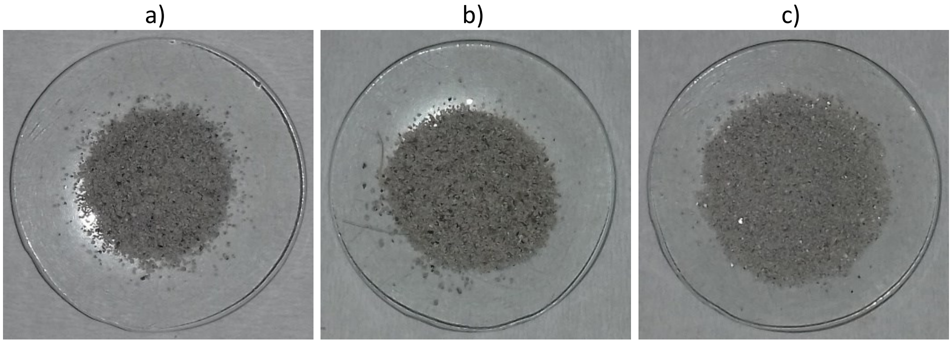
a) b) c)

Figure 1 Prepared CWM samples: a) C1, b) C2, and C) F [7]

Sorption affinities of selected C&DW components were investigated using single-metal solutions with increasing initial metal concentration. Solutions of the specified concentration were prepared by dissolving the adequate masses of Sr^{2+}, Co^{2+}, and Ni^{2+} nitrate salts in distilled water. The initial cation concentrations were varied in the range 10^{-4} to $8 \cdot 10^{-3}$ mol/L. Sorption equilibrium was achieved by contacting 0.1 g of sorbent with 20 mL of a solution on a rotary shaker at 10 rpm, and ambient temperature for 24 h. The preliminary experiments showed that 24 h of contact time was sufficient to achieve sorption equilibrium under specified experimental conditions. Investigated solutions had natural pH between 5.0 and 5.6, and they were applied without adjustments.

The affinity of CWM to bind Sr^{2+}, Co^{2+}, and Ni^{2+} ions was defined based on sorption isotherms, i.e., the relationships between sorbed amounts of pollutants (Q_e) and residual concentrations in a liquid phase (C_e), at equilibrium. The concentrations of Sr^{2+}, Co^{2+}, and

Ni^{2+} ions were determined using an Atomic Absorption Spectrometer (AAS), model 3100, Perkin Elmer. For the instrument calibration, standard solutions were prepared from a single-element Perkin Elmer standard (1000 mg/L). The calibration was re-checked after every ten measurements.

RESULTS DISCUSSION

Sorption experiments were conducted in triplicate, and the results are presented as mean values with corresponding standard deviation in Figures 2–4.

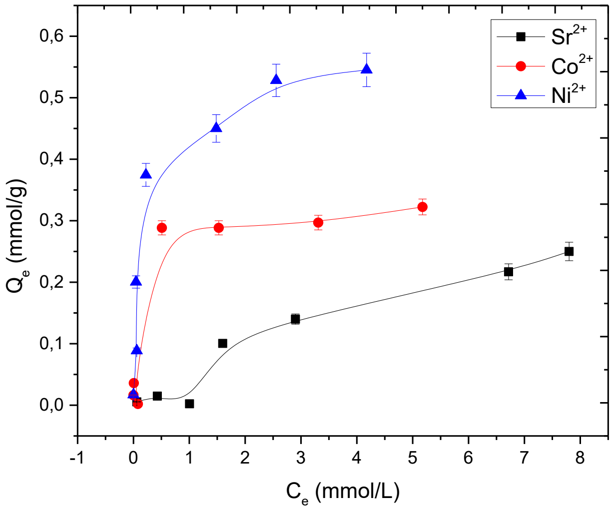

Figure 2 Sorption isotherms of Sr^{2+}, Co^{2+}, and Ni^{2+} ions onto the C1 sample [6,7]

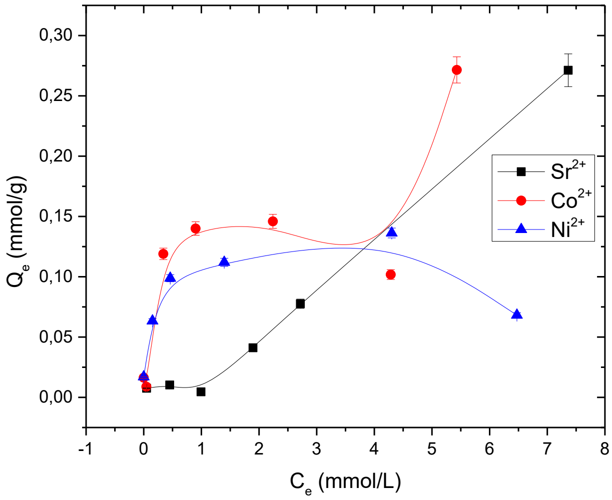

Figure 3 Sorption isotherms of Sr^{2+}, Co^{2+}, and Ni^{2+} ions onto C2 sample [5,7]

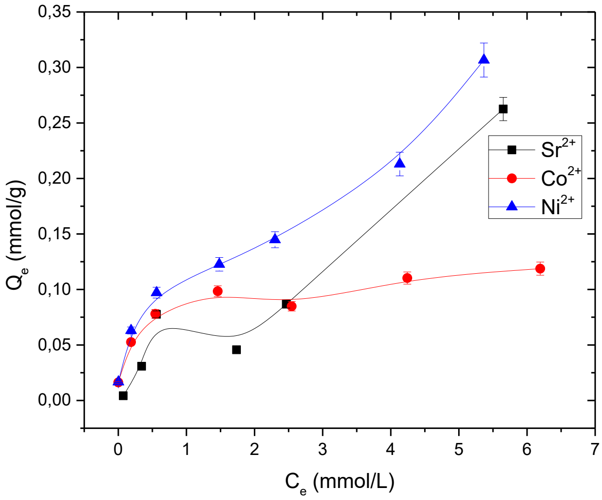

Figure 4 Sorption isotherms of Sr^{2+}, Co^{2+}, and Ni^{2+} ions onto F sample [5,7]

All samples have shown a significant affinity for sorption of Sr^{2+} cations, with an equivalent capacity of approximately 0.25 mmol/g [5-7]. Since the sorption process was followed by a linear dependence, the maximum sorption capacity was not reached and it could be expected to gain a higher value with increasing of initial cation concentrations. However, the obtained results agree with the sorption capacity of Sr^{2+} ions onto C-S-H (calcium silicate hydrate) that are the main components of hardened cement paste [11-13]. Also, the substantial sorption capacity of concrete and façade toward Sr^{2+} ions can be associated with their carbonate content [5].

The highest efficiency of Co^{2+} ions binding was achieved using samples C1 and C2 (0.32 and 0.27 mmol/g, respectively) [5-7]. The sorption capacity of Co^{2+} ions for sample F was found to be 0.12 mmol/g [5-7]. The most effective sorption of Ni^{2+} ions was onto the C1 and F samples, with a sorption capacity of 0.55 and 0.30 mmol/g, respectively. However, sample C2 showed significantly lower sorption with a maximum sorbed amount of 0.13 mmol/g [5-7]. The obtained results are in accordance with the high sorption capacities of C-S-H material according to the radioactive Co^{2+} and Ni^{2+} ions [11,12]. It might be presumed that Co^{2+} and Ni^{2+} ions sorption was the most effective onto cement-based samples, due to high equilibrium pH values [5].

Generally, the highest Co^{2+} and Ni^{2+} ions removal efficiencies were achieved using concrete sample C1, while the Sr^{2+} uptake was equal on all samples. Thus, CWM showed satisfactory performance in radionuclide removal. This feature might be primarily related to the alkaline reaction of CWM in water, which provokes dissociation of protonated surface groups, the increase in the negative surface charge, and facilitates the cation removal by precipitation in some cases [14].

Taking into account chemical compatibility with mixtures commonly used for the solidification of LRW and expressed a high affinity for studied cations, CWM has shown great potential and possibilities for further research, e.g. modification of sorbents and, in particular, the variation of experimental conditions. Also, the recent studies on Sr^{2+},

Co^{2+}, and Ni^{2+} removal by various C&DW components such as bricks, ceramic and roof tiles, and asphalt pavements relative to concrete and façade materials have indicated the highest sorption affinity of cement-based materials [5-7,9]. The sorbents of this type could very effectively replace the more expensive natural or artificially synthesized sorbent materials for radioactive isotopes from LRW.

CONCLUSION

In the present study, the suitability of CWM as a sorbent for the solidification of LRW was presented, through the sorption potential of common radioactive contaminants.

The alkaline nature and mineral composition of CWM proved to be a solid foundation for Sr^{2+}, Co^{2+}, and Ni^{2+} ions immobilization, although the highest Co^{2+} and Ni^{2+} ions removal efficiencies were achieved using old wall concrete (sample C1). Out of investigated species, Sr^{2+} ions exhibited the least effective sorption capacity. The satisfactory results were obtained using CWM due to the favorable mineral composition and alkalinity. The chemical compatibility of CWM with LRW solidification matrices must be emphasized as an advantage over natural or artificial high-capacity sorbents, which use might be environmentally inappropriate. The further removal efficiency of radionuclides testing from the real LRW in order to optimize the process conditions should be the focus of future research.

ACKNOWLEDGEMENT

This work was supported by the Ministry of Education, Science and Technological Development of the Republic of Serbia.

REFERENCES

1. Dimović, S., Šljivić-Ivanović, M., Jelić, I. (2019) Utilization of Waste Materials in Heavy Metals and Radionuclides Immobilization by Sorption. Tehnika, 19 (3), 337-344.
2. Grace, M., Clifford, E., Healy, M. (2016) The potential for the use of waste products from a variety of sectors in water treatment processes. Journal of Cleaner Production, 137, 788-802.
3. Ojovan, M.I., Lee, W.E. (2014) An Introduction to Nuclear Waste Immobilization, Second edition, Elsevier.
4. Stefanovsky, S., Yudintsev, S., Giere, R., Lumpkin, G. (2004) Nuclear waste forms. The Geological Society of London, UK.
5. Jelic, I., Sljivic-Ivanovic, M., Dimovic, S., Antonijevic, D., Jovic, M., Mirkovic, M., Smiciklas, I. (2018) The Applicability of Construction and Demolition Waste Components for Radionuclide Sorption. Journal of Cleaner Production, 171, 322-332.
6. Sljivic-Ivanovic, M., Jelic, I., Dimovic, S., Antonijevic, D., Jovic, M., Mrakovic, A., Smiciklas, I. (2018) Exploring innovative solutions for aged concrete utilization: treatment of liquid radioactive waste. Clean Technologies and Environmental Policy, 20 (6), 1343-1354.
7. Jelić, I. (2017) Application of Composite Construction Waste for Immobilisation of Radionuclides and Heavy Metals by Sorption. Ph.D. dissertation, Singidunum University, Belgrade, Serbia.

8. Sljivic-Ivanovic, M., Dimovic, S., Antonijevic, D., Jovic, M., Vujovic, Z., Smiciklas, I. (2019) Radionuclides Immobilization by Sorption onto Waste Concrete and Bricks – Experimental Design Methodology. Water, Air & Soil Pollution, 230 (10), 242.
9. Jelic, I., Sljivic-Ivanovic, M., Dimovic, S., Antonijevic, D., Jovic, M., Serovic, R., Smiciklas, I. (2016) Utilization of Waste Ceramics and Roof Tiles for Radionuclide Sorption. Process Safety and Environment Protection, 105, 348-360.
10. Sljivic-Ivanovic, M., Jelic, I., Loncar, A., Nikezic, D., Dimovic, S., Loncar, B. (2017) The application of experimental design methodology for the investigation of liquid radioactive waste treatment. Nuclear Technology & Radiation Protection, 32 (3), 281-287.
11. Hietanen, R., Kaemaeraeinen, E., Alaluusua, M. (1984) Sorption of strontium, cesium, nickel, iodine and carbon in concrete. Voimayhtiöiden Ydinjätetoimikunta, Helsinki, Finland.
12. Noshita, K., Nishi, T., Matsuda, M. (1998) Improved Sorption Ability for Radionuclides by Cementitious Materials. In: Symposium on Waste Management WM'98, Tucson, Arizona, USA, Proceedings, 1880-1886.
13. Tits, J., Wieland, E., Müller, C., Landesman, C., Bradbury, M. (2006) Strontium binding by calcium silicate hydrates. Journal of Colloid and Interface Science, 300, 78-87.
14. Sljivic-Ivanovic, M., Smičiklas, I. (2020) Utilization of C&D waste in radioactive waste treatment—Current knowledge and perspectives. In Advances in Construction and Demolition Waste Recycling, Woodhead Publishing, Elsevier, 475-500.

XIV International Mineral Processing
and Recycling Conference
Belgrade, Serbia, 12-14 May 2021

APPLICATION OF FLY ASH TO GET PORTLANT CEMENT

Blagica Cekova[1], Viktorija Bezhovska[2#], Filip Jovanovski[2]
[1] MIT University, Faculty of ecological resources management,
Skopje, Macedonia
[2] University St. Cyril and Methodius, Faculty of Technology and Metallurgy,
Skopje, Macedonia

ABSTRACT – The idea of using fly ash as a raw material in the production of Portland cement is due to its chemical composition which is very similar to the clay component. Fly ash contains the oxides SiO_2, Al_2O_3, Fe_2O_3 and CaO. Portland cement with the addition of fly ash produces less heat of hydration compared to ordinary Portland cement. Combines with lime released during cement hydration, resulting in increased resistance. Its use in cement is also known to reduce water permeability during prolonged water hardening.

Keywords: Fly Ash, Portland Cement, Chemical Composition, Hydration.

INTRODUCTION

The chemical composition of the ash depends, as well as its physical properties, on the type of coal used in the thermal power plant. [1] Based on the literature data, [2,3] it can be concluded that both classes of ash contain in their composition as the most important chemical compounds SiO_2, Al_2O_3, Fe_2O_3 and CaO and to a lesser extent MgO, MnO, Na_2O, K_2O, SO_3, N, C. In some ashes to a lesser extent TiO_2 and Pb_2O_5 can be found. Lignite ash usually shows a $SiO_2 + Al_2O_3 + Fe_2O_3$ content of over 50% (Table 1).

Table 1 Common chemical composition of fly ash

Oxide	Bituminous coal (%)	Sub - bituminous coal (%)	Lignite (%)
SiO_2	20 – 60	40 – 60	15 – 45
Al_2O_3	5 – 35	20 – 30	10 – 25
Fe_2O_3	10 – 40	4 – 10	4 – 15
CaO	1 – 12	5 – 30	15 – 40
MgO	0 – 5	1 – 6	3 – 10
SO_3	0 – 4	0 – 2	0 – 10
Na_2O	0 – 4	0 – 2	0 – 6
K_2O	0 – 3	0 – 4	0 – 4
LOI	0 – 15	0 – 3	0 – 5

The mineral composition of fly ash in a broader sense includes the following components:

[#] corresponding author: bezhovska@gmail.com

1. inorganic constituents, crystalline and amorphous;
2. organic suppositories derived from coal;
3. liquid, gaseous and liquefied gas inclusions in the inorganic and organic component.

The minerals from coal during the combustion process pass into crystalline and amorphous phases of which ash is composed. It is thought that calcite mainly converts to CaO, which in some cases may react with SO_2 and CO_2 to form anhydrite and later calcite. Clay matter, like feldspars, melts and transforms into glass, sometimes under the action of smelters such as FeO and CaO. Kaolinite usually turns into mulite, glass and sometimes cristobalite while other types of clay and feldspar turn into glass. Quartz partially melts, but some quartz grains lag behind. Thus, in addition to the amorphous phase that is characteristic of electrofiltration ash, the crystalline mineral species mainly include quartz, mulite, feldspar of K – and Ca – type, anorthite, calcite, gelenite, hematite, magnetite, and in smaller quantities can wollastonite, spinelles, and corundum also occur. Ashes with lower Ca content usually contain quartz, mulite, hematite, and ashes with high Sa content may also contain mineral species such as melilite $[(Ca,Na)_2(Mg, Al, Fe)(Si,Al)_2O_7]$ and mervinite $[Ca_3Mg(SiO_4)_2]$.

The northern particles that make up the glassy (amorphous) part of the ash are generally thin, hollow, ceramic microspheres and are called price particles (Figs. 1,2). The composition of their solid crusts includes aluminosilicate glass, mulite (Figure 3), quartz, calcite, Fe - oxides, Ca - silicates and sulfates. These spheres are created under specific conditions, such as molten drops of clay minerals, feldspar and quartz. Spheres are usually filled with gases created by the combustion of organic matter, the decomposition of carbonates, the dehydration of clay minerals, and the evaporation of water from the pores. These are mainly CO_2, N_2, O_2 and H_2O. These spheres are assumed to form at temperatures between 1,230 and 1,400 °C. Cenospheres in the cavities of which smaller particles are located are called pleurospheres (Figure 4). In the ash of lignite, bituminous and attractive coals there are also ferrospheres (Figure 5), which consist of ferrispinels, solid solutions of magnetites containing Mg, Mn and Ca, hematite, maghemite and to a lesser extent ilmenite and chromite. Ceramic price spheres, as well as magnetic ferrospheres can be concentrated by special methods and as such find their industrial application. Ferrous metals, for example, are used as catalysts in high-temperature metal conversion processes. In addition to the amorphous and crystalline phases, smoke particles and sometimes minerals such as barite, anglesite, apatite, and monacite can be found in the ashes [4].

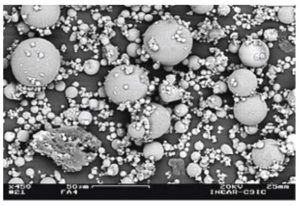

Figure 1 Amorphous phase, composed of alum - silicate amorphous particles in the electrofilter fly ash

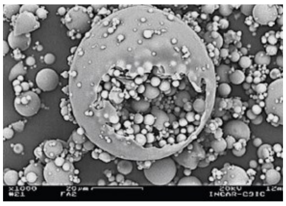

Figure 2 Alum - silicate spherical particle

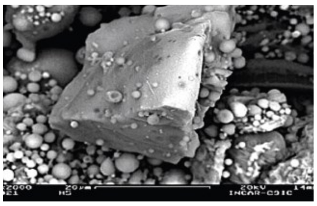

Figure 3 Quartz grain in ash

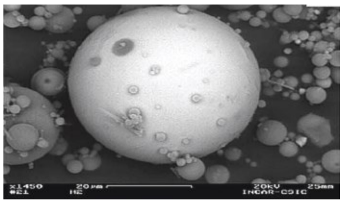

Figure 4 Alum - silicate pleerosphere in ash

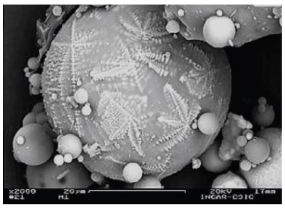

Figure 5 Ferrosphere with dendritic magnetic crystallization

POSSIBILITIES FOR USING FLYING ASH

Huge amounts of flying ash, which from the beginning followed the work of thermal power plants around the world, sought to find an opportunity to use it, so that flying ash has been researched and used for 70 years. For example, in 1984 the United States produced about 48 million tons of ash, of which 8 million tons were used for various purposes, which is about 17%. In 2001, about 71.2 million tons of flying ash were deposited. Today, more than 35% of these quantities are used in the United States, half of which is mainly used as an additive in cement and concrete. Given the fact that the amount of ash produced globally is estimated at around 200 million tons per year, it is clear that unused waste in the form of landfills remains a problem, primarily in environmental terms. However, new and attractive ways of using this ash are constantly used in the world [5].

ASH A PORCELANIN ADDITIVES FOR PORTLAND CEMENT AND CONCRETE

According to the standard definition, pozzolanic materials are natural or artificial silicates, silicon-aluminates, silicon-carbonate substances or their combinations, which finely ground in the presence of water react with dissolved calcium hydroxide to create products that have hydraulic properties. This means that the pozzolanic materials themselves do not have to have pozzolanic properties, but in the presence of water they will react with the corresponding compound ($Ca(OH)_2$) and will upgrade the insoluble compounds - hydrates, with binding properties. Natural Pozzolanic materials are mainly pyroclastic rocks, ie volcanic ash or tuffs, and artificial Pozzolanic materials include blast furnace slag and, of course, electrostatic precipitated ash from thermal power plants.The mechanism of the pozzolanic reaction consists in the reaction of SiO_2 and Al_2O_3 from the pozzolan, with $Ca(OH)_2$ formed as a product of hydration of the mineral cement clinker (tri – and dicalcium silicates). As products of this reaction, new amounts of insoluble calcium – silicon carbohydrates are created, ie new amounts of C – S – H phase. It is interesting to note that the C – S – H phases that are created as a product of the pozzolanic reaction contribute to a better development of hardness than the C – S – H phases that occur primarily as products of the hydration of minerals from cement clinker. Chemically, it can be represented as follows:

CH = $Ca(OH)_2$
S = SiO_2
H = H_2O
CSH = calcium silicon hydrate

The process of hydration of cement with flying ash, as a Pozzolan additive, includes two processes:

- hydration of cement clinkers;
- pozzolanic reaction between fly ash and $Ca(OH)_2$, released by hydration of cement clinker.

Theoretically, both of these reactions are thought to aid each other in the process of hydrating the cement with fly ash: $Ca(OH)_2$ is released by hydration of the clinker, thus creating the conditions for the pozzolanic reaction. The Pozzolan reaction absorbs $Ca(OH)_2$ and thus accelerates its regeneration by hydrating the clinker. This reaction does not change the hydration process of the cement clinker but complements it, as the result is a lower content of $Ca(OH)_2$ and a higher content of calcium silicon hydrate. Interestingly, ash additive cements, compared to standard Portland cement, have a lower heat of hydration in the early hydration period, which is good for the concrete mass.

The addition of fly ash as a pozzolan to cement is of great significance in modern cement and concrete technology. Above all, it speeds up the hydration process and has other positive effects. As is well known, the most important:

$$xCH + yS + zH = CxSyHx + z \tag{1}$$

Portland cement clinker minerals are tricalcium silicate and dicalcium silicate, which make up about 75% of clinker. In contact with water these minerals form high base calcium silicon carbohydrates (ratio $C/S > 1.5$) and large amounts of $Ca(OH)_2$. These calcium silicon carbohydrates develop lower hardness than low base calcium silicon carbohydrates (ratio $C/S < 1.5$), and this leads to the formation of concretes with lower strength and lower durability. The addition of certain amounts of fly ash, as noted above, reacts SiO_2 from the ash with $Ca(OH)_2$, building low-base calcium silicon carbohydrates in the pozzolanic reaction. That is how it is achieved increasing the quality of the hydrates created, and thus the properties of the concrete thus obtained. Cement concrete structures with ash have been shown to develop greater mechanical strength and are more durable than those of pure Portland cement. In addition to having better durability, such concretes have greater resistance to sulfur corrosion, even when exposed to conditions in chemically aggressive environments, such as the impact of seawater [6].

The properties of the cement paste containing a certain percentage of ash depend to a large extent on the grain size of the ash. For these applications, fine-grained ash with low content of unburned coal is mainly used. The pozzolanic activity of the ash also depends on the ratio of the crystalline and amorphous components in the ash. Better properties are obtained for finer ash particles, which in addition to giving the cement paste greater density and homogeneity, also increase the number of nucleation centers that lead to precipitation of hydration products, and this accelerates the reaction of hydration. Incompletely reacted ash particles also increase the density of the paste because they fill the cavities. Very good compressive strength was shown by mortars obtained from ash cements with a particle size below 10 µm. In order to crush the ash particles and get better results, the ash can be mechanically activated. It has been found that the grinding, ie the mechanical activation of the ash improves its pozzolanic activity. By adding pre-activated ash to the mortar, together with cement, higher strengths, lower porosity and better corrosion resistance of the resulting concrete are also achieved. Hardness after 28 days increases by about 27% after which ash is added to the paste which is ground in a ball mill for 6 hours.

Depending on the combustion temperature of the coal, the type of coal and some other factors, the same flying ashes show different particle sizes. This means that different ash grain sizes show different properties. However, this is not of particular importance for Pozzolanic purposes, because when the grains are classified by size and added to the cement paste, the ashes have no greater effect on the hardness of the resulting mortars than the mortar obtained by adding one ash in which all particle sizes in cement paste. F (combustion of bituminous coals) and C (combustion of lignites) class ashes are used equally as a pozzolanic cement additive. By adding any of the ash classes in the mortar are achieve improved properties of concretes. For the F-class the activator is usually the Portland cement CaO, while for the C – class it is self – bonding. One of the first applications of fly ash was in cement factories, where, thanks to the properties of ash, it began to be used as a mineral pozzolanic additive and a substitute for cement. The main reasons for using this material as a Pozzolan additive in cement were primarily economic and environmental in nature, as ash is a relatively inexpensive material and replaces the more expensive Portland cement. Ash is very useful for improving the strength and durability of concrete, the use of ash has thus gained technological justification, which of course encourages the production of cement with pozzolanic additives.

USE OF FLAY ASH AS A RAW MATERIAL COMPONENT FOR THE PRODUCTION OF PORTLAND CEMENT

The idea that fly ash was used as a raw material in the production of Portland cement is not new worldwide. The ash can be used for these purposes because in its chemical composition it is very similar to the clay component used to prepare raw materials in the cement industry, i.e., it consists of SiO_2, Al_2O_3, Fe_2O_3 and CaO. Danish researchers as early as 1981 at the Seventh International Congress of Cement Chemistry presented various ways of fly ash in the cement industry, one of which was the use of this material as a raw material component. However, when a modern system of precalcinators was installed in the late 1980s and the procedure was upgraded, the ash completely replaced the clay component. That way about 400,000 tons of fly ash and other waste materials used in the cement industry as a raw material have been recycled in Denmark.

Favorable results from the use of ashes as raw materials in the cement industry were published during the 1990s and the beginning of the 21st century by researchers from Romania, the Czech Republic, Poland, Italy, Australia, Turkey, India and others.

In addition to solving the serious environmental problem, it is very important to achieve better clinker firing and better hydraulic properties of the cement obtained in this way. Some researchers have gone a step further in their research, using ash to obtain special types of cement, such as white cement, sulfoaluminate cement, sulfoaluminate – white cement, expansive cement, and others. [7]

CONCLUSION

Fly ash is generated as a waste product in the process of burning coal in thermal power plants. The characteristics of electrostatic precipitators depend on the type of coal and the method of ash collection with electrostatic precipitators. It is generally a fine, very fine-grained, powdery material. The flying ash produced in R. Macedonia is of class F or silicate ash with a content of SAO up to 15%.In the construction industry, low and high construction, electro filter ash is found in a wide and varied application and range of products, as a mineral pozzolanic additive and cement substitute. The main reasons for using this material as a Pozzolan additive in cement are primarily of economic and environmental nature, as ash is a relatively inexpensive material and replaces the more expensive Portland cement. Flying ash is very useful for improving the strength and durability of concrete, the use of ash with this gets technological justification, which of course encourages the production of cement with pozzolanic additives.

In the regular production in R. Macedonia produces four types of cement. One of the Portland cements is the so-called "Pure" i.e. made only of clinker, while all other types of cement in addition to clinker have mineral additives (flying ash and natural nozzles) as basic ingredients that improve certain characteristics of cements.

REFERENCES

1. Singh, M., Garg, M. (1999) Cementitious binder from fly ash and other industrial wastes, Cement and Concrete Research, 29, 3, 309-314.
2. Poon, C. S., Qiao, X.C., Lin, Z.S. (2003) Pozzolanic properties of reject fly ash in blended cement pastes, Cement and Concrete Research, 33, 11, 1857-1865.
3. Vassilev, S. V., Menendez, R., Alvarez, D., Diaz-Somoano, M., Martinez-Tarazona, M.R. (2003) Phase – mineral and chemical composition of coal fly ashes as a basis for their multicomponent utilization. 1. Characterization of feed coals and fly ashes, Fuel, 82, 14, 1793-1811.
4. Sokol, F.V., Kalugin, V.M., Nigmatulina, E.N., Volkova, N.I., Frenkel, A.E., Maksimova, N.V. (2002) Ferrospheres from fly ashes of Chelyabinsk coals: chemical composition, morphology and formation conditions, Fuel, 81, 7, 867-876.
5. Fernandez-Jimenez, A., Palomo, A. (2003) Characterization of fly ashes. Potential reactivity as alkaline cements, Fuel, 82, 18, 2259-2265.
6. Saraswathy, V., Muralidharan, S., Thangavel, K., Srinivasan, S. (2003) Influence of activated fly ash on corrosion – resistance and strength of concrete, Cement and Concrete Composites, 25, 7, 673-680.
7. Bhatty, J.I., Gajda, J., Miller, F.M. (2003) Commercial Demonstration of High-Carbon Fly Ash Technology in Cement Manufacturing, International Ash Utilization Symposium, Center for Applied Energy Research, University of Kentucky, Paper no.38, http://www.flyash.info/2003/38bha.pdf.

XIV International Mineral Processing
and Recycling Conference
Belgrade, Serbia, 12-14 May 2021

EFFECT OF FUEL ASH ON RAW MIX IN CLINKER PRODUCTION

Marinko Pavlović[#], Nikola Đokić, Taras Kulyk, Stefan Krstić
Moravacem Ltd, Popovac, Serbia

ABSTRACT - When raw meal is in the sintering zone in a rotary kiln, the ash from the fuel is incorporated into the clinker, which then changes its quality. Effect of ash needs to be calculated before preparation of raw meal, and constant quality of clinker production should be ensured. A way to control the effect ash has on the clinker, depending on the fuel mixture, is presented in this paper.

Keywords: Raw meal, Ash, Fuel, Clinker.

INTRODUCTION

By sintering the raw meal in a rotary kiln, during the production of clinker, the ash from the combustion of energy is incorporated into the clinker and change quality. In order to ensure constant quality of clinker, the impact of ash is controlled in phases in the production of raw meal.

The parameters which control the quality of clinker and raw meal or raw mixture are modules: LSF (lime saturation factor), SR (silicate ratio) and AR (aluminate ratio).

$$\boldsymbol{LSF} = CaO/(2.8SiO_2 + 1.18Al_2O_3 + 0.65Fe_2O_3) \quad (1)$$

$$\boldsymbol{SR} = SiO_2/(Al_2O_3 + Fe_2O_3) \quad (2)$$

$$\boldsymbol{AR} = Al_2O_3/Fe_2O_3 \quad (3)$$

The plan for the extraction of raw materials for creation of raw mixtures, in the current year, represents the starting phase of the control of the impact of ash. The plan defines the percentage of all components of raw meal. With the quality and percent of ash of the planned energy sources, the given extraction plan is controlled and adopted by the budget. Depending on whether the ash is acidic or basic, it is incorporation into clinker, changes the ratios. The corrective components (High Grade Limestone(HGL), quartz sand and iron corrective) are changed before raw mill and are limited by dosages. For this reason, it is necessary to regularly monitor the impact of fuel ash, in order to ensure the required quality of raw mix.

The raw mix is defined by the plan, constantly checked and harmonized in production, depending on the fuel mix percentage and quality of ash. The percentage of corrective components in raw meal is indirectly related to the quality of fuel ash in percentage.

[#] corresponding author: marinko.pavlovic@moravacem.rs

EXPERIMENTAL

Based on complete exploration, testing of marl and limestone for cement production, all necessary atributes have been defined in detail.

Four main oxides play a key role in the composition of raw materials for the production of raw meal: CaO, SiO_2, Al_2O_3 and Fe_2O_3. Based on the 3D block model of both deposits was implemented, all quality and quantity atributes were defined of each blocks for strategic and short-term planning.

The plan for the extraction of raw materials for the mixture, was made with the AthosGeo Blend software. An overview of the affected blocks, and the percentage of raw material components is shown in Figures 1, 2. and 3.

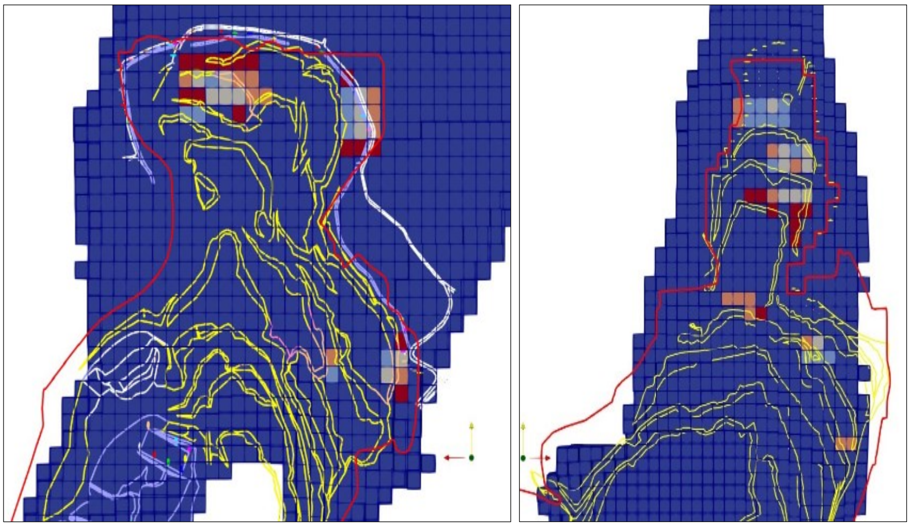

Figure 1 Plan of extraction for marl quarry (left) and limestone quarry (right)

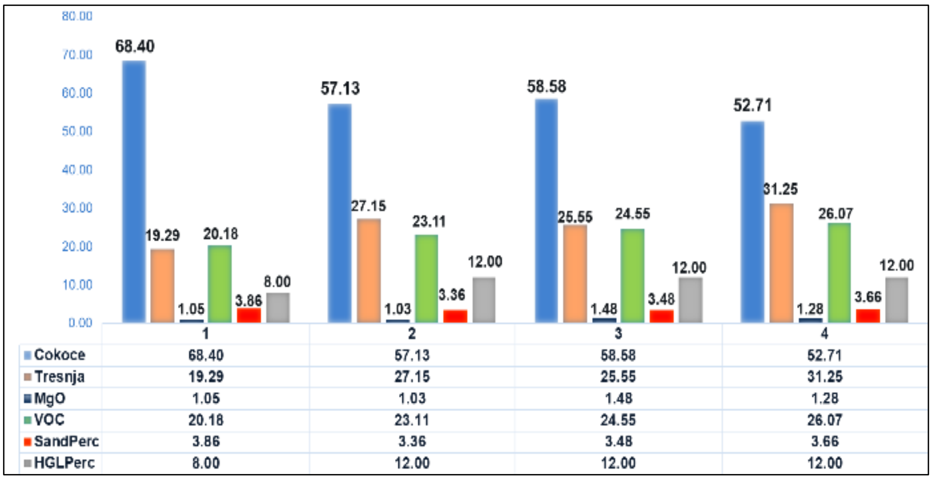

	1	2	3	4
Cokoce	68.40	57.13	58.58	52.71
Tresnja	19.29	27.15	25.55	31.25
MgO	1.05	1.03	1.48	1.28
VOC	20.18	23.11	24.55	26.07
SandPerc	3.86	3.36	3.48	3.66
HGLPerc	8.00	12.00	12.00	12.00

Figure 2 Overall per periods-Raw meal

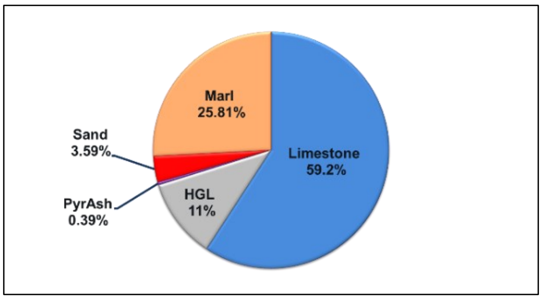

Figure 3 Overall, raw materials and correctives for 2021 - Raw meal

Planned fuels used for sintering raw meal in a rotary kiln consist of traditional (TF) and alternative fuels (AF). Traditional fuels includes: coal and petroleum coke, and alternative fuels: waste car tires, sorted municipal waste, industrial waste, agricultural waste, shredded rubber waste, electronic recycling waste. Their mix is defined depending on the energy value of TF and AF, as well as economy.

Table 1 Calorific values of fuel

Material	**Ash chemistry**						**Others**		**Heat value**	**CV Cont.**
	SiO_2	**Al_2O_2**	**Fe_2O_3**	**CaO**	**MgO**	**K_2O**	**Ash %**	**Fuel %**		
Petcoke	47.27	17.73	4.10	10.24	0.68	1.56	1.73	20.54	7404	1520.8
AF	33.19	16.05	6.17	28.08	5.41		16.4	41.10	4612	1895.5
Tyre			25				25.0	6.85	6210	425.4
coal	56.5	21.9	3.14	8.48	0.79	1.74	39.4	31.51	4588	1445.7
Fuel mix	44.43	18.2	5.88	14.06	2.19	1.04	21.22	100	5287.4	5287.4
Kiln Economy			**854.1 Kcal/kg-clinker**				% fuel on clinker			**16.2**
							Ash eq CK %			**3.43**

Alternative fuels are controlled (Table 2).

Table 2 AF mix analized

Fuel ash_ alternative fuels								
Date	**Supplier**	**Tipe AF**	**SiO_2**	**Al_2O_2**	**Fe_2O_3**	**CaO**	**MgO**	**Ash**
		%	%	%	%	%	%	%
10.03.2021 09:00	Sapphire	participation of the type of fuel from 04.-10.03.2021	23.22	17.25	6.67	35.47	6.03	17.57
17.03.2021 09:00	Sapphire	participation of the type of fuel from 11.-17.03.2021	25.66	16.44	5.93	33.66	6.22	17.74
24.03.2021 09:00	Sapphire	participation of the type of fuel from 18.-24.03.2021	30.66	15.70	7	37.09	6.67	16.99

In addition to deliveries, the daily mix of TF ash in percentage, seven days composite and ash quality are also controlled (Table 3).

Table 3 TF mix analized with ash

Fuel ash_traditional fuels										
Date, time	**Sample ID**	**Mix fuels**	**SiO_2**	**Al_2O_2**	**Fe_2O_3**	**CaO**	**MgO**	**K_2O**	**Na_2O**	**Ash**
			%	%	%	%	%	%	%	%
8.3.2021 09:00	NP21004922	A-60%,P-40%								28.24
9.3.2021 09:00	NP21005081	A-60%,P-40%								31.03
10.3.2021 10:00	NP21005222	A-55%,P-45%								35.25
11.3.2021 09:00	NP21005341	A-55%,P-45%								32.06
12.3.2021 09:00	NP21005493	A-58%,P-42%								32.47
13.3.2021 10:00	NP21005605	A-60%,P-40%								34.97
14.3.2021 08:00	NP21005722	A-60%,P-40%								35.35
14.3.2021 10:00	***Average 07.-14.03.2021***	***A-60%,P-40%***	***53.43***	***19.1***	***2.87***	***11.4***	***0.7***	***1.8***	***0.38***	***32.77***

RESULTS AND DISCUSSION

Based on the planned fuel mix (TF and AF), the extraction plan for the current year - the first phase is checked. If the results are acceptable, if it is possible to achieve the required quality: raw mix, mixture of marl and limestone, raw meal, raw mix and corrective components (HGL, quartz sand, iron corrective), clinker, raw meal, fuel ash and filter dust, the plan is adopted. The check is shown in Table 4 and 5.

Table 4 Raw materials

Raw Materials (unit:%)													
Material	**SiO_2**	**Al_2O_3**	**Fe_2O_3**	**CaO**	**MgO**	**LOI**	**SO_3**	**K_2O**	**Na_2O**	**Total**	**LSF**	**SR**	**AR**	**Moist.**
R mix	9.35	3.37	1.34	45.27	1.07	35.65	0.19	0.50	0.21	96.95	145.59	1.99	2.51	8.08
Ironox	4.63	12.61	75.89	1.26	0.32	2.67	2.60	0.23	0.19	100.40	1.63	0.05	0.17	20.53
Sand	95.34	1.18	0.85	0.24	0.09	1.76	0.03	0.61		100.10	0.09	46.97	1.39	5.81
H limestone	1.75	0.87	0.22	42.21	0.45	54.75	0.11	0.09	0.02	100.47	693.45	1.61	3.95	1.00

Table 5 Raw mix desing

	tones	%	SiO_2	Al_2O_2	Fe_2O_3	CaO	MgO	LOI	SO_3	K_2O	Na_2O	Ms	AR	Total
S.pile		100.0	13.28	3.38	1.83	43.33	0.90	35.65	0.27	0.60	0.21	2.55	1.85	97
s.pile		83.7	13.28	3.38	1.83	43.33	0.90	35.65	0.27	0.60	0.21	2.55	1.85	99
Ironox		0.3	4.63	12.61	75.89	1.26	0.32	2.67	2.60	0.23	0.19	0.05	0.17	100
Sand		2.0	95.34	1.18	0.85	0.24	0.09	1.76	0.03	0.61	0.00	46.97	1.39	100
Hlimestone		14.0	1.31	0.54	0.17	53.68	0.66	42.96	0.15	0.05	0.01	1.85	3.18	100
Rmeal	*135*	100.0	13.22	2.97	1.80	43.79	0.85	35.90	0.26	0.52	0.18	2.77	1.65	99
Fuel ash		3.43	44.43	18.20	5.88	14.06	2.19	0.00	0.00	1.04	0.00	1.84	3.09	86
DUST		14.00	11.31	3.77	1.83	43.84	0.90	35.51	1.02	0.90	0.26	2.02	2.06	99
Clinker	*86.54*		21.01	5.26	2.92	66.41	1.36		0.55	0.90	0.29	2.57	1.80	99
Clinker	C3S	C2S	C3A	C4AF	SR	A/F	ALK		DBC	LSF	Alk/SO3	%LIQ	RM/CK	FCaO
Minerals	63.5	12.3	9.0	8.9	2.57	1.80	0.88		-2.03	99.2	0.48	24.9	1.56	1.5

For each produced mixture, the quality adjustment of raw mix, raw meal and clinker is checked, based on ash quality for seven days in relation to the produced amount of clinker (t/h) (Figure 4, Figure 5 and Table 6).

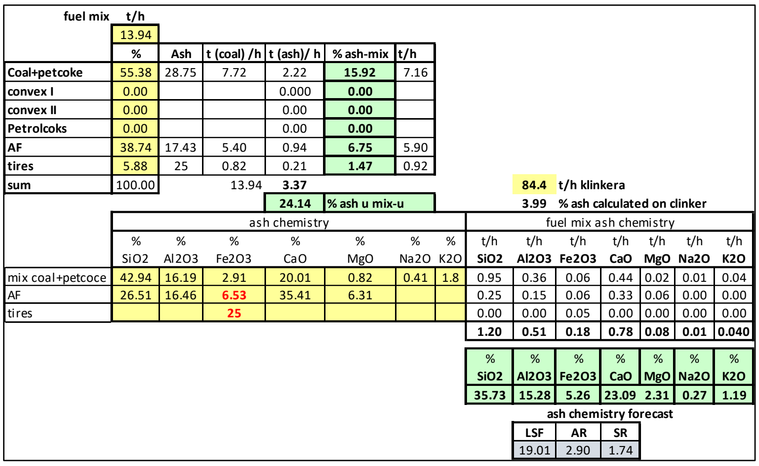

fuel mix	t/h					
	13.94					
	%	Ash	t (coal) /h	t (ash)/ h	% ash-mix	t/h
Coal+petcoke	55.38	28.75	7.72	2.22	15.92	7.16
convex I	0.00			0.000	0.00	
convex II	0.00			0.00	0.00	
Petrolcoks	0.00			0.00	0.00	
AF	38.74	17.43	5.40	0.94	6.75	5.90
tires	5.88	25	0.82	0.21	1.47	0.92
sum	100.00		13.94	3.37		
				24.14	% ash u mix-u	

84.4 t/h klinkera

3.99 % ash calculated on clinker

	ash chemistry							fuel mix ash chemistry						
	% SiO2	% Al2O3	% Fe2O3	% CaO	% MgO	% Na2O	% K2O	t/h SiO2	t/h Al2O3	t/h Fe2O3	t/h CaO	t/h MgO	t/h Na2O	t/h K2O
mix coal+petcoce	42.94	16.19	2.91	20.01	0.82	0.41	1.8	0.95	0.36	0.06	0.44	0.02	0.01	0.04
AF	26.51	16.46	6.53	35.41	6.31			0.25	0.15	0.06	0.33	0.06	0.00	0.00
tires			25					0.00	0.00	0.05	0.00	0.00	0.00	0.00
								1.20	0.51	0.18	0.78	0.08	0.01	0.040

% SiO2	% Al2O3	% Fe2O3	% CaO	% MgO	% Na2O	% K2O
35.73	15.28	5.26	23.09	2.31	0.27	1.19

ash chemistry forecast

LSF	AR	SR
19.01	2.90	1.74

Figure 4 Ash mix fuel for the stock pile

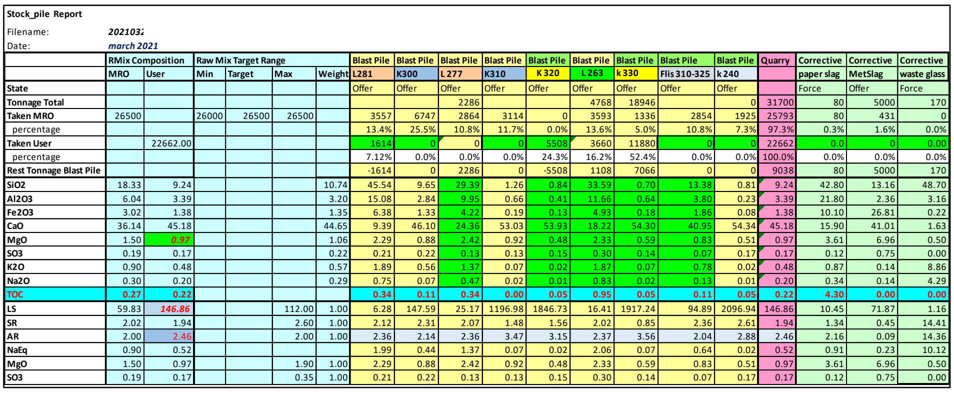

Stock_pile Report

Filename: 2021032

Date: march 2021

	RMix Composition		Raw Mix Target Range				Blast Pile	Blast Pile	Blast Pile	Blast Pile	Blast Pile	Blast Pile	Blast Pile	Blast Pile	Blast Pile	Quarry	Corrective	Corrective	Corrective
	MRO	User	Min	Target	Max	Weight	L281	K300	L 277	K310	K 320	L 263	k 330	Flis 310-325	k 240		paper slag	MetSlag	waste glass
State							Offer	Offer	Offer	Offer	Offer	Offer	Offer	Offer	Offer		Force	Offer	Force
Tonnage Total									2286			4768	18946		0	31700	80	5000	170
Taken MRO	26500		26000	26500	26500		3557	6747	2864	3114	0	3593	1336	2854	1925	25793	80	431	0
percentage							13.4%	25.5%	10.8%	11.7%	0.0%	13.6%	5.0%	10.8%	7.3%	97.3%	0.3%	1.6%	0.0%
Taken User		22662.00					1614	0	0	0	5508	3660	11880	0	0	22662	0.0	0	0.00
percentage							7.12%	0.0%	0.0%	0.0%	24.3%	16.2%	52.4%	0.0%	0.0%	100.0%	0.0%	0.0%	0.0%
Rest Tonnage Blast Pile							-1614	0	2286	0	-5508	1108	7066	0	0	9038	80	5000	170
SiO2	18.33	9.24				10.74	45.54	9.65	29.39	1.26	0.84	33.59	0.70	13.38	0.81	9.24	42.80	13.16	48.70
Al2O3	6.04	3.39				3.20	15.08	2.84	9.95	0.66	0.41	11.66	0.64	3.80	0.23	3.39	21.80	2.36	3.16
Fe2O3	3.02	1.38				1.35	6.38	1.33	4.22	0.19	0.13	4.93	0.18	1.86	0.08	1.38	10.10	26.81	0.22
CaO	36.14	45.18				44.65	9.39	46.10	24.36	53.03	53.93	18.22	54.30	40.95	54.34	45.18	15.90	41.01	1.63
MgO	1.50	0.97				1.06	2.29	0.88	2.42	0.92	0.48	2.33	0.59	0.83	0.51	0.97	3.61	6.96	0.50
SO3	0.19	0.17				0.22	0.21	0.22	0.13	0.13	0.15	0.30	0.14	0.07	0.17	0.17	0.12	0.75	0.00
K2O	0.90	0.48				0.57	1.89	0.56	1.37	0.07	0.02	1.87	0.07	0.78	0.02	0.48	0.87	0.14	8.86
Na2O	0.30	0.20				0.29	0.75	0.07	0.47	0.02	0.01	0.83	0.02	0.13	0.01	0.20	0.34	0.14	4.29
TOC	0.27	0.22					0.34	0.11	0.34	0.00	0.05	0.95	0.05	0.11	0.05	0.22	4.30	0.00	0.00
LS	59.83	146.86			112.00	1.00	6.28	147.59	25.17	1196.98	1846.73	16.41	1917.24	94.89	2096.94	146.86	10.45	71.87	1.16
SR	2.02	1.94			2.60	1.00	2.12	2.31	2.07	1.48	1.56	2.02	0.85	2.36	2.61	1.94	1.34	0.45	14.41
AR	2.00	2.46			2.00	1.00	2.36	2.14	2.36	3.47	3.15	2.37	3.56	2.04	2.88	2.46	2.16	0.09	14.36
NaEq	0.90	0.52					1.99	0.44	1.37	0.07	0.02	2.06	0.07	0.64	0.02	0.52	0.91	0.23	10.12
MgO	1.50	0.97			1.90	1.00	2.29	0.88	2.42	0.92	0.48	2.33	0.59	0.83	0.51	0.97	3.61	6.96	0.50
SO3	0.19	0.17			0.35	1.00	0.21	0.22	0.13	0.13	0.15	0.30	0.14	0.07	0.17	0.17	0.12	0.75	0.00

Figure 5 Raw mix

Table 6 Raw mix desing

	tones	%	SiO_2	Al_2O_2	Fe_2O_3		CaO	MgO	LOI	SO_3	K_2O	Na_2O	Ms	AR	Total
S.pile		100.00	13.28	3.38	1.83		43.33	0.90	35.65	0.27	0.60	0.21	2.55	1.85	100.
s.pile		83.7	13.28	3.38	1.83		43.33	0.90	35.65	0.27	0.60	0.21	2.55	1.85	99
Ironox		0.3	4.63	12.61	75.89		1.26	0.32	2.67	2.60	0.23	0.19	0.05	0.17	100
Sand		2.0	95.34	1.18	0.85		0.24	0.09	1.76	0.03	0.61	0.00	46.97	1.39	100
Hlimest.		14.0	1.31	0.54	0.17		53.68	0.66	42.96	0.15	0.05	0.01	1.85	3.18	100
Rmeal	135	100.0	13.22	2.97	1.80		43.79	0.85	35.90	0.26	0.52	0.18	2.77	1.65	99
Fuel ash		4.15	45.42	17.39	4.94		14.67	1.93	0.00	0.00	1.24	0.26	2.03	3.52	86
DUST		14.00	11.31	3.77	1.83		43.84	0.90	35.51	1.02	0.90	0.26	2.02	2.06	99
Clinker	*88.74*		20.14	5.52	2.94		64.01	1.40		0.45	0.82	0.29	2.38	1.88	99
Clinker	C3S	C2S	C3A	C4AF	SR		A/F	ALK		DBC	LSF	Alk/SO3	%LIQ	RM/CK	FCaO
Minerals	58.9	12.3	9.0	8.9	2.57		1.80	0.88		-2.03	99.2	0.48	24.9	1.56	1.5

CONCLUSION

The extraction plan is made by AtosGeo Blend software, in accordance with the technical mining documentation, the mix of energy plan (TF and AF). Verified extraction plan on the impact of fuel ash is the starting point for good control of ash quality on clinker.

In the process of production of raw mix, raw meal and clinker, regular and representative control of energy quality (TF, AF) and ash quaility is necessary.

The raw mix defined by the plan, is constantly checked and harmonized in production, depending on the fuel mix and the percentage and quality of ash.

The percentage of corrective components in raw meal is indirectly related to the percentage and quality of ash from fuel.

Continuous monitoring of the impact of ash on the quality of raw mix, raw meal and clinker through daily and seven days fuel analyzes, enables stable and continuous quality of clinker.

REFERENCES

1. Pavlović, M. (2010) Planning the exploitation of activities for the application of KM in the NP, Popovac. (In Serbian)
2. Elke, S., et al. (2008) Novi Popovac: Raw Material Investigation and Evaluation of Cokoce Limestone and Tresnja Marl Deposit, Holderbank.
3. Pavlović, M. (2015) Unification of quality of input raw materials for the needs of cement production in Holcim cement plant (Serbia), Bor. (In Serbian)
4. Blaha, P. (2019) Implementation og AtosGEO Blend, Novi Popovac.
5. Pavlović, M., Đokić, N. (2021) Exttraction Plan. CRH (Serbia)

XIV International Mineral Processing
and Recycling Conference
Belgrade, Serbia, 12-14 May 2021

DISSOLUTION OF GLASS MADE FROM COAL FLY ASH, GLASS CULLET AND CALCIUM CARBONATE

Veljko Savić[1#], Vladimir Topalović[1], Jelena Nikolić[1], Srđan Matijašević[1], Snežana Zildžović[1], Snežana Grujić[2], Sonja Smiljanić[2,3]
[1] Institute for Technology of Nuclear and Other Mineral Raw Materials, Belgrade, Serbia
[2] Faculty of Technology and Metallurgy, Belgrade, Serbia
[3] Institute "Jožef Stefan", Ljubljana, Slovenia

ABSTRACT – Coal fly ash represents huge ecological problem and its reutilization should be considered. Vitrification of coal fly ash could be one of the solutions. The glass was obtained by melting a mixture of coal fly ash, glass cullet and $CaCO_3$ at T = 1500 ^oC and quenching the melt in air. The chemical durability of the glass was determined by dissolution test in distilled water, HCl and NaOH at T = 95 ^0C for t = 2 h. It was shown that dissolution rate of glass in distilled water and NaOH is negligible, while in HCl solution was shown significant mass loss.

Keywords: Coal Fly Ash, Glass, Dissolution.

INTRODUCTION

In Serbia, around 8 million tons of ash and slag, each year, has been generated (thermal power plants burn about 40 million tons of lignite annually and produce about 6 million tons of fly ash) [1], where about 2.5% is used in the cement industry. The development of glass and glass-ceramic based on various waste materials is an important area of research because the waste materials can be used to obtain glassy or glass-ceramic materials whose properties are comparable to the properties of commercially available materials.

Fly ash is generated in the process of burning coal in thermal power plants. The incombustible part of the coal matter after combustion stays at the bottom of the furnace as bottom ash and slag, and the part leaves the plant with flue gases and is collected on electrostatic filters, and is called fly ash. Fly ash is mostly disposed of in landfills, but due to its chemical composition where SiO_2, Al_2O_3, CaO, and Fe_2O_3 are dominant oxides, it can be used for road construction, in the cement industry and for obtaining glass and glass-ceramic. Therefore, it is important to find a solution for recycling the generated fly ash and remediation of landfills.

Worldwide, more than 65% of fly ash produced from coal power stations is disposed of in landfills and ash ponds. Large quantities of fly ash are deposited in landfills, which have to be wet to minimize the spread of dust into the environment. In all countries in the world, this is a huge economic and environmental problem. The negative

---

[#] corresponding author: v.savic@itnms.ac.rs environmental impacts of fly ash landfilling are primarily connected with toxic metals that it contains.

The goal in the European Union is to phase-out coal consumption by 2030 and to increase the production of energy from renewable sources [2]. Some European and Western Balkans countries will still use coal thermal power plants after 2030 to produce energy. Even after the closing of currently operating coal-fired thermal power plants, there will be fly ash that isn't reutilized as secondary raw material and is disposed of in landfills or ponds. Landfills and ponds take great areas of land and represent a potential problem for human health, underground water, nearby crops and the whole ecosystem.

From the ecological point of view, during the high-temperature treatment of the fly ash in order to obtain glass, the destruction of the organic pollutants occurs. Vitrification is a known technology for the inertisation of various industrial residues that permits to obtain stable glasses [3,4]. By properly selecting the glass composition and thermal treatment this method gives possibility for re-utilization of the glass or glass-ceramic as raw material for different industrial applications. Additionally, heavy metals present in the glass batch can be successfully immobilized in the glassy matrix. These products can be classified as inert materials, which supports their potential use as eco-friendly building construction materials. Obtaining the glass by recycling of coal fly ash in the glass production includes three main advantages: using a zero cost material, the conservation of natural resources and the elimination of fly ash. The fly ash based glass materials can be used in building and construction, as well as a raw material for making glass-ceramic products [5].

Due to a good mechanical, chemical, and thermal properties, a wide application of glass and glass- ceramic materials made from industrial waste is possible, especially in the building industry.

EXPERIMENTAL

The glass was prepared by a standard melt quenching procedure. Coal fly ash, glass cullet from bottle glass and $CaCO_3$, were mixed and homogenized in an agate mortar in 37.5:37.5:25 ratio. The melting was performed in an electric furnace in zirconium silicate crucible at $T = 1500$ °C for $t = 1$ h and the glass was obtained by quenching of the melt on a steel plate. The obtained dark sample was black without visible gas bubbles. The chemical analysis was performed using spectrophotometer AAS PERKIN ELMER Analyst 703. The powder X-ray diffraction (XRD) analysis confirmed that the quenched melts were vitreous. The chemical durability of glass was estimated in distilled water, 0.01 M HCl and 0.01 M NaOH, respectively. In these experiments 2 g grained samples with sizes from 0.3 to 0.5 mm were placed in contact with 70 ml solution for 2 h at $T = 95$ °C [6]. Solutions were analyzed and loss of elements from glass was determined. The microstructure of the glass samples before and after leaching tests was examined using scanning electron microscope (MIRA3 XM TESCAN). The samples were gold coated using Leica SCD005 device.

RESULTS AND DISCUSSION

The chemical composition of the coal fly ash and glass cullet is shown in Table 1. Due to low concentration of glass network modifier cations viscosity of melted fly ash and glass cullet is very high, and it is imposible to pour it.

Table 1 Chemical composition of the coal fly ash and glass cullet

Sample	**oxides**	**SiO_2**	**Al_2O_3**	**CaO**	**MgO**	**Na_2O**	**K_2O**	**Fe_2O_3**	**TiO_2**	**Cr_2O_3**	**L.o.i**
Coal fly ash	mass%	55.33	25.11	6.26	1.42	0.32	1.23	7.08	0.50	/	2.52
Glass cullet	mass%	71.8	2.46	10.21	2.05	12.74	/	0.42	/	0.117	0.2

In order to make melt pourable chemical composition of batch should be altered introducing modifier cations in the batch using calcium carbonate.The homogenous dark glass was obtained by melt casting on steel plate is shown in figure 1.

Figure 1 Obtained glass sample

XRD patterns are shown in Figure 2.

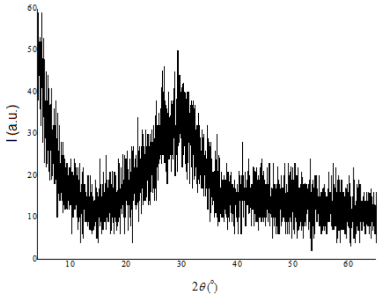

Figure 2 XRD patterns of the obtained glass sample

No crystalline phase was found which confirms that obtained material is amorphous. The chemical composition of the glass sample is shown in Table 2.

Table 2 Chemical composition of obtained glass

Oxide	**SiO_2**	**Al_2O_3**	**CaO**	**MgO**	**Na_2O**	**K_2O**	**TiO_2**	**Fe_2O_3**	**Cr_2O_3**
Mass %	49.54	10.58	32.88	1.58	1.44	0.72	0.34	2.68	0.08

Obtained glass has high concentration of glass network modifier cations which enabled optimal viscosity for melt to be poured.

The results of dissolution test are shown in table 3.

Table 3 Dissolution test of fly ash glass

Solution	Weight loss (%)
Distillated water	negligible
0.01 M NaOH	negligible
0.01 M HCl	20.15

The dissolution of glass matrix is a complex process that consists of several characteristic steps. There are two possible mechanisms, explaining the release of cations from the glass structure in different aqueous solutions, ion-exchange leaching, and matrix dissolution [7].

In alkaline media, the dissolution of the Si-glass network by which the glass dissolves directly into the solution takes place.

In neutral and acid media, the initial dissolution is characterized by ion exchange processes between protons in solution and glass network modifier cations, resulting in the formation of a hydrated layer, through which the aqueous species diffuse. Therefore, in neutral and acid media, the initial stage of the reactions is the diffusion of alkali ions through the glass network and across the leached layer into the solution [8].

At the same time, the glass network composed of network forming tetrahedrons hydrolyzes, causing the release of cations into solution. As a consequence, the complete destruction of the polyanionic glass network occurs.

In figure 3 is shown the percentage of elements released during leaching in acid media and in figure 4 is shown SEM micrograph of glass surface before and after leaching in acid media.

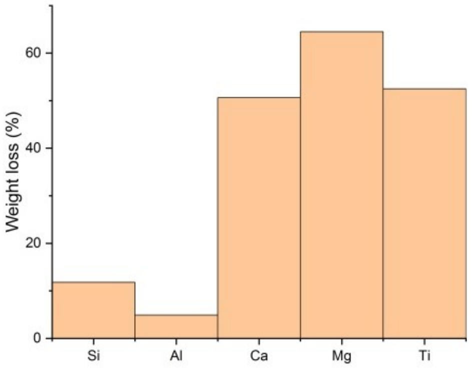

Figure 3 Weight loss of elements of glass sample leached in acid media

Results from figure 3 have shown that ion exchange process between protons in solution and glass network modifier cations is dominant mechanism of glass dissolution. More than 50% of glass network modifier cations leached in acid solution.

In figure 4 is shown change of glass surface after leaching test in acid media. Gel - like structure is formed on the surface of the glass, probably due the destruction of the polyanionic glass network.

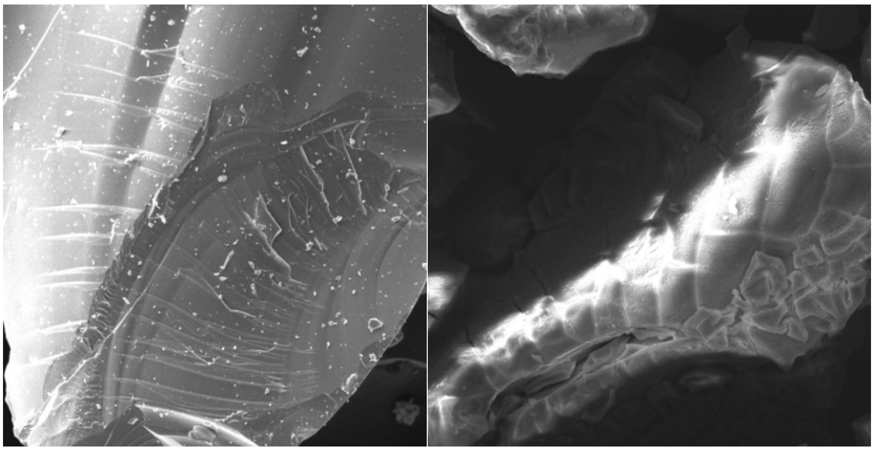

a) b)

Figure 4 SEM micrographs a) before and b) after dissolution test in acid media

CONCLUSION

The glass was successfully obtained using coal fly ash, glass cullet and $CaCO_3$ as raw materials. The results of laboratory experiments have shown that the vitrification process can be considered as promising solution for utilization of industrial waste. The results of dissolution test of grained glass samples revealed a high durability in distilled water and in alkali solution. Weight loss determined after dissolution in HCl solution has shown a poor acid durability of the glass. Analysis of acid solution after leaching test has showed that ion exchange processes between glass network modifier cations and acid solution is dominant mechanism of glass dissolution. Obtained glass can find potential application as thermal and sound insulator, construction materials and wall tiles.

ACKNOWLEDGEMENT

This research was supported through the Ministry of Education and Science of the Republic of Serbia, grant contract No.: 451-03-9/2021-14/200023.

REFERENCES

1. http://www.eps.rs/lat/Stranice/proces-proizvodnje-uglja.aspx, (January 2021.).
2. IEA(2020),EuropeanUnion2020,IEA,Parishttps://www.iea.org/reports/europeanuuon-2020, (January 2021.).
3. Colombo, P., Brusatin, G., Bernardo, E., Scarinci, G., (2003) Inertization and reuse of waste materials by vitrification and fabrication of glass-based products. Curr. Opin. Solid StateMater.Sci., 7, 225–239.
4. Bingham, P.A., Hand, R.J., (2006) Vitrification of toxic wastes: a brief review. Adv. Appl. Ceram., 105, 21–31.
5. Rincon Romero, A., Salvo, A. M., Bernardo, E. (2018) Up-cycling of vitrified bottom ash from MSWI into glass-ceramic foams by means of ‘inorganic gel casting’ and sinter-crystallization. Constr Build Mater., 192, 133-140.

6. Karamanov A., Pelino, M., Salvo, M., Metekovits, I. (2003) Sintered glass-ceramics from incinerator fly ashes. Part II. The influence of the particle size and heat-treatment on the properties. J. Eur. Ceram. Soc., 23, 1609–1615.
7. White, W. B. (1992) Corrosion of glass, ceramics and ceramic superconductors, Noyes Publications, New Jersey.
8. Gin, S. , Jégou, C., Frugier, P., Minet, Y. (2008) Theoretical consideration on the application of the Aagaard–Helgeson rate law to the dissolution of silicate minerals and glasses. Chem. Geol., 255, 14-24.

XIV International Mineral Processing
and Recycling Conference
Belgrade, Serbia, 12-14 May 2021

UTILIZATION OF SECONDARY RAW MATERIALS FROM MINE TAILINGS AND INDUSTRIAL LANDFILLS

Irma Dervišević[1#], Jovana Galjak[1], Ivica Ristović[2]
[1] University of Priština, Faculty of Technical Science Kosovska Mitrovica,
Kosovska Mitrovica, Serbia
[2] University of Belgrade, Faculty of Mining and Geology, Belgrade, Serbia

ABSTRACT – Recovery of metals from secondary raw materials generated in mining, industrial and other waste aims to reduce negative impacts of tailings and landfills on the environment and human health through multiple benefits: reducing the amount of landfilled waste while reducing environmental pollution, more efficient use of materials, preserving natural resources and promoting future sustainable development. The circular economy is essential to develop a sustainable, low carbon, resource efficient, and competitive economy in the developed countries. The recovery of critical, precious, and other materials from extractive waste and landfills, highlighting technological innovations contributions to more efficiency and economic, energy and environmental sustainability. This work aims to identify the best available technologies for material recovery in order to avoid landfill solutions. Within this scope are presented recycling and the recovery of some valuable and rare metals and salts. Finally, future perspectives are provided to advance understanding of this anthropogenic waste as a source of resources, yet tied to safeguards for the environment.

Keywords: Mining and industrial landfills, Recovery, Utilization of secondary raw materials, Environmental protection.

INTRODUCTION

Proper waste management is one of the most important goals of sustainable development [1, 2]. At all stages of metal production, waste is generated which can be composed of natural materials that are only crushed (ordinary mining waste, unusable mineralized materials) or of natural materials that have been processed to varying degrees, during phase of concentration and processing of concentrates, which contain chemical, inorganic and organic additives [3]. Ore extraction and concentrate production operations produce large quantities of unsuitable materials (mineral waste), most of which are usually disposed of in landfills (coarse material) and tailings (fine material) [4]. Mining and industrial waste landfills occupy huge areas of land. Inadequate waste management, which is often reflected, first in the wrong choice of disposal sites, then inadequate treatment and disposal of waste, leads to negative impacts on the quality of all environmental media [5]. Depending on the amount, composition and manner of temporarily or permanently disposed waste, the degree of endangerment of a given locality or region depends. Heavy metals, which are often constituents of mining and industrial tailings/dumps, are high on the scale of pollutants that can seriously endanger the environment, flora and fauna and human health [6]. Intensive technological

---

[#] corresponding author: Irma.dervisevic@pr.ac.rs development leads to: accelerated consumption of primary raw materials, increased energy consumption, progressive generation of huge amounts of waste and environmental pollution [7]. Is very unlikely that recovery processes can target one or just a few specific materials of great interest and disregard other elements or bulk matrixes. Especially in case of very low concentrations, most of the mineral resources and other bulk materials in which they are embedded must be valorized in order to increase economic viability and minimize waste generation. As recovery processes can be very energy intensive, environmental and land use related aspects are also particularly relevant in that environmental gains may also occur and, moreover, land space can be liberated and reused for new purposes and services [8]. From the report of the Environmental Protection Agency, it was generated only in 2019 in the Republic of Serbia almost 12 million tons (11,976,125 tons) of waste, (not counting waste from mining activities) of which 70% of waste ($8.3 \cdot 10^6$ tons) refers to waste from thermal processes. Of the total amount of waste produced in 2019, 78,413 t is hazardous waste, which is 11.3 kg/dwelling/year [9]. It is necessary to prevent further environmental pollution and promote sustainable production and consumption, so that economic growth does not cause a proportional increase in environmental degradation. Sustainable economic growth is based on the efficient use of natural resources and a high level of protection and improvement of the quality of the environment [10]. There is a growing importance of the so-called "internal reserves", i.e. secondary raw materials, which, in addition to investing in research, provide opportunities for their processing into useful products. Insight into the data of the total world production of some non-ferrous metals from primary and secondary raw materials in the period from 1990 to 2019, it is noticed that there is no significant deviation in the production of these metals from secondary sources; where the share of produced Al from secondary raw materials ranged from 30-34.90%, the share of produced Cu for the same period ranged from 13.12-20.13%, the share of Zn production 20.55-22.09%, Sn from 5.04-7.34, while the highest increase in the share of production from secondary sources recorded in the case of Pb and ranged from 41.90-68.00% [11].

CIRCULAR ECONOMY

Managing waste and secondary raw materials in an efficient way is the first step towards a circular economy, in which it is necessary that all products and materials are used, recycled or reused more efficiently. This legal framework sets very ambitious goals for recycling and safe waste disposal. Since 2016, a shift in the focus of policy has been applied, from improving resource efficiency - to the broader perspective of the circular economy [12]. Many aspects of these two approaches overlap in policies, such as waste management and waste prevention, in particular with environmental and sustainable development strategies, innovation policies and economic programs. This shift is expected to be further strengthened in the future, as broader EU actions are under way at the moment, especially with the newly adopted EU Circular Economy Action Plan, which is one of the key parts of the Green European Agreement [12]. The industry sector provides many important economic and social benefits such as the production of goods and products, the provision of employment and tax revenues. On the other hand, the industry participates in emissions of pollutants, land degradation, waste generation, intensive energy consumption, etc. The importance of using secondary raw materials, in addition to preserving resources and the environment, contributes to lower processing costs and relatively small investments. The costs of production of certain metals from secondary raw materials are up to ten times lower than the production of the same from primary resources, primarily due to lower consumption of electricity and energy in general. The problems of environmental pollution in the Republic of Serbia are largely the result of outdated technology and equipment, as well as low energy and raw material efficiency, which is partly due to the lack of financial resources to improve the existing situation.

POTENTIAL OF SECONDARY RAW MATERIALS

EU Raw Materials Initiative = EU Raw Materials Policy. The goal is to ensure sustainable stocks of raw materials - Launched in 2008, consolidated in 2011. Refers to non-energy, non-agricultural raw materials. Linking EU foreign and domestic policy is an integrated strategy based on three main pillars: 1. Increasing resource efficiency through recycling; 2. Sustainable supply of raw materials from domestic sources; 3. Ensuring a level playing field for access to resources in third countries.

Intensive mining activities in the exploitation of mineral resources in the last few decades have contributed to the economic and social development of the region, but have resulted in significant negative impacts on the environment: generating huge amounts of industrial waste and pollutant emissions into all media.

New and more modern technological solutions open the perspective of more efficient use of materials, processing of waste sludge and sludge from current or previous production, as well as exploitation of old tailings dumps, which today represent a significant potential of secondary raw materials.

These materials contain significant amounts of various non-ferrous, rare, precious and valuable metals, which were left in earlier periods because the technological knowledge at the time was insufficient to solve the problem of their economic exploitation.

In addition to platinum group metals, rare metals are of great importance and application in the most advanced technologies, and many of them are of strategic importance due to their application in military technologies. Due to geochemical properties, rare earth elements are usually dispersed and are rarely found in concentrated, economically viable exploitative forms, obtained by processing various output sediments and sludge’s in which they are concentrated in hydrometallurgical production of non-ferrous metals. Conventional methods of metal production and processing consume large amounts of chemicals and energy and lead to significant emissions and immissions of various hazardous substances, polluting all environmental media.

The choice of the most favorable option for metal recovery depends on criteria such as: quantitative and qualitative content of secondary raw material, ability to efficiently extract metal, capital investment, effort, time required for recovery, energy consumption, environmental compatibility, appropriate expertise. Traditional methods of metal recovery, by processing secondary raw materials containing some valuable and rare metals are insufficiently selective, efficient and environmentally friendly. In order to prevent and control pollution, it is necessary to reconstruct and innovate existing technological processes, by introducing the best available techniques and best practices for the environment.

ESTIMATION OF QUANTITATIVE AND QUALITATIVE COMPOSITION OF SECONDARY RAW MATERIALS

Representative material is sampled by extensive drilling. Often the deposit does not show any pronounced layered structure. Mineralogical analyzes show a relatively homogeneous distribution of minerals. Deviations in the concentrations of targeted valuable substances are relatively low. Some metals are part of oxides, others of sulfides, silicates or other constituents.

The computer model of deposits, which are highly developed and represent the basis for quantifying potential raw materials, is often used in estimating the amount of individual metals. The estimation is based on the concentration of elements, their representation and all fractions, and the total mass estimates give the available potentials.

PHYSICAL-CHEMICAL SEPARATION PROCESSES OF SECONDARY RAW MATERIALS

Physical-chemical separation processes are applied in the pre-treatment of secondary raw materials. They include grinding techniques - crushing, fine grinding, sieving, enrichment techniques - sorting, gravitational concentration, magnetic separation, electrostatic separation finely dusted and dried samples, flotation, leaching, etc.

Conventional flotation separation procedures, using innovative technologies such as microwaves and ultrasound, contribute to greater efficiency of the selective separation process. Microwaves cause direct heating of the reaction solution and selective activation of the constituents. The goal is a controlled and economical heating process, because in this way the activated substances from the solution contribute to the interaction with microwaves and / or ultrasound, the formation of radicals, which can reduce the required reaction time and the amount of chemicals.

RECOVERY METHODS OF SOME METALS

Previous knowledge indicates that mechanical-chemical leaching of metals is very selective and brings the best experimental results. Recovery of metals begins with fine mechanical comminution of slag with the aim of activating the surface of the particles while simultaneously separating the target elements with the help of poorly concentrated inorganic acids, or bases, or organic complex agents.

Oxide to sulfide forms of the target metals are often present in the starting material. They are represented by: Al, Si, Ca, Mg, $CaCO_3$. Components of slag can be some Alkali metals, such as Sodium, as well as oxygen as a result of oxidation.

The iron present in the secondary raw materials acts as a collector metal in the processes of melting platinum group metals that need to be recovered.

By fine grinding and increasing the temperature in mechanical-chemical processes, the solubility of Al, Si, Zr decreases, if present, and the solubility of Ca, Ce, La increases.

In solution after 1 h of mechanical-chemical treatment using less concentrated acid, the result obtained is comparable to dissolved metals in the aqua region (HCl: HNO_3 3: 1) after 12 h. For comparison, significantly less cerium could be isolated from conventionally extracted samples: a cerium concentration of 2.85% can be obtained by extraction in the aqua regia for 12 h, and 85% of the Ce thus extracted (2.42%) by mechanochemical washing, 1M HCl in for 1 h. Classical rinsing after pretreatment in a ball mill gives only 42%, or 1.2% recycling success, or only 15% (0.43) when using a rotary mill. Aqua regia is used only in laboratory conditions for environmental and economic reasons.

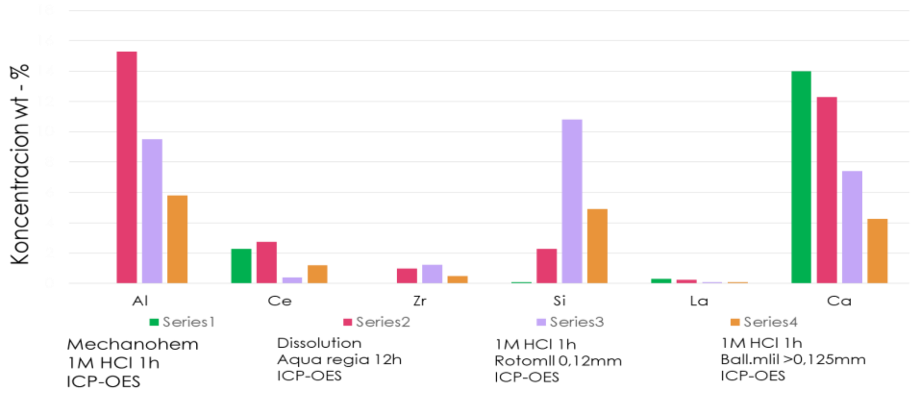

Figure 1 Concentration of Ce, La, Al, Zr, Si and Ca ions in the extraction process based on classical and mechanochemical leaching

The method of "solid gases" offer the possibility of selective separation of valuable metals that can be converted into a gaseous compound. In this cases, conditions for sublimation should be provided - conversion of metal from solid to gaseous state. Most oxides can be transformed into gaseous metal chlorides by chlorination. Suitable processes are hot chlorination with chlorine or ammonium chloride or carbochlorination. In the process of carbochlorination, metals: Nb, Ti and Zr pass into the gas phase at 800 °C, and rarely earth metals only at 1,000 °C.

For selective recovery matals, must condense from the gas phase. From an economic point of view, it is necessary to apply methods with lower energy consumption for complex access to gas and simpler control of the sublimation process.

One of the innovative methods of extraction of some metals is the use of cloth/textiles with polyelectrolytes, which are capable of selective separation and filtration of some rare metals from waste streams. Polyelectrolytes with such selective capabilities should be permanently attached to textile supports using simple methods of classical finishing, which will help more efficient recovery and recycling of valuable and important metals. By controlling process parameters, such as pH, selective precipitation of their compounds or metals can be realized, while the target metal can be completely removed from the remaining solution by means of an innovative cloth depending on the filtration rate.

CONCLUSION

Metal recovery efficiency is improved by using a combination existing and new technologies, such as fine-grained, efficient separation, dielectric heating, traditional and microwave baking, ozonation washing and ultrasonic washing. Innovative highly selective technologies for the recovery of target metals (low concentrations) without disturbing the properties of the rest of the matrix materials for valorization, require a radical new approach with a smart combination of modern methods that provide optimization of efficiency, economy, greening of the process with stable and sustainable future development.

ACKNOWLEDGEMENT

This research is conducted as a part of project No. III 43007 and No 37016 and is supported by the Ministry of Education, Science and Technological development of the Republic of Serbia.

REFERENCES

1. Law on Waste Management of the Republic of Serbia, Official Gazette 36/ 009-115, 88/2010-170, 14/2016-17, 95/2018-267.
2. Law on Environmental Protection of the Republic of Serbia, Official Gazette 135/ 2004-29, 36/2009-144, 36/2009-115, 72/2009-164, 43/2011-88 (US), 14/2016-3, 76/2018-3, 95/2018-267.
3. BRGM: Management of mining, quarrying and ore processing waste in the European union, Decembar 2001.
4. Chan BKC, Bouzalakos S, Dudeney A.W.L, Integrated waste and water management in mining and metallurgical industries, Transaction of Nonferrous Metals Society of China, Vol. 18, 1497-1505.
5. Talens Peiro, L., Nuss, P., Mathieux, F. and Blengini, G., (2008) Towards Recycling Indicators based on EU flows and Raw Materials System Analysis data, EUR 29435 EN, Publications Office of the European Union, Luxembourg, 2018.
6. Ardente, F., Mathieux, F., (2014) Identification and assessment of product measures to improve resource efficiency: the case-study of an Energy using Product. J. Clean. Prod. 83, 126–141.
7. EC - European Commission, (2017). European Innovation Partnership on Raw Materials: Annual Monitoring Report 2016, EUR 28839. ed. Publications Office of the European Union, Luxembourg. doi:10.2760/057300.
8. Jones, P.T., Geysen, D., Tielemans, Y., Van Passel, S., Pontikes, Y., Blanpain, B., Quaghebeur, M., Hoekstra, N., (2013). Enhanced Landfill Mining in view of multiple resource recovery: a critical review. J. Clean. Prod. 55, 45–55.
9. Report of the Environmental Protection Agency 2020.
10. Parker D., Petavratzi E., Petavratzi, Mankelow J., Waugh R., Bertrand G (2015) EU raw materials statistics on resources and reserves, Report number: EC—11 331 Minventory Final Report.
11. European Commission 2020, Study on the EU's list of Critical Raw Materials (Non-Critical Raw Materials Factsheets)- European.
12. EU Circular Economy Action Plan, A new Circular Economy Action Plan for a Cleaner and More Competitive Europe https://ec.europa.eu/environment/circular-economy/dec.2020

XIV International Mineral Processing
and Recycling Conference
Belgrade, Serbia, 12-14 May 2021

OPPORTUNITIES FOR CHOOSING RAW MATERIALS FOR ECOLOGICALLY ACCEPTABLE LUBRICANTS AND PRACTICAL EXPERIENCE

Branko Despotović[1#], Branka Dugić Kojić[1], Pero Dugić[2]
[1] Oil Refinery Modriča, Modriča, Bosnia and Herzegovina
[2] University of Banja Luka, Faculty of Technology, Banja Luka, Bosnia and Herzegovina

ABSTRACT – When selecting the raw materials for lubricant, in addition to functional properties, the criteria of the origin of raw materials and the impact on the environment are increasingly important. Limiting the use of products based on mineral oils, imposes the need to find new substances and improve the characteristics of many previously developed components. Today, we have a wide range of base fluids which are formed from renewable sources and with satisfying degree of biodegradability.

This paper presents the characteristics of different types of synthetic esters that can be potential raw materials for different group of products such as hydraulic lubricants, fire resistant fluids, etc.

Keywords: Lubricant Formulation, Mineral Oils, Synthetic Esters.

INTRODUCTION

Reducing of world's crude oil reserves and rising prices are the first drivers that led to the research of new substances that can be used for the production of raw materials for the lubricants formulation. Problems and questions related to the disposal of used oil products and their impact on the environment led to accelerated activities around development of a new group of lubricants, more environmentally friendly lubricants. Lubricants that are labeled as "environmentally" are described in several ways, like "environmentally friendly", "environmentally safe", ect. In this paper the used term will be "environmentally friendly".

Environmentally friendly lubricants, in addition to biodegradability, must also meet the requirements for ecotoxicity, bioaccumulation, renewability, impact on safety and protection of human health [1]. Lubricants are complex mixture of different chemical compounds, which composition is designed to fulfill specific application tasks. Liquid lubricants consist of base oils and additives, while lubricating greases contains also a thickener. Different combination of anti-wear and extreme pressure additives, antioxidants, viscosity and viscosity index improvers, corrosion protection additives, detergents, dispersants, emulsifiers and antifoams can be used as additives.

Type, chemical type and content of individual additive components and base oils that participate in formulation of final lubricants depend on the purpose of the products. Industrial lubricants represent special but very large group of liquid agents for certain application such as: hydraulic systems, turbines, transformers, heating and

---

[#] corresponding author: bane@modricaoil.com

cooling systems, thermal and mechanical metal processing. Special group of lubricants are lubricating greases. In order for an environmentally acceptable lubricant to meet the requirements set by the new regulations and at the same time meet the performance for certain product groups, researchers are faced with great challenges. In order to be able to formulate such lubricant, the characteristics of the base fluid must first be taken into consideration.

Replacing mineral base oils with biodegradable more environmentally friendly fluid is one way to reduce the harmful effects on the eco system and humans. As the best choice for environmentally acceptable lubricants, ester bases based on synthetic and vegetable base oils are used as base fluids. In the field of synthetic esters development, as one of the most suitable fluids that can replace mineral base oil as base raw material in ecological lubricant, great improvement is achieved.

EXPERIMENTAL

Raw materials and test methods

The paper presents testing results of several different synthetic esters whose characteristics have enabled application in several significant groups of lubricants. The impact of esters on the environment has been extensively investigated and it has been concluded that they have very low toxicity and so they have found application in environmentally friendly lubricants [2]. Many researchers are working on testing of new substances for synthesis of esters and depending on the availability of raw materials, they differ in many characteristics [3]. Development of biodegradable fluids with very high termal and oxidation stability is the main challenge for lubricant manufacturers [4].

Several commercial synthetic esters from different manufacturers were available. They all differ in chemical composition and origin of acids and alcohols for synthesis. When choosing esters, the goal was complete ecological acceptability which, in addition to biodegradability, requires esters to use raw materials from renewable sources. Their physical-chemical characteristics were studied and six synthetic esters were selected, of which five are oleochemical polyol esters and one is complex polyol ester. All used esters have high viscosity index values, good polarity, lower volatility, low pour point, satisfactory biodegradability and reproducibility.

Complex polyol ester marked SE1 was selected because of higher viscosity value and it was used in formulations for viscosity rising, up to ISO VG 46. It is a polymer ester derived from polyol and dicarboxylic acid and it has high thermo-oxidative stability [5]. The chemical composition of ester SE2 is saturated polyol ester, a modified TMP ester [6]. The Non-Polarity Index (NPI) is very important characteristic for ensuring a range of usable esters characteristics. In SE2 NPI is very low, which indicates that this ester has an extremely good polarity. Adhesion of the esters on metal surface gives good lubricity, better protection against oxidation and corrosion. Low NPI affects the possibility of better solubility of additives in this ester [7]. Ester SE3 is unsaturated polyol ester with good low-temperature characteristics, which provided the degree of unsaturation. Although it has lower viscosity, it has lower volatility. The NPI is significantly higher than in most other esters. In combination with heavier ester, it gives poorer oxidative stability. Esters SE4 is saturated polyol ester, with good oxidative stability, but have slightly higher pour point. The NPI is higher then ester SE1, but in tests it have been shown to have good lubricity. Ester SE5 is unsaturated standard TMP polyol ester, which has enabled higher viscosity values to be achieved with ester combination. NPI is very high and this value gives the data that in combinations with other esters its higher participation will significantly affect the solubility of additives that would enable better oxidative stability. Ester SE6 is unsaturated polyol ester intended for fire-resistant hydraulic fluids.

Table 1 shows the characteristics of esters used in biohydraulic oils, lubricating greases, fire-resistant hydraulic fluids and water-soluble metalworking fluids.

Table 1 Characteristics of esters

Esters label		SE 1	SE 2	SE 3	SE 4	SE 5	SE 6
Type of esters	Test methods	Complex ester	Saturated polyol ester	Unsaturated polyol ester	Saturated polyol ester	Unsaturated polyol ester	Unsaturated polyol ester
Viscosity at 40ºC, mm^2/s	BAS EN ISO 3104	495	20.0	19.1	46.0	90	48
Viscosity index	BAS ISO 2909	153	140	145	148	144	187
Iodine number, gL/100g	ISO 3961	3	0.5	1	2	58	84
Flash point, °C	BAS ISO 2592	300	250	240	280	290	300
Pour point, °C	BAS ISO 3016	-34	-39	-60	-27	-24	-15
Biodegradability OECD 301B, %	OECD 301 B	65	75	71	85	65	84
Renewability, %	calculate	87	78	80	85	87	86
NPI (Non Polarity Index)	calculate	-	61	160	130	186	-

Figure 1 shows the comparison of NPI values for esters incorporated into lubricant formulation where this characteristic is important.

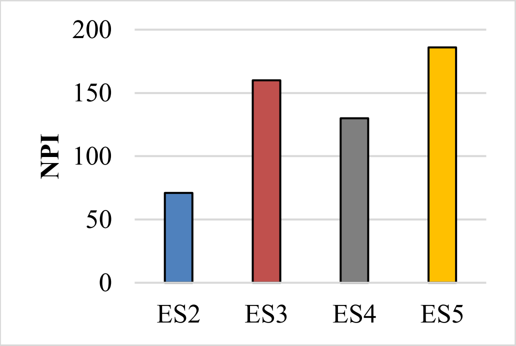

Figure 1 A comparative view of NPI

Environmentally friendly hydraulic fluids

Hydraulic fluids are the main group of products in the field of environmentally friendly lubricants and they are used in hydraulic systems used in environmentally sensitive areas (agriculture, construction, forestry) due to frequent accidents of hydraulic installation and leaks into the environment [8].

For this study, four formulations of environmentally friendly hydraulic fluids were prepared, which differ in the combination of different synthetic esters used as base raw materials. The added additives to improve performance in all four formulations are the same and in the same amount.

From the combination of mentioned esters four formulations of hydraulic fluids ISO VG 46 based on oleochemical polyol estres were prepared. A combination of additives consisting of an ash-free anti-wear additive containing phosphorus ester, a corrosion and oxidation inhibitors package and a passivator for non-ferrous metals was added to each HEES fluid in the same percentage.

The oxidation test of fluids shows that all samples have good oxidation resistance. Compared to mineral based hydraulic fluids, samples BH1, BH3 and BH4 have a significantly longer service life.

NPI with lower values in selected esters enabled better dissolution possibilities of all additives, especially anti-wear and oxidation inhibitors. Hydraulic fluids marked as BH2 and BH4 have been successfully used in road and forestry machinery, and fluid marked as BH1 and BH3 can be used in more demanding lubrication places where operating temperatures are elevated, for example in the steel industry.

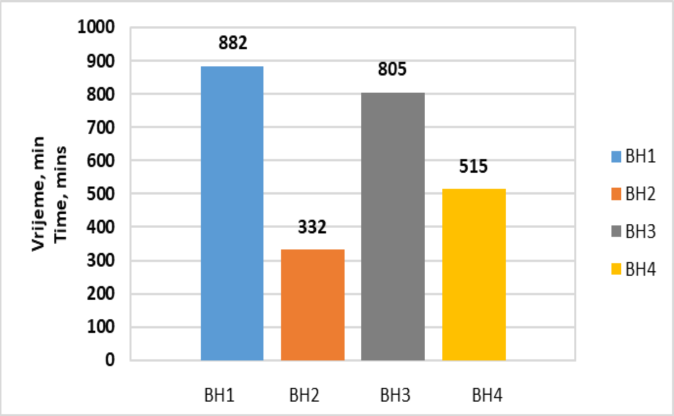

Figure 2 A comparative view of environmentally friendly fluid's Oxidation stability (ASTM D 2272)

Environmentaly friendly lubricating greases

In the field of lubricating greases in recent years, it is possible to formulate not only biodegradable but also more environmentally friendly greases. By developing synthetic esters, it is possible to formulate environmentally friendly greases that have a wider range of application temperatures and all other performances that are required by application place. By using a complex ester marked as SE1 and ester SE5, lithium greases of higher NLGI grades were formulated. With the addition of additives consisting of ash-free anti-wear additives containing phosphorus ester, packages of corrosion and oxidation inhibitors and passivators of non-ferous metals, such greases are successfully used for lubrication of vital parts in road, forestry and construction machinery.

Fire-resistant hydraulic fluids

Although mineral oil is not easy flammable, in environments where there are potential sources of ignition such as sparks, open flames or hot metal, it could cause a fire. Due to such situations at the places of application (mines, iron and steel industry, etc) it is necessary for hydraulic fluid to have adequate “fire resistance”.

In this paper, formulated HFDU fire resistant hydraulic fluids based on synthetic polyol ester marked as SE6 and corresponding additives to achieve all usable characteristics were tested. The basic characteristics of this fluid come from unsaturated polyol ester which is produced from renewable raw materials. The chemical composition provided high thermal and oxidative stability and good resistance to hydrolysis. High polarity provided reduced volatility and better lubricity. Low toxicity to aquatic organism, biodegradability and origin from renewable raw material are additional advantages of these synthetic esters, but their high price determines that are used only where necessary.

Water-miscible metal-working fluid

In this field of lubricants, the advantages of some synthetic esters can be used to improve the anti-wear properties of final product, and at the same time to improve solubility of other substances from the formulation. To investigate the influence of esters in the formulation of metalworking fluids, a typical universal formulation for various mechanical metalworking operations was chosen. A part of naphtenic base oil was replaced with 10% synthetic ester based on trimethylpropane derivates and fatty acids.

The selected ester, in addition to its good ability to dissolve functional additives, is characterized by excellent low temperature characteristics, high degree of biodegradability, low volatility and is produced from renewable raw materials and it has a degree of reproducibility of about 80%.

The polarity of base oil affects tribological performances of lubricants and coolants and lubrication in mechanical metalworking. NPI of ester SE7 is 185 and it is lower than the in mineral base oil, which has NPI of about 250. Thanks to their good properties, these esters improve the stability of the working emulsion, as well its functional properties in more demanding operations, such as drawing, milling and threading, where the emulsions should allow good machining, efficient chip removal from the machined surface without sticking to tools and the parts that are machined, with good cooling of the workpiece and tools. The low volatility of the esters greatly reduces the formation of the oil mist which is released by the action of elevated temperatures in the cutting area.

Table 2 Characteristics of ester SE7

Characteristics of ester SE7	Test methods	Results
Viscosity at 40 ^oC, mm^2/s	BAS EN ISO 3104	19.0
Saponifiication number, mg KOH/g	BAS ISO 6293–1.2	309
Biodegradability, %	OECD 301 B	60
Renewability, %	Calculate	80
Volatility, % weight loss	DIN 51581	3.6
Non polarity index (NPI)	Calculate	185

CONCLUSION

Today's modern lubricants have very complex formulation and their development is continuously going into direction of improving performance and longer-term use, while meeting all environmental criteria. Biodegradable hydraulic lubricants and their performances described in this paper follow this development trend.

When selecting hydraulic fluid where there is a risk of fire, in addition to the requirenments for usable characteristics (range of operating pressures and temperatures, compatibility of all components) fire resistance is extremely important factor. With the development of polyol esters, many performance improvements have been achieved, and environmental requirements have also been met.

The use of synthetic esters in formulation of fluids for lubrication and cooling in machining operations can improve the stability of the formulation and reduce wear.

REFERENCES

1. Rhee, I.S. (1996) Evaluation of environmentally acceptable (EA) hydraulic fluids, NLG1 Spokesman, 60 (5),28–35.
2. Randles S.J., Eastwood J. (2007) An overview of high performance biodegradable ester lubricants from sustainable and non-sustainable feedstock's. Croda Repor.
3. Mirci, L. (2010) Syntetic Complex Esters Lubricants. 17th International Colloquium on tribology, TAE, Ostfildern, Germany.
4. Scherer, M., Rettemeyer, D., Rinklieb, R., Patel, R. (2010) Latest Trends in Biohydraulic Fluids. 17th International Colloquium on tribology, TAE, Ostfildern, Germany.
5. Mortier, R.M., Fox, M.F. and Orszulik, S.T. (2010). Chemistry and technology of lubricants. 3rd ed., 268. Springer Science and Business Media.
6. Lamsa, M., Kosonen, K. (2008) Third Generation Biohidraulics. 16th International Colloquium on tribology, TAE, Ostfildern, Germany.
7. Rudnick, L., Shubkin, R. (1999) Syntetics Lubricant and High-Performance Functional Fluids, 2nd ed., Dekker, 85.
8. Mang, Th. and Dresel, W. (2007) Lubricant and Lubrication. Weinheim,119-129.

XIV International Mineral Processing
and Recycling Conference
Belgrade, Serbia, 12-14 May 2021

TECHNO-ECONOMIC ANALYSIS OF CHERRY OIL BIODIESEL PRODUCTION

**Marija Tasic[1#], Jelena Jovanović[1], Milan Kostić[1], Olivera Stamenković[1],
Vlada Veljković[1,2]**
[1] University of Nis, Faculty of technology, Leskovac, Serbia
[2] The Serbian Academy of Sciences and Arts, Belgrade, Serbia

ABSTRACT – The biodiesel competitiveness in the fuel market largely depends on the feedstock price. Cherry pits are a significant waste in the fruit processing industry of Serbia. In this study, a techno-economics of the cherry oil heterogeneous biodiesel production was performed using the Aspen Economic Analyzer. The plant CAPEX and OPEX were 1.26 million US$ and 3.85 million US$, respectively. A maximum annual profit (4.9 million US$) was achieved at a biodiesel price of 0.99 US$/kg. For the biodiesel price below 0.44 US$/kg, the production was unfeasible. With the advanced technology of removing leached calcium ions, cheaper biodiesel could be obtained.

Keywords: Biodiesel, Cherry Pits, Waste, Economics.

INTRODUCTION

Fruit processing is among the leading industry sectors worldwide, with significant waste quantities (8% of the total food waste in Europe) every year [1]. While the fraction of discarded waste in the large-scale fruit processing industries is typically known, those more numerous from micro and small-scale fall under statistics and are thus of negligible value. However, regardless of processing size or aggregate state (liquid or solid), fruit waste contains much water and has a high biological oxygen demand (BOD), making it an excellent medium for microbial growth and brings huge environmental pollution problems. Therefore, science is currently focused on potential waste utilization. The fruit processing waste is commonly used to extract phenolic compounds, pigments, dietary fiber, proteins, oil, and more recently in biofuel production.

According to the last decade's statistics, widely grown fruits in Serbia are apples, plums, watermelons, grapes, and cherries [2]. However, the waste amounts from the fruit processing industry are unavailable, probably because of insufficient study. Cherry processing generates solid waste, pits, containing kernels rich in oil. Cherry oil has already shown the potential as a biodiesel feedstock [3,4] because of its lower price compared to the refined oils commonly used in most of the existing biodiesel plants. Despite this, no study has been dealing with the simulation and economics of biodiesel production from cherry oil.

This paper aims at the conceptual design, simulation, and techno-economic analysis of a cherry oil-based biorefinery that includes biodiesel production. This novel process

---

[#] corresponding author: marijat14@yahoo.com; mtasic@tf.ni.ac.rs was designed using a rigorous computer simulation for getting the consistent mass and energy balances, equipment sizing, and the involved process costs.

METHODS

Simulation of the cherry oil biodiesel production was performed using the Aspen Plus® v8.63 software (Aspen Technology Inc., Cambridge, Massachusetts, USA), which provides a costing basis for economic analysis. The process simulation and design involve defining chemical components, thermodynamic, reaction, and operating unit models, creating process flowsheets, and setting up the input operational conditions. Since the simulation of cherry oil biodiesel production was done for the first time, the process flowsheet and data on the unit operations conditions were based on the experimental data [4].

Process equipment sizing and capital cost estimating were carried out through vendor quotes and estimations for the 1st quarter of 2014, from Aspen Economic Analyzer® v8.6 software. The cherry oil plant was grass-root located in North America, with the annual capacity of biodiesel production and operation time of 8870 tonnes and 8766 h, respectively. The plant operation and maintenance labor were set as three shifts per day. The costing basis and investment parameters were summarized in Table 1.

Table 1 Costing basis for economic analysis

Investment parameters specifications	
Economic life of project	10 years
Tax rate	40%/year
Desired rate of return/Interest rate	20%/year
Salvage value	20% of initial capital cost
Depreciation method	Straight line
Project capital escalation	5%/year
Products escalation	5%/year
Raw material escalation	3.5%/year
Operating and maintenance labor escalation	3%/year
Utilities escalation	3%/year
Working capital percentage	5%/year
Operating supplies	10% of maintenance/year
Laboratory charges	25% operating labor/year
Plant overhead	50% of operating labor and maintenance costs/year
G&A expenses	8% of subtotal operating costs/year
Facility type	Chemical processing facility
Operating mode	Continuous Processing - 2 operators per shift
Length of start-up period	20 weeks
Process fluids	Liquids, gases and solids

Chemicals prices specifications (US$/kg)	
Cherry oil	0.200
Methanol	0.269
H_2SO_4	0.640
CaO	0.067
Na_2SO_4	1.170
Na_2CO_3	1.200
Biodiesel	0.990
Wastewater treatment	0.091
Utilities prices specifications (US$/kJ)	
Hot oil	$3.5\ 10^{-6}$
High pressure (HP) steam	$2.5\ 10^{-6}$
Medium pressure (LP) steam	$2.2\ 10^{-6}$
Cooling water	$2.12\ 10^{-7}$
Electricity	0.0775*

*US$/kWh.

RESULTS AND DISCUSSION

The process flowsheet for the cherry oil biodiesel production was presented in Figure 1. The flowsheet includes oil esterification and methanolysis, methanol recovery, catalyst separation, and biodiesel purification. Due to a relatively high acidic number (14.2%) of cherry oil [4], the esterification was done before the methanolysis catalyzed by CaO. Biodiesel was treated with a mixture of Na_2CO_3 and methanol to remove leached Ca^{2+} ions.

Based on the simulation results and the assumptions presented in Table 1, the techno-economic analysis of the cherry oil biodiesel (8870 tons/year) production was performed. The distribution of the costs among the raw materials and utility sources is shown in Figure 2. The costs of cherry oil and Na_2CO_3 were the highest. Despite the heat integration, the energy consumption for heating (hot oil, HP, and MP steam) dominated among the utility costs.

The use of cherry oil resulted in a low feedstock cost despite its high fraction (65%) in the total raw material costs. The cherry oil cost was 30% and 11% lower than the cost of castor [5] and canola [6] oil, respectively. With the assumption that the cherry oil biorefinery was a grass-root plant and add-in to the fruit processing plant, waste cherry pits would be free of costs. Therefore, the cherry oil costs could be even lower if the seed extraction technology would be highly efficient. Also, a large amount of Na_2CO_3 was consumed for the regeneration of leached Ca^{2+} ions, which significantly affected the process's economics. The highest operating cost was related to the distillation column for recovery of methanol which is applied in removing leaching Ca^{2+}ions.

The solid catalyst leaching has not been included in the previous simulations of the biodiesel technologies [5-8], which could mislead the interpretation of the total production costs.

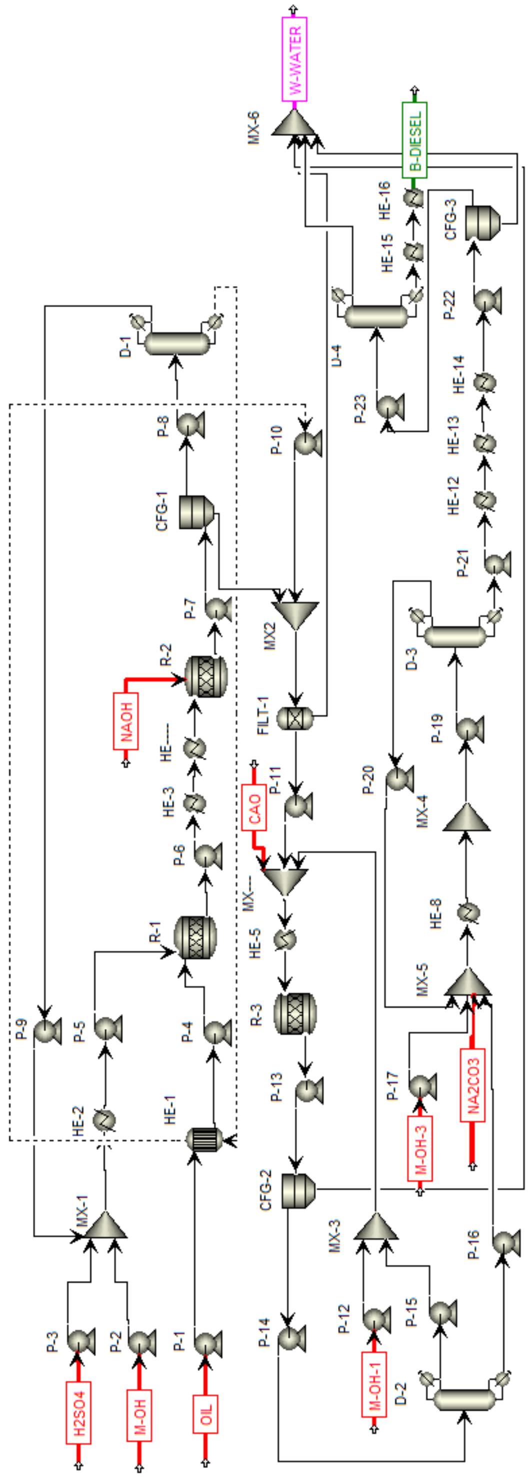

Figure 1 Process flowsheet of cherry oil biodiesel production

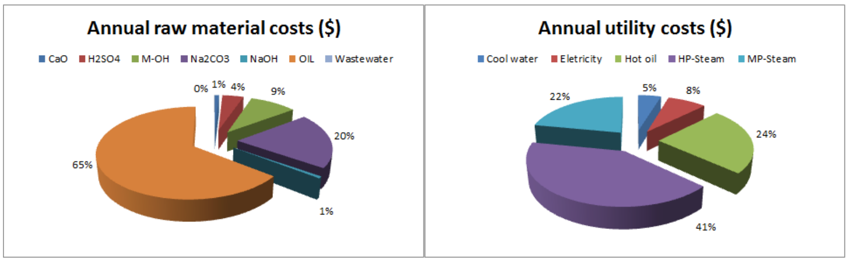

Figure 2 Distribution of annual raw material and utility costs in cherry oil biodiesel production

For a construction period of 45 weeks, the CAPEX and OPEX of the cherry oil biodiesel plant were 1.26 million US$ and 5.94 million US$, respectively. These values were lower than those obtained for waste cooking [7,8], canola [6], and castor [5] oil. The cherry oil biodiesel plant's life cycle is ten years, and the initial capital would be returned for a year and a half, with a payback period of 20%. Table 2 shows the selling price for biodiesel obtained from various oily feedstocks.

Table 2 Profitability analysis

Feedstock	**Biodiesel price (US$/kg)**	**Annual profit (million US$**	**Ref.**
Cherry oil	0.990	4.93*	This study
Castor oil	0.905	4.16	[5]
Canola oil	1.000	1.39	[6]

*A maximum annual profit.

The cherry oil biodiesel price of 0.990 US$/kg was calculated for the maximum annual plant profit. The decline in the price of biodiesel was characterized by a lower profit and a higher payback period. However, the sensitivity analysis showed that the price of biodiesel could decrease to 0.44 US$/kg, while a further decrease made the process unprofitable. Thus, the cherry oil biodiesel technology is shown feasible because fossil diesel price is in the range from 0.97 US$/kg to 1.88 US$/kg [8].

CONCLUSION

The new scientific trends are focused on potential waste utilization. In this paper, the techno-economics of large-scale cherry oil biodiesel production was studied. Cherry pits are agricultural waste, so converting them to biodiesel could be profitable in large cherry production areas. Based on the biodiesel's total cost and the obtained price, it can be concluded that the heterogeneous process of biodiesel production from cherry oil is an economically viable and highly competitive technology. The price of raw materials (cherry oil and Na_2CO_3) and higher heating energy amounts had a decisive impact on higher production costs. The process is eco-friendly because wastewater is treated before released into the environment. Based on these analyzes, it can be concluded that the profitability of cherry oil biodiesel production depends on several factors, but that the improvement of technology for oil extraction and the removal of leached Ca^{2+} ions are crucial.

ACKNOWLEDGEMENT

This work was financially supported by Republic of Serbia - Ministry of Education, Science and Technological Development, Program for financing scientific research work, number 451-03-9/2021-14/200133 (assigned to the Faculty of Technology, Leskovac, University of Niš, researchers' group III 45001).

REFERENCES

1. Banerjee, J., Singh, R., Vijayaraghavan, R., MacFarlane D., Patti, A.F., Arora, A. (2017) Bioactives from fruit processing wastes: Green approaches to valuable chemicals. Food Chemistry, 225, 10–22.
2. FAOSTAT (2020) Crops, http://www.fao.org/faostat/en/#home, (accessed 18 Feb 2021).
3. Demirbas, A. (2016) Biodiesel from kernel oil of sweet cherry (*Prunus avium* L.) seed. Energy Sources, Part A: Recovery, Utilization, and Environmental Effects, 38, 2503–2509.
4. Blagojević, D. (2013) Biodiesel production from kernel seeds oils (*Prunus cerasus* L.), Master thesis, Faculty of Technology, University of Nis, Leskovac.
5. Dimian, A.C., Iancu, P., Plesu, V., Bonet-Ruiz, A.E., Bonet-Ruiz, J. (2019) Castor oil biorefinery: Conceptual process design, simulation and economic analysis. Chemical Engineering Research and Design, 141, 198–219.
6. Baroi, C., Dalai, A.K. (2015) Process sustainability of biodiesel production process from green seed canola oil using homogeneous and heterogeneous acid catalysts. Fuel Processing Technology, 133, 105–119.
7. Dimian A.C., Kiss, A.A. (2019) Eco-efficient processes for biodiesel production from waste lipids. Journal of Cleaner Production 239, 118073.
8. Lee, J.C., Lee, B., Ok, Y.S., Lim, H. (2020) Preliminary techno-economic analysis of biodiesel production over solid-biochar. Bioresource Technology 306, 123086.

ARSENIC REMOVAL FROM WATER BY ADSORPTION – A SHORT REVIEW

Jovana Bošnjaković[1#], Vladimir Pavićević[2], Vesna Radojević[2], Jovica Sokolović[3]
[1]Research and Development Institute Lola Ltd., Belgrade, Serbia
[2]University of Belgrade, Faculty of Technology and Metallurgy, Belgrade, Serbia
[3]University of Belgrade, Technical Faculty in Bor, Bor, Serbia

ABSTRACT – Arsenic, one of the most toxic elements, is present in nature, atmosphere, water, organisms. Human and animal health is highly endangered even at low concentrations of arsenic in water. Therefore, the World Health Organization (WHO) has recommended that the maximum permissible concentration of arsenic in drinking water is 10 μg/L. Many studies in the last ten years have been done to reduce the concentration of arsenic in drinking water and there is still a need to develop new, sustainable procedures. This paper presents the removal of arsenic from water by a relatively simple and inexpensive adsorption process.

Keywords: Adsorption, Arsenic, Water, Removal, Coagulation, Precipitation.

INTRODUCTION

Arsenic (As), a metalloid, is one of the most toxic elements in the world. It is in the Va group of the periodic table. The atomic number of arsenic is 33. Its atomic mass is 74.92, specific gravity is 5.73 g. The boiling point is 613 ˚C, the melting point is 817 ˚C, while at 372 ˚C the vapor pressure is 1 mm Hg [1]. It can be found in the atmosphere, nature, rocks, soil, organism, natural waters. It is present in a small percentage of the Earth's crust. With the help of wind and rain, arsenic reaches natural watercourses and agricultural land. It is also present in traces with metal ores, such as lead, cobalt, zinc, nickel, etc.

Inorganic and inorganic compounds, which are found in the environment, arsenic can be found in different valence states (-3, 0, +3, +5). Arsenites, arsenates, methyl arsenic acid, dimethyl arsinic acid, belong to the ecological forms of arsenic. As (III) forms complex compounds with nitrogen and oxides, while As (V) with sulfides forms complex compounds [2]. Biological activities, burning of fossil fuels, erosion, volcanic eruptions, belong to natural sources and contribute to the increase of arsenic concentration in natural waters above 10 μg/L. Many studies have been done in the last ten years to reduce the concentration of arsenic in drinking water. There is still a need to develop new, economically viable techniques and procedures that are used to reduce the concentration of arsenic in water. Coagulation, flocculation, adsorption, precipitation, ion exchange, and membrane filtration are among the conventional methods. In addition to conventional methods, alternatives are used, such as ozone oxidation, bioremediation, electrochemical treatment.

[#]corresponding author: jocabosnjakovic@yahoo.com

Table 1. Countries where the concentration of arsenic in water is increased [3]

Country	Maximum permissible limits (μg/L)
Argentina	50
Bangladesh	50
China	50
Chile	50
India	10
Mexico	50
Nepal	50
New Zealand	10
Taiwan	10
USA	10
Vietnam	10

ARSENIC COMPOUNDS IN WATER

All arsenic compounds belong to the first group of carcinogenic compounds according to the Agency for Research on Cancer [4]. The form in which arsenic will be present in aquatic systems depends on the pH value, oxidoreduction conditions of the environment, bioprocesses, primarily those involving bacteria. The toxicity of As (III) is about 60 times higher than that of As (V) [5]. The mobility of As (V) is less than the mobility of As (III) because the probability of adsorption of As (V) on the mineral surface is higher compared to neutral As (III) [6]. As (III), in the form of H_3AsO_3, $H_2AsO_3^-$, $HAsO_3^{2-}$ and AsO_3^{3-}, is present under reducing conditions, while As (V), present in the oxidation medium, in surface waters, in the form of H_3AsO_4, $H_2AsO_4^-$, $HAsO_4^{2-}$and AsO_4^{3-} [7]. In the neutral medium, As (III) is in the form of H_3AsO_3 molecules, while As (V) is represented in the ionic form of $H_2AsO_4^-$ and $HAsO_4^{2-}$. The presence of arsenic in groundwater depends on the pH value, the redox potential of the system, the flow rate of water in the aquifer. In seafood and fish, a higher concentration of arsenic in organic form is present. The content of arsenic in groundwater, surface water, and sediments can be controlled thanks to the binding of arsenic to oxides of iron and aluminum, which are found in sediments. For the analysis of arsenic compounds present in water, arsenic and arsenic acid is mostly used.

THE IMPACT OF ARSENIC ON HUMAN HEALTH

When we say the toxicity of arsenic, we mainly mean its inorganic compounds, which predominate in aqueous systems. This property dates back to the ancient period. The toxicity of arsenic in water depends on the valence state, the way it is introduced into the body, the kinetics, the concentration of arsenic and its compounds in water, the general state of the organism, primarily gender, age, sensitivity, etc [8]. Water-soluble arsenic compounds are toxic, unlike metallic arsenic, which is non-toxic. Inorganic forms, As (III) and As (V), in most people are very quickly transported and absorbed into the bloodstream, other parts of the body, kidneys, lungs, muscles, bones, etc [9]. About 70% of arsenic is removed through urine [10,11]. Arsine gas, H_3As, which is not part of water, is considered to be the most toxic inorganic form of arsenic per human.

Consuming water high in arsenic can cause problems with the central nervous system, kidney function, skin, liver, and lungs in humans [12]. It can also lead to problems with the cardiovascular system, hypertension and greatly affect the vascular system [13]. It leads to the appearance of hyperkeratosis on the skin, there is a change in pigmentation [14]. The maximum allowable concentration of arsenic in water varies from country to country. Drinking water with a concentration higher than 10 μg/L poses a very great danger to human health.

REMOVAL OF ARSENIC FROM WATER BY ADSORPTION

Today, there are a large number of techniques used to remove arsenic from drinking water, but conventional physicochemical processes are the most common. Conventional physicochemical processes include oxidation, coagulation, flocculation, membrane filtration, ion exchange, and sorption [15,16]. Bioremediation, electrochemical treatment, ozone oxidation are also used, but their use requires detailed research before their use [7]. These methods are widely used but have several disadvantages: high operating costs, high reagent consumption, and large amounts of sludge [17]. Unlike these processes, the adsorption process has a very great advantage due to low cost, ease of operation, and high efficiency [18].

The adsorption process is applied to remove relatively small amounts of pollutants that cause significant effects or cannot be removed by other methods. Pollutants include highly toxic substances, oils, dyes, agents that affect the smell, taste of water, etc.

Adsorption is the process of ion accumulation from fluid on the surface of a solid phase. Further spreading of a substance over the entire volume of a material is called absorption. During the adsorption process, the substance is concentrated at the interfacial boundary surface. The size of the interfacial region is approximately several molecular diameters. The adsorbent is a substance on the surface of which there is an increase in the concentration of one of the components, while the substance that is adsorbed is an adsorbate. Since the process takes place on the surface of the adsorbent, its surface must be maximally developed. Therefore, a solid, porous phase with highly developed surfaces is always used as the adsorbent.

Since the adsorption process occurs spontaneously, it means that at the phase boundary only parts of the system will be adsorbed which contributes to the reduction of the specific surface energy of the system. The processes of adsorption and absorption are called sorption processes by one name because they often take place together. Sorption can be divided into physical sorption or physisorption and chemical sorption or chemisorption.

Adsorption in physicochemical terms means the ability to bind ions or molecules to a specific surface. Physisorption is reversible and occurs due to the action of Van der Waals forces between the adsorbent molecules and the adsorbent surface. In the case of physical adsorption, due to the action of Van der Waals forces, a higher molecular layer of adsorbents may form on the surface of the adsorbent, which leads to the appearance of multilayer adsorption. Activated carbon sorption is an example of physical sorption.

In the process of water purification, granular activated carbon is mainly used. Adsorbents, such as activated carbon, silica gel, activated clays, infusoria, and activated earth, allow control of adsorption and desorption processes.

In the activated carbon adsorption process, the wastewater enters from the top of the device and moves to the bottom, through a layer of granular coal. The moment the wastewater comes into contact with the activated carbon, the dissolved organic compounds are adsorbed on the surface of the activated carbon. Contaminants are absorbed very quickly in the upper layers. As the number of wastewater increases, the adsorption zone moves to the bottom until it reaches the bottom of the activated carbon layer. In this way, a saturation of all adsorption layers is achieved.

After saturation of the activated carbon in the column, it is removed and regenerated. Activated carbon and other adsorption agents, primarily synthetic, are subjected to the regeneration process. The regeneration process means the process of desorption of adsorbed substances

In some cases, it is more economical to replace activated carbon than the regeneration process. The adsorption mechanism is complex. It is a combination of chemical, physical and electrostatic interactions between organic compounds and activated carbon. The problem with the adsorption process arises when treating wastewater that is very variable in composition and concentration of pollutants. In this case, the adsorption of one compound can lead to desorption of another.

Unlike physical adsorption, in the process of chemical adsorption (chemisorption), there are chemical bonds between adsorbent molecules and adsorbent molecules. The chemical bond is formed as a consequence of a chemical reaction that takes place on the surface of the adsorbent. This reaction is irreversible and fast, unlike physisorption. During chemisorption, a monomolecular layer of adsorbateis formed, due to the establishment of a chemical bond between the adsorbate and the adsorbent.

SORBENTS USED IN ARSENIC REMOVAL BY ADSORPTION PROCESS

The adsorption process is becoming increasingly important in the treatment of drinking water. A large number of commercial sorbents are used to remove arsenic from water. Waste or natural materials can be used as sorbents. With the help of newer technologies, a large number of synthetic sorbents have been developed, which are used in special industrial processes. Synthetic sorbents include hybrid ion exchange resins, high point zeolites, hydroxides, and oxides of iron, aluminum, and manganese. Natural ones include sand, natural zeolites, raw manganese ores, and iron.

In addition to the most commonly used natural ones, waste materials from industrial processes and food production, in water purification, are increasingly attracting attention. From the food industry, rice husk is the most represented. Studies have shown that with the help of rice husk in the flow system removed 20 µg As (III) / g and 7µg As (V) / g. From the production of bio-oil, a process that includes the pyrolysis of pine, oak, and bark, waste carbonized materials were tested, as sorbents for the removal of As^{3+}, Cd^{2+}, Pb^{2+} from water [7]. With the help of waste ash from thermal power plants, waste sludge based on chromium and iron from refrigeration systems, waste from blast furnaces in steel production, the removal of arsenic from the water was tested. Also, due to specific chemical and physical properties, the removal of arsenic from the water was examined with the help of red sludge, which was formed as waste material in the process of aluminum production from aluminum bauxite ore. Red sludge showed higher efficiency for the removal of As (III) in the base medium, and in the acid medium towards As (V) [7].

As for natural sorbents, hydrated silicates of sodium, calcium, and potassium form zeolites. Clinoptiolite, abazite, mordenite, erionite, ferrierite, analcime and filipsite are the most common in nature. These seven natural zeolites, which are the most represented, have a satisfactory level of purity, so they can be used in the treatment of water purification. Studies have shown that zeolite chabazite has a higher affinity for As (V) than for As (III). 50% As (V) and 30% As (III) were removed with the help of chabazite [7]. Clays belong to the group of aluminosilicates. The efficiency and mechanism of arsenic sorption, As (V), were studied on kaolinite, illite, and montmorillonite. Feldspar and hematite showed a very high affinity for As (V).

Recently, research related to the adsorption of arsenic from water with the help of some other natural materials has been reported, such as ion exchange resins, various types of activated carbon, including anthracite.

Activated carbon is a carbon-based adsorbent. Activated carbon production began in the first decade of the 20th century. Activated carbon can be used in the chemical, petrochemical, and military industries. Due to high water and air pollution, carbon adsorbents are becoming increasingly important in the environment. When it comes to water treatment, activated carbon is used as an adsorbent for the adsorption of organic matter, as already described. Activated carbon can be in powdered and granular form. When treating groundwater, granular activated carbon (GAU) is preferred, due to more efficient removal of organic matter, better utilization of adsorption capacity, and the possibility of reactivation and reuse.

Granular activated carbon a granular, porous structure. It has active centers, which can adsorb organic matter that is dissolved in water. Due to its granular structure, it is used as a filtration medium. Which is an extremely good adsorbent, it is also a very good substrate for microorganisms, so that in addition to adsorption processes, biological processes take place on it, such as biosorption and biodegradation. GAU an be obtained from various raw materials, such as coke, wood, coal, peat, oil.

CONCLUSION

Various methods, which are more or less effective, are used to remove arsenic from water. In addition to the efficiency of the process, the choice of technology to be used for water purification is influenced by other equally important factors. The complexity of the system is one of the key factors influencing the choice of technology when removing arsenic from water. This factor is of great importance in smaller settlements, where there is no skilled workforce to monitor the plant daily. The adsorption process is simple, efficient and does not require continuous supervision by a skilled workforce. There are a large number of natural and waste sorbents that can be used in water purification. The scientific and professional challenge, when it comes to the sorption of arsenic from water, is to find new, cheap, easily available alternative materials.

ACKNOWLEDGEMENT

This research has been supported by the research grants No. 451-03-9/2021-14/200066 of the Ministry of Education, Science and Technological Development of the Republic of Serbia.

The research presented in this paper was done with the financial support of the Ministry of Education, Science and Technological Development of the Republic of Serbia, within the funding of the scientific research work at the University of Belgrade, Technical Faculty in Bor, according to the contract with registration number 451-03-9/2021-14/ 200131.

REFERENCES

1. Verma, P., Agarwal, A., Singh, V.K. (2014) Arsenic removal from water through adsorption-A Review. Recent Research in Science and Technology, 6 (1), 219-226.
2. Bodek, I., Lyman, W.J., Reehl, W.F., Rosenblatt, D.H. (1998) Environmental In organic Chemistry: Properties, Processes and Estimation Methods, 1st Edition, Pergamon Press, USA.
3. Charles, U., Pittman, J. (2007) Arsenic removal from water/waste water using adsorbents. Journal of Hazardous Materials, 142, 1-53.
4. Jomova, K., Jenisova, Z., Feszterova, M., Baros, S., Liska, J., Hudecova, D., Rhodes, C. J., Valko, M. (2011) Arsenic: toxicity, oxidative stress and human disease. Journal of Applied Toxicology, 31 (2), 95-107.
5. Wong, K. V. (2017) Nanotechnology and energy, 1st Edition, Jenny Stanford
6. Pan, B. J., Pan, B. C., Zhang, W. M., Zheng, S. (2009) Development of polymeric and polymer-based hybrid adsorbents for pollutants removal from waters. Chemical Engineering Journal, 151 (1-3), 19-29.
7. Jovanović, B., Ljubisavljević, D., Rajaković, Lj. (2011) Uklanjanje arsena iz vode adsorpcijom na nekonvencionalnim materijalima. Vodoprivreda, 43, 127-150.
8. Agusa, T., Fujihara, J., Takeshita, H., Iwata, H. (2011) Individual Variations in Inorganic Arsenic Metabolism Associated with AS3MT Genetic Polymorphisms. International Journal of Molecular Science, 12 (4), 2351-2382.
9. Hong, Y.S., Song, K.H., Chung, J.Y. (2014) Health effects of chronic arsenic exposure. Journal of Preventive Medicine and Public Health, 47 (5), 245-252.
10. Hughes, M.F., Beck, B.D., Chen, Y., Lewis, A.S., Thomas, D.J. (2011) Arsenic exposure and toxicology: a historical perspective. Toxicological Sciencse, 123, 305-332.
11. Abdul, M.K.S., Jayasingheb, S.S., Chandanaa, E.P.S., Jayasumanac, C., Mangala, P., De Silva, C.S. (2015) Arsenic and human health effects: A review. Environmental Toxicology and Pharmacology, 40, 828–846.
12. Monrad, M., Ersbøll, A.K., Sørensen, M., Baastrup, R., Gammelmark, A., Tjønneland, A., Overvad, K. Raaschou - Nielsen, O. (2017) Low-level arsenic in drinking water and risk of incident myocardial infarction: A cohort study. Environmental Research, 154, 318-324.
13. Kazi, T.G., Brahman, K.D., Baig, J.A., Afridi, H.I. (2018) A new efficient indigenous material for simultaneous removal of fluoride and inorganic arsenic species from groundwater. Journal of Hazardous Materials, 357,159-167.
14. Awual, M.R., Shenashen, M.A., Yaita, T., Shiwaku, H., Jyo, A. (2012) Efficient arsenic(V) removal from water by ligand exchange fibrous adsorbent. Water Research, 46 (17), 5541-5550.

15. Mondal, P., Bhowmick, S., Chatterjee, D., Figoli, A., Van der Bruggen, B. (2013) Remediation of inorganic arsenic in groundwater for safe water supply: A critical assessment of technological solutions. Chemosphere, 92, 157-170.
16. Nicomel, N.N., Leus, K., Folens, K., De Voort, P.V., Laing, G.D. (2016) Technologies for Arsenic Removal from Water: Current Status and Future Perspectives. International Journal of Environmental Research and Public Health, 13, 1-24.
17. Hokkanen Repo, S., Song Lou, E., Sillanpä, M. (2015) Removal of arsenic(V) by magnetic nanoparticle activated microfibrillated cellulose. Chemical Engineering Journal, 260, 886-894.
18. Chowdhury, R. (2016) Using adsorption and sulphide precipitation as the principal removal mechanisms of arsenic from a constructed wetland – a critical review. Chemistry and Ecology, 33 (6), 560-571.

XIV International Mineral Processing
and Recycling Conference
Belgrade, Serbia, 12-14 May 2021

CONTAMINATION OF RIVERS WATERCOURSES IN BOR DISTRICT WITH As AND Cd IONS

Radmila Marković[1#], Ljubiša Obradović[1], Vojka Gardić[1], Renata Kovačević[1], Zoran Stevanović[1], Adriana Isvoran[2], Vladan Marinković[1]
[1] Mining and Metallurgy Institute Bor, Bor, Serbia,
[2] West University of Timisoara, Department of Biology-Chemistry and Advanced Environmental Research Laboratories, Timisoara, Romania

ABSTRACT – Four sampling campaigns are realized in the period from 10.09.2019 to 10.09.2020 aim to determine the As and Cd ions concentration in the rivers watercourses in Bor District. Sampling points are selected according to the influence on the water quality of Bor River, Krivelj River, Timok River and Danube River. Metallurgical wastewater has the dominant influence on the Cd ions concentration in the selected surface water. As ions distribution in the rivers watercourses is depend of the As ions concentration in the both type of wastewater, acid mine drainage and metallurgical wastewater.

Keywords: Wastewater, Amd, Arsenic, Cadmium.

INTRODUCTION

The common challenge of all human society is to reduce the pollution and environmental damages produced by different processes.

Based on the fact that the copper is an essential metal for many industries, there is an increasing necessity for production of this metal but copper ore mining and metallurgy activities conduct to environmental damages and health effects. Even if they are stopped, the accumulated waste continuously pollutes the environment.

Based on the historical data, in the immediate vicinity of Bor City, about 750 million tons of open pit overburden and 350 million tons of flotation tailings are delayed. Those delayed waste contains dangerous metals such as copper, nickel, arsenic, zinc, cadmium, iron, etc [1]. In the area of disposal the mining waste, the acid mine water (AMD) is generated as a consequence of the chemical reaction the sulfide rich minerals, with water and O_2. Sulphide oxidation process generated the sulphuric acid and decreasing the pH in solution. Generally, the pH drops to values below 4, which causes dissolving of the metal ions [2].

Copper and iron ions are dominant in the AMD from the area of active or closed copper mines. The concentration of the other heavy metal ions (As, Mn, Cd, Zn, Pb, Ni, etc.) is much lower than the concentration of copper or iron ions [3,4].

During the metallurgical treatment of copper ore, harmful and dangerous materials also are generated and discharged into the local watercourses [2].

All of the wastewater from the Bor mine area is released out to natural environment

---

[#] Corresponding author: radmila.markovic@irmbor.co.rs and through the Bor River and Timok River tributaries flowing in Danube River.

The aim of this work is to determine the As and Cd ions concentration in the rivers watercourses in Bor District. Starting point sample is the Bor River with the AMD tributaries. Fifteen sampling points are defined for monitoring the heavy metals contamination in a period from 10.09.2019 do 10.09.2020.

EXPERIMENTAL

Materials and methods

Wastewater generated in Bor copper mine area pollutes the Bor and Krivelj rivers. Bela River arises after confluence of Bor and Krivelj rivers downstream from the village of Slatina. After inflows of Ravna River in Bela River, a Bela River inflow in Timok River and Timok River flows in Danube River.

Bor and Krivelj rivers are polluted by the wastewater originating from the active copper mining activities or by the wastewater generated from delayed mine overburden and flotation tailings. Krivelj River is polluted with the wastewater originating from the active mines (Bor pit, Veliki Krivelj, Cerovo, tailing dam in operation), as well as with the wastewater from the waste dump and flotation tailings which are not in operation during the long period (field 2 of the large flotation tailings Veliki Krivelj). Bor River is polluted by the Bor municipal wastewater, by the metallurgical wastewater from copper ore processing plant (metallurgical plant), by the wastewater from the mine tailings dump of the old Bor mine and by the part of Bor flotation tailing (RTH tailing), as well as, from the old flotation tailings in Bor.

The sampling points that are selected for the As and Cd ions concentration monitoring (presented in Figure 1) are:

- W1 Robule accumulation (AMD),
- W2 Robule accumulation 1 (AMD),
- W3 AMD from flotation tailing dam RTH (AMD),
- W4 Metallurgical wastewater,
- W5 Bor River divided into fourteen profiles,
- W6 Krivelj River,
- W7 Bela River after the confluence of Bor and Krivelj rivers,
- W8 Ravna River,
- W9 Bela River after flows of Ravna River,
- W10 Bela River before of confluence with Timok River,
- W11 Timok River before of confluence with Bela River,
- W12 Timok River after confluence with Bela River (near the village Rajac),
- W13 Timok River (near the village Mokranje),
- W14 Timok River (near the village Bukovce),
- W15 Danube River (near the village Radujevac).

Sampling is realized fourth times (quarterly) during the period from 10.09.2019 to 10.09.2020, by a hand tools, according to the sampling methods: SRPS EN ISO 5667-1; SRPS EN ISO 5667-3; SRPS ISO 5667-4; SRPS ISO 5667-6. Measurement of the samples pH values was conducted in the field.

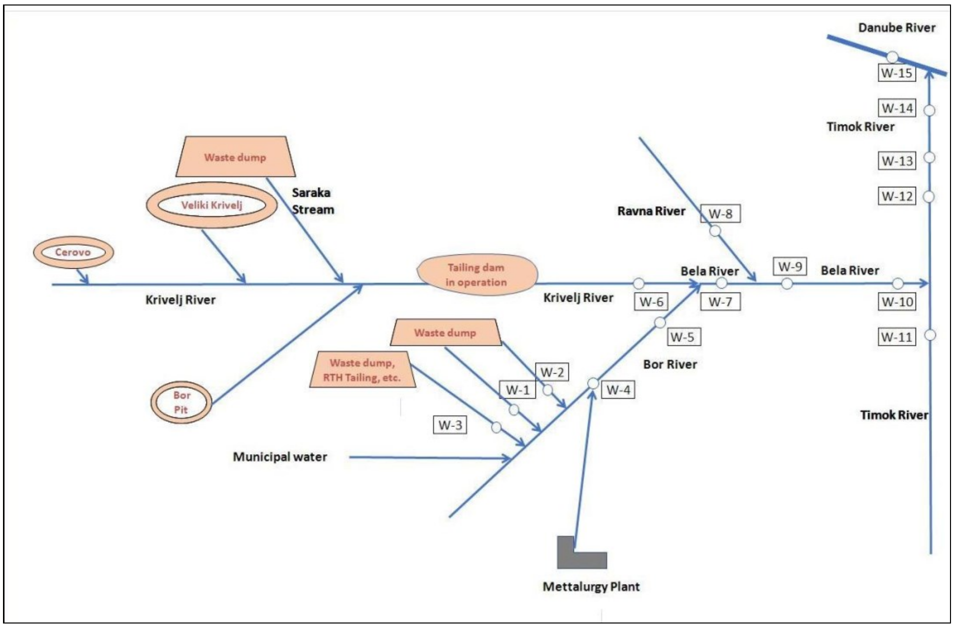

Figure 1 Sampling points in Bor District

The concentration of As and Cd ions in the water samples was determined in the laboratories of Mining and Metallurgy Institute Bor using atomic emission spectrometer with inductively coupled plasma (ICPAES), model Spectro Ciros Vision. The method of calibration curve was used. All reagents used for the chemical analyses were of high purity grade. The certified reference material (CRM) and blank samples were used for quality control of chemical analysis.

RESULTS AND DISCUSSION

In this paper will be discussed results for pH values as so as the values for As and Cd ions concentration. Measured pH values for the all sampling points are presented in Figure 2. pH value for the sampling point W5 (Bor River) is the average pH value obtained based on the data for each profile. From the Figure 2 it can be seen that pH has the lowest values for the sampling point W4 (metallurgical wastewater). Also, the pH values for the sampling points: W1 Robule accumulation, W2 Robule accumulation 1, W3 AMD from flotation tailing dam RTH, W4 Metallurgical wastewater, W5 Bor River divided into fourteen profiles, W7 Bela River after the confluence of Bor and Krivelj rivers, W9 Bela River after flows of Ravna River are lower than the allowable pH values regarding to Serbian legislation (range from 6.5 to 8.5) [5,6,7]. pH values for water samples W10 Bela River before of confluence with Timok River are lower than MAC values during the two quarters. pH values for other sampling points are in accordance with legislation.

In Figure 3 are presented the results of the As ions concentration in the water samples from the selected points.

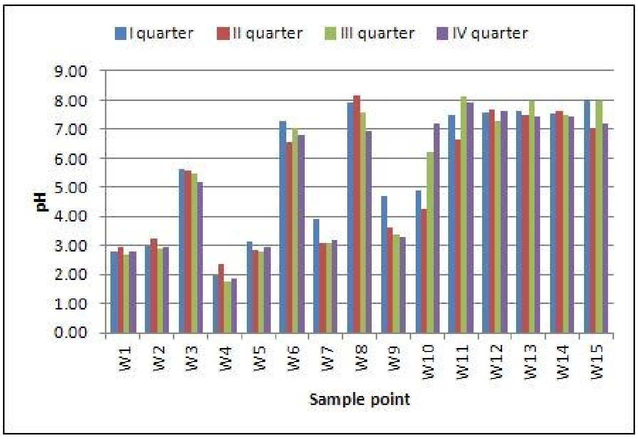

Figure 2 pH values for different sampling quarters

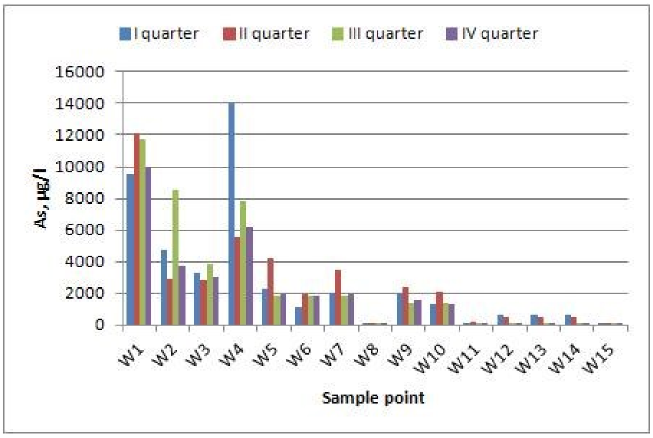

Figure 3 As ions concentration for different sampling quarters

The maximal value of As ions concentration is recorder for the sampling point W4 Metallurgical wastewater but this value is registered only in one sampling campaign. Samples marked as: W1 Robule accumulation, W2 Robule accumulation 1 and W3 AMD from flotation tailing dam RTH also have the high values of As ions concentration and the maximal value is about 120 times higher than the maximal allowed concentration (MAC) according to the Serbian legislation for the IV class waters (MAC = 100 µg/l). Only for a sampling point W11 Timok River before of confluence with Bela River, the concentration of As ions is below the MAC value in a two quarters, according to the river classification (Timok River: III surface water class). For all other sampling points the values for As ions concentration are the much higher than the MAC values.

Maximal value of Cd ions concentration is registered in the sample W4 Metallurgical wastewater and this value is about 6,000 times higher than MAC value. Based on the data presented in Figure 4, increased Cd ions concentration in Bor River and Bela River is consequence of the Cd ions content in metallurgical wastewater. In the water sample from location W11 Timok River before of confluence with Bela River not registered the

Cd ions and in the samples from location W15 Danube River (near the village Radujevac) concentration of Cd ions was lower than MAC value for II surface water class.

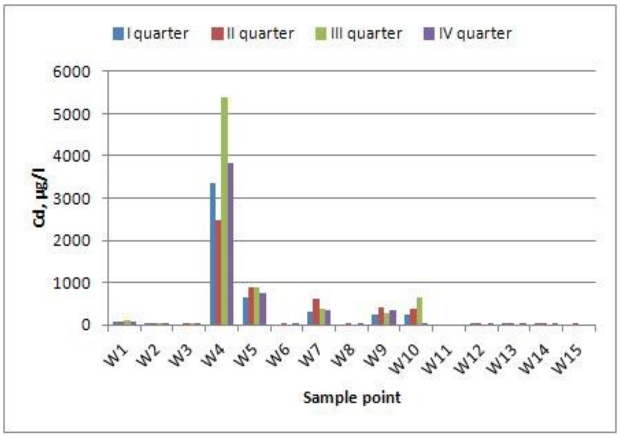

Figure 4 Cd ions concentration for different sampling quarters

CONCLUSION

Obtained results for As and Cd ions concentration in the rivers watercourses in Bor District are confirmed the negative impact of mining and metallurgy activities in the Bor copper mine area. As ions concentration is increased in the each water samples except in the sampling point W11 Timok River before of confluence with Bela River. Obtained results confirmed that presents of As ions in the rivers watercourses in Bor District is a consequence of the impact of two type of wastewater (AMD and metallurgical wastewater). Results for concentration of Cd ions in all samples are confirmed that the metallurgical wastewater has the main impact on the Cd ions concentration.

ACKNOWLEDGEMENTS

We acknowledge the financial support of the Project RoRS 337- ROmania Serbia NETwork for assessing and disseminating the impact of copper mining activities on water quality in the cross-border area (RoS-NET2), implemented under the Interreg-IPA Cross-border Cooperation Romania-Serbia Programme that is financed by the European Union under the Instrument for Pre-accession Assistance (IPA II) and co-financed by the partner states in the Programme.

This work was also financially supported by the Ministry of Education, Science and Technological Development of the Republic of Serbia, Grant No. 451-03-9/2021-14/ 200052.

REFERENCES

1. Project name: ROmania Serbia NETwork for assessing and disseminating the impact of copper mining activities on water quality in the cross-border area, Programme 2014 - 2020 Interreg IPA CBC Romania - Serbia, https://keep.eu/projects/22351/ROmania-Serbia-NETwork-for--EN/

2. Stevanović, Z., Obradović, Lj., Marković, R., Jonović, R., Avramović, Lj., Bugarin, M., Stevanović, J. (2013) Chapter 2: Mine Waste Water Management in the Bor Municipality in order to Protect the Bor River Water, Advances in Waste Water-Treatment Technologies and Recent Analytical Developments, Edited by Dr. Fernando Sebastian Garcia**,** Edited by Fernando Sebastian García Einschlag and Luciano Carlos**,** Published by InTech, First published January, 41-63.
3. Masuda, N., Marković, R., Bessho, M., Božić, D., Obradović, Lj., Marinković, V., Ishiyama, D., Stevanović, Z. (2017) A new approach to recover dissolved metals in AMD by two-step pH control on the neutralization method, 13th International Mine Water Association Congress – Mine Water & Circular Economy, 25-30 June 2017, Lappeenranta, Finland, proceedings, 1111-1118.
4. Marković, R., Bessho, M., Nobuyuki, M., Stevanović, Z., Božić, D., Apostolovski Trujic, T.Lj., Gardic, V. (2020) New Approach of Metals Removal from Acid Mine Drainage, Appl. Sci., 10, 5925.
5. Regulation on the categorization of watercourses ("Official Gazette of the SRS", no.3/1968) (In Serbian).
6. Regulation on Pollutant Limit Values into Surface and Groundwater and Sediment and Deadlines for their Achievement ("Official Gazette of the RS", no.50/2012) (In Serbian).
7. Regulation on Limit Values Priority and Priority Hazardous Substances that Pollute Surface Water and Deadlines for Achieving them, ("Official Gazette RS", no.24/2014) (In Serbian).

XIV International Mineral Processing
and Recycling Conference
Belgrade, Serbia, 12-14 May 2021

UNPRECEDENTED COPPER SMELTING ACTIVITY IN THE VERY CENTRE OF BOR - POOR AIR QUALITY

Snežana Šerbula[#], Jelena Kalinović, Jelena Milosavljević,
Ana Radojević, Tanja Kalinović
University of Belgrade, Technical Faculty in Bor, Bor, Serbia

ABSTRACT – Air quality was analysed after the modernisation of copper production technology. The concentrations of SO_2, PM_{10} and toxic elements As and Pb in PM_{10} samples were monitored at 5 different sites in relation to the copper smelter, in the period 2010-2020. The air quality evaluation was performed concerning the corresponding limit and target values defined by the Serbian and European legislation, as well as the World Health Organization Air Quality Guidelines. Although exceedances were not as pronounced as in the period before the implementation of the new technology, the episodes of extreme air pollution with SO_2, PM_{10}, As and Pb, persisted on the annual basis.

Keywords: Copper Smelter, Sulphur Dioxide, Particulate Matter, Arsenic, Lead.

INTRODUCTION

The greatest anthropogenic sulphur dioxide (SO_2), particulate matter (PM), arsenic (As) and lead (Pb) emission results from pyrometallurgical production of non-ferrous metals, combustion of fossil fuels and the use of pesticides. It has been estimated that anthropogenic emission is three times higher than the natural [1]. The International Agency for Research on Cancer (IARC) has classified As as Group 1 human cancerogen, based on a great deal of epidemiological evidence [2]. Elemental arsenic, lead, and its compounds have been classified as dangerous substances for the environment by the European Union [3]. Besides being toxic, As and Pb form stable compounds that are characterised by their ability to bioaccumulate in the living organisms.

In the atmosphere, arsenic exists predominantly absorbed on PM and is usually present as a mixture of arsenite As(III) and arsenate As(V) [4]. One of the main anthropogenic sources of arsenic in PM (usually present in a form of a sulphide) is copper smelting [5]. The major sources of Pb emissions have historically been motor vehicles (such as cars and trucks) and industrial sources. Today, the highest levels of lead in the air are usually found near smelters [4].

The moisture and sulphur dioxide in the air combine in a photochemical reaction to form sulphurous or sulphuric acid, which are constituents of acid rain. In the Air Quality Guidelines of the WHO the proposed 24-hour mean limit value for SO_2 is 20 $\mu g\ m^{-3}$ [1]. The 24-hour limit value for SO_2 defined by the EU Directive is 125 $\mu g\ m^{-3}$ and should not be exceeded more than three times a year [3]. According to the Environmental Protection Act of the Republic of Serbia, the daily limit value for SO_2 in residential areas

---

[#] corresponding author: ssherbula@tfbor.bg.ac.rs is 125 μg m^{-3}, whereas the annual limit value is set at 50 μg m^{-3} [6].

Note that, knowing the level of air pollution with hazardous materials which derive from mining-metallurgical production is essential for the purpose of environment protection and global sustainable development. This paper presents the results of ten years monitoring of the concentrations of the polluting substances in the air of Bor and its surroundings. The inhabitants of the study area are exposed to a great health risk since it is under the influence of various polluting substances such as sulphur dioxide and suspended particulate matter with a high content of Cu, Zn, As, Pb, Cd, Hg, Mn and Ni [7,8]. The copper smelter, which is a part of the Mining and Smelting Complex, is the major pollution source apart from the open pit, flotation waste heap and ore waste heap. The greatest and most frequent annual exceedances of the limit value (LV) are recorded for As and SO_2.

EXPERIMENTAL

In order to increase the technological utilisation of copper, to decrease the operational costs, as well as to resolve long-term environmental pollution problems, the outdated technology for copper smelting was replaced with an autogenous flesh smelting. The improvements would not be possible without a new sulphuric acid plant, which was also built. The new smelting technology was fully operational in 2016. The Serbian Environmental Protection Agency (SEPA), as the national institution, is obligated to collect, update and process the results of the air quality monitoring from the national network of Automatic Air Quality Monitoring Stations (AAQMS) for the purposes of reporting on the national and the European Union level, since Serbia is the EEA's cooperating country. By fulfilling the obligations of informing the public about the air quality, the SEPA presents the results of the air quality monitoring in the national network of AAQMS in real time. The assessment of the air quality in Serbia is given in the form of Annual Reports [7].

In the study area, SO_2 monitoring was conducted during a calendar year. Concentrations of PM_{10} and toxic elements (As and Pb) in PM_{10} samples were monitored in the form of indicative monitoring, which referred to minimum 14% of total days during a calendar year [6,8]. The monitoring of concentrations of SO_2, PM_{10}, as well as As and Pb in PM_{10} samples during ten years was performed at the five measuring sites. A detailed description of the measuring sites is given in the previous papers [4,9]. The measuring sites Technical faculty (TF), Jugopetrol (JP) and Slatina (SL) are a part of the local Air Quality Monitoring (AQM) network that is operated by the municipality of Bor, whereas the measuring sites Town Park (TP) and Institute (IN) are a part of the national AQM [8] network that is operated by the SEPA [7].

RESULTS AND DISCUSSION

The average annual concentrations of SO_2, PM_{10}, As and Pb, with the exceedances of the limit (LV) and target values TV) defined by the Serbian Regulation during the 10–year period, are presented.

From Figure 1, it can be seen that the poorest air quality was observed at the suburban site JP, considering the highest exceedances of the annual LV [6]. The reason of the high air pollution at the urban–industrial site TF was attributed to the vicinity of the copper smelter. However, the exceedances of the annual LV for SO_2 in the period 2015-2020 were not as pronounced as in the previous period 2010-2015, which was the period before the implementation of the new smelter [9,10].

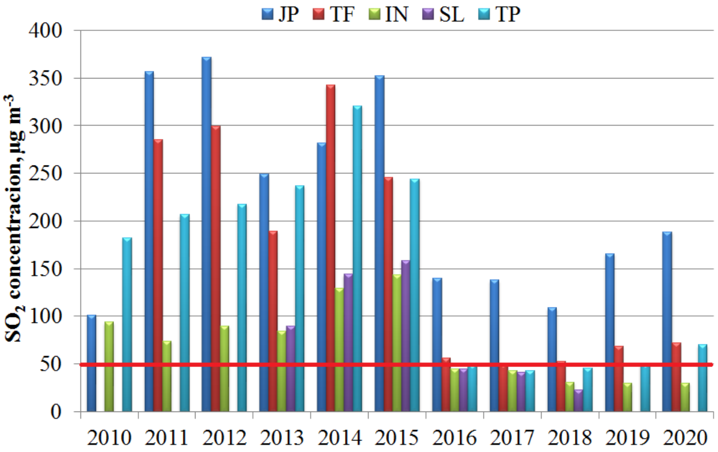

Figure 1 Average annual SO_2 concentrations at five measuring sites in the Bor area during period 2010-2020. Limit values (LV) (red horizontal line) is defined for SO_2 and is 50 µg m^{-3} [6]

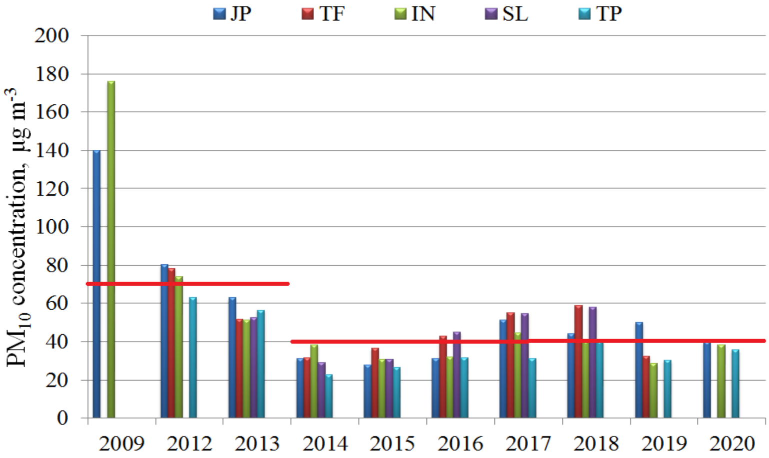

Figure 2 Average annual PM_{10} concentrations at five measuring sites in the Bor area during period 2009-2020. Limit values (LVs) (red horizontal lines) for PM_{10} were 70 µg m^{-3} until 2013, and after that they were defined at 40 µg m^{-3} [6]

Average annual PM_{10} concentrations at five measuring sites in the Bor area during the period 2009-2020 are shown in Figure 2. Limit value was 70 µg m^{-3} until 2013, and after that it was reduced to 40 µg m^{-3}, according to the rules defined by the Serbian Regulation. In both periods, there were exceedances of the average annual values [6].

From Figure 3 it can be seen that all the available annual As concentrations in the air of Bor and the surroundings exceeded the TV defined by the Serbian Regulation and the European Commission Regulation [3,6]. However, the exceedances of the annual TV for As in the period 2015-2020 were more pronounced than in the previous period 2010-2015, which is the period of application of the new smelter [9,10]. Maximum annual As concentrations measured at the site JP during 2019 was 550 μg m^{-3}, which is more than 90 times the allowable value.

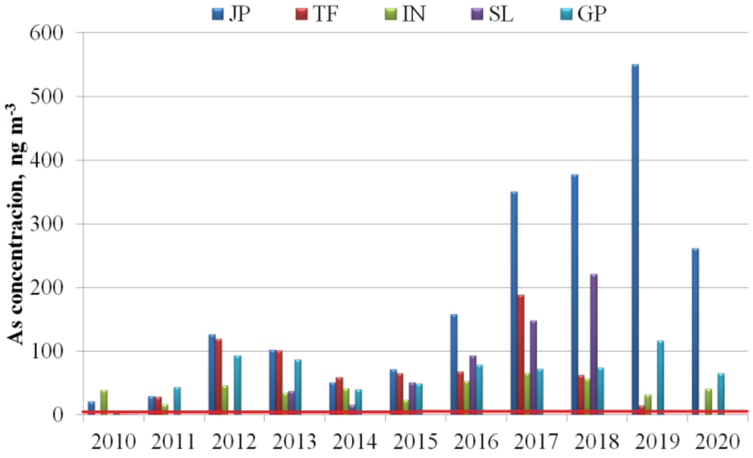

Figure 3 Average annual As concentrations in PM_{10} at five measuring sites in the Bor area during the period 2010-2020. Target value (TV) (red horizontal line) is defined at 6 ng m^{-3} [6]

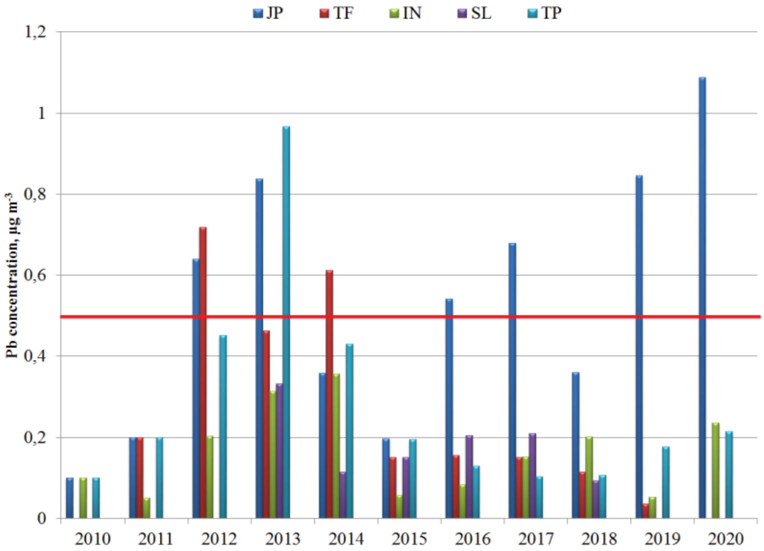

Figure 4 Average annual Pb concentrations in PM_{10} at five measuring sites in the Bor area during the period 2010-2020. Limit value~~s~~ (LV) (red horizontal line) is defined for Pb at 0.5 μg m^{-3} [6]

The annual Pb concentrations exceeded the annual LV of 0.5 µg m^{-3} [6] during 2012 at the sites JP and TF, during 2013 at the sites JP and TP, during 2014 at the site TF, and during 2016, 2017, 2019 and 2020 at the site JP. In the period of application of the new smelter, since 2016, the limit values have been exceeded at the measuring site Jugopetrol.

CONCLUSION

The modernisation of environmentally unacceptable pyrometallurgical copper production in the Mining–Metallurgical Complex Bor was highly needed for the purpose of extensive solution to the problems of air, water and soil pollution with SO_2 and toxic elements. However, the short–term episodes of extreme daily levels of air pollutants still persisted, with undoubtedly adverse human health impact.

Taking into account PM_{10} concentrations in the Bor area for the study period, the exceedances of the annual LV were more pronounced during 2017 and 2018.

During the last ten years, not a single average annual As concentration at the five sampling sites in Bor has been within the annual limit.

With the increase of the number of vehicles, there is no proportional increase of Pb concentration in the air, which means that the primary source of air pollution with the lead is the mining-metallurgical complex.

In toxicological risk assessment it should be taken into consideration that the inhabitants of Bor are simultaneously exposed to other types of pollutants, which also increase the health risk. High concentrations of sulphur dioxide, arsenic, heavy metals and their compounds in suspended particles are constantly present in the atmosphere of Bor.

ACKNOWLEDGEMENT

The authors are grateful to the Ministry of Education, Science and Technological development of the Republic of Serbia for financial support, within the funding of the scientific research work at the University of Belgrade, Technical Faculty in Bor, according to the contract with registration number 451-03-9/2021-14/ 200131. Our thanks also go to English language teacher Mara Manzalovic from the University of Belgrade, Technical Faculty in Bor, for providing language assistance.

REFERENCES

1. WHO, (2006) Air quality guidelines for particulate matter, ozone, nitrogen dioxide and sulfur dioxide. Global Update 2005. Regional Office for Europe, Copenhagen, Denmark.
2. IARC, (2012) International Agency for Cancer Research. Agents Classified by the IARC Monographs. Vol. 1–124.
3. EC, (2008) Council Directive 2008/50/EC of the European Parliament and of the Council on ambient air quality and cleaner air for Europe. Off. J. Eur. Union L152 (31).
4. Šerbula, S.M., Antonijević, M.M., Milošević, N.M., Milić, S.M., Ilić, A.A. (2010) Concentrations of particulate matter and arsenic in Bor (Serbia), Journal of Hazardous Materials, 181, 43-51.

5. Pfafflin, J.R., Ziegler, E.N. (2006) Encyclopedia of Environmental Science and Engineering, fifth ed., Taylor and Francis Group, Boca Raton, Florida.
6. Official Gazette of Republic of Serbia, (2013) Regulation on the conditions for monitoring and requirements of the air quality. No 11/10, 75/10, 63/13 (in Serbian).
7. SEPA, (2010-2020) Annual Reports on the State of the Air Quality in the Republic of Serbia, Belgrade, Ministry of Agriculture and Environmental Protection, (In Serbian).
8. MMI, (2010-2020) Mining and Metallurgy Institute Bor, Annual reports about quality of ambient air in Bor. Sector for Measuring and Control of Gaseous and Dust Parametres. Department Chemical–Technical Control, Bor, Serbia (in Serbian).
9. Serbula, S.M., Milosavljevic, J.S., Radojevic, A.A., Kalinovic, J.V., Kalinovic, T.S. (2017) Extreme air pollution with contaminants originating from the mining–metallurgical processes, Science of the Total Environment, 586, 1066-1075.
10. Serbula, S.M., Milosavljevic, J.S., Kalinovic, J.V., Kalinovic, T.S., Radojevic, A.A., Apostolovski Trujic, T.Lj., Tasic V.M. (2021) Arsenic and SO_2 hotspot in South-Eastern Europe: An overview of the air quality after the implementation of the flash smelting technology for copper production, Science of the Total Environment, 777, 145981.

INVESTIGATION OF THEOBROMINE USING A PENCIL GRAPHITE ELECTRODE

Žaklina Tasić[#], Ana Simonović, Marija Petrović Mihajlović,
Milan Radovanović, Milan Antonijević
University of Belgrade, Technical Faculty in Bor, Bor, Serbia

ABSTRACT – In addition to high–performance liquid chromatography and ultraviolet spectroscopy, electrochemical methods are widely used to determine various electroactive species. In this paper, the electrochemical behavior of theobromine in phosphate buffer solution as a supporting electrolyte was studied. Pencil graphite electrode as a low-cost material with good characteristics such as electrochemical reactivity, conductivity, and sensitivity was used. Cyclic voltammetry and square wave voltammetry methods were performed. Under experimental conditions, the oxidation process of theobromine was irreversible as well as the same number of protons and electrons are involved in the oxidation mechanism.

Keywords: Theobromine, Pencil Graphite Electrode, Sensor, Square Wave Voltammetry.

INTRODUCTION

Theobromine (TB; 3,7-dihydro-3,7-dimethyl-1H-purine-2,6-dione), caffeine and theophylline belong to xanthine-based alkaloids [1]. Plant species such as coffee and cocoa are sources of them [2,3]. Methylxanthines have different physiological effects including vasodilatation effect, diuretic, and smooth muscle relaxation effects [4]. According to Yoneda *et al.* [5], theobromine has less effect on central nervous system stimulation compared to theophylline and caffeine. Various methods have been used to determine and measure theobromine concentration including high–performance liquid chromatography (HPLC) [3] and ultraviolet spectroscopy [6]. Furthermore, the electrochemical behavior of theobromine was studied using different kinds of electrochemical systems and different methods. Also, different electrodes are used in the electrochemical investigation of these xanthines [1,7,8]. Pencil graphite electrode (PGE) is a low-cost material and has good electrochemical reactivity, conductivity, and sensitivity due to the sp^2 hybridized carbon [9]. Compared to other electrodes, pencil graphite electrodes are a less expensive material. Accordingly, the aim of this paper is to investigate the electrochemical behavior of theobromine at PGE.

EXPERIMENTAL

Pure theobromine was purchased from Thermo Fisher (Germany). Phosphate buffer solutions were prepared using the compounds $Na_2HPO_4·7H_2O$ and $NaH_2PO_4·H_2O$.

[#] corresponding author: ztasic@tfbor.bg.ac.rs

Various pH values (4.22, 7.38, 8.20, 9.84, and 10.50) for the phosphate buffer solution were adjusted by the addition of NaOH or H_3PO_4 solutions. All experiments were carried out at room temperature. Electrochemical measurements were performed using a potentiostat (IVIUM XRE) with the appropriate software in a three-electrode system. Pencil graphite leads (HB) with length of 60 mm and diameter of 0.5 mm were used as the working electrode, while a standard calomel electrode (SCE) and a platinum wire were used as the reference and auxiliary electrodes, respectively. The cyclic voltammetry and square wave voltammetry were used in this investigation. Square wave voltammetry was conducted under the following conditions: scan rate 100 mVs^{-1}, amplitude 50 mV, and frequency 15 Hz. Theobromine solutions were prepared by dissolving the required amount of TB in a phosphate buffer solution to obtain a concentration of $1 \cdot 10^{-3}$ M. Lower concentrations of TB were obtained by diluting this solution.

RESULTS AND DISCUSSION

To reveal the optimal pH value of supporting electrolyte (phosphate buffer solution) square wave measurements were performed in the pH range from 4.22 to 10.5. According to Figure 1, the plateau potentials were shifted towards negative values as the pH increased due to the involvement of protons in the process [10]. The best current response and the best plateau shape are obtained at pH 10.5 and this pH value was chosen as optimal for further investigation. The plateau potential (Ep) plot as a function of pH is shown in Figure 2. According to the linear relationship between Ep and pH, the slope is determined (Equation 1). The obtained value of slope 55.8 mV pH^{-1} is approximate to the theoretical value of 59 mV/pH which indicates that the number of electrons and protons participating in the process which takes place at the electrode are equal [10].

$$E_p(V) = 1.7164 - 0.05583pH \quad (R^2 = 0.9912) \tag{1}$$

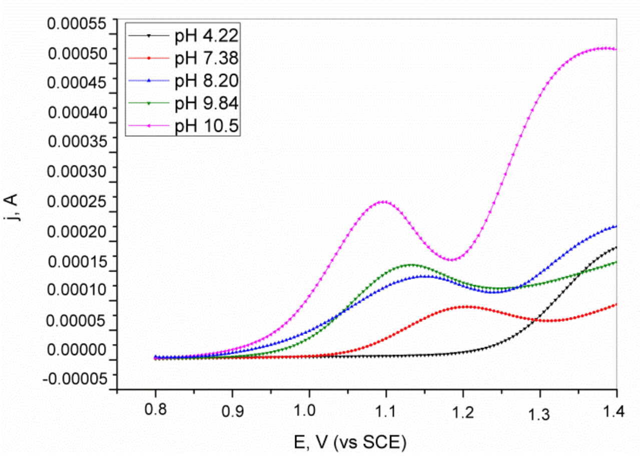

Figure 1 Square wave voltammetry curves of $1 \cdot 10^{-3}$M TB in phosphate buffer solution at different pH values

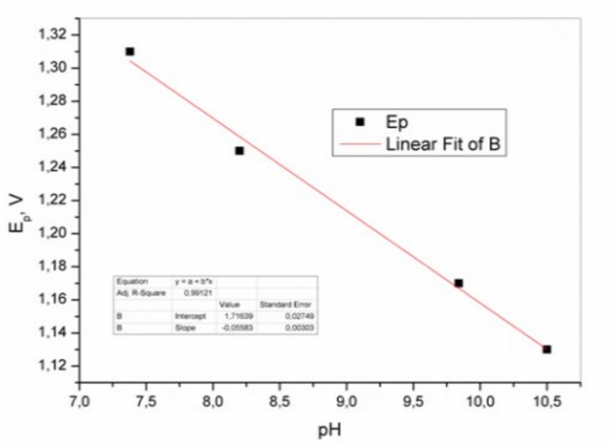

Figure 2 Dependence of plateau potential of 1·10^{-3}M TB on pH value of the phosphate buffer solution, scan rate 100 mVs^{-1}

Cyclic voltammetry measurements are used to investigate the electrochemical behavior of TB at PGE, as well as the effect of scan rate on the shape of the voltammogram and on the recorded current density value. Figure 3 shows the sensitivity of the pencil graphite electrode for theobromine since there is a current plateau at about 1.148 V (vs SCE) compared to the phosphate buffer solution. The current plateau appearance is due to the oxidation of theobromine while the reduction peak was not observed in the reverse scan implying the irreversible nature of the electrochemical process.

Figure 4 presents cyclic voltammograms recorded at different scan rates in the range of 5–200mV/s while the concentration of theobromine was constant, 1·10^{-3} M. It can be seen that peak current increases with the scan rate increase. As shown in Figure 5, the plateau current is linear with the square root of scan rate and that is the characteristic of a diffusion-controlled process. Data fit obeys Equation (2).

$$I_p(A) = 3.6223 \cdot 10^{-5} + 1.5133 \cdot 10^{-5} v^{1/2}\ (V^{1/2}s^{-1/2})\quad (R^2 = 0.9440) \tag{2}$$

Furthermore, the linear dependence of the logarithm of plateau current versus the logarithm of scan rate with a slope of 0.3734 confirms the diffusion control of the process (Figure 6) and obeys Equation (3) [10]:

$$log\ I_p = -4.4663 + 0.3734\ logv\ (Vs^{-1})\ (R^2 = 0.9620) \tag{3}$$

If the slope is close to 1 it is about adsorptive character while the slope value close to 0.5 indicates the diffusion-controlled process. The irreversible process is characterized by the shift of the plateau potential towards the positive value with an increase in scan rate due to the adsorption or double-layer formation at the electrode surface [9].

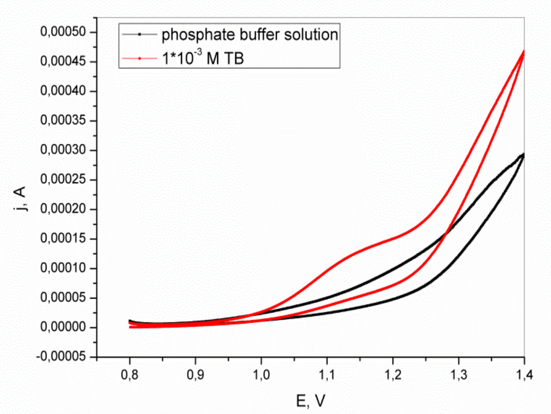

Figure 3 Cyclic voltammetry curves at PGE in phosphate buffer solution (pH 10.5) in the absence and in the presence of $1{\cdot}10^{-3}$ M TB, scan rate 100 mVs^{-1}

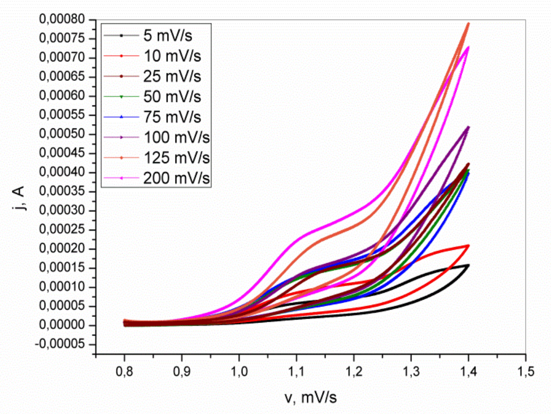

Figure 4 Cyclic voltammetry curves of $1{\cdot}10^{-3}$M TB in phosphate buffer solution (pH 10.5) at different scan rates

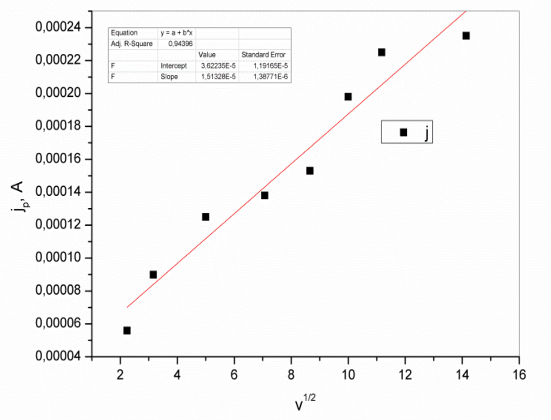

Figure 5 Dependence of plateau current of $1{\cdot}10^{-3}$M TB on the square root of scan rate

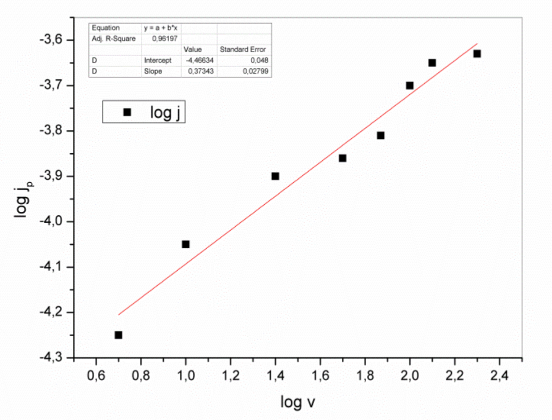

Figure 6 The plot of logarithm of plateau current of $1 \cdot 10^{-3}$ M TB versus logarithm of scan rate

Based on the slope of 55.8 mV per pH unit shown in Figure 2, indicating the involvement of the same number of protons and electrons in the oxidation mechanism of theobromine, an oxidation mechanism is proposed. Since theobromine and theophylline have a similar chemical structure, the oxidation mechanism of theobromine is proposed in Figure 7. According to the literature [10], it was observed that the oxidation mechanism of theophylline is two-electron a two-proton process.

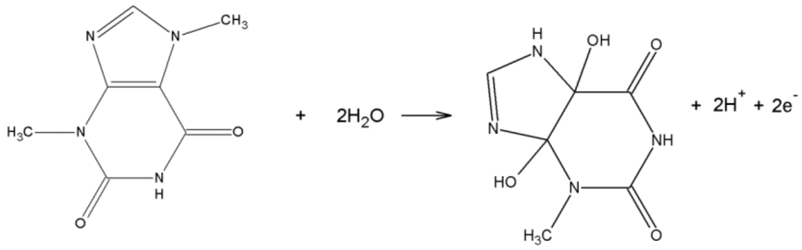

Figure 7 Proposed mechanism for electrode reaction of theobromine

CONCLUSION

Electrochemical behavior of theobromine in phosphate buffer solution at pencil graphite electrode is studied, using cyclic voltammetry and square wave voltammetry.

To reveal the optimal pH value of phosphate buffer solution square wave measurements were performed in the pH range from 4.22 to 10.5. According to the results, the plateau potentials were shifted towards negative values as the pH increased due to the involvement of protons in the process. The best current response and the best plateau shape are obtained at pH 10.5

The effect of changing of scan rate is observed by comparison of cyclic voltammetry curves recorded under different experimental conditions and it can be concluded that the increase of scan rate leads to anodic plateau current increase. The electrooxidation process is under diffusion control.

ACKNOWLEDGEMENT

The research presented in this paper was done with the financial support of the Ministry of Education, Science and Technological Development of the Republic of Serbia, within the funding of the scientific research work at the University of Belgrade, Technical Faculty in Bor, according to the contract with registration number 451-03-9/2021-14/ 200131.

REFERENCES

1. Spataru, N., Sarada, B.V., Tryk, D.A., Fujishima, A. (2002) Anodic Voltammetry of Xanthine, Theophylline, Theobromine and Caffeine at Conductive Diamond Electrodes and Its Analytical Application. Electroanalysis, 14(11), 721-728.
2. Andreeva, E.Y., Dmitrienko, S.G., Zolotov, Y.A. (2012) Methylxanthines: properties and determination in various objects. Russian Chemical Reviews, 81(5), 397-414.
3. Chorti, P., Ntousikou, M., Economou, A. (2019) A linear gradient sequential injection chromatography method exploiting programmable fluidics for the determination of three methylxanthines. Talanta, 202, 514-519.
4. Abuirjeie, M.A., El-Din, M.S., Mahmoud, I.I. (1992) Determination of theobromine, theophylline, and caffeine in various food products using derivative UV-spectrophotometric techniques and high-performance liquid chromatography. Journal of Liquid Chromatography and Related Technologies, 15(1) 101-125.
5. Sharma, V., Gulati, A., Ravindranath, S.D., Kumar, V. (2005) A simple and convenient method for analysis of tea biochemicals by reverse phase HPLC. Journal of Food Composition and Analysis, 18(6), 583-594.
6. Yoneda, M., Sugimoto, N., Katakura, M., Matsuzaki, K., Tanigami, H., Yachie, A., Ohno-Shosaku, T., Shido, O. (2017) Theobromine up-regulates cerebral brain-derived neurotrophic factor and facilitates motor learning in mice. The Journal of Nutritional Biochemistry, 39, 110-116.
7. Svorc, L., Tomcik, P., Svitkova, J., Rievaj, M., Bustin, D. (2012) Voltammetric determination of caffeine in beverage samples on bare boron-doped diamond electrode. Food Chemistry, 135(3), 1198-1204.
8. Wang, T., Randviir, E.P., Banks, C.E. (2014) Detection of theophylline utilising portable electrochemical sensors. Analyst, 139, 2000-2003.
9. Purushothama, H.T., Arthoba Nayaka, Y., Vinay, M.M., Manjunatha, P., Yathisha, R.O., Basavarajappa, K.V. (2018) Pencil graphite electrode as an electrochemical sensor for the voltammetric determination of chlorpromazine. Journal of Science: Advanced Materials and Devices, 3(2), 161-166.
10. Tadesse, Y., Tadese, A., Saini, R.C., Pal, R. (2013) Cyclic Voltammetric Investigation of Caffeine at Anthraquinone Modified Carbon Paste Electrode, International Journal of Electrochemistry, 2013, Article ID 849327 http://dx.doi.org/10.1155/2013/849327

XIV International Mineral Processing
and Recycling Conference
Belgrade, Serbia, 12-14 May 2021

SPECIFIC SOIL ENZYME ACTIVITIES AND ENZYME-BASED SOIL QUALITY INDICES IN THE LONG-TERM POLLUTED ANTHROPOGENIC ECOSYSTEM

Jelena Milosavljević#, Snežana Šerbula, Jelena Kalinović, Ana Radojević, Tanja Kalinović, Boban Spalović
University of Belgrade, Technical Faculty in Bor, Bor, Serbia

ABSTRACT – The study aims to evaluate specific soil enzyme activities and the selected enzyme-based soil quality indices in the anthropogenic ecosystem polluted by mining-metallurgical activities. Specific enzyme activities of ß-glucosidase, arylsulphatase, and acid phosphatase were the highest in the soil from the control site characterised by the lowest soil organic carbon content. The highest value of the GME index was observed at site 3, while the lowest value of the AI3 index was noted for site 4, whereby both sites were located near the pollution sources. The AlP/AcP ratio optimal for plant growth was noted for the control site.

Keywords: Specific Enzyme Activity, Soil Quality, Copper Smelter.

INTRODUCTION

The balance of the anthropogenic ecosystems is determined by soil physico-chemical, biological, and biochemical properties. Thus, changes in these properties must be considered in the soil quality assessment [1,2]. Soil biological and biochemical properties, which respond rapidly to environmental stresses, are recommended to be used in the soil quality estimation, contrary to the soil properties which change very slowly to the environmental alterations. Soil properties that are directly related to the activity of the soil microbiota, or the properties associated with soil organic compounds decomposition and nutrient release (i.e., soil enzyme activities), are readily used in the soil quality assessment [1,3].

The understanding of the response of soil enzyme activity to anthropogenic disturbances is important, considering their enrolment in the maintenance of soil functions that support the ecosystem. Soil enzymes are involved in the decomposition and synthesis of the soil organic matter, cycling, and availability of soil nutrients and biodegradation of pollutants. Soil enzyme activity determination is considered relatively easy and inexpensive, thus representing an important tool for the indication of changes in bioelements (C, N, S, and P) cycling [1,2,4].

Recent studies revealed the importance of the evaluation of the soil enzyme activities in relation to the soil organic carbon (SOC) content, which is known as the specific enzyme activity [1,4,5]. The specific enzyme activity is a useful and sensitive indicator that can be used to detect and reflect soil changes, while specific enzyme activity alterations provide a practical means to detect alterations in soil biochemical processes

---

[#] corresponding author: jmilosavljevic@tfbor.bg.ac.rs and microbial community structure [4,5]. Besides soil specific enzyme activities, other soil properties which can be used as soil quality indices include the geometric mean of enzyme activities (GMea) [4,6,7], the alteration index 3 (AI3) [2,8], and the enzymatic pH indicator (AlP/AcP ratio) [2].

The objective of this study was to investigate the specific activities of ß-glucosidase, urease, arylsulphatase, acid and alkaline phosphatase, involved in C, N, S, and P cycles, respectively. Also, the GMea, the AI3, and the AlP/AcP ratio were also used as soil quality indices.

MATERIALS AND METHODS

Soil sampling and analysis

A sampling of *Plantago* spp. root zone soil was performed at five sites in the Bor area characterised by the long-term pollution originating from the mining-metallurgical copper production activities (primarily copper smelter). Sampling site 1 (Town park) represents an urban-industrial zone, sampling site 2 (Brezonik) represents a suburban zone, sampling sites 3 (Oštrelj) and 4 (Slatina) represent a rural zone, while sampling site 5 (Gornjane) represents control zone. Detailed description of the pollution sources and the sampling sites is given in Milosavljevic *et al*. [9].

Soil enzyme activities expressed as micrograms of product per gram of oven-dry weight soil (i.e., absolute activity) [9] and soil organic carbon content (SOC) determined on the basis of the soil organic matter content by using the conversion factor of 2 [10] were used to calculate the specific soil enzyme activities. The specific activities of enzymes were calculated to normalize the activity to the magnitude of the SOC content [11]. The specific enzyme activity was calculated by dividing soil enzyme activity by the SOC content (g kg^{-1}) at the given sampling site [4,5].

Calculation of enzyme-based indices of soil quality

Soil enzyme activities (i.e. absolute activity) [9] were used to calculate the GMea, the AI3, and the AlP/AcP ratio. The GMea represents a general index that integrates the information from variables with different units and variation ranges [12]. The GMea index was calculated according to the following expression [2,6,12]:

$$GMea = (Glu \cdot Ure \cdot Arl \cdot AcP \cdot AlP)^{1/5} \tag{1}$$

where Glu, Ure, Arl, AcP, and AlP represent ß-glucosidase, urease, arylsulphatase, acid and alkaline phosphatase activities, respectively.

The activities of Glu, AcP, and Ure were used to calculate the AI3 index [2]:

$$AI3 = (7.87 \cdot Glu) - (8{,}22 - AcP) - (0{,}49 \cdot Ure) \tag{2}$$

The activities of AcP and AlP were used to calculate the enzymatic pH indicator [2]:

$$AlP/AcP \tag{3}$$

Data visualisation

Data visualisation was performed in the R statistical environment [13] by R package ggplot2 [14].

RESULTS AND DISCUSSION

Specific activity of soil enzymes

Figure 1 represents the specific activity of the investigated soil enzymes. The specific activities of Glu (Figure 1a), Arl (Figure 1c), and AcP (Figure 1d) were the highest at the control site. This site was not influenced by the mining-metallurgical activities, and it was characterised by the lowest SOC content [9,10]. The obtained results were in accordance with the literature [3,4] indicating that higher soil-specific enzyme activities were observed in soils with low organic carbon/matter content. Soil organic matter is regarded as an organic carrier of soil enzymes, which immobilizes and protects them [2,3]. Losses of soil organic matter might generate stresses to the soil microorganisms, resulting in higher enzyme activities in soil affected by environmental disturbances and stresses [1,4]. Similarly, Trasar-Cepeda *et al*. [1] indicated that deprivation of organic matter resulted in higher specific enzyme activity, although it was expected that a decrease in the soil organic matter content resulted in the reduction of the enzymatic activity. This could be explained by the fact that soil alterations generate stress for the microbiota resulting in the increase of the soil enzyme activities. Raiesi *et al.* [4] indicated that the increase in the soil-specific enzyme activities may reflect a reduction in soil organic carbon rather than the soil enzyme activity reduction.

On the other hand, the highest specific activities of Ure (Figure 1b) and AlP (Figure 1e) observed at site 3 were three and more than two times higher, respectively, compared to the corresponding values at the control site. Also, the specific activity of AlP at site 2 was around 1.3 times higher compared to the control site. Certain studies [2,8] showed that lower enzyme activities were observed in the soils with low organic matter content, which was noted for the specific activities of Ure and AlP at the control site. The reduction in the soil enzyme activity caused by the decrease in the soil organic matter content could be explained by the presence of the organo-enzyme complexes or by stimulation of microbial and subsequently enzymatic activity by organic substances present in the soil [8].

Enzyme-based soil quality indicators

The calculated values of the GMea, the AI3, and the AlP/AcP ratio are given in Table 1. The GMea index integrates data from various soil enzymes and represents an early indicator of soil quality changes [6]. The values of GMea varied between sampling sites, whereby the lowest value was observed at sampling site 2, while the highest value was noted at sampling site 3. As Lemanowicz *et al*. [2] stated, higher GMea values indicated better soil quality, which was not noted in this study since site 3 was located in the vicinity of the flotation tailing ponds. Contrary to our results, Batista *et al*. [7] observed that the GMea index decreased in the mine tailings compared to the reference soil.

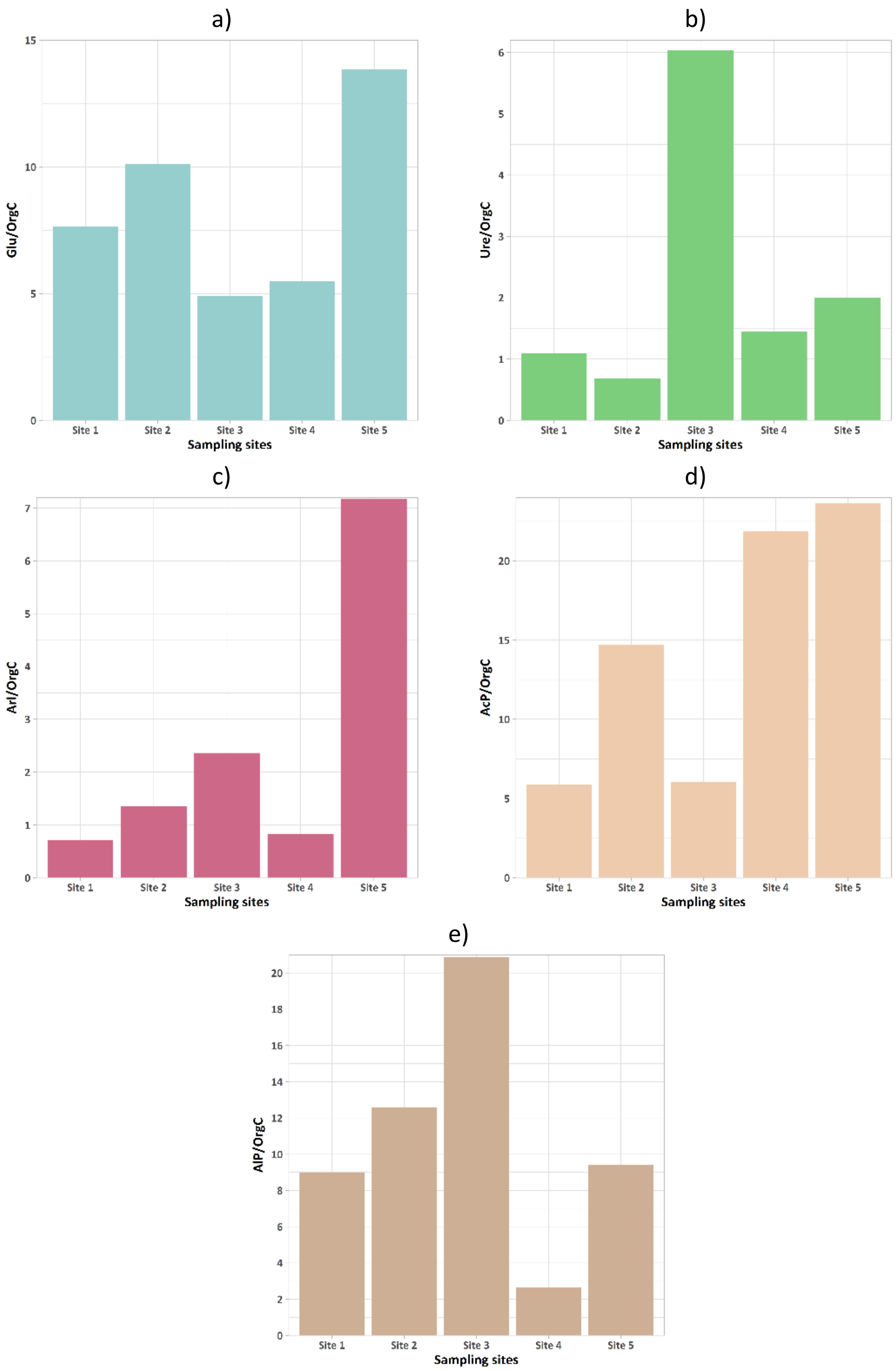

Figure 1 Specific soil enzyme activities in *Plantago* spp. root zone soil (Glu, Ure, Arl, AcP and AlP represent ß-glucosidase, urease, arylsulphatase, acid and alkaline phosphatase activities, respectively, and OrgC represents soil organic carbon content)

It should be emphasized that the GMea index calculation was based on the soil enzyme activities, without including other soil properties [1,2].

Table 1 Enzyme-based soil quality indices

Sampling site	**GMea**	**AI3**	**AlP/AcP ratio**
Site 1	175.08	621.06	1.53
Site 2	146.62	-1375.31	0.86
Site 3	287.74	-663.08	3.44
Site 4	181.70	-7576.85	0.12
Site 5	159.21	-1618.50	0.40

The AI3 index quantifies the balance between Glu, Ure, and AcP activities, and this index is sensitive to the soil alterations due to the anthropogenic disturbances [2]. The lowest value of the AI3 index was observed at site 4, while the highest value was observed at site 1 (Table 1). The low values of the AI3 index could indicate better soil [2], which was not observed in this study. The values of the AI3 index at the sites in the vicinity of pollution sources were higher compared to the value for the control site.

The AlP/AcP ratio is an enzymatic indicator of the pH level of the investigated soil [2]. The lowest value of this indicator was observed at site 4, while the highest was observed at site 3 (Table 1). According to Lemanowicz *et al*. [2], soil pH at which this ratio is about 0.5 could be considered as optimal for plant growth and development, which was observed only at the control site (the value of AlP/AcP ratio was 0.4).

CONCLUSION

Soil quality assessment in anthropogenic ecosystems is of great importance. The highest specific activities of Glu, Arl, and AcP were noted at the control site. The lowest organic carbon content in this site could have contributed to a high specific activity of these enzymes. On the other hand, the specific activity of Ure and AlP was the highest at site 3 located in the vicinity of the pollution sources (i.e. the flotation tailing ponds). Based on the values of the GMea and the AI3 indices, soil quality can be assessed, whereby high and low values of these indices, respectively, indicate good soil quality. However, the highest value of the GMea index was noted for site 3, while the lowest value for the AI3 index was noted for site 4, with both sites located in the close vicinity to the pollution sources. The control site could be regarded as optimal for plant growth, according to the AlP/AcP ratio.

ACKNOWLEDGEMENT

The authors are grateful to the Ministry of Education, Science and Technological development of the Republic of Serbia for financial support, within the funding of the scientific research work at the University of Belgrade, Technical Faculty in Bor, according to the contract with registration number 451-03-9/2021-14/ 200131. Our thanks go to English language teacher Mara Manzalovic from the Technical Faculty in Bor (University of Belgrade) for providing language assistance.

REFERENCES

1. Trasar-Cepeda, C., Leirós, M.C., Gil-Sotres, F. (2008) Hydrolytic enzyme activities in agricultural and forest soils. Some implications for their use as indicators of soil quality. Soil Biology & Biochemistry, 40, 2146-2155.
2. Lemanowicz, J., Haddad, S.A., Bartkowiak, A., Lamparski, R., Wojewódzki, P. (2020) The role of an urban park's tree stand in shaping the enzymatic activity, glomalin content and physicochemical properties of soil. Science of the Total Environment, 741, 140446.
3. Wang, B., Xue, S., Liu, G.B., Zhang, G.H., Li, G., Ren, Z.P. (2012) Changes in soil nutrient and enzyme activities under different vegetations in the Loess Plateau area, Northwest China. Catena, 92, 186-195.
4. Raiesi, F., Beheshti, A. (2014) Soil specific enzyme activity shows more clearly soil responses to paddy rice cultivation than absolute enzyme activity in primary forests of northwest Iran. Applied Soil Ecology, 75, 63-70.
5. Zhang, X., Dong, W., Dai, X., Schaeffer, S., Yang, F., Radosevich, M., Xu, L., Liu, X., Sun, X. (2015) Responses of absolute and specific soil enzyme activities to long term additions of organic and mineral fertilizer. Science of the Total Environment, 536, 59-67.
6. Raiesi, F., Salek-Gilani, S. (2018) The potential activity of soil extracellular enzymes as an indicator for ecological restoration of rangeland soils after agricultural abandonment. Applied Soil Ecology, 126, 140-147.
7. Batista, É.R., Carneiro, J.J., Pinto, F.A., dos Santos, J.V., Carneiro, M.A.C. (2020) Environmental drivers of shifts on microbial traits in sites disturbed by a large-scale tailing dam collapse, Science of the Total Environment, 738, 139453.
8. Paz-Ferreiro, J., Trasar-Cepeda, C., Leirós, M.C., Seoane, S., Gil-Sotres, F. (2009) Biochemical properties in managed grassland soils in a temperate humid zone: modifications of soil quality as a consequence of intensive grassland use. Biology and Fertility of Soils, 45, 711-722.
9. Milosavljevic, J.S., Serbula, S.M., Cokesa, D.M., Milanovic, D.B., Radojevic, A.A., Kalinovic, T.S., Kalinovic, J.V. (2020) Soil enzyme activities under the impact of long-term pollution from mining-metallurgical copper production. European Journal of Soil Biology, 101, 103232.
10. Milosavljević, J., Šerbula, S., Kalinović, T., Kalinović, J., Radojević, A., Spalović B. (2020) The relations between soil physico-chemical properties and soil enzyme activities in long-term contaminated area, In: 28th International conference ecological truth and environmental research – EcoTER'20, Kladovo, Serbia, Proceedings, 66-71.
11. Xu, Z., Yu, G., Zhang, X., He, N., Wang, Q., Wang, S., Wang, R., Zhao, N., Jia, Y., Wang, C. (2017) Soil enzyme activity and stoichiometry in forest ecosystems along the North-South Transect in eastern China (NSTEC). Soil Biology & Biochemistry, 104, 152-163.
12. García-Ruiz, R., Ochoa, V., Hinojosa, M.B., Carreira, J.A. (2008) Suitability of enzyme activities for the monitoring of soil quality improvement in organic agricultural systems. Soil Biology & Biochemistry, 40, 2137-2145.
13. R Core Team, (2018) R: A language and environment for statistical computing. R Foundation for Statistical Computing, Vienna, Austria, https://www.R-project.org/
14. Wickham, H., (2016) ggplot2: Elegant Graphics for Data Analysis. Springer-Verlag New York, https://ggplot2.tidyverse.org/

XIV International Mineral Processing
and Recycling Conference
Belgrade, Serbia, 12-14 May 2021

ASSESSMENT OF METAL(LOID) POLLUTION IN THE URBAN–INDUSTRIAL, TOURIST AND TRAFFIC ZONES OF BOR, USING COMON HAZEL

Ana Radojević[#], **Snežana Šerbula, Jelena Kalinović, Jelena Milosavljević, Tanja Kalinović**
University of Belgrade, Technical Faculty in Bor, Bor, Serbia

ABSTRACT – The level of pollution of the urban–industrial zone (site UI), tourist zone (sites T1 and T2) and traffic zone (site TR) in the city of Bor was assessed in comparison to the background zone (site B). The content of As, Cr, Cu, Fe, Mn, Ni, Pb and Zn was determined in the samples of plant material (roots, branches, washed leaves and catkins) of common hazel (*Corylus* spp.). The results indicated Cu enrichment of the plant parts, especially the washed leaves, which could be directly attributed to the emissions from the copper smelter.

Keywords: Pollution, Metal(loid), Bor, Hazel, Enrichment.

INTRODUCTION

Non–ferrous metal production, which involves primarily mining of ores and secondary pre– and post–smelting operations, is known as one of the most significant anthropogenic pollution sources of the environment [1]. During the mineral processing phase, waste crushed rock (consisting of silicates, oxides, hydroxides, carbonates, sulfides, etc.) and processing fluids from mills, washeries and concentrators (called tailings) are generated. The amount of solid fraction of the tailings consists of 95–99% of the copper ore input [2], since the ore grade is low, usually in the range of 0.5–1.0% [3]. In the refining and processing step of mineral concentrates, significant quantities of atmospheric deposition, containing heavy metals and metalloids, are discharged into the atmosphere [4]. As Etller [1] found, prevailing wind direction is a key factor affecting the dispersion of smelter emissions and their subsequent deposition on the soil, especially in the arid areas. Contaminants associated with particulates emitted from mining operations are usually concentrated in the fine (<2 mm), whereas from smelting operations they are concentrated in the ultrafine (<0.5 mm) fraction, which may travel by wind at greater distances [1].

Surface soils represent direct “sinks” for airborne contaminants. However, soils around mines have commonly natural mineralised backgrounds, and it is often difficult to differentiate among individual pollution sources, such as smelters [1]. The bioavailability of contaminants in soil is under the influence of various factors. Milosavljevic *et al.* [5] showed that soil enzyme activities decreased with high heavy metal content and varied depending on soil physico–chemical properties, especially the soil pH value, thus indicating the alteration of soil nutrient cycling and soil quality. On the

---

[#] corresponding author: aradojevic@tfbor.bg.ac.rs other hand, Opekunova *et al.* [6] found that the high buffer capacity of soils, characterised by high humus content and neutral pH, caused the low mobility and stabilised the biogeochemical cycles of Cu, Zn, Fe, Mn, Ni, Pb, Cd, Co and Cr.

Heavy metals and metalloids (metal(loid)s) including Pb, Cd, As, and Cr, due to their persistence and toxicity, even at low levels, are considered environmentally hazardous by numerous environmental or health related standards. Thus, concerns about dry and wet atmospheric deposition containing metal(loid)s have increased, as they can directly and/or indirectly impact ecosystems and human health [7].

The objective of the paper was to estimate the difference of the contamination level of four zones of sampling by analyzing metal(loid) content (As, Cr, Cu, Fe, Mn, Ni, Pb and Zn) in parts of common hazel (*Corylus* spp.), sampled in the city of Bor and its surroundings.

EXPERIMENTAL

Study area

The city of Bor and its surroundings (Eastern Serbia, Balkan Peninsula) was selected for sampling, since the mining–metallurgical operations, associated with copper production (Figure 1), had been dominant pollution sources over a long period of time [8], which corresponded well to the aim of the survey.

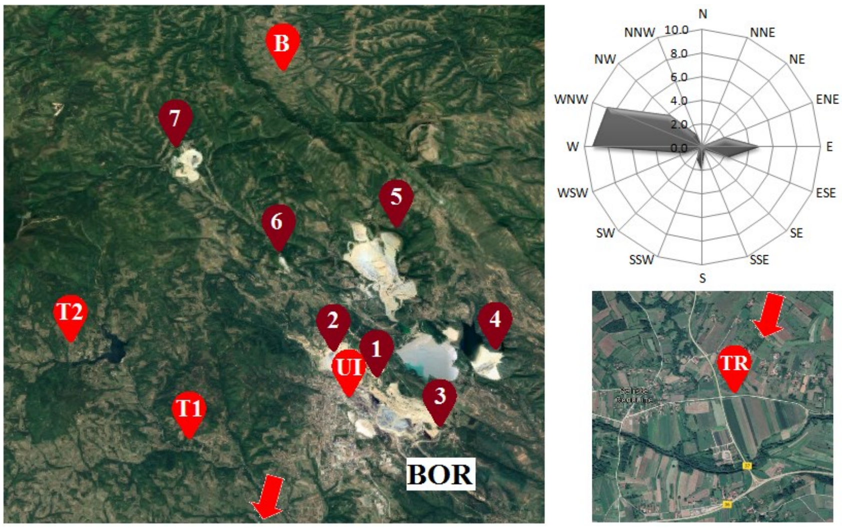

Figure 1 The map of the study area showing dominant pollution sources (1-copper smelter, 2-old open pit Bor, 3 and 4 -flotation tailing ponds, 5-Krivelj copper mine, 6-quarry, 7-Cerovo copper mine), location of the sampling sites (UI, T1, T2, TR, B) and frequency wind rose diagram during the sampling year

The sampling was performed in four sampling zones, including the background. The urban–industrial (UI), traffic (TR) and background (B) zones were represented by one sampling site each, while the tourist zone (T) was represented by two sites. As can be seen from Figure 1, the site UI was located in the city of Bor, in the proximity of the copper smelter (marked with 1), while the sites T1 and T2 were located in the area of Brestovac spa and Bor Lake, respectively. The site TR was located 17 km SSW from the mining–metallurgical complex, predominately characterised with traffic pollution, since the sampling was carried out a few kilometres along the main road which leads to the city of Bor (from the intersection called Selište). Due to its position behind the mountain ranges of Veliki and Mali Krš, which provided a natural shield against air pollution from the copper smelter, the rural settlement Gornjane was selected for the background site.

Concentrations of seven metals (Cr, Cu, Fe, Mn, Ni, Pb and Zn) and one metalloid (As) were determined in the plant material (washed roots, unwashed branches, washed leaves and unwashed catkins) of common hazel (*Corylus* spp., predominantly *Corylus avellana*). Over the time, the considered metal(loid)s were present in the atmosphere of the city of Bor and its surroundings in the form of particulate matter and/or atmospheric depositions, mostly as a result of smelting [8]. The sampling and the analysis of the collected material were performed according to the standard procedures, as previously explained in detail in Radojevic *et al.* [9]. It should be noted that, in the time of the sampling (during the fall of 2013), the "old" copper smelter in the mining–metallurgical complex was operational.

Data analysis

Enrichment Factor (EF_{plant}) was calculated for the obtained concentrations of the selected metal(loid)s (µg/g of dry weight) in the plant material according to the equation (1).

$$EF_{plant} = C_s/C_b \tag{1}$$

where:

C_s – metal(loid) concentration (µg/g);

C_b – corresponding metal(loid) concentration (µg/g) at the background site.

According to the EF values, enrichment of the plant parts with the studied metal(loid)s is observed at values higher than 2 [10].

RESULTS AND DISCUSSION

Concentrations of the selected metal(loid)s in the plant parts of hazel are presented in Figure 2. By comparing, the values detected in the samples of washed leaves of hazel to the deficit/normal/toxic concentrations in the mature leaves of plants [9], we could conclude that, in the study area, metal(loid)s were present mostly in the normal range. The exceptions were noted for: the concentration of As at the site UI, the concentrations of Cu at the sites UI, T1 and T2, the concentration of Mn at the site B and the concentration of Fe at the site UI, which all referred to the corresponding toxic range. However, it should be emphasised that the suggested literature deficit/normal/toxic ranges represent very wide ranges of concentrations summarised for various plant species.

Catkins were the samples of hazel in which metal(loid)s were below the limit of detection (LD) at the sites T2, TR and B. Since hazel branches have very smooth bark (unlike other deciduous trees), the lower concentrations were noticed in the samples of branch compared to other hazel parts at all the sites, with a few exceptions, regardless of the fact that branch samples were not washed before the analysis. The concentrations of As and Cu, as the main pollutants in the study area, were higher at the sites UI and T1, also at the site T2 in the case of Cu, due to unfavourable wind rose. At the site TR, the concentrations of As and Cu were very low. Despite the long usage of leaded gasoline, the Pb concentrations were also lower at the TR compared to the UI site. The data from the site TR are indicating predominant origin from smelting operations of As, Cu and Pb.

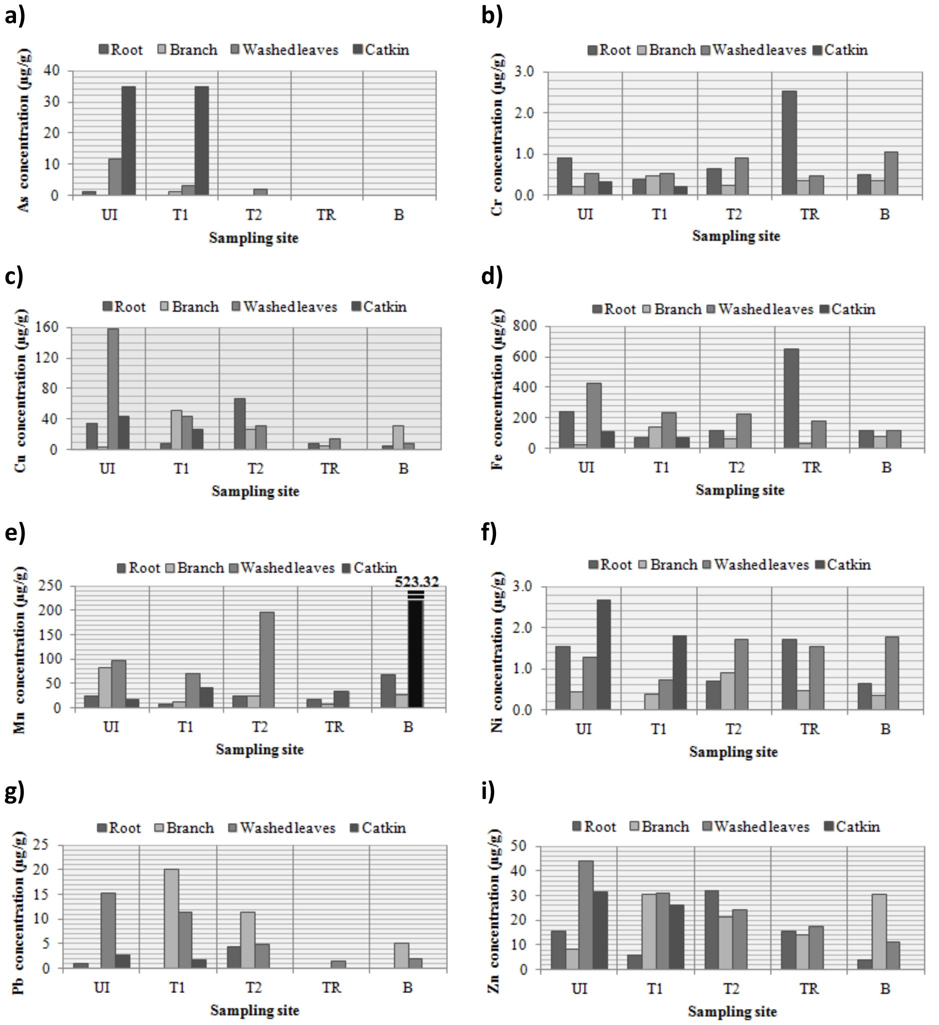

Figure 2 Metal(loid) concentrations (μg/g) in the parts of hazel sampled at five sampling sites in the study area of Bor and its surroundings **a)** As; **b)** Cr; **c)** Cu; **d)** Fe; **e)** Mn; **f)** Ni; **g)** Pb; **i)** Zn (in the case of missing bars, concentrations were below the corresponding LDs)

The concentrations given in Figure 2 were used to calculate EF$_{plant}$, and the results are presented in Table 1. The catkins were excluded from the analysis of the plant enrichment since most of the concentrations were below the corresponding LDs, as previously said. Also, the metal(loid) concentrations at the background site were used for the calculation, hence they are not given in the Table 1.

Table 1 Enrichment Factor (EF$_{plant}$) for metal(loid)s in the parts of hazel at the four sampling sites in Bor and its surroundings

Site	**Metal(loid) / Sample**							
	As	**Cr**	**Cu**	**Fe**	**Mn**	**Ni**	**Pb**	**Zn**
				Roots				
UI	>1	1.9	**7.7**	**2.1**	0.4	**2.4**	>1	**3.8**
T1	/	0.8	1.9	0.6	0.1	**>3.2**	/	1.5
T2	/	1.4	**15.1**	1.0	0.4	1.1	**>4**	**7.8**
TR	/	**5.2**	1.8	**5.5**	0.2	**2.6**	/	**3.8**
				Branches				
UI	/	0.6	0.1	0.3	**3.0**	1.2	/	0.3
T1	>1	1.3	1.6	1.9	0.5	1.1	**4.0**	1.0
T2	/	0.7	0.8	0.9	0.9	**2.5**	**2.2**	0.7
TR	/	1.0	0.2	0.4	0.3	1.3	/	0.5
				Washed leaves				
UI	**>11**	0.5	**21.9**	**3.6**	0.2	0.7	**8.0**	**3.9**
T1	**>3**	0.5	**6.0**	**2.0**	0.1	0.4	**6.0**	**2.8**
T2	**>2**	0.9	**4.4**	1.9	0.4	1.0	**2.5**	**2.1**
TR	/	0.4	**2.1**	1.5	0.1	0.9	0.8	1.6

The values of EF>2 are shown in bold; the values with “>” were obtained by dividing the metal(loid) concentration with the corresponding LD since the concentration at the background site; “/” no data since both metal(loid) concentrations were below the corresponding LDs.

Minimal enrichment was generally observed for the branch samples for most of the studied metal(loid)s, except for Mn, Ni and Pb enrichment in urban–industrial and tourist zones. The enrichment of the root samples was somewhat higher, with the average highest enrichment for Cu (for all the sampling sites) compared to other elements, reaching 15.1 at the T2 site. In the study area, the highest enrichment was observed for the samples of washed leaves, the enrichment was especially high for Cu, As, as well as for Pb and Zn. The highest EF value, amounting to 21.9, was noted for Cu at the UI site.

CONCLUSION

Regarding the zone distribution of metal(loid)s in the plant parts, clear influence of copper production could be seen in the case of As and Cu contents in the hazel material, which are the pollutants of the highest concern in the study area. The concentrations of As, Cu and Pb at the background and traffic related site were much lower compared to the site in the proximity of the copper smelter, i.e. UI. The enrichment of the analysed plant parts generally decreased in the following order: washed leaves>roots>branches. The sites T1 and T2, although belonging to the local tourist area, were also characterised with high plant enrichment with the studied metal(loid)s, mostly due to unfavourable wind rose. High values of EF_{plant} indicated that accumulated metal(loid)s in the plant parts of hazel were a result of the copper smelter emissions, which had generally left consequences on plants growing in the area of the city of Bor and its surroundings.

ACKNOWLEDGEMENT

The authors are grateful for the financial support provided by the Ministry of Education, Science and Technological Development of the Republic of Serbia, within the funding of the scientific research work at the University of Belgrade, Technical Faculty in Bor, according to the contract with registration number 451-03-9/2021-14/200131. Our thanks go to English language teacher Mara Manzalović from the Technical Faculty in Bor, for providing language assistance.

REFERENCES

1. Ettler, V. (2016) Soil contamination near non-ferrous metal smelters: A review. Applied Geochemistry, 64, 56-74.
2. Beylot, A., Villeneuve, J. (2017) Accounting for the environmental impacts of sulfidic tailings storage in the Life Cycle Assessment of copper production: A case study. Journal of Cleaner Production, 153, 139-145.
3. Alvarado, S., Maldonado, P., Jaques, I. (1999) Energy and environmental implications of copper production. Energy, 24, 307-316.
4. Kang, M.–J., Kwon, Y.K., Yu, S., Lee, P.–K., Park, H.–S., Song, N. (2019) Assessment of Zn pollution sources and apportionment in agricultural soils impacted by a Zn smelter in South Korea. Journal of Hazardous Materials, 364, 475-487.
5. Milosavljevic, J.S., Serbula, S.M., Cokesa, Dj.M., Milanovic, D.B., Radojevic, A.A., Kalinovic, T.S., Kalinovic, J.V. (2020) Soil enzyme activities under the impact of long-term pollution from mining-metallurgical copper production. European Journal of Soil Biology, 101, 103232.
6. Opekunova, M., Opekunov, A., Somov, V., Kukushkin, S., Papyan, E. (2020) Transformation of metals migration and biogeochemical cycling under the influence of copper mining production (the Southern Urals). Catena, 189, 104512, 12p.
7. Feng, W., Guo, Z., Peng, C., Xiao, X., Shi, L., Zeng, P., Ran, H., Xue, Q. (2019) Atmospheric bulk deposition of heavy metal(loid)s in central south China: Fluxes, influencing factors and implication for paddy soils. Journal of Hazardous Materials, 371, 634-642.
8. Serbula, S.M., Milosavljevic, J.S., Radojevic A.A., Kalinovic, J.V., Kalinovic, T.S. (2017) Extreme air pollution with contaminants originating from the mining–metallurgical processes. Science of the Total Environment, 586, 1066-1075.
9. Radojevic, A.A., Serbula, S.M., Kalinovic, T.S., Kalinovic, J.V., Steharnik, M.M., Petrovic, J.V., Milosavljevic, J.S. (2017) Metal/metalloid content in plant parts and soils of *Corylus* spp. influenced by mining–metallurgical production of copper. Environmental Science and Pollution Research, 24, 10326-10340.
10. Mingorance, M.D., Valdes, B., Rossini Oliva, S. (2007) Strategies of heavy metal uptake by plants growing under industrial emissions. Environmental International, 33, 514-520.

XIV International Mineral Processing
and Recycling Conference
Belgrade, Serbia, 12-14 May 2021

ASSESSMENT OF THE SOIL CONTAMINATION LEVEL IN BOR AND ITS SURROUNDINGS (SERBIA) BASED ON DIFFERENT POLLUTION INDICES

Jelena Kalinović#, Snežana Šerbula, Jelena Milosavljević, Ana Radojević, Tanja Kalinović
University of Belgrade, Technical Faculty in Bor, Bor, Serbia

ABSTRACT – Assessment of the level of soil contamination with toxic elements in the city of Bor and its surroundings were carried out with several indices of soil pollution. According to the obtained data of geo-accumulation index (I_{geo}), single factor pollution index (SFPI), comprehensive pollution index (CPI, Nemerow index) and pollution load index (PLI), the soil in the study area was heavily affected by the pollution from the mining and smelting activities.

Keywords: Copper Smelter, Soil, Pollution Indices.

INTRODUCTION

Mining and smelting activities, urbanisation, agricultural activities, coal combustion and industrialization have increased negative impact on the environment and human health worldwide [1-3]. Territory in the vicinity of non-ferrous metal mining and smelting plants are often characterized by high concentrations of toxic elements [4]. During mining and smelting processes, elements such as Cu, Pb, As and others, which co-exist in Cu ores, are emitted and accumulated in every segment of the environment [5].

The aim of this paper was to assess the level of soil contamination by toxic elements in the city of Bor and its surroundings using different indices of the soil pollution.

MATERIALS AND METHODS

Study area

The city of Bor (Eastern Serbia) has been well-known for mining and pyrometallurgical copper production for more than a century. The copper smelter is located on the northeastern border of the city. The emissions of the large amounts of gaseous and particulate pollutants (PM_{10} and atmospheric depositions) characterised the Bor area as one of the most polluted in Serbia and Europe [6,7].

The samples of root zone soil of *Rosa* spp. (predominantly *Rosa canina* L.) was collected from the sites which were considered as the most affected with toxic elements from the main pollution source according to the previous studies [6,7]. The urban sampling site (U) was located >2.5 km SW from the copper smelter, the urban-industrial sampling site (UI) was located in the range of 0.5–2.5 km SW from the copper smelter,

---

[#] corresponding author: jkalinovic@tfbor.bg.ac.rs the suburban sampling site (SU) was located in the suburban settlement 2.5 km NW from the copper smelter. The sampling sites R1 and R2 were located in the rural settlements 4.5 km ESE and 6.5 km SE from the copper smelter, respectively. For the background sampling site (B) the rural settlement 17 km in the N direction from the copper smelter was chosen. This site is physically protected by the mountain massifs (Veliki and Mali Krš) from the air pollution originating from the copper smelter. Detailed description of the pollution sources, sampling sites, sampling and analytical procedures is given in Kalinovic *et al.* [6].

Data analyses

The soil contamination level with toxic elements was evaluated with several pollution indices, such as geo-accumulation index (I_{geo}), single factor pollution index (SFPI), comprehensive pollution index (CPI, Nemerow index) and pollution load index (PLI).

Geo-accumulation index (I_{geo}) reports about soil contamination by comparing the content of toxic elements with the corresponding background concentration [3,8,9]. I_{geo} is expressed by an equation (1):

$$I_{geo} = log_2 \frac{C_n}{(1.5 \ x \ B_n)} \tag{1}$$

where:

C_n is the concentration of the analysed element in the sampled soil (mg/kg);

B_n is the geochemical background concentration of the same element (mg/kg);

1.5 is the factor used for the reduction of the influence of natural pedogenic processes.

Based on the I_{geo} values, there are seven different categories of soil contamination level: unpolluted ($I_{geo} \leq 0$); unpolluted to moderately polluted (0–1); moderately polluted (1–2); moderately to highly polluted (2–3); highly polluted (3–4); highly to extremely polluted (4–5), and extremely highly polluted ($I_{geo} \geq 5$) [3]. In this paper, the concentration of the analysed elements in the soil samples from the background site was used for the geochemical background concentration (B_n).

Single factor pollution index (SFPI) is used to estimate the level of soil pollution in the study area. The SFPI is obtained by the following equation [8,10]:

$$SPFI = \frac{C_i}{S_i} \tag{2}$$

where:

C_i is the concentration of the analysed element in the sampled soil (mg/kg);

S_i is the permitted standard of the same element (mg/kg).

According to Ghayoraneh and Qishlaqi [10], the SFPI could indicate: no pollution ($SFPI \leq 1$); slight pollution ($1 < SFPI \leq 2$); moderate pollution ($2 < SFPI \leq 3$), and heavy pollution ($SFPI > 3$).

Comprehensive pollution index (CPI or Nemerow index), which is applied to estimate the contributions of toxic elements to the soil pollution, was calculated by the equation (3) [8,10]:

$$CPI = \sqrt{\frac{SFPI_{max}^{2} + SPFI_{ave}^{2}}{2}} \tag{3}$$

where:

SFPI$_{max}$ refers to the maximal value;

SFPI$_{ave}$ refers to the average value of SFPI among all target toxic elements.

According to the comprehensive pollution index, soil can be classified as [8]: low level of pollution (CPI≤1); moderate level of pollution (1<CPI≤2); high level of pollution (2<CPI≤5); and extremely high pollution (CPI>5).

Pollution load index (PLI) is used to evaluate the overall toxicity status of the soil sampled in the study area using the following equation [1,9]:

$$PLI = (CF_1 \ x\ CF_2 \ x\ CF_3 \ x\ CF_4 \ x\ \ldots\ x\ CF_n)^{1/n} \tag{4}$$

where:

CF is a contamination factor of each element calculated as: CF = C_i/B_i in which C_i represents the concentration of the element determined in the soil, and B_i is the background value of the same element;

n is a total number of elements.

Based on the value of PLI, soil is classified as [1]: unpolluted (PLI<0.7); slightly polluted (0.7<PLI<1); moderately polluted (1<PLI<2); severely polluted (2<PLI<3) and heavily polluted (PLI>3).

RESULTS AND DISCUSSION

The calculated I$_{geo}$ values for the analysed elements in the sampled soil are shown in Figure 1. I$_{geo}$ of Al, Fe and Zn were in the category of unpolluted and unpolluted to moderately polluted, except for Zn at the U site where high pollution of soil was noted. I$_{geo}$ value of As indicated moderate pollution at the U site, moderate to high at the UI and SU sites and high at the R1 and R2 sites. The soil pollution with Pb was in the category of unpolluted to moderately polluted at the SU site, moderate at the UI site, moderate to high at the R1 and R2 sites and extreme to high at U site. The highest I$_{geo}$ value was found for Cu which contributed to the high pollution at the SU site and extreme to high pollution at the U and R2 sites.

According to Kabala *et al.* [3], the calculated values of I$_{geo}$ indicated that there was no soil pollution with Zn, As and Pb in the vicinity of the tailing ponds, while for Cu the mean values of I$_{geo}$ belonged to the category of moderate pollution and the highest values of I$_{geo}$ indicated high pollution of the soil. In the study by Gujre *et al.* [8], the level of contamination and I$_{geo}$ value varied for Zn. At most sampling sites I$_{geo}$ was in the category of moderate pollution and moderate to high pollution, while the I$_{geo}$ for the soil sampled at the site near the metal and glass segregation unit, high level of contamination was noted.

Figure 2 shows the SFPI values of As, Cu, Pb and Zn in the sampled soil. Considering that guidelines for Al and Fe are not defined, so these two elements were excluded from these analyses. The limit values for As, Cu, Pb and Zn in the soil, according to the Serbian Regulation [11] are 29 mg/kg, 36 mg/kg, 85 mg/kg and 140 mg/kg, respectively.

According to the SFPI for As, soil from the control site was not polluted, while the soil from the U site soil was slightly polluted, from SU site moderately and the soil from the UI, R1 and R2 sites was heavily polluted. The SFPI of Cu at all the sampling sites was in the category of heavy pollution, except at the control site (SFPI<1), indicating huge negative impact of the industrial activities on the environment. Heavy pollution of the soil was also noted at the U site for Pb and Zn, and slight-pollution for Pb at the R1 and R2 sites.

In the study by Ghayoraneh and Qishlaqi [10], the SFPI<1 indicated that soil was not polluted with Cu, while the soil contamination with Pb and Zn was relatively heavily polluted (SFPI>3) and decreased with increasing distance from the pollution source.

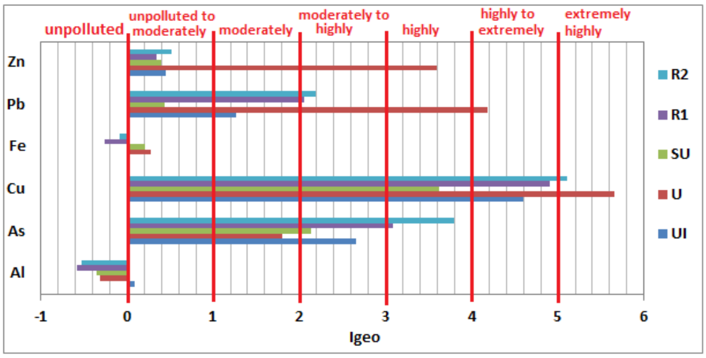

Figure 1 Geo-accumulation index (I_{geo}) of the investigated elements in the study area

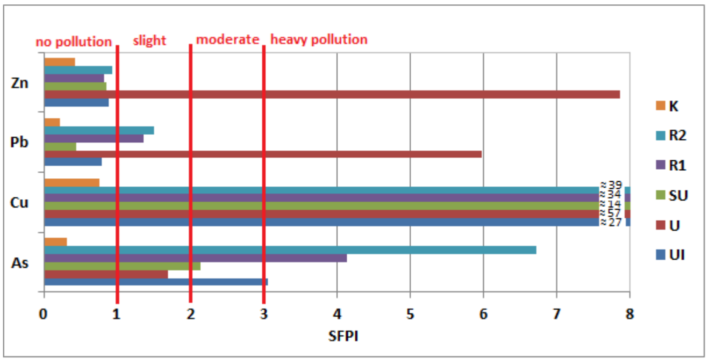

Figure 2 Single factor pollution index (SFPI) of As, Cu, Pb and Zn in the study area

The values of the CPI based on the SFPI for As, Cu, Pb and Zn are presented in Figure 3. The obtained values for CPI indicated that soil sampled at the UI, U, R1 and R2 sites was in the category of extremely high pollution, showing high negative influence of the emissions from the mining-metallurgical complex in the study area. The CPI value was in the category of low pollution only for K site, as expected due to the greater distance of the background site from the main pollution source. According to Ghayoraneh and Qishlaqi [10], based on the CPI values, different pollution zones, depending on the distance from the Pb/Zn smelter, can be identified. For the zone which was the closest to the pollution source, the CPI value was more than 10, while the zone with the CPI<1 was located more than 8,000 m away from the smelter.

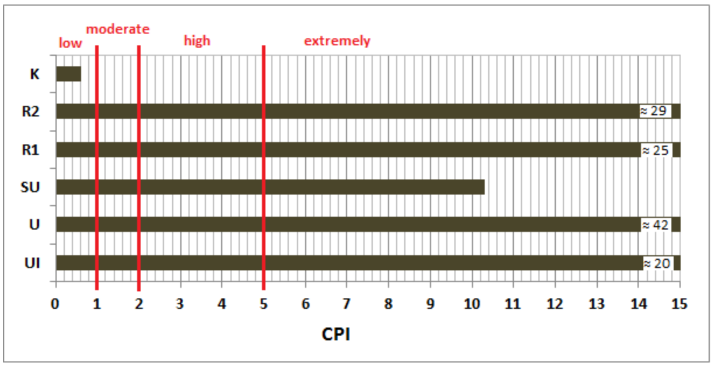

Figure 3 Comprehensive pollution index (CPI) at sampling sites in the study area

The calculated values of PLI also provided information about soil pollution at the selected sampling sites (Figure 4). Based on the obtained values, the soil from all the sampling sites was heavily polluted, with the highest value of the PLI noted at the U site. High PLI values at all the sampling sites could be the consequence of very high CF values obtained particularly for Cu and As, ranging 18–76 and 6.6–21, respectively.

In the study by Okonkwo *et al.* [10] the values of PLI varied from 2.25 to 14.23 suggesting severe to heavy pollution of the soils analysed in the pegmatite mining area, while in the study by Kumar *et al.* [9], the PLI was >1 at two sites.

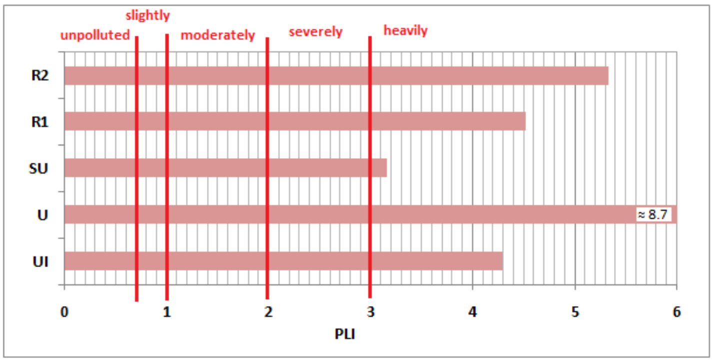

Figure 4 Pollution load index (PLI) of As, Cu, Pb and Zn in the study area

CONCLUSION

In this paper different indices of soil pollution were determined in order to assess the contamination of soil in the city of Bor and its surroundings. Based on the obtained values of I_{geo} and SFPI, it can be concluded that the highest pollution was noted for Cu, As and Pb, while the sites U and R2 could be considered as the most polluted. Regarding the CPI and PLI values, it can be noted that pollution of soil are extreme and heavy at all the sampling sites, except at the control site. Such high values of the soil pollution indices indicated that the mining and smelting activities had high negative impact on the environment. According to the presented data, the soil in the Bor area needs remediation due to the serious pollution with toxic elements.

ACKNOWLEDGEMENT

The authors are grateful to the Ministry of Education, Science and Technological development of the Republic of Serbia for financial support, within the funding of the scientific research work at the University of Belgrade, Technical Faculty in Bor, according to the contract with registration number 451-03-9/2021-14/ 200131. Our thanks go to English language teacher Mara Manzalovic from the Technical Faculty in Bor (University of Belgrade) for providing language assistance.

REFERENCES

1. Okonkwo, S.I., Idakwo, S.O., Ameh, E.G. (2021) Heavy metal contamination and ecological risk assessment of soils around the pegmatite mining sites at Olode area, Ibadan southwestern Nigeria. Environmental Nanotechnology, Monitoring & Management, 15, 100424.
2. Shamsaddin, H., Jafari, A., Jalali, V., Schulin, R. (2020) Spatial distribution of copper and other elements in the soils around the Sarcheshmeh copper smelter in southeastern Iran. Atmospheric Pollution Research, 11, 1681-1691.
3. Kabala, C., Galka, B., Jezierski, P. (2020) Assessment and monitoring of soil and plant contamination with trace elements around Europe's largest copper ore tailings impoundment. Science of the Total Environment, 738, 139918.
4. Xing, W., Liu, H., Banet, T., Wang, H., Ippolito, J.A., Li, L. (2020) Cadmium, copper, lead and zinc accumulation in wild plant species near a lead smelter. Ecotoxicology and Environmental Safety, 198, 110683.
5. Cai, L.-M., Wang Q.-S., Luo, J., Chen, L.-G., Zhu, R.-L., Wang, S., Tang, C.-H. (2019) Heavy metal contamination and health risk assessment for children near a large Cu-smelter in central China. Science of the Total Environment, 650, 725-733.
6. Kalinovic, J., Serbula, S., Radojevic, A., Milosavljevic, J., Kalinovic, T., Steharnik, M. (2019) Assessment of As, Cd, Cu, Fe, Pb, and Zn concentrations in soil and parts of *Rosa* spp. sampled in extremely polluted environment. Environmental Monitoring and Assessment, 191, 15.
7. Kalinovic, T., Serbula, S., Radojevic, A., Kalinovic, J., Steharnik, M., Petrovic, J. (2016) Elder, linden and pine biomonitoring ability of pollution emitted from the copper smelter and the tailings ponds. Geoderma, 262, 266-275.
8. Gujre, N., Mitra, S., Soni, A., Agnihotri, R., Rangan, L., Rene, E., Sharma, M. (2021) Speciation, contamination, ecological and human health risks assessment of heavy metals in soils dumped with municipal solid wastes. Chemosphere, 262, 128013.
9. Kumar, S., Zhao, M., Zhang, H., Rahman, M.A., Luo, C., Rahman, M.M. (2021) Distribution, contamination status and source of trace elements in the soil around brick kilns. Chemosphere, 263, 127882.
10. Ghayoraneh, M., Qishlaqi, A. (2017) Concentration, distribution and speciation of toxic metals in soils along a transect around a Zn/Pb smelter in the northwest of Iran. Journal of Geochemical Exploration, 180, 1-14.
11. Regulation No. 88/10, "The Official Gazette of Republic of Serbia", The soil quality monitoring programme using indicators for assessing the risks from the soil degradation as well as the methodology for working out the remediation programme (2010).

XIV International Mineral Processing
and Recycling Conference
Belgrade, Serbia, 12-14 May 2021

THE IMPACT OF MINERAL RESOURCES EXPLOITATION ON THE ENVIRONMENT

Slavica Mihajlović[1#], Nataša Đorđević[1], Aleksandra Patarić[1], Marina Blagojev[2]
[1] Institute for Technology of Nuclear and Other Mineral Raw Materials,
Belgrade, Serbia
[2] University of Belgrade, Faculty of Mining and Geology, Belgrade, Serbia

ABSTRACT – The paper shows how the exploitation of mineral resources may lead to environmental degradation. Planning the exploitation of certain mineral raw materials requires a detailed analysis of all the necessary works in order to fully eliminate or reduce to a minimum any negative impact on the area where the mining activity is performed. Also, it is important to emphasize that natural resources are very difficult to renew, so in case of uncontrolled exploitation, danger of permanent loss occurs. Therefore, the exploitation of mineral raw materials should be based on the principles of sustainable development, and the measures for the protection of the space where the exploitation is performed should be carried out according to the prescribed rules and legal provisions.

Keywords: Exploitation of mineral raw materials, Sustainable development, Environmental protection.

INTRODUCTION

Environmental pollution, as a consequence of human activities, is increasing progressively. For these reasons, the principles of environmental protection are extremely important in all countries, which contribute to the protection of living and working space on a global level through individual activities. The degradation of living and working environment directly endangers people's health as well as plant and animal species. Also, soil, water and air are contaminated, thus directly affects the quality of food. Therefore, it is extremely important to develop and modernize the monitoring system of all parameters that show quality of soil, water air and food. In order to reduce the level of pollution and disturbance of the natural balance under the influence of anthropogenic factors, it is necessary to have a knowledge about technology that will be applied for certain purposes. When it comes to the exploitation of mineral resources, a multidisciplinary approach to such activities is necessary to completely eliminate or minimize all negative impacts on the area where the necessary actions are performed. Also, it is extremely important to keep in mind that natural resources are non-renewable or difficult to renew, so in case of uncontrolled exploitation, they are in danger of permanent loss.

Connecting all types of production and technological processes with environmental protection has led to the occurrence of an ecological economy. On the other hand, the economic aspect of sustainable development has contributed to the more efficient use

---

[#] corresponding author: s.mihajlovic@itnms.ac.rs of available natural resources, [1,2]. Namely, sustainable development meets the needs of the present without compromising the ability of future generations to meet their own needs, [3]. The concept of sustainable development was created to preserve the environment, to unite all partial measures and separate policies and thus give a better result, [4]. The significance of above mentioned gained in importance when the International Association for the Protection of the Environment and Natural Resources became involved in sustainable development formation with its activities. In 1980, the Association developed an environmental protection strategy, which set the basic task of achieving sustainable development through the protection of natural resources. This concept was later taken over by the World Commission on Environment and Development, better known as the Bruntland Commission, which prepared a report in 1987 called "Our Common Future". The report emphasized a more politically acceptable idea of sustainable development than those promoted in the 1972 "Growth Limits", [5].

The concept of sustainable use and protection of natural values, and thus natural resources, is based on the strategy of spatial development and the national strategy of sustainable use of natural resources and goods. Strategies define the issue and level of research of natural resources and goods by types, spatial distribution, diversity, scope and quality. Also, balance sheet categories are determined, situation changes, valuation method and conditions of sustainable use are predicted, [6].

POSSIBLE NEGATIVE IMPACTS ON NATURE IN MINERAL RAW MATERIALS EXPLOITATION ZONE

The activities carried out during the exploitation of mineral raw materials, which are planned within the mining works, lead to a change in the existing natural state and appearance of the area where they are performed. For these reasons, it is extremely important to make detailed analysis of all works from the aspect of their potentially negative impact on the environment. The company engaged in the exploitation and processing of mineral raw materials has the obligation to adapt its work to modern devices and technological lines in order to minimize the negative impact on the environment, [7,8]. A modern approach to the exploitation of mineral resources must meet the criteria of sustainable use, in order to avoid uncontrolled exploitation and irreversible degradation of the natural ecosystem. During the techno-economic analysis for deposit opening, it is necessary, among other things, to pay attention on two important factors:

1. Economic effects of exploitation;
2. Environmental effects.

For the use of natural resources, the so-called waste-free technologies. Waste-free technologies for benefication of mineral raw materials in their exploitation imply complex utilization of all components from the ore and return by recycling to the process of production of the entire waste material. Furthermore, this technology implies the return to the production process of previously produced final products whose service life has expired, so they appear as waste. Along these lines, the total amount of waste material is reduced, and environmental pollution is scaled down to a minimum. On the Earth is less and less living space, clean air and water, which implies to two important facts, during designing the technology of exploitation of mineral goods: the selected technological line should takes up as little space on the earth's surface and it should have minimal environmental pollution effect.

Generally, it can be said that during the process of exploitation of mineral resources, both underground and surface, the negative impact on the environment can be classified into three groups:

1. Depletion of reserves;
2. Destruction of the natural environment;
3. Environmental pollution.

In areas of underground exploitation, environmental degradation is less noticeable, compared to places with surface exploitation, but it is present indeed. Namely, during underground exploitation, the terrain often subsides due to corridors that are below the surface of the earth, so this should be strictly taken into account. Also, in the vicinity of mines with underground exploitation, tailing dumps, mine facilities with bunkers, workshops and various warehouses, as well as facilities for human habitation, are located on the surface of the earth. Due to the effects of atmospheric precipitation and wind, erosion of the deposited tailings can occur. Acidic mine waters often appear, which can pollute the surrounding land, underground and surface watercourses. Of course, the intensity of each mentioned phenomena as well as the consequences of their action depends on the method of exploitation (surface or underground exploitation), as well as on the type of mineral raw material that is exploited (metals, non-metals, coal). Schematic representation of some of the described negative impacts on the environment during surface and underground exploitation of mineral raw materials are shown in Figure 1, [9].

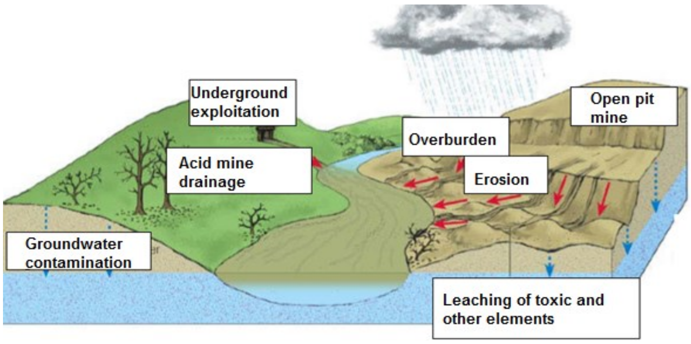

Figure 1 Negative impacts of mineral exploitation on the environment

USE OF NATURAL RESOURCES IN THE REPUBLIC OF SERBIA AND ENVIRONMENTAL PROTECTION

Our country also pays special attention to the protection of the living environment and the controlled use of natural resources. In 2012, the Government of the Republic of Serbia adopted the National Strategy for Sustainable Use of Natural Resources and Goods, which defines the framework for sustainable use and protection of natural values of the Republic of Serbia for coordinated, cross-sectoral management of natural resources, [10]. The Ministry in charge of environmental protection is responsible for the implementation of the Strategies. The goals of the National Strategy for Sustainable Use of Natural Resources and Goods are already largely integrated into the goals of multisectoral strategic documents: National Environmental Protection Program, National Environmental Approximation Strategy for the Republic of Serbia, Cleaner Production Strategy in the Republic of Serbia, Waste Management Strategy and the National Sustainable Development Strategy. The established basic goals of the National Strategy also fit into the goals of the Europe 2020 strategy document (COM (2010) 2020), in the segment of ensuring sustainable growth and providing conditions for less losses due to unsustainable use of natural resources. The main goals to be achieved by implementing this Strategy are:

1. Aiming and providing conditions for sustainable use of natural resources and goods, by creating a basis for setting plans, programs and bases for each individual natural resource or good (within this goal, 32 general sectoral goals are defined);
2. Reducing the negative impact of resource use on the economy and the environment, by establishing basic indicators to be monitored (26 general sectoral objectives);
3. Contribution to directing development towards sustainable production (through less and more efficient use of natural resources) and consumption (change of established consumption patterns) (10 general sectoral goals).

The strategy divides natural resources into 7 categories: mineral resources; renewable resources; forests and forest resources; protected areas, biodiversity, geodiversity and landscape diversity; fish resources; water resources and land resources. For each of these resources, the situation, the existing legal and institutional framework, challenges and goals for their sustainable use and measures for achieving their sustainable use are presented.

In order to better regulate the area of exploitation of mineral raw materials in the Republic of Serbia, an ecological permit for exploitation has been introduced. An environmental permit for a company who wants to engage in the exploitation of a specific mineral resource, at a specific location, aims to confirm the high level of protection that will be implemented, including the protection of water, air and land. There is also a fee for the use of mineral resources. For example, non-metallic mineral raw materials are widely used for the purpose of obtaining construction materials. Therefore, all companies engaged in their exploitation pay a fee for the use of non-metallic raw materials for the purpose of obtaining construction materials. The amount of compensation is determined by the Government of the Republic of Serbia and is clearly defined in a document called the Decree on the amount of compensation for the use of non-metallic mineral raw materials for obtaining construction materials, [11].

Today, the exploitation of mineral raw materials in our country and on a global level, as already mentioned, is increasingly focused on preserving the environment as one of the most important aspects of sustainable development. Having all this in mind, it can be concluded that the criteria for the acceptability of the exploitation activity are becoming stricter, considering its impact on the entire environment. The Republic of Serbia is keeping pace with world trends when it comes to mining practice by implementing measures that balance three important components, namely: economy-ecology-sociological component. The contribution of mining to sustainable development is rationality in the management of mineral resources as the only non-renewable resource. Rationality is implemented through complex planning of mineral resource complex management through strategic, [12]. The strategic document is a product of the development of the management strategy of the mineral complex and has the following three phases:

1. Analysis of the state of potential, reserves, exploitation and consumption of mineral raw materials;
2. Management strategy of the mineral resource complex of the Republic of Serbia in the next 20 years.

During the formation of the Strategy for the Management of the Mineral Resources Complex of the Republic of Serbia, the starting points of the first phase are: Geological potentials and geological reserves; Exploitation of mineral resources; Environmental protection and safety and health at work; Legal and Institutional Framework and the Education System. On the basis of a detailed situational analysis, i.e. analysis of the existing situation, a draft policy of exploitation of mineral raw materials is formed, which is further the framework for defining the Strategy of mineral resource complex management. This strategy has national character and is an integral part of the Economic Development Strategy of the Republic of Serbia. Within the third phase, it is necessary to constantly monitor the implementation of programs, measures and activities, as well as their innovation and updating.

While adopting legal regulations for the field of mining and exploitation of mineral raw materials, it is very important to analyze and compare with legal regulations for other natural resources in Serbia, such as water, forests and agricultural land. However, the fact that mineral raw materials are the only non-renewable natural resources whose location cannot be changed, should always be put in the foreground. Also, in practice, the interest in the exploitation of mineral raw materials most often conflicts with the rebuttable interests of the protection of these resources. Namely, there is an important difference between the legal regulations in the field of mining, which is mainly focused on the conduct of economic activity, mostly on its technical aspect, while the regulations of other related areas focus on resource management, resource protection, resource financing. and economic activity.

CONCLUSION

Necessary activities during the exploitation of mineral raw materials and environmental protection measures form one entirety, which is the only way to contribute to sustainable development. The existence of sustainable development only makes sense when a balance is reached between the use of natural resources on the one hand and nature conservation on the other. The success of a society in this area directly depends on the level of awareness of the population about the importance of a healthy environment and the preservation of natural balance and natural laws. People, as the main link in a complex system where the economy and ecology are closely connected, must always keep in mind the importance of preserving the environment, because they are also part of that environment. By preserving nature, they also preserve themselves in it, with the controlled use of all that nature has given them.

ACKNOWLEDGEMENT

The authors thank the Ministry of Education, Science and Technological Development of the Republic of Serbia for financial support of research (contract 451-03-9 / 2021-14 / 200023).

REFERENCES

1. Mihajlović, S., Blagojev, M. (2019) Eksploatacija prirodnih resursa u funkciji održivog razvoja. In: V naučno-stručni skup sa međunarodnim učešćem „Politehnika“. Beograd, Srbija. Zbornik radova, 188-192.
2. Mihajlović, S., Jovanović, V., Sekulić, Ž., Kašić, V. (2018) Principi održivog razvoja kao direktni faktori u zaštiti životne sredine. In: VI Savetovanje sa međunarodnim učešćem: „Zaštita životne sredine i održivi razvoj“, „Rudarstvo i energetika 2018“. Sremski Karlovci, Srbija, Zbornik radova, 59-63.
3. Štrbac, N., Vuković, M., Voza, D., Sokić, M. (2012) Održivi razvoj i zaštita životne sredine. Reciklaža i održivi razvoj, 5, 18-29.
4. Mladenović, M., Arsić Trajković, M., Mihajlović, M. (2017) Održivi razvoj i zaštita životne sredine. Ecologica, 86, 462-467.
5. Brundtland Report (1987), https://sustainabledevelopment.un.org/content/documents/5987our-common-future.pdf (Accessed on April 24th, 2020).
6. Ilić, B., Mihajlović, D., Omanović, A. (2016) Upravljanje prirodnim resursima i njihova održivost. In: VI Međunarodni simpozijum upravljanja prirodnim resursima, Zaječar, Srbija. Zbornik radova, 25-26.
7. Gligorijević, J., Kostić, M., Kostić, D. (2018) Zaštita životne sredine kao komponenta održivog razvoja sa osvrtom na značaj ekoloških indikatora. Ecologica, 89, 58-62.
8. Cvetanović, D., Nedić, V., Jovović, D. (2018) Regulativa u oblasti zaštite životne sredine, inovativnosti konkurentnost preduzeća. Ecologica, 90, 434-439.
9. http://vtsnis.edu.rs/wp-content/plugins/vts-predmeti/uploads/predavanje-2.pdf (Accessed on April 22nd, 2020).
10. http://www.rsjp.gov.rs/9.9_nacionalna_strategija_odrzivog_koriscenja_prirodnih_resursa_i_dobara.pdf (Accessed on April 20th, 2020).
11. https://www.mre.gov.rs/doc/geologija-rudarstvo/24_Uredba%20o%20visini%20naknade%20za%20koriscenje%20nemetalicnih%20mineralnih%20sirovina%20za%20dobijanje%20gradjevinskog%20materijala.pdf (Accessed on March 20th, 2020).
12. Pavlović, V., Kolonja, B., Ilić, M., Milanović, R. (2010) Održiva strategija upravljanja mineralno-sirovnskim kompleksom Republike Srbije. In: IX Međunarodna konferencija o površinskoj eksploataciji „OMC 2010“, Vrnjačka Banja, Srbija, Zbornik radova, 370-375.

XIV International Mineral Processing
and Recycling Conference
Belgrade, Serbia, 12-14 May 2021

INFLUENCE OF METALLURGICAL ACTIVITIES ON THE CONTENT OF MANGANESE, STRONTIUM AND CHROME IN CHICORY

Aleksandra Papludis, Maja Nujkić[#], Snežana Milić, Dragana Medić,
Slađana Alagić, Sonja Stanković
University of Belgrade, Technical Faculty in Bor, Bor, Serbia

ABSTRACT – The aim of this study was the influence of the Mining and Smelting complex Bor (current ZiJin Bor Copper) on the content of trace elements (manganese, strontium and chromium) in the soil and parts of chicory (Cichorium intybus L.). In order to assess the ability of chicory to accumulate trace elements, its phytoremediation abilities were determined using various biological factors such as: enrichment factor, bioconcentration factor and translocation factor. The phytostabilization condition was achieved for Mn and Sr, on the basis of which it can be concluded that chicory has a potential for phytostabilization of contaminated areas.

Keywords: Heavy Metals, Chicory, Biological Factors, Phytostabilization.

INTRODUCTION

Copper production represents the largest source of environmental pollution in Bor region, more than 100 years. Mine wastes, such as mine overburden, slags and flotation tailings, that were generated during the exploitation and processing of mineral raw materials, are mainly deposited on the Bor surrounding lands. These waste material contains toxic substances, heavy metal ions originating from raw materials and residual flotation reagents that can enter water, air, soil and pollute living organism, such as plant [1, 2].

Numerous plants (mainly herbaceous, weeds and woody) were tested for their potential use in existing phytoremediation procedures. Among the rare examples is the one related to the examination of phytoremediation potential of chicory (*Cichorium intybus* L.) which is known as herbaceous and weed plant.

The aim of this paper is to determine the content of trace elements (manganese, strontium and chromium) in the soil and plant parts of chicory (root and shoot) under real conditions of heavily polluted areas. The level of accumulation of trace elements in plant tissues and their translocation were assessed via several biological factors such as: bioconcentration factor (BCF), translocation factor (TF) and enrichment factor (EF), in order to determine the phytoremediation ability of the examined plant.

MATERIALS AND METHODS

Concentrations of tested trace elements (Mn, Sr and Cr) were determined in topsoil and chicory parts (root and shoot). Samples were collected from eight locations

---

[#] corresponding author: mnujkic@tfbor.bg.ac.rs

(Flotation tailing pond (FJ), Bolničko naselje (BN), Slatinsko naselje (SN), Naselje Sunce (NS), Oštrelj (O), Slatina (S), Dubašnica (D), Minićevo (M)), which are located at different distances from the ZiJin Bor Copper. Minićevo is an unpolluted area and 45 km from the city of Bor, which has choosen as control site. The preparation and mineralization of the samples and their analysis by inductively coupled plasma optical emission spectrometry (ICP-OES Optima 8300; Perkin Elmer, USA) were obtained as it was described by Nujkić et al. [3].

The obtained data were analyzed with the following factors: enrichment factor for the plant (EF_{plant}), bioconcentration (BCF) and translocation factor (TF). The phytoremediation abilities of chicory can be determined from the results of biological factors. Formulas for calculating EF, BCF and TF are given by Alagić et al. [4]. A value of enrichment factor EF>2 may indicate the level of enrichment and pollution of chicory. On the other hand, BCF and TF>1 indicate the potential of the plant species to be used in phytoextraction and BCF>1 and TF<1 suggest that the plant would be useful in phytostabilization of contaminated areas [5].

RESULTS AND DISCUSSION

Soil characteristics

Based on the obtained average pH values for all examined soil samples, which was 6.53, it can be concluded that the soil on the territory of the city of Bor and its surroundings belongs to the category of neutral or slightly alkaline soils. The obtained pH values for the soil at the sites closest to the industrial complex (FJ and BN) of 4.53 and 4.72 indicate that it is extremely acid soil.

The values of electrical conductivity are relatively low (227-446 µS/cm) and similar to the values of 200-800 µS/cm, which are necessary for normal growth and development of plants [6]. The percentage of organic matter in the soil samples ranged from 9% to 14.6%.

Trace elements in soil

The total concentrations of Mn, Sr and Cr in the soil are given in Table 1. The concentrations of Mn in the soil at almost all locations (FJ, BN, NS, O, D) exceed the toxic concentrations of Mn in the soil (300-500 mg/kg) according to Kastori [7].

Sr content is within the normal values of the examined soil of the city of Bor according to Kabata–Pendias and Pendias [8].

The obtained results indicate that the Cr content in the sampled soil was within the limits of the average value in the world (60 mg/kg) [9], except for two locations BN and D, where the values were above the MDK [10].

Trace elements in chicory parts

The content of Mn, Sr and Cr in the parts of the chicory, which were sampled from eight locations are given in Table 1. The toxic value of Mn depending on the plant species ranges from 300-500 mg/kg dry weight [7], while according to Nagajyoti et al.

[11] Mn normal concentrations in plant tissues can be from 15 to 100 mg/kg. The main symptoms of increased Mn concentrations are necrotic brown spots on the leaves and root decay [9]. Mn concentrations in chicory were in the range of normal values at all sites.

Table 1 Concentrations of Mn, Sr and Cr (mg/kg DW) in the soil and chicory parts and soil characteristics from the examined sites of the city of Bor

Sample site	**Total metal concentration (mg/kg)**			**Soil characteristics**		
	Mn	**Sr**	**Cr**	**pH**	**EC (µS)**	**OM (%)**
FJ	851	22.99	53.76	4.53	446	9.2
FJ$_R$	20.92	47.8	40.07			
FJ$_S$	4.85	29.25	28.14			
BN	642	119	65.28	4.72	217	12.4
BN$_R$	29.37	50.2	33.76			
BN$_S$	3.22	74.77	10.37			
SN	384	168	51.33	6.6	444	9.6
SN$_R$	3.55	28.23	10.69			
SN$_S$	5.36	53.86	4.097			
NS	569	277	43.89	6.97	446	9
NS$_R$	90.35	53.71	14.96			
NS$_S$	27.27	54.12	13.37			
O	572	63.98	34.43	6.93	342	9
O$_R$	7.58	20.91	10.44			
O$_S$	3.11	46.27	9.05			
S	189.1	83.71	17.33	7.92	383	12.2
S$_R$	16.18	16.86	34.2			
S$_S$	4.38	78.76	11.175			
D	1228.55	18.26	84.87	7.34	262	11.2
D$_R$	93.28	4.67	14.05			
D$_S$	29.23	3.11	12.81			
M	312.92	43.36	37.58	7.25	340	14.6
M$_R$	12.86	13.88	13.62			
M$_S$	7.82	23.11	10.53			

The maximum values of Sr were recorded in the chicory shoot at the sites S (78.76 mg/kg) and BN (74.77 mg/kg). Strontium is a radionuclide; therefore lower concentrations of this element may indicate a detrimental effect of the test area. The author Sarap [12] points to the fact that ^{90}Sr is an element that originates from nuclear tests and the Chernobyl disaster. Based on the obtained results it can be concluded that this element is still present in the environment of the Republic of Serbia.

The toxicity threshold for chromium is 1 to 2 mg/kg [13], while according to Alloway [14] it is 5 to 30 mg/kg. The obtained results show that Cr content in chicory is higher than the toxic values. Toxic effect is manifested through leaf chlorosis, slow plant growth and seed germination [15]. Increased Cr concentrations were recorded in chicory root at the locations FJ, BN and S, which are closest to the copper smelter and thus exposed to mining and metallurgical activities throughout the year [3]. Particles of Cr (PM_{10} and $PM_{2.5}$) arrive from metallurgical plants, which in this way contaminate the examined areas and beyond [16].

Biological factors

The specific ability of a plant to absorb metal ions from the soil and transport them to shoot can be determined with enrichment factor for the plant (EF_{plant}> 2). EF values for Mn, Sr and Cr in plant parts of chicory (root and shoot) at sites of urban-industrial, urban and rural zones (UI, U and R) are shown in Figure 1.

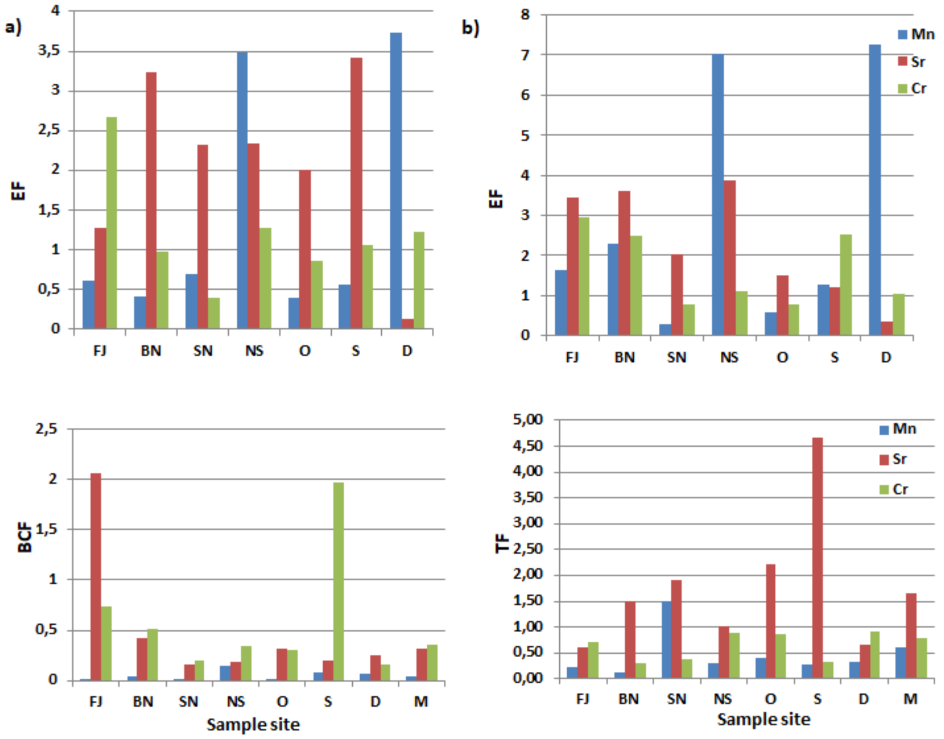

Figure 1 EF (a) root and b) shoot chicory), BCF and TF for Mn, Sr and Cr at the examined sites

The increased values of EF for Mn (EF_{plant}>2) are recorded at the following sites: BN (EF = 2.28 in chicory root), NS (EF = 7.03 in chicory root and EF = 3.49 in chicory shoot) and D (EF = 7.25 in chicory root and EF = 3.74 in chicory shoot).

For Sr, the values of EF greater than 2 were detected at the following sites: FJ (EF = 3.44 in chicory root), BN (EF = 3.62 in chicory root and EF = 3.24 in chicory shoot), SN (EF = 2.03 in chicory root and EF = 2.33 in chicory shoot), NS (EF = 3.87 in chicory root and EF = 2.34 in chicory shoot) and S (EF = 3.43 in chicory shoot).

At some sites, EF values for Cr were below 2, except at three locations in the UI and R zone, such as: FJ (EF = 2.94 in chicory root and EF = 2.67 in chicory shoot), BN (EF = 2.48 in chicory root) and S (EF = 2.51 in chicory root).

Finally, the EF values for Mn and Sr, and in some cases for Cr, indicate the enrichment of all parts of chicory with these elements. Therefore, chicory has good accumulation abilities, because it adopts high concentrations of investigated elements, without visible damages to aboveground parts.

Bioconcentration and translocation factor can be used in assessing the potential of plant species for its use in phytoremediation. The obtained BCF values for Mn in chicory at all examined sites were less than 1, while the TF value was higher than 1 only at the SN location (1.51).

In the case of Sr, the BCF value was higher than 1 only at the FJ location (2.07), while the TF values were higher than 1 at almost all examined sites, except at the FJ and D sites. The values of both BCF and TF for Cr were less than 1 at all investigated sites except for BCF at site S (1.97).

Based on the obtained values of biological factors, it can be concluded that the chicory cannot be used for phytoextraction, but can be applied in phytostabilization of soils which were contaminated with Mn and Sr.

CONCLUSION

Based on the obtained values of biological factors for chicory, both phytoextraction conditions were not met, for any of the analyzed metals. But, the phytostabilization condition for Mn was achieved at the SN site, while the same condition for Sr was achieved at all examined sites, except at the FJ and D sites. Based on the previous, it can be concluded that chicory may be considered as a suitable herb for phytostabilization of Mn and Sr contaminated areas. The obtained results showed that this plant species has the ability to activate defense mechanisms for protection against affect of pollutants, which allows it to develop and grow in adverse conditions. Also, the obtained results for Sr can contribute to the adoption of the Regulations by Republic of Serbia for MAC in soil and medicinal plants, because in our country there is no legislation when it comes to Sr.

ACKNOWLEDGEMENTS

The research presented in this paper was done with the financial support of the Ministry of Education, Science and Technological Development of the Republic of Serbia, within the funding of the scientific research work at the University of Belgrade, Technical Faculty in Bor, according to the contract with registration number 451-03-68/2020-14/ 200131.

REFERENCES

1. Šerbula, S., Stanković, V., Živković, D., Kamberović, Ž., Gorgievski, M., Kalinović, T. (2016) Characteristics of Wastewater Streams Within the Bor Copper Mine and Their Influence on Pollution of the Timok River, Serbia. Mine Water and the Environment, 35(4), 480–485.
2. Panias, D. (2006) Consequences of environmental issues on sustainability of metal

industries in Europe: the case study of Bor. Metalurgija, 12(4), 239–250.

3. Nujkić, M. M., Dimitrijević, M. M., Alagić, S.Č., Tošić, S.B., Petrović, J. V. (2016) Impact of metallurgical activities on the content of trace elements in the spatial soil and plant parts of Rubus fruticosus L. Environmental Science: Processes & Impacts, 18, 350–360.
4. Alagić, S. Č., Tošić, S. B., Dimitrijević, M. D., Antonijević, M. M., Nujkić, M. M. (2014) Assessment of the quality of polluted areas based on the content of heavy metals in different organs of the grapevine (Vitis vinifera) cv Tamjanika. Environmental Science and Pollution Research, 22(9), 7155–7175.
5. Yoon, J., Cao, X., Zhou, Q., Ma, L. Q. (2006) Accumulation of Pb, Cu, and Zn in native plants growing on a contaminated Florida site. Science of the Total Environment, 368, 456–464.
6. Sadhu, K., Adhikari, K., Gangopadhyay, A. (2012) Effect of mine spoil on native soil of Lower Gondwana coal fields: Raniganj coal mines areas, India. International Journal of Environmental Science and Technology, 2, 1675–1687.
7. Kastori, R., Petrović, N. (1993) Teški metali i pesticidi u zemljištima Vojvodine. Poljoprivredni fakultet, Institut za ratarstvo i povrtarstvo, Novi Sad, 113–125.
8. Kabata–Pendias, A. and Pandias, H. (2001) Trace Elements in Soils and Plants. third Edition, CRC Press, LLC, Boca Raton, Florida
9. Kabata-Pendias, A. (2011) Trace elements in soils and plants. fourth edition, CRC Press. Taylor and Francis Group, LLC, Boca Raton, London, New York
10. Službeni glasnik Republike Srbije br. 23/94, 11/92 i 32/2002.
11. Nagajyoti, P. C., Lee, K. D., Sreekanth, T. V. M. (2010) Heavy metals, occurrence and toxicity for plants: A review. Environmental Chemistry Letters, 8(3), 199–216.
12. Sarap, N. (2017) Praćenje distribucije radionuklida ^{90}Sr u poljoprivrednom zemljištu i biljnim kulturama metodom spektrometrije beta zračenja. Doktorska disertacija, Univerzitet u Beogradu
13. Vamerali, T., Bandiera, M., Mosca, G. (2010) Field crops for phytoremediation of metal-contaminated land, A review. Environmental Chemistry Letters, 8, 1–17.
14. Alloway, B. (2013) Heavy metals in soils: Trace metals and metalloids in soils and their bioavailability. Environmental Pollution (22), third edition, Springer New York
15. Jakšić, S., Vučković, S., Vasiljević, S., Grahovac, N., Popović, V., Šunjka, D., Dozet, G. (2013) Akumulacija teških metala u Medicago sativa L. i Trifolium pratense L. na kontaminiranom fluvisolu. Hemijska industrija, 67(1), 95–101.
16. Dimitrijević, M.D., Nujkić, M.M., Alagić, S.Č., Milić, S., Tošić, S.B., (2016) Heavy metal contamination of topsoil and parts of peach-tree growing at different distances from a smelting complex. International Journal of Environmental Science and Technology, 13, 615–630.

DEGRADED AREAS RECULTIVATION ON LOCATION OF OPEN PIT ZAGRAĐE 5

Miomir Mikić[#], Sandra Milutinović, Miroslav Ilić, Ivan Jelić, Miloš Ilić
Mining and Metallurgy Institute Bor, Serbia

ABSTRACT – In order to protect the environment and improve the landscape, the degraded areas created by the exploitation of limestone at the open pit Zagrađe 5, will be recultivated. The goal of recultivation is to "return" in some form, through the projected activities, what was previously borrowed from nature through exploitation. Recultivation will take place according to the following phases of recultivation: technical, agrotechnical, and biological phase. In this way, i.e. by applying biological recultivation, seedlings of black ash, hornbeam and lilac are planned. The alternating combination of these plant species enables the binding of the substrate and gives a beautiful aesthetic appearance to the environment.

Keywords: Environment, Recultivation, Exploitation.

INTRODUCTION

The limestone deposit of Zagrađe is located 12 km east of Bor. The exploitation of limestone in the area of Zagrađe began in 1962 and took place in open pits 1, 2, 3, 4, and currently only the open pit Zagrađe 5 is active, which was opened in 1970.

The main goal of obtaining limestone is the production of baked lime in lime kilns for the needs of flotation in Bor and Veliki Krivelj in order to regulate the pH value during the flotation of copper ore. In addition to industrial lime, the lime plant produces hydrated ground lime for construction and gravel. When crushing limestone, smaller fractions are obtained than needed for lime kilns. During the firing of limestone, lime filler was obtained as waste, which is used in agriculture to repair the pH value of the soil.

The location of Zagrađe is located in the area between the village of Slatine (west), the village of Rgotina in the east and the village of Donja Bela Reka (in the north) (figure 1). The area where the open pit and Krečana Zagrađe are located is sparsely populated. There are small huts, which have been abandoned, because their owners have houses in the surrounding villages for permanent residence. The access road to the Zagrađe limestone plant (K + 220 m) is separated from the regional asphalt road Bor - Majdanpek at K + 195 m (road 166).

The surface mine Zagrađe 5. is located 2.5 km from the lime production plant in Zagrađe and is located at about K+410 m. During the exploitation of limestone, barren material was obtained, which is disposed of to the east in relation to the surface mine, at the existing tailings dump.

The lime production plant is located at K + 220 m above sea level. The access road to the Zagrađe plant is separated at K + 195 m from the asphalt road Bor - Majdanpek.

[#] corresponding author: miomir.mikic@irmbor.co.rs

Figure 1 Location of the mining complex Zagrađe

DEGRADED SURFACES

A discontinuous exploitation system will be applied at the open pit Zagrađe 5. Exploitation of limestone at the open pit Zagrađe 5 implies degradation of the surrounding land during the formation of the projected contours of the open pit.

The existing location east of the Zagrađe-5 mine was chosen for the disposal of tailings obtained during the exploitation of limestone (Figure 2). The soil material obtained by expanding the open pit in the southeastern part will be deposited at a new location, landfill placed south of the open pit Zagrađe-5 (Figure 2). Also, before the advance of the tailings dump continues, the existing quantities of soil material will be moved from the current location to the new location of the soil landfill.

This is important because the soil material can later be used as a final layer when performing biological recultivation of degraded areas.

The total area that has been degraded is 241370 m^2. The projected tailings dump occupied an area of 54.370 m^2, and the projected area of open pit is 187.000 m^2.

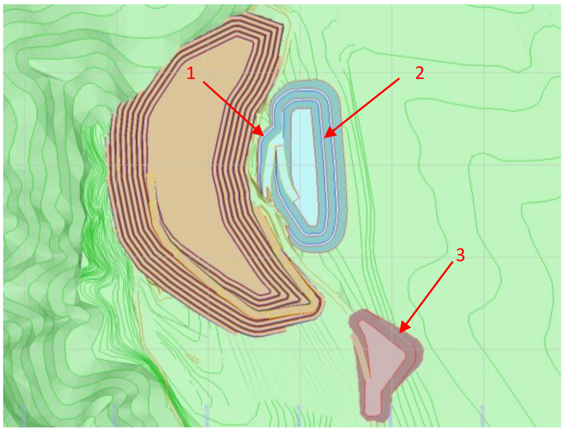

Figure 2 Spatial layout of facilities: open pit (1), tailings dumps (2) and landfill of soil material (3)

CHOICE OF RECULTIVATION METHOD

The main goal of recultivation of physically, chemically and biologically damaged soils is to establish the function of land management, as a resource that is disturbed by anthropogenic activities.

The goal of recultivation is to "return" in some form, through the activities envisaged by the recultivation project, what was previously borrowed from nature through exploitation.

The share of nutrients in the substrate of surface digging and tailings at the dump is insufficient for normal plant development and in order to quickly green the degraded areas created by surface exploitation of limestone and tailings dump, the soil material should be used for biological recultivation. In the world and in Serbia, three categories of recultivation are used. For recultivation in Zagrađe, recultivation with afforestation and grassing methods is proposed. Recultivation works take place in the following phases of recultivation:

1. Technical phase of recultivation,
2. Agrotechnical phase of recultivation,
3. Biological phase of recultivation.

TECHNICAL PHASE OF RECULTIVATION

The technical phase of recultivation at the tailings dump at PK Zagrađe 5. represents the stage of preparatory works (subsequent leveling of the dump final plane), which enable the implementation of agro-technical and biological recultivation. Subsequent planning or leveling of the dump final plane is done with a bulldozer before the start of recultivation. During the final process of disposal of the last excavated piles of tailings on the final level, due to the stability of the landfill, they are not leveled (the piles do not allow the formation of ponds and lakes during atmospheric precipitation and infiltration of water in the landfill body).

The next stage involves the application of soil material. Earth material will be used for:

- formation of a 0.5 m high layer on a dump final plane;
- filling pits when planting seedlings;
- formation of a 0.5 m height layer at the bottom of the open pit;
- application of a 0.25m height layer at the dump slopes and benches.

The introduction of organic matter in the form of humus into the substrate accelerates the microbiological process and enables a continuous influx of assimilators for plant development. The technical phase of recultivation includes loading soil from the soil landfill, transport and planning on the final level of the tailings dump K + 420m and the lowest benches ie. bottom of the open pit K + 335 m. Also, the soil will be transport from location of soil landfill to all benches of open pit.

The agrotechnical phase of recultivation includes leveling and planning of the soil layer along the tailings dump final plane, slopes and benches and the bottom of the open pit and the phase of drilling and blasting in order to form (excavate) pits (funnels) for seedlings on the benches of the open pit. In order to optimize the works, the works of the agro-technical and technical phase are supplemented, and thus the maximum utilization of machines and shortening of the time of completion of works are obtained.

AGROTECHNICAL RECULTIVATION

The agrotechnical phase of recultivation includes leveling and planning of the soil layer along the tailings dump final plane, slopes and benches and the bottom of the open pit and the phase of drilling and blasting in order to form (excavate) pits (funnels) for seedlings on the benches of the open pit. In order to optimize the works, the works of the agro-technical and technical phase are supplemented, and thus the maximum utilization of machines and shortening of the time of completion of works are obtained.

BIOLOGICAL PHASE OF RECULTIVATION

The biological phase of recultivation implies a complex of biotechnical and phytomeliorative measures for growing grass and forest crops on the prepared surfaces of open pit and tailings dump in order to green and restore ecosystems.

The most effective measures to prevent erosion and improve the stability of the landfill is afforestation [1]. Development of seedlings comes into a better binding of substrate in the landfill, thus preventing erosion and also raising dust from the landfill through the wind [1]. Seedlings with crowns and green leaves prevent drying, whereby micro-climatic conditions become more favorable. Falling of leaves in autumn and their retention in the denuded areas and rotting over the winter, create conditions for formation of humus and opportunities of auto-recultivation and occurrence of terrestrial flora.

The biological phase of recultivation includes the following works:

- On the final plane of the tailings dump, grassing and afforestation according to the mosaic arrangement of crops;
- On the slopes and floors of the tailings dump, grassing and afforestation according to a triangular pattern;
- At the open pit bottom, grassing and afforestation according to the mosaic arrangement of crops;
- Afforestation on the benches surfaces of the open pit.

The final level of the tailings dump for the purpose of landscaping is filled with a 50 cm height layer of humus. After that, the grassing of this area will be done. Planting of plant crops: black ash, lilac and hornbeam will be done according to the mosaic schedule.

Along the perimeter of the outer slope of the landfill, soil material is poured in a layer of 0.25 m. The slope is grassed. After that, a protective belt of lilac, hornbeam and black ash is formed.

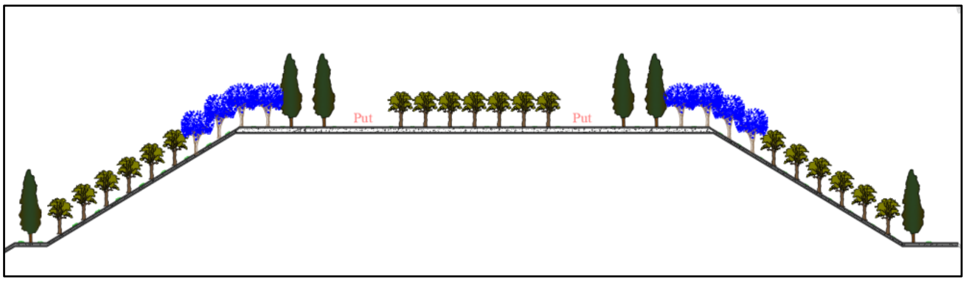

Figure 3 Cross-section of landfills with crops

On the slope of the landfill (405/390), in horizontal rows according to the triangular pattern, black ash is planted in round pits with a diameter of 40 cm and a depth of 40 cm at the landfill benches, and on the slopes horbeam seedlings and at the top of the slope lilac.

Black ash will be planted on the open pit benches, in horizontal rows as shown in Figure 4. The open pit bottom will be worked in several phases. First, a layer of soil material in the height of 0.5 m will be applied. After that, the entire surface will be grassed. Planting culture: black ash, hornbeam and lilac is planned to be done according to a mosaic arrangement (Figure 4).

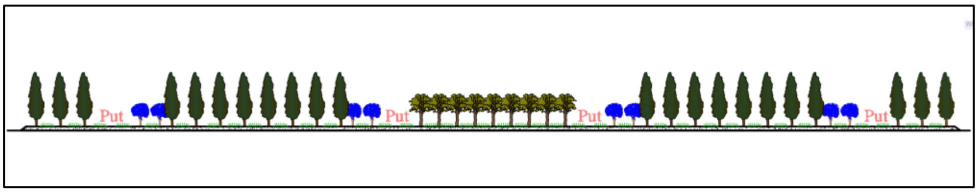

Figure 4 Cross- section of open pit bottom with crops

SELECTION OF SEEDLINGS

It was concluded for the biological stage of recultivation the degraded areas that it is best to apply the species growing in natural conditions in the same or similar fields in Serbia, and they are: lilac, hornbeam and black ash.

Number of plants per hectare is 1100 of black ash and lilac and hornbeam of 2,000 seedlings per hectare respectively.

SELECTION OF GRASS-LEGUMINOUS MIXTURE

The grass mixtures should be used to raise the grass areas, as follows: white clover.• yellow star, cat's tail, real meadows. The required amount of grass-leguminous mixtures for planting the predicted area is 25 kg/ha.

The following properties were taken into consideration in selection the above given grass-leguminous mixture to raise the lawn: resistance to the specific environmental conditions, tolerance to the climatic conditions, prevalence, ground cover, binding capacity of the substrate, etc.

CONCLUSION

The effects of recultivation of degraded areas are reflected in the fact that:

- Forest plantations enable better binding of the soil, stimulate the development of ground flora, activate pedological processes in the substrate by the root system, prevent insolation and drying of the soil, blowing strong winds and raising dust.
- The application of grass cover on the final planes aims to prevent the erosion of humus (soil) applied in a layer 50 cm high and to enable the creation of grass surfaces that could be used for recreational purposes.

- Afforestation of degraded areas contributes to environmental protection, improvement of the microclimate and aesthetic appearance of the environment.

ACKNOWLEDGEMENT

This work was financially supported by the Ministry of Education, Science and Technological Development of the Republic of Serbia, Grant No. 451-03-9/2021-14/ 200052.

REFERENCE

1. Mikić, M., Petrović, S., Jovanović, I., Rajković, R. (2016) Recultivation the inner landfill of the coal open pit Cementara in Pljevlja, Montenegro. 48th International october conference on mining and metallurgy. Universitet of Belgrade Technical Faculty Bor. Bor, Serbia. ISSN / ISBN 978-86-6305-047-1. DOI 226011916. pp. 285-288.

REMEDIATION AND RECLAMATION OF DEGRADED AREA IN THE SOUTH-EASTERN PART OF THE MARLSTONE QUARRY “TREŠNJA”

Stefan Krstić[#], Marinko Pavlović, Nikola Đokić, Taras Kulyk
Moravacem Ltd, Popovac, Serbia

ABSTRACT – Before privatization of the cement plant in Novi Popovac, due to bad mining operational plan, big area in south-eastern part of the marlstone quarry was degraded. This paper will describe remediation and reclamation of degraded area in this part of the quarry.

Keywords: Remediation, Reclamation, Degraded Area.

INTRODUCTION

In the south-eastern part of the deposit of the “Trešnja” marl mine, there are currently inactive floors that were previously unplanned exploited for many years. Due to the quality requirements of the mixture and targets related to the emission of harmful gases, this part of the marl mine is not exploited due to the high content of harmful components.

As such, the degraded areas in this part of the mine are intended for tailings disposal and reclamation of these areas. Degraded areas amount to about 5.1 ha, and the total volume of disposed tailings is about 50,000 m^3.

Tailings were disposed of in accordance with the project, where tailings disposal, technical, agro-technical and biological reclamation are envisaged.

Also, the areas themselves are maintained according to the project, mowing the tailings, maintenance of seedlings, watering, fertilizing, replacement of dried and planting new ones. On these areas, in the part of biological reclamation, cherry seedlings were also planted, as a symbol of the eponymous marl surface mine.

EXPERIMENTAL

For the selection of species for afforestation, care was taken to adapt them to the conditions of the substrate, climate, good reception during planting and resistance to the action of basic natural factors. A pioneer species was chosen - acacia, which has so far given good results in reclamation on degraded areas with unfavorable conditions.

Acacia will be planted on flat and sloping surfaces, which corresponds to the placement of a square or triangular network of pits with a distance of 2.24 m (Figure 1). Acacia as a pioneer species is very adaptable to shallow rocky, dry habitats, is well received when planting, successfully withstands drought, frost, wind, stabilizes slopes and at the same time repairs the soil.

[#] corresponding author: stefan.krstic@moravacem.rs

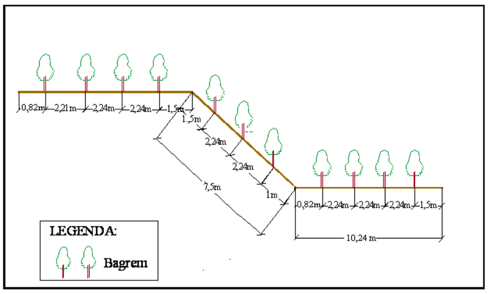

Figure 1 Surface mine profile showing planted crops

Due to its ability to develop a large number of surface veins, it binds the soil on which it is located very well.

Surface veins can reach a length of up to 20 m, and due to its shoot abilities, a new plant can grow from the roots at that distance from the parent plant. Since it belongs to the Fabacene family, it binds biosphere N (nitrogen) to the soil and thus enriches it.

RESULTS AND DISCUSSION

Location, size and shape of tailings

The tailings are located in the souyh-eastern part of the surface marl mine. It extends in a northwest-southeast direction on the mentioned part of the mine. It covers a part of inactive floors that are at elevations +221, +228 and +235. It is about 500 m long and 150 m wide. It occupies an area of about 5.1 ha, and the volume of disposed tailings is about 50,000 m^3. (Figure 2)

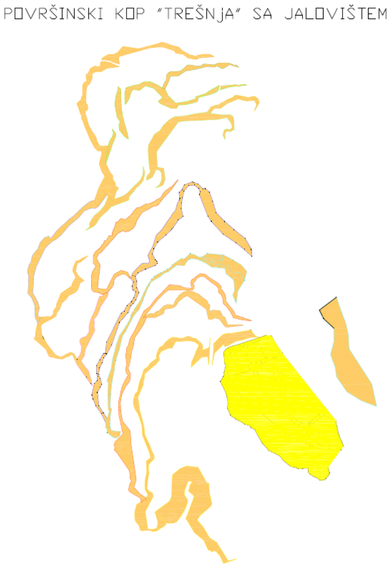

Figure 2 Surface mine of marl "Trešnja" with tailings

Tailings disposal

The disposal of tailings was performed on several occasions, depending on the excavation positions on the active floors in the marl mine and the removal of the humus layer, which was later deposited on the mentioned tailings. Also, marl which does not meet the quality targets and which due to physical-mechanical characteristics and moisture cannot be crushed through the crushing plant is also deposited on site as tailings. Loading and transport of tailings is performed by the existing mechanization in the marl mine, hydraulic excavator CAT 5080 and dump trucks CAT 773E. Leveling and tailings planning is done with a CAT D9R bulldozer and a CAT 12H grader.

Recycling of tailings

Reclamation consisted of three phases: technical, agrotechnical and biological.

1. Agro-technical reclamation

Technical reclamation included anti-erosive works - construction of channels for drainage of atmospheric water, mitigation of slopes of floors, preparation of plateaus for access of dumpers and disposal of tailings. The construction of the canal and the work on the preparation of the plateau was done by mechanization of surface mines.

2. Technical reclamation

This phase of reclamation includes leveling of tailings, loading, transport of humus and application of humus. The total area for reclamation was 48,525 m^2.

Table 1 shows the dynamics of works on technical reclamation.

Table 1 Technical reclamation dynamics

Year	Equipment working hours, h				Price for equipment €/h	Buldozer working hours €	Total cost €
2016-2018	Buldozer	excavator	Dump truck	Total			
	4	20	27	51	170	11,330	20,000

3. Biological reclamation

In order to protect the environment, the method of grassing the surfaces and plantations of corporate forest tree species was chosen: hornbeam, oak, ash, linden and cherry.

The grass-legume mixture was chosen for grassing, depending on the altitude and the quality of the substrate. For grassing areas on tailings, the following were adopted: true meadow grower (8kg) 14.8%, tall screw (20kg) 37.0%, red screw (20kg) 37.0%, white clover (6kg) 11.2% in total kg) 100%. This mixture has the property of binding the substrate and its protection from water and aeolian erosion.

Grassing works are: manual cross-sowing of grass mixtures in a given ratio, sowing depth ranged between 1-1.5 cm, rolling of sown areas, fertilization of sown areas with

NPK (15:15:15) and fertilization (watering) of sown areas until the grass sprouts and then depending on the meteorological conditions.

Table 2 shows the dynamics of work on biological reclamation.

Table 2 Biological reclamation dynamics

Year	Area ha	Amount of grass needed, kg	Price for grass €/kg	Amount of fertilizer kg	Price for fertilizer €/kg	Work days			Maintaining €	Work day price €	Total cost €
						Sowing	Fertilizing	Total			
2019	5.1	262	5	970	0.3	102	35	137	2,000	30	7,711

Tailings reclamation works are shown in Figure 3.

Figure 3 Works on recultivation of "Trešnja" tailings

The last phase of works was done in 2019: planting of new seedlings, replacement of dried ones, fertilization, watering and mowing.

CONCLUSION

Due to the quality of marl, ie the content of unfavorable components for the cement industry, such as pyritic sulfur and magnesium, it is not possible to continue exploitation in this part of the surface mine, an excellent opportunity to use these surfaces for tailings disposal. The project clearly defines the area and volume of tailings that will be disposed of here, where in the end comes the technical agro-technical and biological reclamation.

The research of marl and limestone deposits, the development of a 3D block model, and the implementation of a software package (AthosGEO Blend) in the field of raw materials management, enables optimal design of the raw mix from the aspect of environmental protection. Taking into account the reduction of emissions (by limiting pyritic sulfur, TOC and VOC from marl), tailings are excluded during the exploitation of marl, except humus. This creates a favorable environment for the remediation and reclamation of tailings.

The goal of tailings reclamation is to protect the environment.

Measures of agro-technical reclamation have contributed to the improvement of resistant and deformable characteristics of tailings, which directly affect the increase of erosion stability of slopes.

Technical measures, together with agro-technical ones, contribute to faster achievement and maintenance of permanent stability of tailings.

Biological measures contribute to the stability and maintenance of reclaimed areas, but are much more important from the aspect of spatial revitalization and establishment of natural biocenoses. In biological reclamation, the choice of tree species is based on the existing pedological, hydrological and climatic conditions, having in mind the original species of natural habitat of the locality.

The total cost of reclamation is € 30,000 (work dynamics 3 years).

REFERENCES

1. MMI Bor, (2014) Technical mining project of recultivation of the degraded area of marl quarry “Trešnja“.
2. Pavlović, M., (2014) Sanation and recultivation of marl quarry „Trešnja“ tailings pond as contribution to sustainable development Holcim (Serbia) Ltd. In: Recycling technologies and sustainable development. Zaječar, Serbia

XIV International Mineral Processing
and Recycling Conference
Belgrade, Serbia, 12-14 May 2021

THERMOELECTIC MATERIALS APPLICATION AND THEIR CONTRIBUTION TO PROVIDING CLEANER ENERGY

Emina Požega[1#], Danijela Simonović[1], Saša Marjanović[2], Milenko Jovanović[1], Zdenka Stanojević Šimšić[1], Slađana Krstić[1], Miomir Mikić[1]
[1] Mining and Metallurgy Institute Bor, Bor, Serbia
[2] University of Belgrade, Technical Faculty in Bor, Bor, Serbia

ABSTRACT – The $Bi_2Te_{2.88}Se_{0.12}$ single crystal was grown using the Czochralski technique. Hall and Van der Pauw method were used for the monocrystal characterization. Mobility and concentration of charge bearers majority and Hall coefficient of single crystal were determined. For the sample of BiTe doped with selenium Hall effect was measured at room temperature with an applied magnetic field strength of 0.37 T at different current intensities. The Hall coefficient value is negative, which shows that the samples are n type and that the charge carriers majority are electrons. The fact that the samples are n type was also confirmed by the hot point method.

Keywords: Czochralski Technique, Hall and Van der Pauw Method, Doping.

INTRODUCTION

Thermoelectric materials have unique dual capability of directly converting heat into electricity or electrical power into cooling or heating. They receiving increasing attention due to their potential to make important contributions to the effort on reducing CO_2 and greenhouse gas emission and providing cleaner forms of energy [1,2]. The best known commercially used thermoelectric material (TE) in the bulk form for cooling and power generation applications at ambient temperature is bismuth telluride (Bi_2Te_3), including p-type $Bi_xSb_{2-x}Te_3$ and n-type Bi_2Te_3-ySey [3]. The Bi_2Te_3 based single crystal bulks have the lamellar structure and the weak Van der Waals bonding between Te(1)-Te(1), which is responsible for the easy cleavage along the planes perpendicular to the c-axis. Because this unique structural anisotropy, thermoelectric properties of n-type Bi_2Te_3-*y*Se*y* single crystal solid solutions prepared by traveling heater method shows strong anisotropy. The electrical and thermal conductivities along the cleavage planes (perpendicular to the *c*-axis) are about four and two times larger than those along the *c*-axis, respectively.

Hall effect measurements are important to semiconductor material characterization. From the Hall voltage, the conductivity type, carrier density, and mobility can be derived. With an applied magnetic field, the Hall voltage can be measured.

The Van der Pauw method was first propounded by Leo J. van der Pauw in 1958 [4,5]. This technique commonly used to measure the Hall coefficient of a sample and the resistivity. This method employs a four-point probe placed around the perimeter of the sample. This allows the van der Pauw method to provide an average resistivity of the

---

[#] corresponding author: emina.pozega@irmbor.co.rs sample. From the measurements made, the resistivity of the material, the doping type, the number of majority carriers per unit area and the mobility of the material majority carrier can be calculated. The measurements require that four ohmic contacts be placed on the sample. Sample thickness must be much less than the width and length. Symmetrical of the sample reduce errors in the calculations.

In this paper we report results for $Bi_2Te_{2.88}Se_{0.12}$ single crystal obtained by Hall and Van der Pauw method.

EXPERIMENTAL METHOD

Hall-based measurements were performed on an Ecopia device, HMS-3000. The Hall Effect Measurement System HMS-3000, manufactured by Ecopia, is designed to measure the concentration of charge carriers, mobility, specific resistance and Hall coefficient, with the aim of enabling easier and simpler observation of the semiconductor samples electrical characteristics.

Ecopia HMS-3000 set (Figure 1) consists of an adjustable constant current source, software part system, low temperature measurement system and a source of magnetic flux density in the form of a permanent magnet (magnetic set). The system for measuring at different temperatures and the source of magnetic flux density in the form of a permanent magnet (Figure 1 b) physically represent one whole, which has, in addition to the stated roles, also the task of the input part of the whole system (main role).

Figure 1 Ecopia HMS-3000 set

An important property of this measurement system is that different data can be calculated and displayed automatically at once (graphically and tabular), after the measurement has been performed on a material single sample. The data obtained after the measurement are: surface carrier concentration, mobility, specific resistance, conductivity, Hall coefficient, magnetic resistance (occurrence of resistance change when the sample is exposed to a magnetic field), alpha (horizontal / vertical resistance ratio), etc., as well as a graphical representation of voltage dependence and current resistance (U-I, R-I graphs).

RESULTS AND DISCUSSION

The samples tested by the Hall and Van der Pauw method were cut from different parts of the ingot normally to the crystallization direction (⊥). In the following, these samples will be referred to as 1/5 (⊥) and 2/2 (⊥), respectively.

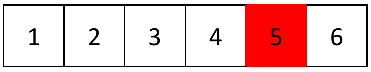

1	2	3	4	5	6

Figure 2 Schematic representation of the location from which the 1/5 (⊥) sample was cut from the ingot

The sample 1/5 (⊥) of circular cross-section is 2.05 mm thick. On Figure 2 the crystal growth beginning is the location one.

Before the measurement starting, it is necessary to prepare the samples and connect them to the PCB holders. The samples on which the measurements were performed had a uniform thickness and did not have any irregularities on them. They prepared to be in the form of thin disc (Figure 4) cut perpendicular to the long axis of a single crystal ingot. All samples were carefully inspected for cavities and scratches and polished if necessary. All measurements were carried out at room temperature (T=300 K). The source of magnetic field applied perpendicular to the Hall element was a permanent magnet of 0.37 T. Hall effect measurements were done to obtain transport properties.

For resistance measure, voltage and current contacts were attached to 4 fixed contact terminals located at the sample ends and at different current intensities. Schottky contacts were used for tests performed at room temperature. The change of transport and electrical parameters with increasing current intensity was also monitored.

Table 1 The results of the Hall and Van der Pauw method for the sample 1/5 (⊥)

Current intesity I [mA]	Bulk carrier concentration n_b [/cm^3]	Sheet carrier concentration n_S [/cm^2]	Mobility μ [cm^2/Vs]	Average Hall coefficient R_H [cm^3/C]
0.1	-1.010x10^{18}	-2.070 x10^{17}	6.698x10^{2}	-6.180 x10^{0}
0.5	8.546x10^{18}	1.752x10^{18}	2.892x10^{2}	7.304x10^{-1}
1	-7.684x10^{18}	-1.576x10^{18}	2.517x10^{2}	-8.124x10^{-1}
5	-2.268x10^{19}	-4.650 x10^{18}	1.356x10^{2}	-2.752 x10^{-1}

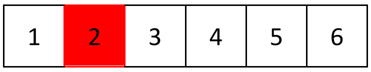

1	2	3	4	5	6

Figure 3 Schematic representation of the location from which the 2/2 (⊥) sample was cut from the ingot

The sample 2/2 (⊥) of circular cross-section is 1.9 mm thick.

Table 2 The results of the Hall and Van der Pauw method for the sample 2/2 (⊥)

Current intesity I [mA]	Bulk carrier concentration n_b [/cm^3]	Sheet carrier concentration n_S [/cm^2]	Mobility μ [cm^2/Vs]	Average Hall coefficient R_H [cm^3/C]
0.1	7.828×10^{17}	1.487×10^{17}	1.082×10^{3}	7.974×10^{0}
0.5	-2.525×10^{18}	-4.797×10^{17}	6.982×10^{2}	-2.472×10^{0}
1	-3.659×10^{19}	-6.951×10^{18}	5.810×10^{1}	-1.706×10^{-1}
5	-1.050×10^{19}	-1.996×10^{18}	2.238×10^{2}	-5.943×10^{-1}

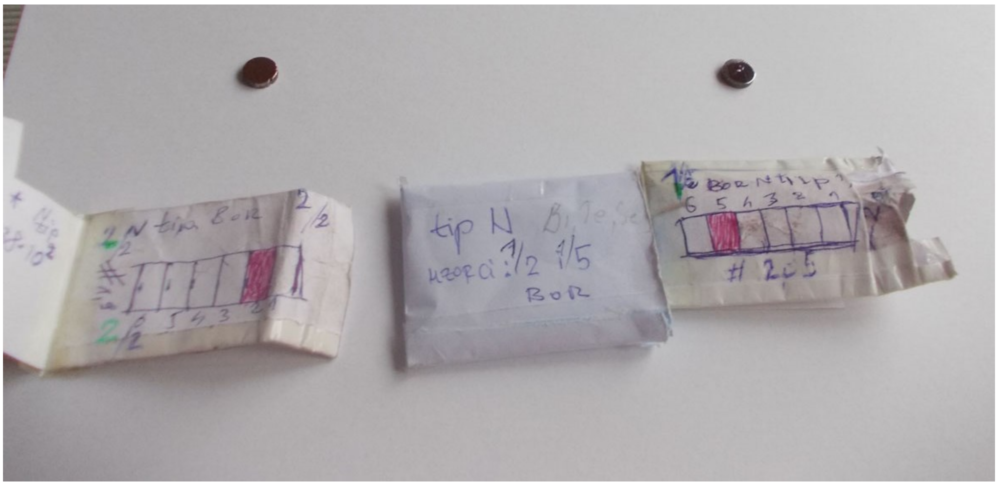

Figure 4 Cross-sectional view of a circular samples 1/5 (⊥) and 2/2 (⊥), cut from the ingot

The calculated data from the measurement results of the transport quantities for samples 1/5 (⊥) and 2/2 (⊥) with a Schottky diode at room temperature (25 °C) and magnetic induction of the permanent magnet B = 0.370 T are given in Tables 1 and 2. Measurements were performed at currents of: 0.1; 0.5; 1; and 5 mA. The concentration of the carrier charge increases with increasing current for both samples and ranges from 1017 to 1019 cm^{-3}. The power factor is related to the concentration of the carrier charge and is maximized by nb~1020 cm^{-3} in semiconductors [6,7]. The Hall coefficient values are negative except for the sample 1/5 (⊥) at a current of 0.5 mA and for the sample 2/2 (⊥) at a current of 0.1 mA. This indicates that the samples are of n type and that the charge carriers majority are electrons. That the samples are of n type was also confirmed by the hot point method. The mobility of most charge carriers decreases with increasing current, which indicates that the temperature of the samples increases, which affects on the mobility. For the sample 1/5 (⊥) the value of μ is less than the value of n type bismuth telluride mobility which is 510 cm^{2}V^{-1}s^{-1} [8].

CONCLUSION

This paper was the result of the properties testing of an selenium doped bismuth telluride semiconductor monocrystalline compound. Hall's and Van der Pauw's methods were used for material characterization.

An selenium doped bismuth telluride monocrystal was synthesized. The electrical properties of this crystal were measured and the mobility, concentration of the charge carriers majority and Hall coefficient were observed. On the basis of the Hall coefficient, it was determined that in the monocrystal the majority carriers are electrons. The measured electrons mobility was significantly less than the electron mobility in pure bismuth telluride.

The results of these studies show that the selenium doped bismuth and tellurium monocrystal was successfully synthesized by the Czochralski method, and significantly complement existing bismuth telluride single crystals knowledge.

ACKNOWLEDGEMENT

Authors wish to thank Professor Academician Pantelija Nikolić on big and selfless efforts and assistance in all stages of investigations. As well authors wish to thank Stevan Vujatović, a specialized technician. This work was financially supported by the Ministry of Education, Science and Technological Development of the Republic of Serbia, Grant No. 451-03-9/2021-14/ 200052.

REFERENCES

1. Yan, X., Poudel, B., Ma, Y., Liu, W.S., Joshi, G., Wang, H., Lan, Y., Wang, D., Chen, G., Ren, Z. F. (2010) Experimental Studies on AnisotropicThermoelectric Properties and Structures of n-Type $Bi_2Te_{2.7}Se_{0.3}$. Nano Letters, 10, 3373–3378.
2. Bell, L.E. (2008) Cooling, heating, generating power and recovering waste heat with thermoelectric systems. Science*,* 321, 1457-1461.
3. Saleemi, M., Toprak, M.S., Li, S., Johnsson, M., Muhammed, M. (2012) Synthesis, processing, and thermoelectric properties of bulk nanostructured bismuth telluride (Bi_2Te_3). Journal of Materials Chemistry, 22, 725-730.
4. Van der Pauw, L.j. (1958) A method of measuring specific resistivity and Hall effect of discs of arbitrary shape. Philips Research Reports*,* 13, 1–9.
5. Van der Pauw, L.j. (1958) A method of measuring the resistivity and Hall coefficient on lamellae of arbitrary shape. Philips Technical Review*,* 20, 220–224*.*
6. Snyder, G., Toberer, E. (2008) Complex thermoelectric materials. Nature materials 7, 105-114.
7. Požega, E. (2018) Sinteza i karakterizacija monokristala bizmuta i telura dopiranih selenom, cirkonijumom i arsenom (Doktorska disretacija). Univerzitet u Beogradu, Tehnički fakultet u Boru, Bor.
8. Gol'cman, B.M., Kudinov, V.A., Smirnov, I.A. (1972) Semiconductor thermoelectric materials based on Bi_2Te_3. 2nd ed. Moskva: Nauka (in Russian).

XIV International Mineral Processing
and Recycling Conference
Belgrade, Serbia, 12-14 May 2021

HYBRID GEOMATERIALS

**Milenko Jovanović[#], Miomir Mikić, Radmilo Rajković,
Daniel Kržanović, Emina Požega**
Mining and Metallurgy Institute Bor, Bor, Serbia

ABSTRACT – Waste is a big (global) problem, which has been accumulating more and more over the years, so it needs to be stored somewhere permanently. However, it should be disposed of in the prescribed manner - it's not the same where and how we dispose of waste. Various variations of geosynthetics have been playing this most important role lately. Geosynthetics play a major role in soil protection whether it is a landfill or some other surface pollution. Geosynthetics has been developing in the last four decades and all products in this field can still be considered relatively new, which certainly does not mean that they have not proven themselves on many demanding projects (applications) in various occasions and requirements, especially in mining and construction.

Keywords: Geosynthetic, Geogrids, Hybridgeomaterials, Slope, Landfill.

INTRODUCTION

In accordance with the technical documentation of the Law on Mining, the obligation to recultivate the land is determined, according to the valid Project. The amendment of the Law and its harmonization with international standards (EN ISO 10318-1: 2015 CEN / TC 189) and articles (ISO 10318-1: 2015 ISO / TC 221) related to ecology and safety of works envisages the introduction of "new" security and protection measures. Mining facilities and surroundings. One of them is the application (installation) of geosynthetics (various types), as (in the future) a mandatory measure for securing mining and construction facilities (landfills, securing slopes, embankments, canals, etc.). [1,2]

A special part of this area refers to geogrids and geotextiles made of organic material (from nature), which, along with some variations in the use of building materials, is the main topic of this paper. Organic geogrids have unique characteristics, consisting of biologically and chemically degradable natural fibers. They are designed to keep the land in place until natural vegetation is established. On the other hand, geogrids and geotextiles made of synthetic materials have much greater strength, elasticity and durability. [1,3,4]

By combining these types (materials) of geogrids and geotextiles in the form of a certain hybrid technology of making these products, we obtain usable parameters suitable in the field of environmental protection and the necessary mechanical and temporal usability (long-lasting).

Seemingly contradictory requirements, by applying these hybrid geomaterials, can be effectively fulfilled.

[#] corresponding author: milenko.jovanovic@irmbor.co.rs

EXPERIMENTAL

Geogrids - materials, differences and types

Geogrids (Fig. 1) are made of polymeric materials such as polyethylene, polyester and polypropylene and are characterized by high tensile strength. The original geogrids were made by drilling holes in the sheet of material. Today, such geogrids are made by the so-called extrusion process. We now have geogrids made of polyester fibers coated with polyethylene. A multitude of continuous fibers are joined into a thread, which is then woven in the longitudinal and transverse direction with a certain distance between the ribs, and the folds are additionally strengthened, and then the fibers are coated. Geogrids are most often used to strengthen and stabilize poorly bearing soil. Apart from stabilizing and strengthening poorly bearing soil, geogrids are also used to strengthen asphalt by installing a geogrid between the layers of asphalt. The geogrid takes over the action of forces and prevents the formation of cracks on the newly installed layer of asphalt. The third important purpose of geogrids is to protect against soil erosion. For this purpose, there are two-dimensional geogrids that have small eye openings and three-dimensional geogrids. Depending on the manufacturer, geogrids may differ, but their primary function and mode of operation are the same: [1,3,5]

- absorb the kinetic energy of erosive elements (rain, wind) and stabilize the soil surface, creating numerous micro-dams over it,
- keeps seeds and hydrosowing materials in place, even on a steep slope of the soil, which leads to successful seed germination,
- helps water penetrate through the soil and retain moisture, leading to better seed germination and good grass growth.

The use of anti-erosion geotextiles can increase and support the effect of erosion control in areas with particularly steep slopes or in substrates susceptible to erosion. [1,3,5,6,7]

Figure 1 Setting up a geogrid

Organic geogrids

The greatest role of vegetation in the protection of slopes from erosion and its stabilization is provided when its surface enables the establishment of a given vegetation and allows water to flow at a certain speed and intensity on the surface and thus prevents the degradation of vegetative cover. Organic geogrids have unique characteristics, consisting of biologically and chemically photo degradable natural fibers. They are designed to keep the land in place until vegetation is established. The organic geogrid has the following roles:

- To absorb the kinetic energy of erosive elements (rain, wind).
- To facilitate the penetration of rain into the ground.
- To retain moisture from rain: In addition to being eco-friendly, they can absorb water about five times the dry weight.
- Allows to avoid loss or dispersion of seeds necessary for revegetation.
- Provides radical establishment of plant species.
- Allows control of soil temperature by mitigating its natural oscillations: so that they can mitigate extreme temperatures and create a pleasant micro-climate for vegetation growth.
- Allows to reduce the loss of soil moisture.

Organic geogrids are more flexible than most types of synthetic geogrids. This allows them to easily follow the contour of the soil surface. The ability to make direct contact between the fibers and the soil and enable the development of a connection between them, enables the reduction of soil loss by 90% or more. In addition to the above, organic geogrids act as "mulch" and thus improve the establishment of vegetation. After degradation, they do not leave any toxic material. [4,8,9]

Geo-network of Jute – Jute is an annual plant that requires a very warm climate and a lot of moisture. Utah geogrid (Fig. 2) is used to cover slopes and protect against erosion. Jute yarns are thick with pronounced 3D characteristics and provide a number of barriers, thus reducing the rate of water runoff. The openings of the jute net retain the displacement of the clearings of the soil. The jute net has an excellent ability to shape and follow the contours of the land on which it is placed. It absorbs water up to almost 4-5 times its dry weight, storing water from the rain and preventing the soil from separating. In humid conditions, its flexibility increases due to water absorption. The jute mesh provides surface stability on steep slopes and slopes with an angle of about 45 degrees. When vegetation begins to grow it takes on the role of a jute net. It takes about 2 years for the biodegradation of the jute network. [4,6,9]

Figure 2 Jute geogrid

Figure 3 Coconut geogrid

Coconut geogrid – Geotextile made of organic material (coconut) is a natural and 100% biodegradable solution for erosion control using a coconut fiber geotextile mat. Permeable geotextile provides a natural system of assistance (improvement of characteristics) to the soil (soil) and vegetation. Coconut fiber is obtained from the coconut shell. They are naturally strong, durable and biodegradable.

The coconut geogrid (Fig. 3) is a very strong and durable network. Open weaving allows the planting of seeds and vegetation both before and after the installation of the mat, and offers strong support to the vegetation. The lifespan of a coconut fiber mat is four to six years. Period, enough for strengthens with consolidation. After that time, the mat slowly biodegrades. This geogrid has high tensile strength (35 kn/m) and elasticity and can be installed even on very steep slopes around 70 degrees. On steep slopes, which are more prone to erosion, organic geogrid can be placed in combination with metal nets. Organic geogrids are best for protection against erosion through vegetative growth. When vegetation is established, organic geogrids no longer serve as protection. Metal mesh remains permanently as active or passive slope protection. The geogrid can be set up to 60 degrees, with the support of a metal mesh, while the coconut geogrid in combination with metal can also be placed on vertical slopes. [4,6,9]

Synthetic geogrids

Synthetic geogrids are synthetic products (geosynthetics) used to stabilize the terrain. The polymeric nature of the products makes them suitable for use in a country where high levels of durability are required. This type of geogrid is available in a wide range of shapes and (synthetic) materials. In difficult conditions (such as slopes with a critical angle, channels with high flow, etc.), the vegetative cover, even when it is well placed, will not be able to survive under the erosive power of water. Therefore, for the purpose of stabilization and strengthening of the terrain, the law should define the obligation to use (install - install) geogrids or geosynthetic networks and thus increase the resistance to erosion and thus the protection of the natural environment. [3,8,9]

RESULTS AND DISCUSSION

Types of materials – fibers

Primary properties of fibers

In order for the fibers to be further processed into more complex textiles (materials) and for the final products to meet the intended purpose, the fibers must meet certain requirements. Some characteristics reflect the behavior of fibers under the action of external forces and influences. The mechanical properties (characteristics) describe the behavior of fibers under the action of various types of forces and loads. Physical properties represent the response of fibers to various external physical influences, such as the action of heat, various types of radiation, the atmosphere, etc. Another type of feature is related to the appearance of the fiber, its dimensions and surface characteristics. These properties are very specific to fibers - as a form of material, but also different and characteristic of certain types of fibers. The characteristics of this group are also important for processability, and based on them, many differences in the behavior of textile products in application result. Behavior during the action of chemical agents is important for the implementation of various physico-chemical processes, and resistance to certain chemicals is an important characteristic. It is common for numerous characteristics of fibers, on which the possibility of their processing and suitability for a certain purpose depend, to be classified into two groups: primary and secondary properties. [4,6,8,9]

Fineness of fibers

Fineness is a measure of the cross-sectional area of a fiber (Tab. 1). The smaller the surface, the finer the fiber, which means that it is thinner. Therefore, when determining the fineness, it would be correct to determine the size of the cross section. The fibers are very fine, so these surfaces are very small and difficult to measure. Due to this difficulty in determining the cross-sectional size of the fibers, the fineness is expressed by the length of mass, i.e. by the mass contained in a unit length of fiber. [4,6,9,10]

Table 1 Classification of textile fibers

Fine fineness [dtex]	**Fiber group designation - according to fineness**
More than 7	Coarse fibers
2.4 - 7	Medium fine fibers
1 – 2.4	Fine fibers
0.3 - 1	High Fine Fibers
0.4 and less	Microfibers

Fiber strength

Strength reflects the behavior of fibers under the action of various forces and loads. The stronger the fibers, the more loads they can withstand. The strength must be such as to enable the unobstructed processing of the fibers into various more complex textile products (as intended) and to ensure sufficient durability of those products during their use. In order to find out the strength of fibers, the maximum force that a fiber can withstand is measured. Breaking force [cN]. Different types of fibers differ significantly in strength, which is evident from the above data (Tab. 2). It should be noted that even within one type of fiber there are different types of strength. [4,6,8,10]

Table 2 Fiber strength under normal conditions

Fiber	**Fiber Strength [cN/dtex]**	**Fiber**	**Fiber Strength [cN/dtex]**
Raw cotton	3 – 4.9	Viscose - standard type	0.7 – 3.2
Linen	2.6 – 7.7	Viscose - HWM type	2.5 – 5
Hemp	5.8 – 6.8	Polyester (PES)	4.6 – 9.5
Juta	3 – 5.8	Polyamide (PA)	2.5 – 8.3
Ramia	5.5	Acrylic (PAN)	2 – 4.5
Silk	2.4 – 5.1	Modacrylic (MAC)	2.5 – 3.5
Wool	1 – 1.7	Polypropylene (PP)	3 – 7.5
Asbestos	2.5 – 3.1	Glass	6.3 – 7.2

Division of fibers according to origin

According to the origin, all fibers can be classified into two groups - a group of natural and a group of artificial fibers. Within its group, natural fibers are divided according to the type of natural source in which the fiber is formed, and in the group of artificial fibers we distinguish fibers from organic polymers and fibers that are made of inorganic material. Fibers from organic polymers are usually further classified according to the origin of the polymer, where it is important to distinguish artificial fibers from natural polymers and artificial fibers from synthetic polymers.

- Natural fibers: - vegetable: fibers from seeds, fruits, bark and leaves; - animal: hair, wool and silk and - mineral: asbestos.
- Man-made fibers: artificial silks: viscous copper nitrate and nitrate, copper, acetate; - cellulose wool and - protein fibers: animal and vegetable.
- Synthetic fibers: polymerization and polycondensation. Natural fibers - Plant fibers.
- The main ingredient in plant fibers is cellulose. [8,9,10]

CONCLUSION

Geosynthetics have proven to be the most efficient material of wide application. Its building elements provide great quality and multi-purpose use in civil engineering, building construction, mining, environmental protection.

Geogrids and geotextiles made of organic material are a natural and 100% biodegradable solution for erosion control using geomaterials mats made of coconut fibers. Organic geogrids have unique characteristics, consisting of biologically and chemically photodegradable natural fibers. They are designed to keep the land in place until vegetation is established. Geogrid or permeable geotextile provides a natural system of assistance (improvement of characteristics) to the soil and vegetation.

The installation of these efficient systems (geogrids, geotextiles, geomembranes…) in various branches of the ecology and industry and their expediency directly depends on the materials from which they are made. The application and selection of types and materials in road construction is important for (savings) improvements in the field of faster, safer and more efficient construction of road. It also refers to the protection and stabilization (strengthening) of surfaces (slopes) of landfills and other mining facilities, where the cover layer depends on the deposited material, size and shape too. [4,6,9]

As a possible saving solution in many cases, where an efficient result is required, both on the ecological and on the construction, safety, field security plan, there is a hybrid approach to the use of construction materials. Namely, by using (cross - hybrid) different types of materials in the production of geogrids or geotextiles, we can solve the seemingly contradictory requirements in their application. [4]

Special attention in further development should be paid to the use of new natural materials and hybrid technology (type) of geomaterials, as products of the future.

ACKNOWLEDGEMENT

Study research II & III - Preparing a topic for the Doctoral (- Doctoral dissertation)/ Scientific work.

REFERENCES

1. Bogićević, M. (2008) Construction. Belgrade, Serbia.
2. SRPS EN ISO 10318: (2015) Geosintetics - Terms and definitions. (ISO 10318: 2015).
3. Jovanović, M. (2019) Study research II (Doctoral dissertation): "Geosynthetics - purpose and application (in mining)", University of Belgrade, Technical Faculty in Bor.
4. Jovanović, M. (2019) Study research III (Doctoral dissertation): Organic geogrids, University of Belgrade, Technical Faculty in Bor.
5. Nonveiler, E. (1987) Slope sliding and stabilization. School book, Zagreb.
6. Veinović, Ž., Kvasnička, P. (2007) Surface landfills. Internal script. Faculty of Mining, Geology and Petroleum Engineering, University of Zagreb, Zagreb.
7. Zidar, M. (2009) Landslide remediation methods. Faculty of Geotechnics, University of Zagreb, Varaždin.
8. Sandra, L. (2009) Final paper work (PhD): Application of geosynthetics in landscaping - Faculty of Geotechnics, University of Zagreb, Varaždin [k 3 6].
9. Lukavečki, I. (2010/2011) About geosynthetics and applications in landfill remediation"; Final paper work; 1821.
10. Đorđić, D. (2016) Research of deformation characteristics of nonwoven geotextile materials made of polyester and polypropylene fibers" - Doctoral Dissertation.

STRUCTURE, ORGANIZATION AND FUNCTIONING OF A SUSTAINABLE DEVELOPING METALLURGICAL PLANT

Lyubomir Ilchev[#], Nadezhda Davcheva-Ilcheva
University of Chemical Technology and Metallurgy, Sofia, Bulgaria

ABSTRACT – Sustainable development helps the transition of industrial enterprises from "open" to "closed" type of economy, solving their contradictions with the environment and the biosphere. Therefore, the future belongs to those industrial enterprises that will comply with and put into practice the concept of sustainable development. The authors propose a conditional structural and functional schemes of a metallurgical plant (for example, copper pyrometallurgy or/and production of semi-finished products) in accordance with the requirements of the main UN and EU documents for sustainable development. Management, as a major production factor, together with one of its main tools - feedback, have the task to change the ongoing processes to this desired goal. A network of industry indicators accounting for the effectiveness of systems management and the progress made is also pointed out.

Keywords: Sustainable Development, Structure, Organization, Functioning, Management Toolkit.

INTRODUCTION

Like most anthropogenic systems, industrial enterprises are structured, organized and operate on a "linear" basis, i.e. as an "open" type of economy, carrying with it huge risks and disadvantages. Sustainable development (SD) - development in harmony with the environment, in a market economy solves problems such as: quality, material and energy efficiency, waste, markets, prices, problems in the social sphere. It helps the transition of industrial enterprises from "open" to "closed" type - circular economy. The future therefore lies with those industrial enterprises which will comply with and put into practice the concept of sustainable development [1].

REQUIREMENTS OF SUSTAINABLE DEVELOPMENT TO THE STRUCTURE AND ORGANIZATION OF METALLURGICAL PLANTS

Metallurgical plants must be structured in such a way as to perform well their main specific objectives and tasks. Sustainable development imposes some additional requirements on their structure and organization, in order to improve their internal strengths and opportunities for development and strengthen their viability. These requirements in terms of the main factors of production are [1]:

- conservation and proper management of natural resources and raw materials;
- continuous increase of energy efficiency;
- introduction of non-waste, environmentally friendly technologies;
- environmental protection (EP);

[#] corresponding author: lubomirilchev@abv.bg

- achieving management for sustainable development of plants.

It is necessary for their organization to comply with the basic principles of sustainable development. More important of them are [2,3]:

- Integrity - uniting the economic and social development of the metallurgical plants with the protection and development of the environment. This means that the problems of protecting and improving the environment must be an integral part of those related to the development of raw materials, energy, technology and management.
- Synergy - important for the three main pillars of sustainable development - economic, social and environmental, one of the most influential but also the most underestimated principles of modern development of the information society. For metallurgy, synergy must be achieved both between the main production factors for the sustainable development of plants and throughout the value chain.
- Homeostasis - an important organizational principle for industrial systems, allowing metallurgical plants in today's dynamic conditions of a constantly changing environment to be maintained, to be internally stable and to develop sustainably. The organization must help them, like the ecosystems in the biosphere, to self-regulate and self-control. This is possible when there is well-organized feedback in the system.
- Succession - metallurgical plants should not exclude it, but provide and encourage it, similar to the development in the biosphere. Their inertia must be overcome and the structural elements must be replaced quickly, and, if necessary, entire systems that hold back their sustainable development. The goal is to continuously improve their competitiveness and sustainability, regardless of changes in external conditions, such as climate and others.

CONDITIONAL FUNCTIONAL DIAGRAM OF SUSTAINABLY DEVELOPING METALLURGICAL PLANTS

The conditional functional diagram of a sustainably developing metallurgical plant (on the example of copper pyrometallurgy and/or production of semi-finished products) is shown in fig.1. There are high requirements and strict control over incoming raw materials, energy and other important resources. Continuous improvement of their quality is required. Important for its sustainable development is the use of "green" energy, full utilization of waste energy and, if possible, the use of its own alternative energy from renewable sources with the application of modern co- and three-generative energy systems.

The production capacity of the plant must be constantly balanced with the market needs and capabilities of the feeding ecosystems. Its production and technological schemes should be resource and energy efficient, subject to the principle of prevention, recovery or, in extreme cases, harmless disposal of waste. Recycling, recovery and purify systems serve to prevent and minimize waste, be able to generate new by-products.

Final emissions and waste in terms of quality and quantity must be non-adverse for the environment, within the limits of its absorbing and neutralizing possibilities. Waste storage facilities must be designed in such a way as to create opportunities for further additional treatment of the waste deposited in them, with the possible creation of new innovative technologies for this purpose.

The quantity and quality of the produced products must meet the high market needs and requirements, ensuring and maintaining high competitiveness of the plant.

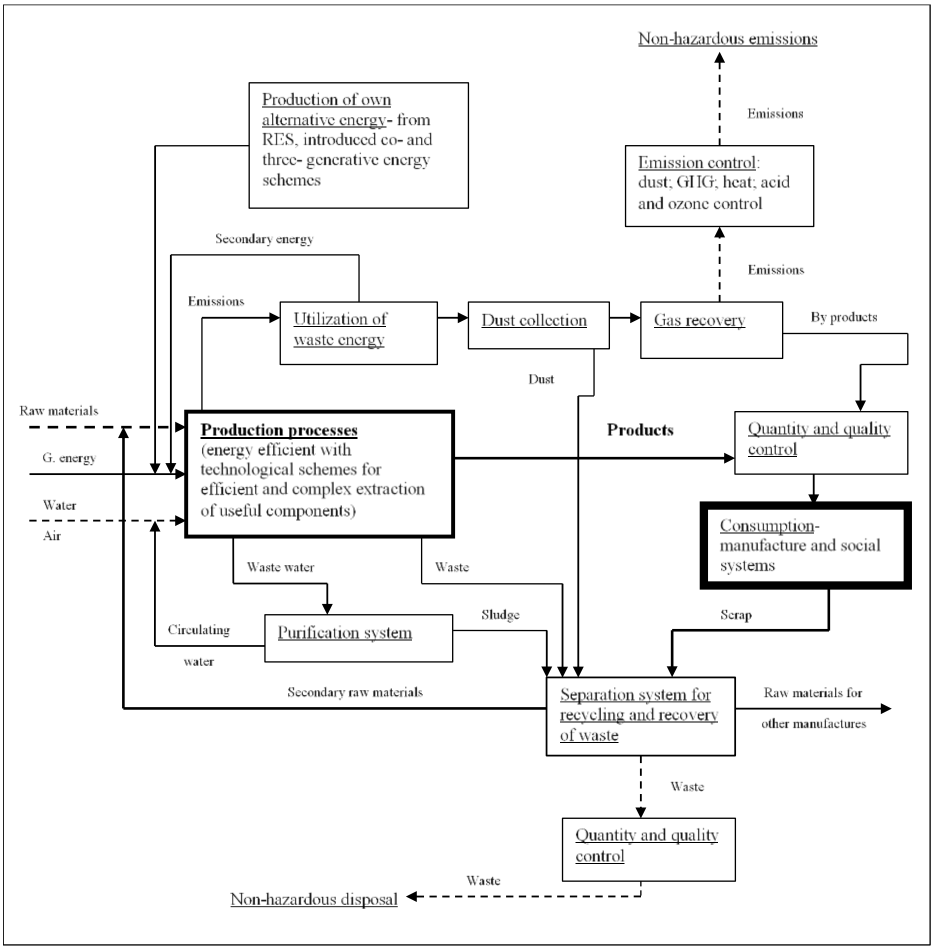

Figure 1 Conditional functional scheme of a sustainably developing metallurgical plant
Abbreviations: G. energy - green energy

MANAGEMENT INCLUDING FEEDBACK - A KEY FACTOR FOR ACHIEVING SUSTAINABLE DEVELOPMENT

The management of the plant has the task to change the ongoing processes according to the changing environment and social requirements for sustainable economic development - fig. 2. Economic conditions should help the management of industry, in innovative solutions, to change the existing market relations and requirements in the direction of sustainable development (fig. 2-the dotted line SD & EP).

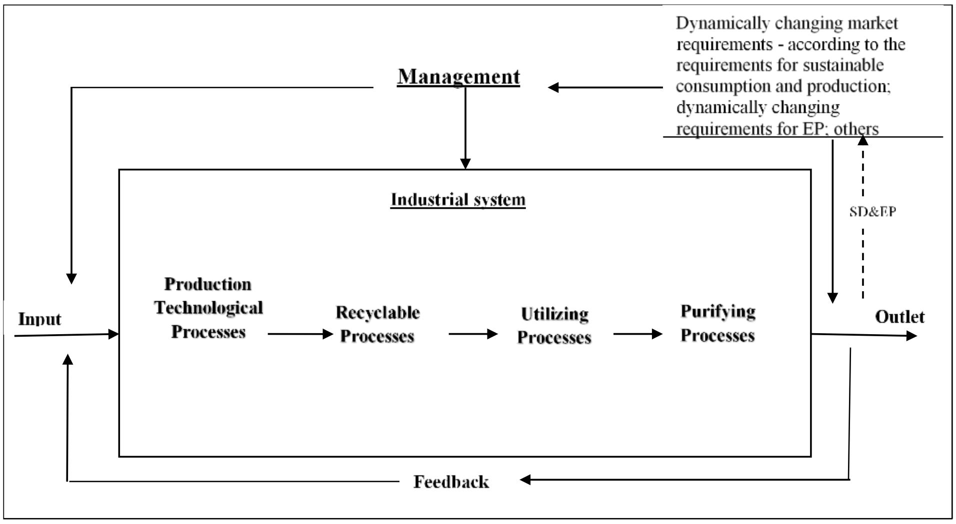

Figure 2 Conditional functional scheme for sustainable management of an industrial system

Industrial indicators accounting the effectiveness of systems management and the progress made

A management toolkit for sustainable development is in the early stages of building up. It was launched by Scientific Advise Group (SAG)-an EU Expert Group, which has developed and proposed a network of important industrial sustainability indicators, with units of measurement [4]. We complimented a SAG`s set of indicators with some common and specific indicators and units of measurements concerning branches with pressure upon environment as metallurgy [5]. They are consistent with the most important areas of pressure on the environment from metallurgical enterprises-Table 1-5.

Table 1 Indicators for air pollution

Indicator	Unit of measurement	Proposed by
Emissions of SO_2	tones yr^{-1} kg ton^{-1} of raw material kg ton^{-1} of product	SAG authors authors
Emissions of NO_x	tones yr^{-1} kg ton^{-1} of raw material kg ton^{-1} of product	SAG authors authors
Emissions of dusts	tones yr^{-1} kg ton^{-1} of raw material kg ton^{-1} of product	SAG authors authors
Emissions of heavy and toxic metals (Cu, Pb, As, Cd etc.):	kg ton^{-1} of product	authors
Fugitive emissions*	tones yr^{-1}	authors

* Indicators have to be introduced after adoption of proper method for their measurement.

Table 2 Indicator for climate changes

Indicator	Unit of measurement	Proposed by
Emissions of CO_2:	tones yr^{-1} kg ton^{-1} of raw material kg ton^{-1} of product	SAG authors authors

Table 3 Indicators for resource depletion

Indicator	Unit of measurement	Proposed by
Production of non- ferrous metals from raw, non- recycled resources	tones yr^{-1}	SAG
Increase in territory permanently occupied by infrastructure and waste-tipping	ha yr^{-1}	SAG
Use of fossils	m^3 or tones yr^{-1} toe ton^{-1} of raw material toe ton^{-1} of product	authors authors authors
Surface water abstraction	m^3 yr^{-1} m^3 ton^{-1} of raw material m^3 ton^{-1} production	SAG authors authors
Ground water abstraction	m^3 yr^{-1} m^3 ton^{-1} of raw material m^3 ton^{-1} production	SAG authors authors

Table 4 Indicators for industrial waste

Indicator	Unit of measurement	Proposed by
Waste	tones yr^{-1} tones yr^{-1} of raw materials tones yr^{-1} of product	SAG authors authors
Hazardous waste	tones yr^{-1} ton ton^{-1} of raw materials ton ton^{-1} of product	SAG authors authors
Waste converts to products	tones yr^{-1}	authors
Waste recycled	tones yr^{-1}	authors
Total waste recycled/ total quantity of raw materials	%	authors

The industrialization of a given area must be preceded by preliminary ecological background studies on the state of nature, its resources and the environment, which should be the basis for determining the ecological pressure of the realized production activity.

In a market economy, additional environmental friendly investments in production and output must generate added value for the plant. They need to have an exact economic equivalent and find a place in the most important economic indicators for the functional activity of plant [6,7,8]:

- Operation costs;
- $\frac{\text{Profit}}{\text{Total Incom}}$ Ratio;
- ROCE = $\frac{\text{Pre-tax Operating Profit}}{\text{Capital Employed}}$;
- Return on Investmants = $\frac{\text{Profit on Investments-Investments Costs}}{\text{Investments Costs}}$;
- Online time (% of available time).

Table 5 Indicators for water pollution & water resources

Indicator	Unit of measurement	Proposed by
Emissions of heavy and toxic metals (Cu, Pb, As, Cd etc.):	tones yr^{-1} g m^{-3} of water g ton^{-1} of product	authors
Acid emissions (SO_4)	tones yr^{-1}	authors
Waste waters	1000m^3 yr^{-1} m^3 ton^{-1} of raw material m^3 ton^{-1} production	authors
Water recycling	1000m^3 yr^{-1} m^3 ton^{-1} of raw material m^3 ton^{-1} production	SAG authors authors
Total of waste water treated by industry/total quantity of water used	%	SAG
Recycled water/ total water used	%	authors

CONCLUSION

The management tools proposed for us for sustainable development must be developed and enriched according to the specifics of the respective production. Analyzes for harmonious development of the enterprises with nature are in the initial stage. With the help of systematic observations and research in these areas, a cadaster of environmental problems can be created for industry on a regional and national scale. This will help unite efforts to address them and achieve environmentally friendly and sustainable operation of metallurgy.

REFERENCES

1. Ilchev L. (2018) Managing Sustainable Development of the Copper Life Cycle in the Republic of Bulgaria, (Dissertation). University of Chemical Technology and Metallurgy, Department of Environmental Engineering, Sofia, 192.
2. Brundtland (1987) Our Common Future: Report of the World Commission on Environment and Development, Oslo.
3. Давчева-Илчева, Н., Илчев, Л. (2005) Екология. Устойчиво Развитие. Околна Среда, Издателство „Изток-Запад", София, 162.

4. Eurostat (2010) Measuring Sustainability- Sustainable Development Indicators, Indicators for Decision Making, Policy Performance Indices- a challenge to the GDP.
5. Ilchev, L., Davcheva-Ilcheva, N. (2015) Indicators Describing Pressures on Environment from Industry. Journal of Chemical Engineering and Chemistry Research, 2 (6), Ethan Publishing Company, USA, 635-640.
6. Aspola, L. (2008) Sustainability Indicators in Copper Smelting Processes, M.Sc. Thesis. Helsinki University of Technology.
7. Jeffrey M. Perloff, Klaas T. van`t Veld (1994) Modern Industrial Organization, Second edition, Harper Collins.
8. Kenneth D. George, Caroline Joll, E. L. Lynk (1992) Industrial Organization-Competition, Growth and Structural Change, Fourth edition, Rout ledge.

BIODIVERSITY CONSERVATION NEAR THE ADA TEPE MINE - MISSION POSSIBLE

Elisaveta Valova[#]
Dundee Precious Metals Krumovgrad, Krumovgrad, Bulgaria

ABSTRACT – Assessing its net impact, Dundee Precious Metals Krumovgrad started a long-term initiative to study and preserve the population of two species of tortoises, which are protected under the Habitats Directive of the European Commission. Being the most sensitive biodiversity indicator within the Ada tepe Natura-2000 mining site, extensive research, awareness and collaboration with community added valuable knowledge to a previously under-researched scientific field.

Keywords: Natura-2000, Tortoise, Mining, Protection, Biodiversity.

INTRODUCTION

Dundee Precious Metals Krumovgrad EAD is a Bulgarian gold-mining company. Winning community support over a comprehensive and extensive stakeholder engagement process, it developed and now operates the first greenfield mine in Bulgaria in the last 40 years. DPM willingness to change and adapt its mining project to accommodate community expectations and nature preservation recommendations turned the Ada tepe, Krumovgrad project into a model for the long-term conservation of the populations of two protected local tortoise species. Following NGO experts' Compatibility Assessment recommendations to mitigate negative impact, DPM reduced two-fold the mine area size, applied innovative waste management to protect rare species and preserve forests, transforming a mining project into a EU case study under the Habitats directive.

EXPERIMENTAL

"WE SUCCEED BECAUSE WE CARE"

Changing to meet experts' recommendations and community expectations

The monitoring of animal species and the choice of monitoring areas are based on various surveys carried out throughout the years in relation to the investment project of Dundee Precious Metals Krumovgrad EAD for the Mining and Processing of Auriferous Ores from the Ada Tepe Prospect, Khan Krum Deposit. Since 2019 Ada tepe mine is a fully operational mine.

Ada Tepe mine is within a large Natura 2000 zone (Rodopi iztochni – 21,700ha), hosting important natural forest types and mammals. The baseline document for

---

[#] corresponding author: elisaveta.valova@dundeeprecious.com

defining the monitored animal species and their habitats is the "Assessment of Project Compatibility with the Conservation Objectives of the East Rhodopes Protected Site and the Krumovitsa Protected Site".

Guided by the “We succeed because we care” principle, coupled with consistent transparency, allowed DPM to successfully go through a nearly 15-year process of interaction with community, local administration and NGO, permit the first greenfield mine and commence operation.

In the course of studies, experts assessed negative impact on numerous rare amphibians, reptiles and invertebrates and two types of protected tortoise species – Testudo graeca, and Testudo hermanni.

Acknowledging experts and community concerns and in line with its principles, DPM responded by:

- Reducing production footprint – DPM developed an innovative solution for mine waste management that involved an Integrated mine waste facility. Use of agricultural land or private land was no longer needed and a phased-out rehabilitation process was possible. The footprint of the mine site was reduced two-fold -from 187 ha to 85 ha, or just 0.04% of the protected BG0001032 Rhodopes-East area. The new facility allows for 100% water recycling and reuse, no discharge to the Krumovitsa river and negligible impact on natural habitats – including fish, bats, tortoises, invertebrate and mammal species, trees.
- Constructing water treatment plant and committing to ensure that any discharge of industrial wastewater meets drinking water quality standards.
- Maintaining a buffer zone between facilities and the surrounding forestry area, keeping existing trees and protecting biodiversity.

SPECIAL MEASURES TO PRESERVE AND STUDY THE POPULATIONS OF THE PROTECTED TORTOISES

Biodiversity is part of DPM Corporate Responsibility strategic imperatives. It is not only a commitment under the EIA and a promise to the community but also an integral part of DPM Environment and Sustainability policy that can be traced as a material issue in GRI-consistent reporting.

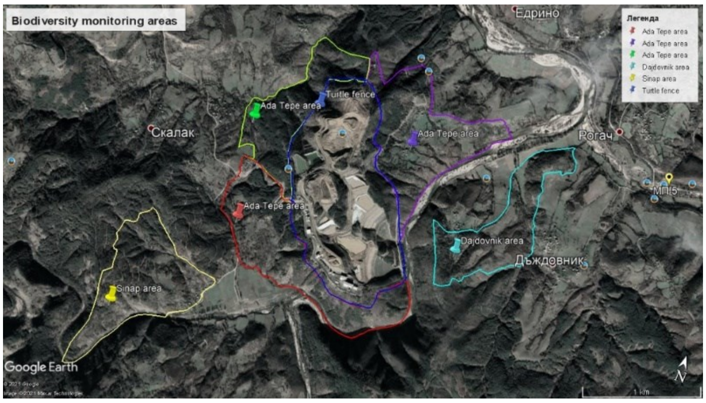

Figure 1 Map of biodiversity monitoring areas

While the mine was commissioned in 2019, as early as 2012 work started to collect grassroot information about the tortoise population. The areas designated for biodiversity monitoring are divided into reference zones and Ada Tepe Zone (Figure 1). Over 7 years 2472 individual alive tortoises from the two protected species were found, marked, measured, recorded, GPSed, and photographed. Their population has been assessed against morphometric data, population number and density. All data has been thoroughly recorded over the years as per the National System for Monitoring of Biodiversity requirements and filled in GIS data base to allow analyses.

As a first step the future mine site was fenced (Figure 2), tortoises within the site were collected, marked and placed in an appropriate, pre-assessed area, similar to their natural habitat. Community was involved in educational programs, trainings and information campaigns as well as in the process of collecting and relocating the species as a way of securing conservation process sustainability.

The methodology applied follows several key indicators – age and size profile, weight index, territorial distribution, gender structure, mortality and birth rate.

Over 3600 hours were spent in field research over the spring, summer and autumn months and 1500 km walked in search of animals. By the end of 2013, 403 tortoises were moved from the project area. The fence (Figure 2) was carefully inspected to ensure no animals return to the future mine site. Following a comprehensive biodiversity plan in 2017, 9 sites were developed to support the nourishing of the tortoises. These sites in the area of relocation, each 2,5 decares, were planted with 324 fruit trees and bushes. Besides there were planned activities for cleaning of fountains, wells and springs that sustain 93 key turtle sites in the Ada Tepe.

Figure 2 Initial fence placed to impede returning of relocated individuals

Continuous monitoring followed also tortoise hatchlings. These have been successfully established in the new territories. At the end of 2020 a total of 2603 individual tortoises from the two species have been captured, marked and researched.

The academic approach to the monitoring of the populations of Testudo graeca and Testudo hermanni made it possible to not only research in depth and compile knowledge related to the biology and habits of terrestrial tortoises, an under-studied species, but also provided a clear understanding of the interactions in place in an area that hosts Natura-2000 site and a mining site (Figure 3).

Figure 3 Finding and measuring individual on an annual basis

Along with the monitoring of the status of the tortoise population a number of additional initiatives were carried to support the conservation process - training of local volunteers, information campaigns to reduce poaching, consultation with local authorities to coordinate conservation activities, maintaining an aggregate database, development of educational programs in cooperation with local schools and eco-clubs, regular trainings of personnel of companies subcontracted by Dundee Precious Metals on the company procedures applied for the protection of tortoises.

The consistent efforts of Dundee Precious Metals to support the studying of the Testudo graeca and Testudo hermanni, the focused investment in the accumulation of scientific database and analyses of the interconnection Natura-2000 place – mining site, the implementation of a biodiversity plan allow for a better understanding of the factors that influence the habitats of the tortoise species as well as provide measurable data on the relationship of biodiversity conservation activities around the Ada Tepe mine and the concentration of various mammals and the formation of new biotopes.

RESULTS AND DISCUSSION

The primary task of the biodiversity work supported by Dundee Precious Metals is to evaluate the status, review the trends and then come up and implement the most adequate strategy and measures to mitigate unfavorable impacts from mining. Based on the capture-mark-recapture methodology, summarized are the results of the project.

The 2020 tortoise monitoring involved 47 days of fieldwork. Fieldwork took approx. 380 hours and 246 km in search of reptiles. For more information see Table 1 - "n" are the GPS points marked upon finding a tortoise for the first time, "x" - upon finding the animal for a second time, "c" - are the locations with remnants of a dead animal, and finally "e" - the locations with a hatchery (tortoise eggs).

Table 1 General Field Data 2012-2020

General field data								
Year	No. of records	n – points	x – points	c – points	e – points	Field hours (approx.)	Man-days	Distance (km)
2012	125	119	6	-	-	650	131	-
2013	676	482	194	-	-	600	100	-
2014	495	245	141	51	58	190	27	209
2015	1035	538	383	22	92	380	48	290
2016	934	369	459	23	83	360	47	285
2017	1096	323	674	25	74	370	45	252
2018	939	201	617	30	91	380	47	236
2019	1004	195	697	23	89	380	47	231
2020	979	131	762	22	64	380	47	
Total	**7283**	**2603**	**3933**	**196**	**551**	**3690**	**539**	

CONCLUSION

Collected and analyzed data demonstrate a steady population of tortoises in the monitored zones. The biodiversity plans implemented at the sites show positive results on the animals and their habitats.

Being the most sensitive biodiversity indicator within the Ada tepe Natura-2000 mining site, extensive research, awareness and collaboration with community added valuable knowledge to a previously under-researched scientific field.

REFERENCES

1. Duhalov, D. (2015) Reptile Monitoring Report of Ada Tepe Prospect, Khan Krum Deposit.
2. Duhalov, D. (2016) Reptile Monitoring Report of Ada Tepe Prospect, Khan Krum Deposit.
3. Duhalov, D. (2017) Reptile Monitoring Report of Ada Tepe Prospect, Khan Krum Deposit.
4. Duhalov, D. (2018) Reptile Monitoring Report of Ada Tepe Prospect, Khan Krum Deposit.
5. Duhalov, D. (2019) Reptile Monitoring Report of Ada Tepe Prospect, Khan Krum Deposit.
6. Duhalov, D. (2020) Reptile Monitoring Report of Ada Tepe Prospect, Khan Krum Deposit.

THE AWARENESS OF IMPORTANCE OF RECYCLING AMONG HIGH SCHOOL AND UNIVERSITY STUDENTS IN BOR

Zoran Štirbanović[1#], Zorica Trkulja[2], Sandra Vasković[1], Sanja Popović[2], Jelena Milutinović[2]
[1] University of Belgrade, Technical Faculty in Bor, Bor, Serbia
[2] Secondary School for Mechanical and Electrical Engineering, Bor, Serbia

ABSTRACT – Serbia in general and city of Bor in particular are known for many environmental issues, and bad waste management is one of them. Recycling is one of the main aspects of waste management. In order to achieve better results in recycling in the future, it is necessary to educate and promote recycling among general population, youth in particular.

The aim of this paper was to investigate the awareness of importance of recycling among high school and university students in Bor. Online poll was created and over 600 students participated in the survey. The results showed that young people in Bor are highly aware that recycling is very important, but bad recycling infrastructure, such as lack of organized waste selection in households, no separate bins for different waste materials, etc., prevents them from doing more in practice.

Keywords: Recycling, Poll, Students, High school, University.

INTRODUCTION

The constant increase in human population along with modern consumerism are causing the generation of large amounts of waste each year. According to the World Bank [1], 2.01 billion tons of municipal solid waste is being generated in the world annually and it is estimated to grow up to 3.40 billion tons by 2050.

Waste is already causing huge environmental problems, since it is mainly being deposited in open dumps and landfills without proper collecting of landfill gases or drainage waters. Degradation of plastic waste and creation of micro and nano plastic particles that could cause water, soil, and plants pollution [2, 3] and even health problems for animals and humans [4] represent especially large problem.

One of the possible ways for minimizing problems with waste is proper waste management whose integral part is recycling. Recycling represents recovery of waste materials in production process for the original or other purposes, except for energy purposes [5]. According to The national waste management strategy for the period 2010-2019 [5], approximately 60% of municipal solid waste is being collected in the Republic of Serbia, mainly in the urban areas, but separation and recycling of waste is not systematically organized even though there are legislations that define the primary recycling in Serbia and envisages separation of paper, glass, and metal in specially labeled containers.

[#] corresponding author: zstirbanovic@tfbor.bg.ac.rs

Besides legislations, one of the very important aspects of proper waste management, i.e. recycling, is its promotion, especially among younger school population. Primary and secondary school systems in Serbia do not have in their curriculum any courses dealing with this subject, but it is being partially mentioned in biology or some other classes. Exceptions are Technical schools in Bor, Smederevo, and Užice that are engaged in training for the profession of recycling technician. As for higher education, College of Vocational Studies – Belgrade Polytechnic has department of Recycling technologies and also, Technical Faculty in Bor, which is part of University of Belgrade, has a module Recycling technologies and sustainable development, educating future engineers to deal with problems in the field of recycling.

The aim of this paper was to investigate the level of knowledge and awareness of importance of recycling among high school and university students in Bor municipality.

EXPERIMENTAL

Online poll was created with two groups of questions: general information (age, gender of respondents, etc.) and questions about recycling. The poll was created in Google Forms and it was placed on the internet so all students could accessed it. Students were informed about the poll by their teachers and professors and they were able to take the survey for one week.

The aim of the poll was to find out what is the perception of the recycling among youth in city of Bor and its surroundings. Respondents were asked to give grades or rate the importance for some particular matter in some questions, but also, in some cases, they were able to give their own opinion about the improvement of recycling in city of Bor and Serbia in general.

RESULTS AND DISCUSSION

The number of students that participated in the survey was 606. High response showed high interest in this subject, since the participation in the poll was on voluntarily basis.

General information about respondents is given in Figure 1. As can be seen from Graph in Figure 1a, the ratio of the male vs. female respondents was 49.40%:50.60%, i.e., almost half-half which is good from the perspective of the representativeness of the sample. The vast majority of the respondents (82.10%) were in the age group from 15-18 years old, following by 16.20% of students older than 18 years, while 1.70% was younger than 15 years. Graph in Figure 1c shows that 71.90% of respondents live in urban area and 28.10% in rural. Students from all high schools in Bor and also Technical Faculty in Bor participated in the poll. Students from Secondary School for Mechanical and Electrical Engineering Bor (MEŠ) were the most represented in the poll with 56.90%, followed by students from Secondary School of Economics and Trade Bor (ETŠ) with 19.70%, Gymnasium "Bora Stanković" Bor (GBS) with 7.30%, Technical School Bor (TŠB), Technical Faculty in Bor (TFB) with 7.10%, and others with 1.90%.

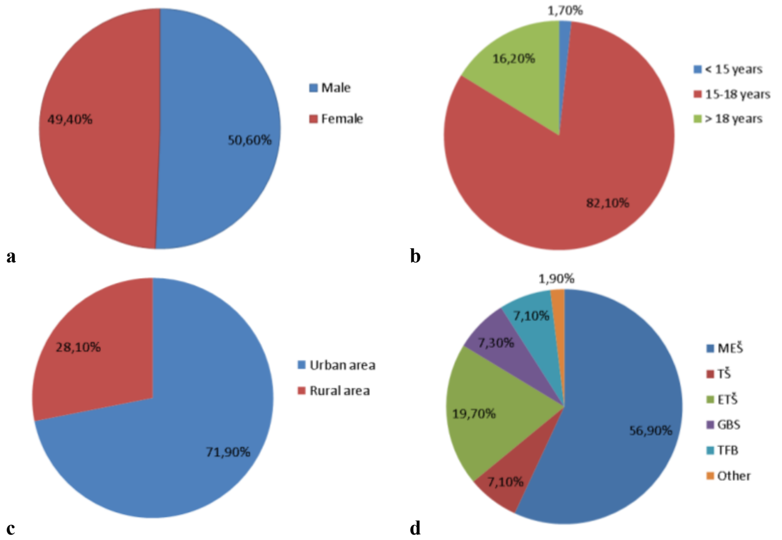

Figure 1 General information: a – gender; b – age; c – area of residence; d – attending school/university)

Figure 2 shows how respondents rated their knowledge of recycling and importance of recycling and also what their main source of information about recycling was.

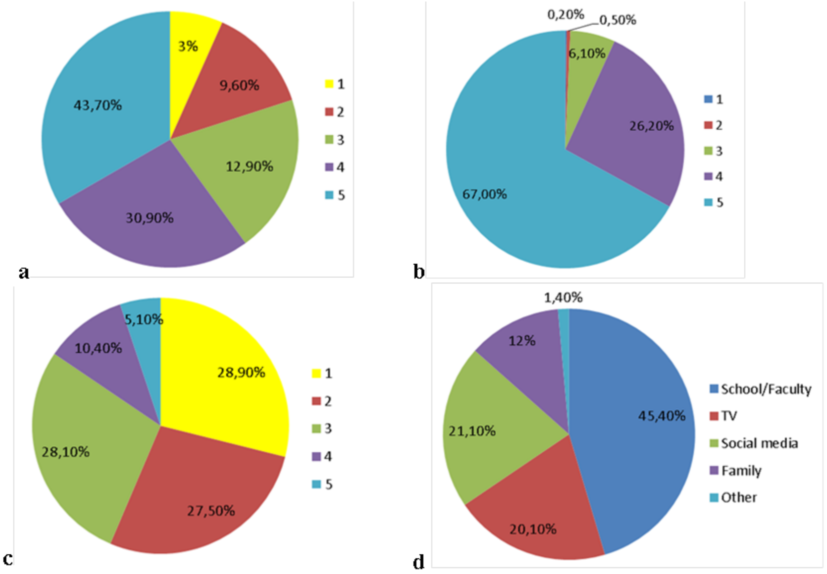

Figure 2 Knowledge of recycling and its importance
a – Rate your knowledge about recycling; b – Rate the importance of recycling; c – Rate the care about recycling in your city/village; d – From which source do you get the most information about recycling?

The students were asked to rate their knowledge of recycling (Figure 2a) and 43.7% rated their knowledge 5, meaning their knowledge was very good, 30.9% rated their knowledge as good (4), 12.9% as medium (3), 9.6% as bad (2), and 3% as very bad (1). The importance of recycling (Figure 2b) was rated as very high (5) by 67% of respondents, while 26.2% considered that recycling had high importance (4), 6.1% medium (3) and 0.5% low (2), i.e. 0.2% very low (1). On the other side, majority of students (28.9%) think that care about recycling in their local community was very bad (1), 27.5% rated it as bad (2), 28.1% as medium, 10.4% as good (4), and only 5.1% as very good (5). The most information about recycling, 45.4% of respondents got from school and/or university (Figure 2d). Other sources of information about recycling were social media (21.1%), TV (20.1%), but also family (12%). This results show that even though the curriculum does not include recycling, teachers and professors talk about it with students. The interesting fact is that family is also one of the significant sources of information about recycling.

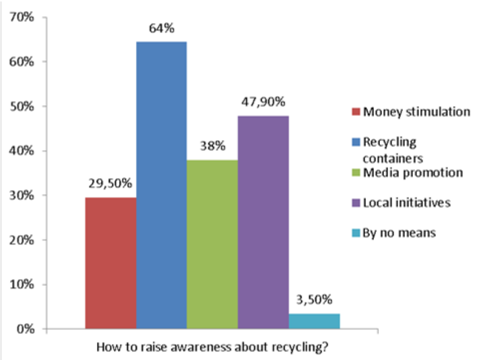

Figure 3 How to raise awareness of recycling?

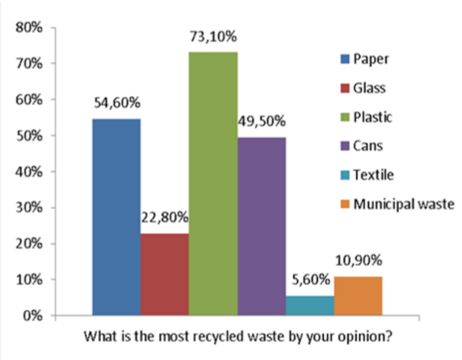

Figure 4 What is the most recycled waste by your opinion?

It is possible to raise awareness about recycling by setting up separate recycling containers, in opinion of 64% of respondents (Figure 3). Local initiatives were marked by 47.9% as important also, following by media promotion (38%), and money stimulation (29.5%), while 3.5% thought that by no means it was possible to raise awareness of recycling.

The next question the students were asked was to mark the most recycled waste in their opinion (Figure 4). Plastic was considered as the most recycled by 73.1% of respondents, followed by paper (54.6%), cans (49.5%), glass (22.8%), municipal waste (10.9%), and textile (5.6%).

Graph in Figure 5 shows that only 20.8% of students recycled regularly, while on the other side 33.2% did not recycle at all. Majority of respondents (46%) recycled sometimes and only some kind of waste. This can be connected to the lack of recycling infrastructure. Exceptions are some supermarkets where you can bring used batteries, paper, plastic etc. It is also important to mention “cap for handicap” initiative, which has established good network for collecting plastic bottle caps which are then recycled and the money is used for helping children with disabilities.

Figure 6 shows answers for the following question: What kind of waste do you recycle? As can be seen from Graph in Figure 6, 50.8% of students said that they recycled plastic and 48.7% paper. Cans were also recycled by 38.4% of respondents, followed by glass 15.8%, batteries 7.9%, textile 6.6%, and electronic/metal waste 6.1%.

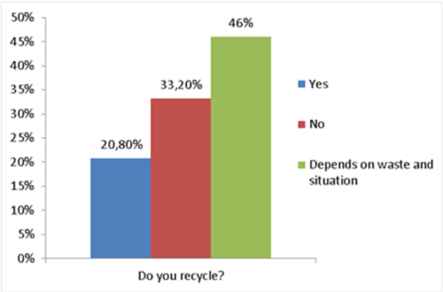

Figure 5 Do you recycle?

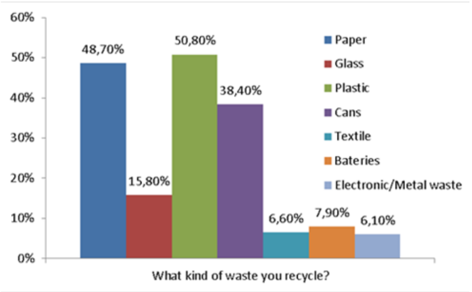

Figure 6 What kind of waste do you recycle?

“How many plastic bottles do you throw away in one week” was the next question whose answers are shown on Figure 7. Majority of students (54.6%) said that they threw away less than 5 bottles a week, 22.1% threw 5-10 bottles, while 6.9% threw more than 10 plastic bottles a week. There was also large number of students, 16.4%, who said that they did not throw away plastic bottles at all.

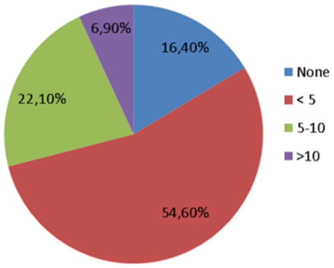

Figure 7 How many plastic bottles do you throw away in one week?

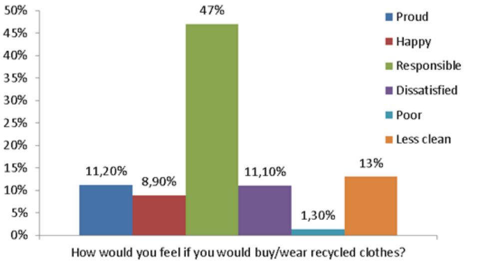

Figure 8 How would you feel if you would buy/wear recycled clothes?

When it came to recycling of textile, 47% of students said that they would feel “responsible” if they would buy and wear recycled clothes. Some other answers were “less clean” 13%, “proud” 11.2%, “dissatisfied” 11.1%, “happy” 8.9%, and “poor” 1.3%.

It was encouraging to hear that majority of students, almost 70%, had positive attitude towards wearing recycled clothes, which showed their social awareness of sustainability and importance of recycling.

CONCLUSION

Recycling as an integral part of waste management is not sufficiently developed in Republic of Serbia, therefore in city of Bor as well. Even though there are legislations regulating this area, their implementation is not carried out throughout. There is no organized primary selection of waste in households, and also there is a lack of recycling infrastructure such as separate containers for each type of waste, etc.

One of the problems is also insufficient promotion of recycling in all kinds of media and also in school system. Local initiatives, like organized collection of waste paper in primary and secondary schools which was regular in the 80's and 90's in 20th century, have become very rare now. Exception is initiative "cap for handicap", aiming to help children with disabilities by collecting and selling plastic bottle caps.

The aim of the research presented in this paper was to investigate the awareness of importance of recycling among high school and university students in Bor, bearing in mind all mentioned above. The online poll was created and students' response was high, over 600 of them participated in the survey, showing high interest in the subject. The students showed satisfactory knowledge about recycling and its importance. Over 45% of respondents identified the school or University as the main source of information about recycling. Almost 80% of students said that they recycle regularly or occasionally, which could be considered high, knowing that there are no favorable circumstances for that. The most recycled waste materials are plastic, paper, and cans. Also majority of students showed positive attitude towards buying and wearing recycled clothes, thus showing high social responsibility. The general conclusion is that most students would recycle more if the recycling system was better organized and if the adequate recycling infrastructure existed.

ACKNOWLEDGEMENT

The research presented in this paper was done with the financial support of the Ministry of Education, Science and Technological Development of the Republic of Serbia, within the funding of the scientific research work at the University of Belgrade, Technical Faculty in Bor, according to the contract with registration number 451-03-9/2021-14/ 200131.

REFERENCES

1. https://datatopics.worldbank.org/what-a-waste/trends_in_solid_waste_management.html (Accessed: March 15, 2021)
2. Iqbal, S., Xu, J., Allen, S. D., Khan, S., Nadir, S., Arif, M. S., Yasmeen, T. (2020) Unraveling consequences of soil micro- and nano-plastic pollution on soil-plant system: Implications for nitrogen (N) cycling and soil microbial activity. Chemosphere, 260, 127578.
3. Helinski, I. K., Poor, C. J., Wolfand, J. M. (2021) Ridding our rivers of plastic: A framework for plastic pollution capture device selection. Marine Pollution Bulletin, 165, 112095.
4. Zarus, G. M., Muianga, C., Hunter, C. M., Pappas, R. S. (2021) A review of data for quantifying human exposures to micro and nanoplastics and potential health risks. Science of The Total Environment, 756, 144010.
5. The national waste management strategy for the period 2010-2019 ("Official Gazette of RS" no. 29/2010).

XIV International Mineral Processing
and Recycling Conference
Belgrade, Serbia, 12-14 May 2021

CURRENT METHODS AND MODELS IN PROCESS SAFETY AND RISK MANAGEMENT

Aleksandra Jelić, Nebojša Ćurčić, Novak Milošević, Marina Stamenović[#],
Marta Trninić, Slaviša Putić
Academy of technical vocational studies - Department Belgrade Polytechnic,
Belgrade, Serbia

ABSTRACT – The aim of this paper is to review historical advances in fields of process safety and risk control approaches and models and to outline recent research developments. For many industries, process safety is of special significance. The role of safety management is to reduce or eliminate accidents. It is noticeable that the latest study focus has been in the field of intrinsic safety, complex and operational risk assessment, the introduction into the risk assessment of human and organizational variables, and the integration into the risk assessment of a safety management layer. In this article, the authors discussed current hazard identification and analysis, risk assessment, and safety management models and methods.

Keywords: Process Safety, Risk Management, Hazard, Inherent Safety, Accident Modeling.

INTRODUCTION

As the world's technical and social growth continues, energy, chemicals and food are in high demand. As a result, the scale and sophistication of processing plants grows. This has ultimately culminated in new dangers and heightened risk, which must not be sacrificed for the sake of economic gain; rather, but minimised and mitigated. Regrettably, injuries of various degrees of magnitude take place. The Flixborough explosion in 1974 was the largest explosion in the United Kingdom during peacetime. According to the reanalysis, the failure was triggered by a two-step process involving the failure of only one bellows, the release of about 10-15 tonnes of cyclohexane, and the detonation of the resultant vapour cloud with an explosive impact of about 280 tonnes of TNT [1].

In 1974, another terrible accident occurred when a Turkish Airlines DC-10 crashed south of Paris killing all 346 passengers and crew members. A broken rear cargo door blew open at an altitude of 12,000 feet causing rapid freight cabin depressurization [2]. The Bhopal tragedy, which occurred in 1984, involved a chemical plant owned by the American multinational Union Carbide, which specialised in pesticide manufacturing. A methyl isocyanate storage tank explosion inside the plant resulted in killing over 3,000 people and infecting tens of thousands more. However, it was discovered that there was a deficiency of security and measures in the safety operations [3]. The Chernobyl nuclear power plant incident was the worst industrial accident involving radiation in the twentieth century. In certain aspects, the magnitude and long-term prevalence of

---

[#] corresponding author: mstamenovic@politehnika.edu.rs radiation pollution poses a threat to the affected population [4, 5]. In 2001, in Toulouse, a catastrophic ammonium nitrate explosion occurred at the AZF plant of the TotalFinaElf Group's Grande Paroisse Company. The blast of between 20 and 120 tons of ammonium nitrate residue caused the deaths of 30 people and the injuries of up to 2242 others [6]. The BP Texas City Refinery experienced an explosion and fire in 2005 due to many pre-existing latent issues and protection system defects. As a distillation tower overfilled and liquid and vapour hydrocarbons were released into the atmosphere, fifteen employees were killed and 180 others were harmed [7].

Several research papers have been written on various aspects of process safety and risk control, including hazard recognition, risk evaluation and prevention, accident simulation, and intrinsic safety [8-10]. The aim of this paper is to provide a historical analysis of process protection and risk management, as well as current research trends. To achieve a deeper understanding of current concepts, methodologies, and procedures related to process safety and risk management, multiple classification criteria are used. The study is limited to areas specifically applicable to process safety and risk management that have been published in peer-reviewed journals.

PROCESS SAFETY ORIGIN

Although, the United States Center for Chemical Process Safety (CCPS), which provides leadership and resources to support and advance PSM, claims that Process Safety began on the banks of the Brandywine River at the E. I. du Pont black powder works in the early 1800s, it is believed that as industrialization and technology accelerated in the early twentieth century, a trend of periodic disasters started to arise leading to the first process safety thinking.

In 1976, a fire and explosion occurred at a small chemical processing plant operated by ICMESA in Seveso, about 25 kilometres north of Milan, resulting in the release of dioxins and poisoning of 2,000 people. This event caused a great deal of attention. The European Community passed the Seveso Directive in 1982, which implemented much tighter industrial controls, in response to a huge and pervasive public uproar about industrial plant safety. In the United Kingdom, the Seveso Directive was revised in 1999, amended again in 2005, and is now known as the Seveso II Directive or Control of Major Accident Hazards Regulations (COMAH) [11].

In 2005, the Buncefield Depot (Hertfordshire, United Kingdom), an oil storage terminal, was hit by a series of explosions that were more powerful than the Flixborough disaster, and were described as the largest of their kind in peacetime Europe. The original investigation, which was sent to the UK's Health and Safety Committee and the Environment Department, came to general conclusions on the need for action in three areas: storage site construction and operation, emergency response to accidents, and planning authority guidance. Legislative reforms were also in process [12].

Scientific studies on process safety and risk began at the same time, and the 1970s was widely regarded as the golden age of process safety and risk research [13]. The American Institute of Chemical Engineers (AIChE) founded the Center of Chemical Process Safety (CCPS) in 1985, shortly after the Bhopal disaster, to create protocols, strategies, criteria, and healthy work practises for chemical process industries [14]. With the aim of fostering best process safety practises across Europe, the European Federation of Chemical Engineering (EFCE) founded the European Process Safety Center (EPSC) [15].

After a major train derailment crash in which a rail car burned, spilling extremely toxic chemicals such as styrene, toluene, propane, caustic soda and chlorine, the Canadian Chemical Producers Association (CCPA) released guideline standards to responsibly handle hazardous content [16]. Methods and models focused on hazard detection and risk management were developed in addition to protocols, processes, and policies.

QUALITATIVE ANALYSIS

Hazard and Operability Analysis (HAZOP) is a well-known and commonly employed qualitative hazard detection tool that investigates not just a system's hazards but also its operability concerns through examining the results of any deviations from design conditions. In 1963, Imperial Chemical Industries (ICI) developed and used the HAZOP for the first time to recognize hazards and understand machinery faults that lead to accidents [13]. There are research initiatives underway to broaden the reach of the HAZOP analysis and change some of its functionality to prevent the study's applicability being limited to highly complex process systems. HAZOP was initially designed to rely on continuous production process/unit processes, but later, the automated tool CHECKOP was developed to increase the reliability and precision of batch process hazard detection [17]. The standard HAZOP protocol was later adapted to perform hazard detection for multifunction electronic devices, and the modified procedure became known as Chazop [18]. Later on, an integrated HAZOP/FMEA (Failure Mode and Results Analysis) approach was developed for risk management in the semiconductor industry [19]. In 2012, scientists created HELPHAZOP, a new HAZOP analysis assistant software. The aim of HELPHAZOP was to address several issues that arose during the functional implementation of the HAZOP analysis, such as the succession instrument of experience information, the classification of accident causes, the recurrence of the analysis procedure, and the verification of analysis outcomes [20].

Major Hazards Analysis (MHA), a modern process hazard analysis technique, was introduced in 2003. Using a categorization scheme and strategizing of triggering incidents that can lead to significant hazards, it offered an effective and thorough identification of major danger scenarios [21].

RISK MANAGEMENT

Understanding why injuries happen and how to keep them from occurring again is crucial to increasing safety in every sector. Obtaining this information necessitates assessing whether a certain set of circumstances, situations, and behaviour result in a certain result, i.e. accident investigation. Analysis models reflect the principle of accident causation conceptually, while investigation approaches show how to put it into practise. Heinrich was the first to create the Domino theory for risk analysis that was later upgraded to Loss causation model theory which puts greater focus on management and operational causes [22]. Johnson's Management Oversight and Risk Tree (MORT) approach produces an idealised control strategy, which is described as a logic tree and includes basic control and management variables [23].

The Swiss cheese model, which showed how individual and systemic deficiencies affected the accident mechanism by taking multi-causality into account, was the most important advance of accident modelling in the early 1990s. A collection of walls prohibit hazards from suffering human casualties in a dynamic environment, according to this metaphor. Each barrier has unintentional defects, or gaps – therefore the Swiss cheese analogy [24, 25].

Later, the idea of "inherent protection" was introduced in risk assessment with the goal of defining inherent dangers and applying inherent safety architecture criteria to eliminate or monitor the danger [26]. Human, management, and operational considerations, including technological and mechanical factors, play an important role in process safety and risk evaluation. Although it is considered that if the roles of the operators and the features of the technology used were understood, human error could be predicted, there are a variety of methodological difficulties in modelling operational variables in safety efficiency.

SAFETY MANAGEMENT FRAMEWORK

System safety monitoring requires the planning of safety cases. Accident scenario design, cause-and-effect review, and safety measure recommendations are all part of the safety case formulation process. In order to avoid serious incidents, early warning and danger thresholds are critical in risk assessment. Similar to the extent and form of dangerous situations present in the environment, a Hazard/Risk Identification Evaluation Preparation (HARP) method was proposed to select the right risk assessment and management strategies [27].

RISK ASSESSMENT

A rigorous risk evaluation not only ensures that all actual threats are recognized, but it also analyses risks minimizing unreal risks and prevent wasting resources by excluding them. An effective risk evaluation often specifies activities in a manner that allows them to be completed efficiently. A simple risk index was suggested, beginning with a basic description of risk, which was the combination of the likelihood of incident and the magnitude of the effects, which was made up of four elements: frequency/probability of accident, dangerous effects of the accident, chemical released inventory, and plant scale [28].

CONSEQUENCE ANALYSIS

The aim of a cause-and-effect study of hazards is to gain a better understanding of them. In order to determine the result of different failures, effect research necessitates a clear understanding of the materials/hazards involved. The physics and chemistry of the results are needed to build mathematical models that can be used to quantify the impact on objects and humans. Heat radiation, food/water contamination, poisoning, contamination from nuclear weapons, and explosions are forms of flammable and harmful releases [29].

CONCLUSIONS

The structured description of the developed methods and models, from their inception to current study, serves as a guide to possible research directions. Around 1960 and 1990, major injuries prompted the adoption of process safety concepts in industrial practise. It has been noted that the number of quantitative innovations is steadily increasing over time. To cope with the complexity of stochastic quantification, a range of mathematical and analytical techniques have been developed. Present process safety and risk growth patterns indicate that research is increasingly based on issues such as data volatility, knowledge scarcity, and process system complexity. However, an increase in the number of technical disasters in developing countries as the globalization process progresses, followed by the transition of technology from developed to developing economies is still possible.

REFERENCES

1. Venart, J.E.S. (2004) Flixborough: the Explosion and its Aftermath. Process Saf Environ Prot 82:105-127.
2. Durbin, P. (1991) Critical Perspectives on Nonacademic Science and Engineering. Lehigh University Press.
3. Di Nardo, M., Madonna, M., Murino, T., Castagna, F. (2020) Modelling a Safety Management System Using System Dynamics at the Bhopal Incident. Appl Sci 10:903.
4. Liland, A., Skuterud, L. (2013) Lessons Learned from the Chernobyl Accident in Norway. pp 159–176.
5. Saenko, V., Ivanov, V., Tsyb, A., Bogdanova, T., Tronko, M., Demidchik, Y., Yamashita, S. (2011) The Chernobyl Accident and its Consequences. Clin Oncol 23:234–243.
6. Dechy N, Mouilleau Y (2004) Some lessons of the Toulouse disaster, 21st september 2001. In: Loss Prevention Bulletin. Praha, pp 2353–2363
7. MacKenzie, C., Holmstrom, D., Kaszniak, M. (2007) Human Factors Analysis of the BP Texas City Refinery Explosion. Proc Hum Factors Ergon Soc Annu Meet 51:1444–1448.
8. Bowonder B (1987) An analysis of the Bhopal accident. Proj Apprais 2:157–168 . https://doi.org/10.1080/02688867.1987.9726622
9. McCreary, J., Pollard, M., Stevenson, K., Wilson, M.B. (1998) Human factors: Tenerife revisited. J Air Transp World Wide 3.
10. Venart, J.E.S. (2007) Flixborough: A final footnote. J Loss Prev Process Ind 20:621–643.
11. Besserman, J., Mentzer, R.A. (2017) Review of global process safety regulations: United States, European Union, United Kingdom, China, India. J Loss Prev Process Ind 50:165–183.
12. Manion, M., Evan, W.M. (2002) Technological catastrophes: their causes and prevention. Technol Soc 24:207–224.
13. Kletz, T.A. (1999) The Origins and History of Loss Prevention. Process Saf Environ Prot 77:109–116.
14. Berger, S. (2009) History of AIChE's Center for Chemical Process Safety. Process Saf Prog 28:124–127.
15. Pasman, H.J., Fabiano, B. (2021) The Delft 1974 and 2019 European Loss Prevention Symposia: Highlights and an impression of process safety evolutionary changes from

the 1st to the 16th LPS. Process Saf Environ Prot 147:80–91.

16. Creedy, G.D. (1990) The CCPA manufacturing code of practice. Plant/Operations Prog 9:238–241.
17. Dunjó, J., Fthenakis, V., Vílchez, J.A., Arnaldos, J. (2010) Hazard and operability (HAZOP) analysis. A literature review. J Hazard Mater 173:19–32.
18. Schubach, S. (1997) A modified computer hazard and operability study procedure. J Loss Prev Process Ind 10:303–307.
19. MacGregor, R.J. (2017) Results matter: Three case studies comparing and contrasting PFFM and HazOp PHA reviews. J Loss Prev Process Ind 49:266–279.
20. Wang, F., Gao, J., Wang, H. (2012) A new intelligent assistant system for HAZOP analysis of complex process plant. J Loss Prev Process Ind 25:636–642.
21. Baybutt, P. (2003) Major hazards analysis: An improved method for process hazard analysis. Process Saf Prog 22:21–26.
22. Wang, J., Yan, M. (2019) Application of an Improved Model for Accident Analysis: A Case Study. Int J Environ Res Public Health 16:2756.
23. Johnson, W.G. Rare Event/Accident Research Methodology. In: Pezoldt VJ (ed) Proceedings of a Workshop held at the National Bureau of Standards. Gaithersburg, Maryland
24. Perneger, T.V. (2005) The Swiss cheese model of safety incidents: are there holes in the metaphor? BMC Health Serv Res 5:71. https://doi.org/10.1186/1472-6963-5-71
25. Larouzee, J., Le Coze, J.-C. (2020) Good and bad reasons: The Swiss cheese model and its critics. Saf Sci 126:104660.
26. Nolan, D.P. (2019) Philosophy of Protection Principles. In: Handbook of Fire and Explosion Protection Engineering Principles for Oil, Gas, Chemical, and Related Facilities. Elsevier, pp 51–64
27. Reniers, G. (2009) An optimizing hazard/risk analysis review planning (HARP) framework for complex chemical plants. J Loss Prev Process Ind 22:133–139.
28. Al-Sharrah, G.K., Edwards, D., Hankinson, G. (2007) A New Safety Risk Index for Use in Petrochemical Planning. Process Saf Environ Prot 85:533–540.
29. Smith, D.J. (2005) Risk assessment (QRA). In: Reliability, Maintainability and Risk. Elsevier, pp 130–141

XIV International Mineral Processing and Recycling Conference
Belgrade, Serbia, 12-14 May 2021

THE IMPACT OF LANDSLIDES AND EROSIONS ON THE MULTI-RISK ASSESSMENT IN THE MUNICIPALITY OF SMEDEREVO

Martina Petković[1], Anita Klikovac[2], Dragan Knežević[3], Biljana Nikolić[1]
[1] Kosovo and Metohija Academy, Department Zvečan, Serbia
[2] Department of Emergency Situations in Smederevo, Sector for Emergency Situations, Ministry of the Interior, Serbia
[3] LOGOS Center, Mostar, Bosna and Hercegovina

ABSTRACT – In the urban area and in the wider vicinity of Smederevo, where loose and irresistible lake sediments are present, there are typical examples of landslides, which, according to the dynamics of movement and surface, are among the largest landslides in Serbia. Therefore, it is important to correctly calculate the multi-risk in order to anticipate adequate organizational and technical measures for the preservation of the ecological equilibrium. Therefore, it is necessary to carry out a multi-risk assessment, which in principle acts and processes, with a specific example of assessment. The paper made a multi-risk assessment for the municipality of Smederevo, which had a major problem with floods and erosions in the past, using GIS.

Keywords: Multi-Risk Assessment, Floods, Erosions.

INTRODUCTION

Landslide hazard, vulnerability, and risk-zoning maps are considered in the decision-making process that involves land use/land cover (LULC) planning in disaster-prone areas. The accuracy of these analyses is directly related to the quality of spatial data needed and methods employed to obtain such data. In this study, we produced a landslide inventory map that depicts 164 landslide locations using high-resolution airborne laser scanning data. The landslide inventory data were randomly divided into a training dataset: 70% for training the models and 30% for validation. In the initial step, a susceptibility map was developed using logistic regression approach in which weights were assigned to every conditioning factor. A high-resolution airborne laser scanning data (LiDAR) was used to derive the landslide conditioning factors for the spatial prediction of landslide hazard areas. The resultant susceptibility was validated using the area under the curve method. The validation result showed 86.22 and 84.87% success and prediction rates, respectively. In the second stage, a landslide hazard map was produced using precipitation data for 15 years. The precipitation maps were subsequently prepared and show two main categories (two temporal probabilities) for the study area (the average for any day in a year and abnormal intensity recorded in any day for 15 years) and three return periods (15-, 10-, and 5-year periods). Hazard assessment was performed for the entire study area. In the third step, an element at risk

---

[#] corresponding author: martina.petkovic@akademijakm.edu.rs map was prepared using LULC, which was considered in the vulnerability assessment. A vulnerability map was derived according to the following criteria: cost, time required for reconstruction, relative risk of landslide, risk to population, and general effect to certain damage. These criteria were applied only on the LULC of the study area because of lack of data on the population and building footprint and types. Finally, risk maps were produced using the derived vulnerability and hazard information [1,2]. Thereafter, a risk analysis was conducted. The LULC map was cross-matched with the results of the hazard maps for the return period, and the losses were aggregated for the LULC. Then, the losses were calculated for the three return periods. The map of the risk areas may assist planners in overall landslide hazard management.

THE LANDSLIDES IN SMEDEREVO

Serbia belongs to the areas that are endangered by landslides and landslides, 30% of the territory of Serbia is susceptible to landslides. In order to reduce the damage, it is important to get acquainted with this natural disaster of seismological and lithospheric character. Landslides represent the movement of earth, stones and other sediments. They are activated and develop quickly, when water accumulates in the soil as a result of heavy and heavy rains, groundwater, melting snow and inadequate land exploitation. They can occur as a result of poor treatment of land, especially in mountainous areas, canyons or near the coast, and they also occur as a result of earthquakes and floods. Rural settlements in the higher parts of the city's terrain are potentially endangered by landslides and landslides due to the danger of torrential floods and torrential phenomena in the tributaries of the Danube and Velika Morava rivers. Although natural landslides can occur in any year, the most common ones are in the period February-May (85%), while only 4% occur in the summer period, and 9% in the autumn, which is in accordance with the hydrological conditions. The picture shows a map of the landslide in Smederevo. Mapping of erosion processes in the area of the city of Smederevo was performed during the fall 2005. Based on the reconnaissance of the terrain and later calculations, an erosion map was made, from which it can be concluded that more than 70% of the area under 22 agricultural crops is affected by erosion processes of various types and categories of destruction. Landslides are the most severe form of erosion. It most often appears on the terrains of Neogene sediments. The big landslide is on the territory of the city settlement known as Kraljevi vinogradi, in the area of the villages Udovice and Seone, especially on the slopes towards the Danube. Surface erosion of medium intensity occurs in practically all arable land and vineyards on slopes steeper than 5%, but due to annual cultivation, it cannot be easily observed [3,4].

In the city area and in the wider vicinity of Smederevo, where loose and irresistible lake sediments are present, there are typical examples of landslides, which, according to the dynamics of movement and surface, are among the largest landslides in Serbia. Preconditions for landslides are especially favorable on the right valley side of the Danube. Unbound sediments, the slope of the layers towards this river, the constant reminder and removal of the accumulated material by the work of the Danube and the disturbance of the stability of the sliding mass, condition the permanent development of the sliding process. In the narrower area of Smederevo, there are a large number of landslides that differ spatially, morphologically and genetically. Larger landslides represent a permanent problem of the overall functioning of the city, because they endanger the road infrastructure, residential buildings, industrial capacities, sports and cultural facilities, the water supply and sewerage system and others.

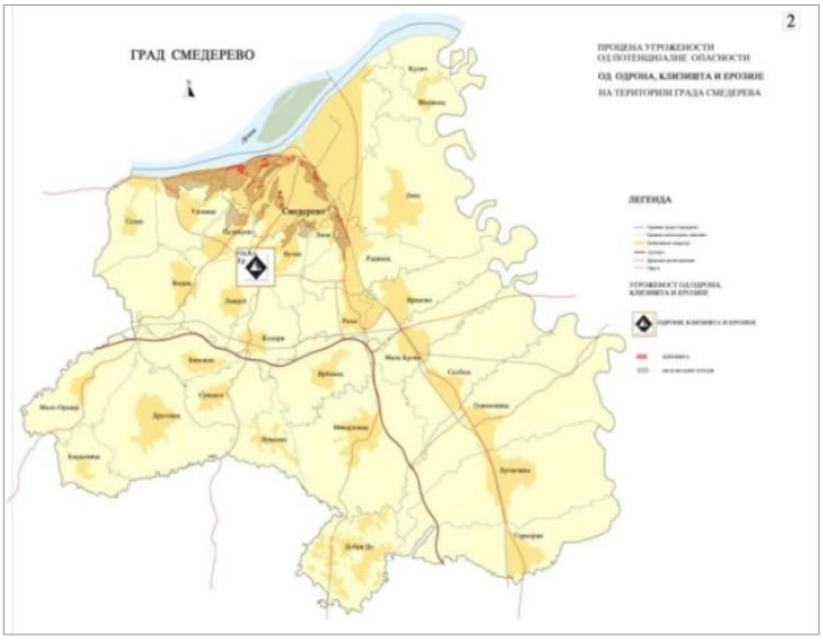

Figure 1 The Landslides In Smederevo

List of Cadastral Municipalities or their parts on the territory of the city of Smederevo under erosion area: KO Smederevo, KO Seone, KO Udovice, KO Vodanj, KO Landol, KO Vučak, KO Malo Orašje, KO Binovac, KO Badljevica, KO Drugovac, KO Suvodol, KO Kolari, KO Mihajlovac and KO Dobri do. The narrower city zone of Smederevo has a large number of larger and smaller landslides, mainly activated by the construction of infrastructure facilities (roads, House of Culture, stadium, sports center, water supply), but also by cutting the landslides by mechanical work of the Danube. In the wider vicinity of Smederevo, landslides occur in the Ralja and Konjska rivers. Landslides in the narrower territory of the city of Smederevo. [4]

1. Landslide in Moračka Street in Jugovo On the upper part of Moračka Street in the settlement of Jugovo, there was a sudden start, activation of the secondary landslide. The landslide is located in a partially urbanized part of the settlement, on a hillside just above the regional road R100 Smederevo - Belgrade. The landslide is shell-shaped, about 5 meters wide and about 20 meters long. The depth of the sliding plane is estimated at about 2 meters. At the beginning of March 2010, in the part of Moračka Street, that is, in its upper part, next to the steep section located on the left side of the street, in the length of about 20 m, a part of the land material along the street was torn off and washed, as well as parts of the road construction. The cause of such landslides and landslides is certainly the sudden melting of the snow that fell at the beginning of the year.

Figure 2 Landslide in Moračka Street in Jugovo

2. Landslide in the settlement of Jablan on Udovicki put In the settlement "Jablan", which is located on the right side of Udovicki put, directly on the part of the slope above this settlement, at the beginning of March 2010, a large amount of land material was torn off and started (sliding). The landslide is frontal, about 30 meters wide and about 80 meters long. The depth of the sliding plane is estimated at about 2 meters. At the beginning of March 2010, on the part of the old Udovicki put, ie in its upper part, directly on the slope of the hill, a part of the land material was torn off and washed away, ie the secondary landslide was activated. The cause of this landslide and splitting of the soil is the appearance of sudden and constant wetting of the earth with atmospheric and shallow groundwater, which appeared primarily after the melting of the snow that fell at the beginning of that year [4].

Figure 3 Landslide in the settlement of Jablan on Udovicki put, Expected degree of negative consequences for nature, material goods and people

Road infrastructure is extremely susceptible to the latent harmful effects of landslides, landslides and erosion. These damages can be caused by the sudden appearance of the collapse of road sections in the length of several tens of meters, as well as the local sinking of the entire width of the road. Underground infrastructure refers to the underground electrical distribution network, water supply and sewerage network and installations, telecommunications network, as well as hot water external distribution network. Underground infrastructure is particularly sensitive to landslides, landslides and erosion because they are difficult to detect and adequate preventive measures cannot be implemented in order to avoid accidents [4].

The city of Smederevo is very sensitive to the occurrence of damage to roads and underground infrastructure, because there may be a standstill or complete interruption of all functions. The following is an overview of the negative consequences of the identified landslides in the city of Smederevo.

Table 1 Consequence of the landslide

Landslide	Consequence
Landslide in Moračka street in the South	The cause of such landslides and landslides is certainly sudden melting snow that fell at the beginning of the year. Except for part of the road in Moračka Street, not a single building was damaged. By activating landslide in March 2010, there was a landslide streets, during which about 300 cubic meters were launched material. Plumbing installations in the hull of the road on that occasion are not damaged. In the area above and below the mentioned street there are a number of objects, but they are not noticeable on them damage. Other buildings in the area are not damaged
Landslide in the settlement Jablan on Udovicki Putu	Several individual buildings are currently threatened by this the occurrence of landslides, and at a distance of about half a meter from the object whose owner is Dragoslav Zlatković, a large scar appeared, whereby the overall stability of this facility is significantly impaired. Currently, no road facility is endangered by this phenomenon. On the mentioned area, except for the building owned by Dragoslav Zlatković (the building is prone to collapse), other buildings are not damaged, but are endangered by further activation of the landslide. Other facilities in the wider area are neither endangered nor damaged.

CONCLUSION

The city of Smederevo is very sensitive to the occurrence of damage to roads and underground infrastructure, because there may be a standstill or complete interruption of all functions. There may be a complete interruption of traffic and communal infrastructure, economic activities of HBIS GROUP Serbia Iron & Steel d.o.o. (Ironworks) and sports facilities-stadiums. Potentially active landslides are in the zone of Plavinac, Dunavska, Majdan. 10-25% of important infrastructural and economic facilities are endangered. Normal functioning for up to 15 days has been disrupted. It takes 30-60 days to normalize the supply. At the same time, with landslides, landslides and erosion, there is a danger of floods, chemical accidents at plants with hazardous substances, epidemics and small-scale epizootics (infectious diseases for humans and animals), plant infectious diseases. At the same time, with the occurrence of landslides, there is a danger of floods in the northern part of the territory next to the Danube River, there is also the possibility of technical and technological accidents at plants with hazardous substances and their transport in the presence of fire. Companies on the territory of the city of Smederevo in their technological processes use about 180 types of hazardous substances with very different physical and chemical properties. They are stored in the prescribed warehouses, but there is always a danger of various chemical accidents, both when handling hazardous substances and during their transport. The area affected by landslides in the area called Plavinac, is limited in the north by the road R 100 Smederevo - Belgrade, in the south by Gorička Street, in the east by Izletnička Street, and in the west by Udovicki Road, due to the activation of this landslide this part of the road may be damaged. Occurrence of technical-technological accidents during transport of dangerous goods. Since the preconditions for landslides are especially favorable on the right valley side of the Danube, unbound sediments, slope of layers towards this river, constant reminding and removal of accumulated material by the Danube and disturbing the stability of the landslide condition, cause permanent landslide process. Due to the landslide in this part, almost all factories and plants located in the northern part of the city, right next to the river Danube ("NIS-GASPROMNEFT"; "Nafta" JSC; "Messer Tehnogas" a. d., "HBIS Group" d.o.o., there are also the following companies: "Du integral"; "Linzer-agro trade" d.o.o; "Eko-mineral" d.o.o .; " Feranex "a.d .;). Also, due to the occurrence of landslides in the territories where there are companies that have hazardous substances, the spillage of hazardous substances and their impact on the environment is expected. Due to the activation of landslides in the city center, damage to residential and commercial buildings is possible, especially traffic, water, sewage, electrical network damage and all this can lead to epidemics and small episodes (infectious diseases for humans and animals), as and plant infectious diseases.

ACKNOWLEDGEMENT

The city of Smederevo is very sensitive to the occurrence of damage to roads and underground infrastructure, because there may be a standstill or complete interruption of all functions. There may be a complete interruption of traffic and communal infrastructure, economic activities of HBIS GROUP Serbia Iron & Steel d.o.o. (Ironworks) and sports facilities-stadiums. Potentially active landslides are in the zone of Plavinac, Dunavska, Majdan. 10-25% of important infrastructural and economic facilities are endangered. Normal functioning for up to 15 days has been disrupted. It takes 30-60 days to normalize the supply. At the same time, with landslides, landslides and erosion, there is a danger of floods, chemical accidents at plants with hazardous substances, epidemics and small-scale epizootics (infectious diseases for humans and animals), plant infectious diseases.

REFERENCES

1. Petković, M., Garvanov, I., Knežević, D., Aleksić, S. (2020) Optimization of Geographic Information Systems for Forest Fire Risk Assessment. 2020 21st International Symposium on Electrical Apparatus & Technologies (SIELA), 3-6 June 2020, Bourgas, Bulgaria, 1-4.

2. Petković, M., Nikolić, B., Božović, M. (2019) The Importance of Multi-Hazard Risk Assessment. Proceedings from the 16th International Conference of Occupational Health and Safety, 9-12 October 2019, Ohrid, North Macedonia, Univerzitet Goce Delčev, Štip.
3. Petković, M., Garvanov, I., Nikolić, B., Knežević, D., Aleksić, S., Milošević, L., Haznadarević, N. (2019) Use of information technologies for calculation of multi risk in The Municipality of Knjaževac, Serbia. ICAT 2019: 8th International Conference on Advanced Technologies (ICAT'19), 26-30 August 2019, Sarajevo, Bosnia and Herzegovina.
4. Klikovac, A. (2020) Izvestaj o klizištima Smederevo, Sektor za VS, 2020.

2021 IMPRC INTERNATIONAL MINERAL PROCESSING & RECYCLING CONFERENCE

XIV International Mineral Processing and Recycling Conference
Belgrade, Serbia, 12-14 May 2021

ANALYSIS OF THE STABLE FIRE EXTINGUISHING SYSTEMS IN UNDERGROUND EXPLOITATION AND MINING

Martina Petković[1#], Milenko Petrović[2], Dragan Knežević[3], Akaid Saradak[3]
[1] Kosovo and Metohija academy, Department Zvečan, Serbia
[2] Faculty of technical sciences, Kosovska Mirovica, Serbia
[3] LOGOS Center, Mostar, Bosna and Hercegovina

ABSTRACT – The paper deals with the dangers of underground exploitation and mining with emphasis on fires and explosions. All causes of fires and explosions in mining, their prevention and control are listed. The fire extinguishing systems is guaranteed total protection against fire emergencies since they are known to significantly minimize damage and prevent loss of life. The Law on Fire Protection and Regulations in this area provide precise requirements for the design and construction of special fire extinguishing systems. The paper presents a comparative analysis of individual fire extinguishing systems in underground exploitation and mining, with innovative solutions in this area.

Keywords: Fire Protection, Fire Extinguishing System, Sprinklers.

INTRODUCTION

Fire is a serious hazard in mines and outbreaks of fire underground can be particularly dangerous due to the:

- confined nature of excavations,
- potential quantity of smoke and noxious fumes,
- restricted ability to evacuate quickly from the mine.

Employers have a duty of care to provide and maintain a safe working environment.

The prevention of fires is a priority for underground mines as they can lead to entrapment, smoke inhalation, serious or fatal burns, asphyxiation and other serious consequences such as explosions.

All underground mines should have a documented underground fire risk assessment that is current and specific to its operations, with appropriate controls in place to manage the risks.

FIRE SAFETY IN MINING

The fire safety problems in mines are in many ways very similar to the problems discussed in road, rail and metro tunnels under construction. There is usually a limited amount of escape routes and the only safe havens are the safety chambers consisting of steel containers with air supply within and rescue rooms which have a separate ventilation system and will withstand a fire for at least 60 minutes. Rescue operation is hard to perform when the attack routes often are equal with the possible path for smoke

---

[#] corresponding author: martina.petkovic@akademijakm.edu.rs to reach the outside. The possibilities for a safe evacuation and a successful fire and rescue operation are strongly linked to the fire development and the smoke spread in these kinds of constructions. For mining companies the problems with evacuation and rescue operations in case of fire are closely linked to policies, work environment protection and their systematic fire safety work. An accident not only can cause injuries, or in the worst case deaths, but also large costs due to production losses, reparations and loss in good-will. The main problem with mines today is that they have become more and more complicated, with endless amount of shafts, ramps and drifts, and it is difficult to control the way the smoke and heat spread in case of a fire. The ventilation strategy is of the greatest importance in such cases in combination with the fire and rescue strategies [1]. Since there are very few fires that occur, the experience of attacking such fires in real life is little.

EXPERIMENTAL

New knowledge about fire and smoke spread in complicated mines consisting of ramps is therefore of importance in order to make reasonable strategies for the personnel of the mining company and the fire and rescue services. The main experience from fighting mine fires comes from old coal mines, which are usually quite different in structure compared to mines in Sweden which mainly work with metalliferous rock products. In Sweden the mines consist of either active working mines with road vehicle traffic and elevator shafts for transportation of people and products or old mines allowing visitors. In some cases it is a combination of both types. As the mine industry is changing and the challenging techniques are developed, the measures to guarantee the safety of personnel need to be adjusted. The new technology means new types of fire hazards, which in turn requires new measures to cope with the risks. New equipment means new types of fire development. The knowledge about fire developments in modern mines is relatively limited. The fire development of vehicles transporting material inside the mines is usually assumed to be from ordinary vehicles, although the vehicles may be considerably different in construction and hazard. The difference may mainly be in the amount of liquid (e.g., hydraulic oil) and the size of the rubber tyres. A relatively straightforward conclusion here is that the need for improvements is great and so is the challenge ahead of us [2].

Mine sites across Serbia and other countries are both broad and varied in how they operate as well as the critical natural resources that they search for. However, all have in common, highly expensive and mission critical equipment that typically operate day and night under extreme hostile conditions, in vast, remote and difficult to access environments, especially on underground equipment. The last thing a mining operation can afford is a fire. Not only will it threaten the safety of operators and destroy vital equipment, a devastating fire most certainly will be catastrophic to production and profits. This is why it is so important to ensure that all these mission critical equipment are protected by appropriate fire protection systems. Fire safety in the industry On a mine site, fire hazards may occur in and around process plants, underground conveyors, static and mobile plants, draglines, workshops, substations, monitored control rooms and switch rooms. In many cases non-gaseous and gaseous fire suppression systems are the preferred systems installed to protect the high value assets, safeguard operators and processes so as to guarantee business continuity. Systems and equipment used Non-gaseous systems are primarily used on mobile plant and are usually not scheduled extinguishing agents under the Ozone Protection and Synthetic Greenhouse Gas Management Act 1989 (the Act). Gaseous fire suppression systems typically encompass extinguishing agent stored in pressurised cylinders that are connected to a network of discharge pipework and nozzles that deliver the extinguishing agent to an enclosure to be protected. Typically, they also include dedicated fire detection and control systems which provide an automatic discharge if a fire starts [2].

These systems are best used to primarily protect delicate electronic and electrical equipment against fire due to their quick detection of a fire event, and rapid suppression & extinguishment capabilities.

An additional benefit is the extinguishing agents used do not leave any residue after discharge, and hence sometimes are referred to as ‘clean agents’. There are two broad groups of extinguishing agents:

- Inert gases-are naturally occurring gases such as nitrogen, argon, carbon dioxide or combinations of these (e.g.IG541, IG55). They extinguish fires by reducing the available oxygen to a level below that which a fire needs to burn (typically less than 15%).
- Synthetic gases–are manmade manufactured gases and they extinguish fires by reducing heat and using chemicals to interfere with the fire chain reaction.

Both types of extinguishing agents have their own advantages and disadvantages. This means that choosing the most suitable fire extinguishing agent for a specific application will depend on a range of factors including their impact on the environment.

Scheduled extinguishing agents A number of synthetic extinguishing agent sareo zone depleting substances(ODS), i.e. when released into the atmosphere they will deplete the stratospheric ozone, and/or synthetic greenhouse gases(SGG), i.e. when released into the atmosphere they will contribute to global warming.

As such, these are defined as scheduled agents under the Actand the Ozone Protection and Synthetic Greenhouse Gas Management Regulations 1995 (the Regulations). The Regulations stipulate certain obligations in how they are to be acquired, stored, used, handled, disposed of and maintained safely to minimise their impact on the environment. Under the Act, a scheduled extinguishing agent can only be discharged where the product containing the extinguishing agent is being used for its designed purpose, in other words in response to an actual fire. Discharge for testing or training purposes are not permitted unless the person meets the requirements in the Regulations, and has been granted a fire protection industry permit to do so by the Fire Protection Industry (ODS & SGG) Board (the Board). It is very important that all mine owners, facility managers, and operators understand the potential environmental impacts of scheduled extinguishing agents if released into the atmosphere.

The types scheduled extinguishing agents in the mining industry Scheduled extinguishing agents that are most typically used on mine sites are:

Typically they will be contained in fixed fire suppression systems located in or around the fire risk areas such as control rooms, data centers, electrical switch rooms, and process control rooms. Large mobile plants including large excavators, shovels, draglines, haul trucks and wheeled loaders may also have fire suppression systems installed that may contain such agents. The primary scheduled extinguishing agent used on mine sites isFM-200®/ FE-227™ (with some minimal use of NAF S-III and NAF P-III). Halon systems (halon 1301, halon 1211) have been phased out dueto its significant ozone depleting and global warming impact to the environment are now typically not found on mining sites. The use of halon has been restricted to only “essential use”, and a halon special permit must be held. If you are aware of a halon system installed in your facility (easily identified by its yellow cylinders) you should arrange for the system to be decommissioned and the cylinders sent to the National Halon Bank for disposal [2, 1].

Table 1 The types scheduled extinguishing agents

Product name	Uses	Other name
FM-200® FE-227™	Function is total flooding agents. Typical applications could include chemical storage areas, clean rooms, communication facilities, laboratories, museums, robotics and emergency power facilities.	Heptafluoropropane HFC-227ea
NAF-P-III	Tipically used as a streaming agent. It is a replacement for halon-1211. Effective on Class A, B and C type fires.	HCFC Blend C
NAF-S-III	Tipically used as a total flooding agent. It is a replacement for halon-1301. Effective on Class A, B and C type fires.	HCFC Blend A

Ensuring correct servicing and installation of fire protection systems All fire equipment and systems including gaseous fire suppression systems need to be regularly tested, serviced and maintained to help ensure that they will be ready to operate as intended at the event of a fire. Australian Standard, AS 1851-2012 Routine service of fire protection systems and equipmentsets out these requirements. The objective of AS 1851 is to maximise the reliability of fire protection systems and equipment such that the systems and equipment meet the requirements of the relevant design, installation and commissioning standards and are likely to continue to do so until the next scheduled activity. Section 7 of the standard contains the inspection and testing requirements for gaseous fire suppression systems. Under the Regulations, to minimise the environmental impact for accidental discharge of scheduled extinguishing agents it mandates that work on such systems (including the installation, decommissioning and servicing) must be performed by an appropriate licensed technician [3].

Mining fire safety summary For gaseous fire suppression systems to operate effectively on mining site, it is recommended that: -Owners, facility managers, only have technicians working on gaseous fire suppression systems that hold the appropriate Extinguishing Agent Handling licence (EAHL) when installing, decommissioning, servicing or handling scheduled extinguishing agents. -Owners of gaseous fire suppression systems use a maintenance log book to record all maintenance activity. The use of logbooks will establish a process for documentation and provide a full life-cycle chain of custody documentation for all installed systems. A log book would record all maintenance activity and record the details of the licensed technician who is servicing the system. -Ongoing maintenance of systems will greatly improve the efficiency and longevity of the system.

CONCLUSION

Fire protection requirements related to mining are extensive and differing since the industry is defined by large operations and complex production processes. Fires and explosions pose a constant threat to miners and to the production capacity of mines. A fire in a mine can have awful ramifications for human lives and economic viability. Storage, handling and use of flammable and combustible materials pose ever-present fire hazards in all sectors of the mining process. Moreover, vehicles used in mining and other heavy equipment in both surface and underground operations are usually diesel-powered and a large percentage of mining related fire incidents have involved fuel used by these machines. Likewise, fire protection systems and contingency plans are required for other key operational assets such as machinery, electrical rooms, UPS rooms to safeguard the working environment and to offer assurance for business continuity. Mine operators demand a compact fire protection system that is effective, robust and autonomous. FirePro can help in the fire detection and suppression of fires related to power generation equipment, vehicles and electrical equipment. Our systems can considerably reduce hazards to personnel and prevent financial losses due to down times. FirePro modular mining related systems are sensitive to issues of running costs, effectiveness, durability and personnel safety.

ACKNOWLEDGEMENT

Fire protection requirements related to mining are extensive and differing since the industry is defined by large operations and complex production processes. Fires and explosions pose a constant threat to miners and to the production capacity of mines. The fire risk assessment will help managers determine what type of fire-fighting equipment is appropriate and where to site it. In selecting fire-fighting equipment, managers will need to take account of the nature of the fire hazard. This is particularly important if the fire might involve electrical equipment and/or flammable liquids.

REFERENCES

1. Fire Safety in Mines and Underground Constructions, SVEMin 2009, The Swedish Mining Industry's Health and Safety Committee.
2. http://www.fpaa.com.au/media/203619/mining_industry_article.pdf
3. https://www.hse.gov.uk/mining/feguidance.pdf

XIV International Mineral Processing
and Recycling Conference
Belgrade, Serbia, 12-14 May 2021

NOISE SOURCES AND CONTROL IN UNDERGROUND METAL MINING

Miomir Mikić[#], Milenko Jovanović, Daniela Urošević, Radmilo Rajković
Mining and Metallurgy Institute Bor, Serbia

ABSTRACT – Application of modern technologies in the mining industry through energy efficiency, higher labour productivity, adopting continuous production methods, operational flexibility, resulted the use of machinery and equipment of high capacity. Parallel to this, the result was a significant increase in the number of noise sources and noise levels in open pit and underground mining. The paper presents noise sources, the impact of noise on labour and suggestions to reduce noise impact in the workplace.

Keywords: Noise, Level, Impact, Mining.

INTRODUCTION

Noise or noise disturbances are caused by excessive noise that can harm the activities or balance of human or animal life [1]. The source of most of the world's external noise is mainly caused by machines and transport systems, motor vehicles, planes and trains [1]. This type of noise is briefly summarized as environmental noise. Poor urban planning can lead to increased noise, as both industrial and residential buildings can lead to noise pollution in populated areas.

External noise can be caused by machines, due to construction activities, and musical performance, especially in some workplaces. Hearing loss due to noise can be caused by external (e.g. trains) or internal (e.g. music) noise.

High noise levels can contribute to cardiovascular effects in humans and increase the incidence of coronary heart disease [2]. In animals, noise can increase the risk of death due to the inability to detect and avoid predators, obstructed reproduction and navigation, and contribute to permanent hearing loss [3].

NOISE IN MINING

Work being carried out to expand productivity in mining has indicated the need to use larger machines in parallel with improvements in technology. The increase in mechanization has led to an increase in noise levels. Professional noise in underground mines has reached unbearable levels of noise due to the natural propagation of sound in narrow spaces. Therefore, it is difficult to find an environment for workers with relatively low noise levels.

In reality, the noise that occurs during exploitation works (drilling-blasting, excavation, loading and transport of excavations) that take place at underground mines is significant when it comes to the health of workers and their performance at work, because noise has the highest rate of disease and illness in mining, which leads to

---

[#] corresponding author: miomir.mikic@irmbor.co.rs permanent or temporary hearing impairment of workers [4].

In addition, noise appears to be the cause of an accelerated heart rate, high blood pressure and narrowing of blood vessels. Workers exposed to noise sometimes complain of nervousness, insomnia and fatigue [5]. Therefore, it is crucial to conduct research on this issue and to make suggestions to the mine management in order to preserve the health of the workers. Compared to the level of noise exposure in different industries (airport, wood industry, cement industry, foundries, textile industry, printing, ship engine room, etc.), the noise levels encountered in mining are second only to the noise generated by jets. engines at airports [6].

Noise-induced hearing loss most commonly occurs at high frequencies (3000, 4000, or 6000 Hz) and then spreads to low frequencies (500, 1000, or 2000 Hz) [7].

Kinds of noise sources depend on the technology applied in an open cast mining. Apart from blasting works, which are the source of short-lived noises, there are also continuous noises. Sources of this kind of noise constitute machines and devices used in the excavation processes, transporting, dumping and crushing of raw materials.

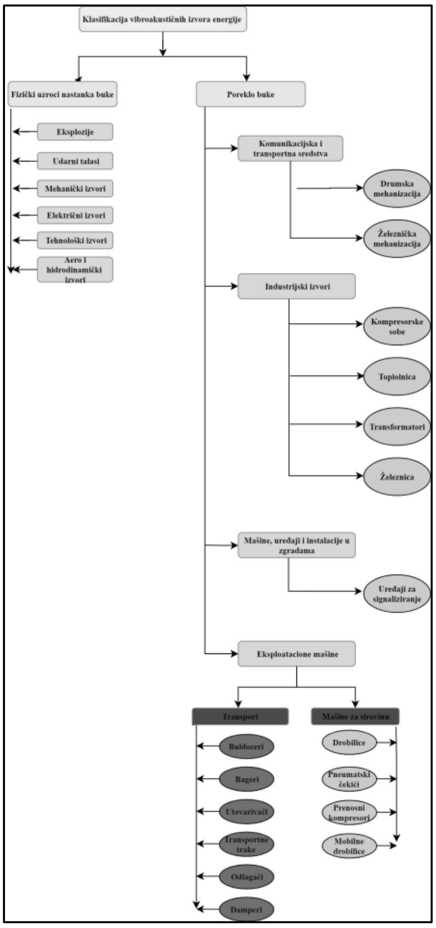

Figure 1 Classification of vibroacoustic energy sources

Each machine, device or means of transportation has many elementary vibroacoustic energy sources. The vibroacoustic energy source is understood as a mechanical or acoustic system generating acoustic vibrations. Properties of such source can be assessed in two ways:

- considering the properties of an acoustic field generated by the source, which provide the so-called external or field characteristics of the source,
- considering the properties of the source itself as the vibroacoustic energy emitter.

The collection of such properties constitutes the so-called internal characteristics of the source. [8].

External characteristics of the source are used for assessment of an acoustic effect generated by the source, while internal characteristics - for assessment of the source itself [8].

Sources can be classified from many points of view. The basic division consists of: theoretical models of radiation, physical reasons of noise generation and the noise origin.

Classification of vibroacoustic energy sources occurring in underground mines of mineral raw materials, performed when taking into account two criteria: physical causes of noise generation and the noise origin - is given in Figure 1. The machines which emit most vibroacoustic energy: are mining machines, especially: Haul Trucks, crushers, pneumatic hammers, drilling rigs, excavators, dumping conveyers and belt conveyers. The most annoying sources of vibroacoustic energy are explosions at blasting works, which are also the sources of shortlived noises.

NOISE LEVELS

The noise levels emitted by haul trucks, load-haul-dump vehicles (LHD) and jumbo drills and bolters are presented in this paper.

Haul trucks are constructed with various sound absorbing materials, such as vinyl-covered material installed in the area in front of the operator; Also, engine enclosures and sealing gaps are having more – less absorbing role.

Performed testing on haul trucks represents results in table 1.

Table 1 Sound level at the haul truck operator's position, underground measurement [9]

	Without vinyl-covered material (dB[A])	With vinyl-covered material in canopy only (dB[A])	With all vinyl-covered material (dB[A])	Noise reduction with vinyl-covered material in canopy (dB[A])	Noise reduction with all vinyl-covered material (dB[A])
Low idle	83.2	82.4	82.6	0.8	0.6
High idle	100.6	100.0	99.6	0.6	1.0

Load-haul-dump vehicles (LHD) similar like haul trucks are constructed with various sound absorbing materials. The engineering noise controls on the machine consisted of a partial engine enclosure and sound-absorbing material in the engine compartment and in the cab. The used materials are thick steel panels, thick fiberglass sound-absorbing material, thick rubber.

Comparing the surface and underground measurements, the underground environment adds about 3 to 4 dB(A) to the sound level at the operator's ear. The table 2 shows the application of all controls in the underground environment resulted in an attenuation of 1.5 dB(A) at the operator position.

Table 2 Sound level for LHD at the operator's position, high idle [9]

	Surface measurement			Underground measurement		
	Without enclosure (dB[A])	With enclosure (dB[A])	Noise reduction (dB[A])	Without enclosure (dB[A])	With enclosure (dB[A])	Noise reduction (dB[A])
Both sides on or off	91.9	90.8	1.1	95.8	94.3	1.5
Right side off, Left side on or off	91.6	90.8	0.8	95.1	94.3	0.8

Noise controls for jumbo drills and bolters consisted of several motor covers or barriers, treatments applied inside the cabs, and different cab windshield designs.

Table 3 shows the sound levels without and with noise controls applied to the electric-motor-powered hydraulic pumps. It should be noted that the sound levels generated with only the electric motors on were less than 85 dB(A). Sound levels during drilling and bolting can exceed 100 dB(A).

Table 3 Sound level for jumbo drills and bolters at the operator's position, underground [9]

Motors	Noise control	Without control (dB[A])	With control (dB[A])	Noise reduction (dB[A])
Bolter	0.25-inch-thick heavy conveyor belt	84.9	83.2	1.7
Bolter	1.5-inch-thick fiberglass blanket	77.3	76.9	0.4
Face drill	0.5-inch-thick heavy conveyor belt	79.4	77.2	2.2
Face drill	1.5-inch-thick quilted fiberglass absorptive material	79.9	79.5	0.4
Face drill	0.25-inch-thick Plexiglas	84.3	81.9	2.4

Table 4 shows the sound levels without and with the material and the resulting noise reduction achieved by applying it to the canopy. The face drill measurements were taken underground during the drilling cycle, and the bolter results were measured above ground with the percussive hammer operating. The data show the sound-absorbing material did not significantly change the sound levels at the operator's position in this case.

Table 4 Sound level of jumbo drills and bolters at the operator's position [9]

Motors	Without absorptive material (dB[A])	With absorptive material (dB[A])	Noise reduction (dB[A])
Bolter	97.4	97.3	0.1
Face drill (with windshield)	99.6	99.6	0.0
Face drill (without windshield)	100.3	100.1	0.2

Table 5 shows the sound levels with and without the absorptive material placed around the operator and the resulting noise reduction. The data indicate that the absorption around the operator has essentially no effect on the sound level during the drilling process.

Table 5 Sound level of jumbo drills and bolters at the operator's position, absorptive material around operator [9]

	Without quilted material around operator area (dB[A])	With quilted material around operator area (dB[A])	Noise reduction (dB[A])
Bolter (drilling)	97.5	97.6	-0.1
Bolter (bolting)	98.4	98.7	-0.3
Face drill (motor)	78.1	77.2	0.9

CONCLUSION

Basic noise controls include barriers and sound-absorbing materials. A barrier is a solid obstacle that is somewhat impervious to sound and that interrupts the direct path from the sound source to the receiver. For the best reduction in sound level, the barrier should be:

- placed as close as possible to either the source or receiver;
- assembled to be as tall and wide as practical so it extends well beyond the direct source-receiver path; and
- constructed of a material that is solid and airtight.

Sound-absorbing treatments reduce reflections and the resulting echoes and reverberation. Usually, these materials are porous. Compared to high frequency sounds, low frequency sounds are more difficult to absorb with materials and to block with barriers. Therefore, it is important to know the frequency content for a particular noise problem.

Based ol noise levels shown at tables 1-5, we can concluded that usage of sound absorbing materials is good for noise control. Mainly because they are inexpensive and simple to attach to existing surfaces.

Also, windshields and environmental cabs can be highly effective noise controls, especially for high frequency noise.

For the noise reduction benefits of existing barriers plugging gaps in machine panels and windshields with a material that creates an airtight seal can greatly enhance.

Noise levels survey sampling is necessary to determine any overexposure in order to effectively eliminate or reduce them [1]. Additionally, reduction of occupational noise in mines is an effective factor to ensure adequate and productive working conditions [1].

ACKNOWLEDGEMENT

This work was financially supported by the Ministry of Education, Science and Technological Development of the Republic of Serbia, Grant No. 451-03-9/2021-14/ 200052.

REFERENCES

1. Mikić, M., Rajković, R., Rajković, B., Jovanović, M. (2018) REVIEW OF Noise sources in mining, the impact of noise in the working environment and measures for its control, Mining and geology today ii international symposium, pp. 259 - 264, 978-86-82673-14-9 (RI), Beograd, 1. - 2. Dec, 2018.
2. Hoffmann, B., Moebus, S., Stang, A., Beck, E.M., Dragano, N., Möhlenkamp, S., Schmermund, A., Memmesheimer, M., Mann, K. (2006) Residence close to high traffic and prevalence of coronary heartdisease. European Heart Journal, 27 (22), pp. 2696–2702.
3. Results and Discussion Effects Noise Effect On Wildlife Noise Environment FHWA. www.fhwa.dot.gov. Decembar 2015.
4. Scott, D. F., Grayson, R. L., Edward, A. (2004) Disease and Illness in U.S. Mining, 1983-2001. J. of Occup. & Env. Medicine 46 (12), pp.1272.
5. U.S. Dept. of labor, Noise Control – A Guide for Workers and Employers, Occup. Safety & Health Administration, pp.119 (no date).
6. Sensogut, C., Cina, R. I. (2007) An Empirical Model for the Noise Propagation in Open Cast Mines – A Case Study, Applied Acoustics, 68, pp. 1026.
7. Chen, J.D., Tsai, J.Y. (2003) Hearing Loss among Workers at an Oil Refinery in Taiwan. Archives of Environmental Health, ISSN 003-996, 58 (1), pp.55.
8. Jacek, R., Engel, Krzysztof Kosala. (2007) Sources of vibroacoustic hazards in open-pit mines of mineral raw materials. Archives of acoustics 32, 2, pp.251-262.
9. Noise Control in Underground Metal Mining.

ABSTRACTS

TROUBLESHOOTING OF THE SECONDARY VIBRATING SCREEN AT THE GOHAR-ZAMIN IRON ORE COMPLEX BY MONITORING THE 3D CLOGGING PATTERNS

Hamid Reza Shirazi, Hamid Khoshdast[#]**, Mohammad NaeimZeidabadi Nejad**
Higher Education Complex of Zarand, Kerman, Iran

ABSTRACT – In this research, the performance of the vibrating banana screen used in the HPGR circuit of Gohar-Zamin Iron Ore Complex was evaluated by monitoring the clogged apertures of both screening decks. In order to plot the three-dimensional pattern of clogging of each deck, the proportion of free and clogged apertures of every individual to the longitudinal and transverse sections of the screen were measured separately for each deck. For each measurement step, the screen was stopped after about 500 hours of operation and restarted immediately after all panels were photographed to avoid any interruption in the production process. In order to analyze more precisely the influence of different parameters on the screening efficiency, the number and position of the replaced panels at each stop stage were also taken into account. Examination of 3D clogging patterns showed that most of the upper deck damages were related to the primary panels, which were subject to high input loads. In the case of the lower deck, most of the damage is related to a row of panels beneath the upper deck panels with larger apertures. The 3D pattern plots also provide other useful information, such as the time-dependent impact of wash water failures, poorly installed components, varying quality of installed panels, and tonnage input to the screen.

Keywords: Screen, Vibrating, HPGR, Iron ore.

[#] corresponding author: khoshdast_hamid@yahoo.com

XIV International Mineral Processing
and Recycling Conference
Belgrade, Serbia, 12-14 May 2021

INTELLIGENT SIMULATION OF METALLURGICAL RESPONSE OF GOHAR-ZAMIN IRON ORE PROCESSING COMPLEX USING BIOGEOGRAPHY-BASED ANN METHOD

Alireza Gholami, Mohammad NaeimZeidabadi Nejad, Hamid Khoshdast[#]
Higher Education Complex of Zarand, Kerman, Iran

ABSTRACT – In this study, the prediction of metallurgical parameters of the production in Gohar-Zamin Iron Ore Processing Plants based on selected feed parameters was evaluated by artificial neural networks (ANN) method using Biogeography algorithm. Grade, tonnage and yield of concentrate were considered as production responses and grade, tonnage and characteristic size (d80) of feed were chosen as input parameters. To develop the models, production data during one operating year from the first processing plant were collected systematically and used to train the developed network. The mean squared error (MSE), root mean squared error (RMSE), percentage error and coefficient of determination (R2) were used to evaluate the performance of different models. Evaluations showed that the best prediction results were achieved using structure [4-2-1] for Fe and FeO, and structure [4-5-1] for concentrate tonnage and yield. Models were validated using data collected over three consecutive months of production, and the results showed that the developed models provide over 98% fit for all responses. This study revealed that using the ANN method can significantly contribute to more accurate and intelligent production management.

Keywords: Prediction, Modeling, Process, Control, ANN.

[#] corresponding author: khoshdast_hamid@yahoo.com

XIV International Mineral Processing
and Recycling Conference
Belgrade, Serbia, 12-14 May 2021

CADASTRE OF MINING WASTE FROM ABANDONED MINES IN SERBIA 2020, EU/IPA FUND - PRELIMINARY REMARKS

Bogoljub Vuković[#]
EPS, RB Kolubara, Lazarevac, Serbia

ABSTRACT – The history of modern mining in Serbia dates back to the end of the 19th century. Initially, underground pit mining was primarily on metal and coal ores. After WW II reset and additionally start as open pit mining, also first mines start on non-metals. Numerous mines were in operation; after decades of operation they were closed. The opening, operation and closing of these pits was sometimes not accompanied by a binding legal procedure, and if it was, the documentation was lost. Particular attention was paid to mining tailing during excavation and ore processing. After many years, these mines have been forgotten, as have their tailing. The paper provides an overview of these forgotten mines, tailing and sites.

Keywords: Mining, Waste, Cadastre, Serbia.

[#] corresponding author: bogoljub.vuckovic@eps.rs

XIV International Mineral Processing
and Recycling Conference
Belgrade, Serbia, 12-14 May 2021

THE ROLE OF ALGERIAN LEGISLATION IN MANAGEMENT OF HEALTHCARE WASTE

Cherifa Benzidane[#]
University of Oran 02, Algeria

ABSTRACT – The Algerian legislation has given an importance to treatment of healthcare waste within the framework of respecting the principles of public health and the environment, as Algeria is aiming to improve the capabilities of treating waste management by 0.4 million Dollars annually, with imposing the laws and taxes in order to reduce many environmental and health damages that result from mismanagement waste of health institutions, especially that Algeria has recorded an increase of health institution workers who are infected of blood diseases by more than 50%, which may result the risk of developing immunodeficiency diseases and hepatitis.

Keywords: Waste, Healthcare, Management, Algeria.

[#] corresponding author: benzidanecherifa1989@gmail.com

XIV International Mineral Processing
and Recycling Conference
Belgrade, Serbia, 12-14 May 2021

THE STRATEGY OF UNITED ARAB EMIRATES IN DEVELOPING RENEWABLE ENERGIES

Cherifa Benzidane[#]
University of Oran 02, Algeria

ABSTRACT – The leadership in renewable energies is no longer confined to Western countries, UAE has been able to develop strategy for developing renewable energies aims to achieve a sustainable environment in terms of air quality, water conservation, reliance on clean energy and the application of green development, and reducing the energy generated from gas from 98% in 2012 to less than 76% in 2021 by diversifying energy include clean and renewable sources and increasing use efficiency. The strategy also aims to increase using of renewable energy between 25% to 30% by focusing on nuclear energy, solar energy and electricity production.

Keywords: Renewable, Energy, Sources, Efficiency.

[#] corresponding author: benzidanecherifa1989@gmail.com

XIV International Mineral Processing
and Recycling Conference
Belgrade, Serbia, 12-14 May 2021

SIMULATION OF CHERRY OIL BIODIESEL PRODUCTION

Marija Tasić[1#], Katarina Stamenković[1], Milan Kostić[1], Olivera Stamenković[1], Vlada Veljković[1,2]
[1] University of Nis, Faculty of technology, Leskovac, Serbia
[2] The Serbian Academy of Sciences and Arts, Belgrade, Serbia

ABSTRACT – Cherry pits (waste from the fruit processing industry, rich in oil) can be a valuable biodiesel feedstock. This study aimed at simulating the steady-state biodiesel production from cherry kernel oil based on the mass and energy balances, using Aspen Plus (v.8.6) software. The process units were simulated based on the literature's experimental works. The annual production was assumed to be 8015 tons of biodiesel. The simulation results showed that the production plant processed 19677 tons of raw material and consumed 10 GW of energy yearly. This study is the first attempt to evaluate large-scale biodiesel production from cherry kernel oil.

Keywords: Cherry pits, Biodiesel, Oil, Production.

[#] corresponding author: marijat14@yahoo.com; mtasic@tf.ni.ac.rs

AUTHORS INDEX

AUTHOR INDEX

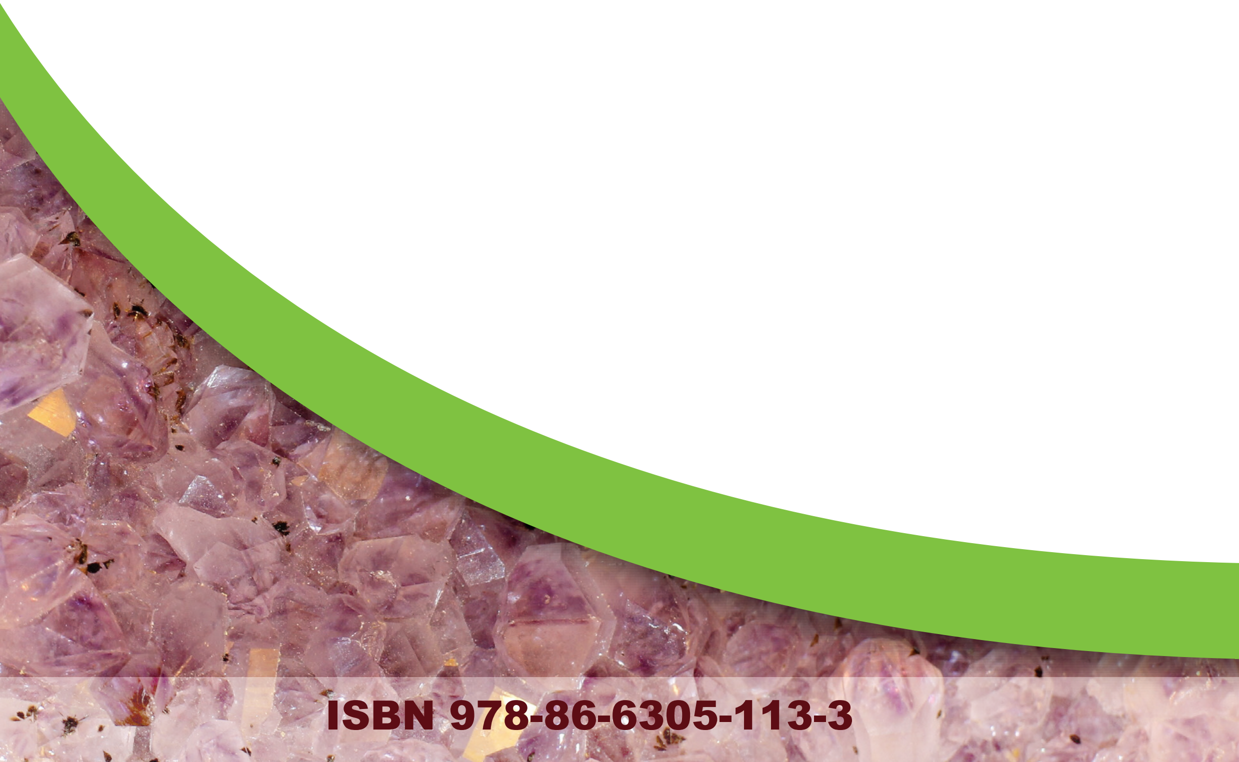

ISBN 978-86-6305-113-3